Author:
Hartley, April E

Title:
Understanding the Role of Bone in the Pathogenesis of Osteoarthritis

Understanding the Role of Bone in the Pathogenesis of Osteoarthritis

April Elizabeth Hartley

A dissertation submitted to the University of Bristol in accordance with the requirements for award of the degree of PhD in the Faculty of Health Sciences, September 2020.

Word count: 81,385

ABSTRACT

There is strong evidence that higher bone mineral density (BMD) is a risk factor for osteoarthritis (OA), although the association with OA progression is unclear. It is uncertain if observational associations reflect a causal effect of bone on joint deterioration, or shared underlying biology.

I examined the role of BMD in OA progression by determining change in radiographic sub-phenotypes (osteophytes, joint space narrowing) at the hip and knee in individuals with high bone mass (HBM, L1 and/or total hip Z-score≥+3.2), comparing progression to their relatives without HBM (Chapters 6,7). HBM individuals had increased progression of radiographic OA sub-phenotypes at both joints, compared to their relatives. Metabolomics analysis did not identify any metabolic traits, and thus metabolic pathways, which could mediate the association between HBM and OA (Chapter 8).

I next performed multivariable Mendelian randomization (MVMR) in UK Biobank to determine if BMD exerts a causal effect on OA, independent of confounding by body mass index (BMI) (Chapter 9). MVMR identified a BMI-independent causal effect of BMD on hip and knee OA (26% and 36% increased odds per SD increase, respectively).

Subsequently, I analysed the underlying biological pathways contributing to both BMD and OA, by calculating the proportion of variance in hospital-diagnosed hip and knee OA explained by genetic variation in the Wnt signalling, TGFβ superfamily and osteoclast differentiation pathways (Chapter 10). This analysis provided evidence for a BMD-independent contribution of these pathways to OA. Further MVMR analyses identified a BMI-independent causal effect of circulating IGF-1 on risk of hospital-diagnosed hip and knee OA (49% and 22% increased odds per SD increase, respectively, Chapter 11).

This work suggests a role of BMD in structural OA progression at the hip and knee, reflecting a direct role of bone in joint deterioration, as well as shared underlying pathways, such as the IGF-1 axis.

ACKNOWLEDGEMENTS

First of all, I am extremely grateful to the Wellcome Trust for funding this PhD, including my research and personal development, for the past four years.
I am truly grateful to my supervisors, Dr Celia Gregson, Dr Lavinia Paternoster and Professor Jon Tobias, for their time and guidance over the past four years. I am grateful to Dr Raquel Granell, who provided supervision during my second year. I am also extremely grateful to Professor Joyce van Meurs, Erasmus Medical College, for her expertise and for providing access to Rotterdam data and. I am also thankful to Dr Sarah Hardcastle, for volunteering her time to share her knowledge of grading radiographic osteoarthritis.

HBM follow-up imaging and questionnaire administration was co-ordinated with the help of Mrs Karen Ireland, High Bone Mass study Administrator. I am extremely thankful for Karen's support during my early PhD. I am also extremely grateful to the High Bone Mass study PIs and collaborators at the participating follow-up sites, including Maxine Osgerby, Karen Blesic, Dr Margaret Paggiosi and Jacqueline Shipley. I also wish to thank the High Bone Mass study participants for giving up their valuable time to participate in the follow-up study.

I would also like to acknowledge the technical guidance provided by members of the MRC Integrative Epidemiology Unit and the wider research community. I am grateful to my mini project supervisors and collaborators, namely Dr Kim Hannam, Dr Evie Stergiakouli, Dr Hannah Jones, Dr Diana Santos-Ferreira, Dr Emma Anderson, and Professor Deborah Lawlor, for teaching me the skills and techniques to form a solid foundation for my main research project. I am also grateful to all the peer reviewers who improved my manuscripts with their insightful feedback.

Finally, I am extremely appreciative for the support of my family and friends over the past four years. I am especially thankful for the advice and support provided by Dr Monika Frysz, whose words of wisdom from her own recent PhD experience were essential for the success of this PhD.

AUTHOR'S DECLARATION

I declare that the work in this dissertation was carried out in accordance with the requirements of the University's Regulations and Code of Practice for Research Degree Programmes and that it has not been submitted for any other academic award. Except where indicated by specific reference in the text, the work is the candidate's own work. Work done in collaboration with, or with the assistance of, others, is indicated as such. Any views expressed in the dissertation are those of the author.

SIGNED: ..... DATE:.....

PUBLICATIONS RELATED TO THIS WORK

Work from this thesis has been published in three peer-reviewed publications. All manuscripts contain my own work, with all analyses performed by myself. I wrote the first full draft of each manuscript before comments and edits were provided by co-authors. Copies of the published papers, including full statements of contribution, are provided in Appendix 1-Appendix 4.

Peer-reviewed manuscripts

1. **Hartley A**, Hardcastle SA, Paternoster L, McCloskey E, Poole KES, Javaid MK, *et al*. Individuals with high bone mass have increased progression of radiographic and clinical features of knee osteoarthritis. Osteoarthritis and cartilage. 2020. Published online ahead of print.
   This paper contains results presented in Chapter 6.
2. **Hartley A**, Hardcastle SA, Frysz M, Parkinson J, Paternoster L, McCloskey E, *et al*. Increased development of radiographic hip osteoarthritis in individuals with High Bone Mass: a prospective cohort study. Arthritis Research and Therapy. 2021. Published online ahead of print.
   This paper contains results presented in Chapter 7.
3. **Hartley A**, Paternoster L, Evans DM, Fraser WD, Tang J, Lawlor DA, *et al*. Metabolomics analysis in adults with high bone mass identifies a relationship between bone resorption and circulating citrate which replicates in the general population. Clinical endocrinology. 2020;92(1):29-37.
   This paper contains results presented in Chapter 8.
4. **Hartley A**, Sanderson E, Paternoster L, Teumer A, Kaplan R, Tobias JH, and Gregson CL. Mendelian randomization provides evidence for a causal effect of higher serum IGF-1 concentration on risk of hip and knee osteoarthritis. Rheumatology. 2021. Published online ahead of print.
   This paper contains results presented in Chapter 11.
5. **Hartley A**, Gregson CL, Paternoster L and Tobias JH. Osteoarthritis: insights offered by the study of bone genetics. Current Osteoporosis Reports. Accepted November 2020.
   This review was adapted from Chapter 3 by Professor Jon Tobias and I commented on the manuscript.

Conference abstracts

The following conference abstracts have been published in *Osteoarthritis and Cartilage*, April 2020 and are provided in Appendix 5, Appendix 6.

1. **Hartley A**, Sanderson E, Granell R, Paternoster L, Zheng J, Southam L, Zeggini E, Gregson CL, and Tobias JH. Using multivariable mendelian randomization to estimate the BMI-independent causal effect of bone mineral density on osteoarthritis.
   This abstract contains results presented in Chapter 9.
2. **Hartley A**, Sanderson E, Paternoster L, Granell R, Tobias JH, and Gregson CL. Mendelian randomization identifies a causal role for serum insulin-like growth factor-1 in hip osteoarthritis.
   This abstract contains results presented in Chapter 11.

The following abstract was published in JBMR Volume 32, Supplement 1.

1. **Hartley A**, Paternoster L, Murphy A, Hardcastle S, Tobias JH, and Gregson CL. Circulating sclerostin is associated with preserved joint space in non-weight bearing joints in a population enriched for high Bone Mineral Density.
   This abstract contains results presented in Chapter 10.

Manuscripts in preparation

1. **Hartley A**, Sanderson E, Granell R, Paternoster L, Zheng J, Davey Smith G *et al.* Using multivariable mendelian randomization to estimate the causal effect of bone mineral density on osteoarthritis risk, independent of body mass index.
   This manuscript contains results presented in Chapter 9.

STATEMENT OF CONTRIBUTION

Technical guidance on extracting SNP dosage data from VCF files was provided by Dr Joost Verlouw, Erasmus MC. GWAS scripts were adapted from Dr Lavinia Paternoster's (https://github.com/epxlp/GWAS_scripts). '*EasyQC*' scripts were provided by Dr Jie Zheng, University of Bristol.

As I was working on the High Bone Mass study as a study Administrator prior to commencement of my PhD, I was able to design the questionnaire and submit the amendment application to the Research Ethics Committee prior to my PhD commencement date and the date of REC approval therefore predates my PhD commencement.

TABLE OF CONTENTS

LIST OF TABLES

LIST OF FIGURES

LIST OF APPENDICES

LIST OF ABBREVIATIONS

1SMR	One Sample Mendelian Randomization
2SLS	Two Stage Least Squares
2SMR	Two Sample Mendelian Randomization
AC	Articular Cartilage
ACL	Anterior Cruciate Ligament
ADAMTS	A Disintegrin And Metalloprotease with Thrombospondin Motifs
ALSPAC	Avon Longitudinal Study of Parents And Children
AOGC	Anglo-Australasian Genetics Consortium
AP	Anteroposterior
BCAA	Branched Chain Amino Acid
BMC	Bone Mineral Content
BMD	Bone Mineral Density
BMI	Body Mass Index
BML	Bone Marrow Lesion
BMP	Bone Morphogenetic Protein
BMU	Basic Multicellular Unit
BTM	Bone Turnover Marker
BUA	Broadband Ultrasound Attenuation
BWHHS	British Women's Heart and Health Survey
CHARGE	Cohorts for Heart and Aging Research in Genetic Epidemiology
CHECK	Cohort Hip Cohort Knee
CI	Confidence Interval
CMC	Carpometacarpal
CV	Coefficient of Variation
CTX-1	C-terminal Telopeptide of Type 1 Collagen
DAG	Directed Acyclic Graph
DIP	Distal Interphalangeal
DXA	Dual X-ray Absorptiometry
EA	Effect Allele
EAF	Effect Allele Frequency
eBMD	estimated Bone Mineral Density
ECM	Extracellular Matrix
eQTL	expression Quantitative Trait Locus
FAI	Femeroacetabular Impingement
FM	Fat Mass
FN	Femoral Neck
FOM	Focus On Mothers
FRAX	Fracture Risk Assessment Tool
FRP	Frizzled Related Protein
GAG	Glycosaminoglycan
GC	Genomic Control
GCP	Genetic Causality Proportion

GDF5	Growth Differentiation Factor-5
GEE	Generalized Estimating Equations
GEFOS	Genetic Factors for Osteoporosis
GIANT	Genetic Investigation of Anthropometric Traits
GO	Genetics of Osteoarthritis
GP	Growth Plate
GWAS	Genome Wide Association Study
HA	Hyaluronic Acid
HBM	High Bone Mass
HCS	Hertfordshire Cohort Study
HDL	High Density Lipoprotein
HES	Hospital Episode Statistics
HRC	Haplotype Reference Consortium
HRT	Hormone Replacement Therapy
HR-QoL	Health Related Quality of Life
HWE	Hardy-Weinberg Equilibrium
IBS	Identical By State
ICC	Intraclass Correlation Coefficient
ICD	International Statistical Classification of Diseases and Related Health Problems
IGF-1	Insulin-like Growth Factor-1
IGFBP-3	IGF Binding Protein-3
IHH	Indian Hedgehog
IL	Interleukin
IMD	Index of Multiple Deprivation
IPAQ	International Physical Activity Questionnaire
IQR	Interquartile Range
IVW	Inverse Variance Weighted
JoCo	Johnston County Osteoarthritis Project
JSN	Joint Space Narrowing
KL	Kellgren-Lawrence
KNHANES	Korean National Health and Nutrition Survey
LCV	Latent Causal Variable
LD	Linkage Disequilibrium
LDL	Low Density Lipoprotein
LM	Lean Mass
LMM	Linear Mixed Model
LMWM	Low Molecular Weight Metabolites
LRP	Low-density lipoprotein Receptor-related Protein
LS	Lumbar Spine
MAF	Minor Allele Frequency
MCP	Metacarpophalangeal
M-CSF	Macrophage Stimulating Factor
MET	Metabolic Equivalent Task
MetS	Metabolic Syndrome
MGP	Matrix Gla Protein

mJSW	minimal Joint Space Width
MMP	Matrix Metalloproteinase
MPC	Mesenchymal Progenitor Cell
MR	Mendelian Randomization
MRI	Magnetic Resonance Imaging
MrOS	Study of Osteoporotic fractures in Men
MRU	Musculoskeletal Research Unit
MSC	Mesenchymal Stem Cell
MVMR	Multivariable Mendelian Randomization
NBT	North Bristol NHS Trust
NCP	Non-Collagenous Protein
NEA	Non-Effect Allele
NHS	National Health Service
NMR	Nuclear Magnetic Resonance
NTX-1	N-terminal Telopeptide of Type 1 Collagen
OA	Osteoarthritis
OAI	Osteoarthritis Initiative
OARSI	Osteoarthritis Research Society International
OPC	Osteochondral Progenitor Cell
OPG	Osteoprotegerin
OR	Odds Ratio
OSQ	Osteoporosis Screening Questionnaire
OSX	Osterix
P1NP	N-terminal Propeptide of Type 1 Collagen
PA	Physical Activity
PBMC	Peripheral Blood Mononuclear Cell
PC	Principal Component
PIP	Proximal Interphalangeal
POC	Primary Ossification Centre
pQCT	peripheral Quantitative Computed Tomography
PRS	Polygenic Risk Score
PTH	Parathyroid Hormone
PTHrP	Parathyroid Hormone-related Protein
QC	Quality Control
RANK	Receptor Activator of Nuclear factor Kappa-B
RANKL	Receptor Activator of Nuclear factor Kappa-B Ligand
RCI	Reliable Change Index
RCT	Randomised Controlled Trial
REC	Research Ethics Committee
RS	Rotterdam Study
RUNX2	Runt-related transcription factor-2
SD	Standard Deviation
SE	Standard Error
SEKOIA	Strontium Ranelate in Knee Osteoarthritis
SES/SEP	Socio-Economic Status/Position
SF	Synovial Fluid

SNP	Single Nucleotide Polymorphism
SOC	Secondary Ossification Centre
SOF	Study of Osteoporotic Fractures
SOS	Speed Of Sound
SOX9	SRY-Box Transcription Factor-9
StR	Strontium Ranelate
TASOAC	Tasmanian Older Adult Cohort
TB	Total Body
TBFM	Total Body Fat Mass
TBLM	Total Body Lean Mass
TGFβ	Transforming Growth Factor-β
TH	Total Hip
THR	Total Hip Replacement
TJR	Total Joint Replacement
TKR	Total Knee Replacement
TNF	Tumour Necrosis Factor
TRAcP	Tartrate Resistant Acid Phosphatase
TREAT-OA	Translation Research in Europe Applied Technologies for OA
VEGF	Vascular Endothelial Growth Factor
VIBE	Vertical Impacts on Bone in the Elderly
VLDL	Very Low Density Lipoprotein
WOMAC	Western Ontario and McMaster Universities Arthritis Index

CHAPTER 1. OSTEOARTHRITIS

1.1. Joints

Joints occur at the margin between two bones. Joints are an organ consisting of multiple interdependent tissues. There are two main types of joints: synovial and solid joints (1). Synovial are the most common type of joint and are found at the ends of human long bones and are distinguished by the presence of a cavity surrounding the joint components (1,2) (section 1.1.1). Solid joints have no capsule and instead the components of the joint are bound by connective tissue (1).

Joints can be further classified by shape and movement (1). The different shapes of joints are plane, hinge, pivot, bicondylar, condylar, saddle and ball and socket (1). Bicondylar joints are named as such as there are two contact points in the joint; an example is the knee joint (1). In terms of movement, joints can be uniaxial, biaxial, or multiaxial (1). Multiaxial joints are named due to their ability to move along multiple axis; an example is the 'ball and socket' hip joint (1).

1.1.1. Features of a synovial joint

Figure 1 presents the structure of a knee joint, an example of a synovial joint. The knee consists of the common features of a synovial joint: the synovium which encapsulates the joint, a synovial cavity consisting of synovial fluid (SF), articular cartilage (AC), subchondral bone and tendons and ligaments (all discussed in detail below) (3). The knee joint is highly specialised to provide frictionless movement despite being a weight-bearing joint and has additional features (the menisci and the fat pad) (3), which are discussed below.

Figure 1: Structure of a synovial joint (the knee).

Reproduced from (3).

Features common to all synovial joints

Articular cartilage

AC is an avascular and aneural tissue of up to 3mm thickness (3). This tissue allows movement of the joint with limited friction and dissipates load to protect the underlying subchondral bone (3). There is one cell type present in the AC: the chondrocyte. Chondrocytes secrete an extracellular matrix (ECM) consisting mainly of type II collagen and proteoglycans, along with water to maintain the pressure within the cartilage, to withstand mechanical load (3). The main proteoglycan, aggrecan, has glycosaminoglycan (GAG) chains which bind to water, generating the stiffness of cartilage, whilst collagen provides the strength (3). The majority of AC is uncalcified, with the exception of a thin layer adjacent to the subchondral bone; where this layer meets the uncalcified cartilage is called the tidemark. The calcified region of cartilage is involved in the transition of mechanical properties between cartilage and bone (3).

Capsule and synovium

The capsule is a fibrous structure which encapsulates the joint, providing blood vessels which bring nutrients to the joint, as well as lymphatic vessels and nerve fibres (3). The capsule supports the synovium, which is a thin layer of cells (maximum two cells deep), which maintains an aseptic environment in the joint, through type A synovial cells (3). The synovium is involved in joint lubrication by the synthesis and secretion of hyaluronic acid (HA) and lubricin by the type B synovial cells (3). The capsule and synovium are a source of mesenchymal progenitor cells (MPCs, also referred to as MSCs), which can differentiate into chondrocytes (3).

Synovial fluid

SF coats the joint surface and provides nutrition to the joint (3). There are two main constituents of SF: HA and lubricin. Lubricin is synthesized in response to mechanical forces in the joint and provides lubrication (3). HA is involved in lubrication and nutrient transfer to cartilage (4).

Subchondral bone

The subchondral bone plate is the layer of cortical bone underlying the joint, at the end of the long bones. It is thinner and less stiff than other cortical bone, with its thickness related to cartilage thickness and the thickness of the trabecular bone underneath, rather than body size (3). Underlying the bone plate is the subchondral trabecular bone, which provides support and absorbs forces (5). Cortical and trabecular bone are described in section 2.1.2.

Tendons and ligaments

The ligaments of a joint connect the two bones, providing stability, whilst the tendons connect the bone to muscle, converting muscle contractions into movement of the joint (6). Both tendons and ligaments are composed of collagen fibres (mainly type I).

Knee-specific features

Infrapatellar fat pad

The fat pad between the patella and femur, also known as Hoffa's fat pad, provides a source of MPCs, which differentiate into chondrocytes (3).

Menisci

Medial and lateral menisci in the knee joint, formed mainly of type I collagen fibrils, are responsible for dissipating mechanical load (particularly during knee flexion), absorbing impact and maintaining stability, to prevent joint injury (6). Aggrecan in the centre of the meniscus provides stiffness.

1.2. Osteoarthritis

1.2.1. Definition

Arthritis is a disease of the joints and osteoarthritis (OA) is the most common form of arthritis. OA is colloquially known as 'wear and tear' arthritis, although as discussed in section 1.2.2, this is an outdated term. OA used to be thought of as cartilage degradation, but evidence has since lead to the current thinking that OA is a disease of the whole joint (7). Osteoarthritis Research Society International (OARSI), proposed the following definition in 2015 (8):

"Osteoarthritis is a disorder involving movable joints characterized by cell stress and extracellular matrix degradation initiated by micro- and macro-injury that activates maladaptive repair responses including pro-inflammatory pathways of innate immunity. The disease manifests first as a molecular derangement (abnormal joint tissue metabolism) followed by anatomic, and/or physiologic derangements (characterized by cartilage degradation, bone remodelling, osteophyte formation, joint inflammation and loss of normal joint function), that can culminate in illness".

OA can be defined as primary or secondary depending upon its aetiology. Secondary OA is caused by joint injury or comorbid disease. Primary OA develops without injury or comorbid disease, most likely due to a combination of risk factors (discussed in section 1.2.5). OA can further be defined as either atrophic or hypertrophic based on radiographic features. Atrophic OA describes severe cartilage loss without features of extra bone formation, whereas hypertrophic OA is characterized by excess bone formation without cartilage loss (9). These radiographic features will be discussed in more detail in section 0.

1.2.2. Pathogenesis

OA used to be known as 'wear-and-tear arthritis' due to the prior belief that the pathogenesis of OA was solely based on the degeneration of AC. It is now widely accepted that OA is a condition affecting all tissues of a synovial joint, caused by an imbalance between anabolic and catabolic processes within the joint (10). This

has led to the hypothesis that OA is a syndrome, whereby a range of pathogenic pathways lead to an end-stage phenotype of joint destruction (10). The pathogenic processes of OA are presented in Figure 2 and detailed below.

Figure 2: Pathogenic processes occurring in an OA joint.

Reproduced from (11).

Cartilage degeneration

Chondrocytes normally maintain matrix integrity by producing matrix degrading enzymes such as the metalloproteinases (MMPs) or aggrecanases (such as A Disintegrin And Metalloproteinase with Thrombospondin motifs [ADAMTS]4/5) to degrade the damaged tissue and producing new matrix to replace the damaged tissue (11-14). However, in OA, the production of matrix-degrading enzymes exceeds the anabolic processes leading to progressive cartilage loss (15). The disequilibrium between the anabolic and catabolic processes in OA is thought to be caused by mechanical injury, inflammation or age-related declines in the anabolic properties or number of chondrocytes (13-15). Additionally, receptors on chondrocytes can bind to advanced glycation end products, which accumulate with age, causing a shift to catabolism (11).
When catabolism exceeds anabolism, loss of aggrecan due to the action of aggrecanases reduces the concentration of GAGs in the matrix, altering the water content of the cartilage and making it less able to withstand mechanical loading and increasingly vulnerable to further damage (16). During the pathogenic process of OA, chondrocytes start to produce inflammatory mediators, such as cytokines and chemokines (15,16). These inflammatory mediators, along with the accumulation of products of cartilage degradation, stimulate MMP and ADAMTS synthesis by the chondrocytes (Figure 2) (14-16). Accumulation of these inflammatory mediators, in addition to abnormal loading due to reduced cartilage integrity, leads to chondrocyte hypertrophy. Hypertrophic chondrocytes, which are terminally differentiated, produce less type II collagen

but produce catabolic factors such as MMP13 (17). As cartilage is aneural, initial cartilage degeneration does not cause pain. However, as OA progresses, vascular invasion of the cartilage from the subchondral bone (see below), mediated by vascular endothelial growth factor (VEGF), and innervation occurs, contributing to pain severity (10,16,18,19).

Osteophyte formation

Formation of additional bony 'spurs' at the joint margin, known as osteophytes, is a characteristic feature of OA, visible on a radiograph (section 0). These form due to the reactivation of endochondral ossification (the process of forming bone from cartilage, described in section 2.1.3) (10). It is thought that formation of osteophytes is stimulated by growth factors such as insulin-like growth factor-1 (IGF-1) and transforming growth factor-β (TGFβ); both can be produced by chondrocytes or subchondral osteoblasts, and expression levels of both have been correlated with OA severity (15,16,18). It has been hypothesized that osteophyte formation represents an attempt to repair the joint by increasing the surface area, to dissipate load and prevent irreparable damage to the cartilage (19). Alternatively, animal studies suggest that osteophytes form due to blood vessel penetration into degrading cartilage (15).

Subchondral bone remodelling and sclerosis

Subchondral bone plays a key role in OA pathogenesis, although it is currently unknown if changes in subchondral bone remodelling precede, or are a consequence of, cartilage degeneration (14,18). Increased bone remodelling early in OA, where bone resorption exceeds formation, leads to thinning of the subchondral bone plate (18). This could reflect a response by osteocytes to repair microcracks in the bone, or a response to cytokines produced by deteriorating cartilage (18). Endochondral ossification is re-established at the tidemark, creating multiple tidemarks, and thickening of the calcified cartilage, reducing the area of the non-calcified cartilage (11,18). Bone marrow lesions (BMLs) can be seen on a magnetic resonance imaging (MRI) scan early in the disease process,

these are a feature of microdamage to the subchondral bone and associated increased vascularity (19).

As OA progresses, subchondral bone formation increases, but the bone is poorly mineralized. This is due to the production of TGFβ by the subchondral osteoblasts, increasing production of the Wnt inhibitor Dickkopf-related protein-2 (DKK-2), which inhibits mineralization (the Wnt signalling pathway is described in section 2.1.3) (18). The composition of α chains in type I collagen (section 2.1.1) is altered, which further contributes to hypomineralization (14). An increase in thickness of the subchondral bone plate with poor mineralization generates a sclerotic bone plate which is stiff and creates greater pressure on the underlying cartilage (16). This is known as subchondral sclerosis and can be visualized on a radiograph (section 0) as a marker of severe and irreparable damage (19). The trabecular number and volume of the underlying trabecular bone is increased (14). Subchondral bone cysts can occur at the later stage of disease, where complete cartilage loss has occurred; cysts reflect the entry of SF into bone marrow (14).

Synovitis

Synovitis, which refers to synovial inflammation, is believed to be occur secondary to initial joint damage, due to the degradation products of both cartilage and bone, such as type II collagen fragments. Synovitis is therefore often localized to regions of damaged cartilage or bone (11,15,16). These degradation products cause an immune response in the synoviocytes, which produce cytokines, MMPs and aggrecanases leading to further cartilage degeneration (11,20). Synovitis leads to excess SF secretion which causes swelling and joint effusion (15). Synovitis is also characterized by hyperplasia of the synovial membrane due to proliferation of the synoviocytes, which increases synovial vascularity (10,15).

Inflammation

Although OA used to be thought of as a non-inflammatory condition, recent evidence suggests a role of chronic low-grade inflammation in OA pathogenesis

(15). Damage-associated molecular patterns in the joint, produced due to the breakdown of the cartilage ECM, trigger an innate immune response and subsequent production of inflammatory mediators (21). This leads to increased synthesis of MMPs and ADAMTSs and reduced synthesis of type II collagen (15,16). IL1β, a proinflammatory cytokine, stimulates IL6 production by chondrocytes (16). IL6 stimulates osteoblasts in subchondral bone to produce matrix-degrading enzymes, which can diffuse into AC, leading to further cartilage degradation (16). Synoviocytes additionally produce these proinflammatory cytokines in response to collagen degradation products (11,14). However, it is currently unknown if inflammation is a cause or response to cartilage damage, as joint inflammation (*e.g.* due to injury) could be the initial factor causing the initial imbalance between anabolic and catabolic processes (15). Despite clear *in vitro* evidence and biological plausibility for a role of the proinflammatory mediators IL1β and TNFα in OA pathogenesis, trials of drugs targeting these cytokines have not demonstrated efficacy, suggesting that one cytokine alone is not key to OA pathogenesis (21). Alternatively, as inflammation is often present prior to development of radiographic features, it may be that these pro-inflammatory cytokines have a more important role in initial disease development rather than progression (21).

Hypothesized model of pathogenesis

Although it is now widely accepted that OA is a disease of the whole joint, it is currently unclear whether pathogenic changes in the subchondral bone or changes in AC occur first. Burr and Gallant (18) generated a hypothesized model of OA pathogenesis, whereby repetitive joint loading leads to initial subchondral bone remodelling. This in turn leads to vascular invasion of the deeper layers of cartilage, allowing cartilage access to chondrolytic enzymes. Products of cartilage degeneration potentially stimulate synovitis and loss of cartilage integrity, leading to increased subchondral bone formation as an adaptive response to the greater loads. This would generate a pathological cycle as the increased subchondral bone formation would lead to subchondral sclerosis (densification

of the subchondral bone plate) and further cartilage loss. Burr and Gallant's hypothesized model is presented in Figure 3.

Figure 3: Hypothesized timeline of processes in OA pathogenesis.

Reproduced from (18).

1.2.3. Diagnosis

There is no laboratory test to specifically diagnose OA. In a clinical setting, diagnosis generally occurs upon presentation of a patient to a healthcare setting due to symptoms (11). Diagnosis of OA is normally based on either radiographic features and/or clinical symptoms (22). Common symptoms of OA include pain, especially after use of the joint, which often improves on rest, and stiffness of the joint upon wakening in the morning. Clinical signs often examined to aid clinical diagnosis of OA include crepitus, bony enlargement, a reduced range of movement, tenderness upon palpation of the joint and malalignment and/or instability (22). Criteria for diagnosing OA of the hand, hip and knee have been developed by the American College of Rheumatology and these are summarised in Table 1.

Table 1: American College of Rheumatology criteria for diagnosis of OA of the hand, hip, and knee.

	Clinical and laboratory	**Clinical and radiographic**	**Clinical**
Hand	Hand pain, aching or stiffness plus at least two of: • Hard tissue enlargement of at least two joints • Hard tissue enlargement of two or more distal interphalangeal joints • Less than three swollen metacarpophalangeal joints • Deformity of at least one joint Joints assessed: 2nd/ 3rd distal interphalangeal, 2nd/3rd proximal interphalangeal, first carpometacarpal of both hands		
Hip	Hip pain plus at least two of: • Erythrocyte sedimentation rate <20mm/hour • Femoral or acetabular osteophytes		

	• Superior, axial, or medial joint space narrowing		
Knee	Pain plus at least five of: • Aged 50+ years • Stiffness <30 minutes • Crepitus • Bony tenderness • Bony enlargement • No palpable warmth • Erythrocyte sedimentation rate <40mm/hour • Rheumatoid factor <1:40 • Synovial fluid signs of OA	Pain, osteophytes plus at least one of: • Aged 50+years • Stiffness <30 minutes • Crepitus	Pain plus at least three of: • Aged 50+ years • Stiffness< 30 minutes • Crepitus • Bony tenderness • Bony enlargement • No palpable warmth

Adapted from (23-25).

Radiographic OA in a research setting

Radiographic definition using plain X-ray is currently the most common method for assessing OA in research settings, although MRI methods are more sensitive to change over time. MRI can detect early features in the pathogenic process and features unobservable on a radiograph, such as early cartilage changes and BMLs, and MRI is likely to become the standard way for diagnosing OA in research studies in the future (9,11,16).

Several key features of OA can be viewed on a standard radiograph: loss of joint space (used as a marker of cartilage degeneration), osteophytes, subchondral sclerosis, and subchondral cysts (26). Malalignment at the knee and deformity of the femoral head are additional features of OA which can be visualized on a radiograph. Not all features may be present. The tibiofemoral joint of the knee is imaged using an anteroposterior (AP) knee X-ray and the patellofemoral joint is imaged with a lateral view. Radiographic knee OA in most epidemiological studies refers to tibiofemoral OA. Knee X-rays are normally performed in a weight-bearing position (*i.e.* standing), to observe narrowing of the joint space. This can be with the knee in a semi-flexed or extended position, with the semi-flexed position generating more accurate measures of medial minimal joint space width (mJSW) (27). Hip OA is normally viewed on an AP pelvis radiograph, performed with the patient in a supine position. Examples of hip and knee

radiographs, with and without features of OA, are presented in Figure 4 and Figure 5. X-rays of the hand can be performed to diagnose hand, finger, or thumb OA, normally with a posteroanterior view (Figure 6). OA most commonly affects the distal interphalangeal (DIP), carpometacarpal (CMC, the thumb case) and the proximal interphalangeal (PIP) joints of the hand (Figure 6) (28).

Figure 4: AP knee radiographs showing the tibio-femoral joint.

Image removed for copyright purposes

The radiograph on the left is normal (i.e. no features of OA evident). The radiograph on the right displays large osteophytes of the tibia and femur margins, both medially and laterally, and severe medial joint space narrowing. Reproduced from (29).

Figure 5: AP pelvic radiographs showing the hip.

Image removed for copyright purposes

The radiograph on the left is normal (i.e. no features of OA evident). The radiograph on the right displays large osteophytes of the femur and acetabulum, both superior and inferior, and severe medial joint space narrowing. Reproduced from (29).

Figure 6: Joints of the hand commonly affected by OA (left) and a radiograph of a DIP joint severely affected by OA (osteophytes and JSN).

Image removed for copyright purposes

Reproduced from (28,29).

In research settings, Kellgren-Lawrence (KL) grading is commonly used to define OA severity (30). KL grading evaluates OA severity on a scale of 0-4, with zero representing a joint with no radiographic features of OA, and four representing severe OA, with a cut-off of two and above used to define the presence of OA (30). The radiographic criteria for each of the grades for knee OA, originally proposed by Kellgren and Lawrence in 1957, are presented in Table 2. However, various interpretations of the gradings now exist (31). A 2008 review identified five different interpretations of the KL grades for knee OA across 18 cohort studies, mainly differing in the level of joint space narrowing (JSN) required for grades two and three (32). Radiographic atlases have been generated to

standardize the grading of the individual radiographic sub-phenotypes (*i.e.* osteophytes, JSN, subchondral sclerosis) (29,33). Quantitative measures of JSW, performed on the medial aspect of the knee or the superior aspect of the hip, can be used as more sensitive measures of change in cartilage thickness over time.

Table 2: Grading criteria for radiographic knee OA originally proposed by Kellgren and Lawrence (29).

Grade	Radiographic features
0	No radiographic features of OA observed
1	Doubtful JSN, possible osteophytes
2	Definite osteophytes, possible JSN
3	Moderate osteophytes, JSN, some sclerosis, possible deformity of bone ends
4	Large osteophytes, severe JSN, severe subchondral sclerosis, deformity of bone ends

1.2.4. Epidemiology

Prevalence

Data from the Global Burden of Disease study 2010 generated worldwide prevalence estimates of 3.8% for knee and 0.9% for hip OA (34). Prevalence is increasing; data from the US highlighted that the number of people with clinical hand, hip or knee OA increased from approximately 21 million in 1995 to 27 million in 2005 (35). This reflects an ageing population and the increasing prevalence of risk factors such as obesity (section 1.2.5) (36).

Prevalence estimates vary by joint studied, with much higher estimates for hand, compared to hip or knee OA, and a higher prevalence of knee compared to hip OA. Analyses of individuals aged 50 years or older from the Framingham population determined a prevalence of 20% for radiographic hip OA in the cohort from 2002-2005, with a much lower prevalence of symptomatic hip OA, at 4.2% (37). Prevalence estimates for radiographic knee OA of 31% for men and 34% women have been measured in an earlier Framingham cohort (1983-1985) (38). In the Rotterdam study, the prevalence of radiographic OA in at least one hand joint was 67% for women and 55% for men (39). However, prevalence of

symptomatic OA of the hand is much lower, with 14% women and 7% of men diagnosed with symptomatic hand OA in the 1992-1995 Framingham cohort (40).

Estimates for the prevalence of OA vary depending upon the definition used, for example the prevalence of radiographic OA is higher than the prevalence of symptomatic OA, as radiographic OA is commonly required alongside symptoms to define symptomatic OA (41,42). There is discordance between radiographic and symptomatic evidence for OA and it is estimated that up to 50% of individuals with radiographic OA do not have symptoms (43). Prevalence estimates even vary within definitions; although a KL grade of two or more is normally used to determine OA, other thresholds can be used (44,45). As discussed earlier, a KL grade of two can be interpreted in different ways and Kerkhof *et al* identified four different interpretations for knee OA and two for hip OA in the Translation Research in Europe Applied Technologies for OA (TREAT-OA) consortium (45). When the definitions were standardized across studies, the maximum prevalence estimates decreased from 55% to 25% for knee OA and from 33% to 10% for hip OA (45).

The prevalence of radiographic OA varies by population, with African Americans displaying a greater prevalence of both radiographic and symptomatic hip and knee OA compared to Caucasians in the Johnston county OA project (JoCo) (46,47). Analyses of a Chinese population in Beijing identified a lower prevalence of hip and hand OA compared to US Caucasian populations, but Chinese women had a higher prevalence of knee OA (48-50).

Incidence

Generally, studies of the incidence of OA have been based either on incidence of radiographic OA in cohorts drawn from the general population (Framingham and Chingford) (40,51,52) or data extracted from routine healthcare records (53-57). Data derived from both sources have revealed a higher incidence for women compared to men (51,53-57) and studies investigating site-specific incidence consistently show a greater incidence of knee, compared to hip and hand OA (Figure 7) (53,56,57).

Figure 7: Incidence of OA at the hand, hip and knee across age groups and stratified by sex.

Reproduced from (10).

The largest study of the incidence of hand, hip and knee OA in the general population was performed by Prieto-Alhambra *et al,* who utilised primary care record data covering approximately 3.3 million individuals, representing approximately 80% of the population of Catalonia, Spain (56). They observed an overall incidence of 2.4 per 1000 person-years for hand, 2.1 per 1000 person-years for hip and 6.5 per 1000 person-years for knee OA (56). The incidence of both hip and knee OA increased with age up until age 80, with a steep increase in incidence seen between ages 50 and 70 years for knee OA (Figure 7) (56). The incidence of hand OA in women rose steeply between ages 45 and 55 years, reflecting the menopausal period (56). A decrease in incidence of knee OA after age 80 years may reflect survivor bias, whereby individuals who are less likely to develop knee OA (*e.g.* because they are not obese) are more likely to survive to this age (56). Analysing primary care records from Staffordshire, UK, Yu *et al* also identified an increasing incidence rate for individuals aged 35-44 years, from 0.3 per 1000 person-years in 2003 to 2.0 per 1000 person-years in 2010 (57). This increasing risk in younger individuals likely reflects an increasing prevalence of risk factors such as obesity (section 1.2.5).

Estimates of the incidence of radiographic OA in cohort studies are slightly higher at 2-3% per year (51,52). This probably reflects the use of radiographic definitions in cohort studies, where everyone is X-rayed even if they do not display symptoms. The inclusion of those with possible radiographic features at baseline (*i.e.* KL=1) in the population at risk in cohort studies may also increase incidence rates. Leyland *et al* identified a five-times greater odds of incident knee OA in those with a KL grade of one at baseline compared to those with a KL grade of zero (52).

Burden

OA conveys a significant socioeconomic burden worldwide. The economic costs can be separated into direct and indirect costs (36). Direct costs include the costs to healthcare services, of which the majority is attributable to total joint replacement (TJR) surgery (58). The estimated direct cost of OA in the UK in 2010 was £1billion (58). Indirect costs can be experienced at both a societal and an individual level and represent the cost related to lost productivity due to the disease. This includes being absent from work and having reduced capability when present at work, for both the individual with OA and their caregiver(s) (59). The total economic cost of OA in the UK has previously been estimated at 1.1% of the gross national product (60). These costs do not include the costs of associated comorbidities.

The social burden attributable to OA can be measured using the number of years lived with disability. OA is estimated to cause 2.8% of worldwide disability (61) and is estimated to account for 2.4% of all years lived with disability (36). This made OA the 12th greatest cause of global years lived with disability worldwide in 2016 and it is expected to rise to the fourth greatest this year (2020) (62,63). The social burden includes costs such as reduced quality of life (QoL), depression and pain (36).

1.2.5. Risk factors

Risk factors for OA can be categorised as systemic or joint-level risk factors. These risk factors are summarised in Figure 8 and detailed below.

Figure 8: Summary of key risk factors for OA.

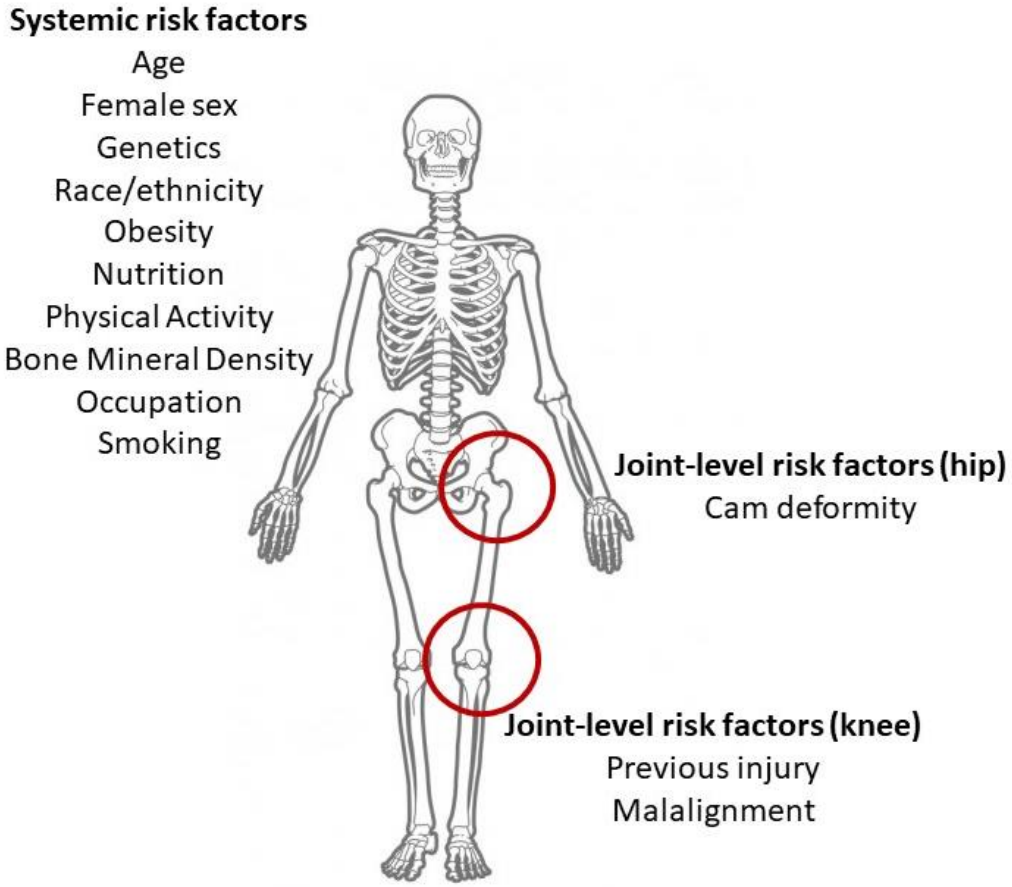

Individual-level factors

Age

Age is arguably the strongest risk factor for developing OA. As discussed in section 1.2.4, incidence rates for hip, knee and hand OA increase with age up until the eighth decade (42). This pattern reflects the accumulation of other risk factors with time (42), such as cumulative exposure to mechanical damage from joint loading (physical activity [PA], obesity). It further reflects the reduced ability of the joint to react to mechanical injury, for example the loss of muscle mass and strength with ageing will reduce mechanoprotective gait responses (64). Reduced cartilage matrix synthesis and increased activation of degradation pathways may contribute to the association between age and OA risk (64).

Sex

It is well-established that women have a much greater risk of developing OA of the hand and knee compared to men, with less of a sex contribution to hip OA risk (10,56,65). Risk differences between men and women for hand OA peak around the age of the menopause (Figure 7) (56). This suggests a key role of postmenopausal declines in oestrogen in OA pathogenesis in women, particularly for hand OA (56). Consistent with a protective role of oestrogen, a randomised controlled trial (RCT) of oestrogen use, in women who had undergone a hysterectomy from the Women's Health Initiative, identified a lower risk of TJR in those taking oestrogen compared to placebo (66).

Sex differences in cartilage volume could explain the greater risk of OA in women. Lower cartilage volume in women compared to men has been observed at the hip and knee (67-70). Differences in knee cartilage volume have been observed in both children and adults, with these differences independent of bone and body size and levels of PA. The sex difference increased after age 55 years, suggesting a role of sex hormones in cartilage maintenance in later life (69,70). Sex differences in OA risk could alternatively be explained by postmenopausal bone loss (the role of bone in OA pathogenesis is detailed in Chapter 3) or reduced muscle strength in women (71).

Genetics

OA is highly heritable, but heritability varies by joint. A study of discordance between monozygotic and dizygotic female sibling pairs from the UK generated a heritability estimate of 58% for radiographic hip OA, with a higher heritability estimate of 64% for hip JSN specifically (72). Heritability estimates for the knee were lower in female twin pairs recruited from the same population (44%) (73) and higher in mixed-sex twin pairs recruited from an Australian population (61%) (74). In another study of patients receiving a total knee replacement (TKR) from Nottinghamshire, UK, and their siblings, the overall heritability estimate for knee OA was 62%, with evidence for a stronger genetic component in men than women (78% *vs* 49%) (75). Spector *et al* estimated the heritability for radiographic

hand OA at 65% in a population of British women and identified larger heritability estimates for osteophytes at the hand and knee (72%) compared to JSN in the same joints (46%) (73). OA-related loci identified from genetics studies are detailed in section 1.2.6.

Race/ethnicity

As highlighted in section 1.2.4, the prevalence and incidence of OA varies by race/ethnicity. Racial/ethnic differences could reflect differences in the frequency of genetic variants conferring a greater risk for OA (section 1.2.6) or differences in other risk factors, for example a greater prevalence of valgus malalignment in Chinese men (see below) (76). Racial/ethnic differences in OA risk could also reflect behavioural differences such as differences in levels of PA or differences in diet (see below).

Obesity

There is strong evidence to suggest that a high body mass index (BMI) is a risk factor for knee OA, with a dose-response relationship whereby obese individuals appear to be at a greater risk than overweight individuals (77,78). A higher BMI has also been related to an increased risk of hip OA, although the magnitude was weaker than seen for the knee (79). Further evidence for a key role of obesity in OA pathogenesis is the improvement of OA symptoms observed in weight loss intervention studies (80).

Sex appears to modify the effect of BMI on risk of knee OA, with a stronger relationship observed in women than men (77,79). However, modification of the effect of BMI on risk for hip OA by sex is less clear, with one large Norwegian registry-based study observing an increased risk of total hip replacement (THR) with increasing BMI for women (81), whereas another observed a stronger magnitude for men (82). A dose-response relationship with duration of time being overweight has been observed, suggesting that high BMI throughout the lifecourse confers a greater risk for OA (79). This is consistent with the Norwegian registry-based analysis of over 1 million individuals, identifying that obesity prior to age 25 years was a strong risk factor for THR in later life (82).

A strong relationship between BMI and knee and hip OA can be explained by increased loading on the joint, increasing stress on AC. However, there is some evidence for a relationship between BMI and hand OA (83), suggesting that joint loading is not the sole mediator of the relationship between BMI and OA. BMI is a measure of adiposity (*i.e.* amount of adipose tissue). Adipose tissue synthesizes and releases adipokines, which are signalling molecules that can be pro-inflammatory (84,85). These adipokines include adiponectin, leptin, and the cytokines IL6 and TNFα, discussed in section 1.2.2. Leptin receptors have been observed on chondrocytes and increased leptin has been measured in the cartilage and SF in OA (84). It has been suggested that leptin is required for chondrocyte hypertrophy, a key process in OA pathogenesis (84). Adiponectin production is lower in obese individuals; adiponectin has been shown to downregulate chondrocyte MMP13 production *in vitro*, suggesting that obesity may contribute to cartilage destruction through reduced adiponectin production (84).

Nutritional factors

Diet may be involved in OA pathogenesis, not just through its influence on BMI, but through the effect of diet on the production of pro-inflammatory mediators (86,87). For example, the classic Western diet is rich in red meat, dairy and refined grains, which leads to higher levels of cytokines such as IL6 (86). In terms of individual nutrients, higher omega-6 fatty acid intake has been associated with BMLs and higher total fat intake has been associated with increased knee JSN in a study of individuals with OA (87). Lipids can accumulate in AC and therefore may contribute to cartilage degeneration (87). Positive relationships between hypercholesterolaemia and knee/hand OA have been observed in cross-sectional analyses and statins, which lower cholesterol, may be beneficial in reducing risk of incident clinical OA and progressive knee OA (87). There is some evidence to suggest that vitamin C supplements may prevent incident knee OA (86,87). Vitamin K, which is involved in bone and cartilage mineralization, deficiency may be a risk factor for hand and knee OA, with an intervention study suggesting that there is a beneficial effect of vitamin K supplementation on hand

JSN in those with vitamin K deficiency (86). Magnesium deficiency has been related to OA risk; it is hypothesized that magnesium deficiency may lead to crystal formation in, and hence damage to, AC (86). Finally, small benefits of vitamin D supplementation have been reported in some clinical trials, although several others have observed no beneficial effect of vitamin D supplementation on cartilage volume or pain severity (86,88).

Physical activity

There is evidence to suggest that both high levels of PA, as well as physical inactivity, could be risk factors for OA (13). High levels of PA can subject the joint to repeated abnormal loading and increase the risk of joint injury (13) (discussed below). This could explain the greater risk of knee OA in elite footballers (89). Conversely, physical inactivity is related to obesity, which is a strong risk factor for OA (see above). Furthermore, PA may be beneficial in reducing pain and increasing function in those with lower limb OA (90,91). This may be through improved muscle strength, reducing further joint stress. The effect of PA may differ across different pathogenic features of OA; higher levels of PA are positively related to osteophyte formation but inversely related to cartilage defects (89).

Bone mineral density

The evidence suggesting that higher bone mineral density (BMD) is a risk factor for OA is discussed in Chapter 3.

Occupation

Individuals working in certain occupations are at a higher risk of OA, particularly at the knee and hip (77,92-95). Kellgren and Lawrence first observed, in 1952, that miners were at a greater risk of knee OA, compared to office or manual workers (96). Since then, evidence has consistently suggested that individuals in occupations such as manual labour, agriculture, fishing, construction, and machine operation are at a greater risk of lower-limb OA (77,92,94,97). The relationship between occupation and OA is not limited to lower limb OA; occupations with repetitive hand movements, such as dentistry,

are associated with a higher risk of hand OA and occupations involving heavy loading are associated with a higher risk of spine, neck and hand OA (92).

The mechanism by which certain occupations increase risk of OA is based on the movements required to perform the role and the abnormal mechanical loads these movements transmit through the joint (see below). For example, it has been estimated that kneeling leads to a transmission of 70% of the body weight through a small surface area of the tibia/patella (95). A recent review concluded that roles involving repeated kneeling, squatting, lifting, and climbing are associated with the development of knee OA or the aggravation of pre-existing knee OA (95). Heavy lifting appeared to be the main factor contributing to hip OA (95).

Smoking

Whether smoking is a risk or protective factor for OA is currently unclear. There is limited evidence to suggest that smoking increases risk of knee cartilage degradation and pain (98). However, there are several studies suggesting that current smoking may be related to a reduced odds of OA, particularly at the knee (99-101). The most recent meta-analysis of 38 studies addressing the role of smoking on knee OA identified a 20% reduced risk of knee OA in ever smokers compared to non-smokers, as well as a dose-response relationship with number of cigarettes per day (101). The authors hypothesized that this relationship could reflect the anti-inflammatory properties of nicotine (101). However, the authors did note that the inverse relationship between smoking and knee OA could be explained by BMI, as smokers tend to be thinner than non-smokers (101). Some studies adjusted for BMI, however, this is complicated by potential collider bias, as BMI may be a common outcome of both smoking and other risk factors for OA, leading to spurious inverse relationships between smoking and these other risk factors (102). Another explanation for the inverse relationship between BMI and smoking is that these meta-analyses included studies from a hospital setting, where controls are often selected from non-musculoskeletal patients, who are more likely to have smoking-related illnesses (98).

Joint-level factors

Joint biomechanics

Repeated abnormal mechanical loading of the joint can lead to damage of AC, as well as the ligaments and the meniscus (93). Anatomical factors, such as altered joint morphology or limb alignment (see hip shape and knee malalignment, below), as well as poor muscle function in the muscle groups near to the joint (*e.g.* poor quadriceps function and knee OA) are chronic contributors to abnormal mechanical loading of the joint (11,103). Age-related degeneration of the meniscus can also contribute to altered biomechanics at the knee by increasing load (103).

Joint injury

Although previous joint injury is traditionally thought of as a cause of secondary OA, joint injury is an acute cause of altered biomechanics and can lead to an extreme alteration in load distribution across the joint, for example through reduced stability due to loss of the cruciate ligament, traumatic damage to the cartilage or meniscal damage (103,104). Knee injuries such as anterior cruciate ligament (ACL) tears could lead to OA development through knee instability, altering the mechanical forces through the joint (105). ACL tears due to injury are often associated with damage to other tissues, including cartilage and the meniscus, further contributing to altered joint biomechanics (103). Alternatively, injuries including ACL tears and meniscal tears could lead to OA via an inflammatory response (93). Evidence for a role of abnormal loading includes a case-control study by Englund *et al*, which identified a greater prevalence of knee OA in the contralateral knee in patients who had undergone meniscectomy, compared to the controls from the general population (106).

Two meta-analyses have concluded that knee injury is associated with subsequent development of knee OA (93,100,107), although there is currently no evidence to suggest that knee injury leads to an increased risk of knee OA progression (108). Silverwood *et al* identified 13 cohort studies determining the relationship of knee injury to onset of knee OA, 12 of which identified an

increased risk. Upon meta-analysis of these studies, the odds of developing knee OA were 2.8 times higher in those with a previous knee injury (100). Similarly, in a meta-analysis of 24 studies of knee OA, knee pain and/or knee OA progression, Muthuri *et al* generated a similar magnitude of effect for cohort studies (107).

Hip shape

Developmental abnormalities of the hip increase the risk of hip OA development; individuals with mild developmental dysplasia of the hip are 10 times more likely to develop hip OA (109). Femeroacetabular impingement (FAI), which causes abnormal contact between the femur and acetabulum, is highly prevalent in European populations (109). FAI can be categorized as either a cam deformity, where the femoral neck (FN)-femoral head junction is extended, leading to reduced sphericity of the femoral head, or a pincer deformity, characterised by acetabular over-coverage (Figure 9) (109,110). There is strong evidence for a role of cam deformity in hip OA development, but less evidence for a role of pincer deformity (110-112). A recent analysis of approximately 4,500 individuals from the Rotterdam study, with follow-up over approximately nine years, observed an association between cam deformity and incident hip OA only in those aged 55-65 years in stratified analyses (112), suggesting that cam leads to earlier development of hip OA.

Figure 9: Illustration of a cam-type deformity (left) and a pincer-type deformity (right) compared to a normal hip (middle).

Reproduced from (113).

More recently, research addressing the role of hip shape in hip OA development has focused on the contribution of subtle variations in hip shape within the general population. Several studies have employed statistical shape modelling to quantify these subtle changes in hip shape, for example an analysis of the Chingford and Cohort Hip-Cohort Knee (CHECK) populations consistently identified a relationship between a flatter FN to head junction, along with a flatter greater trochanter and more prominent acetabular wall, with hip OA (110,111). However, the limitation of most analyses aimed at determining the role of hip shape in OA development is that hip shape measurements are generally performed in populations of older adults and there is a possibility that the presence of osteophytes can alter measurements (*i.e.* reverse causality), particularly the alpha angle used to assess cam deformities (112).

Knee malalignment

Varus (bowleg) and valgus (knock-knee) malalignment are risk factors for knee OA progression, with more severe cartilage defects and greater changes in tibial cartilage volume observed by MRI in those with more severe varus malalignment (114). The effect of malalignment on OA progression is likely to be mediated by abnormal joint loading, providing extra stress on the cartilage and meniscus (115). There have been fewer studies of malalignment and incident knee OA, but those few have found stronger evidence for a role of varus, compared to valgus, malalignment (116-118). Weight may modify the effect of malalignment on the knee joint: Brouwer *et al* observed a stronger relationship between malalignment and incident knee OA in overweight individuals compared to normal/underweight individuals (116).

1.2.6. Genetics

Established loci

The first locus associated with OA risk was a single nucleotide polymorphism (SNP) located in the 5′ untranslated region of the Growth Differentiation Factor-5 (*GDF5*) gene (119). This SNP was associated with hip OA at genome-wide significance in two independent Japanese populations and knee OA in Japanese and Han Chinese populations (119). As it was known that GDF5 is involved in joint formation (120), the authors identified the SNP by sequencing variants within this specific gene, rather than a genome-wide approach. The association between the *GDF5* locus and knee and hip OA was later replicated in European populations (121-123). GDF5 is a ligand in the TGFβ signalling pathway (section 2.1.3,3.3.2).

Since the discovery of *GDF5*, 18 genome-wide association studies (GWAS) of OA phenotypes have been published according to the GWAS catalog (124-142). These GWAS have identified 96 novel OA-associated loci (Figure 10). These identified loci are mainly common variants which have small effects on OA risk, with the exception of three rare variants (minor allele frequency [MAF]<5%), annotated to *COMP, CHADL* and *EP300*, which had an odds ratio (OR)>5 for hip OA (135,140). The *COMP* and *CHADL* variants were identified by whole genome sequencing of THR cases and controls in an Icelandic population and represent missense and frameshift mutations, respectively (135).

Other loci identified include *SMAD3,* encoding a transcription factor in the TGFβ signalling pathway (137), *TGFB1* and *BMP5* which encode ligands for the TGFβ signalling pathway (141), and *PTHLH* (also known as *PTHRP*) (131). PTHLH is an important regulator of cartilage mineralization during endochondral ossification and stimulates proliferation of immature osteoblasts (143). An analogue of PTHLH is used as an osteoporosis treatment (abaloparatide, section 2.2). Estimates from the latest (and largest) GWAS meta-analysis of up to 77,052 cases and 378,169 controls suggest that the current identified loci explain 14.7% of the narrow-sense heritability (*i.e.* the heritability due to additive, but not

dominant variants, and excluding gene-gene interactions (144)) for knee OA and 51.9% for hip OA (141).

To maximise sample size, most of these GWAS have been based on OA defined by one of several methods (TJR, clinical definition/hospital diagnosis, self-report or radiographic) (124,127,128,130,132,139,141,145). This heterogeneity may explain the low proportion in narrow-sense heritability currently explained. Only three of the published GWAS have been based purely on a radiographic definition of OA, but these studies did not identify any loci associated with radiographic OA at genome-wide significance (125,126,134). However, it should be noted that these studies were small (N<10,000). To-date, only one GWAS has been published aiming to identify loci associated with individual radiographic sub-phenotypes. A meta-analysis of hip mJSW identified four loci: *TGFA, PIK3R1, SUPT3H-RUNX2* and *DOT1L,* of which the *TGFA, SUPT3H-RUNX2* and *DOT1L* loci were also related to hip OA (146).

Figure 10: Summary of the novel genome-wide significant loci identified over the last 12 years.

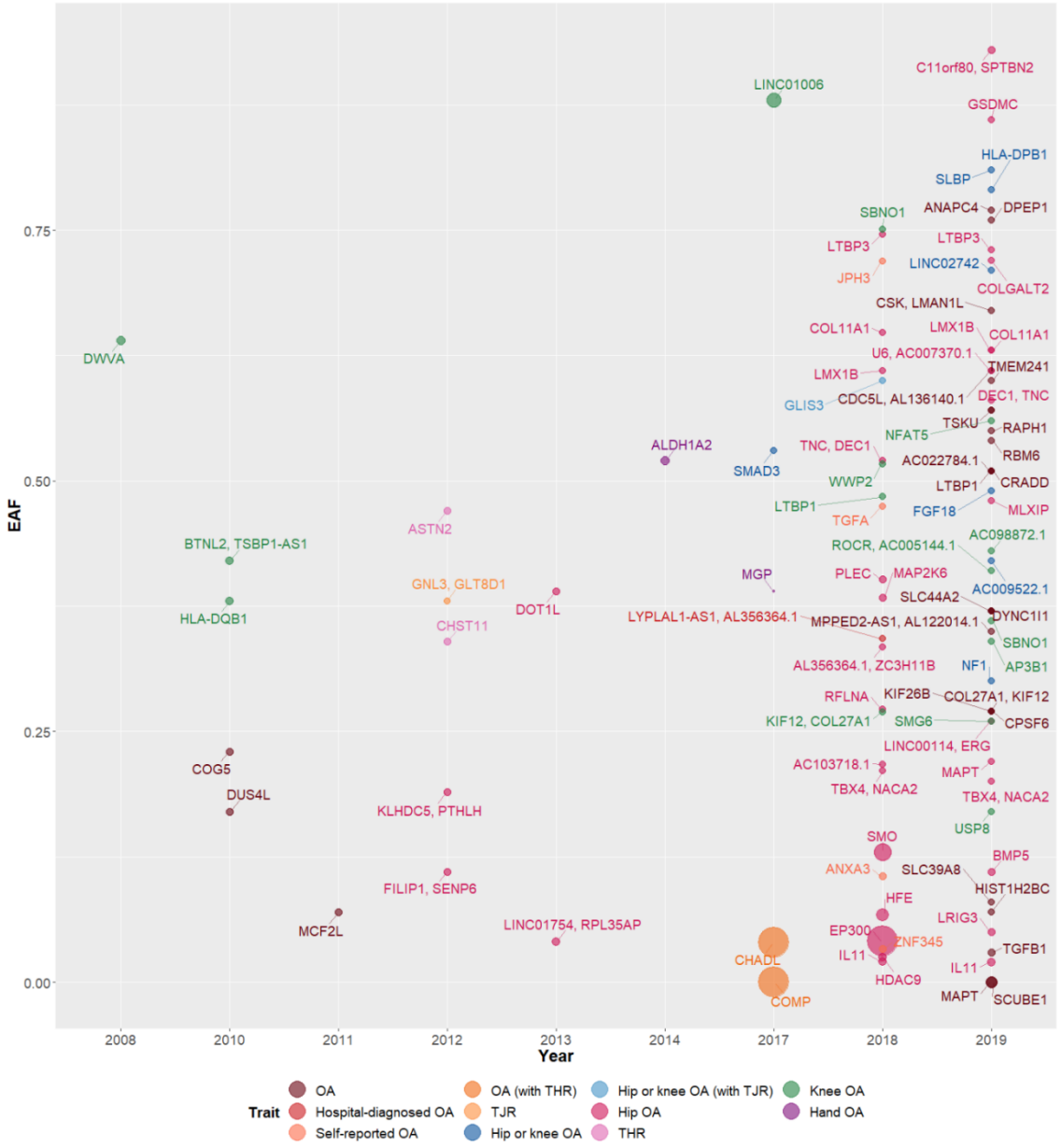

Point sizes are proportional to the effect size (OR). Named genes represent the annotated genes provided from the GWAS catalog (https://www.ebi.ac.uk/gwas/, downloaded 20th February 2020). The ASTN2 locus was initially identified in a female-only analysis of THR (131), but was later associated with OA of the hip in a mixed-gender population (141). The DOT1L locus was identified in relation to hip OA in a male-only analysis (132), but has been identified in a GWAS of hip mJSW including males and females (147). SMAD3 was identified in an analysis of cross-phenotype associations with OA and BMD (137). Figure updated from (148).

In addition to loci identified by GWAS in large populations, whole exome sequencing in three Finnish families has recently identified novel rare variants

segregating with OA within two families (149). One variant was a mis-sense variant in the *OLIG3* gene, of which expression has been linked to Wnt signalling during neuronal development (149). The other variant was a 5' UTR variant of *FIP1L1.*

1.2.7. Management

Treatment of OA mainly focuses on managing symptoms, as treatments to slow joint degeneration, or to repair damaged joints, are currently lacking. Management of symptoms can be achieved using non-steroidal anti-inflammatory drugs to reduce the pain (or opioids in severe cases), via weight loss in obese patients to limit joint loading and reduce structural progression, and by physiotherapy to strengthen the muscles around the joint to reduce abnormal load (22,26). Other aids such as braces and insoles can be used for lower limb OA to stabilise the joint (22). In severe cases, surgical intervention may be required. This normally involves performing a TJR. TJR are performed for most joints affected by OA, but most commonly for the hip, knee, or base of the thumb joint (26). However, joint replacements can be associated with complications such as infections, leg-length discrepancy, and spontaneous dislocations (6) and approximately 9% of patients with THR and 20% with TKR still have chronic pain after surgery (150).

It was previously thought that degenerative changes in cartilage were irreversible (151), hence the focus on management of symptoms. However, evidence from clinical trials of interventions to reduce mechanical loading, such as knee joint distraction which can cause increases in cartilage thickness (152-154), provide hope that cartilage can be repaired, and further treatments can be developed to reverse structural progression in the future.

CHAPTER 2. BONE

2.1. Bone biology

The human skeleton is vital to provide shape, protect organs, for locomotion and is an important store of minerals (particularly calcium) to maintain mineral homeostasis (155). The human skeleton consists of over 200 bones, which can be grouped as long (*e.g.* the femur), short (*e.g.* tarsals), flat (*e.g.* cranial bones), sesamoid (*e.g.* the patella) or irregular (*e.g.* vertebrae) (130,156). Bone is a dynamic tissue, which is constantly remodelled throughout the lifespan, for example to adapt to mechanical strain placed upon it by movement.

2.1.1. Composition of bone tissue

Bone is a composite tissue composed of bone cells and ECM (157). There are three types of bone cells: osteoblasts, osteocytes, and osteoclasts. The ECM is composed of inorganic mineral salts, water, and an organic phase of collagen, non-collagenous proteins, and lipids (157).

Bone cells

Osteoblasts

Osteoblasts derive from mesenchymal stem cells (MSCs) and are the cells responsible for bone formation. Osteoblasts produce type I collagen, which forms over 90% of the organic bone matrix, and regulate mineralization of this matrix (158). Osteoblasts produce receptor activator of nuclear factor kappa-B ligand (RANKL), which binds to RANK on osteoclast precursors, thus triggering osteoclast maturation and bone resorption (section 2.1.4) (158). However, osteoblasts can produce osteoprotegerin (OPG), which binds to RANKL so that it cannot bind to RANK, thus inhibiting bone resorption (158). A number of key transcription factors and pathways regulate osteoblast proliferation, differentiation, and survival; these will be discussed in section 2.1.3. Mature osteoblasts undergo apoptosis, line the surface of bone, or are embedded in the bone matrix where they differentiate into osteocytes.

Osteocytes

Osteocytes are the most common cell type in bone (approximately 90-95%) (159). Osteocytes form large dendritic processes called canaliculi, which connect in a network with other osteocytes, functioning as a system of intercellular communication (159). Osteocytes are mechanosensory cells which produce signalling molecules to signal to osteoblasts and osteoclasts as a response to mechanical loading (160). It has been suggested that RANKL can be expressed along the dendritic processes, stimulating differentiation of osteoclast precursors and thus resorption (159). Osteocytes produce sclerostin, an inhibitor of the canonical Wnt signalling pathway (section 2.1.3), which leads to inhibition of new bone formation by osteoblasts (159). In response to loading, osteocytes reduce sclerostin expression and inhibit osteoclasts, whereas during unloading sclerostin and RANKL are expressed (159). Osteocyte apoptosis is important for bone repair as it stimulates resorption by osteoclasts (159). However pathogenic apoptosis of osteocytes can lead to excessive bone resorption and skeletal fragility (159). Disorientation of canaliculi and decreased connectivity, associated with a loss of osteocyte ability to sense damage and initiate repair, can lead to bone resorption (159).

Osteoclasts

Osteoclasts are multinucleated cells derived from monocytes originating from the bone marrow (161). They are responsible for bone degradation. Two key cytokines regulate the differentiation of osteoclasts: RANKL and Macrophage Stimulating Factor (M-CSF). M-CSF contributes to the proliferation, differentiation, and survival of several cells from the monocyte lineage (161). Attachment of the osteoclast to the bone surface is mediated by integrins, which are cell surface attachment molecules recognizing specific motifs on bone proteins (161). Upon attachment, acidified vesicles containing molecules, such as the lysosomal enzyme Cathepsin-K, are transported to the plasma membrane in contact with the bone (161). Fusion of these vesicles to the membrane results in formation of the ruffled membrane, which is a unique feature of osteoclasts (161).

The contents of the vesicles are then exocytosed into the acidic environment, created by a proton pump and a chloride channel in the membrane (161). This acidic environment mobilizes bone mineral, exposing the type I collagen to degradation by enzymes such as Cathepsin-K (161-163).

Bone matrix

Bone mineral

The inorganic bone mineral is the largest component of the bone matrix and constitutes approximately 65% of the total bone weight (164). The mineral component of the bone matrix is a modified version of the naturally occurring mineral hydroxyapatite, containing calcium and phosphate ions (157). As bone matures, mineral crystals grow in size and become plate-like in structure, aligning in parallel with the collagen fibrils, strengthening the collagen (157,164). Hydroxyapatite forms a source of calcium, phosphate, and magnesium ions, maintaining homeostasis of these ions (157).

Type I collagen

Type I collagen is the most abundant protein in the bone matrix and the major component of the organic component of the bone matrix (~90%) (164). It generates a scaffolding, providing structure to the bone, binding other proteins. Type I collagen is a triple helix structure, formed of two α1 chains and an α2 chain, which aggregate to form fibrils (157,164,165). Each collagen chain is composed of approximately 1000 amino acids, with a Glycine-X-Y repeat, with X and Y commonly representing proline and hydroxyproline respectively, which are essential for helix formation and other properties such as water binding (155). Fibrils are connected by crosslinks (155). The pattern of aggregation of fibrils depends on the type of bone: woven bone contains fibrils arranged in a random formation whereas lamellar bone contains fibrils arranged in sheets (166).

Non-collagenous proteins and other components

Non-collagenous proteins (NCPs) form approximately 10-15% of the protein content of bone (157). NCPs have various roles, including organization of the

ECM, regulating mineralization and co-ordinating interactions of the cells or mineral with the matrix (157). Approximately 25% of these NCPs are derived from non-skeletal sources, particularly from the serum (157). An example of an NCP derived from the serum is albumin, which binds to the hydroxyapatite crystals, inhibiting their growth (157). Proteoglycans, discussed in section 1.1.1, are an NCP present in the bone matrix and function in matrix organization, water and ion retention and regulation of TGFβ signalling (section 2.1.3) (157). Other NCPs include proteins with gla residues, which enhance calcium binding (157). These include matrix gla protein (MGP), which is a negative regulator of mineralization, and osteocalcin, which is a bone specific gla protein which possibly regulates osteoclast activity (157). As osteocalcin is bone-specific, it can function as a marker of osteoblast activity and thus bone formation (section 2.1.4).

Other non-protein components of the bone matrix include water and lipids. Water constitutes approximately 10% of the weight of bone and functions in maintaining the collagen structure of the bone matrix (157). Water can be bound to collagen/mineral or flowing through the osteocyte canaliculi, where it has a suggested role in intercellular signalling in response to mechanical loading (155).

2.1.2. Structure of bone

There are two types of bone present in the adult human skeleton: cortical (compact) and trabecular (cancellous or spongy). Both are types of lamellar bone. These two types of bone differ in their structure. Cortical bone, forming a greater proportion of bone mass, has low porosity, approximately 3-5% (155,164). Cortical bone is composed of Haversian systems which are also known as secondary osteons (155). Secondary osteons are a central canal, containing a blood vessel, nerve fibres and lymphatics, surrounded by concentric sheets of lamellar bone containing osteocytes (Figure 11). The blood vessels in the secondary osteons are connected by Volkmann's canals, which additionally connect the secondary osteons to the marrow vasculature (155). In the long bones, cortical bone is found in the diaphysis surrounding the trabecular bone

(Figure 11), providing strength, support, and protection in response to load bearing (155,164).

Trabecular bone is formed of plates and rods of lamellar bone, running roughly parallel to the bone surface, with approximately 75-85% porosity, which is filled with bone marrow (155,164). The vertebrae and ribs are composed of predominantly trabecular bone (155). The periosteum is a thin membrane covering the outer surface of the diaphysis of a long bone and contributes to bone formation along the outer surface (Figure 11). The endosteal surface lines the marrow cavity within the diaphysis (155).

Figure 11: Structure of a long bone (left) and the cortical and trabecular bone components (right).

Image removed for copyright purposes

Reproduced from https://training.seer.cancer.gov/anatomy/skeletal/.

2.1.3. Bone formation

There are two main types of bone formation during skeletogenesis: endochondral and intramembranous ossification. Intramembranous ossification does not involve a cartilage structure; it occurs when MSCs, migrated to ossification centres, condense to form osteoblasts, which lay down osteoid for mineralization (160,167). This process occurs in the formation of the flat bones of the cranial vault and the clavicle (160). Endochondral ossification requires a cartilage structure for ossification (160). This process occurs during skeletogenesis, postnatal growth, modelling and fracture repair and is involved in the formation and growth of long bones.

Endochondral ossification

The process of endochondral bone formation begins with the condensation of MPCs at the site of bone development to form a cartilage model (167). The MPCs proliferate and express cell adhesion molecules, leading to condensation (Figure

12A) (160). Within the condensations, MPCs differentiate into chondrocytes, which produce ECM leading to the formation of a cartilage structure (160). A sheath called the perichondrium forms around the cartilage from peripheral spindle-shaped cells (168). The perichondrium becomes the primary source of chondroblasts for the cartilage structure (Figure 12B). Chondrocytes near the centre of the developing limb flatten and align into columns and further differentiate into hypertrophic chondrocytes (Figure 12C) (160). Hypertrophic chondrocytes produce signalling molecules such as VEGF, leading to vascularization and calcification, as well as growth factors responsible for osteoblast differentiation, marrow cavity formation and formation of the primary ossification centre (POC, Figure 12D) (160). Chondrocytes secrete MMPs to degrade the cartilage matrix and hypertrophic chondrocytes transdifferentiate into osteoblasts (160). The degrading cartilage forms a scaffold for further bone formation (160). Vascular invasion allows osteoblast precursor cells to migrate to the POC and deposit type I collagen, which later mineralizes to form bone (Figure 12E). Growth plates (GP) form at the end of the growing long bone, which are a site of continuous bone formation in the growing skeleton. The GP is separated from the AC at the joint margin by a secondary ossification centre (SOC) during early postnatal growth (160). At the end of puberty, these cartilaginous GPs are converted to bone and the only cartilage that remains is the AC at the joint margin.

Figure 12: The key stages of endochondral ossification.

Image removed for copyright purposes

Orange cells in stage (A) represent mesenchymal progenitor cells and in stage (B) represent perichondral progenitors. In stages (C-E) orange cells represent late-stage hypertrophic chondrocytes. Blue cells represent chondrocytes, purple cells are prehypertrophic chondrocytes and green cells represent hypertrophic chondrocytes. Light blue cells in stage (E) represent articular chondrocytes. Red lines represent blood vessels and black lines represent osteoblasts/ bone matrix. Reproduced from (160).

Regulation of endochondral ossification

SRY-Box Transcription Factor-9 (SOX9) and RUNX Family Transcription Factor-2 (RUNX2) are key transcription factors regulating whether osteochondral progenitor cells (OPCs) differentiate into osteoblasts or chondrocytes (Figure 13) (160). OPCs are differentiated from MPCs due to β-catenin mediated gene expression (169). SOX9 is the "master regulator of cartilage formation", regulating OPC differentiation into chondrocytes (160). RUNX2 is essential for the differentiation of OPCs into preosteoblasts (160). RUNX2 controls expression of osteoblast specific genes, including type I collagen and osteocalcin (169). The key role of RUNX2 in osteoblast differentiation is demonstrated by knockout mice models, who have an unmineralized cartilage skeleton due to no osteoblasts (169). The transcription factor Osterix (OSX) is a key regulator of later differentiation of preosteoblasts into mature osteoblasts (160). *Osx* expression is regulated by RUNX2, but knockout mice lack osteoblasts, suggesting that OSX is essential for osteoblast differentiation (169).

Figure 13: Key signalling pathways and transcription factors regulating endochondral ossification and differentiation of MPCs to osteoblasts or chondrocytes.

Image removed for copyright purposes

Reproduced from (160).

The five key signalling pathways regulating endochondral ossification are Wnt signalling, Bone Morphogenetic Protein (BMP) and TGFβ signalling (which form

the TGFβ superfamily), Notch signalling and Indian Hedgehog (IHH) signalling. The role of each of these pathways is discussed below.

Other modulators of osteoblast activity include parathyroid hormone (PTH) and PTH-related protein (PTHrP), which can activate several intracellular pathways, leading to bone formation or bone loss depending on their intermittent or continuous presence, respectively (169). Growth factors, such as IGF-1, also play a role in bone development (169).

The Wnt signalling pathway

Ligands for the Wnt signalling pathway are Wnt glycoproteins (169). These act through frizzled-related transmembrane receptors and low-density lipoprotein receptor-related protein (LRP) co-receptors (169). There are two sub-pathways to the Wnt signalling pathway: canonical and non-canonical (Figure 14). The canonical pathway, involving β-catenin and the receptors LRP5/6, has a key role in osteoblast differentiation (170). β-catenin forms a complex with APC, GSK3 and CK1 in the cytoplasm in the absence of Wnt ligands, where GSK3 phosphorylates β-catenin, leading to its degradation (169,170). In the presence of Wnt ligands, this complex dissociates and β-catenin translocates to the nucleus, where it interacts with transcription factors, leading to transcription of genes involved in osteoblast differentiation (169). Canonical Wnt signalling is regulated by secreted frizzled-related proteins (FRPs), which interact extracellularly with Wnts, blocking their interaction with Frizzled receptors, as well as sclerostin and dikkopf-1 (DKK-1), which bind to LRP5/6 and block Wnt interaction (170).

Figure 14: The canonical (a) and non-canonical (b) Wnt signalling pathways.

Image removed for copyright purposes

Reproduced from (171).

The TGFβ superfamily

The TGFβ superfamily can be separated into two key signalling mechanisms: canonical, SMAD-dependent signalling, and non-canonical signalling via p38-MAPK (172,173). TGFβ signalling regulates expression of *RUNX2* and *SOX9*

(160,172,173). The TGFβ pathway can be further divided into the TGFβ receptor-dependent and the BMP receptor-dependent pathways. These two pathways differ in their receptors, ligands and the SMADs that they activate (the TGFβ-specific pathway activates SMAD2/3 whereas the BMP-specific pathway activates SMAD1/5/8 [SMAD8 is also known as SMAD9]) (169). However, the receptors and ligands are similar, and they share a common signalling mechanism (Figure 15). The ligands form dimers to interact with a type 1 and type 2 serine/threonine kinase receptor (169,174). The type 2 receptor then phosphorylates and activates the type 1 receptor, which then phosphorylates the pathway-specific SMAD, allowing interaction with SMAD4 (common to both pathways), leading to translocation of the SMAD complex to the nucleus, association with target transcription factors and expression of target genes (169,174). These target genes vary between ligands, for example BMP2 ligand is involved in regulation of *OSX* expression (169).

Figure 15: Diagram summarizing the TGFβ and BMP signalling pathways.

Reproduced from (175).

Notch signalling

The role of the Notch signalling pathway in promoting or inhibiting osteoblast differentiation appears to vary, possibly depending on the stage of differentiation (169). There are three Notch ligands (delta, serrate and Lag2), which bind to transmembrane notch receptors (169). This leads to cleavage of the intracellular domain by presenilin which then translocates into the nucleus, forming a complex with CSL family DNA binding proteins and the recruitment of co-activators, ultimately leading to the transcription of target genes (169).

Ihh signalling

Indian hedgehog signalling leads to expression of *RUNX2* via the transcription factor GLI2 (169). In the presence of the IHH ligand, inhibition of the Smoothened receptor by the Patched-1 receptor is depleted, allowing signalling via the GLI2 transcription factor (169). Ihh signalling also leads to expression of *PTHRP*, which in turn downregulates chondrocyte hypertrophy at the growth plate (176). Mice deficient in Ihh lack osteoblasts in new bone formed by endochondral ossification (169).

2.1.4. Bone metabolism

There are two processes of bone metabolism: bone modelling and bone remodelling. Bone modelling occurs when either bone formation occurs without prior resorption, or bone resorption occurs without subsequent formation (177). Bone modelling alters the size and/or shape of bone and is important for periosteal expansion during growth (177). Bone remodelling is a coupled process of bone resorption and formation and is important to repair microdamage and maintain mineral homeostasis in adulthood (177,178).

Bone remodelling

Bone remodelling occurs at a structure called a basic multicellular unit (BMU) and consists of five stages (178):

1. Activation: osteoclast precursor cells are recruited to the site of resorption, fuse to form multinucleated osteoclasts and are activated. The activated osteoclasts then bind to the bone matrix (section 2.1.1), creating a sealing zone for resorption (Figure 16A).
2. Resorption: the process of bone resorption by osteoclasts (section 2.1.1) lasts approximately two weeks and ends with the programmed cell death of the osteoclasts (Figure 16B). A resorption cavity is created.
3. Reversal: unmineralized matrix on the resorbed bone surface is removed and a non-collagen mineralized matrix is deposited, called the cement line, to enhance the adherence of osteoblasts (Figure 16C). This stage lasts for approximately one month.
4. Formation: new osteoid is deposited by osteoblasts and subsequently mineralized (Figure 16D). This is the longest stage of the bone remodelling process (177).
5. Termination: bone formation is stopped by apoptosis of osteoblasts or their differentiation into osteocytes or bone lining cells (Figure 16E).

Figure 16: The bone remodelling cycle.

Reproduced from (179).

Regulation of bone remodelling

The OPG-RANK-RANKL system (described in section 2.1.1) is a key regulator of the activation and resorption stages. Osteoclasts are initially recruited due to microdamage in the bone matrix disrupting osteocyte canaliculi, leading to the release of cytokines, such as RANKL, responsible for osteoclast recruitment (178). RANKL expression by bone lining cells is increased during the activation phase

(180). Glucocorticoid use and continuous use of PTH also upregulate RANK/RANKL expression (178). Oestrogen is an important regulator of bone remodelling. Oestrogen receptors are expressed on all bone cells (177). Reduced oestrogen levels can lead to osteocyte apoptosis, releasing pro-inflammatory cytokines which promote osteoclast recruitment (177). The TGFβ superfamily (section 2.1.3) is involved in the coupling of bone resorption and bone formation. Active forms of TGFβ ligands are released during resorption, leading to the recruitment and differentiation of OPCs during reversal and formation (174).

Measuring bone metabolism

Based on the knowledge of the structure of the bone matrix and the processes involved in bone remodelling, assays have been developed to measure specific products of both bone formation and resorption, to give an estimate of the current rate of bone turnover. These bone turnover markers (BTMs) can be used to predict major osteoporotic fractures or to determine response to, and the ideal dosage for, medications for osteoporosis (section 2.2) (181). Telopeptides at the N-terminal (NTX-1) and C-terminal (CTX-1) of type I collagen are cleaved during bone resorption and released into the circulation (164). NTX-1 or CTX-1 levels can therefore be measured in serum or urine to provide an estimate of the level of bone resorption (181). CTX-1 can be measured in the non-isomerized (α) form, which is mainly derived from new bone, but more commonly the β isomer (β-CTX) is measured, which reflects breakdown of older bone (182). N-terminal propeptide of type I collagen (P1NP) is released into the circulation by posttranslational cleavage of type I procollagen and can therefore be used as a measure of osteoblast function and thus bone formation (181). However, measurement of BTMs is affected by circadian variations, diet, and seasonality and therefore measurements should be taken from fasting samples following a standardized protocol (181).

2.2. BMD and osteoporosis

BMD is a measurement of the bone mineral content (BMC) per unit of bone area and low BMD is used clinically to identify individuals with osteoporosis, at high risk of fracture. BMD is commonly assessed through Dual X-ray Absorptiometry (DXA) scanning. DXA scanning is the preferred method for assessing BMD clinically as it is relatively quick, with low radiation and DXA-assessed BMD correlates with fracture risk, the clinical endpoint that interventions for osteoporosis are trying to prevent (183,184). Every DXA scanner, regardless of manufacturer, has a radiation source which emits two energy levels. The difference in attenuation of these two energy levels, as they pass through different tissues with varying composition, is detected by a radiation detector and transferred to computer software linked to the scanner, which allows an image to be generated and quantitative measurements of BMD and soft tissue mass to be calculated (184).

In the UK, DXA scanning is performed on the National Health Service (NHS) if an individual is determined to be at risk of low density (*e.g.* due to long-term steroid treatment, use of aromatase inhibitors for breast cancer, previous fracture). A T-score for the number of standard deviations (SDs) below a sex-matched young adult population mean is generated (185). A BMD T-score $\leq$-2.5 is used by the World Health Organization to determine osteoporosis. Osteoporosis is a metabolic bone disorder characterized by low bone mass and reduced bone strength, leading to an increase in bone fragility and risk of fracture (186,187). Most cases are caused by age-related bone loss due to a decline in bone formation, relative to resorption, at BMUs, as a consequence of a reduced number of MSCs to differentiate into osteoblasts (177). This is usually caused by an overall increase in bone turnover, with the increase in bone resorption greater than the increase in formation. There is overall loss of bone strength, as newly formed bone is hypomineralized, increasing fracture risk (177).

2.2.1. Treatments for osteoporosis

Several drug therapies have been developed and routinely used for treatment of osteoporosis. These can be split into two categories: antiresorptives and anabolic drugs. Antiresorptive drugs increase BMD by reducing osteoclast activity. Bisphosphonates are the first therapy normally given to postmenopausal women with osteoporosis (188). Bisphosphonates bind to hydroxyapatite, where they are released during bone resorption, taken up by osteoclasts, leading to reduced bone resorption due to inactivation or apoptosis of the osteoclasts (188). As discussed in section 2.1.4, bone resorption is coupled, so the decrease in bone resorption due to use of bisphosphonates is followed by a decrease in bone formation, but the decrease in the rate of bone formation is slower than the decrease in the rate of formation (188). Denosumab is a monoclonal antibody specific for RANKL, inhibiting RANKL binding to the RANK receptor on osteoclasts (189). Denosumab therefore reduces bone resorption, leading to an overall decrease in bone turnover (189).

Anabolic drugs increase bone formation by increasing osteoblast activity. Evidence suggests that anabolic drugs may cause greater increases in BMD, particularly at the spine, compared to antiresorptive drugs (190). Teriparatide is an anabolic drug routinely used to treat osteoporosis. Teriparatide is an amino terminal fragment of PTH (190). Despite continuous administration of PTH increasing bone resorption, intermittent administration can stimulate bone formation by downregulation of Wnt signalling antagonists (178,191). Romosozumab is the latest osteoporosis drug to be licenced in the UK. Romosozumab is an anti-sclerostin antibody, reducing Wnt antagonism and increasing bone formation and suppressing bone resorption (192).

2.3. High bone mass

As discussed in section 2.2, a T-score threshold $\leq$-2.5 is used to define osteoporosis. However, an equivalent threshold has not been set to define high BMD (high bone mass [HBM]). There are cases where a high BMD value on a

DXA scan does not necessarily mean a lower fracture risk (193). For example, artefactual elevations in lumbar spine (LS)-BMD measured by DXA scan can occur due to the presence of osteophytes and subchondral sclerosis (section 1.2.2). Artefactual elevations in BMD due to osteophytes can be determined by progressive increases in BMD with decreasing LS vertebrae (193). Other conditions artefactually elevating LS-BMD include diffuse idiopathic skeletal hyperostosis and ankylosing spondylitis, which are associated with an increased fracture risk, and vascular calcification of the abdominal aorta (193). The presence of surgical metalwork can lead to artefactual BMD measurements (193).

2.3.1. Rare monogenic HBM disorders

In addition to artefactual elevations in BMD, there are several known monogenic disorders causing extremely high BMD measurements on DXA scans. These can be separated into two types: disorders characterised by reduced osteoclastic bone resorption (the osteopetroses) and disorders characterized by increased bone formation (193). Although osteopetroses are associated with dense bones, bones are brittle and liable to fracture (193). An example of osteopetrosis is pycnodysostosis, caused by non-synonymous mutations leading to inactivation of Cathepsin-K (194).

An example of a monogenic condition leading to excess bone formation is sclerosteosis, caused by a loss-of-function mutation in the *SOST* gene (193). Features of sclerosteosis include a reduced fracture risk, gigantism, mandible enlargement and compressed cranial nerves leading to hearing loss and headaches (193). Van Buchem's disease is a milder version of sclerosteosis caused by an intronic deletion in *SOST* (193). Mutations in the *LRP4* gene also cause sclerosteosis, by inhibiting the interaction between LRP4 and sclerostin (195). A similar phenotype is observed for activating *LRP5* mutations (193), of which 13 have been identified as associated with HBM (196).

2.3.2. The HBM study

Approximately one-third of HBM observed on routine DXA scans is not explained by artefactual elevations or the monogenic disorders described in section 2.3.1 (193). The HBM study was therefore set up to identify the underlying genetic aetiology causing unexplained HBM, to further understand how bone mass is regulated, with the hope of identifying novel therapeutic targets for osteoporosis.

The HBM study is a multi-centre study of individuals with unexplained generalized high BMD, and their family and relatives without HBM, recruited from 15 NHS centres across England and Wales (1). Recruitment of this cohort began with a screen of 335,115 DXA scans on NHS databases at 13 centres (2 centres recruited patients prospectively) for a T-score or Z-score $\geq$+4. Identified scans were visually inspected; 49.4% had elevated BMD due to degeneration and 9.7% had artefacts or were unverifiable. The overall prevalence of unexplained HBM was 0.18% (197).

To determine the effect of osteoarthritic changes on BMD at the LS, 562 LS scans with a Z-score $\geq$+4 at the largest centre, Hull, were graded for OA severity using KL grading (198). BMD of each vertebra was associated with OA grade, except for the L1 vertebra, for which BMD was not associated with OA (198). Therefore, the definition of HBM was based on L1-BMD. It was assumed that both the L1 vertebra and total hip (TH) would be affected, but not necessarily to the same extent. A definition based on that previously published by Little *et al* (199) was therefore used, with HBM being defined as either [1] L1 BMD Z-score $\geq$+3.2 plus TH Z-score $\geq$1.2 or [2] TH Z-score $\geq$3.2 plus L1 Z-score $\geq$1.2. Overall, 41% (258) of identified HBM individuals were recruited (Figure 17).

Figure 17: Screening and recruitment of the HBM study population.

Image removed for copyright purposes

Reproduced from (197).

Index cases were asked to invite their first-degree relatives and spouses to participate in the study. Recruitment ran from July 2005 to April 2010. The aim of including relatives was to determine the pattern of inheritance of HBM (monogenic or polygenic). 236 relatives and 61 spouses were recruited to the study (Figure 17). All participants were aged 18-90 years and all but three were Caucasian. To characterize the HBM phenotype, index cases and relatives/spouses were invited to their local HBM centre for a detailed clinical assessment and interview. In first-degree relatives, HBM case status was defined as summed TH plus L1 Z-score $\geq$+3.2, to overlap the index case distribution. HBM in spouses was defined as for index cases. Ninety-four first-degree relatives and three spouses had HBM.

2.3.3. The HBM phenotype

Compared to relatives/spouses without HBM, individuals with HBM (including index cases and relatives with HBM) had an enlarged mandible, broad frame, were more likely to have misshapen or extra bone at tendon or ligament insertions and a reduced odds of reporting a family history of fracture. These features were suggestive of a mild skeletal dysplasia (197).

Bone phenotype of HBM

Peripheral quantitative computed tomography (pQCT) analyses of 98 HBM individuals and 65 controls at the largest centre, Hull, identified higher trabecular and cortical bone area, periosteal circumference, trabecular and cortical BMD, and strength-strain index at the distal tibial site in HBM individuals (200). The same pattern was not seen at the radius, suggesting that there is an interaction between HBM status and weight-bearing activity on cortical/trabecular BMD, which suggests that individuals with HBM have an increased responsiveness to mechanical strain (200). The inverse relationship between TB-BMC and age in female HBM individuals was much weaker than relatives without HBM, suggesting that HBM individuals are less likely to lose bone as they age (201).

Metabolic phenotype of HBM

Initial phenotyping of HBM individuals identified a higher BMI than relatives and spouses without HBM (197). Further assessment of body composition on DXA scans found that HBM individuals had a higher percentage of total body fat mass (TBFM) compared to relatives/spouses without HBM (201). Adjustment for TH-BMD attenuated the relationship between HBM and TBFM, whereas adjustment for TBFM only minimally attenuated differences in BMD between HBM individuals and relatives/spouses without HBM, suggesting that BMD mediates the relationship between HBM and increased TBFM, rather than increased TBFM responsible for the higher BMD. There was also a trend towards lower bone turnover in HBM individuals, with lower levels of osteocalcin. Osteocalcin knockout mice have been observed to be insulin resistant with greater fat mass (FM) (202). Therefore, it has been hypothesized that HBM individuals may have a genetic tendency for lower bone turnover, leading to reduced serum osteocalcin and increased TBFM (201). However, adjustment for bone turnover did not attenuate the relationship between HBM and TBFM, although it should be noted that BTMs measured at one timepoint will not be reflective of bone turnover during growth and development. It has been hypothesized that bone formation is increased in early life in HBM which leads to suppression of bone turnover in later life (201).

2.3.4. Genetics of HBM

Sequencing of *LRP5, LRP4* and *SOST* in HBM individuals identified three known missense *LRP5* mutations and two novel missense *LRP5* mutations in 11 adults from 7 families, all of which were heterozygous and the highest BMD of all HBM individuals (196). All mutations identified were predicted to have functional consequences resulting in decreased Wnt antagonism. Two mutations in the SOST binding site had the most extreme phenotypic consequences. A novel nonsense mutation in exon two of *SOST* was identified, as well as a previously reported SNP in exon one in eight cases and two intergenic SNPs in nine cases

(196). A novel intronic mutation near exon 25 of *LRP4* was identified, as well as a common *LRP4* SNP in 56 individuals (196).

A lack of mutation in genes known to cause monogenic HBM disorders in the majority of HBM individuals led to the hypothesis that HBM could be caused by the polygenic inheritance of multiple loci known to influence BMD in the general population (203). A GWAS in the HBM population (combined with individuals from the Anglo-Australasian Genetics Consortium (AOGC) with a TH-BMD Z-score $\geq$1.5 and low bone mass controls (Z-score$\leq$-1.5) identified that the observed *p*-values for 49 known BMD loci (204) were smaller than expected by chance (*i.e.* there was an over-representation of common BMD variants in the HBM population) (203).

Whole exome sequencing and pedigree analysis of HBM individuals (without *LRP5* or *SOST* mutations) identified a novel autosomal dominant mutation in *SMAD9* (205). This variant was additionally found in two unrelated individuals, one from HBM and one from the AOGC high TH-BMD population. The variant was not present in the AOGC low BMD population and is rare in the general population (MAF=0.002). The mutation is within the DNA-binding MH1 domain (205).

CHAPTER 3. THE RELATIONSHIP BETWEEN BONE DENSITY AND OSTEOARTHRITIS

3.1. Epidemiological evidence for a relationship between BMD and OA

Foss and Byers first observed, in 1972, that OA of the hip was rarely present in cases of hip fracture and that those with OA of the hip had above average metacarpal BMD, suggestive of an inverse relationship between osteoporosis and OA (206). Since then, the relationship between BMD and radiographic OA has been extensively studied. Evidence for an association between BMD and prevalent OA has been generally consistent, despite the variation in site of BMD (LS, hip, total body [TB], radius, calcaneus) and OA (hip, knee, hand) assessment (Figure 18). However, evidence for associations with incident/progressive OA has been less consistent (207). This section summarizes the epidemiological evidence for relationships between BMD and prevalent, incident, and progressive OA at various skeletal sites.

3.1.1. Cross-sectional evidence

Prevalent OA

Evidence from cohort studies

The relationship between BMD and prevalent radiographic OA has been investigated in a wealth of cohorts sampled from the general population (Figure 18). Analyses in women from the study of osteoporotic fractures (SOF), the first Rotterdam study (RS) population (RS1), men from the study of osteoporotic fractures in men (MrOS) and female twins from the St Thomas UK adult twin register, all identified positive relationships between hip or FN-BMD and *hip* OA (208-211). There is consistent evidence for a relationship between hip OA and BMD of the LS, radius, and calcaneus (208).

Positive relationships between BMD and *knee* OA have also been identified. The first analysis was performed on a population of 932 individuals from the Framingham study (212). This study assessed OA of the knee four years prior to BMD measurement at the femur and radius. This study found a higher FN-BMD

in women with a KL grade of 1 or 2, compared to those with no features of OA. This study also identified higher BMD in women, but not men, with knee osteophytes (212). Subsequent analyses identified positive relationships between hip/FN BMD and knee OA in Chingford women, the RS population, women from the Michigan Bone Health study, and the Korean National Health and Nutrition Examination Survey (KNHANES) (209,213-215). Associations between knee OA and LS-BMD have been identified in Chingford women, women from the Michigan Bone Health Study and both men and women from KNHANES (213-215). However, analysis of the Dong-gu Korean cohort identified an inverse relationship between FN-BMD and knee OA, reflecting an inverse relationship with JSN (216).

The relationship between BMD and prevalent *hand* OA is less well characterised. A study of 979 Chingford women identified a higher mean LS-BMD in those with OA at the DIP or CMC and greater FN-BMD in those with CMC OA (213). A further study of women from the Michigan Bone Health Study identified a positive relationship between TB-BMD and overall hand OA severity score (217). As observed at the knee joint in the Dong-gu cohort, FN-BMD was inversely related to hand JSN in this population, but hand osteophytes and sclerosis were positively related to BMD (216).

Figure 18: Summary of evidence for associations between BMD and radiographic OA from cross-sectional and longitudinal analyses.

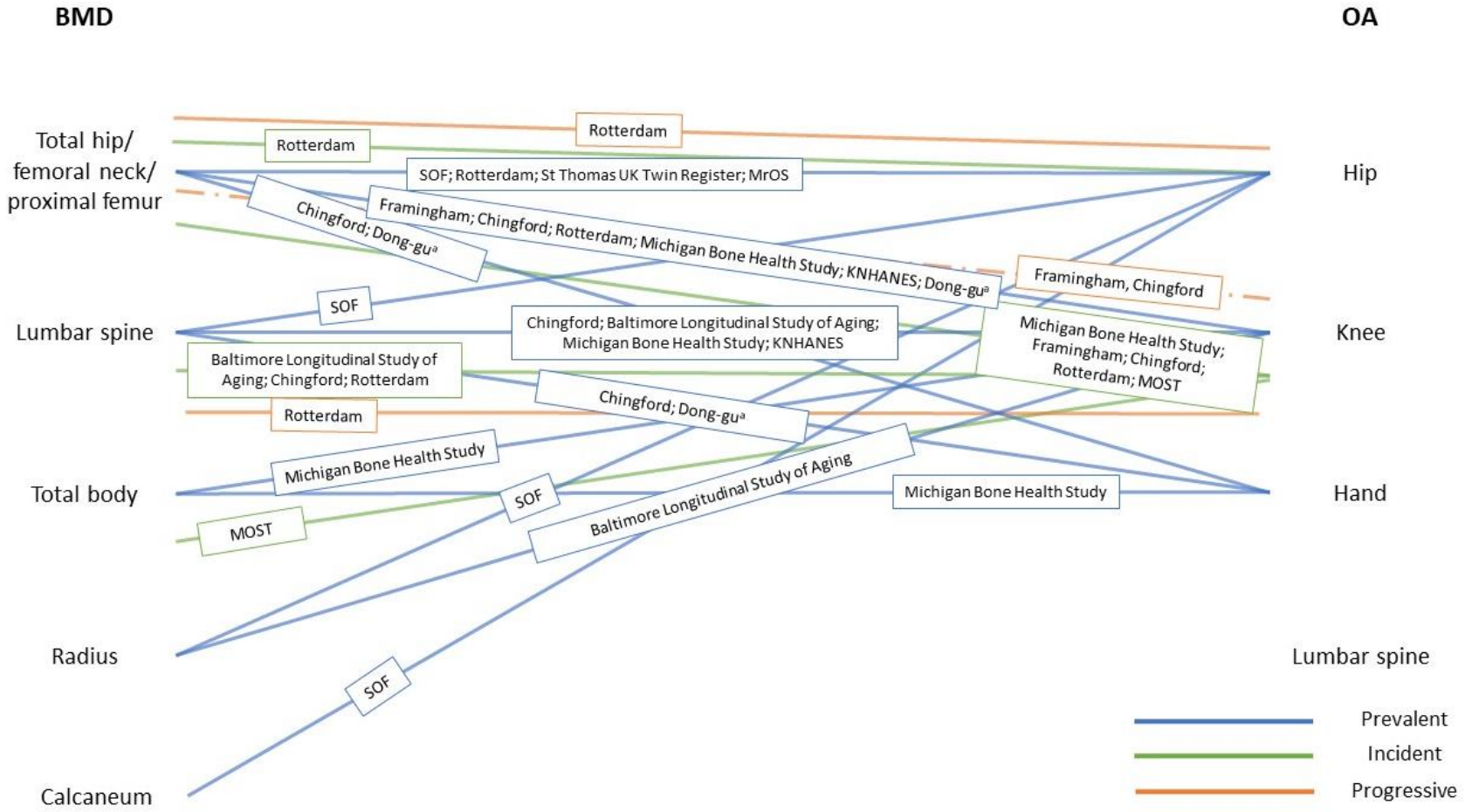

Solid lines represent positive associations, dashed lines represent inverse associations. [a] represents an inverse association.

Evidence from case-control studies

In addition to cohort studies of the relationship between BMD and prevalent OA, some studies have collected opportunistic BMD data in OA patient populations, for example pre-operative THR or TKR patients with confirmed OA, and have compared BMD in these patients to age-matched control populations. Arokoski *et al* measured FN and calcaneus BMD in 27 men with unilateral or bilateral hip OA and 30 age-matched controls but did not find evidence for a difference in BMD between cases and controls, although they did find that FN-*BMC* and *volume* were 18% higher in hip OA cases compared to controls (218). Iwamoto *et al* observed a higher BMD at the radius in 305 postmenopausal women with knee OA compared to 369 controls without knee OA, and a positive correlation between BMD and KL grade up to grade 3, after which BMD decreased (219). Glowacki *et al* compared hip BMD between hips of 34 individuals undergoing unilateral THR and observed a higher FN and trochanteric BMD in the hip due to be replaced, compared to the contralateral hip, but did not observe a difference in TH-BMD between the two hips, suggesting artefactual elevations in FN-BMD due to features of OA (220). Similarly, Goerres *et al* compared TH-BMD in 161 unilateral knee OA cases and found a *lower* hip BMD in the same leg as the affected knee, compared to the contralateral hip (221). Several papers by Karlsson and colleagues have determined differences in TB-BMD Z-scores between 62 hip OA cases and 187 controls (222), 112 knee OA cases and 243 controls (223,224) and 39 hand OA cases (defined as OA of the DIP and/or CMC joints) and 164 controls (225). Cases were referred to a hospital in Sweden and controls were randomly selected from Statistics Sweden population records. In all papers, TB-BMD was higher in cases compared to controls for both men and women (222-224), with the exception of male hand OA cases, who did not have higher BMD than male controls (225).

HBM and prevalent OA

An increased prevalence of overall radiographic hip and knee OA in individuals with HBM (section 2.3.2) compared to relatives and general population controls has been observed, with age-, sex- and BMI-adjusted ORs of 1.52 (95% CI 1.09, 2.11) and 1.62 (1.22, 2.16) for hip and knee OA, respectively (226,227). Adjustment for BMI made little difference to the results for hip OA but attenuated the OR for knee OA from 2.38, suggesting that the increased FM of HBM individuals partially mediates the relationship between HBM and knee OA, with mediation analysis suggesting that 45% of the effect of HBM on knee OA is mediated by BMI (227).

When analysing the individual radiographic sub-phenotypes of OA (osteophytes, JSN, subchondral sclerosis), an increased odds of osteophytes in HBM individuals was observed at both joints and an increased odds of subchondral sclerosis was observed at the hip. However, there was no difference in odds of JSN, between individuals with and without HBM, at either joint (226,227). These associations are suggestive of a 'bone-forming' phenotype in HBM individuals. The same pattern of increased odds of osteophytes but not JSN in individuals with HBM compared to unaffected relatives was also observed in the (non-weight-bearing) DIP and CMC joints (228).

3.1.2. Longitudinal evidence

Incident OA

In epidemiological studies, incident radiographic OA is normally defined as a joint with a KL grade $\geq$2 at follow-up, which had been free of OA at baseline (KL<2). The relationship between BMD and incident OA of the hip and/or knee has been studied in the following cohorts: the Michigan bone health study, the Framingham study, the Chingford study, RS, the Baltimore longitudinal study of aging, the MOST study and JoCo. Overall, there is relatively consistent evidence to suggest higher BMD is associated with incident knee OA, but less clear evidence to suggest a relationship with incident hip OA.

The first longitudinal analysis of the relationship between BMD and incident OA was published by Sowers *et al* in 1999, who studied the incidence of hand and knee OA in 482 women, with a mean age of 37 years, from the Michigan bone health study (214). The authors observed a 0.8SD higher mean FN-BMD Z-score in those with incident *knee* OA within three years of follow-up, compared to those who did not develop knee OA during follow-up; however, the authors did not find evidence for a relationship between BMD and incident hand OA (214). An association between FN-BMD and incident knee OA was also observed in a population of 473 women with a mean age of 71 from the Framingham study, followed-up over approximately nine years (229). In a population of 119 men and 76 women, with mean age 61 years, from the Baltimore longitudinal study of aging, higher LS, but not FN, BMD predicted an increased odds of incident knee OA over an average of 10 years of follow-up (230). In a population of 975 individuals aged over 45 years from the JoCo study, a higher risk of developing incident knee OA over a median of 6.5 years was observed in those with intermediate, but not high, TH-BMD, suggesting a non-linear relationship between TH-BMD and incident knee OA (231). Bergink *et al* studied the relationship between BMD and incident knee OA in a population of 619 women and 496 men from RS, over on average 6.5 years. They observed that the difference in baseline FN and LS-BMD between those with and without incident knee OA at follow-up was greater for men than women (232).

Studying the individual radiographic phenotypes of OA, Hart *et al* identified a 6.3% higher mean LS-BMD and 3.9% higher mean FN-BMD in women with incident knee *osteophytes*, but evidence for higher BMD at either site was much weaker in those with incident *JSN* amongst Chingford women (233). However, in the MOST study cohort, BMD was associated with an increased odds of JSN (defined by change in JSN grade of at least half a grade) and an increased odds of osteophyte worsening (increase of one grade for any osteophyte) in those without OA at baseline, suggesting that BMD is related to the incidence of both osteophytes and JSN (234).

Fewer studies have examined the relationship between BMD and incident *hip* OA. In the JoCo analysis by Barbour *et al*, amongst 928 adults free of hip OA at baseline (KL<2), TH-BMD was unrelated to incident hip OA, as defined by radiographic criteria. However, an *inverse* relationship between TH-BMD and incident symptomatic radiographic OA (*i.e.* symptoms and radiographic evidence of OA in a hip without both at baseline) was observed (231). In RS, no evidence was found to support a linear relationship between FN-BMD and incident hip OA, although when the population was divided by quartile of FN-BMD, there was a higher odds of incident OA in the highest quartile compared to the lowest quartile only, suggesting a threshold effect (235).

Progressive OA

Evidence supporting an association between BMD and progressive OA is limited and inconsistent (207). Zhang *et al* studied the relationship between FN-BMD and *knee* OA progression in a female population from the Framingham study. They defined OA progression as an increase of KL grade in those with a KL grade of at least two at baseline. They found a lower odds of OA progression with increasing BMD quartile (229). When analysing the individual sub-phenotypes, they found evidence that higher BMD was associated with a reduced odds of JSN progression but there was no dose-response relationship between BMD quartile and osteophyte progression (229). Hart *et al* similarly found a lower hip, but not LS, BMD in those with progressive OA and JSN in women from the Chingford study (233). An analysis of the RS population failed to identify an association between FN-BMD and progressive knee OA but did observe a relationship between LS-BMD and knee OA progression (232). Further analyses of RS identified an increased odds of *hip* OA progression per SD increase in FN-BMD (235).

Summary of evidence

Overall, the evidence from both cross-sectional and longitudinal observational analyses provides consistent evidence for a relationship between high BMD and

risk of OA. However, the role of BMD in OA progression is less clear. One possible explanation is that studies of OA progression have been performed in case-only populations. This could result in a selection bias whereby risk factors for disease incidence can be spuriously inversely associated due to 'conditioning' on case status, leading to spurious inverse associations of risk factors with progression if there are unmeasured confounders related to both incidence and progression (236). Alternatively, there may truly be an inverse relationship between BMD and OA progression due to a positive relationship between BMD and cartilage thickness, meaning higher BMD is related to reduced progression of JSN. To progress from KL grade two to three or four at the knee, JSN needs to occur. The results of Zhang *et al* suggest that higher BMD is specifically associated with reduced JSN, but not osteophyte, progression. Therefore, further analyses of progression of the individual radiographic sub-phenotypes of OA are required.

HBM, BMD and joint replacement

Joint replacement surgery can be used as an indicator of severe OA, as OA is the most common reason for performing TKR/THR (237). TJR reflects a combination of pain and reduced function, along with radiographic features of OA (238). In an analysis of the HBM population, Hardcastle *et al* identified a higher odds of TJR at any site in HBM individuals compared to their relatives without HBM, reflecting a greater than 4.5 times higher odds of hip replacement (partial or total) (239). Evidence for an increased odds of knee replacement was much weaker. When comparing the prevalence of TJR at any site in the HBM population, aged over 65 years, with general population data from the Health Survey for England, a higher prevalence of TJR in HBM individuals was observed, whereas there was no difference in prevalence between the relatives without HBM and the general population (239). These findings are consistent with a more recent analysis in TASOAC, which identified a positive relationship between LS and TB-BMD and risk of THR, but no relationships between LS, TH or TB-BMD measures and TKR were observed (240). The authors did, however,

observe a relationship between medial tibia *subchondral* BMD and risk of TKR. Overall, the findings of these two studies suggest that higher BMD is related to a greater risk of severe, end-stage OA at the hip, suggestive of a *positive* relationship between BMD and hip OA progression.

3.2. Bone turnover and OA

Evidence from observational studies

Several cross-sectional and longitudinal analyses have examined the relationship between BTMs (section 2.1.4) and OA, with inconsistent findings. As bone turnover is inversely related to BMD, one may expect to see lower levels of BTMs in those with OA. Peel *et al* found evidence for inverse relationships between BTMs and severity of spinal OA (241) and Sowers *et al* found lower osteocalcin levels in both knee and hand OA cases (214). Garnero *et al* similarly reported lower osteocalcin, as well as lower CTX-1, in outpatients with knee OA compared to controls, and identified an inverse relationship between osteocalcin levels and severity of OA symptoms assessed by total Western Ontario and McMaster Universities OA (WOMAC) index (242).

Inconsistent with these studies suggesting increased bone turnover is related to a reduced risk of OA, Stewart *et al* identified higher osteocalcin levels in cases with clinically diagnosed hip OA, compared to controls (243). Bettica *et al* identified higher levels of urinary CTX-1 and NTX-1 in Chingford women with progressive knee OA, compared to controls without OA or osteoporosis (244). However, CTX-1 and osteocalcin were unrelated to knee OA in a population of men from the Hertfordshire Cohort Study (HCS) (245). Hunter *et al* studied twin pairs from the St Thomas twins registry and identified a higher concentration of deoxypyridinoline, a marker of bone resorption, in individuals with knee OA, compared to those without knee OA, but no difference in osteocalcin (246). Min *et al* identified higher OPG levels in those with KL grade 4 knee OA compared to those with a KL grade 2 or 3, suggestive of higher bone turnover in those with more severe OA (247).

Inconsistencies in these studies could reflect the fact that they are measuring systemic bone turnover, rather than bone turnover localized to the subchondral bone. Dieppe *et al* found evidence for a relationship between subchondral bone turnover, as assessed by bone scintigraphy, and progression of JSN (248). A similar relationship with radiographic changes was observed at the hand (249). Nwosu *et al* compared levels of serum tartrate resistant acid phosphatase 5b (TRAcP5b), produced by osteoclasts, to the density of TRAcP-positive osteoclasts in the subchondral bone and found a positive relationship, suggesting that serum BTMs correlate with subchondral bone turnover. The authors further identified a positive relationship between TRAcP5b and WOMAC pain scores and subchondral sclerosis (250).

Evidence from clinical trials

Further evidence for a role of bone turnover in OA progression is provided by clinical trials of drugs affecting bone turnover. Strontium ranelate (StR) is an osteoporosis treatment suggested to reduce bone resorption whilst increasing bone formation. A post hoc analysis of 1,105 women from a clinical trial for spinal osteoporosis, who also had spinal OA, found that StR improved back pain compared to those taking placebo and resulted in a 42% reduction in progression of radiographic OA compared to placebo (251). Another post-hoc analysis of 2,617 women from a StR osteoporosis trial identified a reduction in CTX-II, a marker of cartilage degradation, over three years in women taking StR (252). This evidence led to the design of the StR in knee OA (SEKOIA) trial, which was a three-year double-blinded trial to determine if StR protects from knee OA progression (253). The trial recruited 1,371 patients with knee OA and found evidence for reduced cartilage degeneration in the treatment group compared to the placebo group, and those taking a higher dose also had improvements in WOMAC pain and physical function scores compared to those taking the placebo (254,255). A further MRI analysis also identified that those taking the higher dose had reduced cartilage volume loss and attenuated BML progression compared to those taking the placebo (256). Hypothesized mechanisms by which

StR protects from OA progression include reduced subchondral bone remodelling or a direct effect on reduced chondrocyte apoptosis (257).

Evidence from clinical trials of the bisphosphonate risedronate have similarly suggested a possible role of bone turnover in OA progression. The first one-year trial of 231 patients with knee OA from the UK determined the effect of two doses of risedronate, compared to placebo, on radiological changes and changes in symptoms. Improvements in total WOMAC scores, reflecting improvement in symptoms, were observed for both doses compared to placebo (258). There was also an improvement in the patient global assessment of disease for the higher dose of risedronate, compared to placebo (258). A larger, two-year, trial, including North American and European individuals with medial compartment knee OA did not observe differences in the change in WOMAC scores between those taking risedronate and those taking the placebo, nor did they observe differences in change in mJSW (259), suggesting potential population-specific effects of risedronate on OA symptoms. It should be noted that decreases in average pain scores were observed in all groups, of similar magnitude to previously observed (258). However, a decrease in CTX-II was observed (259), which was subsequently related to reduced radiological progression at two years (as defined by change in mJSW) (260).

3.3. Insights from genetic studies

3.3.1. Determining the causal effect of BMD on OA risk

Although there is a wealth of evidence to suggest an observational relationship between BMD and OA, it is currently unclear whether this represents a true causal effect of BMD on OA, or shared underlying biological pathways contributing to bone and joint development and homeostasis.

Consistent with a direct causal effect of BMD on OA, Funck-Brentano *et al* identified a causal effect of FN-BMD on both hip and knee OA using Mendelian randomization (MR) analyses for causal inference (MR is described in section

5.3.3) (261). However, the authors did not determine the causal effect of hip and knee OA on FN-BMD; lack of evidence for this direction of effect would strengthen the evidence for a direct causal effect of BMD on OA. MR analyses have also provided some evidence for a causal effect of LS-BMD on knee OA (139,261). In a study of knee OA cases and controls from OA Initiative (OAI) and JoCo, Yerges-Armstrong *et al* identified an association between four BMD-associated SNPs and knee OA (262). The four SNPs associated with knee OA were among the most strongly associated BMD, which is as expected of a causal relationship (one would expect, in the case of a true causal effect, for the SNP-outcome association to increase as the SNP-exposure association increases).

3.3.2. Evidence for shared aetiology

Converse to a direct causal effect of BMD on OA, when exploring the genome-wide genetic correlation between BMD and OA, Hackinger *et al* identified a genetic correlation between LS-BMD, but not FN-BMD, and combined OA (hip and/or knee OA), with weaker evidence for a genetic correlation with hip and knee OA individually (137). One could hypothesize that a genetic correlation specific to LS-BMD reflects artefactual elevation of BMD, in the presence of OA, by spinal osteophytes. However, the authors also found some evidence for a genetic correlation between TB-BMD measured in childhood and combined OA (137). TB-BMD measurement during childhood will not be affected by features of OA, which suggests that there may be a true genetic correlation between BMD and OA, reflecting shared genetic aetiology. In this section I will discuss the evidence for shared biological pathways contributing to BMD and OA.

The Wnt signalling pathway in OA pathogenesis

There is overwhelming evidence to suggest that the Wnt signalling pathway, outlined in section 2.1.3, plays a role in OA pathogenesis (171,263-265), which is consistent with shared underlying biology between BMD and OA. Evidence suggests that both overactivation of, as well as a reduction in, Wnt signalling can be deleterious for the joint structure, particularly cartilage.

Wnt antagonists and OA

An early OA genetic analysis by Loughlin *et al* identified a SNP (rs7775) in exon 6 of *FRZB* (encoding a Wnt antagonist), which was more frequent in females with hip OA undergoing THR, compared to controls without hip OA (266). Lane *et al* later determined the relationship between rs7775 and radiographic hip OA phenotypes in SOF; the minor allele was associated with a slight increased risk of JSN in this population (267). Individuals with the minor allele, in combination with the minor allele for another variant in exon 4 (rs288326), had an increased risk of severe JSN (267). The MAF for rs7775 was increased in individuals from RS with generalized OA, compared to controls without OA (268). Rs7775 was related to diminished Wnt signalling antagonism *in vitro* (266), providing evidence for a role of Wnt inhibitors in reducing OA risk. In a large meta-analysis of the TREAT- OA consortium, rs288326 was related to hip OA (122) ; rs288326 was also associated with reduced Wnt antagonism *in vitro* (266), providing further evidence for a role of reduced Wnt antagonism in hip OA. Consistent with a role of *FRZB* in reducing OA risk, lower *FRZB* mRNA in osteoarthritic cartilage samples, compared to healthy cartilage, has been demonstrated (269), as well as an inverse correlation between *FRZB* expression and expression of markers of cartilage degeneration (270).

DOT1L, a histone methyltransferase, is involved in the downregulation of Wnt signalling and cartilage preservation (271). Further suggestive of a role of Wnt inhibition in reducing OA risk, a SNP in the *DOT1L* gene was associated with hip mJSW with genome-wide significance (147), and the same SNP has been associated with a reduced risk of hip OA (147,272).

Additionally, several studies of human cartilage samples suggest that *DKK1* expression is lower in OA cartilage compared to healthy cartilage (247,269), although others have suggested than *DKK1* expression is higher in damaged cartilage (273,274). Using a mouse model, Funck-Brentano *et al* observed lower *DKK1* expression in the non-calcified zone of damaged cartilage compared to healthy cartilage (275); however, expression was higher in the subchondral bone

of knees with OA, with the authors concluding that increased expression in bone maintains cartilage homeostasis via the regulation of bone factors such as VEGF (275). Consistent with this theory, Zarei *et al* observed higher expression in subchondral bone underlying partially damaged cartilage, compared to normal or fully defected cartilage in femoral heads extracted during THR (276).

Studies of *SOST* knockout mice showed that the knockouts had more severe cartilage lesions compared to wildtype mice (277). Chan et al (2011) provided evidence that SOST may protect against cartilage proteolysis (278). However, others have found no difference in cartilage lesions in *SOST* knockout mice (279), whilst Zhou *et al* identified more rapid OA development following surgical induction of OA in mice overexpressing *SOST* (280). Sclerostin expression has been found to be decreased in osteocytes of the subchondral bone in OA (278,279,281) and this decreased expression was associated with subchondral bone thickening (278). However, other studies have shown increased sclerostin staining in bone tissue and cartilage from tibial plateaus of TKR patients, compared to healthy control samples (282).

Wnt receptors, ligands and downstream targets and OA

In addition to studies of the role of Wnt antagonists in OA pathogenesis, the role of Wnt receptors and downstream signalling molecules have been investigated. Blom *et al* identified higher expression of *WISP1*, a Wnt responsive gene, in human OA cartilage and synovium (283). Nalesso *et al* observed more severe OA in *Wnt16* knockout mice compared to wildtype, suggesting that the Wnt16 ligand has a role in preserving cartilage after joint injury (284). However, Van den Bosch *et al* provided evidence to suggest that *Wnt16* overexpression in the synovium of a mouse model leads to increased expression of markers of cartilage degeneration (270), whereas Tornqvist *et al* found no change in OA severity in transgenic mice specifically overexpressing *Wnt16* in osteoblasts (285). *Lrp5* knockout mice displayed more cartilage degeneration compared to wildtype mice (286), although analyses by a different group have suggested the opposite (287).

The TGFβ super-family

As discussed in section 1.2.6, the first genetic locus associated with OA risk was linked to the *GDF5* gene. *GDF5* encodes a ligand for the TGFβ superfamily signalling pathway (section 2.1.3). In addition to *GDF5,* genetic analyses have identified other TGFβ and BMP ligands, mediators, and inhibitors with a potential role in OA pathogenesis. Two SNPs in the *BMP2* gene were linked to an increased odds of knee JSN in Chingford women (288). Yamada *et al* identified a relationship between a polymorphism in the *TGFβ1* gene and risk of spinal osteophytosis; the same allele related to increased osteophytosis was also related to a reduced risk of osteoporosis (289). More recently, a cross-phenotype meta-analysis identified a novel locus in the *SMAD3* gene, which is related to both LS-BMD and hip/knee OA (137). Another study found higher expression of *TGFβ1* and *SMAD3* in human OA cartilage samples compared to healthy cartilage samples, but reduced expression of *BMP2* (290). *GREM1*, encoding an inhibitor of the BMP signalling pathway, mRNA levels were lower in cartilage from osteoarthritic joints compared to cartilage extracted from healthy individuals (269). Further evidence for a role of expression of *GREM1* in OA pathogenesis is the identification of a SNP, located 80kb downstream of the gene in a gene regulatory region, as related to hip OA in RS (291). A genetic variant in the *ASPN* gene, encoding a TGFβ pathway inhibitor, has been linked to OA risk in several populations (175).

With regards to experimental evidence for a role of the TGFβ signalling in OA pathogenesis, mice with mutations resulting in loss-of-function of *Smad3* had a joint phenotype characterized by osteophyte formation and loss of cartilage (292). The same phenotype was observed in mice with cartilage-specific knockout of *Alk5*, encoding a TGFβ receptor (293), as well as mice with cartilage-specific deletion of *Tgfbr2* (294). Furthermore, mice with cartilage-specific overexpression of Smurf2, a TGFβ inhibitor, generated osteophytes and subchondral sclerosis and had a reduced cartilage area (295). Conversely, in another study, mice with cartilage-specific loss of *Tgfbr2* expression, resulting in loss of TGFβ signalling,

displayed reduced cartilage loss after destabilization of the medial meniscus, compared to wildtype mice (296). In a human RCT, injection of human chondrocytes expressing TGFβ1 from a viral vector into AC of knee OA patients reduced progression of cartilage loss, but not osteophyte progression, compared to injection of a placebo (297). In a mouse study, treatment with an inhibitor of the ligands TGFβ1 and TGFβ3 resulted in reduced osteophyte formation but also reduced cartilage proteoglycan content and cartilage volume (298), suggesting that TGFβ signalling may have opposing effects on osteophyte formation and cartilage maintenance.

Experimental evidence suggests that the TGFβ-specific *vs* the BMP-specific pathway may be involved at different stages of OA pathogenesis; in a guinea pig model, the number of Smad2/3-expressing chondrocytes decreased with OA progression, whereas the number of chondrocytes expressing Smad1/5/8 increased (299). As well as the action of TGFβ signalling on expression of chondrogenic transcription factors, BMP signalling pathway may be involved in OA pathogenesis via cross-talk with the canonical Wnt signalling path; chondrocytes treated with BMP2 displayed increased expression of the Wnt inhibitors *FRZB* and *DKK1* (269) and increased *LRP5* expression and activated nuclear β-catenin (300).

Overall, there is clear evidence for a key role of both the BMP and TGFβ signalling pathways in OA pathogenesis. However, it is unclear the exact contribution of each pathway to individual features of OA pathogenesis.

Cathepsin-K

Evidence suggests a role of Cathepsin-K in OA pathogenesis. A locus annotated to *CTSK* was associated with hip OA in a recent GWAS (141). In addition to degradation of type I collagen of bone, Cathepsin-K is able to cleave type II collagen of cartilage (301). Cathepsin-K is expressed by human chondrocytes (301) and mRNA levels have been observed to be higher in OA cartilage (302), with levels correlated to OA severity (303). A *CTSK* knockout mouse showed delayed development of OA after surgery, compared to wildtype mice (304). An

RCT of a Cathepsin-K inhibitor, MIV-711, in individuals with knee OA from across Europe found evidence for reduced MRI-assessed features of structural progression in those taking either of the two doses of the intervention, compared to placebo (305). Improvements in pain score, which was the primary outcome, were not observed in those taking either dose of the inhibitor, although the duration of the trial was only six months (305).

3.4. PhD aims

The overall aim of this PhD thesis is to develop understanding of the role of bone in OA pathogenesis. In order to do this, I firstly aim to clarify the role of BMD in knee and hip OA progression by determining the relationship between HBM and OA progression. I aim to determine if there are differential associations of HBM with osteophyte progression, compared to JSN progression, as seen for prevalent OA sub-phenotypes. Secondly, I aim to perform metabolomics analysis to identify metabolic traits associated with both HBM and OA sub-phenotypes and determine if these metabolic traits mediate the relationship between high BMD and OA. Any metabolic mediators of the BMD-OA relationship could represent metabolic pathways involved in the pathogenesis of bone-forming OA. Thirdly, I aim to use bidirectional MR to clarify the direction of causality between BMD, OA, and BMI. If bidirectional causal associations are observed, this could indicate that biological pleiotropy explains the BMD-OA observational relationships. However, if I observe a causal effect of BMD on OA, without a bidirectional causal pathway, this will strengthen the evidence for a direct causal role of BMD on OA. Fourthly, I aim to perform pathway-specific genetic analyses to determine the role of pathways in bone development and homeostasis in OA pathogenesis. Pathways of interest include the Wnt signalling pathway, the TGFβ superfamily (both involved in osteoblast development and hence bone formation, as discussed in section 2.1.3), the pathway regulating osteoclast differentiation (and thus bone resorption) and the IGF-1 axis which regulates endochondral ossification and hence skeletal development. The aims of this PhD are summarized in Figure 19.

Figure 19: Diagram of the aims of this thesis and the corresponding chapters.

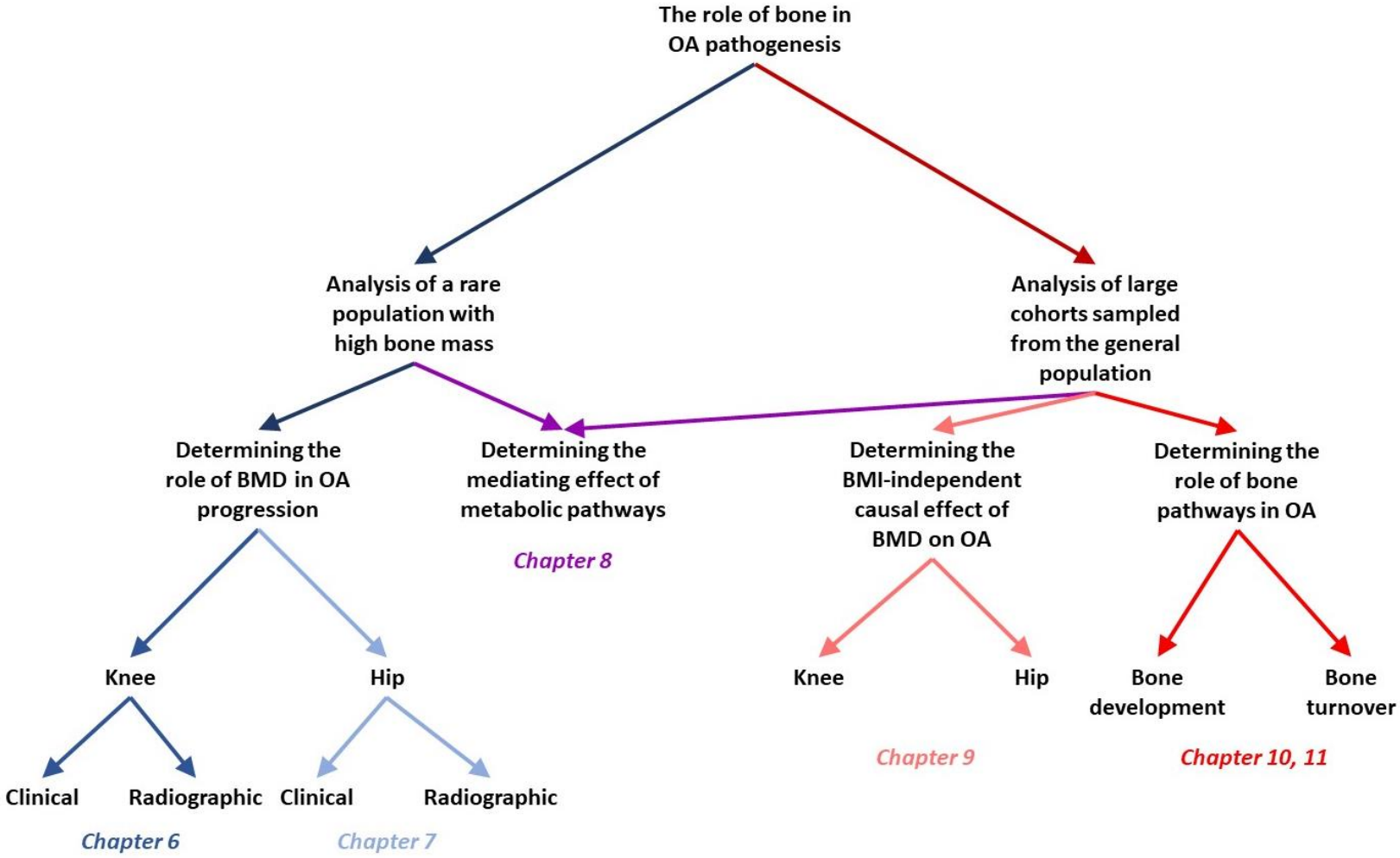

The aims of this PhD thesis can be split into six key research questions, each representing a separate results chapter:

Question 1: Is HBM related to radiographic and clinical features of knee OA progression? (*Chapter 6*)

In this chapter, I use baseline and follow-up knee radiographs from the HBM study population to determine the relationship between HBM and progression of the individual radiographic sub-phenotypes (*i.e.* osteophytes and JSN). I use data collected from the postal questionnaires, completed at follow-up, to determine the relationship between HBM and knee pain, stiffness, and functional limitations.

Question 2: Is HBM related to radiographic and clinical features of hip OA progression? (*Chapter 7*)

As described for knees, I will use baseline and follow-up pelvic radiographs from the HBM study population to determine the relationship with hip OA sub-phenotype progression and will use questionnaire data to determine the relationship between HBM and symptoms of hip OA.

Question 3: What are the metabolic predictors of radiographic OA sub-phenotypes of the hand, hip and knee and do these metabolic traits mediate the HBM-OA relationship? *(Chapter 8*)

In Chapter 8, I will use metabolomics to determine relationships between multiple metabolic traits and radiographic OA sub-phenotypes. I will determine if the metabolic traits are related to HBM, BMD and bone turnover. I aim to replicate any observed associations in cohorts sampled from the general population to determine generalizability, and to determine if any HBM/BMD and OA-related metabolic trait mediates the HBM-OA relationship.

Question 4: Is BMD a causal risk factor for OA, independent of BMI? (*Chapter 9*)

In this chapter, I firstly aim to use bidirectional MR analyses to determine the causal effects of BMD and BMI on hospital-diagnosed hip and knee OA in UK Biobank (and vice versa). If any causal effects are identified, I aim to

use multivariable MR (MVMR) to determine independent causal effects. I will then use BMD polygenic risk scores (PRS) to determine if BMD has specific causal effects on individual radiographic sub-phenotypes.

Question 5: What is the contribution of key bone pathways to OA risk? (*Chapter 10*)

In this chapter, I will calculate the proportion of variance explained in OA risk and OA sub-phenotypes by key bone pathways. I will compare the proportion of variance explained to the proportion of variance explained in BMD estimated from heel ultrasound (eBMD). I will also determine the relationship between circulating sclerostin levels and OA sub-phenotypes.

Question 6: Is IGF-1 a risk factor for hand, hip, or knee OA? (*Chapter 11*)

My final research question will be answered in Chapter 11, by determining the observational associations between serum IGF-1 and hospital-diagnosed hand, hip, and knee OA in the UK Biobank population. MR will be performed to determine if there is a causal effect of IGF-1 on OA.

CHAPTER 4. METHODS: HBM STUDY- NEW DATA COLLECTION

As outlined in section 3.4, a key aim of this PhD is to determine the relationship between HBM and radiographic and clinical features of OA progression. Addressing this involved novel data collection in the HBM study population (section 2.3.2). I collected follow-up data from all alive and contactable individuals from the HBM study population. I designed a questionnaire to characterize clinical features of OA progression, such as pain and TJR, arranged follow-up X-rays to determine changes in radiographic features of OA, and follow-up DXA scans to assess body composition in this population. In this chapter, I will outline how these data were collected and cleaned ready for analysis, which will be discussed in the next chapter.

4.1. Ethical considerations

4.1.1. Application for research ethics committee (REC) approval

The follow-up questionnaire (section 4.2), along with the plan for follow-up radiographic data collection (section 4.3,4.4) were submitted for approval to the South West-Central Bristol REC. The flowchart detailing the process for participant contact for the follow-up studies is displayed in Figure 20. Due to the time lapse between the initial and follow-up data collection (up to 12 years), the REC requested an additional step be added to the follow-up data collection process, whereby all individuals who were alive and had not withdrawn consent were contacted in writing, asking them to sign a consent form if they were happy to still be contacted about the study. Only when an individual had provided written consent for future contact could they be contacted about the study questionnaire and invited for imaging. Ethical approval for the follow-up study was provided on 18th August 2016 (REC reference 05/Q2001/78-amendment 21) and Health Research Authority approval on 19th October 2016.

Figure 20: Flowchart detailing the follow-up data collection process.

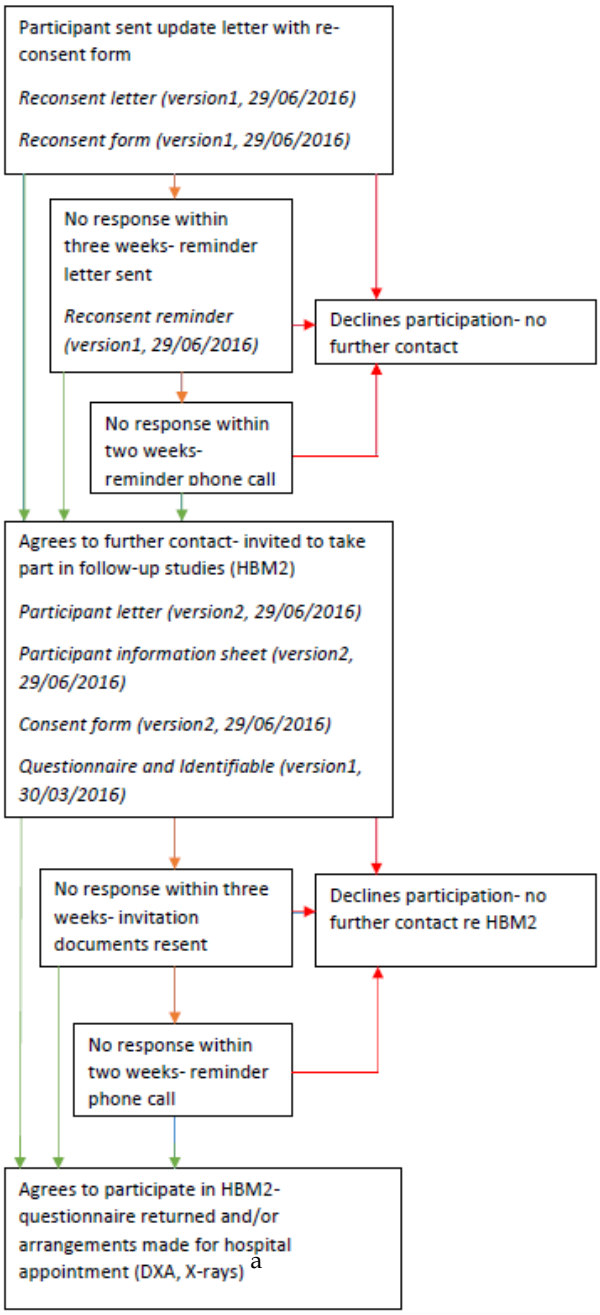

[a]Arrangements were made for those originally recruited at the seven centres able to perform follow-up DXA/X-rays (plus those from Yeovil were invited to attend Bath); those recruited at other centres were still invited to complete the questionnaire.

4.2. Questionnaire design

To assess clinical progression of OA (in terms of pain and TJR surgery), I designed a postal questionnaire. The overall aim for the questionnaire was to collect data on measures of OA severity, such as pain, and collect data on relevant covariates. However, it was important to ensure that the questionnaire was not too long, as this would reduce participant compliance.

4.2.1. Rationale for question selection

To ensure reliability and validity of the data collected, the questionnaire collated questions from questionnaires previously used by other cohort studies or validated specific-use questionnaires. I will discuss the selection and previous use of these questions. The questionnaire is provided in Appendix 7.

Bones and Joints

Arthritis questions from the British Women's Heart and Health Survey (BWHHS)

BWHHS is a prospective cohort study investigating risk factors for heart disease in 4,286 women randomly selected from 23 towns in England, Scotland, and Wales (306). Four postal questionnaires have been sent to consenting participants. The questions taken from BWHHS questionnaires were deemed to be valid due to the prior publication of analyses using these data, and the observed relationships of arthritis with BMI and prevalent and incident locomotor activity limitation (307-309). The questions reproduced included '*Have you ever been told by a doctor that you have arthritis*?', '*If yes, please give the type of arthritis*' and '*Which joints are affected?*' These questions were included to allow participants to self-report OA, as self-reported OA could potentially identify more severe cases (*i.e.* painful enough to seek medical help).

WOMAC

The WOMAC index is a widely used and validated questionnaire employed in OA research as a measure of pain, stiffness, and limitation of physical function (310). The questionnaire consists of three subscales: five questions for pain; two questions for stiffness and 17 for physical function. Each question is answered on a five-point scale, from 0 representing no pain/stiffness/difficulty performing an activity, to 4 representing extreme pain/stiffness/limitation of activity. The WOMAC index can be used to produce a pain score, a stiffness score and a physical function score for the hip and knee separately. A short-form version of the WOMAC function index was proposed by Whitehouse *et al* to reduce participant burden by limiting the physical function section to the seven most important questions (based on data analysis and the opinion of Rheumatologists) (311). This questionnaire has been validated in patients with varying severities of OA (311,312). Due to the relevance of including all three WOMAC sections for both the hip and knee, I decided to use the short version of the WOMAC in this questionnaire, significantly reducing the number of questions and page count of the questionnaire.

Arthritis procedure questions from the HCS (EPOSA) questionnaires

HCS includes a population of 2,997 people living in Hertfordshire, who were born between 1931 and 1939 (313). The EPOSA sub-study is a collaboration of six European cohorts with the aim of determining the impact of OA (314). Four hundred and 44 HCS participants have been recruited into this sub-study (314). A question about surgical procedures for knee OA was taken from the follow-up study of knee OA questionnaire. These procedures included steroid injection, cartilage operation and knee washout/lavage/arthroscopy. This question was included firstly because it indicates clinical OA, in that pain was severe enough to require surgical intervention, but secondly knee OA procedures could reduce the symptoms recorded in the questionnaire. The question was adapted to read '*have you ever had any of the following procedures performed on your knee(s) for*

arthritis?' instead of '*for osteoarthritis*' so that participants who did not know what type of arthritis they had would not skip this question.

Mobility questions from the Osteoporosis Screening Questionnaire (OSQ)

The OSQ is currently used by the North Bristol Trust (NBT) DXA service to aid calculation of a fracture risk (FRAX) score for patients (315). The questionnaire has been developed based on the advice of Rheumatologists and Geriatricians and asks about a variety of factors which may affect fracture risk. Due to the regular use and refinement of this questionnaire, to aid interpretation of DXA scan results and inform treatment, the questions selected from the questionnaire were deemed to be sufficiently reliable. Questions taken from the OSQ include a mobility aid and a walking distance question, which can be used as two further clinical measures of OA severity, as the further the participant can walk unaided, the less severe their lower-limb OA is likely to be. Regular use of a mobility aid indicates that mobility is severely affected, potentially by painful OA. The walking unaided question was adapted from the OSQ to quantify distance rather than time. The large age range of the cohort added the problem of deciding whether to use metric or imperial measures of distance. '*Unaided*' was adapted to '*before you need to stop and rest*' as the question follows the mobility aid question, and it may have caused confused the participant to ask how far they can walk unaided immediately after them selecting the mobility aid they use. This wording of the question made it possible for those who cannot walk without a mobility aid, such as a walking stick, to still answer the question.

Health and demographics

Vertical Impacts on Bone in the Elderly (VIBE) questionnaire

The VIBE study is a multi-centre epidemiological study investigating the effect of vertical impacts, achieved during habitual PA, on bone parameters such as BMD (316). The education question '*What is the highest level of education or training that you have successfully completed?*', and the relevant categories (e.g. CSE/ School Certificate, GCSE/O Level, Apprenticeship *etc.*), were adapted from this

questionnaire. The VIBE questionnaire specifically asks which education level achieved by the age of 26, but due to the large age range of the HBM participants and the youngest participant being below the age of 26, the question was adapted to be highest education level ever achieved. This was based on the advice of Dr Rachel Cooper from the National Survey for Health and Development. Educational attainment, a measure of individual-level socioeconomic status (SES), is a potential confounder when measuring the relationship between HBM and pain. As some participants resided in Wales, and the Index of Multiple Deprivation (IMD) only includes English postcodes, IMD was not a suitable measure. Education was selected over other measures of SES, such as income or occupation, due to the large age range of the HBM population, meaning some participants may not have reached their peak occupation level and others will be retired meaning their current income may not reflect the income they received in the past. Another question adapted from the VIBE questionnaire addressed prior joint replacement. The '*reason for joint replacement*' question was added to ascertain whether the joint replacement was due to arthritis, which is an indicator of OA progression, or another reason such as a fracture.

EQ5D-5L

The EuroQol EQ5D questionnaire is a short and simple standardized questionnaire designed to measure health-related QoL (HR-QoL) for a range of diseases. It is one of the most commonly used generic measures of HR-QoL worldwide (317). This generic measure of HR-QoL was included, along with the disease-specific measure (see WOMAC above), to capture overall health status, including the effect of any comorbid conditions. The questionnaire measures HR-QoL in five domains: pain/discomfort, depression/anxiety, mobility, self-care, and usual activities. Within each domain there are five levels from which to select; no pain/problems/depression to extreme pain/extremely depressed or unable to walk/look after oneself/take part in usual activities. The validity of the five-level version of the EQ5D has been tested in eight patient groups with

chronic health conditions in six different countries, including patients with arthritis (318).

International Physical Activity Questionnaire (IPAQ)

PA is a potential confounder of any relationship between BMD and OA progression. Lifetime and past week PA have previously been measured in the HBM cohort using a postal questionnaire. To update current PA status of participants, the short form version of the IPAQ questionnaire was included in the questionnaire. The short-form IPAQ measures three types of PA over the past week, vigorous activities (such as aerobics), moderate activities (such as carrying light loads) and walking. Participants were asked how many days over the past week they had performed such activities, and if they had, how many hours and minutes spent participating in these activities on an average day, if known. The IPAQ short form has been psychometrically tested in 12 developing and developed countries, by comparison of the score with an objective measure of PA and has acceptable reliability and validity (319).

4.2.2. Questionnaire piloting

Advice on clinical content was sought from Dr Celia Gregson, Professor Jon Tobias, and Dr Emma Clark, who are clinicians with experience in musculoskeletal research. Their advice included adding more clinical OA questions, such as use of mobility aids and adapting questions to make them more patient-friendly (*e.g.* adapting '*osteoporosis*' to '*osteoporosis (brittle bones)*'). Other advice on clinical content was to remove '*due to arthritis*' from the WOMAC questions, so that pain, stiffness, and difficulty performing activities were all captured even if the participant had not had a diagnosis of arthritis. Other questions to assess OA severity, such as effect on walking distance, were recommended and subsequently added to the questionnaire.

Questionnaires were next trialled by two qualitative researchers in the Musculoskeletal Research Unit (MRU). Their advice included adding a contact name and postal address to the front of the questionnaire to remind the

participants who they could contact for help. They advised that it may not be necessary to ask the participant their name, postcode, and date of birth as the questionnaire had been labelled with their unique ID. However, these were still included to check the details were correct and to allow data checking if there were discrepancies with the IDs (*i.e.* human error when labelling the questionnaires with the ID, discrepancies when sending multiple questionnaires from the same household). The cover sheet was removed by the administrator after the questionnaire was returned and stored separately to retain anonymity. They recommended adapting the wording of the WOMAC questions as the questions originally read '*…the amount of pain you are currently experiencing…please enter the pain experienced in the last 48 hours*'. Due to the contradiction of currently and past 48 hours, which could confuse the participant, the question was adapted to '*the amount of pain you have experienced… please enter the amount you have experienced in the last 48 hours*'.

Once the questionnaires had been adjusted based on this advice, the questionnaire was piloted by two members of the Patient Experience Partnership in Research group, a group of Musculoskeletal service users who regularly meet with researchers to aid development of research project literature. Their feedback was positive, with only a few comments, such as to emphasize on the front of the questionnaire that some questions may seem similar but were still important.

4.2.3. Questionnaire formatting

I formatted the questionnaire for scanning using ABBYY FormDesigner and Flexicapture software (Version 10, http://www.abbyy.com/flexicapture/). ABBYY FormDesigner allowed me to format the questionnaire with page anchors and barcodes for page recognition, aiding the design of a project in Flexicapture which automatically recognised text and checkmarks. Completed questionnaires could then be scanned by the study administrator. After scanning, the Flexicapture software checks each individual answer has been recognised correctly. Once verified, the programmed software exports coded variables to a

Microsoft Excel dataset. This methodology limits data entry errors, compared to entering all answers individually into a database, and is much quicker than manual data entry.

4.2.4. Questionnaire data cleaning

Data were exported to a Microsoft Excel file and imported into Stata (Version 13). Variables were renamed with the prefix '*hm2_*' to represent follow-up data when linked with baseline data. Basic data checks were carried out. These included checking for duplicate IDs and discrepancies between gender and gender-specific responses, for which four were found. These four discrepancies were matched to two couples who had accidentally completed each other's questionnaires.

Joints

Free-text answers for '*Other*' types of arthritis were checked and re-coded as necessary: responses including "*wear * tear*" were recoded as '*Osteoarthritis*' and "*zero negative*" was recoded as '*Rheumatoid arthritis*', assuming the participant meant '*sero-negative*'. Individuals stating that their arthritis type was "*osteoporosis*" were recoded as not having arthritis. '*Other*' free text responses were checked for joints affected by arthritis. In one case, "*fingers*" had been stated but the participant had not selected '*Yes*' for arthritis in hands/wrists and therefore this individual was recoded as having hand arthritis. Responses for joint replacements were checked for consistency. In some cases, individuals did not respond to the '*Have you ever had a joint replacement?*' question, or responded as '*No*', but had later stated that they had a knee replacement, so these individuals were recoded as '*Yes*' for joint replacement. Categorical variables were created concerning the reason for joint replacement for each of the left knee, right knee, left hip, and right hip, based on the free text responses. Free text responses of "*arthritis*", "*pain*", "*worn*" and "*wear and tear*" were coded as '*arthritis*', responses of "*fracture*" and "*shattered*" were coded as '*fracture*', and

"*limping*", "*bi-lateral knee replacement*" and "*estimate*" were coded as '*uncategorised*'.

Self-reported arthritis was checked against radiographic OA at baseline. Thirty-one individuals reporting arthritis at follow-up had a knee KL score <2 at baseline and 32 reporting hip arthritis had a Croft score <3 at baseline (*i.e.* no radiographic OA). Of the 31 with self-reported knee arthritis, all had an incident diagnosis (*i.e.* after the date of their first X-ray), a score >25 on at least one WOMAC knee domain or a TKR due to arthritis. All individuals self-reporting hip arthritis had a diagnosis after their first X-ray, a score >25 on at least one of the WOMAC hip domains or a THR due to arthritis. Self-reported joint replacement was validated using baseline TB DXA images, where available. No discrepancies were identified.

WOMAC pain, stiffness and function scores were calculated for both the hip and knee based on the average value for each subscale, multiplied by 25 (320). Total scores for each subscale were subtracted from 100 to give a score from 0 to 100, with 100 representing no pain, stiffness, or limitation of function. If one pain question out of the five was unanswered, the value was imputed as the mean of the other four questions (320). If fewer than four of the function responses were missing, these values were mean imputed based on the answered function questions (320). Although this protocol was developed for the full version of the WOMAC, it has been used for the reduced version (311).

Demographic variables

Education was further sub-categorised to match the categories used by the Avon Longitudinal Study of Parents and Children (ALSPAC) maternal cohort (321) and categories are summarised in Table 3. Additional free text answers when '*Other*' was selected were manually coded as highlighted in italics in Table 3.

Table 3: Categorisation of education responses.

1. CSE/ None	• None of these • CSE/ School Certificate • *Leaving certificate*
2. Vocational	• Apprenticeship • Qualifications in shorthand typing or other skills (e.g. hairdressing) • *Nursery nurse* • *Private secretary* • *Agriculture*
3. O Level or equivalent	• GCSE/ O Level
4. A Level or equivalent	• GCE/ A Level/ Scottish Highers • Other teaching qualification • State enrolled nurse • State registered nurse • Other para-medical qualification • *Top class 6th form (Ireland)* • *National diploma* • *Ordinary National Certificate (ONC)* • *City & Guilds* • *NNEB*
5. Degree Level	• Diploma of Higher Education • Bachelor's degree (e.g. BA, BSc) • Other degree level qualification (e.g. graduate membership of a professional institute) • Higher degree (e.g. Master's/ PhD) • PGCE- Postgraduate Cert. of Education • *Higher National Certificate (HNC)* • *Higher National Diploma (HND)* • *Chartered insurance institute*

Responses in italics represent additional free text answers when 'Other' was selected, which were manually coded.

Health

Responses to the five EQ5D questions were converted to index values using the crosswalk index value calculator and the UK value set (322). For example, an individual responding that they have no problems with mobility, self-care, performing their usual activities and no pain or depression would score '11111' which is given a value of 1.0 and those reporting that they are unable to walk, wash/dress themselves, unable to do their usual activities, with extreme pain and depression would score '55555' which converts to an index value of -0.594. If

an individual were missing a response for any domain, an index value could not be calculated.

Physical activity

The responses to the IPAQ questions were scored following the protocol on the IPAQ website (https://sites.google.com/site/theipaq/scoring-protocol). Values were calculated for total amount of time per day spent doing each activity type in minutes (vigorous, moderate, and walking). As recommended in the guidelines, values of less than 10 minutes were recoded as 0. Capped variables were then generated based on a maximum time of 180 minutes per day. MET-minutes for each activity type were then calculated:

"Walking MET-minutes= 3.3 x capped walking minutes x number of days of walking
Moderate MET-minutes= 4 x capped moderate activity minutes x number of days of moderate activity
Vigorous MET-minutes= 8 x capped vigorous activity minutes x number of days of vigorous activity"

The three values were then summed to generate total weekly MET-minutes.

4.3. DXA data

As discussed in section 2.2, DXA scanning is the most common way to assess BMD and is used routinely in the NHS. In the HBM study, follow-up TB, bilateral TH (or unilateral, scanning the same hip as baseline) and LS DXA scans were performed on consenting participants using standard NHS operating procedures at each hospital. DXA scans additionally assess body composition (TBFM and total body lean mass [TBLM]). Data were transferred in electronic form, anonymised with the study ID, from each site. Paper copies of the DXA scan images were sent to Bristol so that I could inspect the images for positioning errors or metal artefacts (section 4.3.1, 4.3.2), apart from Hull, where the chief DXA technician performing all scans, Maxine Osgerby, had generated a spreadsheet noting positioning errors and metal artefacts.

4.3.1. Coding metal artefacts

Despite being asked to remove metal before scanning, metal artefacts were still common on DXA scan images, namely wedding rings, jewellery/watches, and TJRs. All images were visually inspected for metalwork. Metalwork was coded using the same methodology as baseline (323):

Table 4: Coding of metal artefacts on DXA scans.

Code	Artefact
0	No visible metal artefact on images
1	Rings
2	Other larger jewellery *e.g.* bracelets
3	Joint replacement (any joint)

This generated a variable for adjustment in regression models using the DXA data. However, only one individual had a metal artefact categorised as 'other large jewellery' and therefore categories two and three were combined when using this variable.

4.3.2. Positioning errors

Sometimes, when a patient is obese or particularly tall, their full body does not fit within the DXA field and some tissue is not captured in the TB image. Most commonly, parts of the arm can be missing from the image. DXA technicians can correct the patient's positioning so that at least one half of the body is within the image and then TB values for FM, lean mass (LM) and BMC can be generated by doubling the FM, LM and BMC for the side fully within the image. However, not all DXA technicians will correct for this and in some cases parts of both arms can be missing. All TB scans were visually inspected for this and a code of '*1*' was given if tissue loss was limited to one side and '*2*' if it was missing from both sides.

4.3.3. Standardizing BMD

There are two main manufacturers of DXA scanners: Hologic Inc. (Bedford, MA, USA) and GE-Lunar Inc. (Madison, WI, USA). Scanner type varied by site, with Bath, Bristol, Oxford, Sheffield, and St Georges using Hologic, and Cambridge and Hull using Lunar, scanners. To limit within-person error due to differences in scanner manufacturer and localised protocol at baseline and follow-up, I, with the help of Karen Ireland, tried to ensure that all participants attended their original centre. 10 individuals were unable to attend their original centre due to logistical restrictions or because their original centre (Yeovil) could not perform follow-up scans. However, these 10 individuals attended a site with the same type of scanner used as at their original centre.

Each manufacturer has its own calibration methods, regions of interest and algorithms for calculating BMD, TBFM and TBLM (324). This leads to variation in DXA measurements between scanners; an analysis by Genant *et al* found that total LS-BMD was 11.7% lower when assessed by a Hologic scanner compared to a GE-Lunar scanner (325). Equations have therefore been developed to generate standardized BMD (sBMD, mg/cm^2) for the LS (325) and TH (326). Hui *et al* later optimized these equations (327). The Hui equation for converting LS-BMD to sBMD for Hologic and GE-Lunar scanners is presented in Equation 1 (327). The Hanson equations for converting BMD of the femur are presented in Equation 2 (326).

Equation 1: Conversion of Hologic and GE-Lunar LS-BMD values to sBMD.

$$sBMD = 1000 * \left(1.055 * \left(BMD_{Hologic} - 0.972\right) + 1.0436\right)$$

$$sBMD = 1000 * (0.9683 * (BMD_{Lunar} - 1.1) + 1.0436)$$

Equation 2: Conversion of Hologic and GE-Lunar TH-BMD values to sBMD.

$$sBMD = 1000 * \left(1.008 * BMD_{Hologic}\right) + 0.006$$

$$sBMD = 1000 * (0.979 * BMD_{Lunar}) + 0.031$$

These calibration equations were developed for the old-style pencil-beam DXA scanners, with a single detector. Later DXA scanners use fan-beam technology to assess BMD, which have multiple radiation detectors (184), and this has led to greater variation in technology between the two major manufacturers. Fan *et al* validated the use of the equation for TH sBMD using fan-beam scanners but found that differences still existed between scanners for LS-sBMD (4.1% for L1-L4 BMD) (328). However, I used these equations to generate sBMD for all participants, in line with the sBMD values generated at baseline by Dr Celia Gregson (323).

4.4. Radiographic data collection

X-rays were performed at Hull, Sheffield, Cambridge, Bath, Bristol, Oxford, and St Georges following standard clinical operating procedures. Bilateral AP knee and dominant hand X-rays were performed on all consenting individuals and AP pelvis X-rays performed on all consenting individuals aged over 40 years.

4.4.1. Anonymising radiographs

Systems for data transfer varied by site. Sites were asked to remove all identifiable information from the DICOM images before transfer. Most sites transferred the anonymised DICOM images on discs labelled with a unique identifier and provided an excel spreadsheet to link the disc to the participant ID. Image files were relabelled with an anonymous ID using the same relabelling system as at baseline (329) to ensure that baseline radiographs could not be distinguished from follow-up when grading. An excel spreadsheet linking the filename to the participant ID and timepoint (baseline or follow-up) was generated for data linkage.

To ensure that all files had the same date stamp, so that baseline and follow-up radiographs could not be distinguished, all files were converted to TIFFs using an ImageJ macro designed by Dr Jenny Gregory at the University of Aberdeen. This macro converted the images to TIFFs while retaining the original scaling

information, which was important for accurate quantitative measures of mJSW and tibial plateau width (section 4.4.5).

4.4.2. Choice of radiographic atlas

The HBM radiographs were graded at baseline using the Burnett atlas (33,226,227). As I was going to regrade all baseline radiographs for individuals with follow-up data, I did not need to use the same atlas as previously used. I therefore chose to use the updated OARSI (Altman and Gold) atlas as this atlas includes additional osteophyte variables (*e.g.* grading medial and lateral for both the tibia and femur) (29), providing additional information and increasing phenotypic variability. This atlas was also chosen as it is a widely used atlas for grading radiographic features of OA. Radiographs were compared to the OARSI atlas to determine the semi-quantitative grade for each feature.

4.4.3. Ensuring consistency in radiographic measures

To ensure gradings were not affected by environmental factors such as lighting and computer screen specification, all readings were performed on the same computer, in the same location. To ensure readings were as consistent as possible, all readings at the knee were performed within a fortnight and all readings at the hip were performed within another fortnight. Each grade was determined by comparing the radiographic image to the atlas images, and a grade was only given for osteophytes if the osteophyte was at least as large as that shown in the atlas.

4.4.4. Assessing reliability of measures

Intra-rater reliability determines how reliable measurements by one reader are, by determining the similarity of two measurements of the same construct (*e.g.* measurement of mJSW) by one reader. Higher intra-rater reliability suggests less measurement error. Inter-rater reliability represents the reliability of a measurement of a construct by two different readers. High inter-rater reliability scores suggest that results are reproducible.

Intra- and inter-rater reliability for categorical variables were determined by kappa statistics. Kappa statistics compare the proportion of agreement between observers with the proportion expected by chance using the following formula:

$$\boldsymbol{\kappa = \frac{A_{obs} - A_{exp}}{1 - A_{exp}}}$$

If there is perfect agreement between observers, κ will be 1. If the agreement between observers is the same as expected by chance, κ will be 0 (330). Landis and Koch suggested a classification system to determine strength of agreement (Table 5).

Table 5: Threshold values to determine strength of agreement proposed by Landis and Koch (1977).

Kappa value	Strength of agreement
<0	Poor
0-0.2	Slight
0.21-0.4	Fair
0.41-0.6	Moderate
0.61-0.8	Substantial
0.81-1	Almost perfect

Reliability for continuous variables was determined using the intraclass correlation coefficient (ICC). The ICC is a measure of the ratio of variance between individuals to the variance between different observations of the same individual (*i.e.* measurement error). The ICC is calculated using one-way ANOVA as follows:

$$\boldsymbol{\frac{\sigma_i^2}{\sigma_i^2 + \sigma_o^2}}$$

Where σ^2_i is the variance in measurements between individuals and σ^2_o is the variance between the repeated observations. If there is no variation between observations, the ICC will be 1. An ICC close to one therefore represents highly reproducible results.

Bland Altman plots were generated for continuous measures. These are plots of the mean of the two measurements (x) against the difference between the two measurements (y) (331). A line is plotted at the mean difference and two additional lines at the mean plus or minus the SD of the difference between the two methods/assessors. If agreement between two methods, or between two assessors, is good, all measurements should lie within the two lines either side of the mean. These plots can be inspected for systematic bias, such as the difference increasing with increasing measurements.

4.4.5. Training to grade radiographic knee OA using the OARSI atlas

As a non-clinician, I did not have prior experience of reading radiographs and grading features of OA. I therefore attended one-on-one training sessions with Dr Sarah Hardcastle, a Consultant Rheumatologist, who has extensive experience grading radiographic OA. During these sessions, we discussed a range of radiographs of differing severities, comparing the images to the atlas, and determining if we agreed on the grading for each feature of OA. After three 90-minute sessions, I graded the training set of 30 radiographs which had been specifically picked by Dr Martin Williams, Consultant Radiologist, NBT, as they reflected a range of severities of KL grade. Dr Hardcastle also graded the radiographs and then after a two-week break, I regraded the 30 radiographs. Inter- and intra-rater reliability were determined, as described in section 4.4.4. ICC statistics were calculated using the Stata '*loneway*' command and kappa statistics using the '*kapci*' command. For variables with more than two levels, weighted kappas were calculated, using the parametric weight ('*wgt(w2)*') option, to account for the fact that an osteophyte graded as two versus three would have less of an impact on analyses than grading the same radiograph as a grade zero versus grade two (and the same for JSN). Full inter- and intra-rater statistics are provided in Appendix 8; all intra-rater weighted kappas were >0.8

and inter-rater weighted kappas were >0.6. Dr Hardcastle and I agreed these were sufficient to start grading the full set of images.

Additional quantitative measures

In addition to the semi-quantitative radiographic sub-phenotypes, additional measurements were generated for mJSW (a continuous, indirect measure of cartilage thickness) and maximum tibial plateau width (to enable adjustment for bone size). As the X-rays were performed at NHS hospitals, they were stored as DICOM files, which retained the image scaling information (except a small proportion, 2%, which were compressed), allowing these measures to be performed. The measurements were performed in ImageJ (332) using a macro custom-designed by Dr Gregory. I adapted the macro to include the image filename in the exported Excel file, for data linkage. Measurements were performed using the ImageJ line tool, with the macro providing prompts to ensure measurements were performed on the right side first and that mJSW was measured first. The macro stores the results in a table and prompts the user to save the file (in Excel format) after each measurement.

mJSW was measured at the narrowest gap between the tibial plateau and the medial femoral condyle (Figure 21). When the line was placed in the most appropriate position, '*OK*' was selected on the prompt and then the macro prompts the user to draw a line to measure maximal tibial plateau width. The line was placed at the widest point beneath the tibial plateau, ensuring that any tibial osteophytes were not included in the measurement (Figure 22). After the line was placed, '*OK*' was selected and the macro prompts the user to pan to the left side and repeat the measurements.

Figure 21: Measurement of mJSW using the custom-designed ImageJ macro.

Figure 22: Measurement of maximal tibial plateau width using the custom-designed ImageJ macro.

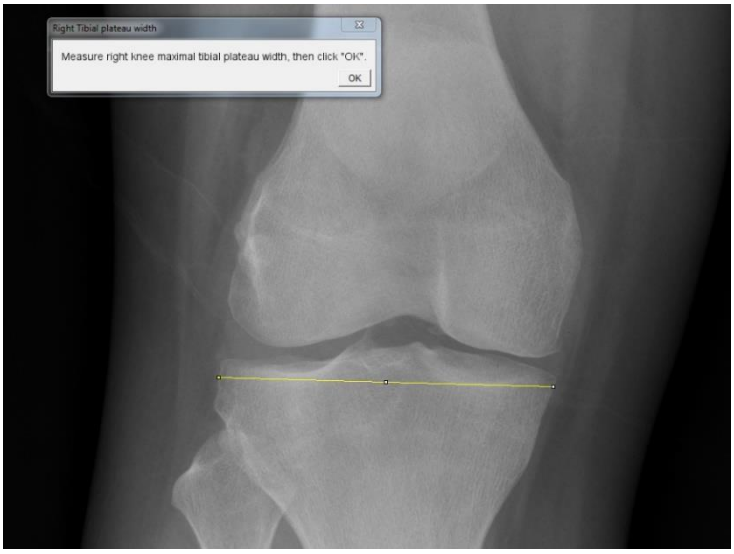

4.4.6. Reliability of full radiographic knee OA readings

Readings of the full HBM set of knees (pooled and anonymised baseline and follow-up radiographs) were performed in December 2018. After grading all available radiographs, a random sample of 18 individuals (10%) were selected using the Stata '*runiform*()' command. To limit possible bias from unblinding, this was carried out by Dr Celia Gregson. Dr Gregson then copied the baseline and follow-up radiographs for the 18 individuals (36 paired knees) to a separate

folder, where I could regrade the images, blind to whether they were baseline or follow-up images. Intra-rater statistics for prevalent OA variables for all 36 pairs, regardless of baseline or follow-up status, are presented in Appendix 9.

The intra-rater reliability was relatively weak for JSN, particularly before weighting (0.42 for medial, 0.24 for lateral). This meant that overall KL grades were also less reliable (0.54), as a knee received a KL grade of 3 only if JSN was present. I identified that the reason for the lower reliability of the JSN grades was that a lot of the knee radiographs were marginally rotated, but not enough to be categorised as grossly rotated and excluded from analyses. However, rotation of the knee can make the joint space appear narrowed. It became clear as I graded the radiographs that I had to be more cautious grading JSN on the rotated radiographs. This meant the later gradings, including the second gradings, were more reliable in terms of JSN compared to the first readings, particularly over the first few days of grading. I therefore repeated the grading of the 10% sample to determine if the lack of reliability for the JSN scores was due to an improvement of detection of rotation throughout the grading process. Intra-rater reliability statistics for the second and third readings are presented in Appendix 10. Kappa scores had increased for all semi-quantitative variables, including osteophytes, and all weighted kappas were >0.8. Hence, I decided to regrade all radiographs for the semi-quantitative features (reliability was already >0.9 for the continuous measures, so to save time these were not repeated). After the full regrading, the 72 radiographs were regraded to check for drift and the final intra-rater reliability statistics are presented in Table 6. Inter-rater reliability was then checked using the readings from the full set of regradings and Dr Hardcastle's readings and reliability statistics are presented in Table 6.

Table 6: Final intra- and inter-rater reliability statistics for knee radiographic gradings.

		Intra-rater				Inter-rater			
	N	**Unweighted**		**Weighted**		**Unweighted**		**Weighted**	
		Kappa	**95% CI**	**Kappa**	**95% CI**	**Kappa**	**95% CI**	**Kappa**	**95% CI**
KL	69	0.731	0.597, 0.860	0.900	0.813, 0.950	0.549	0.399, 0.692	0.847	0.758, 0.914
Medial femoral osteophyte	69	0.755	0.504, 0.943	0.929	0.826, 0.978	0.416	0.205, 0.649	0.830	0.674, 0.922
Medial tibial osteophyte	69	0.765	0.587, 0.907	0.875	0.745, 0.956	0.609	0.448, 0.780	0.860	0.777, 0.919
Lateral femoral osteophyte	69	0.681	0.404, 0.898	0.880	0.693, 0.983	0.697	0.471, 0.911	0.914	0.793, 0.971
Lateral tibial osteophyte	69	0.802	0.571, 1	0.853	0.714, 1	0.677	0.421, 0.875	0.836	0.662, 0.935
Medial JSN	69	0.935	0.710, 1	0.975	0.848, 1	0.440	0.224, 0.655	0.668	0.427, 0.836
Lateral JSN	69	1	1, 1	1	1, 1	0.486	0,1	0.691	0,1
Medial sclerosis	69	0.378	-0.176, 0.932			0.378	-0.176, 0.932		
Lateral sclerosis	69	1	1, 1			0.660	0.038, 1		
Chondrocalcinosis	69	0.881	0.652, 1			0.704	0.387, 1		
Any OA (>=2)	69	0.795	0.641, 0.950			0.774	0.616, 0.932		
Severe OA (>=3)	69	0.872	0.7,1			0.799	0.613, 0.986		
Any osteophyte (>=1)	69	0.795	0.641, 0.950			0.842	0.710, 0.975		
Moderate osteophyte (>=2)	69	1	1, 1			0.722	0.497, 0.947		
Any JSN (>=1)	69	0.939	0.821, 1			0.532	0.319, 0.744		
Moderate JSN (>=2)	69	1	1, 1			0.706	0.394, 1		
Any sclerosis	69	0.549	0.096, 1			0.469	0.027, 0.911		
		ICC	**95% CI**			**ICC**	**95% CI**		
mJSW	139	0.995	0.993, 0.998			0.990	0.985, 0.995		
Maximum tibial plateau width	139	1	1.000, 1.000			1	0.999, 1		

Weighted kappas for *intra-rater* reliability for the semi-quantitative measures were all >0.8, representing almost perfect agreement (333). Unweighted kappas for the binary variables were all >0.795, except for subchondral sclerosis, possibly explained by the fact that this was such a rare finding, with only one case of lateral sclerosis and four cases of medial sclerosis observed. Apart from lateral JSN, weighted *inter-rater* kappas were >0.8. Most of the binary variables had kappas >0.6, representing substantial agreement (333). Again, kappas were low for subchondral sclerosis (particularly medial), representing only moderate (any subchondral sclerosis) or fair (medial sclerosis) agreement. Inter-rater reliability for any JSN was much lower than that for intra-rater reliability, reflecting an undercalling by myself. However, after discussion with Dr Hardcastle, this was deemed acceptable as I was consistent in my gradings of JSN and therefore undercalling JSN at both baseline and follow-up would not systematically bias results.

As the quantitative measurements had been performed using the same methodology by Dr Hardcastle during her analysis of the full set of baseline knee radiographs, I determined the correlation between my full set of measurements on the baseline radiographs and Dr Hardcastle's readings from 2014. There was a strong correlation between my measurements and those performed by Dr Hardcastle (r>0.8, Appendix 11), particularly for maximal tibial plateau width. Bland Altman plots confirmed good agreement between these measurements (Appendix 11). Reassuringly, mJSW measurements decreased with increasing semi-quantitative JSN grade, as assessed by the OARSI atlas at both baseline and follow-up (Figure 23, Figure 24) and there was a greater decrease in mJSW between baseline and follow-up with those with a greater change in semi-quantitative grades (Figure 25).

Figure 23: Boxplot of semi-quantitative medial JSN grade at baseline against measured medial mJSW at baseline.

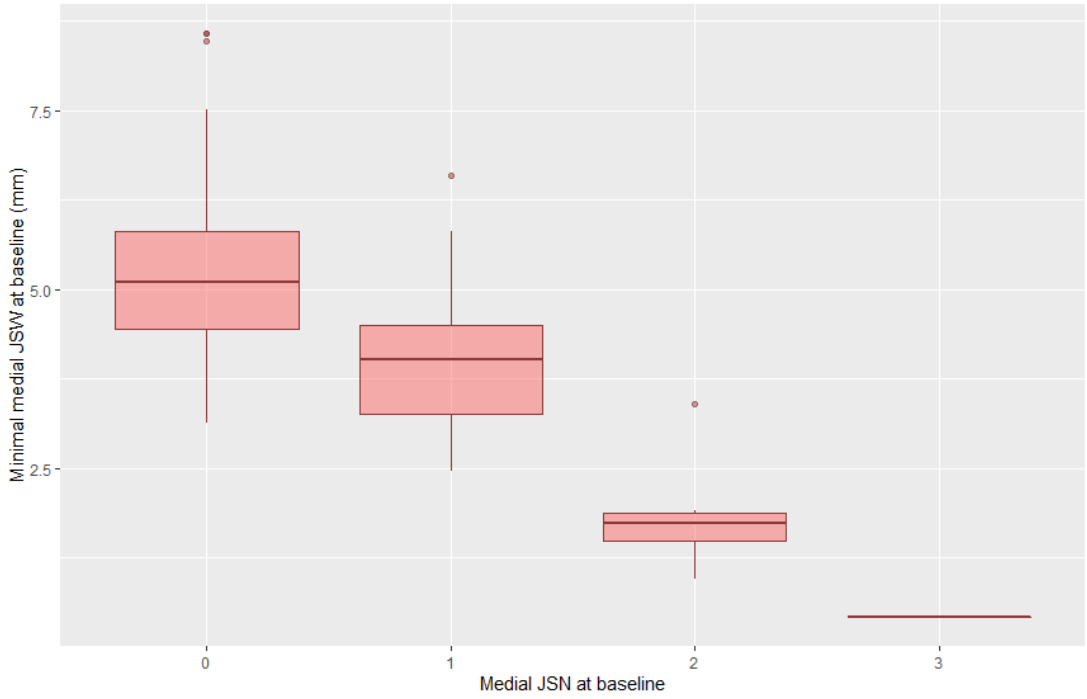

Figure 24: Boxplot of semi-quantitative medial JSN grade at follow-up against measured medial mJSW at follow-up.

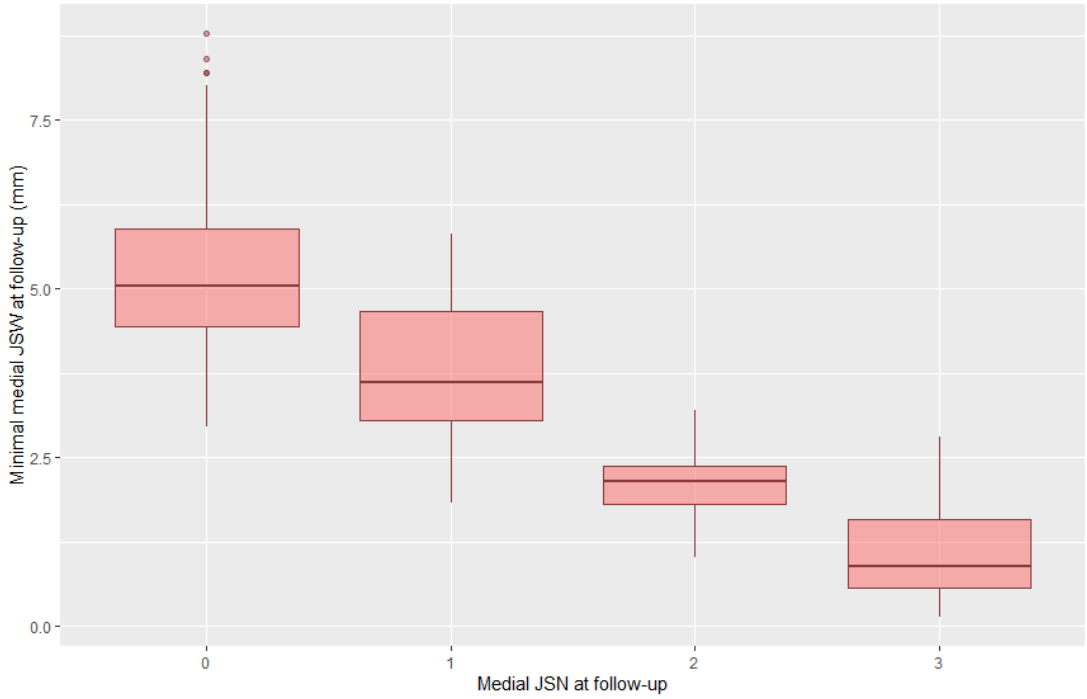

Figure 25: Boxplot of change in summed semi-quantitative JSN score (medial and lateral) against change in measured medial mJSW.

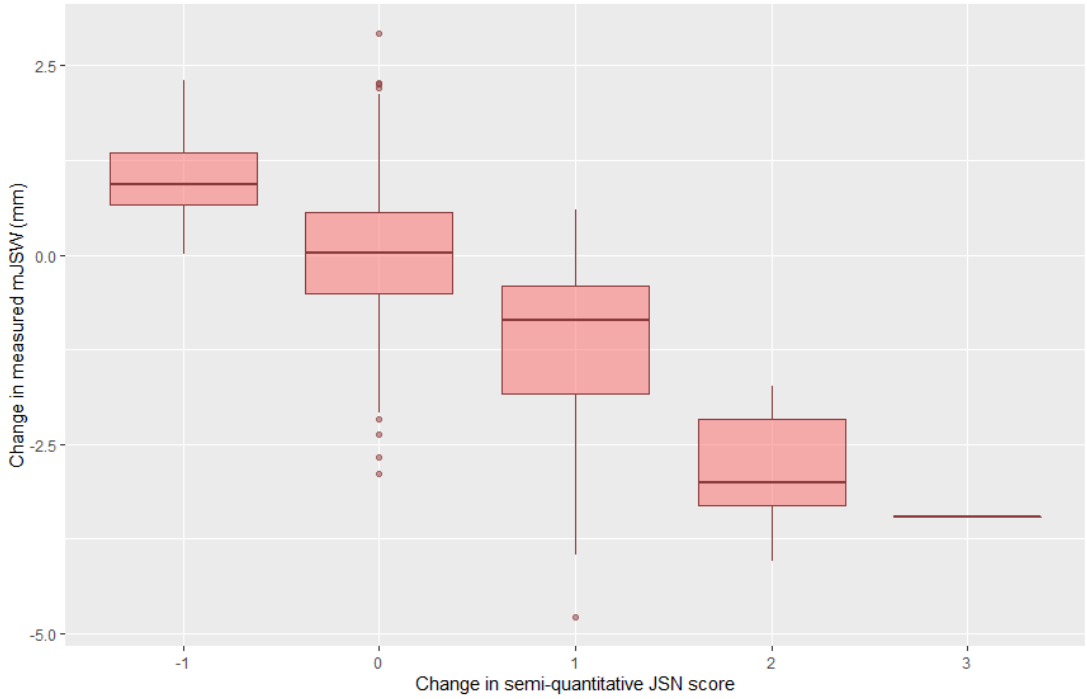

As maximum tibial plateau width is less likely to change over 8 years, I checked agreement between maximum tibial plateau width measured at baseline and follow-up, as a further test of the reliability of the continuous measurements (Appendix 11). Overall, there was a strong correlation between these two variables (r=0.92).

As a final check of the validity of the radiographic sub-phenotype measures, associations between change in summed osteophyte and JSN scores and outcomes expected to be associated with OA progression were determined. This included use of a walking aid and WOMAC pain, stiffness, and functional limitation scores (section 4.2.1). Table 7 displays these associations. Both change in osteophytes and change in JSN were associated with a higher pain score at follow-up. Change in osteophyte score was also associated with more stiffness and functional limitation and there was some evidence for an association between change in JSN score and these outcomes (greater magnitude of effect but wider CIs). No evidence for an association with mobility aid use at follow-up was observed.

Table 7: Associations between change in osteophytes or JSN over 8 years and clinical OA outcomes at follow-up.

	Change in osteophyte score		**Change in JSN grade**	
	OR (95% CI)	**P**	**OR (95% CI)**	**P**
Use of walking aid	1.00 (1.00, 1.00)	0.604	1.00 (1.00, 1.00)	0.307
	β (95% CI)	**P**	**β (95% CI)**	**P**
WOMAC knee pain score	0.39 (0.17, 0.62)	$7.31x10^{-4}$	1.08 (0.05, 2.10)	0.039
WOMAC knee stiffness score	0.48 (0.18, 0.77)	0.002	0.57 (-0.35, 1.49)	0.227
WOMAC knee function score	0.39 (0.16, 0.61)	$7.28x10^{-4}$	0.65 (-0.30, 1.60)	0.178

OR per 1 grade increase in osteophyte or JSN score between baseline and follow-up. β represents the increase in WOMAC score (out of 100) per 1 grade increase in osteophyte or JSN score between baseline and follow-up.

4.4.7. Training to grade radiographic hip OA using the OARSI atlas

Training to grade radiographic features of hip OA followed the same structure as grading knee OA. However, hip radiographs were more difficult to read, particularly when determining JSN, and therefore five 90-minute training sessions were required before grading the training set. Croft scores, rather than KL grades, were used as an overall measurement of OA severity. The advantage of determining Croft score over KL grade at the hip is the additional level to reflect JSN without osteophytes (334).

Measurement of hip mJSW

Hip mJSW was assessed at baseline using HipMorf software (Oxford, UK) (226). However, as access to this software was no longer available, I investigated other options for measuring mJSW. The AUGMENT study uses the software BoneFinder, developed by Claudia Lindner and Tim Cootes at the University of Manchester (http://bone-finder.com/, patent number EP 2893491) to place points around the outline of the hip on a radiograph or DXA image. Points can also be placed along the acetabular eyebrow. Dr Jon Parkinson, University of Manchester, designed a python script to generate a curve from the points around

the femoral head and along the acetabular eyebrow and then calculate the shortest distance between these two curves. Due to time constraints and expertise, points were placed on all baseline and follow-up images by Dr Monika Frysz, University of Bristol. I then placed points on a subset of 36 pairs of hips, which were remarked by Dr Frysz, to calculate inter-rater and intra-rater reliability, respectively. Points were placed starting at the superior lateral curvature of the femoral head (Figure 26). 15 additional points were then placed, evenly spaced, around the femoral head, ending at the superior medial curvature of the femoral head (Figure 27).

Figure 26: The first point was placed at the superior lateral curvature of the femoral head in BoneFinder.

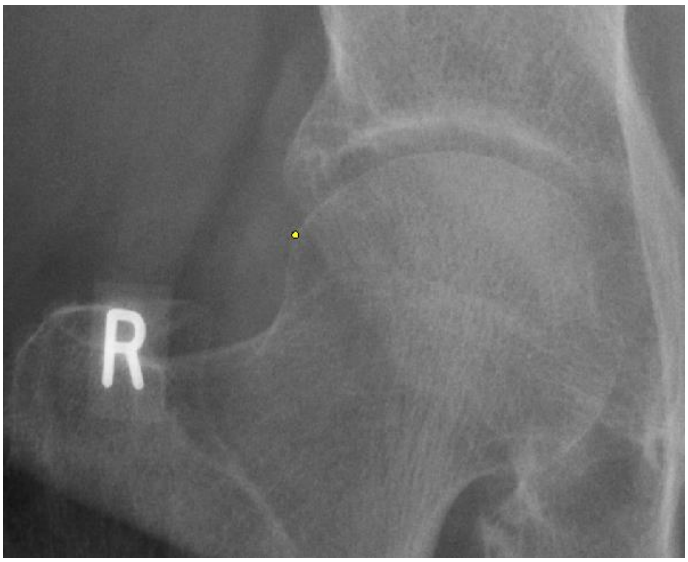

Figure 27: 15 Additional points placed evenly spaced around the femoral head ending at the superior medial curvature.

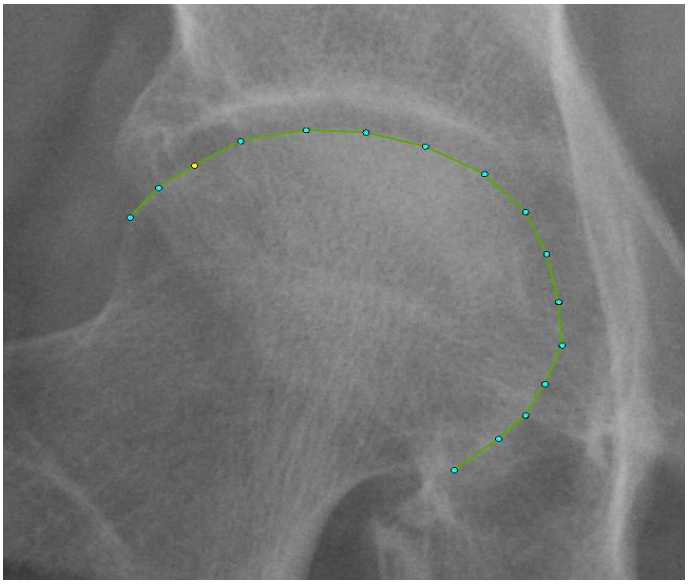

A point was then placed at the lateral edge of the acetabular eyebrow, ignoring any osteophytes, if present. The point was placed at the lowest edge at the most lateral point of the sclerotic line, as displayed in Figure 28. An additional seven points were then placed along the acetabular eyebrow, ending where there was a break in the line or a change in thickness or angle (Figure 29). The protocol for point placement is provided in Appendix 12.

Figure 28: Placement of the first acetabular point in BoneFinder.

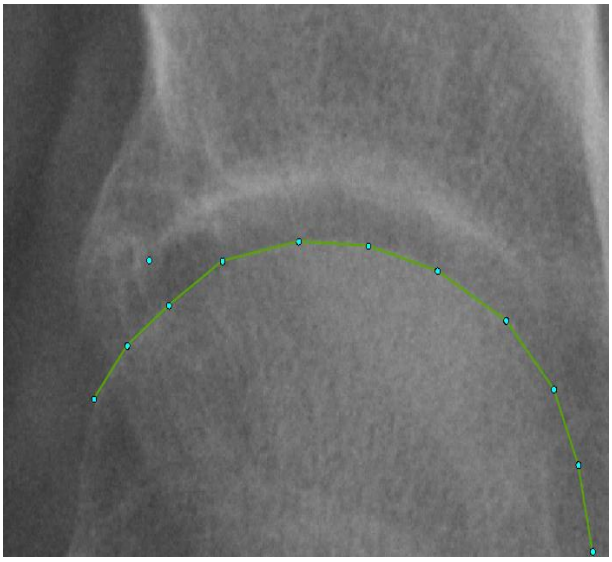

Figure 29: Placement of the additional seven points along the acetabular eyebrow in BoneFinder.

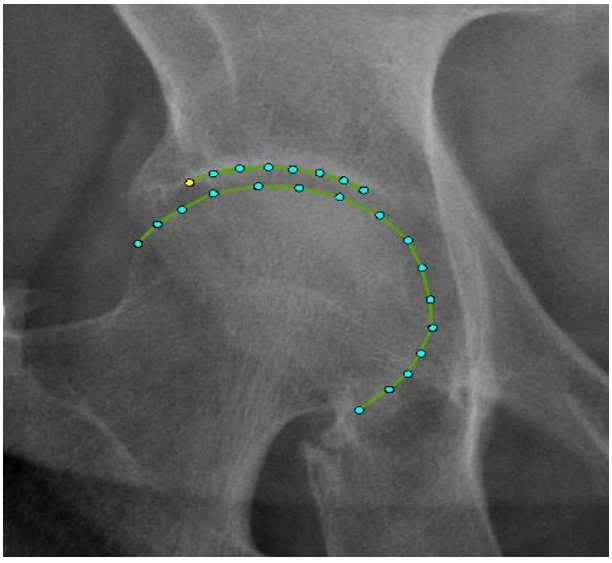

Once all points had been placed on all images, I ran a python script for all points files to generate the measurement of mJSW. The python script extracted pixel spacing from the DICOM image file, so that a measurement in mm was generated, rather than in pixels (for all non-compressed images). The script generated an image of the outline of the femoral head and the acetabulum, showing the point at which mJSW was measured (Figure 30).

Figure 30: Figure generated by the python script showing the point on the curves where mJSW was measured (the narrowest point between the two curves).

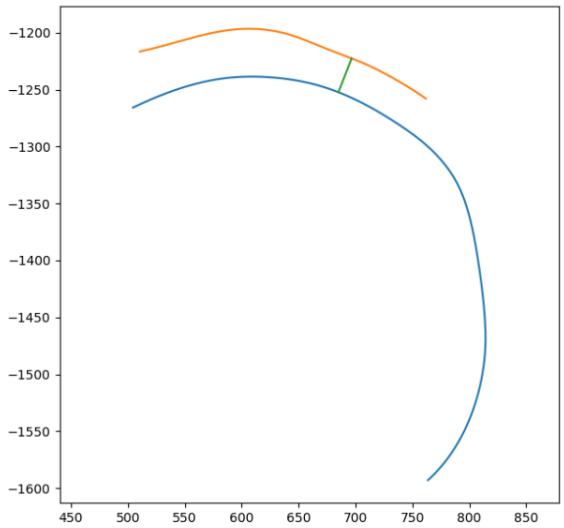

The intra-rater ICC of the mJSW measurements was 0.73 (0.58,0.83) and the inter-rater ICC was 0.68 (0.53,0.82). Baseline measures of mJSW using BoneFinder were compared to Dr Hardcastle's previous baseline measurements from HipMorf (Appendix 13). There was a strong correlation between the BoneFinder and HipMorf measurements (r=0.8) but the ICC was lower (0.35 [0.23,0.46]). It appeared that the BoneFinder method was generally overestimating the value of mJSW compared to HipMorf. However, I was interested in the change between baseline and follow-up rather than the absolute values, I decided to use the measurements of mJSW provided by the Bone Finder method. The BoneFinder measurements, reassuringly, seemed to correlate with the semi-quantitative measurements of hip JSN (
Figure 31-Figure 33) and the Bland-Altman did not identify systematic bias (no systematic increase in difference with increasing or decreasing measurements, Appendix 14).

Figure 31: Relationship between superior JSN grade determined by the OARSI atlas (x) and mJSW measurements determined by BoneFinder (y) at baseline .

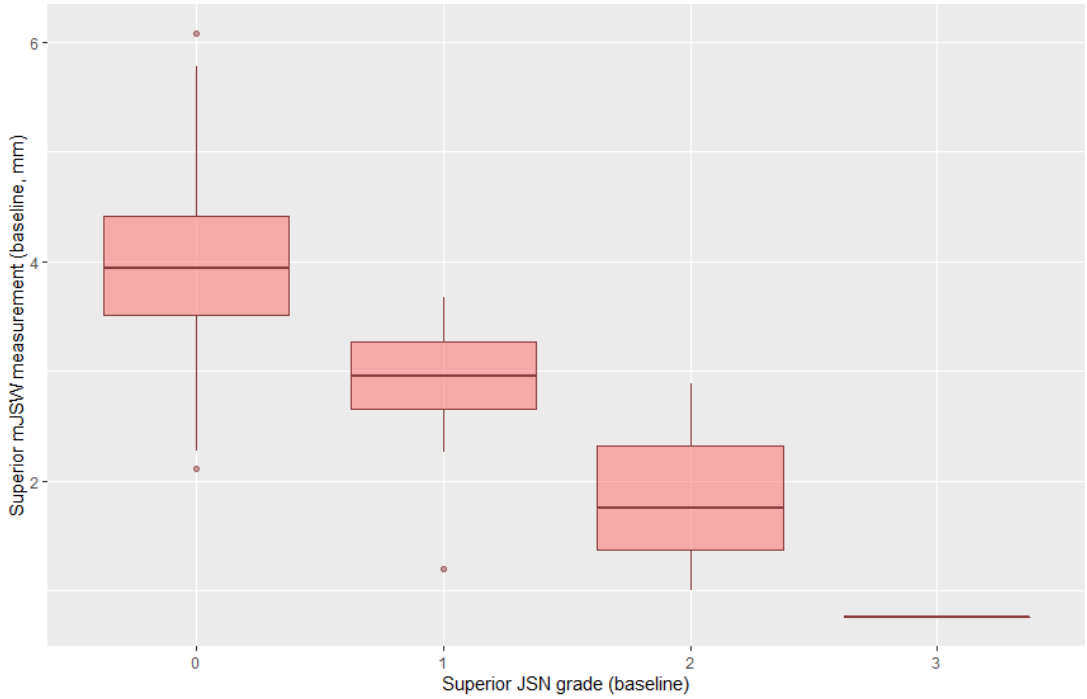

Figure 32: Relationship between superior JSN grade determined by the OARSI atlas (x) and mJSW measurements determined by BoneFinder (y) at follow-up.

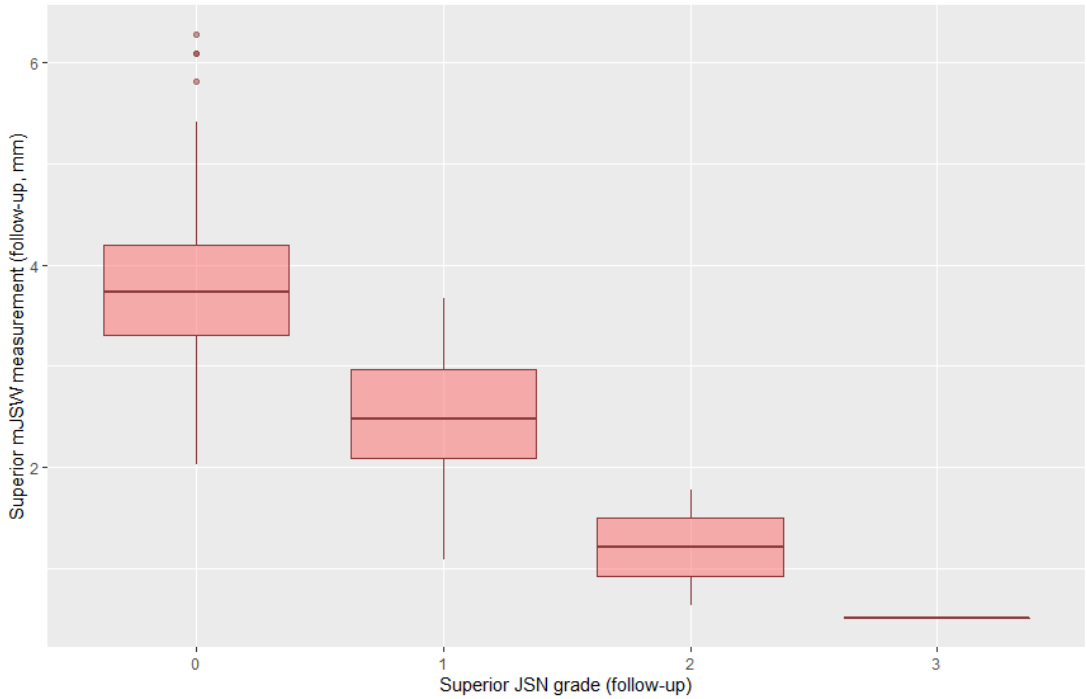

Figure 33: Relationship between change in overall hip JSN grade determined by the OARSI atlas (x) and change in mJSW measurement determined by BoneFinder (y).

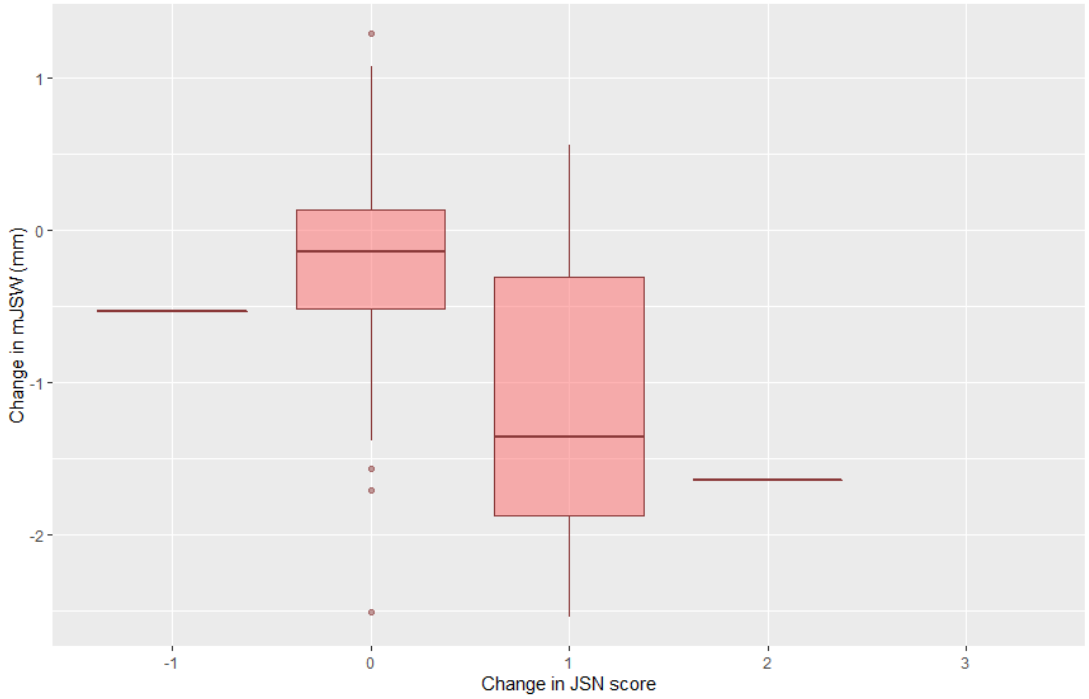

4.4.8. Reliability of hip radiographic gradings

Hip radiograph readings of the full HBM set (pooled and anonymised baseline and follow-up radiographs) were performed in October 2019. After grading all available radiographs, each study ID was imported into Stata with their baseline and follow-up anonymous filename. A random sample of 18 individuals (10%) were selected. Intra- and inter-rater statistics for prevalent OA variables for all hips, regardless of baseline or follow-up status, are presented in Table 8. Both intra- and inter-rater reliability statistics were lower for hips than seen for knees and were particularly low for JSN. JSN was rare in the set of radiographs regraded and where it was present, it was mild, with no hips scoring above grade one. Osteophyte severity were generally less severe than seen at the knees. All intra-rater kappas and all inter-rater kappas, except inferior acetabular osteophytes and superior JSN, represented moderate to substantial agreement based on the thresholds of Landis and Koch (333). As agreement was much better

for the training set (Appendix 15), which represented a range of OA severities, it was agreed that the full set of readings were acceptable to use for analyses.

Table 8: Intra- and inter-rater reliability statistics from grading the full set of HBM hips.

		Intra-rater				Inter-rater			
	N	**Unweighted**		**Weighted**		**Unweighted**		**Weighted**	
Croft score	69	0.611	0.404, 0.772	0.744	0.421, 0.940	0.498	0.305, 0.705	0.627	0.344, 0.836
Superior acetabular osteophytes	69	0.588	0.347, 0.791	0.704	0.338, 0.891	0.528	0.325, 0.802	0.607	0.175, 0.800
Superior femoral osteophytes	69	0.738	-0.018, 1	0.849	0, 1	0.575	0, 0.847	0.733	-0.015, 1
Inferior femoral osteophytes	69	0.883	0.646, 1	0.961	0.793, 1	0.518	0.211, 0.825	0.766	0.422, 0.950
Inferior acetabular osteophytes	69	0.489	-0.111, 1			0.378	-0.176, 0.932		
Medial JSN	69	0.660	0, 1			0.477	0, 0.849		
Superior JSN	69	0.489	0, 1			0.386	0, 1		
Acetabular sclerosis	69	none seen				none seen			
Femoral sclerosis	69	1	1, 1			0*			
Subchondral cysts	69	none seen				0*			
Croft $\geq$3	69	0.793	0.398, 1			0.850	0.561, 1		
Any osteophyte	69	0.688	0.488, 0.888			0.612	0.410, 0.814		
Any JSN	69	0.549	0.096, 1			0.465	0.120, 0.811		

**Observed by SH but not AH.*

As seen at the knee, change in summed osteophyte score was strongly associated with subsequent increased pain, stiffness, and functional limitations (Table 9). Change in JSN score was associated with subsequent WOMAC scores, with a larger magnitude of effect, although CIs were much wider and overlapped the null for hip pain, reflecting the lower variability in change in JSN score (scored out of six *vs* 10 for osteophytes).

Table 9: Associations between change in hip osteophytes or JSN and clinical OA outcomes at follow-up.

	Change in osteophyte score		**Change in JSN grade**	
	OR (95% CI)	***p***	**OR (95% CI)**	***p***
Use of walking aid at follow-up	1.07 (0.74, 1.56)	0.711	1.73 (0.71, 4.22)	0.225
	β (95% CI)	***p***	**β (95% CI)**	*p*
WOMAC hip pain score	2.90 (0.31, 5.48)	0.028	10.0 (-1.97, 22.0)	0.101
WOMAC hip stiffness score	3.13 (0.35, 5.90)	0.027	12.5 (3.45, 21.6)	0.007
WOMAC hip function score	3.23 (0.62, 5.84)	0.015	14.6 (5.64, 23.6)	0.001

OR per 1 grade increase in summed osteophyte or JSN score. β represents the increase in WOMAC score per grade increase. From person-level analyses of 125 individuals, accounting for family-level clustering.

CHAPTER 5. METHODS: DATA ANALYSIS

5.1. Statistical methods

Prior to commencing all analyses presented in this thesis, I generate an analysis plan detailing the variables and methods for analysis and any planned sensitivity analyses. I generated a list of potential confounders from literature searches. The analysis plan was then circulated to my supervisors and collaborators and the plan was refined based on their comments, including suggestions of additional covariates to analyse.

5.1.1. Descriptive statistics

I tabulated all categorical variables prior to analysis to determine variables were coded correctly (*e.g.* to check coding of missing values). Descriptive statistics comparing categorical variables, between those with and without data or between HBM cases and relatives without HBM, were generated as the number and percentage for each category and using χ^2 tests to test between category differences in proportions. I visually inspected all continuous variables using histograms, to determine normality and to detect outliers. I calculated descriptive statistics for normally distributed variables as the mean and SD. Differences in means between HBM cases and relatives were determined using T-tests, or ANOVA for more than two categories. For non-normal variables, I calculated the median and interquartile range (IQR), and differences between groups using non-parametric Mann-Witney U-tests.

5.1.2. Regression analyses

I generated estimates of the effect of binary or continuous exposures on continuous outcomes by linear regression, using multivariable analyses to adjust for potential confounding variables. When analysing binary exposures, the effect sizes generated were differences in the mean outcome between the reference and the alternative category. For continuous exposures, effect sizes were the unit increase in outcome per unit increase in the exposure. Generally, exposure variables were standardized, and units were SDs. Ninety-five percent confidence

intervals (CIs) were calculated for effect estimates, as 1.96 standard errors (SEs) above and below the effect estimate. I analysed binary outcomes using logistic regression, adjusting for potential confounders. Estimates of ORs for binary exposures represent the OR in the alternative compared to the reference category and, for continuous exposures, the OR per unit change in the exposure. Analyses were restricted to those with complete data for all confounders.

Dealing with skewed outcomes

The main continuous outcomes analysed, namely the WOMAC scores and changes in semi-quantitative sub-phenotype grades, were highly positively skewed with many participants having a score of zero (see Chapter 6,Chapter 7). I checked for the most appropriate transformation for each variable using the Stata '*gladder*' command, however many of the continuous variables were heavily zero-skewed and therefore none of the transformations normalized the data. I therefore included the Stata '*robust*' option to generate heteroskedasticity-robust (Huber-White) SEs (335,336).

There was also the possibility of a ceiling effect for some of the outcomes analysed, as WOMAC scores had a limit of 100 (representing the maximum pain/stiffness or limitation of function) and the progression variables had a maximum value of 12 for osteophytes and six for JSN. Tobit regression modelling is an alternative to least-squares regression, which models the outcome as a latent variable and estimates the line beyond the limit of the measurement (337,338). However, tobit models assume that there would be a normal distribution should values have been observed beyond the limit of measurement (339). Tobit modelling is more sensitive to violations of assumptions of homoskedasticity and normally distributed residuals (339). In ordinary least-squares, if assumptions are not met, the SE will be underestimated, leading to CIs that are too narrow. However, in tobit regression, both the beta and SE will be biased by violations of the assumptions (339). I therefore decided to use least-squares linear regression.

Accounting for clustering

To increase sample size and statistical power, all available knees/hips were analysed. That meant that an individual could contribute up to two knees or hips to an analysis. As two knees/hips from the same individual are likely to be more correlated in terms of OA severity and covariates than two knees/hips from different individuals, they are not independent observations, and I needed to account for this 'clustering' in my analyses. Additionally, as non-index cases and controls from the HBM study population were recruited through, and were relatives or spouses of, HBM index cases, there was a need to account for family-level clustering in analyses. OA severity is likely to be more strongly correlated within a family compared to between different families. Individuals from the same family are more likely to share genetic variants that may be associated with HBM or OA, and OA risk factors such as a high BMI (section 1.2.5), than individuals from different families. I selected generalized estimating equation (GEE) models as the most appropriate analyses for clustered data as these are more suitable for binary and skewed outcomes, compared to other methods such as random effects models (330). GEE does not explicitly model clustering in the data to generate an effect estimate for a particular individual, but instead generates an estimate of the average effect for a population (330). SEs are adjusted for clustering. The correlation between observations in a cluster is specified; I used an exchangeable correlation structure as this structure assumes the correlation is the same between all pairs in a cluster (330). In the case of joint-level analysis, this assumption is correct as there are only two observations in a cluster.

I performed all GEE analyses twice: once using all knees/hips and accounting for within-individual correlation and once using the most severely affected knee/hip per individual or the sum of radiographic sub-phenotype severity across both joints (person-level) and accounting for correlation within families. More complex statistical models are available to model the within- and between-individual, as well as within- and between-family, variance in the same model

(*i.e.* three-level multilevel mixed effects models) (340). However, these models are more computationally intensive and complicated to interpret. As I was interested in the overall effect of HBM on OA outcomes, rather than how effects differ between individuals or between families, I used the more straightforward GEE models.

All statistical analyses were performed in Stata version 13/15 (StataCorp, USA) or R version 3.5.1.

5.2. Cohorts

Although analysing the HBM study population represents a novel way to determine observational associations between high BMD and OA progression, the HBM population is relatively small and therefore unsuitable for genetic analyses. Larger populations were therefore studied for genetic analyses. A summary of the contribution of data from each cohort is presented in Table 10. The additional general populations included in this work are described below.

Table 10: Summary of cohorts contributing individual-level data to analyses presented in this thesis.

Cohort	Primary data collection	PI and collaborators	My role	Analysis	Chapters
HBM	Yes, collected by me: see Chapter 4	CI: Prof. Jon Tobias Study co-ordinator: Dr Celia Gregson PIs: Dr Ashok Bhalla, Prof. Kassim Javaid, Dr Katie Moss, Dr Mo Aye, Prof. Eugene McCloskey, Dr Kenneth Poole Collaborators: Mrs Karen Ireland, Dr Sarah Hardcastle, Dr Martin Williams, Ms Maxine Osgerby, Ms Karen Blesic, Dr Margaret Paggiosi, Dr Jacqueline Shipley, Prof. Bill Fraser, Dr Jonathan Tang	Application to REC for ethics approval Questionnaire design Co-ordination of data collection Data management Grading of radiographic OA Data analysis	The association between HBM and knee and hip OA progression Metabolomics of BMD, bone turnover and OA sub-phenotypes The association between plasma sclerostin and radiographic OA sub-phenotypes	6,7,8,10
UK Biobank	No	PI: Dr Celia Gregson Collaborators: Dr Monika Frysz, Dr Benjamin Elsworth, Dr Eleanor Sanderson	Data analysis	Bidirectional/ multivariable MR of causal pathways between BMD/BMI/OA Quantifying the contribution of bone pathways to BMD and OA risk The causal effect of serum IGF-1 on OA risk	9,10,11
The Rotterdam Study	No	PI: Prof. André Uitterlinden Collaborator: Prof. Joyce van Meurs, Dr Cindy Boer, Prof. Fernando Rivadneira, Dr Katerina Trajanoska	Data analysis	Replication of metabolomics of BMD and OA sub-phenotypes The association between eBMD PRS and radiographic OA sub-phenotypes Quantifying the contribution of bone pathways to radiographic OA sub-phenotypes	8,10,11
ALSPAC	No	PI: Prof. Nic Timpson, Prof. Deborah Lawlor	Data analysis	Replication of the relationship between bone resorption and plasma citrate	8

Abbreviations: PI: Principal Investigator; CI: Chief Investigator.

5.2.1. UK Biobank

UK Biobank recruited over 500,000 individuals across the UK, aged 38-73, between 2006 and 2010 (341), to generate a health resource with the aim of "*improving the prevention, diagnosis and treatment of a wide range of serious and life-threatening illnesses*" (342). Participants were selected from a range of locations across the UK to cover the socioeconomic, ethnic and landscape heterogeneity (341). Access to data can be applied for by any researcher registered with UK Biobank; application is submitted via the UK Biobank website (https://www.ukbiobank.ac.uk/). UK Biobank received REC ethical approval (REC reference: 11/NW/0382) and electronic signed consent was provided by all participants. Participants attended one of 22 research centres across the UK for baseline data collection. At the assessment centre, participants filled in touch-screen questionnaires and completed computer-assisted interviews to collect data including lifestyle factors, health status and sociodemographic factors (341,343). Physical and functional measurements were performed, including measurement of height and weight and BMD at the heel using ultrasound (341). Blood samples were collected at the baseline assessment, which have been used for genotyping (section 5.3.1) and biomarker assays (section 11.2.2).

The UK Biobank population contributed to analyses to determine the BMI-independent causal effect of BMD on OA (Chapter 9), analyses to determine the contribution of bone pathways in OA pathogenesis (Chapter 10) and analyses of the causal effect of serum IGF-1 on OA risk (Chapter 11). Analyses were performed under application number 17295, using data released in April 2019.

5.2.2. The Rotterdam study

RS is a prospective cohort of 14,926 individuals aged 45 and above residing in the city of Rotterdam, the Netherlands (344). The aim of the study was to determine risk factors for diseases in the elderly. The total cohort is split into four sub-

cohorts, recruited at different times and with varying levels of follow-up (Figure 34). The first cohort (RS1) included 7,983 adults, aged 55-106, from the Ommoord district, recruited 1989-1993 (344,345). This cohort has been followed up up to five times. In 2000-2001, 3,011 additional individuals from the region who had reached the age of 55 years, or who were aged over 55 and had moved to the district, were recruited as the RS2 cohort. A total of four assessment cycles have been performed for RS2. The RS3 cohort included 3,932 individuals aged 45-54 years from Ommoord, recruited from 2006-2008. This cohort has been followed up once. Recruitment of RS4 began in 2016, recruiting individuals aged 40+ years from Ommoord (344). Ethical approval has been provided by the Erasmus Medical Centre Medical Ethics Committee and the Netherlands Ministry of Health, Welfare and Sports (344). At baseline, a home-based interview and a clinic-based assessment were performed, which included imaging (including DXA and X-rays) and collection of blood samples for biomarker assessment and genotyping.

The Rotterdam data was used to replicate the metabolomics analysis of BMD and OA sub-phenotypes (Chapter 8), to determine the association between BMD PRS and OA sub-phenotypes (Chapter 9) and to determine the contribution of bone pathways to variation in OA sub-phenotypes (Chapter 10).

Figure 34: Diagram of the design and data collection of the Rotterdam study population.

Reproduced from (344).

5.2.3. ALSPAC

ALSPAC is a cohort of 14,541 pregnancies with an estimated delivery date between April 1991 and December 1992, recruited 1990-1992, from the former Avon area, southwest England (346,347). The women and resulting offspring (N=13,988 alive at one year) have been followed up for almost 30 years with questionnaires and clinical assessment. An additional 456 offspring were recruited at age 7 during recruitment phase two, 262 were recruited between ages 8-18 during recruitment phase three and 195 at ages 19-26 during recruitment phase four (348). Ethical approval has been provided by the ALSPAC ethics and law committee and the local REC. The mothers have been invited to attend four research clinics for a variety of outcome assessment measures (including DXA scans): Focus on Mothers (FOM)1 between December 2008 and July 2011, FOM2 between July 2011 and June 2013, FOM3 between March 2013 and March 2014 and FOM4 between April 2014 and March 2015. All children were invited to assessment clinics at age 7, 8, 9, 10, 11, 12.5, 13.5, 15.5, 17.5 and 24 years.

The ALSPAC data was used to replicate the metabolomics analysis of bone turnover presented in Chapter 8, as BTMs have not been measured in either UK Biobank or RS. Analyses were performed under ALSPAC executive committee-approved proposal B3083.

5.3. Genetic analyses

5.3.1. Genotype data and quality control (QC)

UK Biobank

The genotyping and pre-imputation QC methods for the UK Biobank population are described in full elsewhere (349). A summary of the pre-imputation QC and imputation procedure has been published by Mitchell *et al* (350):

"The UK Biobank full data release contains data on all successfully genotyped samples (n=488,377). 49,979 individuals were genotyped using the UK BiLEVE array and 438,398 the UK Biobank axiom array. Pre-imputation QC, phasing and imputation are described elsewhere (349). In brief, prior to phasing, multiallelic and rare SNPs (MAF≤1%) were removed. Phasing of genotype data was performed using a modified version of the SHAPEIT2 algorithm (349). Genotype imputation to a reference set, combining the UK10K haplotype and HRC reference panels (351), was performed using IMPUTE2 algorithms (352). Analyses were restricted to autosomal variants by graded filtering with varying imputation quality according to allele frequency ranges, rarer genetic variants were required to have a higher imputation info score (info>0.3 for MAF>3%; info>0.6 for MAF 1-3%; info>0.8 for MAF 0.5-1%; info>0.9 for MAF 0.1-0.5%) with MAF and info scores having been recalculated on an in-house derived 'European' subset."

QC filtering of the UK Biobank data was conducted by Mitchell *et al* as previously described (350):

"Individuals with mismatches between genetic and reported sex or individuals with sex chromosome aneuploidy were excluded. The sample was restricted to individuals of European ancestry as defined by an in-house k-means cluster analysis performed using the first 4 principal components (PCs), provided by UK Biobank, in R. The current analysis uses the largest cluster from this analysis. Estimated kinship coefficients, using the KING toolset (353), identified pairs of related individuals (349). An inhouse algorithm preferentially removed individuals related to the greatest number of other individuals, until no related pairs remained."

12,321,875 SNPs and 463,005 individuals passed QC and were included in the final dataset.

The Rotterdam study

Genotyping of the three RS cohorts was performed at the Genetics laboratory, department of Internal Medicine, Erasmus Medical College. The RS1 and RS2 cohorts were genotyped using the Illumina HumanHap 550kv3 chip and the RS3 cohort was genotyped using the Illumina HumanHap 610-Quad V1 chip. SNPs with a call rate <98% (*i.e.* SNPs missing in >2% of individuals), with a MAF <1%

or a Hardy-Weinberg *p*-value $<10^{-6}$ were excluded, leaving 512,349, 455,389 and 517,658 SNPs in RS1, 2 and 3, respectively (146,354). Duplicates and first/second-degree relatives were identified using identical by state (IBS) probabilities greater than 97% in PLINK (146,354) and these individuals were excluded. Ethnic outliers were identified using an IBS distance >3SD and excluded. Individuals with sex mismatches with typed X-linked markers or excess autosomal heterozygosity were excluded. Additional genotypes were imputed using the Haplotype Reference Consortium (HRC)v1.1 reference panel and '*minimac3'*. Genotypes of 39,117,478 SNPs were available for 6,291 individuals in RS1, 2,157 individuals in RS2 and 3,048 individuals in RS3. Additional analysis-specific post-imputation QC steps are described in Chapter 9 and Chapter 10.

5.3.2. GWAS

GWAS has been developed as a hypothesis-free scan of millions of genetic variants across the genome, with the aim of identifying common genetic variants robustly associated with a disease/phenotype, which may lead to the identification of novel causal genes for the disease/phenotype in question (355). GWAS tests whether the allele frequency for each genotyped SNP is related to a trait (either binary or quantitative), most commonly using an additive model (*i.e.* assuming a linear relationship with dosage of the effect allele) (355). GWAS of a binary outcome performs millions of individual logistic regression analyses, adjusted for *a priori* confounders, and a GWAS of a quantitative trait performs millions of linear regressions. The assumptions of these analyses are therefore the same as those for a standard linear regression model (*i.e.* homoskedasticity and normality of residuals) (356). In this thesis, I performed GWAS to generate summary statistics for pathway analyses (section 5.3.5) and latent causal variable analyses (LCV, Chapter 9).

Accounting for population stratification

Population stratification can occur because allele frequencies differ between populations with different ancestries. If the disease/trait also varies between

these populations, the allele frequency can appear related to the disease/trait, even if it is not causal (or in linkage disequilibrium [LD] with the causal variant) (356). I performed GWAS in UK Biobank using a linear mixed model (LMM) within the software '*BOLT*' (version 2.3) (357), using the MRC-Integrative Epidemiology Unit pipeline (358). The BOLT-LMM model is advantageous over standard linear regression modelling in that it can account for cryptic relatedness and population stratification and therefore related individuals do not need to be excluded, increasing power (357). The population structure, which is treated as a random effect in the linear mixed model, is modelled from 143,006 genotyped SNPs (selected based on a MAF>0.01, genotyping rate>0.015, Hardy-Weinberg equilibrium (HWE) p-value<10^{-4} and independence based on an r^2 threshold of 0.1, all calculated in PLINKv2.0) (358). The BOLT-LMM model is particularly advantageous in the UK Biobank population as all white Europeans can be included, instead of restricting to white British individuals (358,359). I adjusted for sex and genotyping chip in all GWAS analyses. To ensure population stratification was fully accounted for, I also adjusted for 10 PCs, generated using the software EigenSTRAT (360), which compares the allele frequencies within the study population to HapMap reference populations of different ethnicities (356).

I performed GWAS of the individual radiographic OA sub-phenotypes (binary) in each RS population using the software '*SNPtest*', using an additive model and adjusting for sex and 10 PCs. Post-GWAS QC in RS is described in Chapter 10. I performed GWAS separately for each cohort and then meta-analysed using a fixed-effect inverse-variance weighted meta-analysis in the software '*EasyQC*' (361). I selected a standard logistic model over the linear mixed model in RS as BOLT-LMM is not recommended for sample sizes <5000 (362).

I measured the potential effect of population stratification in each GWAS using the genomic inflation statistic, known as lambda genomic control (λ_{GC}) (363). This statistic measures the ratio of the median test statistic to the median test statistic of a null distribution, with a value of one representing no population stratification (363). A value much greater than one provides evidence for

population stratification. I also generated QQplots of the observed *p*-values against expected *p*-values from a χ^2 distribution (364), to visually inspect for population stratification (deviation of most *p*-values from the χ^2 distribution suggests population stratification), using the R '*qqman*' package (365).

5.3.3. Mendelian randomization

Although every effort was made to collect data on all *a priori* confounders for analyses, there is still the possibility, as in any observational study, that unmeasured confounding or reverse causality may explain any associations observed, rather than a causal effect of BMD on OA.

MR is a form of instrumental variable analysis that has been developed to determine whether a risk factor is causal, using data from large cohorts (366). This methodology is based on the concept of an RCT, the 'gold standard' method for determining a causal relationship (367). In well-designed, unbiased RCTs, patients are randomized to either receive an intervention (*e.g.* a drug) or to the control group (*e.g.* placebo). If successful randomization has occurred, the only difference between the groups should be whether they receive the intervention; all confounding variables should be evenly distributed between groups. The theory of MR is based on Mendel's law of independent segregation of alleles during gamete formation. This leads to a random assortment of alleles in the offspring, which in theory means that the genotype determining a particular exposure of interest should not be associated with confounding variables (except in cases of assortative mating) (368,369). Therefore, if there are genetic variants that are robustly associated with the exposure (*e.g.* from GWAS), these variants can be used as instruments for the exposure of interest, to determine a causal effect of an exposure on an outcome, independent of confounding. Additionally, as alleles are randomly assigned at conception, they will not be influenced by the outcome and therefore reverse causality can be ruled out. If an exposure truly has a causal effect on an outcome, any genetic variant robustly associated with the exposure should be related to the outcome with an effect size proportional to

the SNP-exposure association and the causal effect of the exposure on the outcome (370).

Assumptions of MR

To accurately determine the causal effect using MR, three key assumptions must be met (Figure 35). The first key assumption is that the instrument (genetic variant(s)) is associated with the exposure of interest (IV1). To ensure an instrument meets this assumption, genetic variants are usually taken from the largest possible GWAS for the exposure (any SNP associated with the exposure with genome-wide significance). Although there may be additional variants associated with the phenotype above this stringent *p*-value threshold, the instrument is normally restricted to genome-wide significant SNPs to limit weak instrument bias, which will be described in more detail in the context of one-sample (1S) and two-sample (2S) MR, below. The second assumption is that the instrument(s) is not associated with any confounders of the exposure-outcome relationship (IV2). This assumption can be tested for *measured* confounders by determining the association between the instrument(s) and all *a priori* confounders; instruments can be either the single SNPs or a PRS. The third key assumption of MR is that the instrument is not related to the outcome via a pathway independent of the exposure (IV3). This is known as the exclusion-restriction criteria (371). When an instrument is associated with an outcome through a pathway other than via the exposure it is called horizontal pleiotropy (366,367,371).

Figure 35: Assumptions of MR.

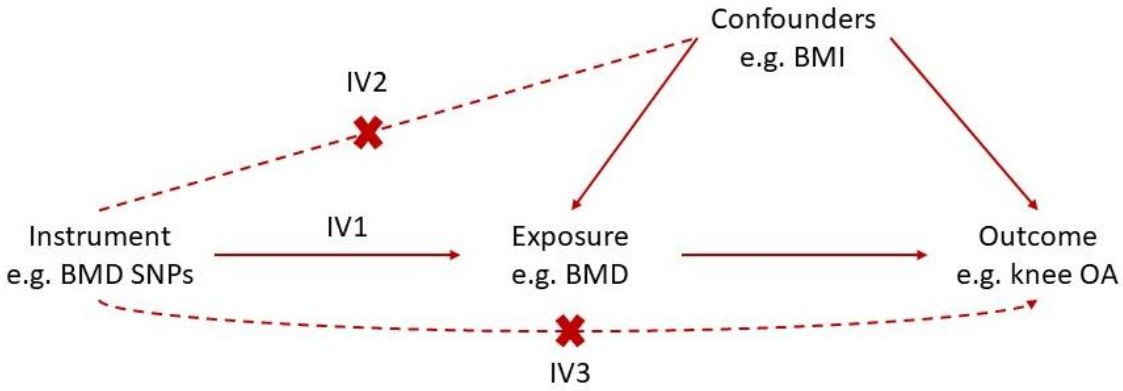

One-sample MR

Where data were available for the exposure and the outcome in the same population (367,369), I performed 1SMR. In 1SMR, the causal effect of the exposure is determined either by a Wald ratio estimator (for a single SNP) or using two-stage least squares (2SLS) regression (367). The Wald ratio estimator is simply the beta of the instrument-outcome association divided by the beta of the instrument-exposure association (367), as displayed in Equation 3.

Equation 3: Calculation of the Wald ratio estimator.

$$\boldsymbol{\beta_{IV}} = \frac{\boldsymbol{\beta_{ZY}}}{\boldsymbol{\beta_{ZX}}}$$

Two-stage least-squares regression was used if multiple instruments were available for the exposure of interest. This was performed in three stages: 1) a regression of the exposure on the instruments was performed; 2) fitted values of the exposure were calculated; 3) the outcome was regressed on the fitted values of the exposure. I performed all analyses using the instrumental-variable regression ('*ivreg*') function of the Applied Econometrics with R package (372) or the Stata '*ivreg2*' package (373).

In 1SMR, I determined the strength of the instrument-exposure relationship using the F-statistic, which is displayed in both the Stata and R output. The F-statistic is calculated from a combination of the sample size, the number of

instruments and the proportion of variation in the exposure explained by the instrument (374). A value of less than 10 was used as evidence for weak instrument bias (367,375). In 1SMR, weak instrument bias would overinflate the estimate, biasing it towards the observational (confounded) estimate (374). I tested the IV2 assumption where data were available for relevant confounders, by determining the association between the instrument(s) and measured confounders using standard regression modelling. However, I was unable to test IV2 for *unmeasured* confounders. I tested IV3, in analyses where I included individual SNPs as instruments, using the Sargan test of overidentification, which determines if the estimates differ between the different instruments (376). If the estimates differ, this is evidence for heterogeneity: *i.e.* pleiotropy (377). 1SMR is still vulnerable to confounding by population stratification. I therefore adjusted for 10 PCs in the 2SLS analysis, along with sex and genotyping chip. 1SMR can be underpowered as analyses are limited to populations with measured exposure, outcome, and genotype data.

Two-sample MR

2SMR has since been developed to make use of publicly available summary statistics from large GWAS collaborations and to allow MR analyses when access to individual-level data is not possible (378,379). For 2SMR analyses, I extracted the summary statistics (effect size, SE, effect allele [EA] and alternative allele [NEA], effect allele frequency [EAF]) for the SNP-exposure and the SNP-outcome associations, for autosomal SNPs associated with the exposure at genome-wide significance, from published GWAS summary statistics. I performed LD-based clumping, using an r^2 threshold of 0.001, with European reference data, so that only the most strongly associated SNP at each locus was retained. Exposure and outcome data were then harmonized to ensure the statistics correspond to the same effect allele. I excluded palindromic alleles with indeterminate allele frequencies *(i.e.* MAF>0.42).

After harmonization, I calculated individual Wald ratios for each SNP and then generated an overall estimate for the causal effect by meta-analysing these Wald

ratio estimates. The meta-analysis was performed using fixed-effects inverse-variance weighted (IVW) meta-analysis, *i.e.* a meta-analysis weighted by the inverse of the SE of the SNP-outcome association (379). I performed all 2SMR analyses in this thesis using the '*TwoSampleMR*' package version 0.4.22 (downloaded from http://www.mrbase.org/) (380).

Numerous methods have been developed to test the IV3 assumption illustrated in Figure 35 and determine if horizontal pleiotropy is biasing results. I used MR-Egger regression to generate an estimate of the causal effect which is not biased by horizontal pleiotropy. Unlike IVW regression, MR-Egger regression can have a value other than 0 for the intercept and this value represents the average effect of the instruments on the outcome not mediated by the exposure (381). Therefore, if this value is not zero, there is evidence that the exclusion-restriction criteria is invalid. The slope from the MR-Egger regression is a pleiotropy-robust estimate of the causal effect of the exposure on the outcome provided the InSIDE assumption holds: the instrument strength does not correlate with the degree of pleiotropy (381). In cases where the exposure is highly correlated with other covariates, this may be violated; for example, when analysing the effect of BMD on OA, the BMD SNPs are likely to be associated with BMI as well. As BMD and BMI are correlated, it is likely that as the strength of the SNP-BMD association increases, so does the strength of the SNP-BMI association. Another limitation of MR-Egger regression is low power (382).

Additional methods have been developed more recently, such as the weighted-median estimator. The IVW estimate is a weighted mean of the Wald ratios for each SNP (379) and is biased if any SNP is an invalid instrument (383). The weighted median estimate, however, is valid as long as at least 50% of SNPs are valid instruments (383). I therefore compared the IVW, weighted median and MR-Egger slope estimates for all analyses to determine if the causal effect estimates are likely to be biased by invalid instruments. If the effect estimates were similar across the three methods, I was more confident that the effect estimate generated was a good, unbiased, approximation of the causal effect of the exposure on the outcome.

Multivariable MR

In analyses where I detected evidence for horizontal pleiotropy, I performed MVMR. MVMR determines the causal effect of one exposure (exp_1) on an outcome when the instrument exerts a pleiotropic effect on another exposure(s) (exp_2) (Figure 36). MVMR requires an additional instrument(s), robustly associated with exp_2. This methodology is particularly useful when trying to determine the causal effect of exp_1 on an outcome when exp_1 and exp_2 are highly correlated traits (377). I performed MVMR in a one-sample setting, by regressing exp_1 on the instrument(s) for both exp_1 and exp_2 and generating predicted values for exp_1 (exp_{1p}). I repeated this process for exp_2, generating exp_{2p}. I then regressed the outcome on exp_{1p} and exp_{2p}, in a multivariable model including potential confounders (sex, genotyping chip and 10 PCs), to give a causal effect estimate for exp_1 on the outcome, independent of exp_2, and vice versa (377). It does not matter if any of the instrument(s) are associated with both exposures, as long as they are associated with at least one exposure. Sanderson-Windmeijer (SW) conditional F-statistics, generated in the Stata '*ivreg2*' output, determined the conditional strength of the instruments, as the instrument must be able to jointly predict both exp_1 and exp_2 (377,384). It should be noted that MVMR can only account for pleiotropy if all pleiotropic variables and their instrument(s) are included in the model.

Figure 36: DAG summarizing the concept of MVMR.

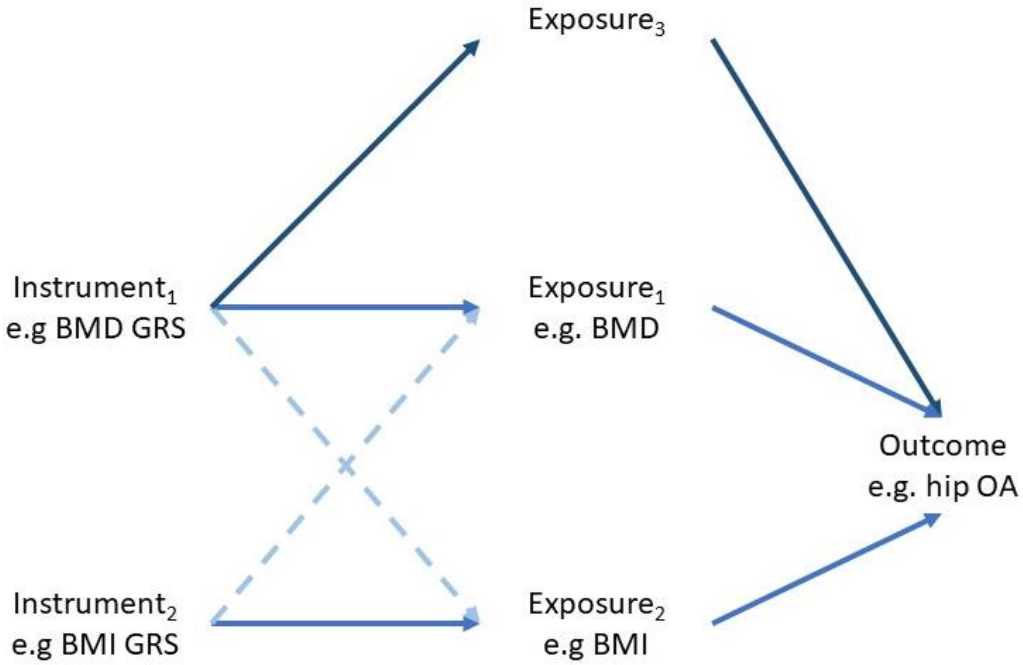

In MVMR, a genetic instrument (or instruments) robustly associated with each exposure is required. It is possible for the instruments to be associated with more than one exposure in the model if the instrument can jointly predict both exposures. MVMR will generate an estimate for the causal effect of exposure$_1$ on the outcome, independent of exposure$_2$ and an effect estimate for exposure$_2$ on the outcome, independent of exposure$_1$. However, if any of the instruments are related to another exposure not included in the model, the effect estimate will still be biased by horizontal pleiotropy (in this instance, if exposure$_3$ is not included in the model, the effect estimate generated for BMD will be independent of BMI but will still be biased).

5.3.4. Polygenic risk scores

Individual variants identified by GWAS normally only explain a small amount variance in the phenotype of interest. PRS sum the alleles for all genome-wide significant loci, generating a variable with increased variability. PRS were first used by Purcell *et al* in their GWAS of schizophrenia: due to a small sample size, their GWAS was underpowered to identify variants with small effects on disease risk and therefore they generated PRS to determine if this would explain a greater proportion of variability in schizophrenia risk (385). PRS can be weighted by the beta (*i.e.* the per-allele effect on the phenotype) from the GWAS, hence

giving greater weight to variants that have a greater effect on the phenotype, further increasing variability.

As discussed in section 3.1, the two major radiographic features of OA (osteophytes and JSN) may have distinct relationships with BMD. I generated PRS using independent BMD loci, from a recent large-scale GWAS of eBMD (386), to determine if genetic burden for eBMD is differentially associated with the radiographic OA sub-phenotypes in the RS population (Chapter 9). PRS are a continuous variable, which I analysed using standard linear and logistic regression analyses. As SNPs are constant from conception, reverse causality and confounding are less of an issue in PRS models. However, population stratification still needs to be accounted for, as described in section 5.3.2. Therefore, I adjusted for 10 PCs in all PRS analyses.

5.3.5. Pathway analysis

In Chapter 10, I aimed to determine the variation in OA, and specifically OA sub-phenotypes, explained by specific biological pathways known to influence both BMD and OA, such as the Wnt and TGFβ signalling pathways described in sections 2.1.3 and 3.3.2. The pathways selected and the methods for extracting a list of genes annotated to each pathway are described in detail in Chapter 10. I extracted variants related to each pathway using two methods:

1. Using all variants within 20kb upstream and 20kb downstream of all genes in the pathway.
2. Using all *cis*-expression quantitative trait loci (eQTLs) associated with gene expression levels in blood in the eQTLgen (significant) December 2019 release data, downloaded from (https://www.eqtlgen.org/cis-eqtls.html).

Variants were restricted to independent SNPs (*i.e.* SNPs in linkage equilibrium) using the Plink '*–indep-pairwise*' function and a pairwise LD≤0.2.

I considered generating PRS based on all variants linked to each pathway and determining the variation explained by each pathway using the r^2 from a linear

regression of the PRS on each sub-phenotype. However, the disadvantage of generating PRS is that you must select an allele to count as the 'effect allele' when summing alleles across multiple loci. Therefore, I generated SNP-specific r^2 estimates using the formula published by Shim *et al* (Equation 4) (387).

Equation 4: Calculation of SNP-specific r^2.

$$r^2_{SNP} = \frac{2 * \beta^2_{SNP} * EAF_{SNP} * (1 - EAF_{SNP})}{2 * \beta^2_{SNP} * EAF_{SNP} * (1 - EAF_{SNP}) + EA^2_{SNP} * 2N * EAF_{SNP} * (1 - EAF_{SNP})}$$

β_{SNP}: per-allele effect estimate for the SNP on the sub-phenotype, estimated from a GWAS, SE_{SNP}: standard error for β_{SNP}, EAF: effect allele frequency.

I then summed values across all independent variants linked to each pathway to generate an estimate of the pathway-specific r^2.

5.4. Metabolomics

Metabolomics is the study of metabolites within a sample. Unlike genetics, which are fixed at conception, metabolites represent the current cellular state within a particular tissue; they are the intermediate or end-stage products produced by metabolic processes of a cell, representing a mix of genetic and lifestyle factors (388).

5.4.1. Determining plasma metabolomic profile using NMR spectroscopy

Metabolomic profiling in all cohorts analysed was performed externally by Nightingale health (formerly Brainshake), Helsinki, Finland, using their custom-designed platform. This is a high-throughput, reproducible, proton-nuclear magnetic resonance (NMR) spectroscopy platform which measures over 200 metabolic traits in serum or plasma, representing systemic metabolism, including low-molecular weight molecules (LMWMs) such as amino acids, lipoproteins and lipid sub-factions (Figure 37) (389). Due to the inclusion of lipids and lipoproteins from 14 subclasses, which are too large to be classed as metabolites

(a mass of less than 1.5kDa is normally used to define a metabolite) (390,391), the measures generated by this platform are referred to as metabolic traits throughout this thesis.

Figure 37: List of the metabolic traits quantified by the Nightingale health platform.

Reproduced from (389).

NMR utilises the magnetic properties of hydrogen ions (*i.e.* protons) within the molecules. Electromagnetic radiation emitted by the spectrometer excites the protons and the energy released as the protons return to equilibrium is recorded (390). A mathematical process called Fourier transformation generates the spectra (392,393), with *x* axis representing chemical shift and *y* axis representing intensity (390). The chemical shift of a proton, compared to the reference, gives information about the environment of a proton (*i.e.* the chemical structure of the molecule) (390). The intensity provides information about the molecule concentration.

The methodology for the Nightingale NMR analysis has been published in detail in several reviews (389,392-394). The NMR spectroscopy was performed on a 96 well plate, including two QC samples: one to measure the consistency of quantification and the other to measure performance of the spectrometer (389). Prior to analysis, blood samples were stored at -80°C within two hours of collection and thawed to 4°C overnight before analysis (390). Samples were then spun in a centrifuge to remove precipitate (3400x*g*) (392). 300µl of sample was mixed with 300µl of sodium phosphate buffer in NMR tubes and samples were heated to 37°C for analysis (394). Analyses were performed using a Bruker AVANCE III spectrometer at 500.36MHz (392,393). The metabolic traits were detected using three molecular windows (Figure 38): LIPO identified lipoproteins and LMWM identified LMWMs. Then lipids were extracted with 0.15M saturated sodium chloride solution, 5ml methanol and 10ml dichloromethane and deuterochloroform, the sample was centrifuged at 4°C for 20 minutes (2400x*g*) and the lipid extracts were moved to separate NMR tubes

for detection by the LIPID window (at 22°C) (389,394). QC and quantification of metabolic traits were performed using proprietary software (395). The quantification of lipids and metabolites measured by standard clinical chemistry assays (such as total cholesterol, triglycerides) is comparable to routine clinical assays (395).

Figure 38: The Nightingale health platform for determination of metabolomic profile.

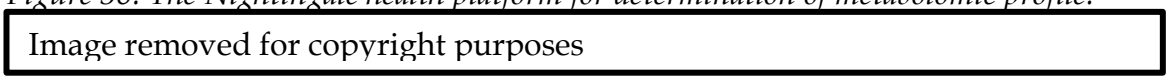

Reproduced from (389).

5.4.2. Analysing metabolomic data

The Nightingale platform generates a measure of the absolute concentration of each metabolic trait (normally in mmol/L, Figure 37) or a percentage for the ratio metabolic traits (*e.g.* apolipoprotein B: apolipoprotein A1). All measures represent continuous variables that were analysed in standard linear/logistic regression analysis, adjusting for covariates such as age and sex. A large proportion of the measures were skewed (Appendix 16). To reduce the complexity of interpreting some metabolic traits in log-transformed units and others on their original scale, analyses were performed with metabolic traits in their original units (or SD units). Regression analyses were performed with heteroskedasticity-robust SEs (section 5.1.2). However, sensitivity analyses were performed with log-transformed metabolic traits (where appropriate) to determine if results were biased by skewed metabolic traits.

CHAPTER 6. THE ASSOCIATION BETWEEN HIGH BONE MASS AND KNEE OSTEOARTHRITIS PROGRESSION

6.1. Background and aims

As discussed in section 3.1, there is strong evidence to suggest that higher BMD is a risk factor for prevalent and incident knee OA (209,212-215,229,230,232,396-398), whereas there is some evidence suggesting that high BMD is protective against knee OA progression (229,233). There are several reasons for this paradox. The first potential explanation is selection bias (also known as collider or index event bias). When studying OA progression based on a binary definition of any increase in overall OA severity in those with OA at baseline (*i.e.* KL≥2), the analysis is restricted to cases. If a variable that causes both OA incidence and progression is not controlled for in a case-only analysis, an inverse association between the confounding variable and high BMD may be induced, causing a backdoor pathway from high BMD to OA progression (Figure 39 illustrates collider bias, using an analysis which has not been adjusted for fat mass as an example).

Figure 39: Illustration of the theory of collider bias in a case-only study.

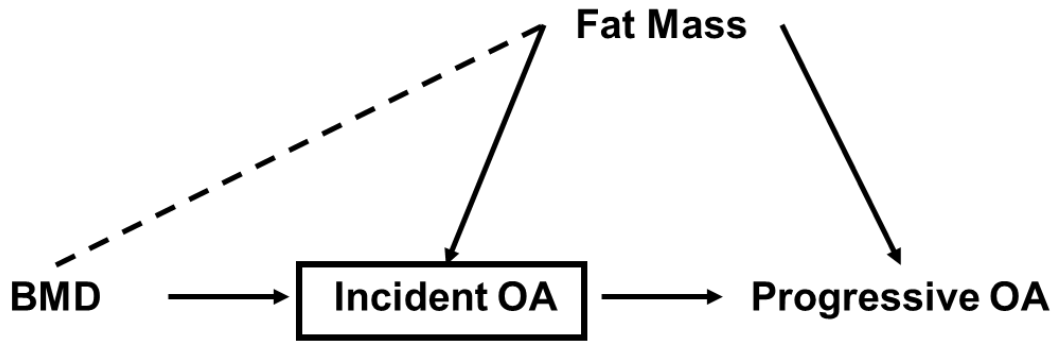

The box around incident OA indicates that incident OA has been 'conditioned on' by restricting the analysis to those with OA at baseline. Fat mass has not been adjusted for in this analysis, leading to a backdoor pathway between BMD and progressive OA. The dashed line represents an induced negative association. Adjusting for fat mass in this example would 'block' this backdoor pathway.

Another reason why basing the definition of OA progression on KL grade could lead to a potentially spurious inverse association between BMD and OA progression is that to progress from a KL grade of two to a grade of three, a knee

must go from displaying 'possible' to 'definite' narrowing of the joint space (32). Therefore, progression from grade two to three reflects incident JSN. Studies that have identified the relationship between BMD and radiographic sub-phenotypes of OA suggest that BMD is related to osteophytes, but not JSN (212,227,233). It is possible that high BMD is also only related to the progression of osteophytes and not progressive JSN; this would not be picked up in a study using overall KL change as an outcome.

Alternatively, there may in fact be a protective effect of BMD against knee OA progression. One reason for this could be that individuals with higher BMD have lower bone turnover. As discussed in section 3.1.2, an analysis in the Chingford population without osteoporosis found that women with progressive OA had higher levels of uNTX-1 and uCTX-1, compared to women with non-progressive OA and women without OA, at three timepoints (244). This suggests that bone turnover may be specifically related to reduced OA progression. Further evidence for a relationship between bone turnover and OA progression was provided by Berry *et al*, who found that higher baseline P1NP, osteocalcin and CTX-1 were associated with a reduced rate of cartilage loss in 132 older Australians (399).

In this chapter, I employ a novel approach to determine the relationship between high BMD and knee OA progression, by examining the HBM population and their relatives without HBM (section 2.3.2). By examining progression of the individual radiographic sub-phenotypes in this population, I can detect any differential associations which may explain the potential spurious associations observed in previous studies of overall OA. To limit the possibility of selection bias from performing a case only study, I analysed change in sub-phenotypes as a continuous variable and included individuals without features of OA at baseline, which also increased variability in the outcome and hence statistical power. As clinical severity (*e.g.* pain) may have differential relationships with OA risk factors, such as BMD, I also aimed to determine if HBM is associated with clinical symptoms of OA, *i.e.* pain, stiffness, functional limitation and reduced HR-QoL, and whether any such symptom is explained by radiographic

OA severity, which would provide insight into the potential clinical relevance of the association between HBM and knee OA (sub-phenotype) progression.

6.2. Methods

6.2.1. Study population

This analysis was performed in the HBM study population (section 2.3.2), who were still alive and contactable and consented to knee X-rays. The follow-up procedure is described in Chapter 4. Of the 437 individuals who originally consented at the eight participating centres, 254 (58%) were still alive and contactable, of whom 217 (85%) completed the questionnaire and 176 (69%) attended for follow-up radiographs. Derivation of the follow-up population and reasons for loss-to-follow-up are presented in Figure 40.

Figure 40: Flowchart of derivation of the study sample for knee OA progression analyses.

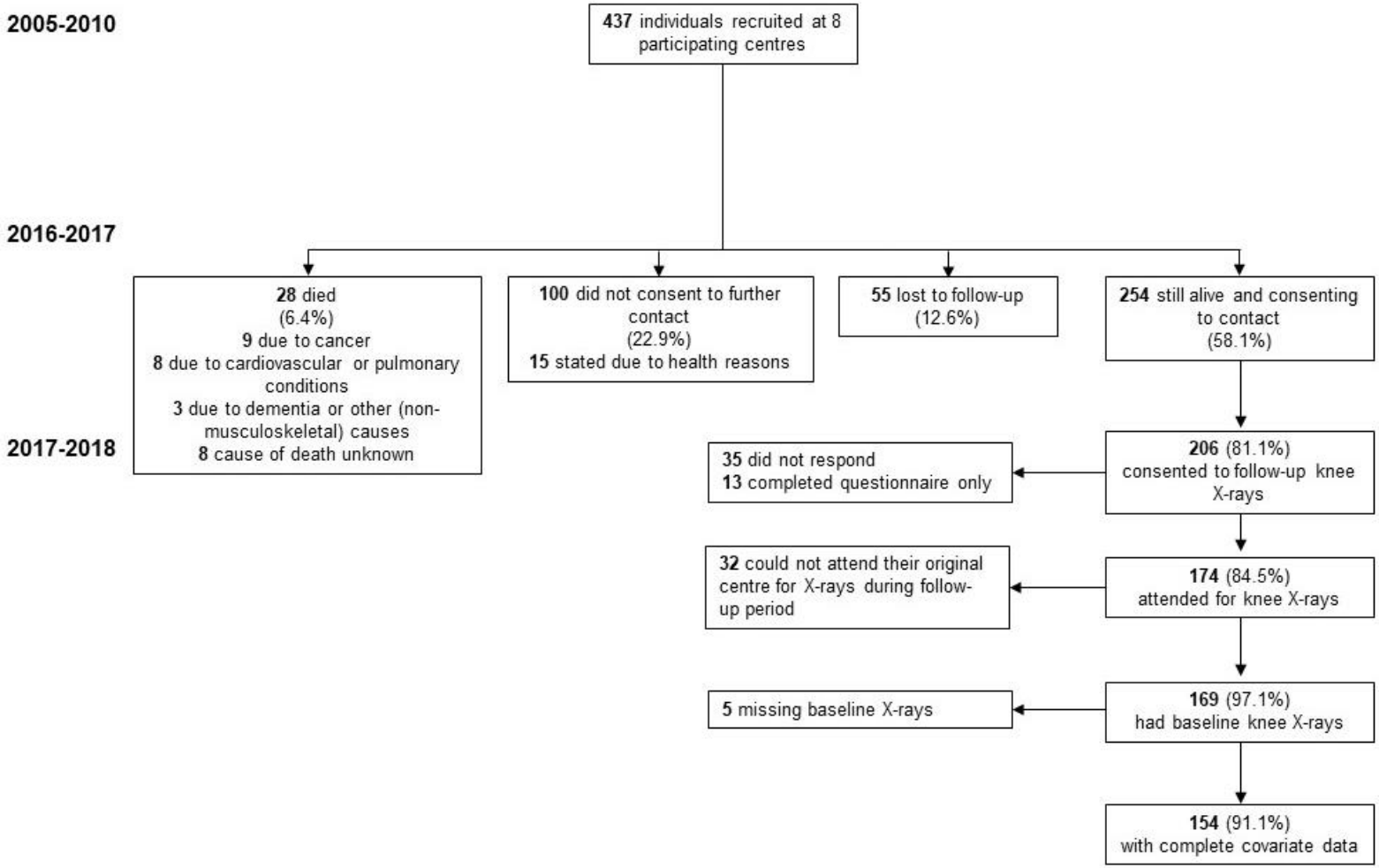

6.2.2. Assessing radiographic OA progression

Methodology for grading radiographic OA progression is described in section 4.4. Overall KL grade at the two timepoints was used to generate a binary variable for overall OA progression, using the standard definition of OA at baseline (KL≥2) and an increase in grade at follow-up. This variable is limited as it does not consider how individuals with doubtful OA at baseline (KL=1) differ from those clear of OA at baseline (KL=0). It is also vulnerable to a ceiling effect as individuals with a KL grade of four at baseline cannot progress.

I summed the semi-quantitative grades for osteophytes at the four regions (tibial and femoral, medial and lateral) and separately for JSN at the two regions (medial and lateral) to generate continuous outcome variables based on change in these summed scores between baseline and follow-up, with higher scores representing worsening osteophytes or JSN. Continuous measures of mJSW at the two timepoints were used to calculate reliable change index (RCI), which determines if the change in mJSW is meaningful over and above measurement error. Methodology for calculating RCI from mJSW measurements is outlined in Equation 5 and has been published elsewhere (400).

Equation 5: Formula for generating RCI from mJSW measurements at two timepoints.

$$RCI = \frac{mJSW_2 - mJSW_1}{\sqrt{(\sigma_1^2 + \sigma_2^2 - 2\sigma_1\sigma_2 r(mJSW_1, mJSW_2))}}$$

The RCI is a Z-score and a level of 1.96 is used to denote a 'true' change over and above measurement error (400). A binary variable for true JSN was therefore generated for those with an RCI<-1.96. A summary of all radiographic variables and how they were derived is presented in Table 11.

Table 11: Variables generated by Kellgren-Lawrence grading and semi-quantitative sub-phenotype grading using the OARSI atlas, and the derived variables used in this analysis.

Variable	Grading	Variable used in analysis
Osteoarthritis (KL grade)	0-4	Progressive OA: KL grade ≥2 at baseline and an increase in grade at follow-up Incident OA: KL grade <2 at baseline and ≥2 at follow-up
Osteophytes		
Medial femoral	0-3	Osteophyte progression: Sum of all semi-quantitative osteophyte grades at follow-up – sum at baseline
Lateral femoral	0-3	
Medial tibial	0-3	
Lateral tibial	0-3	
JSN		JSN progression: Sum of both semi-quantitative JSN grades at follow-up – sum at baseline
Medial	0-3	
Lateral	0-3	
Subchondral sclerosis		Incident sclerosis: no sclerosis (medial or lateral) at baseline and any sclerosis at follow-up
Medial	0, 1	
Lateral	0, 1	
Chondrocalcinosis	0, 1	Incident chondrocalcinosis: no chondrocalcinosis at baseline and chondrocalcinosis at follow-up
mJSW	continuous	Change in mJSW: mJSW at follow-up – mJSW at baseline True JSN: Reliable change index ≤-1.96

6.2.3. Determining clinical features of knee OA progression

Knee pain, stiffness and limitation of function were assessed using the WOMAC index at follow-up (310), as described in section 4.2.1. HR-QoL was determined using the five-level EuroQol EQ5D questionnaire as described in section 4.2.1.

6.2.4. Covariates

Age and sex were considered *a priori* confounders. Baseline grades for continuous sub-phenotype outcomes were also adjusted for, to limit the possibility of a ceiling effect, due to those with higher baseline scores being less able to progress. Due to HBM cases being identified from routine DXA databases, the proportion of postmenopausal women and the proportion with a history of steroid use was higher than the relatives without HBM (197) and as these factors could be related to osteophyte development, these were investigated as potential confounders. History of hormone replacement therapy (HRT) use, PA and time between baseline and follow-up X-rays were also

investigated as potential confounders. As individuals with HBM have higher TBFM than their unaffected relatives, with a hypothesized causal pathway between HBM and TBFM via bone turnover (201), I investigated TBFM as a potential mediator of any observed associations. However, it is also possible that TBFM is a confounder, as there is strong evidence for a causal relationship between higher BMI and higher BMD (401). The directed acyclic graph (DAG) for the hypothesized causal pathway between HBM and osteophyte/ JSN progression is presented in Figure 41.

Figure 41: DAG of the hypothesized causal pathway between HBM and OA sub-phenotype progression, highlighting hypothesized confounders.

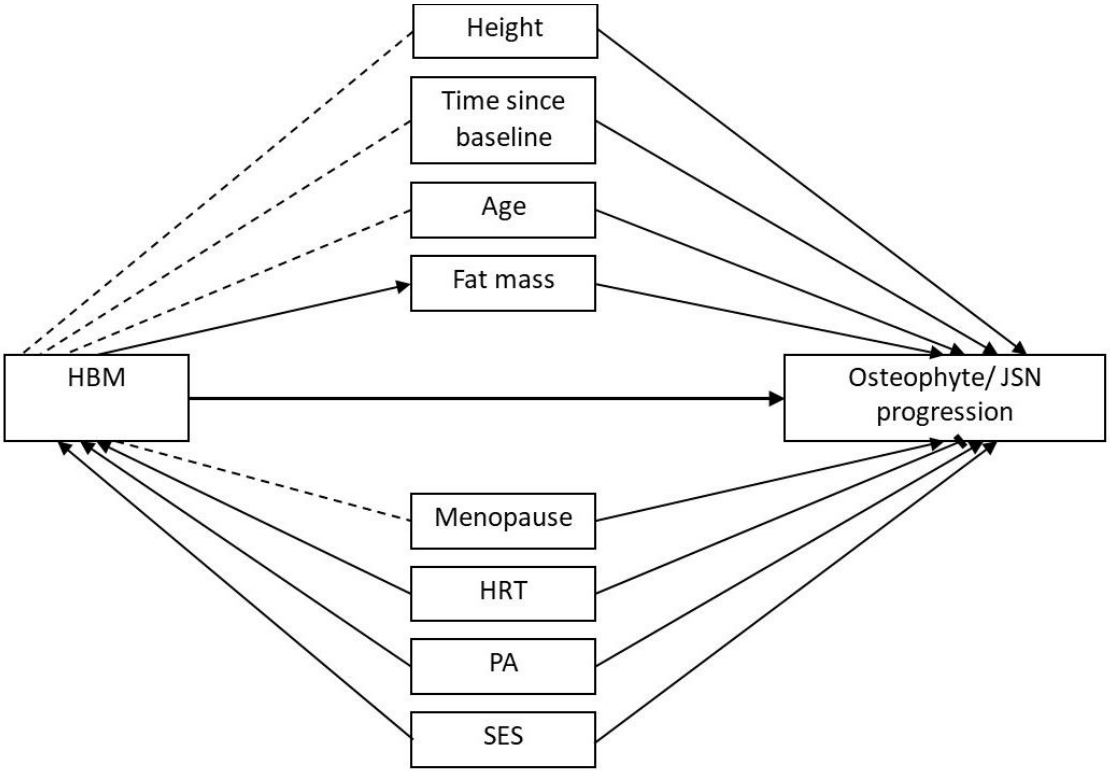

Dashed lines represent induced associations due to participant selection. Arrows represent positive associations and capped lines represent inverse associations.

6.2.5. Statistical analysis

Associations between HBM status (binary) and binary OA incidence and progression variables were determined by multivariable logistic regression,

using GEE to account for clustering due to multiple knee radiographs per person, as described in section 5.1.2. Associations with continuous osteophyte and JSN progression variables were determined by multivariable GEE linear regression, with robust SEs due to non-normal distributions of outcome variables. Analyses were initially performed unadjusted (model 1), then adjusted for age and sex (and baseline score for continuous outcomes) (model 2), then additionally adjusting for height, menopause, and education (model 3). Finally, the mediating/confounding effect of TBFM was determined by additionally adjusting for TBFM in model 4.

6.2.6. Sensitivity analyses

I performed the following sensitivity analyses to assess the reliability of results:

1) As TKRs were excluded from analyses but are likely to be performed due to severe OA, analyses of progressive OA were repeated, assuming that individuals with OA at baseline (KL$\geq$2) and a TKR at follow-up had progressive OA. Those with a KL score <2 at baseline and a TKR at follow-up were coded as incident and progressive OA cases (assuming rapid OA progression led to a TKR within eight years of OA development).
2) Person-level analyses, using the highest value for osteophyte/JSN scores of the two knees.
3) Repeating analyses removing individuals reporting a cartilage operation (12 knees), knee lavage, washout, arthroscopy (16 knees) or a steroid injection (9 knees) in their follow-up questionnaire.
4) An additional model adjusting for metal artefacts on DXA scans (section 4.3.1).
5) An additional model adjusting for bone size as assessed by maximal tibial plateau width.
6) Removing individuals with positioning errors leading to loss of fat mass from the DXA image (section 4.3.2).
7) Removing those visiting a different site for follow-up imaging.

8) To check that conclusions were not invalid due to skewed continuous outcome variables, analyses were repeated with a Poisson model.

6.3. Results

6.3.1. Descriptives of the High Bone Mass radiographic follow-up population

Follow-up and baseline radiographic data were available for 169 individuals, 63% of whom had HBM. Those with follow-up data were more commonly female and more active at baseline and less commonly postmenopausal and diabetic at baseline (Table 12). However, there did not appear to be differential loss-to-follow-up between HBM cases and their relatives, and there was no evidence of a difference in baseline prevalence of knee OA or OA sub-phenotypes or joint replacement between those with and without follow-up radiographic data.

Table 12: Baseline descriptives of individuals from the HBM cohort with and without radiographic follow-up data.

	All N=437	**With follow-up data N=169**	**Without follow-up data N=268**	***p*-value for difference**
		N (%)		
HBM cases	274 (62.7)	107 (63.3)	167 (62.3)	0.833
Female sex	285 (65.2)	124 (73.4)	161 (60.1)	0.004
Postmenopausal	207 (74.2)	85 (68.6)	122 (78.7)	0.054
History of smoking	244 (57.0)	85 (50.3)	159 (61.4)	0.023
Alcohol consumption				
None	87 (20.3)	28 (16.6)	59 (22.7)	
Occasional	52 (12.1)	23 (13.6)	29 (11.2)	0.164
Regular	217 (50.6)	94 (55.6)	123 (47.3)	
Heavy	73 (17.0)	24 (14.2)	49 (18.9)	
Diabetes	44 (10.1)	10 (5.9)	34 (12.7)	0.022
Physical activity category[d]				
Low	66 (17.4)	19 (11.6)	47 (21.9)	0.030
Moderate	129 (34.0)	58 (35.4)	71 (33.0)	
High	184 (48.6)	87 (53.1)	97 (45.1)	
Joint replacement	47 (10.8)	16 (9.5)	31 (11.6)	0.490
KOA (KL $\geq$2)	127 (32.2)	49 (29.5)	78 (34.2)	0.325
Knee osteophyte	127 (32.2)	49 (29.5)	78 (34.2)	0.325
Knee JSN	78 (19.9)	27 (16.3)	51 (22.5)	0.128
Any subchondral sclerosis	17 (4.4)	4 (2.4)	13 (5.8)	0.111
Any chondrocalcinosis	37 (9.6)	15 (9.2)	22 (9.9)	0.812
		Mean (SD)		
Age, years	59.1 (15.4)	57.7 (12.3)	59.9 (17.1)	0.133
Height, cm	168.8 (9.8)	167.7 (9.2)	169.5 (10.1)	0.072
Weight, kg	84.5 (17.1)	82.6 (17.6)	85.6 (16.6)	0.074
L1 Z-score	2.6 (2.1)	2.5 (2.0)	2.7 (2.3)	0.281
Max total hip Z-score	2.0 (1.6)	2.0 (1.5)	2.1 (1.7)	0.846

As expected, individuals with follow-up data and HBM were more commonly female (84% *vs* 55%), more commonly postmenopausal (74% *vs* 53%) and had a greater baseline BMD (mean TH-BMD 1.25g/cm^2 *vs* 0.97g/cm^2) and BMI (30.4 kg/m^2 *vs* 27.7 kg/m^2) than individuals with follow-up data without HBM (Table 13). Individuals with HBM were also less likely to drink regularly (weekly or more frequent) and had a greater loss of BMD between baseline and follow-up, which was explained by age differences.

Table 13: Descriptives of the HBM cohort radiographic follow-up population.

	All N=169	HBM Individuals N=107	Non-HBM Relatives N=62	*p*-value for difference
		N (%)		
Female sex	124 (73.3)	90 (84.1)	34 (54.8)	7.22×10^{-5}
Postmenopausal at baseline	85 (68.5)	67 (74.4)	18 (52.9)	0.037
Menopause transition during follow-up	13 (10.8)	7 (8.1)	6 (17.7)	0.131
History of HRT use	55 (45.5)	44 (50.0)	11 (33.3)	0.151
History of smoking	81 (50.6)	49 (49.0)	32 (53.3)	0.596
Alcohol consumption				0.037
Never	15 (9.0)	7 (6.7)	8 (12.9)	
Monthly or less	60 (35.9)	46 (43.8)	14 (22.6)	
Weekly	49 (29.3)	29 (27.6)	20 (32.3)	
Daily/ most days	43 (25.8)	23 (21.9)	20 (32.3)	
Physical activity at baseline				0.453
Low	19 (11.6)	11 (10.8)	8 (12.9)	
Medium	58 (35.4)	33 (32.4)	25 (40.3)	
High	87 (53.0)	58 (56.9)	29 (46.8)	
Education				0.061
Up to GCSE/ O level	67 (41.4)	50 (48.1)	17 (29.3)	
A level or equivalent	37 (22.8)	22 (21.2)	15 (25.9)	
Degree or equivalent	58 (35.8)	32 (30.8)	26 (44.8)	
		Mean (SD)		
Age at baseline, years	57.7 (12.3)	58.4 (12.6)	56.4 (11.7)	0.303
Age at follow-up, years	65.9 (12.4)	66.7 (12.7)	64.7 (11.8)	0.312
Height at baseline, cm	167.7 (9.2)	166.5 (8.0)	169.8 (10.6)	0.036
Weight at baseline, kg	82.6 (17.6)	84.1 (17.6)	80.0 (17.4)	0.146
BMI at baseline (kg/m^2)	29.4 (5.9)	30.4 (6.2)	27.7 (5.0)	0.003
TBFM (kg)	32.1 (10.9)	33.2 (11.3)	30.0 (10.0)	0.076
Baseline TH Z-Score	2.03 (1.50)	2.96 (0.95)	0.46 (0.80)	8.55×10^{-39}
Baseline TH-BMD, g/cm^2	1.15 (0.19)	1.25 (0.14)	0.97 (0.13)	1.03×10^{-26}
Change in TH-BMD, % per year	-0.31 (0.92)	-0.44 (0.94)	-0.09 (0.84)	0.020
Baseline L1 Z-Score	2.47 (1.96)	3.64 (1.25)	0.44 (1.14)	4.20×10^{-37}
Baseline L1-BMD, g/cm^2	1.26 (0.22)	1.38 (0.15)	1.06 (0.14)	1.39×10^{-29}
Change in L1-BMD, % per year	0.02 (1.19)	0.02 (1.24)	0.02 (1.09)	0.994
Maximum tibial plateau width at baseline, mm	81.4 (7.2)	80.1 (6.3)	83.9 (8.0)	0.001
Follow-up time, years	8.3 (1.0)	8.3 (0.7)	8.2 (1.3)	0.871

6.3.2. Determining potential covariates

Age, sex, educational attainment, height, and weight were *a priori* confounders. As highlighted in section 6.2.4, I investigated time between X-rays, menopause, PA, and HRT use as potential confounders, by determining the association between these variables and OA sub-phenotype progression. As there was some evidence for alcohol consumption differing between HBM cases and relatives without HBM (Table 13), I also determined the associations of alcohol

consumption with the outcomes (Table 14, Table 15). There was evidence for a greater odds of incident OA for women postmenopausal at baseline. Age was related to an increased odds of incident OA, chondrocalcinosis and subchondral sclerosis. Baseline weight was related to an increased odds of incident OA and to change in osteophyte and JSN scores. As BMD is a component of weight, TBFM was included in statistical models instead of weight. Time between X-rays was related to incident chondrocalcinosis and subchondral sclerosis.

Table 14: Associations between potential covariates and incident OA outcomes in the HBM cohort follow-up population.

	Incident OA		**Incident Chondrocalcinosis**		**Incident subchondral sclerosis**	
	OR (95% CI)	***p***	**OR (95% CI)**	***p***	**OR (95% CI)**	***p***
Female	0.83 (0.38, 1.80)	0.637	0.62 (0.22, 1.72)	0.361	0.38 (0.12, 1.16)	0.088
Alcohol consumption (baseline)		*p for trend=0.188*		*p for trend=0.251*		*p for trend=0.864*
None	*Ref*		*Ref*		*Ref*	
Occasional	3.16 (0.68, 14.63)	0.141	0.27 (0.05, 1.57)	0.145	0.81 (0.08, 8.15)	0.856
Regular	3.24 (0.87, 12.16)	0.081	0.42 (0.12, 1.49)	0.179	1.01 (0.27, 3.81)	0.987
Heavy	2.25 (0.51, 9.84)	0.282	0.38 (0.08, 1.80)	0.221	1.13 (0.17, 7.40)	0.902
PA category (baseline)		*p for trend=0.540*		*p for trend=0.545*		*p for trend=0.662*
Low	*Ref*		*Ref*		*Ref*	
Medium	0.54 (0.19, 1.51)	0.238	0.54 (0.08, 3.42)	0.509	2.11 (0.25, 18.0)	0.494
High	0.94 (0.37, 2.35)	0.890	1.09 (0.21, 5.60)	0.917	2.03 (0.25, 16.6)	0.508
Education		*p for trend=0.982*		*p for trend=0.123*		*p for trend=0.294*
up to GCSE/O level	*Ref*		*Ref*		*Ref*	
A level	0.69 (0.27, 1.82)	0.457	0.53 (0.17, 1.64)	0.271	0.77 (0.19, 3.16)	0.719
Degree	0.99 (0.46, 2.14)	0.979	0.40 (0.12, 1.30)	0.127	0.48 (0.12, 1.97)	0.308
Postmenopausal (baseline)	3.40 (1.26, 9.14)	0.015	*all cases postmenopausal at baseline*		4.40 (0.54, 35.9)	0.166
Premenopausal at baseline, postmenopausal at follow-up	0.72 (0.19, 2.81)	0.641	*all cases postmenopausal at baseline*		0.85 (0.10, 6.89)	0.876
History of HRT use (follow-up)	2.13 (0.93, 4.84)	0.072	0.65 (0.19, 2.25)	0.498	0.34 (0.07, 1.76)	0.201
Age (baseline), years	1.06 (1.02, 1.09)	4.70×10^{-4}	1.11 (1.06, 1.16)	2.71×10^{-5}	1.08 (1.03, 1.13)	0.001
Time between X-rays, years	0.78 (0.52, 1.15)	0.211	2.34 (1.20, 4.55)	0.013	1.43 (1.18, 1.74)	3.55×10^{-4}
Height (baseline), cm	1.01 (0.96, 1.05)	0.717	1.00 (0.94, 1.07)	0.977	1.00 (0.91, 1.09)	0.944
Weight (baseline), kg	1.02 (1.01, 1.04)	0.013	1.01 (0.99, 1.03)	0.230	1.03 (1.00, 1.07)	0.056

ORs are per unit increase for continuous covariates.

Table 15: Associations between covariates and progressive OA outcome variables in the HBM cohort follow-up population.

	Change in osteophyte score		Change in JSN grade	
	β (95% CI)	***p***	**β (95% CI)**	***p***
Female	0.38 (-0.09, 0.84)	0.111	-0.08 (-0.26, 0.10)	0.378
Alcohol consumption at baseline		*p for trend=0.860*		*p for trend=0.535*
None	*Ref*			
Occasional	-0.14 (-0.90, 0.61)	0.709	0.04 (-0.19, 0.27)	0.722
Regular	0.04 (-0.62, 0.69)	0.912	0.15 (-0.03, 0.34)	0.111
Heavy	-0.19 (-0.91, 0.52)	0.592	-0.03 (-0.20, 0.13)	0.677
Physical activity category at baseline		*p for trend=0.458*		*p for trend=0.175*
Low	*Ref*		*Ref*	
Medium	0.15 (-0.41, 0.71)	0.601	0.25 (0.09, 0.41)	0.002
High	0.24 (-0.24, 0.72)	0.335	0.22 (0.08, 0.36)	0.002
Educational attainment		*p for trend=0.988*		*p for trend=0.273*
up to GCSE/ O level	*Ref*		*Ref*	
A level	-0.23 (-0.80, 0.35)	0.436	0.07 (-0.11, 0.24)	0.462
Degree	0.01 (-0.52, 0.54)	0.976	0.10 (-0.08, 0.27)	0.274
Postmenopausal at baseline	0.16 (-0.47, 0.79)	0.609	-0.06 (-0.25, 0.12)	0.507
Premenopausal at baseline, postmenopausal at follow-up	0.80 (-0.52, 2.12)	0.236	0.24 (-0.16, 0.64)	0.242
History of HRT use at follow-up	0.18 (-0.37, 0.72)	0.530	0.08 (-0.07, 0.23)	0.291
Age at recruitment, years	0.01 (-4.77×10^{-3}, 0.03)	0.154	4.04×10^{-3} (-7.82×10^{-4}, 0.01)	0.101
Time between X-rays, years	0.15 (-4.38×10^{-3}, 0.29)	0.057	-0.01 (-0.06, 0.04)	0.784
Height at recruitment, cm	-0.02 (-0.04, 3.45×10^{-3})	0.095	4.63×10^{-3} (-4.11×10^{-3}, 0.01)	0.299
Weight at recruitment, kg	0.02 (0.01, 0.03)	0.002	0.01 (2.72×10^{-3}, 0.01)	0.001

Betas represent the difference in the mean change in osteophyte/JSN score between categories or per unit increase in continuous variables. ORs are the odds ratio compared to the reference category or per unit increase for continuous variables. E.g. a beta of 0.38 represents a 0.38-point higher mean change in osteophyte score in females compared to males and a beta of 0.02 represents a 0.02-point higher change in osteophyte score per 1kg increase in weight.

6.3.3. HBM and radiographic OA progression

OA progression based on KL grade

I found limited evidence for a relationship between HBM and incident, but not progressive, OA as defined by overall KL grade (*i.e.* global OA incidence and progression, Figure 42). In analyses adjusted for age, sex, height, educational attainment, and menopause (model 3), HBM was associated with an over two-fold odds of incident OA (OR=2.29 [1.00,5.26]). Additional adjustment for TBFM did not largely attenuate the effect size but widened the CIs (OR=2.17 [0.90,5.23]). However, incident OA analyses were restricted to 213 knees without OA (KL<2) at baseline and progressive analyses were even further restricted to the 76 knees eligible to progress due to the presence of OA at baseline.

Figure 42: Associations between HBM status and global OA incidence and progression.

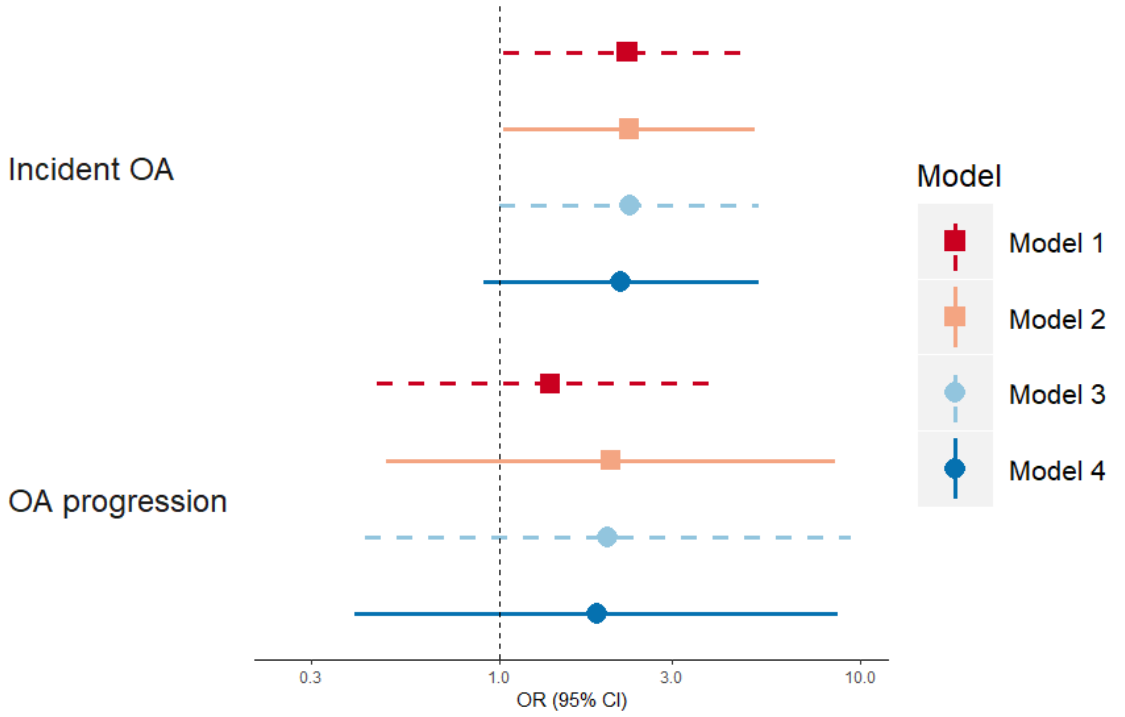

Points represent ORs and horizontal bars represent 95% CIs. Model 1: Unadjusted; model 2: adjusted for age and sex; model 3: model 2 plus height, educational attainment, and menopause; model 4: model 3 plus TBFM.

Sub-phenotype progression

In age, sex, height, education, baseline score and menopause-adjusted analyses (model 3), individuals with HBM had greater changes in osteophyte score between baseline and follow-up (mean difference=0.50 [0.06,0.94], Figure 43). Further adjustment for TBFM explained approximately 10% of this relationship (TBFM-adjusted mean difference=0.44 [0.02,0.87]). Individuals with HBM also had a greater change in JSN score, with an age, sex, height, education, baseline score and menopause-adjusted mean difference of 0.17 (0.03,0.31). This association was robust to additional adjustment for TBFM (mean difference=0.16 [0.02,0.29]). Determining 'true' JSN, based on RCI, individuals with HBM had a greater odds of 'true' JSN, which was not affected by adjustment for TBFM ($OR_{model\ 4}$=9.72 [1.23,76.9]), although the CIs were wide reflecting the low numbers of individuals without HBM displaying this phenotype. I did not find evidence for an association between HBM and incident subchondral sclerosis or chondrocalcinosis, but these phenotypes were rare.

Figure 43: Associations between HBM status and incident and progressive OA sub-phenotypes.

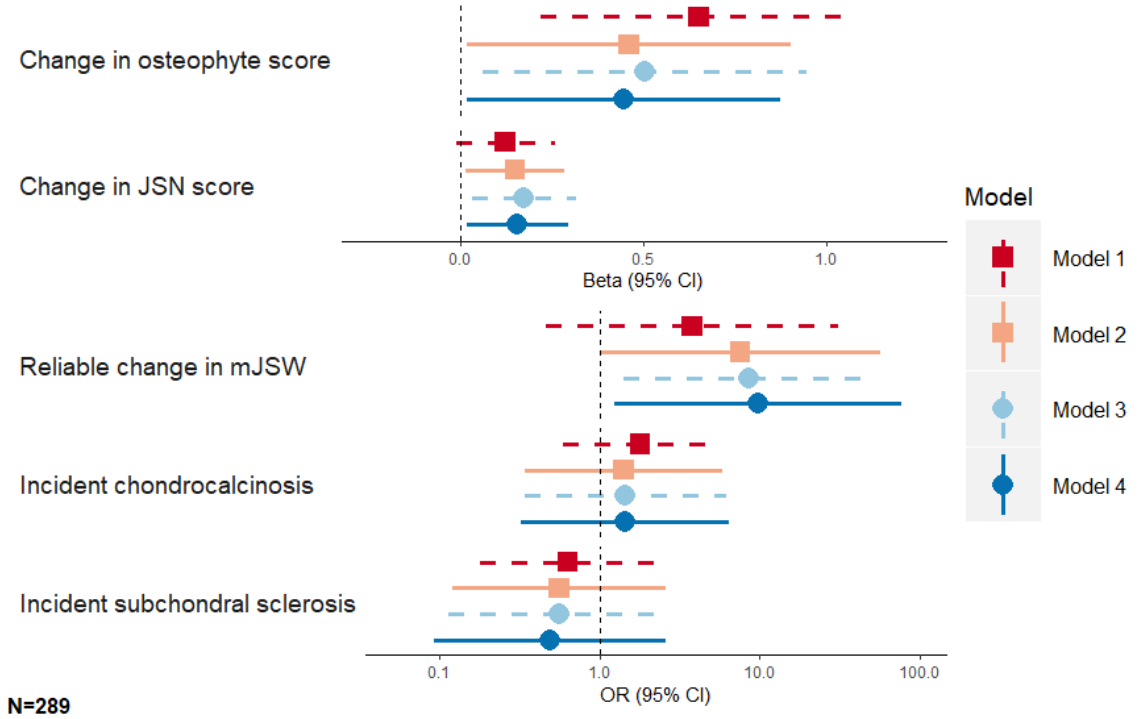

Points for continuous outcomes represent the difference in mean outcome between individuals with and without HBM. Points for binary outcomes represent the OR for individuals with HBM compared to their relatives with normal BMD. Horizontal bars represent 95% CIs. Model 1: unadjusted; model 2: adjusted for age and sex (plus baseline score for continuous outcomes); model 3: model 2 plus height, educational attainment, and menopause; model 4: model 3 plus TBFM. N for reliable change in mJSW=278; N for incident chondrocalcinosis=274; N for incident subchondral sclerosis=287.

6.3.4. HBM and clinical features of OA progression

In unadjusted analyses, individuals with HBM had much greater WOMAC pain, stiffness, and functional limitation scores (mean differences=11.2 [5.4,17.0], 11.0 [4.5,17.5] and 9.7 [4.8,14.7], respectively) and lower HR-QoL index values (mean difference=-0.09 [-0.14,-0.04]). Adjustment for age and sex (model 2) attenuated the strength of the relationship between HBM and WOMAC scores by approximately 30% (Figure 44). Relationships persisted after further adjustment for height, education, and menopause (model 3, mean differences=7.2 [0.7,13.6], 6.9 [0.2,13.6] and 5.9 [0.8,11.0] and -0.07 [-0.13,-0.004] for pain, stiffness, limitation of function and HR-QoL, respectively).

Figure 44: Associations between HBM status and WOMAC pain, stiffness, and functional limitation subscale scores and HR-QoL measured by EQ5D.

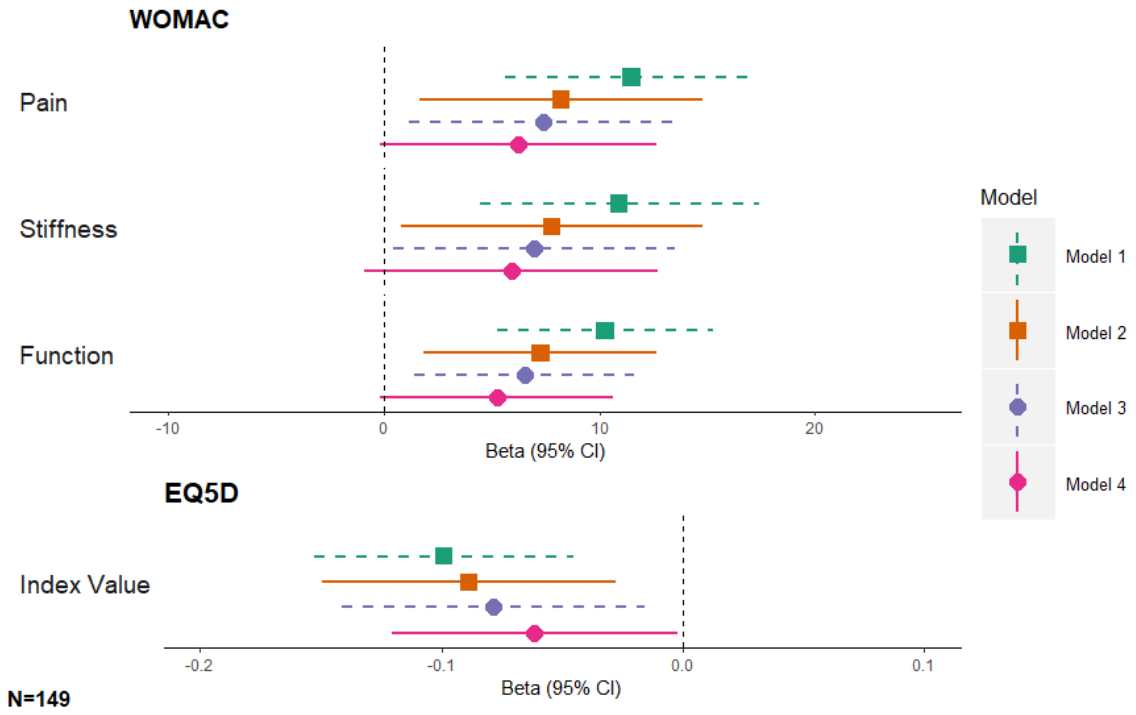

Points represent the mean difference in WOMAC scores or EQ5D values between individuals with HBM and relatives/spouses without HBM. Horizontal bars represent 95% CIs. Results are from a person-level analysis, accounting for clustering in families. Model 1: unadjusted; model 2: adjusted for age and sex; model 3: model 2 plus height, educational attainment, and menopause; model 4: model 3 plus TBFM.

I performed further analyses to determine which of TBFM, osteophyte severity, JSN severity, change in osteophytes or change in JSN were the strongest predictors of increased pain and reduced HR-QoL in HBM individuals (Figure 45). Adjustment for osteophyte severity at follow-up attenuated the association between HBM and pain, stiffness, functional limitations and reduced HR-QoL by the greatest proportion, with follow-up osteophyte score attenuating the relationships by 58%, 67%, 55% and 37%, respectively. Osteophyte progression also attenuated the association between HBM and knee stiffness by 43%. Adjustment for TBFM and JSN severity and progression had little effect on the relationship between HBM and HR-QoL. Adjustment for TBFM attenuated associations between HBM and WOMAC scores by 15-20%, whilst JSN severity at follow-up attenuated these associations by 25-30%.

Figure 45: Associations between HBM status and WOMAC pain, stiffness, and functional limitation scores and HR-QoL, adjusting for radiographic OA sub-phenotypes.

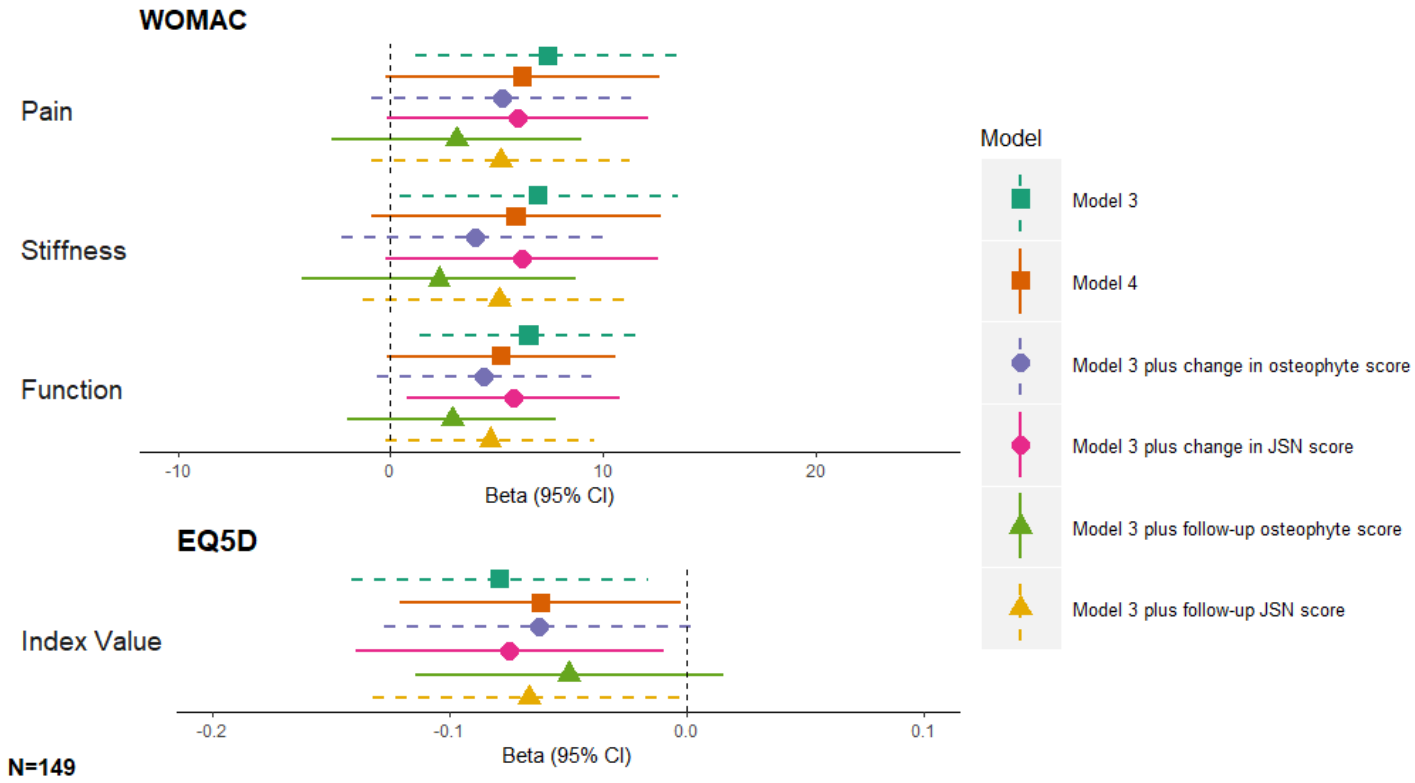

Points represent the mean difference in WOMAC scores or EQ5D values between individuals with HBM and relatives/spouses without HBM. Horizontal bars represent 95% CIs. Results are from a person-level analysis, accounting for clustering in families. Model 3: adjusted for age, sex, height, educational attainment, and menopause; model 4: model 3 plus TBFM. Follow-up osteophyte and JSN score is the highest of the two knees. Change in score is the greatest change of the two knees.

6.3.5. BMD and OA progression

When analysing associations with TH-BMD as a continuous exposure, there was evidence for an association between TH-BMD and incident OA, with an age, sex, height, TBFM, menopause and education-adjusted (model 4) OR of 1.64 (1.04,2.56) per SD increase in TH-BMD (Figure 46). ORs for the association with OA progression were similar, although CIs were much wider and overlapped the null, probably due to the small sample size (N=75). There was no evidence for an association between L1-BMD and incident or progressive OA (Figure 47).

Figure 46: Associations between TH-BMD and global OA incidence and progression in the HBM cohort.

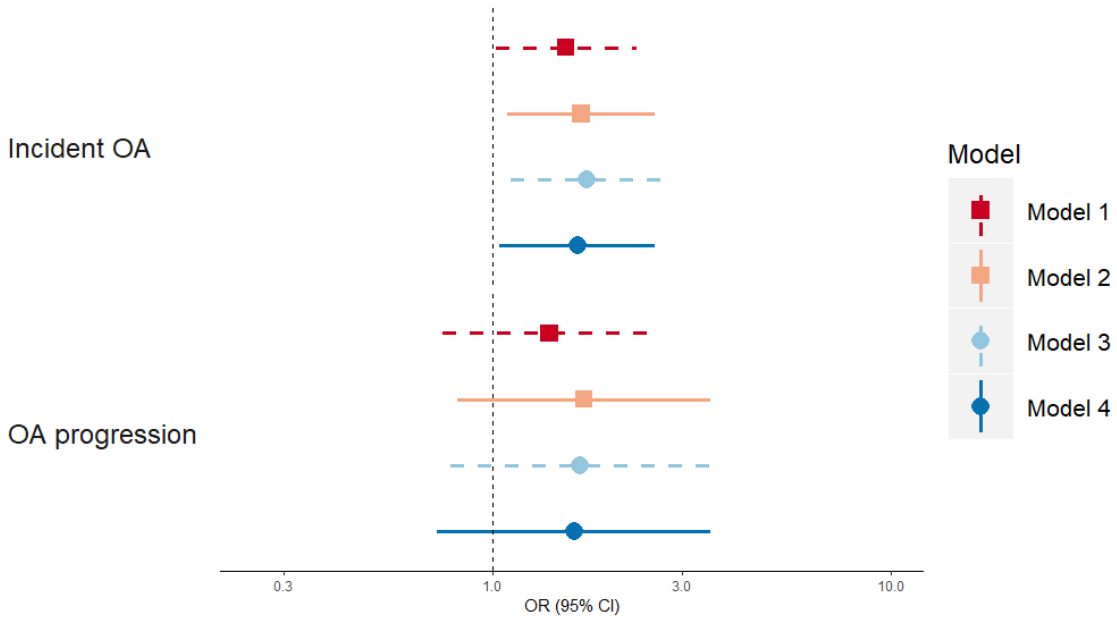

Points represent ORs per SD increase in TH-BMD and horizontal bars represent 95% CIs. Model 1: Unadjusted; model 2: adjusted for age and sex; model 3: model 2 plus height, educational attainment, and menopause; model 4: model 3 plus TBFM.

Figure 47: Associations between L1-BMD and global OA incidence and progression in the HBM cohort.

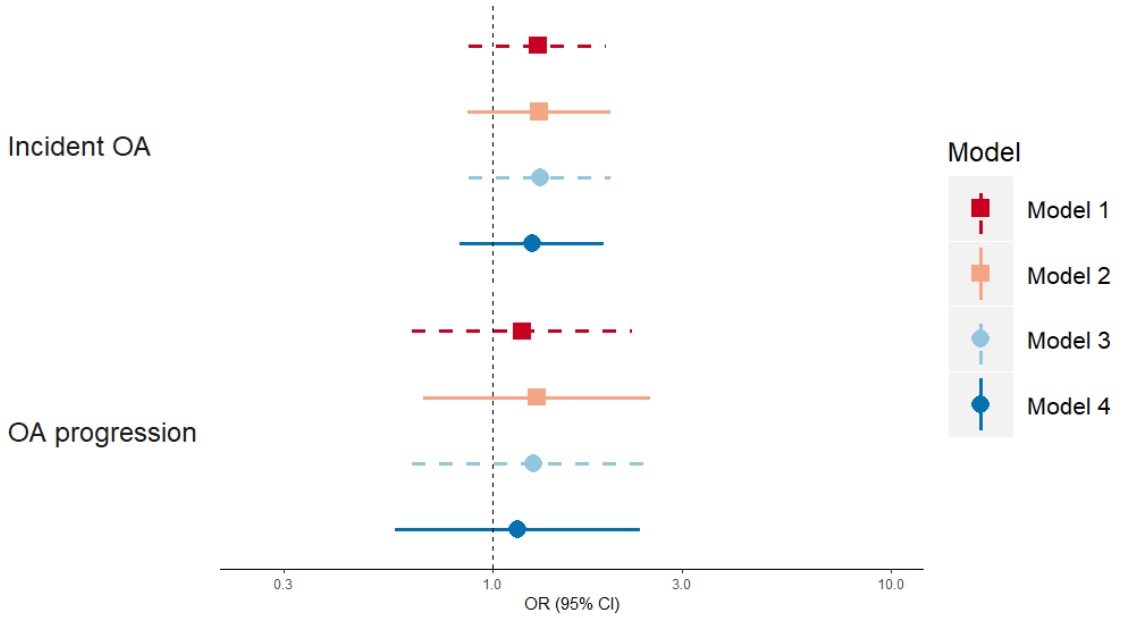

Points represent ORs per SD increase in L1-BMD and horizontal bars represent 95% CIs. Model 1: Unadjusted; model 2: adjusted for age and sex; model 3: model 2 plus height, educational attainment, and menopause; model 4: model 3 plus TBFM.

TH-BMD strongly predicted change in osteophyte score, with an SD increase in TH-BMD associated with a greater change in osteophyte score of 0.28 (0.05,0.51) (Figure 48). Evidence supported an association between TH-BMD and change in JSN score, although much weaker than that seen for osteophytes (β=0.09 [$3x10^{-3}$,0.18]). TH-BMD was also related to an increased odds of 'true' JSN (OR=2.07 [1.14,3.77]). There was limited evidence for an association between L1-BMD and change in osteophyte score only, although CIs overlapped the null (0.17 [-0.05,0.39]) (Figure 49).

Figure 48: Associations between TH- BMD and incident and progressive OA sub-phenotypes in the HBM cohort.

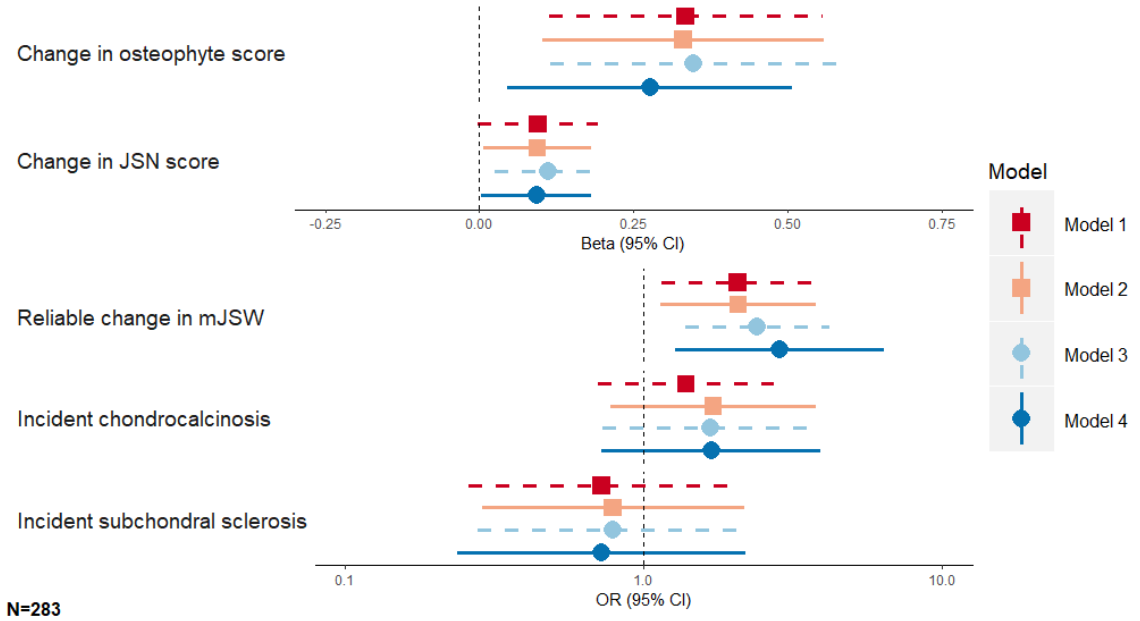

Points for continuous outcomes represent the increase in outcome per SD increase in total hip BMD. Points for binary outcomes represent the OR per SD increase in total hip BMD. Horizontal bars represent 95% CIs. Model 1: unadjusted; model 2: adjusted for age and sex (plus baseline score for continuous outcomes); model 3: model 2 plus height, educational attainment, and menopause; model 4: model 3 plus TBFM. N for reliable change in mJSW=272; N for incident chondrocalcinosis=268; N for incident subchondral sclerosis=281.

Figure 49: Associations between L1-BMD and incident and progressive OA sub-phenotypes in the HBM cohort.

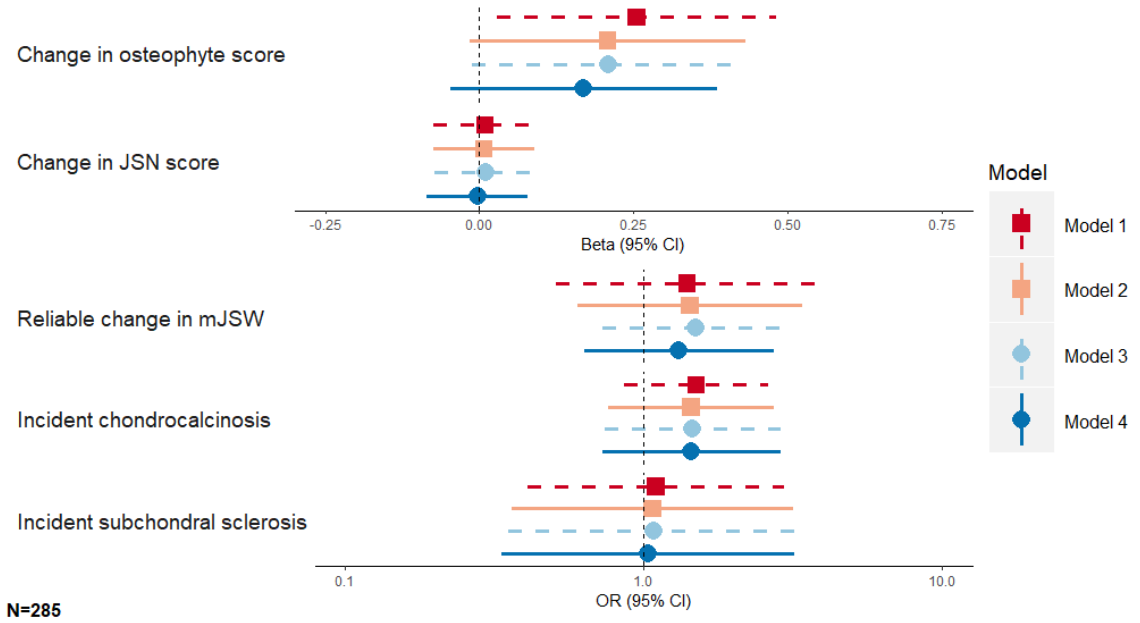

Points for continuous outcomes represent the increase in outcome per SD increase in L1-BMD. Points for binary outcomes represent the OR per SD increase in L1-BMD. Horizontal bars represent 95% CIs. Model 1: unadjusted; model 2: adjusted for age and sex (plus baseline score for continuous outcomes); model 3: model 2 plus height, educational attainment, and menopause; model 4: model 3 plus TBFM. N for reliable change in mJSW=274; N for incident chondrocalcinosis=270; N for incident subchondral sclerosis=283.

I next determined the relationship between change in TH-BMD and L1-BMD, between baseline and follow-up, and progression of OA and OA sub-phenotypes. There was no evidence for a relationship between change in TH-BMD and incident or progressive OA (Figure 50) or incidence or progression of OA sub-phenotypes (Figure 51). There was some evidence for an association between change in L1-BMD and OA progression in the unadjusted model (OR=0.64 [0.41,0.99]) (Figure 52). Adjustment for age, sex, menopause, education, height and TBFM (model 4) did not alter the point estimate but did widen the CIs to include the null. There was no evidence for an association between change in L1-BMD and incidence or progression of OA sub-phenotypes (Figure 53).

Figure 50: Associations between change in TH-BMD and global OA incidence and progression in the HBM cohort.

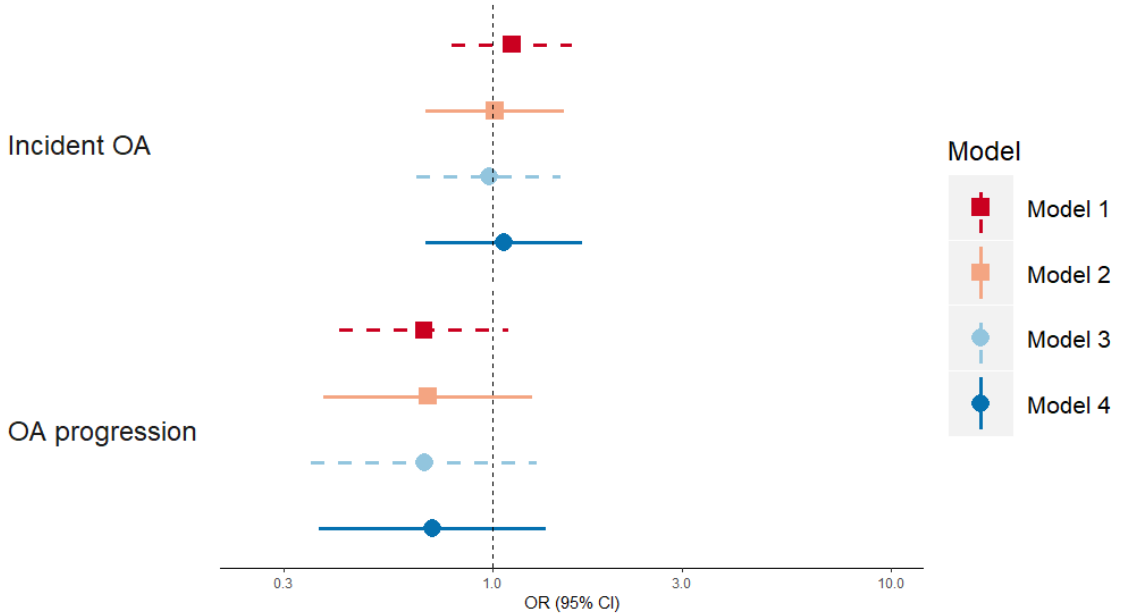

Points represent ORs per SD increase in change in TH-BMD and horizontal bars represent 95% CIs. Model 1: Unadjusted; model 2: adjusted for age and sex; model 3: model 2 plus height, educational attainment, and menopause; model 4: model 3 plus TBFM.

Figure 51: Associations between change in TH-BMD and incident and progressive OA sub-phenotypes in the HBM cohort.

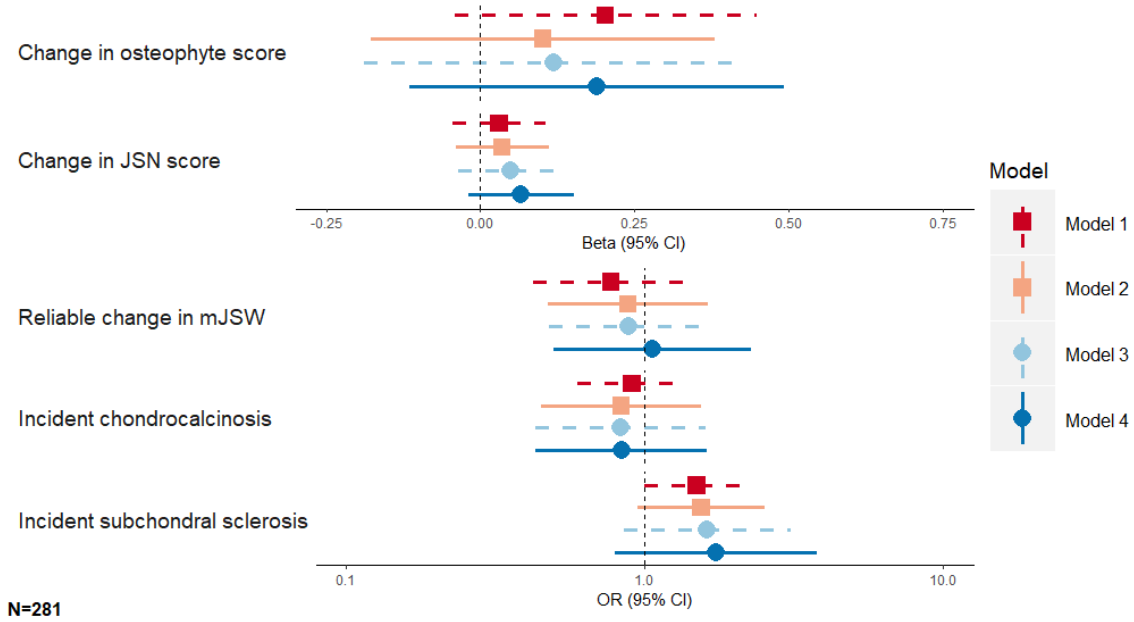

Points for continuous outcomes represent the increase in outcome per SD increase in change of TH-BMD. Points for binary outcomes represent the OR per SD increase in TH-BMD. Horizontal bars represent 95% CIs. Model 1: unadjusted; model 2: adjusted for age and sex (plus baseline score for continuous outcomes); model 3: model 2 plus

height, educational attainment, and menopause; model 4: model 3 plus TBFM. N for reliable change in mJSW=272; N for incident chondrocalcinosis=266; N for incident subchondral sclerosis=279.

Figure 52: Associations between change in L1-BMD status and global OA incidence and progression in the HBM cohort.

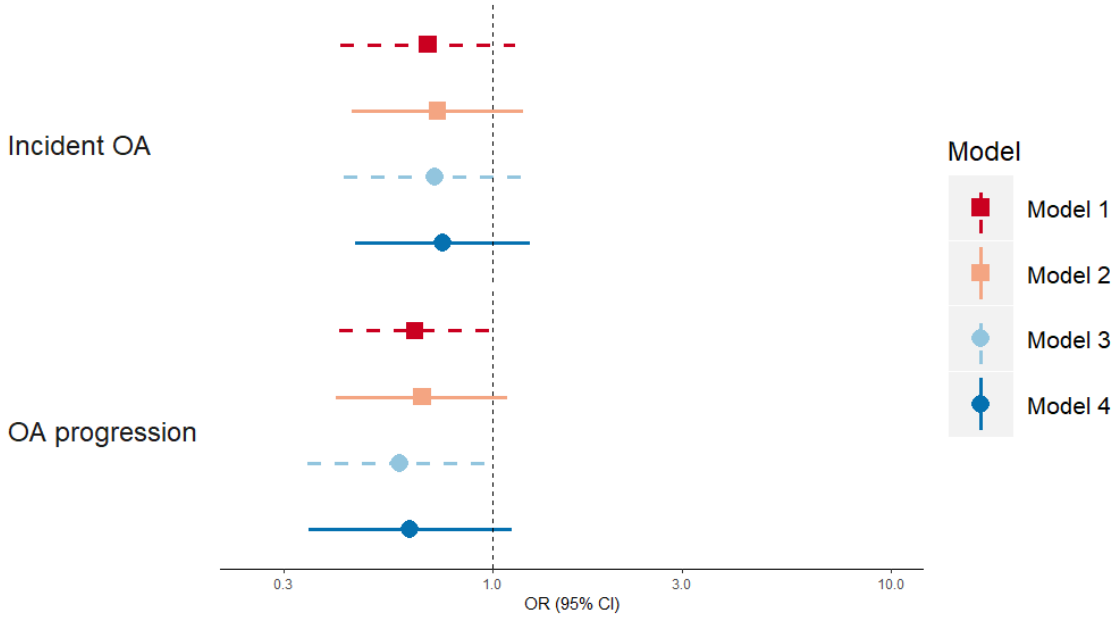

Points represent ORs per SD increase in change in L1-BMD and horizontal bars represent 95% CIs. Model 1: Unadjusted; model 2: adjusted for age and sex; model 3: model 2 plus height, educational attainment, and menopause; model 4: model 3 plus TBFM.

Figure 53: Associations between change in L1-BMD and incident and progressive OA sub-phenotypes in the HBM cohort.

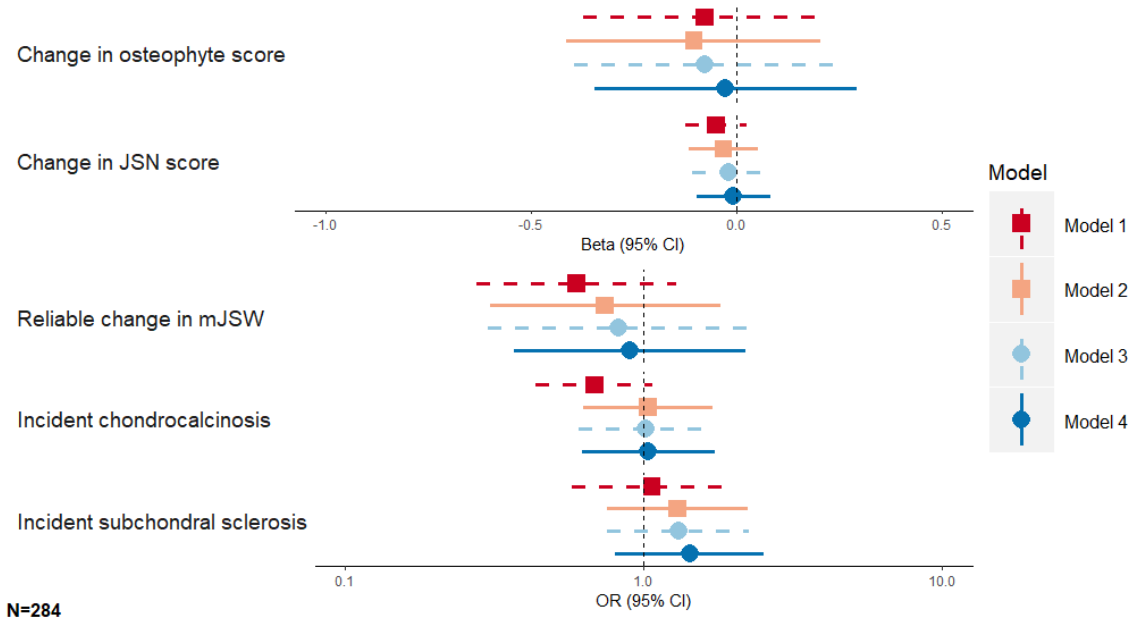

Points for continuous outcomes represent the increase in outcome per SD increase in change of L1-BMD. Points for binary outcomes represent the OR per SD increase in L1-BMD. Horizontal bars represent 95% CIs. Model 1: unadjusted; model 2: adjusted for age and sex (plus baseline score for continuous outcomes); model 3: model 2 plus height, educational attainment, and menopause; model 4: model 3 plus TBFM. N for reliable change in mJSW=273; N for incident chondrocalcinosis=269; N for incident subchondral sclerosis=282.

6.3.6. Investigating dose-response relationships

As one of the Bradford Hill criteria for assessing causality is the presence of a dose-response relationship between exposure and outcome, I next aimed to determine if there was a dose-response relationship between TH-BMD and change in osteophyte score, change in JSN score or WOMAC pain scores. Baseline TH-BMD Z-score was categorized into quartiles, separately for HBM and non-HBM individuals. A non-linear trend between quartile of TH-BMD and change in osteophyte score was observed in the HBM population, with mean change in osteophyte score increasing with increasing quartile until the highest BMD quartile (Figure 54). There was no evidence for an association between BMD quartile and change in osteophyte score in individuals without HBM, nor

was there an association between TH-BMD quartile and change in JSN score in either population. There was strong evidence for a dose-response relationship between BMD and WOMAC pain score in HBM individuals only (*p* for trend <0.001).

Figure 54: Association between quartiles of TH-BMD Z-score and (A) change in osteophyte score, (B) change in JSN score and (C) WOMAC pain scores in individuals with HBM (top) and relatives without HBM (bottom).

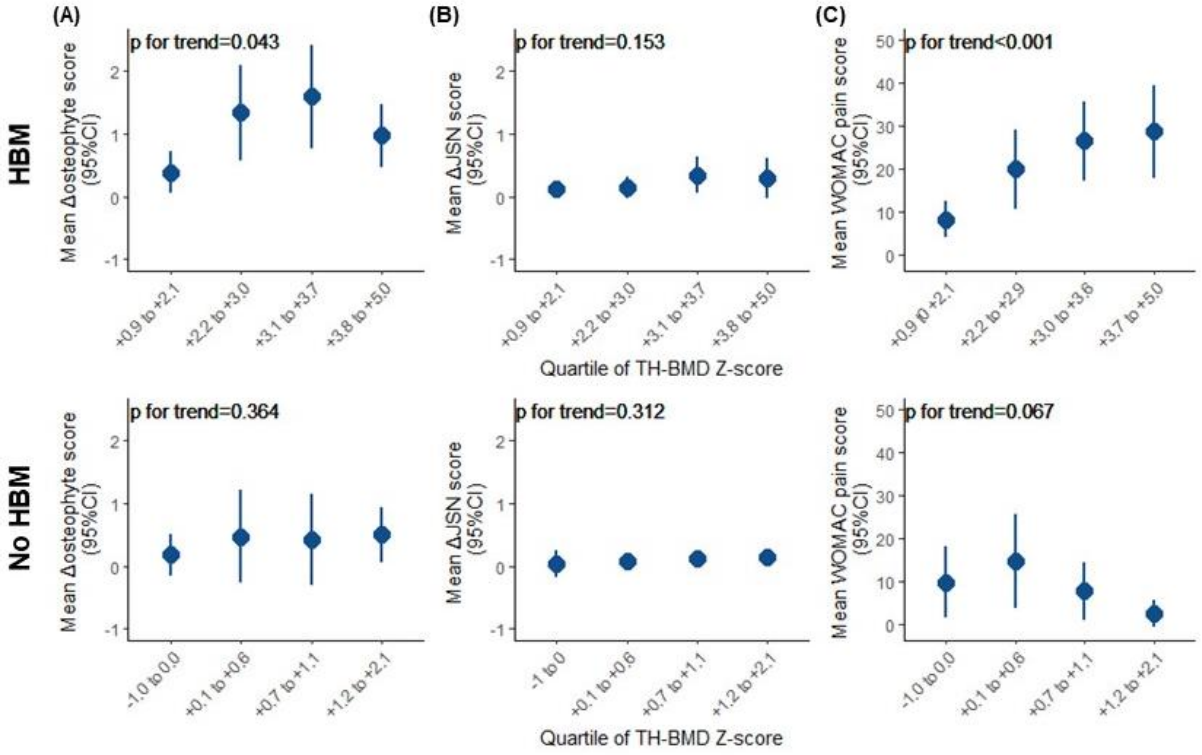

6.3.7. Sensitivity analyses

Including 18 knees with an incident TKR at follow-up as progressive OA cases did not affect conclusions drawn, nor did including three knees with no OA (KL≤2) at baseline and a TKR at follow-up as incident OA cases (Figure 55).

Figure 55: Association between HBM and incident and progressive OA including knees with TKR.

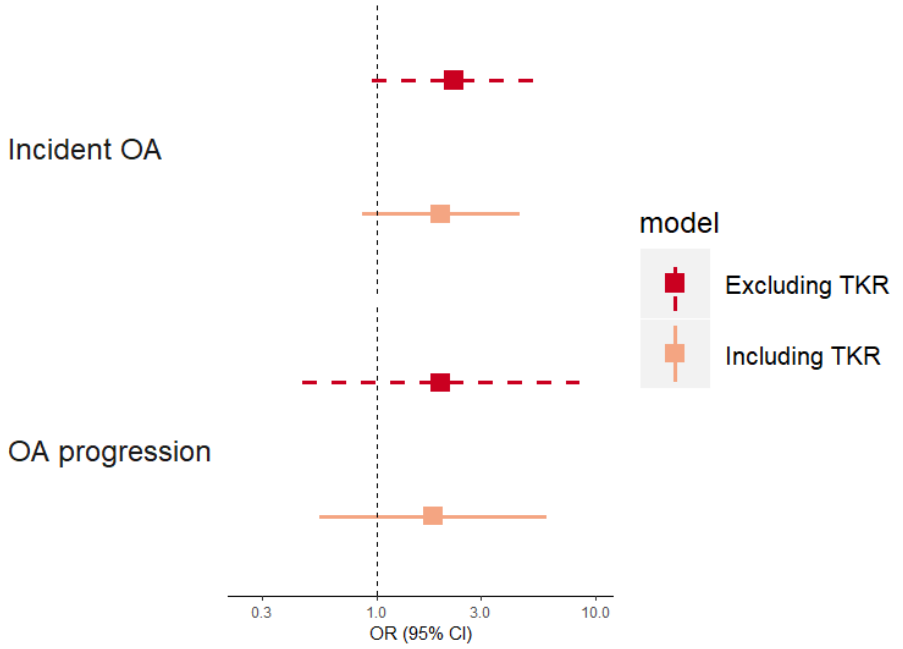

Knees with OA at baseline (KL≥2) and a TKR at follow-up were included as progressive OA cases. Knees without OA at baseline and a TKR at follow-up were including as incident and progressive cases. Adjusted for age, sex, menopause, educational attainment, height, and TBFM. $N_{incident}$=213 without including TKR, 216 including TKR. $N_{progression}$=76 excluding TKR, 94 including TKR.

In person-level analyses, effect sizes were weaker with wider CIs overlapping the null for the relationship with change in osteophyte score ($\beta_{model\ 4}$=0.29 [-0.16,0.75]), although these analyses only included 140 individuals (

Figure 56). There was no evidence for an association between HBM and change in JSN score in person-level analyses, whilst the relationship between HBM and reliable change in mJSW was still present in person-level analyses and of a similar magnitude.

Figure 56: Person-level analyses of the associations between HBM and progression of OA sub-phenotypes.

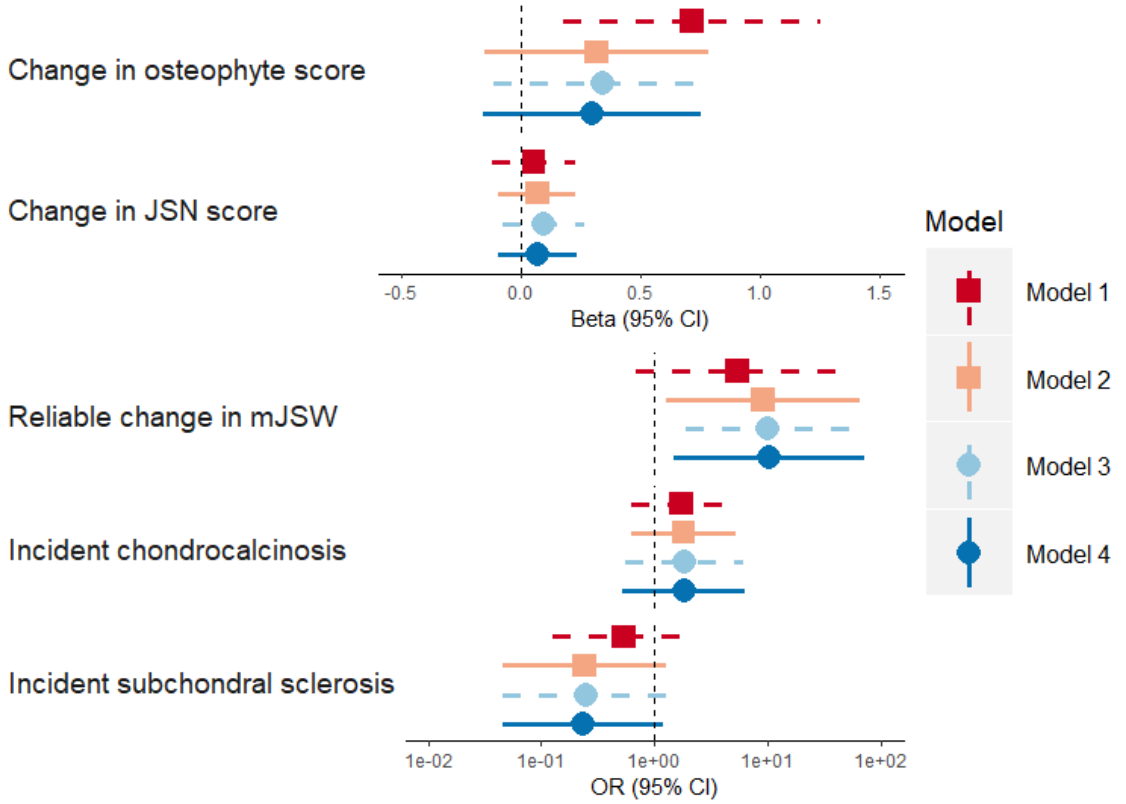

Change in osteophyte and JSN score represent the highest of the two knees. Reliable change in mJSW represents an RCI≤-1.96 in either knee. Incident chondrocalcinosis and subchondral sclerosis represent any incident subchondral sclerosis or chondrocalcinosis in either knee. Model 1: unadjusted; model 2: adjusted for age and sex (and baseline score for change in osteophytes or JSN); model 3: model 2 plus height, menopause, and highest educational attainment; model 4: model 3 plus TBFM. N =140, N_{RCI}=135.

Removing individuals reporting knee procedures did not alter overall conclusions drawn, although this did weaken the evidence for an association between HBM and reliable change in mJSW (Figure 57). Weak evidence for a reduced odds of incident sclerosis in HBM individuals was also present after removing those reporting knee procedures.

Figure 57: Analyses of associations between HBM and OA progression removing individuals who had reported knee procedures.

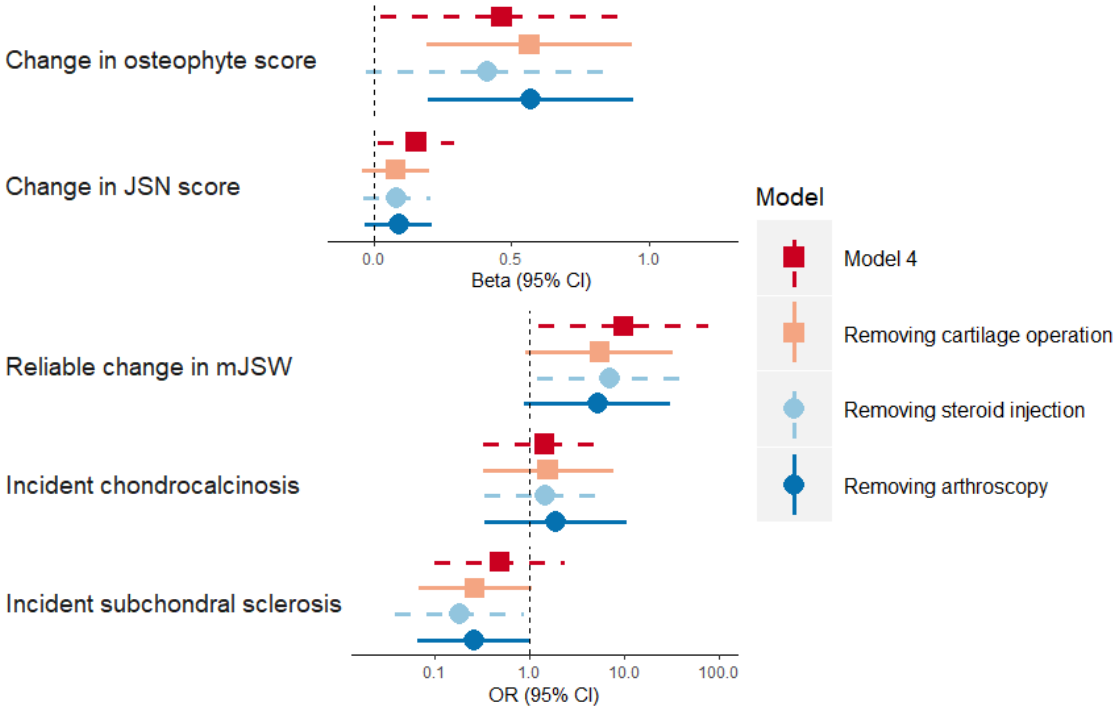

Adjusted for age, sex, baseline score, height, menopause, highest educational attainment and TBFM. $N_{cartilage\ operation}=12$, $N_{knee\ lavage,\ washout,\ arthroscopy}=16$, $N_{steroid\ injection}=9$.

Additional adjustment for metal artefact grade (Figure 58) and maximal tibial plateau width as a marker of bone size (Figure 59) did not alter conclusions.

Figure 58: Associations between HBM and incident and progressive OA sub-phenotypes with additional adjustment for metal artefacts on DXA scans.

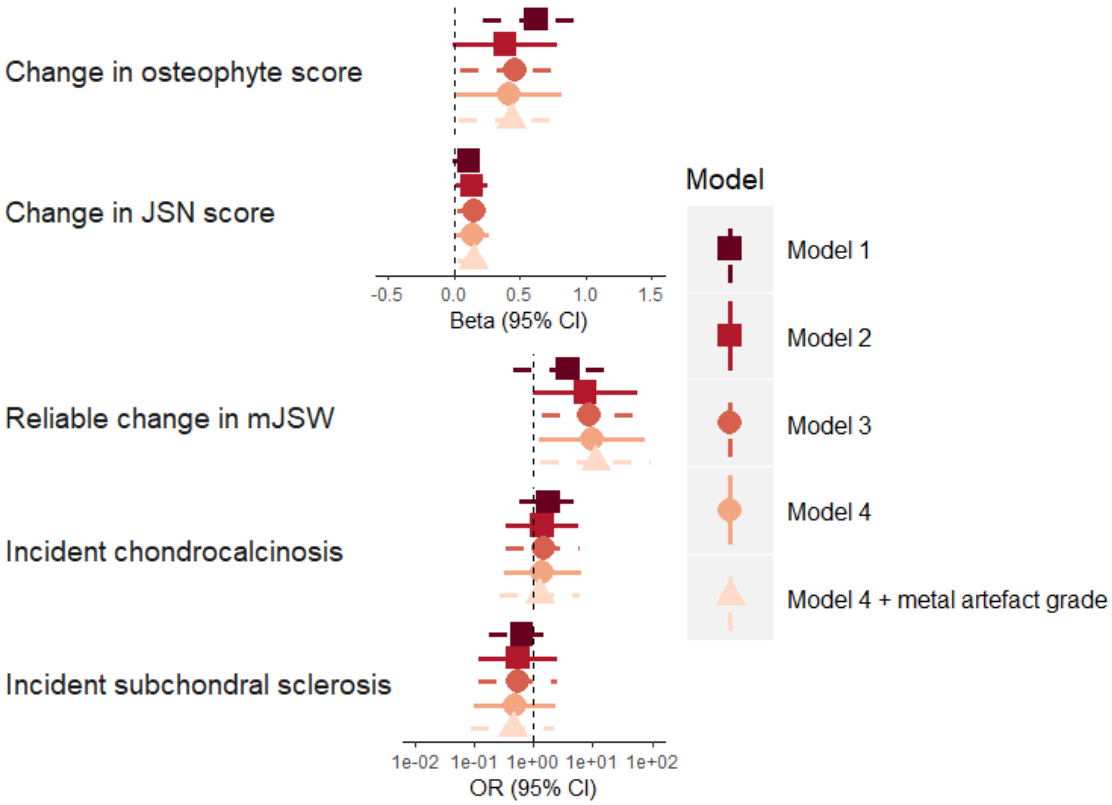

Model 1: unadjusted; model 2: adjusted for age and sex (and baseline score for change in osteophytes or JSN); model 3: model 2 plus height, menopause, and highest educational attainment; model 4: model 3 plus TBFM.

Figure 59: Associations between HBM and incident and progressive OA sub-phenotypes with additional adjustment for maximal tibial plateau width.

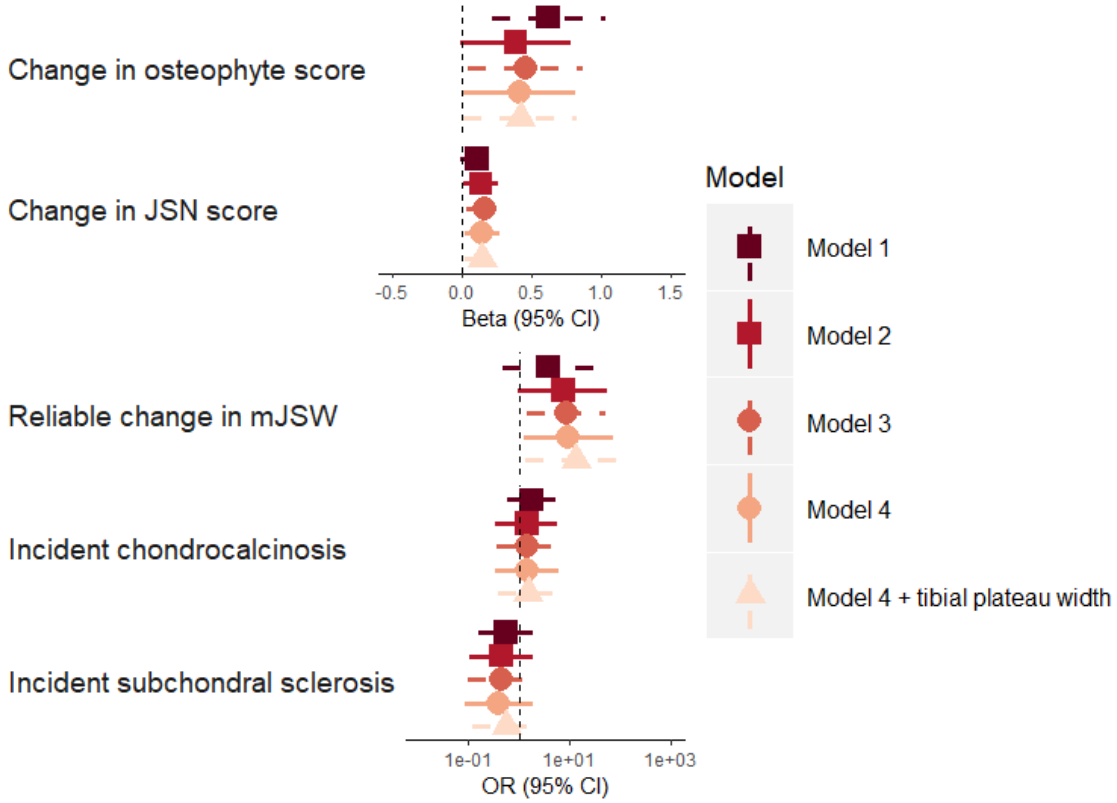

Model 1: unadjusted; model 2: adjusted for age and sex (and baseline score for change in osteophytes or JSN); model 3: model 2 plus height, menopause, and highest educational attainment; model 4: model 3 plus TBFM.

Removing 10 individuals with TB DXA positioning errors, which can lead to loss of TBFM, slightly weakened the evidence for an association with reliable change in mJSW, but otherwise did not alter conclusions (Figure 60), nor did removing 10 individuals visiting a different site at follow-up (Figure 61).

Figure 60: Associations between HBM and incident and progressive OA sub-phenotypes, with and without individuals with TB DXA positioning errors.

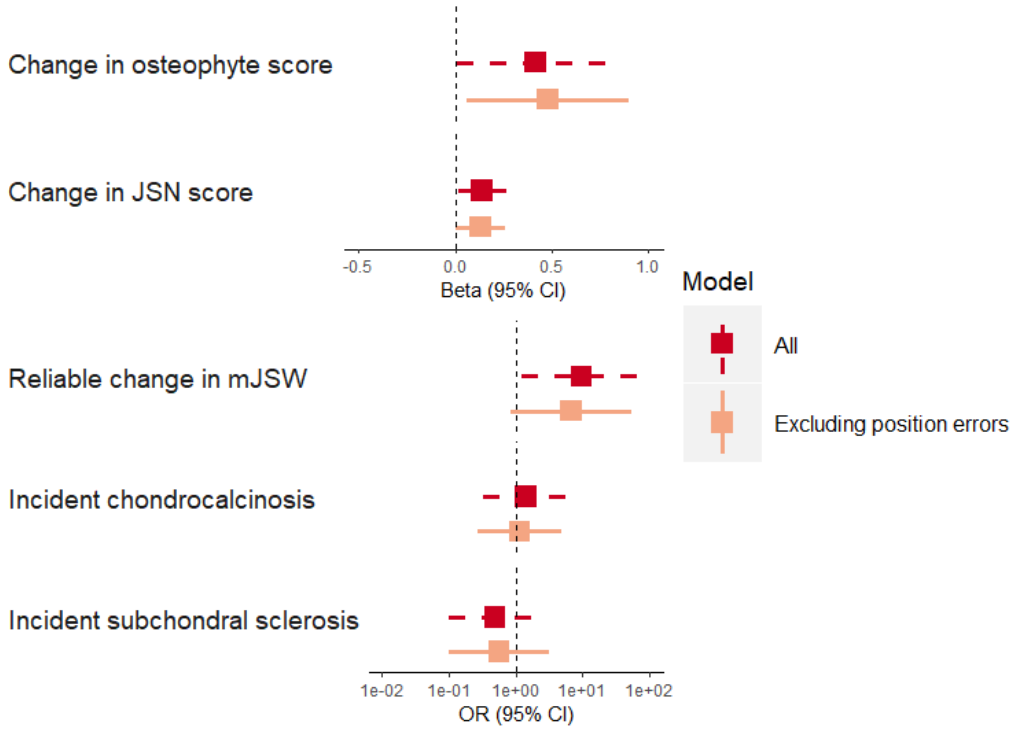

Adjusted for age, sex, menopause, educational attainment, height, and TBFM (model 4).

Figure 61: Associations between HBM and incident and progressive OA sub-phenotypes, with and without individuals attending a different site for follow-up.

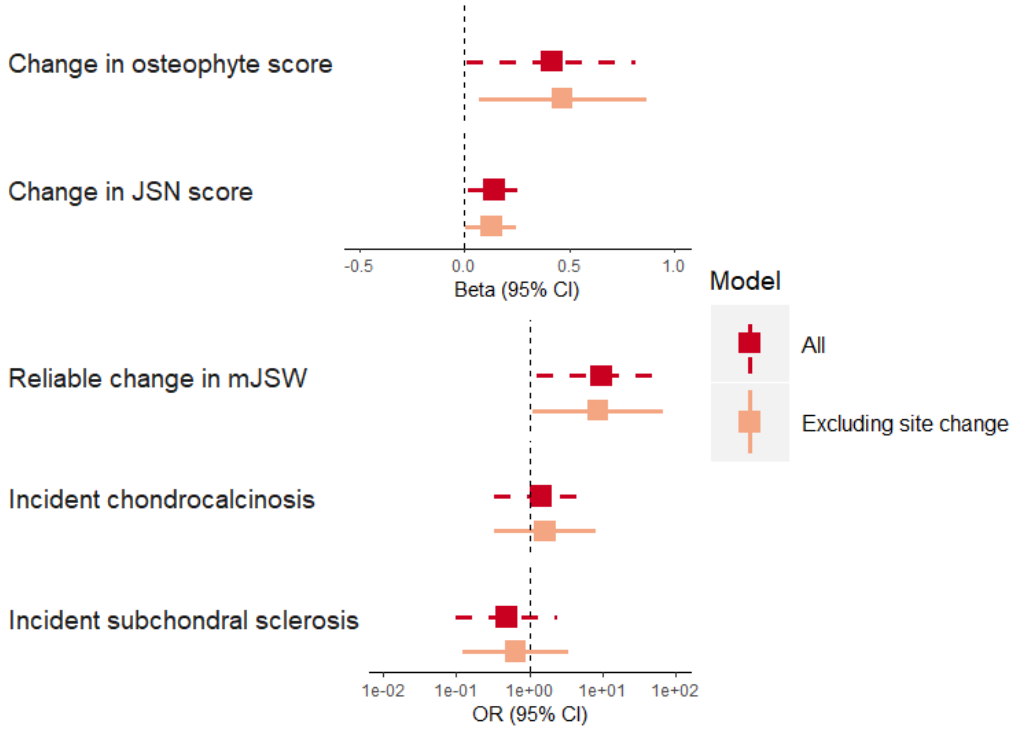

Adjusted for age, sex, menopause, educational attainment, height, and TBFM (model 4).

Evidence for a positive relationship between HBM and osteophyte and JSN progression were observed when using a Poisson model (Figure 62), although CIs overlapped the null ($\beta_{\Delta osteophyte}$= 1.72 [0.88,3.38] and $\beta_{\Delta JSN}$=1.97 [0.99,3.93]). The magnitude of effect was greater for change in JSN, rather than change in osteophytes, when using a Poisson model.

Figure 62: Associations between HBM and change in osteophyte and JSN scores using a Poisson model.

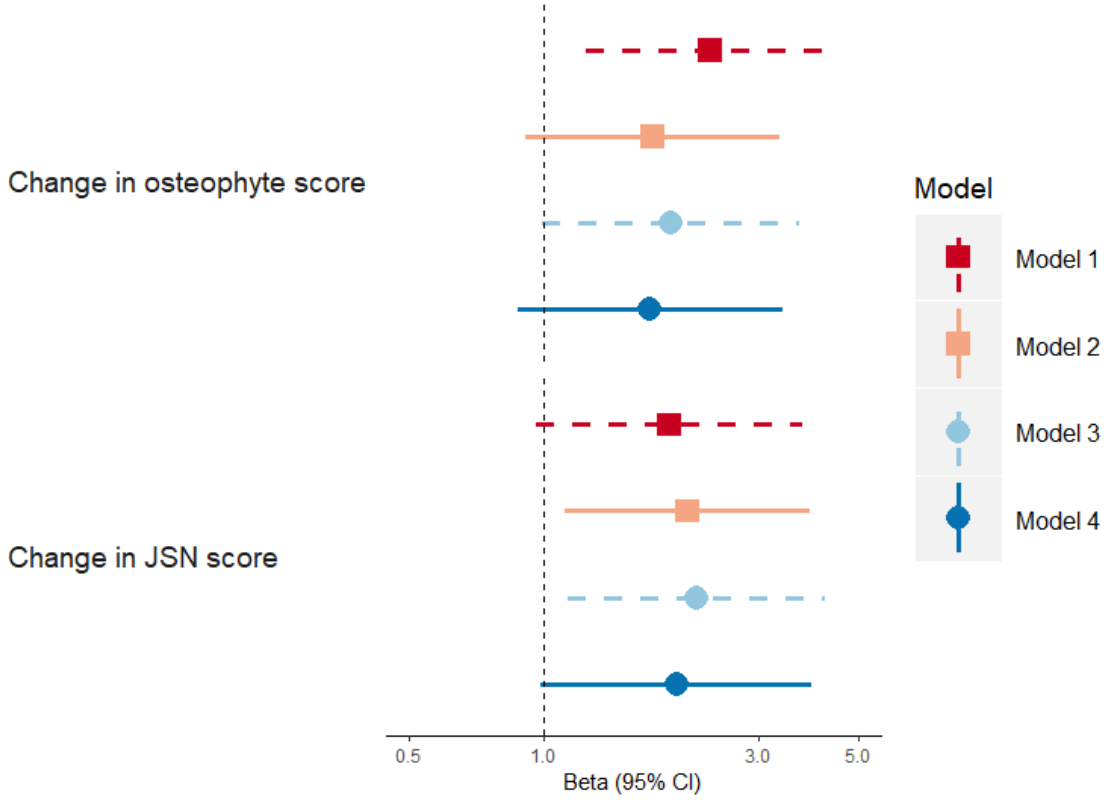

Points represent the difference in predicted count between individuals with and without HBM. Model 1: unadjusted; model 2: adjusted for age and sex (and baseline score for change in osteophytes or JSN); model 3: model 2 plus height, menopause, and highest educational attainment; model 4: model 3 plus TBFM.

6.4. Discussion

6.4.1. Summary of findings

This is the first study to evaluate change in sub-phenotypes of knee OA in a population with HBM. I have identified increased osteophyte development in individuals with HBM, compared to their relatives without HBM, reflecting both initial appearance and subsequent growth of osteophytes. The same direction of effect was observed for JSN, but of weaker magnitude. Furthermore, I have identified that individuals with HBM have worse clinical symptoms of knee OA (pain, stiffness, and limitation of function) and reduced HR-QoL, which is mainly explained by osteophyte severity. These results are consistent with the one general population study which identified a positive relationship between LS-BMD and progression of knee osteophytes (232).

6.4.2. Context of findings

The relationship between high BMI and knee OA is widely acknowledged (78,100). Individuals with HBM have increased TBFM compared to their relatives without HBM (201), with development of HBM likely preceding fat accumulation due to its genetic origin (203). One could therefore hypothesize that increased TBFM mediates the association between HBM and OA progression through increased joint loading, or other metabolic pathways. However, the observed association between HBM and increased osteophyte development was not attenuated by adjustment for TBFM. This finding is consistent with one earlier population-based study of North American women in whom those with low BMD and low BMI had the lowest KL grades, those with high BMD and high BMI had the highest KL grades, and those with low BMI and high BMD had similar KL grades to those with high BMI and low BMD, suggesting that the underlying biological pathway leading to increased osteophyte development in individuals with higher BMD is independent of adiposity (217).

Previous analyses of this HBM population identified an increased presence of enthesophytes, reflecting a 'bone-forming' phenotype (402). Increased osteophyte development over an average of eight years provides further evidence for this phenotype. As both BMD and knee OA are highly heritable (403,404), one possible explanation for this 'bone-forming' phenotype is pleiotropy, whereby the same genetic variants contribute to both phenotypes: genetic analyses in the OAI and JoCo populations identified a positive association between four BMD-associated SNPs and knee OA (262). Such pleiotropy could reflect a causal pathway between BMD and knee OA (*i.e.* vertical pleiotropy), where BMD mediates the relationship between the variants and knee OA, a hypothesis supported by a recent MR study (261), or shared underlying biological pathways contributing to both phenotypes. Individuals with HBM have an over-representation of common BMD-associated variants, including those which annotate to bone-forming pathways *e.g.* Wnt signalling (203), which, as discussed in section 3.3.2, is also linked to OA. However, a more recent genome-wide analysis did not find evidence for a genetic correlation specifically between FN-BMD and knee OA (137).

Differences in subchondral bone texture may explain the positive, albeit weaker, association between HBM and JSN progression (207). Higher trabecular number and thickness plus reduced trabecular separation in subchondral bone have been linked to medial JSN progression (405). Individuals with HBM have greater trabecular density at both the tibia and radius (200); it is currently unknown whether HBM individuals have altered subchondral trabecular bone texture predictive of JSN progression.

An alternative explanation is enhanced endochondral ossification, due to an enrichment of variants annotated to genes involved in this process (203). Endochondral ossification not only contributes to osteophyte formation (406), but also reestablishment of endochondral ossification at the tidemark, which leads to tidemark duplication, reducing the area of non-calcified cartilage (18). However, lack of evidence for a relationship between HBM and incident chondrocalcinosis

suggests that calcification of cartilage is not key to OA pathogenesis in HBM individuals.

In contrast to my analysis, Zhang *et al* found that risk of knee OA progression declined with increasing BMD in the Framingham cohort (229). One possible explanation for this opposite direction of effect is that authors defined knee OA progression as change in KL score in those with prevalent knee OA at baseline. To have prevalent knee OA an individual must present with osteophytes, and to increase KL grade, JSN must occur (30). Therefore, progression from KL=2 to KL=3 relies solely on incident JSN, not worsening of osteophyte grade. Using an increased KL grade to define progression is also vulnerable to bias due to a ceiling effect, as those with a KL grade of 4 at baseline cannot progress. Another potential explanation for the observed inverse association in the Framingham study is 'collider bias', as this analysis was restricted to those with OA at baseline (*i.e.* case only), thereby potentially inducing a negative correlation between BMD and any other variable that influences incident OA. If any such variable is also associated with progression and is not appropriately controlled for in the analysis, a 'backdoor pathway' from high BMD to knee OA progression can be induced. This can manifest as a negative association, when in fact there is none, or even a true positive association (236). Although adjusting for baseline score could also induce collider bias, reassuringly the results did not change between model 1 and model 2.

The weak evidence for an association between HBM and incident OA in this analysis corroborates results from two population-based studies, where an increased risk of incident OA was observed in those with higher BMD (232,234). The weak evidence, with CIs overlapping the null after adjustment for TBFM, is likely due to a lack of power to detect this association due to the small sample size and the fact that the study prevalence of OA was already 33% at baseline, reducing the number of possible incident cases. The small sample size may also explain why I did not observe an association between change in TH-BMD and OA sub-phenotype progression, despite previous studies relating bone loss to prevalent radiographic OA (209) and cartilage loss (407). Unfortunately, I am

unable to make any firm conclusions about relationships between HBM and subchondral sclerosis, which one may expect to be key to OA pathogenesis in HBM individuals, due to the rarity of this phenotype and the lower reliability of gradings.

The finding that individuals with HBM suffer worse clinical symptoms of OA, independent of TBFM, is consistent with a recent MR analysis which identified a causal relationship between FN-BMD and hospital-diagnosed knee OA, even after excluding BMI-associated SNPs from the instrument (261). OA is often diagnosed clinically due to symptoms, such as pain, rather than by radiography (10) and therefore hospital-diagnosed knee OA is likely to reflect symptomatic OA, confirmed by radiographic changes. One Bradford-Hill criterion supporting causal inference is a dose-response relationship (408) and I found increased WOMAC pain scores with increasing TH-BMD quartile, although this relationship was only present in individuals with HBM. The observation that adjustment for osteophyte severity at follow-up attenuated the association between HBM and pain to a greater extent than adjustment for JSN is consistent with the findings of Cicuttini *et al,* who observed that the odds of ever having knee pain was increased in middle-aged women with osteophytes compared to those without osteophytes, and this association was stronger than the association between knee JSN and knee pain (409). However, Neogi *et al* found that JSN, rather than osteophytes, was more strongly related to knee pain in individuals with knees discordant for pain (410).

6.4.3. Strengths of this research

The HBM study is the largest population of individuals with relatively rare, unexplained, generalized HBM (197). Detailed data were collected at baseline and follow-up, allowing for adjustment for *a priori* confounding variables. I analysed change in OA sub-phenotypes separately as well as using KL score, which allowed the identification of the strong relationship with osteophyte development and the weaker relationship with change in JSN. I analysed change in osteophytes and JSN as continuous measures, increasing statistical power to

detect associations, and reducing the possibility of a ceiling effect by increasing the range of possible values to 0-6 for JSN and 0-12 for osteophytes.

6.4.4. Methodological issues and limitations

The method of identifying individuals from NHS DXA databases meant that the average age of the population at baseline was 59 years, ranging from 18 to 90. This meant a large proportion of participants were not able to be followed-up due to death or poor health. Follow-up X-rays could only be performed at seven (albeit the largest) of the original 13 centres, again reducing the size of the follow-up population. Some individuals were able to visit a different centre, but these individuals had to be removed in a sensitivity analysis to confirm that differences in X-ray methodology between baseline and follow-up were not explaining observed associations. Due to the small sample size, I could not evaluate change in osteophyte score in individuals with osteophytes at baseline (*i.e.* progression) separately from those with no osteophytes at baseline (*i.e.* incidence). The stronger magnitude of effect observed for osteophytes, compared to JSN, may purely reflect the greater range of possible values, rather than a stronger effect of BMD on osteophyte progression compared to cartilage loss. I did not read baseline and follow-up radiographs paired and I did observe some negative scores for change in osteophytes and change in JSN, which were included in analyses. Removing these values as 'measurement error' would have biased results as there is likely to be the same proportion of measurement error in the opposite direction, for which I would not be able to account, and may explain why a stronger magnitude of effect was observed for JSN, compared to osteophytes, when using the Poisson model. Reassuringly, the proportion with negative values did not differ between HBM and relatives (data not shown). Radiographic grading of OA sub-phenotypes is subjective; I tried to limit subjectivity by using an established atlas (29). There was good intra-rater and inter-rater agreement for the osteophyte and JSN measures and no evidence of a systematic over-estimation of JSN/osteophytes. Agreement was lower for subchondral sclerosis, but I was not able to draw any clear conclusions about the

relationship between HBM and incident sclerosis due to the rarity of this sub-phenotype. Due to the complexity of the statistical models, age was included as a continuous covariate, under the assumption that it was linearly associated with the outcomes. Although HBM is thought to be largely genetically-determined (203) and therefore a causal relationship between BMD and knee OA progression is inferred, I cannot rule out the possibility that genetic pleiotropy may explain the overlap between BMD and osteophyte progression rather than a causal relationship. Finally, the majority of the HBM population is female, limiting generalizability to male populations.

6.4.5. Future work

There are four key areas of further work to address. The first is to determine if the relationship between high BMD and knee osteophyte progression is a true causal relationship. To do this, a GWAS of osteophyte progression in a large sample with multiple available radiographs would first need to be performed. Summary statistics could then be used for 2SMR analyses. Unfortunately, this analysis was beyond the scope of this PhD. Secondly, the analyses presented in this current chapter should be repeated with hip OA sub-phenotypes as outcomes, to determine if there is an association between HBM and generalized osteophyte progression or whether this is knee-specific (Chapter 7). Thirdly, bidirectional analyses should be performed to determine whether the observed association between HBM and knee OA subphenotype prevalence/progression represents a true causal pathway between BMD and OA, or whether shared underlying biology contributing to both phenotypes explains observational relationships (Chapter 9). Finally, it is important to determine the underlying pathways which contribute to OA sub-phenotype development in HBM (Chapter 10).

6.4.6. Conclusions

In this chapter, I have found evidence that individuals with HBM have increased knee osteophyte and JSN development over eight years, independent of

adiposity, and that a greater number and/or size of osteophytes explains the association between HBM and knee pain, stiffness and functional limitation and reduced HR-QoL.

CHAPTER 7. THE ASSOCIATION BETWEEN HIGH BONE MASS AND HIP OSTEOARTHRITIS PROGRESSION

7.1. Background and aims

As discussed in section 3.1.1, higher BMD has been associated with *prevalent* hip OA in several cross-sectional analyses (208-211,411,412). However, these analyses are complicated by the fact that BMD is often measured at the hip (208-211) and therefore it is hard to determine whether higher BMD is a cause, or feature, of hip OA. Arokoski *et al* identified that FN-BMD was 4% higher in the hip scoring higher for OA in men with discordant hips (218), reflecting a greater FN volume, assessed by MRI. Hip osteophytes can grow across the FN, in a process known as buttressing, which can lead to an increased FN size (226). Despite this, Chaganti *et al* identified a relationship between TH cortical volumetric BMD (measurement of which is not artefactually elevated by bone size) and hip OA in 3,886 men from MrOS (210). Alternatively, BMD can be measured at the LS (208,210,211), which is commonly artefactually elevated by the presence of spinal osteophytes, a feature of spinal OA. However, Nevitt *et al* found that the relationship between LS-BMD and severe hip OA persisted after adjustment for spinal osteophytes. They additionally found a relationship between BMD of the calcaneus (which is less likely to be affected by artefactual elevation due to OA) and hip OA in over 4,000 women from SOF, although of lower magnitude than see for hip BMD (208).

The limitation of not being able to determine the temporal relationship between higher BMD and OA development in cross-sectional analyses can be overcome by studying the HBM population. As discussed in section 3.1.1, individuals with HBM have a greater odds of hip OA than their relatives without HBM and general population controls, reflecting a greater odds of osteophytosis, but not JSN (226). As HBM reflects a generalized phenotype (section 2.3.2), it is unlikely to be an artefact of osteophytosis (197).

As discussed in section 3.1.2, fewer analyses have been performed to determine the relationship between BMD and hip OA *incidence* and *progression*. In Chapter 6, I identified a strong relationship between HBM and worsening *knee* osteophytosis over an average of eight years, with some evidence that knee JSN

incidence and/or progression is increased in HBM individuals. In this chapter, studying the same population, I aim to determine the relationship between HBM and change in radiographic features of *hip* OA over eight years, as well as severity of symptoms of hip OA.

7.2. Methods

7.2.1. Study population

These analyses were performed in the HBM study population (section 2.3.2), who were still alive after eight years, able to be contacted and who consented to pelvic X-rays. Participants aged under 40 years did not have pelvic X-rays and baseline pelvic X-rays were not performed on those who attended the Oxford centre. In total, 363 individuals, aged 40 years or older at baseline, had attended one of the seven centres which was then able to perform follow-up X-rays. Of these individuals, 207 (57%) were still alive and consenting to contact in 2016, of whom 149 (72%) completed the postal questionnaire and attended for follow-up radiographs (Figure 63).

Figure 63: Flowchart of derivation of the HBM cohort follow-up population for the hip analyses.

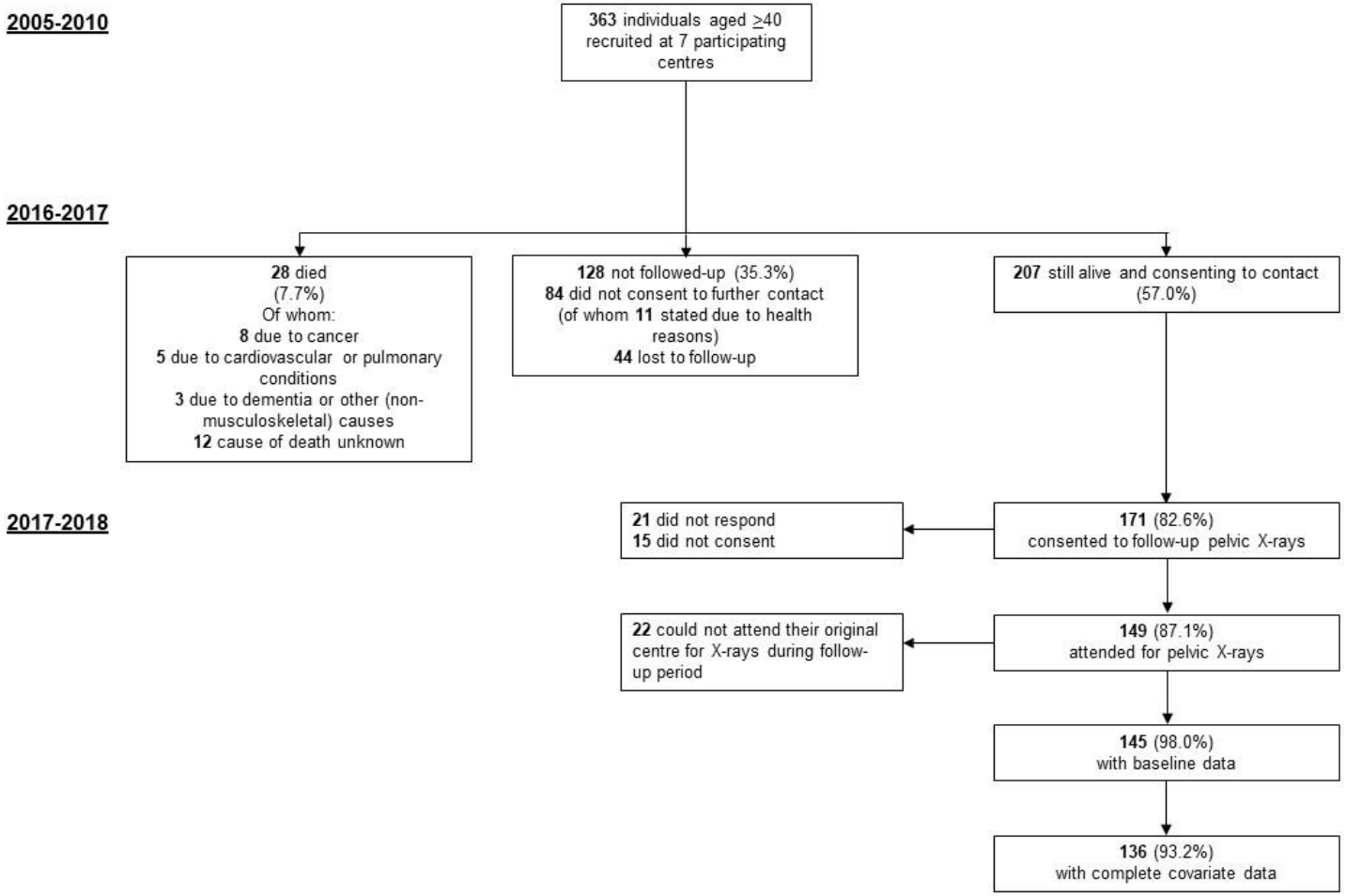

7.2.2. Radiographic OA progression

Methodology for grading radiographic hip OA progression is described in section 4.4. Croft score at baseline and follow-up was used to generate a binary variable for overall OA progression, using Croft≥3 to define OA at baseline and an increase in grade at follow-up. As discussed in Chapter 6, using continuous variables for change in OA sub-phenotypes, instead of binary variables for any progression, avoids the limitations associated with performing a case-only analysis. I therefore summed the semi-quantitative grades for osteophytes at the four regions (inferior and superior, acetabulum and femur) and JSN at the two regions (medial and superior) to generate continuous outcome variables based on change in these summed scores between baseline and follow-up, with higher scores representing worsening osteophytes or JSN. Continuous measures of mJSW at the two timepoints were used to calculate RCI, as outlined in Chapter 6. Table 16 presents a summary of all radiographic variables analysed.

Table 16: Variables generated by Croft scoring and semi-quantitative sub-phenotype grading using the OARSI atlas, and derived variables.

Variable	Grading	Variable used in analysis
Osteoarthritis (Croft score)	0-5	Progressive OA: Croft score ≥3 at baseline and an increase in grade at follow-up Incident OA: Croft score <3 at baseline and ≥3 at follow-up
Osteophytes		
Superior femoral	0-3	Change in osteophyte score: Sum of all semi-quantitative osteophyte grades at follow-up minus the sum at baseline
Medial femoral	0-3	
Superior acetabular	0-3	
Medial acetabular	0-3	
JSN		
Superior	0-3	Change in JSN score: Sum of both semi-quantitative JSN grades at follow-up minus the sum at baseline
Medial	0-3	
Subchondral sclerosis		
Femoral	0, 1	Incident sclerosis: no sclerosis (femoral or acetabular) at baseline and any sclerosis at follow-up
Acetabular	0, 1	
Subchondral cysts	0, 1	Incident cysts: no cyst at baseline and cyst at follow-up
Superior mJSW	Continuous	Change in mJSW: mJSW at follow-up minus mJSW at baseline True JSN: Reliable change index ≤-1.96

7.2.3. Clinical features of hip OA progression

Hip pain, stiffness and limitation of function were determined using the WOMAC questionnaire, as outlined in section 4.2.

7.2.4. Covariates

Age and sex were considered *a priori* confounders, as well as baseline radiographic sub-phenotype grade for osteophyte and JSN outcomes. Height and TBFM were included in the final model to determining their potential confounding or mediating effect. Time between baseline and follow-up, menopausal status and HRT use, history of smoking, baseline PA, education and steroid use were all investigated as potential confounders by determining their relationships with the OA sub-phenotype outcomes.

7.2.5. Statistical analysis

Statistical analysis was performed as outlined for knee OA (sub-phenotype) progression (Chapter 6). Distributions of continuous outcomes are presented in Figure 64-Figure 66. Due to the lower numbers with complete data for hip, compared to the knee, analyses, less variables were included in the statistical models to reduce complexity. Model 1 was unadjusted, model 2 was adjusted for age, sex, baseline score and follow-up time and model 3 was additionally adjusted for height and TBFM.

Figure 64: Distribution of change in osteophyte score between baseline and follow-up in the HBM cohort.

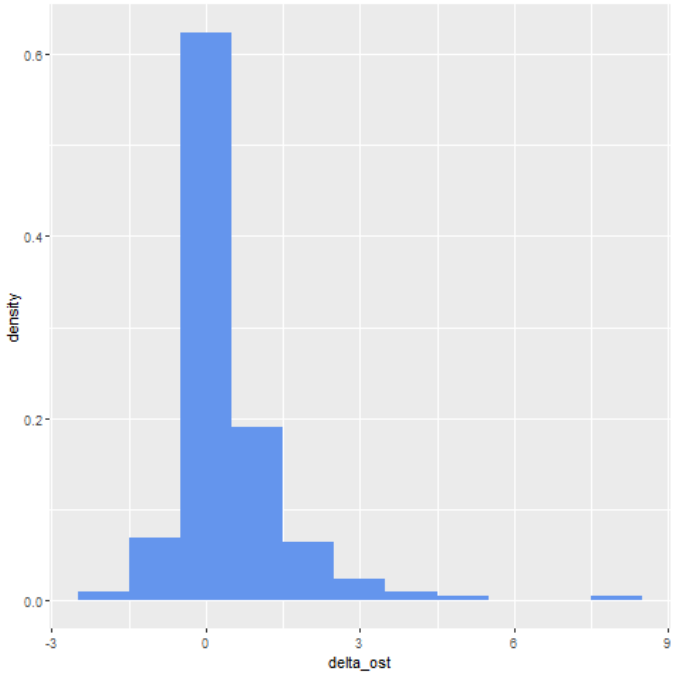

Figure 65: Distribution of change in JSN score between baseline and follow-up in the HBM cohort.

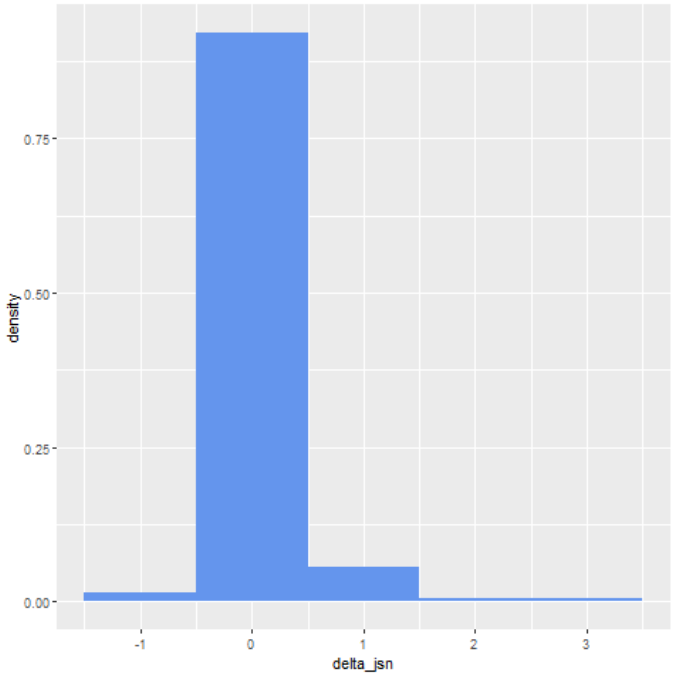

Figure 66: Distribution of change in mJSW between baseline and follow-up in the HBM cohort.

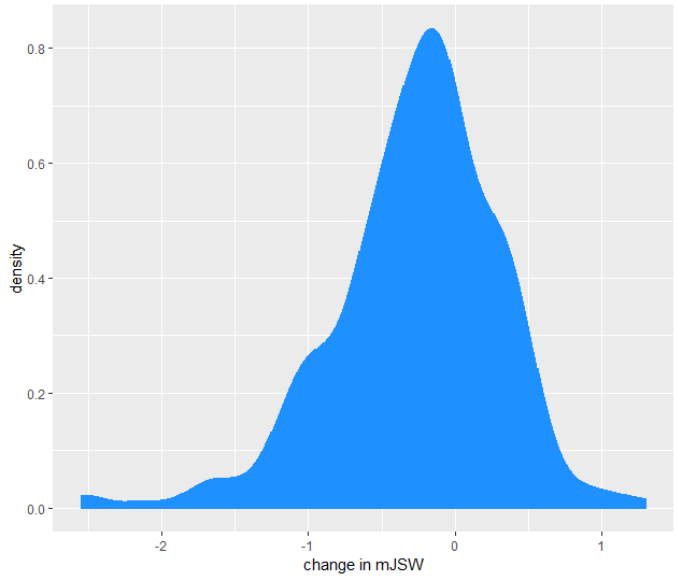

7.2.6. Sensitivity analyses

I performed the following sensitivity analyses to determine the reliability of results:

1. As hips with THR were excluded from analysis, but THRs are likely to be performed due to severe OA, analyses were repeated including those with a Croft grade <3 at baseline and a non-fracture-related THR at follow-up, and counting these as incident and progressive OA cases (assuming rapid OA progression led to a THR within eight years of OA development). Individuals with Croft≥3 at baseline and a non-fracture related THR at follow-up were included as progressive cases.
2. Person-level analyses, using the sum of the osteophyte/JSN scores from the two hips and any incident OA in either hip.
3. Additional adjustment for metal artefacts on DXA scans (section 4.3.1).
4. Removal of individuals with positioning errors leading to loss of fat mass from the DXA image (section 4.3.2).
5. Removal of those visiting a different site for follow-up imaging.
6. Poisson regression analyses, recoding negative values as 0, to check that conclusions were not invalid due to skewed outcome variables.

7. Additional adjustment for FN area (measured at follow-up) to check that associations between HBM and OA sub-phenotype progression were not explained by bone size.

7.3. Results

7.3.1. Descriptives of the HBM radiographic hip OA follow-up population

Complete baseline and follow-up radiographic data were available for 145 individuals, with 64% having HBM. There was no difference in the proportion of HBM individuals in the population with or without follow-up data. Those with follow-up data were younger, were less likely to have had hip OA at baseline, to have ever smoked, to be postmenopausal, but they were more physically active (Table 17).

Table 17: Baseline descriptives of those with and without complete radiographic hip follow-up data in the HBM cohort.

	All **N=363**	**With follow-up data N=145**	**Without follow-up data N=218**	***p*-value for difference**
		N (%)		
High Bone Mass	237 (65.3)	92 (63.5)	145 (66.5)	0.548
Female	240 (66.1)	105 (72.4)	135 (61.9)	0.039
Postmenopausal	197 (84.2)	81 (77.1)	116 (89.9)	0.008
History of smoking	208 (58.8)	74 (51.0)	134 (64.1)	0.014
Alcohol consumption				0.154
None	79 (22.3)	25 (17.2)	54 (25.7)	
Occasional	41 (11.6)	17 (11.7)	24 (11.4)	
Regular	185 (52.1)	85 (58.6)	100 (47.6)	
Heavy	50 (14.1)	18 (12.4)	32 (15.2)	
Physical activity category				0.009
Low	58 (18.1)	16 (11.4)	42 (23.2)	
Moderate	112 (34.9)	47 (33.6)	65 (35.9)	
High	151 (47.0)	77 (55.0)	74 (40.9)	
Hip Osteoarthritis (Croft≥3)	87 (27.5)	28 (19.9)	59 (33.7)	0.006
Any hip osteophyte	248 (77.5)	102 (71.3)	146 (82.5)	0.017
Moderate hip osteophyte	82 (26.0)	30 (21.6)	52 (29.6)	0.110
Hip joint space narrowing	98 (30.8)	36 (25.5)	62 (35.0)	0.068
		Mean (SD)		
Age, years	62.8 (12.0)	59.6 (10.2)	64.9 (12.6)	<0.001
Height, cm	168.1 (9.7)	167.6 (9.5)	168.4 (9.8)	0.476
Weight, kg	83.4 (16.5)	82.1 (16.9)	84.2 (16.1)	0.222
L1 Z-score	2.7 (2.1)	2.5 (2.0)	2.9 (2.1)	0.069
Maximum total hip Z-score[a]	2.1 (1.5)	2.1 (1.5)	2.1 (1.5)	0.953

[a]*Maximum value for TH-BMD of left and right sides.*

Of the 136 individuals who also had complete covariate data, HBM individuals were more commonly female and postmenopausal, with a higher BMI at baseline and higher TBFM at follow-up (Table 18). As expected, mean baseline TH and L1-BMD were higher in HBM individuals compared to relatives without HBM. Relatives without HBM were more highly educated and were taller at baseline.

Table 18: Descriptives of the radiographic hip follow-up population with complete covariate data from the HBM cohort.

	All N=136	**HBM N=86**	**Relatives without HBM N=50**	***p*-value for difference**
		N (%)		
Female gender	98 (72.1)	73 (84.9)	25 (50.0)	<0.001
Postmenopausal[b]	75 (76.5)	59 (80.8)	16 (64.0)	0.087
Menopause transition during follow-up period	11 (11.2)	6 (8.2)	5 (20.0)	0.177
History of HRT use[f]	49 (50.0)	39 (53.4)	10 (40.0)	0.508
History of smoking[f]	66 (48.9)	42 (49.4)	24 (48.0)	0.874
Physical activity category[b]				
Low	14 (10.7)	9 (11.0)	5 (10.2)	
Medium	46 (35.1)	26 (31.7)	20 (40.8)	0.567
High	71 (54.2)	47 (57.3)	24 (49.0)	
Education category[f]				
Up to GCSE/ O level	55 (42.0)	42 (50.0)	13 (27.7)	
A level or equivalent	26 (19.9)	17 (20.2)	9 (19.2)	0.019
Degree or equivalent	50 (38.2)	25 (29.8)	25 (53.2)	
		Mean (SD)		
Age, years[b]	59.2 (10.2)	60.2 (9.9)	57.5 (10.6)	0.136
Height, cm[b]	167.8 (9.6)	166.1 (8.4)	170.8 (10.8)	0.005
Weight, kg[b]	81.5 (17.0)	82.1 (16.0)	80.6 (18.7)	0.619
BMI (kg/m^2)[b]	28.9 (5.5)	29.8 (5.6)	27.5 (5.1)	0.017
TBFM (kg)[f]	31.6 (10.6)	33.0 (10.9)	29.1 (9.5)	0.035
TH-BMD, g/cm^2 [b]	1.143 (0.182)	1.242 (0.129)	0.976 (0.131)	<0.001
L1-BMD, g/cm^2 [b]	1.255 (0.215)	1.377 (0.149)	1.049 (0.141)	<0.001
FN area[f], cm^2	5.28 (0.52)	5.20 (0.52)	5.40 (0.51)	0.029
Follow-up time, years	8.2 (1.0)	8.2 (0.7)	8.2 (1.4)	0.817

[b]*assessed at baseline,* [f]*assessed at follow-up.*

7.3.2. Prevalence, incidence, and progression of hip OA sub-phenotypes

Due to the rarity of baseline OA in this population (6.5%), it was not possible to analyse overall OA progression (Table 19). Incidence and prevalence of both subchondral sclerosis and subchondral cysts were too low to analyse ($N \leq 5$) and

the prevalence of true JSN, based on RCI, was too low in the non-HBM relatives to draw any meaningful conclusions.

Table 19: Proportion of all hips with baseline, follow-up, incident, and progressive OA (sub-phenotypes) in the HBM cohort follow-up population.

	All hips		**HBM hips**		**Non-HBM hips**	
	Total N	**N (%)**	**Total N**	**N (%)**	**Total N**	**N (%)**
OA (Croft≥3)						
Baseline	285	22 (7.7)	179	13 (7.3)	106	9 (8.5)
Follow-up	275	33 (12.0)	173	24 (13.9)	102	9 (8.8)
Incident	257	18 (7.0)	162	15 (9.3)	95	3 (3.2)
Progressive	18	5 (27.8)	11	2 (18.2)	7	3 (42.9)
Hip replacement (identified on radiograph)						
Baseline	290	5 (1.7)	184	5 (2.7)	106	0
Follow-up	290	15 (5.2)	184	11 (6.0)	106	4 (3.8)
Incident	285	10 (3.5)	179	6 (3.4)	106	4 (3.8)
Subchondral sclerosis						
Baseline	285	4 (1.4)	179	3 (1.7)	106	1 (0.9)
Follow-up	275	4 (1.5)	173	3 (1.7)	102	1 (1.0)
Incident	273	3 (1.1)	171	2 (1.2)	102	1 (1.0)
Subchondral cysts						
Baseline	283	1 (0.4)	178	0	105	1 (1.0)
Follow-up	275	5 (1.8)	173	3 (1.7)	102	2 (2.0)
Incident	275	5 (1.8)	173	3 (1.7)	102	2 (2.0)
Osteophyte score						
Baseline	285		179		106	
0		203 (71.2)		126 (70.4)		77 (72.6)
1-4		75 (26.3)		50 (27.9)		25 (23.6)
≥5		7 (2.5)		5 (2.8)		4 (3.8)
Follow-up	275		173		102	
0		161 (58.6)		94 (54.3)		67 (65.7)
1-4		105 (38.2)		73 (42.2)		32 (31.4)
≥5		9 (3.3)		6 (3.5)		3 (2.9)
Delta	275		173		102	
<1		201 (73.1)		121 (69.9)		80 (78.4)
1		48 (17.5)		32 (18.5)		16 (15.7)
>1		26 (9.5)		20 (11.6)		6 (5.9)
JSN score						
Baseline	285		179		106	
0		253 (88.8)		160 (89.4)		93 (87.7)
1-2		27 (9.5)		16 (8.9)		11 (10.4)
≥3		5 (1.8)		3 (1.7)		2 (1.9)
Follow-up	275		173		102	
0		241 (87.6)		149 (86.1)		92 (90.2)
1-2		28 (10.2)		20 (11.6)		8 (7.8)
≥3		6 (2.2)		4 (2.3)		2 (2.0)
Delta	275		173		102	
<1		261 (94.9)		161 (93.1)		100 (98.0)
1		12 (4.4)		10 (5.8)		2 (2.0)
>1		2 (0.7)		2 (1.2)		0 (0.0)
True JSN	245	16 (6.5)	151	13 (8.6)	94	3 (3.2)

	Total N	Mean (SD)	Total N	Mean (SD)	Total N	Mean (SD)
mJSW						
Baseline	283	3.874 (0.791)	179	3.910 (0.784)	104	3.811 (0.802)
Follow-up	247	3.626 (0.842)	151	3.605 (0.820)	96	3.659 (0.877)
Delta	245	-0.275 (0.565)	151	-0.328 (0.606)	94	-0.190 (0.485)
	All individuals		**HBM individuals**		**Relatives without HBM**	
	Total N	**Median (IQR)**	**Total N**	**Median (IQR)**	**Total N**	**Median (IQR)**
WOMAC at follow-up						
Pain	145	0 (0, 25)	92	10 (0, 35)	53	0 (0, 15)
Function	145	3.6 (0, 25)	92	10.7 (0, 30.4)	53	0 (0, 14.3)
	Total N	**N (%)**	**Total N**	**N (%)**	**Total N**	**N (%)**
Hip replacement (self-reported)	145	16 (11.0)	92	13 (14.1)	53	3 (5.7)

7.3.3. Determining covariates

To determine which of the potential covariates (highlighted in section 7.2.4) should be included in analyses, associations between the potential covariates and the three main outcomes (change in osteophyte score [continuous], change in JSN score [continuous] and incident OA [binary]) were determined by GEE linear (for continuous variables) and logistic (for binary outcomes) regression. Low numbers meant very few associations were observed, including lack of evidence for associations with *a priori* confounders sex and weight (Table 20). There was evidence for a greater mean change in JSN score in those with a history of steroid use and a much higher odds of incident OA. Follow-up time was strongly related to change in JSN score. This was not attenuated by adjustment for assessment centre (β=0.04 [0.02,0.06]), meaning this relationship does not reflect systematic differences in follow-up time between study centres. I therefore decided to include age, sex, baseline score (for the continuous outcomes) and follow-up time (except for cross-sectional WOMAC variables for which follow-up time was not included) in the first adjusted model (model 2) before adjusting for height and TBFM in model 3. To limit model complexity, I adjusted for history of steroid use

in sensitivity analyses (section 7.3.8).

Table 20: Associations between potential covariates and hip OA outcomes in the HBM cohort.

	Change in osteophyte score		**Change in JSN grade**		**Incident OA**	
	β (95% CI)	***p***	**β (95% CI)**	***p***	**OR (95% CI)**	***p***
Female	0.221 (-0.135, 0.576)	0.224	-0.010 (-0.129, 0.109)	0.868	2.08 (0.58, 7.52)	0.262
Ever smoked	0.014 (-0.308, 0.335)	0.934	0.019 (-0.084, 0.123)	0.714	1.75 (0.59, 5.18)	0.316
Alcohol consumption at baseline						
None	*Ref*		*Ref*		*Ref*	
Occasional	0.621 (0.066, 1.180)	0.028	0.081 (-0.064, 0.227)	0.273	5.57 (0.53, 59.1)	0.154
Regular	0.180 (-0.125, 0.484)	0.248	0.051 (-0.032, 0.133)	0.231	3.08 (0.38, 25.4)	0.295
Heavy	0.538 (-0.199, 1.270)	0.152	0.049 (-0.180, 0.279)	0.673	0.89 (0.05, 14.6)	0.933
Physical activity category at baseline						
Low	*Ref*		*Ref*		*Ref*	
Medium	-0.227 (-0.905, 0.450)	0.511	-0.010 (-0.290, 0.270)	0.943	0.62 (0.11, 3.49)	0.584
High	-0.153 (-0.786, 0.480)	0.636	-0.037 (-0.304, 0.230)	0.785	0.40 (0.07, 2.27)	0.303
Education						
up to GCSE/ O level	*Ref*		*Ref*		*Ref*	
A level	-0.037 (-0.365, 0.291)	0.826	-0.003 (-0.124, 0.119)	0.966	1.16 (0.30, 4.57)	0.828
Degree	-0.107 (-0.543, 0.329)	0.631	0.012 (-0.121, 0.146)	0.856	0.59 (0.16, 2.22)	0.439
Postmenopausal at baseline	-0.154 (-0.754, 0.447)	0.616	-0.028 (-0.207, 0.151)	0.759	7.71 (0.98, 60.7)	0.052
History of HRT use at follow-up	0.191 (-0.184, 0.566)	0.318	-0.007 (-0.128, 0.113)	0.906	1.71 (0.48, 6.08)	0.409
History of steroid use at follow-up	0.553 (-0.071, 1.180)	0.082	0.305 (0.100, 0.509)	0.004	8.01 (2.37, 27.1)	0.001
Age at baseline, years	0.004 (-0.013, 0.021)	0.622	0.005 (-0.001, 0.010)	0.104	1.08 (1.04, 1.12)	$3x10^{-4}$
Follow-up time, years	0.002 (-0.060, 0.064)	0.944	0.047 (0.029, 0.066)	$5x10^{-7}$	1.72 (0.92, 3.20)	0.089
Height at baseline, cm	-0.009 (-0.025, 0.007)	0.273	-0.002 (-0.006, 0.003)	0.536	0.96 (0.90, 1.02)	0.145
Weight at baseline, kg	-0.002 (-0.010, 0.006)	0.603	-0.001 (-0.003, 0.002)	0.649	0.99 (0.97, 1.01)	0.282

7.3.4. HBM and global radiographic hip OA incidence and progression

Out of 290 hips with repeat radiographs, hip OA was observed in 7.7% of all hips at baseline and 12.0% of all hips at follow-up (Table 19). Out of the 257 hips without OA at baseline, 7.0% developed OA. There was no clear evidence that HBM was associated with an increased odds of overall incident OA measured by Croft score, before (model 1: OR=2.54 [0.66,9.71], Figure 67) or after adjustment for age, sex, and follow-up time (model 2: 1.65 [0.41,6.70]). Due to the low prevalence of hip OA at baseline in the population with follow-up data, I was unable to analyse a binary variable for overall hip OA progression based on a Croft$\geq$3. Using a Croft score $\geq$1 to define OA at baseline, 82 hips were eligible to progress, of which 16 had a higher Croft score at follow-up (12 with HBM). The fully adjusted OR for hip OA progression (model 3) was 4.14 (0.81,21.3).

7.3.5. HBM and the combined incidence and progression of radiographic hip OA sub-phenotypes

Of the total population analysed, 28.8% had at least one osteophyte at baseline, rising to 41.5% at follow-up (Table 19). JSN was much less prevalent than osteophytes at baseline and follow-up (11.3% and 12.4%, respectively). In unadjusted analyses, individuals with HBM had a greater change in osteophyte and JSN score between baseline and follow-up than those without HBM ($\beta_{osteophyte}$=0.30 [0.05,0.54], p=0.019 and β_{JSN}=0.09 [0.01,0.16], p=0.019, β reflects the mean difference in change in score between those with and without HBM). These associations persisted after adjustment for age, sex, follow-up time, baseline score, height and TBFM (model 3,Figure 67). HBM was not associated with change in mJSW ($\beta_{model\ 3}$=-0.07 [-0.24,0.09]).

Figure 67: Associations between HBM and incident OA and change in OA sub-phenotypes.

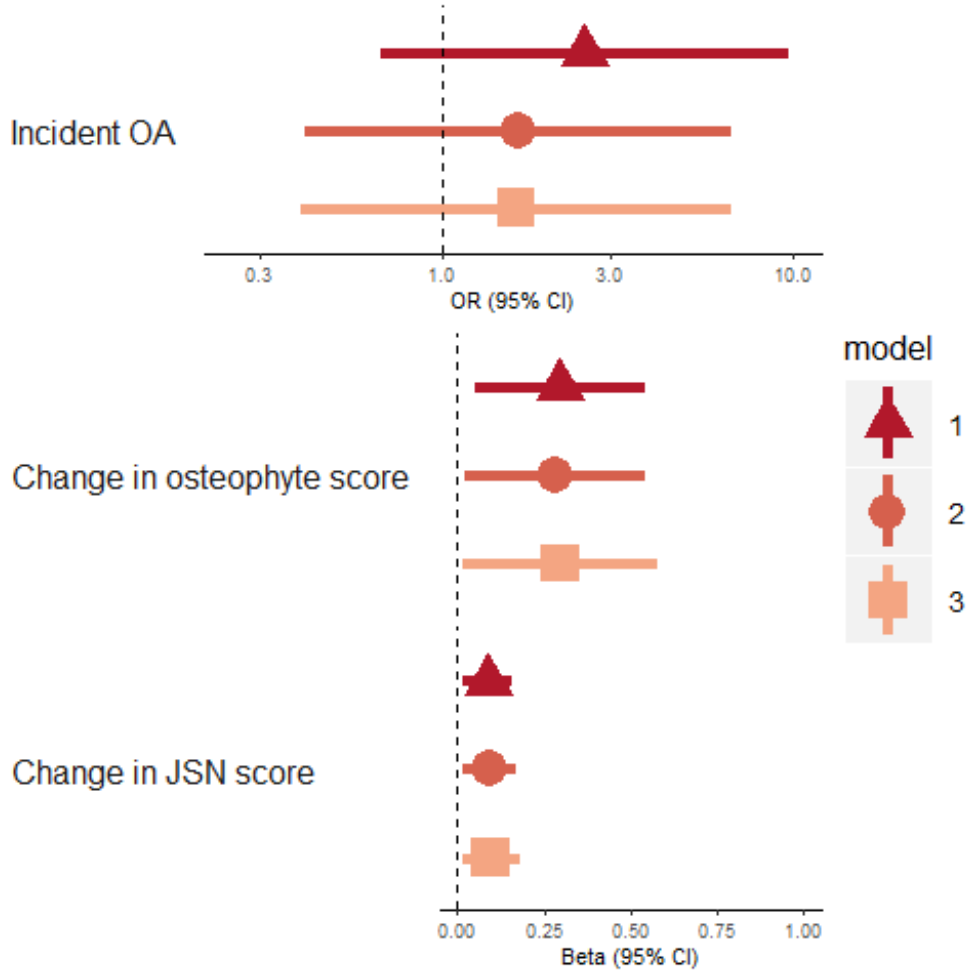

Points for continuous outcomes represent the difference in mean outcome between individuals with and without HBM (e.g. a beta of 1 for change in osteophyte score would represent a 1-point greater increase in summed osteophyte score, which is the equivalent of the appearance of one additional osteophyte or the increase in size of an osteophyte already present). Points for binary outcomes represent the OR for individuals with HBM compared to their relatives without HBM. Horizontal bars represent 95% CIs.

Model 1: unadjusted, model 2: adjusted for age, sex, and follow-up time (plus baseline score for continuous outcomes), model 3: model 2 plus height and TBFM.

$N_{incident\ OA}$*=248;* $N_{continuous\ outcomes}$*=263.*

7.3.6. HBM and clinical features of hip OA

HBM was associated with 12-point (95% CI: 5,18) higher WOMAC pain scores and 13-point (7,19) higher function scores in unadjusted analyses. Adjustment for age, sex, height and TBFM attenuated these relationships by approximately one-third to one-half (β_{pain}=6.4 [-1.4,14.2], p=0.105 and $\beta_{function}$=8.3 [0.7,15.8], p=0.032,

β represents the difference in mean WOMAC score between those with and without HBM). Further adjustment for osteophyte or JSN score at follow-up did not appear to explain these relationships (Figure 68). There was some weak evidence supporting an increased odds of self-reported hip replacement in individuals with HBM who completed the follow-up questionnaire, compared to those without HBM (age, sex, height and TBFM-adjusted OR=4.27 [0.94,19.5], *p*=0.061, N=148).

Figure 68: Associations between HBM status and WOMAC pain, stiffness, and function subscales.

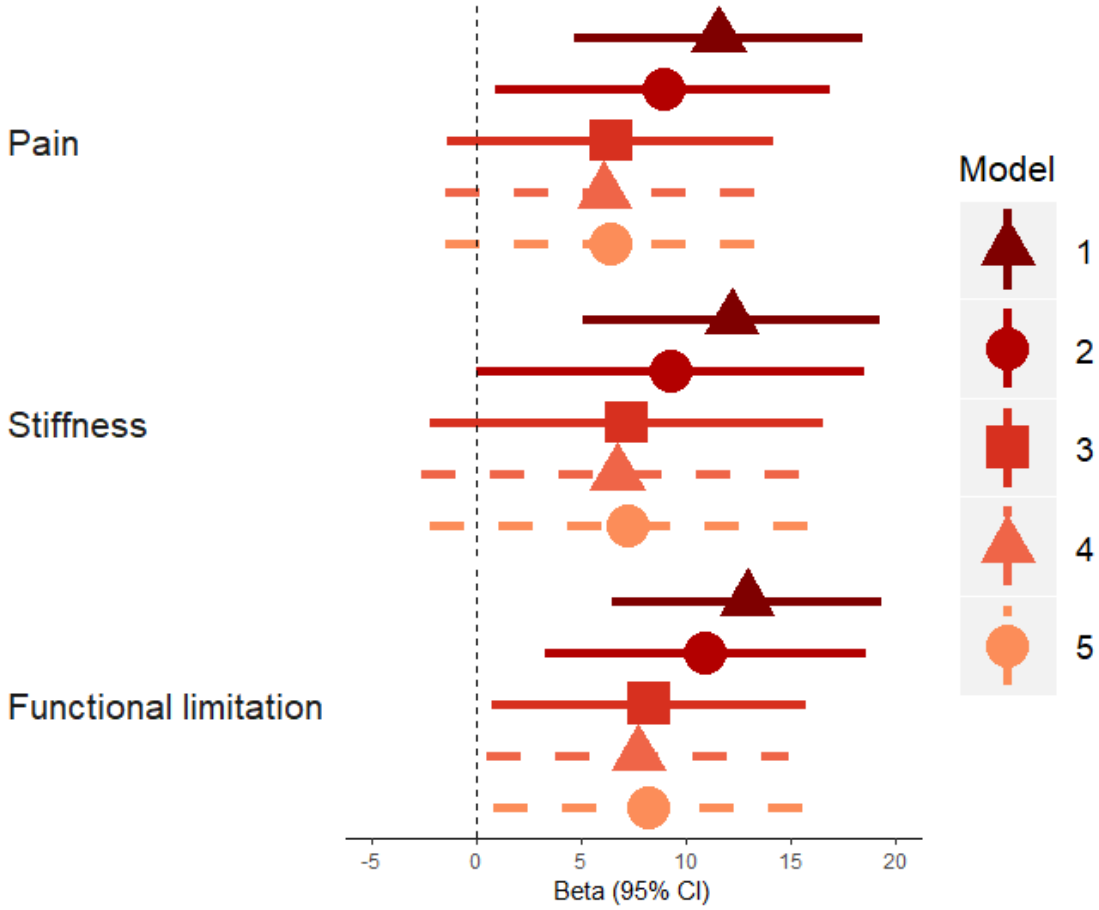

Points represent the mean difference in WOMAC scores between individuals with HBM and relatives/spouses without HBM. Horizontal bars represent 95% CIs. Person-level analysis, accounting for clustering in families. Model 1: unadjusted, model 2: adjusted for age, sex and follow-up time, model 3: model 2 plus height and TBFM, model 4: model 3 plus osteophyte severity at follow-up, model 5: model 3 plus JSN severity at follow-up. N=127.

7.3.7. BMD and hip OA progression

No evidence was detected to support an association of baseline TH or L1-BMD with odds of incident OA or change in sub-phenotype scores (Table 21). However, there was evidence for associations of baseline TH and L1-BMD with WOMAC pain, stiffness and functional limitation scores (Table 21), although CIs overlapped the null after adjustment for TBFM. Magnitudes of associations were stronger for TH, compared to L1, BMD.

Table 21: Associations of L1 and TH-BMD with radiographic and clinical features of OA progression in the HBM cohort.

			Model 1				Model 2				Model 3			
Outcome	**Exposure**	**N**	**β**	**LCI**	**UCI**	**P**	**B**	**LCI**	**UCI**	**P**	**β**	**LCI**	**UCI**	**P**
Incident OA	L1-BMD	245	1.39	0.65	2.97	0.398	1.34	0.57	3.14	0.495	1.34	0.56	3.23	0.513
	TH-BMD	245	1.04	0.53	2.05	0.907	1.08	0.50	2.36	0.844	1.07	0.47	2.40	0.876
Change in JSN score	L1-BMD	259	0.03	-0.01	0.06	0.137	0.03	-0.01	0.06	0.161	0.03	-0.01	0.07	0.184
	TH-BMD	259	0.00	-0.05	0.05	0.953	0.01	-0.04	0.05	0.784	0.01	-0.04	0.05	0.726
Change in osteophyte score	L1-BMD	259	0.11	-0.03	0.26	0.132	0.11	-0.04	0.25	0.145	0.11	-0.04	0.27	0.152
	TH-BMD	259	0.10	-0.04	0.25	0.170	0.11	-0.03	0.26	0.132	0.12	-0.03	0.28	0.107
WOMAC pain	L1-BMD	125	4.20	0.24	8.16	0.038	3.67	-0.03	7.37	0.052	2.04	-1.75	5.82	0.291
	TH-BMD	125	4.84	0.23	9.45	0.040	4.96	0.45	9.47	0.031	3.60	-0.87	8.07	0.115
WOMAC stiffness	L1-BMD	125	4.87	0.38	9.35	0.033	4.37	0.01	8.74	0.050	2.90	-1.74	7.55	0.220
	TH-BMD	125	5.32	0.30	10.3	0.038	5.29	0.41	10.2	0.033	4.10	-0.78	8.98	0.100
WOMAC functional limitation	L1-BMD	125	5.11	1.35	8.87	0.008	4.70	1.20	8.21	0.009	2.80	-0.98	6.59	0.147
	TH-BMD	125	5.49	0.91	10.1	0.019	5.55	1.08	10.0	0.015	4.16	-0.27	8.59	0.066

Estimates are the unit change in outcome (or OR for incident OA and true JSN) per SD increase in BMD.

7.3.8. Sensitivity analyses

Including six individuals with an incident THR and with a Croft score<3 at baseline in the analysis of incident OA did not alter conclusions drawn. Neither did removing 10 hips from individuals who visited a different site for follow-up radiographs (Figure 69), additional adjustment for TB DXA artefact (Figure 69) or removing 10 hips from individuals with DXA positioning errors (Figure 69). Conclusions were unchanged when performing a person-level analysis accounting for within-family clustering, although CIs were wider due to the lower numbers (Figure 70). When recoding the 21 hips with negative scores for change in osteophytes, and the 4 hips with negative scores for JSN, as 0 to enable use of a Poisson model, the association between HBM and change in JSN score was stronger (but with wider CIs) than the association with change in osteophytes (model 3: $IRR_{osteophyte}$=2.10 [1.09,4.02] and IRR_{JSN}=115 [10,1313]). Additional adjustment for FN area (as a measure of bone size) marginally attenuated effect estimates ($\beta_{osteophyte}$ 0.26 [0.01,0.52] attenuated to 0.21 [-0.02,0.44] and β_{JSN} 0.08 [0.01,0.16] to 0.07 [$4x10^{-3}$,0.13]). Additional adjustment for history of steroid use (assessed at baseline) did not alter conclusions.

Figure 69: Results of the hip OA sensitivity analyses in the HBM cohort follow-up population.

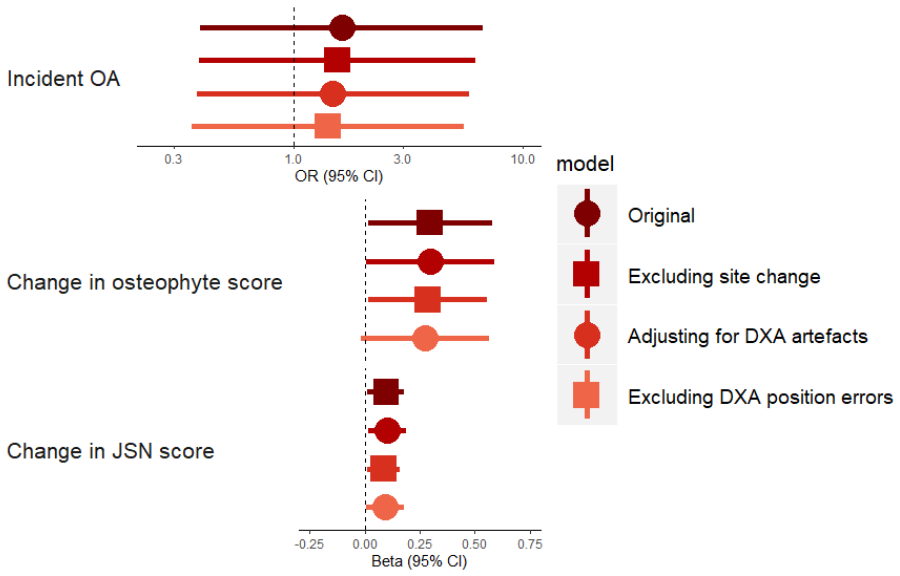

Adjusted for age, sex, follow-up time, height, TBFM, and baseline score for the continuous outcomes.

Figure 70: Associations between HBM and incident OA and change in OA sub-phenotypes in person-level analyses.

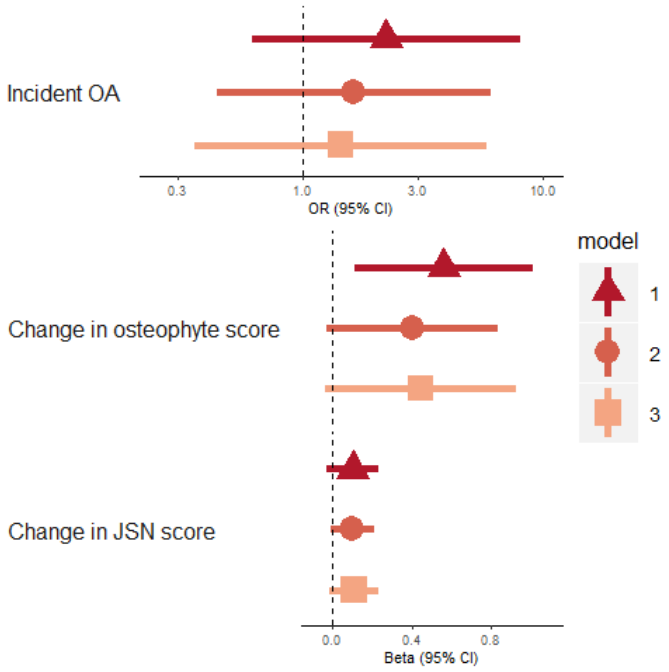

Points for continuous outcomes represent the difference in mean outcome between individuals with and without HBM. Points for binary outcomes represent the OR for individuals with HBM compared to their relatives with normal BMD. Horizontal bars represent 95% CIs.
Model 1: unadjusted, model 2: adjusted for age, sex, and follow-up time (plus baseline score for continuous outcomes), model 3: model 2 plus height and TBFM. $N_{incident\ OA}$*=121;* $N_{continuous\ outcomes}$*=126.*

7.4. Discussion

7.4.1. Summary of findings

In this chapter, I have presented evidence for increased *hip* osteophyte and JSN development, over an average of eight years, in individuals with HBM, compared to their relatives without HBM. Furthermore, I present evidence that individuals with HBM have more hip pain and limitation of function, which provides further evidence for more severe OA in this HBM population, although these clinical relationships were independent of radiographic features of OA. This analysis extends the previous findings of increased radiographic and clinical features of *knee* OA progression in this population (Chapter 6), suggesting that HBM is related to generalized OA progression, although the magnitudes of effect were weaker than seen at the knee.

7.4.2. Context of this research

Few studies have determined the association between BMD and hip OA incidence or progression. Bergink *et al* observed a relationship between FN-BMD and both hip OA incidence and progression in the Rotterdam study population (235). This chapter has extended these findings by determining the relationship between high BMD and the incidence and/or progression of individual radiographic *sub-phenotypes*. Barbour *et al* identified weak evidence for worsening osteophytes with increasing BMD in JoCo, but no evidence for a relationship with JSN progression (231), which is inconsistent with the observed (albeit weak) relationship between HBM and change in JSN score. Hochberg *et al* identified a dose-response relationship between BMD and subsequent incidence of OA in SOF (413). However, this relationship was no longer present when defining incidence based on JSN alone. In this chapter, I did not observe strong evidence for an association between HBM and incident hip OA, possibly due to low numbers, but the direction of effect was consistent with previous findings. The observed relationship between HBM and hip pain is consistent with studies of cohorts sampled from the general population, which have identified a higher

BMD in those reporting hip pain (208). The severity of OA sub-phenotypes did not appear to explain the relationship between HBM and hip pain or functional limitations, suggesting that HBM individuals have an increased risk of clinical OA independent of radiographic severity. The WOMAC questionnaire measures pain over the past 48 hours, which may explain why radiographic OA severity did not explain current pain, as pain could increase during stages of rapid OA progression not captured by radiographs (414). An analysis of the Framingham and OAI populations found that fewer than 25% of individuals with radiographic hip OA reported hip pain, and fewer than 20% of individuals reporting hip pain had radiographic hip OA (415). It is possible that more pain and functional limitations in the HBM population could reflect other conditions of the hip (*e.g.* bursitis (416)), features of a mild skeletal dysplasia, or inflammation not detected on the radiograph.

Increased TBFM in the HBM population (201) did not appear to explain the relationship between HBM and change in radiographic OA sub-phenotypes. Adjustment for FN area, as a measure of bone size, only explained a small proportion of the relationship. Unfortunately, measures of FN width are not available in the HBM population, a risk factor for hip OA progression (417). It is plausible that HBM individuals would have greater FN width due to greater bone mass, meaning measures of FN area may not equate to FN width in this population. Another factor which may mediate the relationship between HBM and development of hip OA sub-phenotypes are differences in hip shape. HBM individuals more commonly have features of cam-type deformity (section 1.2.5), compared to their relatives without HBM (418). There is evidence to suggest that cam-type deformities are related to end-stage hip OA, suggesting that cam-type deformity is a risk factor for hip OA progression (419,420).

As discussed in section 2.3.4, HBM is likely to be caused by the polygenic inheritance of multiple BMD loci (203), or the monogenic inheritance of rare variants (205), indicating that HBM precedes OA development. However, the possibility that biological pleiotropy, rather than a causal effect, explains the current results cannot be ruled out. Previous observations of a greater prevalence

of pelvic enthesophytes in the HBM population led to the hypothesis that HBM individuals may have a genetic predisposition to form extra bone (402). The stronger effect size for the relationship between HBM and change in hip osteophyte score, compared to change in hip JSN score, further suggests a 'bone-forming' phenotype in this population. The genetic correlation between hip OA and LS-BMD (137) is further evidence for pleiotropy.

7.4.3. Strengths

The HBM study constitutes the largest population of individuals with extreme, unexplained, generalized HBM (11). I analysed change in OA sub-phenotypes separately, which allowed me to detect the stronger relationship with osteophyte development compared to change in JSN. I analysed change in osteophytes and JSN as continuous measures, increasing statistical power to detect associations, and reducing the possibility of a ceiling effect by increasing the range of possible values from 0-6 for JSN and 0-10 for osteophytes, and eliminating the possibility of selection bias in a case-only analysis.

7.4.4. Limitations

The method of identifying individuals from NHS DXA databases ascertained a predominantly female and older population, such that a relatively large proportion were unable to be followed-up after eight years, due to death or poor health. Hence there was a lower baseline prevalence of radiographic hip OA in the population able to be followed-up, meaning power to assess hip OA incidence and progression, based on overall Croft score, was limited. Radiographs and DXA scans were performed using standard protocols at each centre but were not standardized across centres. However, as 97% of individuals re-attended the same centre for follow-up, this is unlikely to affect the measures for *change* in radiographic features. Furthermore, measuring change in sub-phenotype variables did not separate hip OA sub-phenotype progression from incidence since these results had to be pooled to optimise sample size. As I did not read baseline and follow-up radiographs paired, I did observe a few negative

scores for change in osteophytes (8%) and change in JSN (1.5%), which were included in analyses, because removing these values as 'measurement error' would have biased results, as there was likely to have been the same proportion of measurement error overinflating change, for which I would not have been able to account (hence the reasoning for not basing conclusions on the Poisson analysis). Radiographic grading of OA sub-phenotypes is subjective, which I limited using an established atlas (19), although the intra-rater and inter-rater reliability were low for a few variables, attenuating the conclusions I can draw from this analysis. As I was blinded to timepoint, it is unlikely that I systematically under-graded at baseline and over-graded at follow-up, meaning measurement error is unlikely to explain these results. WOMAC scores were only collected at follow-up and therefore I cannot draw conclusions about the relationship between HBM and *symptomatic* OA progression.

7.4.5. Future work

As highlighted in Chapter 6, it is important to determine if the relationship between high BMD and hip osteophyte development is a true causal relationship. In Chapter 9, I determine the causal effect of BMD on hip OA, using multivariable analyses to determine if the causal effect is independent of BMI. To determine if BMD has a causal effect on OA (sub-phenotype) progression, a GWAS of hip OA (sub-phenotype) progression in a large sample with multiple available radiographs would first need to be performed. Summary statistics could then be used for 2SMR analyses. Unfortunately, this analysis was beyond the scope of this PhD. Bidirectional analyses should additionally be performed to determine whether the observed association between HBM and hip OA subphenotype prevalence/progression represents a true causal pathway between BMD and hip OA sub-phenotypes, or whether there may be shared underlying biology contributing to both phenotypes (*i.e.* pleiotropy, Chapter 9). Finally, it is important to determine the underlying pathways which contribute to hip OA in people with high BMD (Chapter 10), as knowledge of the underlying biological pathways may lead to the identification of novel druggable targets.

7.4.6. Conclusions

I have found evidence for associations between HBM and worsening radiographic sub-phenotypes of hip OA over eight years. I have found evidence for a greater clinical severity of hip OA in HBM individuals, compared to their relatives without HBM. These associations are independent of the elevated TBFM observed in HBM individuals. Further analyses are required to determine the BMI-independent causal role of BMD in hip OA progression, and to identify the underlying biological pathways explaining these associations.

CHAPTER 8. USING METABOLOMICS TO DETERMINE THE ROLE OF BONE IN OSTEOARTHRITIS PATHOGENESIS

8.1. Background and aims

8.1.1. The association between bone and metabolism

A positive relationship between BMD and BMI is widely accepted, reflecting the beneficial effect of increased loading on the skeleton; MR analysis provided evidence for a causal pathway from higher BMI to increased BMD (401). Obesity is a component of the metabolic syndrome (MetS), along with hyperglycaemia, dyslipidaemia, and high blood pressure (421). Several studies have investigated the link between MetS and BMD (422-424). These studies have produced conflicting results, suggesting that individuals with MetS could have lower, higher or no difference in BMD compared to those without MetS (422-424). Reasons for these inconsistencies could include the differential relationships of each of the MetS components with BMD; a study in the RS population found a positive relationship between elevated glucose and FN-BMD, a positive relationship between high-density lipoprotein cholesterol (HDLc) and FN-BMD in women only and an inverse relationship between waist circumference and FN-BMD in men only (425). More recently, MR analyses have suggested an inverse effect of low-density lipoprotein cholesterol (LDLc) on BMD estimated from heel ultrasound (eBMD); the same association was not observed for HDLc or triglycerides (426).

This recent MR analysis found some evidence for a causal pathway between eBMD and LDLc (*i.e.* bidirectional relationships between eBMD and LDLc) (426). Bone is suggested to play a role in regulating energy metabolism. Osteocalcin is a measure of osteoblast function and thus bone formation (427-429). Osteocalcin deficient mice have increased blood glucose, reduced insulin levels, and an increase in FM compared to wildtype mice (202). In human populations, osteocalcin has been inversely associated with FM and blood glucose levels (430,431). Further evidence for a metabolic effect of high BMD was provided by investigating the HBM population, as discussed in section 2.3.2.

Several human metabolomic studies of BMD have been performed (432-438), but only one has used the targeted metabolomics platform developed by Nightingale health outlined in section 5.4 (434), allowing analyses to be reproduced in other populations. This study, performed in the ALSPAC adolescent population outlined in section 5.2.3, identified inverse relationships between tibial cortical BMD and concentrations of lipoprotein, lipid, and fatty acid traits, as well as a strong inverse relationship with citrate. However, only the association with citrate met the Bonferroni-corrected *p*-value threshold after adjustment for FM and LM (434). Consistent with an inverse relationship between BMD and citrate, a non-targeted metabolomics analysis in a smaller Japanese population observed higher serum citrate in postmenopausal women with low BMD, defined by a T-score<-1, compared to those with a T-score≥-1 (437).

8.1.2. OA and metabolism

As discussed in section 1.2.5, BMI is a strong risk factor for OA. With regards to the relationship between MetS and OA risk, a systematic review concluded that there was insufficient evidence to draw conclusions on the relationship between MetS and hand OA, and that there was no evidence to suggest a relationship between MetS and hip and knee OA, although the majority of studies were cross-sectional (439). In a more recent analysis of the Chingford cohort, the individual components of MetS (hypertriglyceridemia, low HDLc, hypertension and high fasting glucose levels) were associated with painful interphalangeal OA, but not knee OA, independent of BMI (440). An MR analysis including the UK Biobank population (N=376,435) and the Malmo Diet and Cancer Study (N=27,691) provided evidence for a protective effect of LDLc on hip/knee OA (441). This MR analysis did not find evidence for a causal effect of HDLc, triglyceride levels or fasting plasma glucose on OA risk (441).

Several metabolomics studies have been performed of OA, mainly in animal or small case-control settings (388). Several of these studies have determined metabolic profile of SF (442-445). Xu *et al* extracted cartilage samples from osteophytes of postmenopausal women undergoing TKR and compared the

metabolic profiles of these samples to those extracted from the lateral posterior femoral condyle. They identified 28 metabolic variations, many of which corresponded to amino acids, including elevated phenylalanine and proline in the osteophyte samples (446). Whilst this tissue-specific analysis will capture localised metabolic dysregulation, SF and cartilage cannot be easily sampled from large cohorts.

Of the studies determining circulating metabolic profile (*i.e.* plasma or serum), Zhai *et al* identified an increased branched chain amino acid (BCAA) to histidine ratio in the serum of female knee OA cases, compared to controls, from TwinsUK. This association replicated in a population of knee OA cases and controls from the Chingford cohort (447). Zhang *et al* also identified an increased plasma BCAA to histidine ratio in knee OA cases sampled from the mixed sex Newfoundland OA study, compared to controls sampled from the Complex Diseases in the Newfoundland Population: Environment and Genetics study. This ratio, however, did not predict TKR in a separate population sampled from TASOAC, but lysophosphatidylcholine to phosphatidylcholine ratio did predict TKR (448). In another analysis, Zhang *et al* identified lower levels of plasma arginine in knee OA patients undergoing TKR, compared to controls, which replicated in a separate case-control study (449). However, none of these metabolomics studies have determined which circulating metabolic traits are associated with the individual radiographic OA sub-phenotypes. As discussed in Chapter 3, the sub-phenotypes of bone formation and cartilage loss may have different associations with BMD and therefore may display different associations with metabolic traits.

8.1.3. Aims

The cross-sectional association between HBM and knee OA was attenuated by approximately 50% by adjustment for BMI (227). This could be explained by confounding, as BMI is a common cause of both BMD and OA. However, HBM is at least in part genetically determined (203) and in the HBM population, adjustment for TH-BMD partially attenuated the relationship between HBM and

TBFM, whereas adjustment for TBFM only minimally attenuated differences in BMD between HBM individuals and their relatives without HBM, suggesting a causal pathway between HBM and TBFM (201). HBM could therefore be associated with dysregulation of metabolic pathways, via reduced bone turnover (201). I aim to identify metabolic traits cross-sectionally associated with BMD (Aim 1, Figure 71) and OA (Aim 2, Figure 71) in the HBM cohort. These metabolic traits may mediate the relationship between BMD and OA, possibly identifying pathways involved in OA pathogenesis. Due to the suggested role of osteocalcin in insulin sensitivity and adiposity (202), I aim to determine if BTMs (section 2.1.4) alter metabolic profiles (Aim 3, Figure 71) , which could mediate the association between HBM and OA phenotypes, as HBM individuals have reduced bone turnover (201). Finally, I aim to assess the generalizability of any observed results in cohorts more representative of the general population.

Figure 71: Simplified DAG of hypothesized pathways between HBM, bone turnover and OA sub-phenotypes and the hypothesized mediating effect of metabolic pathways.

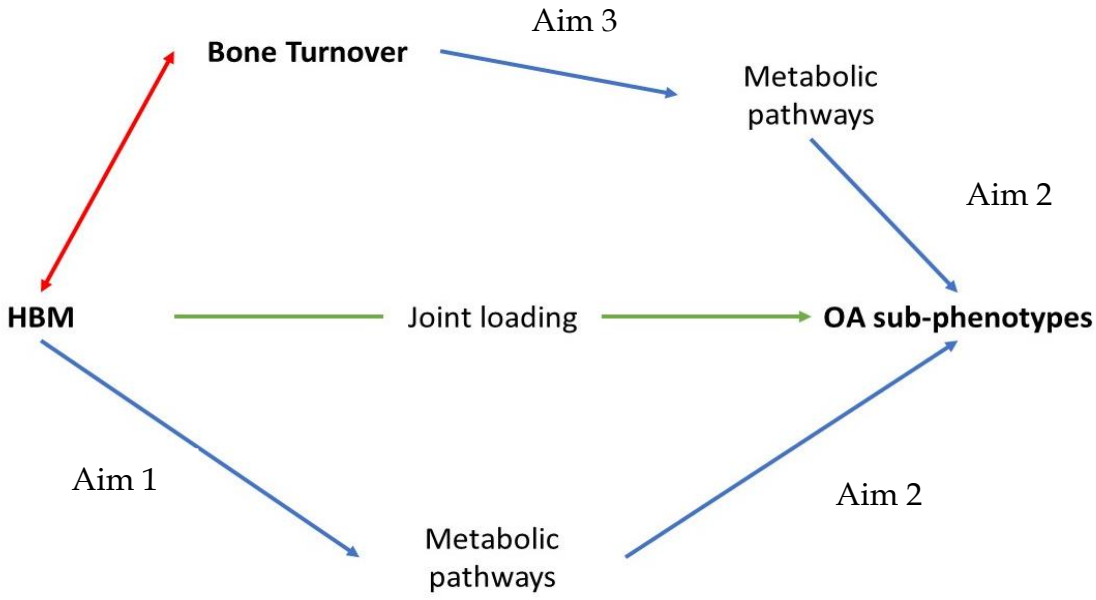

Red arrows indicate an inverse relationship and green arrows represent a positive relationship. The possible direct effect of bone turnover on OA sub-phenotypes is excluded from this DAG as it will not be analysed in this chapter.

8.2. Methods

8.2.1. Study population

Initial analyses were performed in the HBM study population, described in section 2.3.2. Metabolomic profiling was performed on 354 individuals, of whom 229 (65%) were HBM cases and 125 (35%) were relatives/spouses without HBM. Individuals with metabolomic data were recruited from eight of the original centres: Bristol, Cardiff, Bath, Hull, Gwent, Birmingham, Sheffield, and Cambridge.

8.2.2. Metabolomics

Metabolic profiling of the HBM cohort was performed using the Nightingale Health NMR platform (section 5.4.1).

Data cleaning and quality control

Analytical outliers

Histograms were produced for all metabolic traits to detect potential analytical outliers (those which were several orders of magnitude greater than all other measurements and make all other measurements indistinguishable on a scatterplot). Although potential outliers were detected (*i.e.* measurements $\geq$7SD above or below the mean), that could be removed in later sensitivity analyses (section 8.2.5), no analytical outliers were detected. Some metabolic traits, particularly the lipoprotein measures, were heavily zero-skewed. This may not represent true zero concentrations, but a failure to detect the true concentration (450). These zero values were therefore set to missing. Several of the lipoprotein subclass measures were undetectable in many individuals, ranging from 3% missing for the extra-large HDL lipoproteins to 95% for the large and medium HDL lipoproteins (Table 22). The general pattern also appeared to be an increase percentage of missing data in those without HBM compared to those with HBM. Due to the large amount of missing data for the lipoprotein subclass measures, I excluded these variables from all analyses.

Table 22: Number of individuals with available data for each of the metabolic traits in the HBM cohort.

Metabolic Trait		N_{HBM} (%)	$N_{no\ HBM}$ (%)	N_{total} (%)
Extremely large VLDL		187 (82)	87 (70)	274 (77)
Extra-large VLDL		153 (67)	65 (52)	218 (62)
Large VLDL		125 (55)	53 (42)	178 (50)
Medium VLDL		141 (62)	51 (41)	192 (54)
Small VLDL		87 (38)	39 (31)	126 (36)
Very small VLDL		64 (28)	36 (16)	100 (28)
IDL		96 (42)	42 (34)	138 (39)
Large LDL		58 (25)	19 (15)	77 (22)
Medium LDL		32 (14)	7 (6)	39 (11)
Small LDL		32 (14)	8 (6)	40 (11)
Extra-large HDL		222 (97)	120 (96)	342 (97)
Large HDL		15 (7)	1 (1)	16 (5)
Medium HDL		16 (7)	0 (0)	16 (5)
Small HDL		222 (97)	119 (95)	341 (96)
Lipoprotein particle size		229 (100)	125 (100)	354 (100)
Cholesterol				
	Total	229 (100)	125 (100)	354 (100)
	VLDL	229 (100)	125 (100)	354 (100)
	Remnant	229 (100)	125 (100)	354 (100)
	LDL	229 (100)	125 (100)	354 (100)
	HDL	229 (100)	125 (100)	354 (100)
	HDL2	30 (13)	3 (2)	33 (9)
	HDL3	229 (100)	125 (100)	354 (100)
	Esterified	229 (100)	125 (100)	354 (100)
	Free	229 (100)	125 (100)	354 (100)
Glycerides and phospholipids		229 (100)	125 (100)	354 (100)
Fatty acids				
	Degree of unsaturation	34 (15)	9 (7)	43 (12)
	Docosahexaenoic acid	18 (8)	0 (0)	18 (5)
	Linoleic acid	34 (15)	9 (7)	43 (12)
	MUFA	34 (15)	9 (7)	43 (12)
	n-3 fatty acids	34 (15)	9 (7)	43 (12)
	n-6 fatty acids	34 (15)	9 (7)	43 (12)
	PUFA	34 (15)	9 (7)	43 (12)
	Saturated fatty acids	34 (15)	9 (7)	43 (12)
	Total fatty acids	34 (15)	9 (7)	43 (12)
Apolipoproteins		229 (100)	125 (100)	354 (100)
Glycolysis-related metabolites				
	Glucose	228 (99.6)	119 (95)	347 (98)
	Lactate	228 (99.6)	119 (95)	347 (98)
	Citrate	229 (100)	125 (100)	354 (100)
Amino acids				
	Alanine	229 (100)	125 (100)	354 (100)
	Histidine	229 (100)	125 (100)	354 (100)
	Isoleucine	229 (100)	125 (100)	354 (100)
	Leucine	229 (100)	125 (100)	354 (100)
	Valine	229 (100)	125 (100)	354 (100)
	Phenylalanine	216 (94)	119 (95)	335 (95)
	Tyrosine	229 (100)	125 (100)	354 (100)
Ketone bodies				
	Acetate	228 (99.6)	122 (98)	350 (99)

	Acetoacetate	228 (99.6)	125 (100)	353 (99.7)
	Beta-hydroxybutyrate	229 (100)	125 (100)	354 (100)
Fluid balance				
	Creatinine	229 (100)	120 (96)	349 (99)
	Albumin	229 (100)	125 (100)	354 (100)
Inflammation				
	Glycoprotein acetylation	229 (100)	125 (100)	354 (100)

Metabolic traits in bold correspond subclasses of metabolic traits. Numbers were the same for all lipoprotein measures within these subclasses. MUFA: monounsaturated fatty acid, PUFA: polyunsaturated fatty acid.

Storage issues and sample degradation

Unfortunately, due to the time lapse between collection of blood samples and analysis (average 8 years), some samples had degraded, and the quality of the data was reduced (450). Nightingale Health provide variables for quality control tags for sample issues:

- Low glucose/high lactate: samples kept at room temperature during blood collection result in glucose metabolism to lactate or pyruvate. I set glucose and lactate concentrations to missing for individuals with this tag.
- Abnormal macromolecule A: this tag means that signals from abnormal proteins and macromolecules have been detected and accurate quantification of phenylalanine, acetate, and acetoacetate has not occurred. I therefore set phenylalanine, acetate, and acetoacetate concentrations to missing for individuals with this tag.
- Low glutamine/high glutamate: this tag is given when glutamine appears to have degraded, normally due to samples being left at room temperature or being subjected to multiple freeze-thaw cycles. All but three samples had this tag, so glutamine was not analysed.

Due to differences in facilities available at the different HBM centres, some sites were unable to freeze samples in the required amount of time for accurate metabolomic analysis (Bristol, Cardiff, Bath, Gwent, N=28). I analysed differences in metabolite concentrations between sites where the samples could be frozen correctly, and those where there was a delay in freezing, using GEE to account for clustering within families. Mean concentration of most metabolites

were lower in the group where samples were stored correctly (Figure 72). This was not explained by differences in HBM prevalence, age, or social status (IMD) between the sites. Individuals from sites where samples could not be stored correctly were excluded from further analysis, leaving the final maximum sample numbers for each metabolite provided in Appendix 17.

Figure 72: Differences in metabolic trait concentrations between samples that were immediately frozen, compared to those that were not immediately frozen, in the HBM cohort.

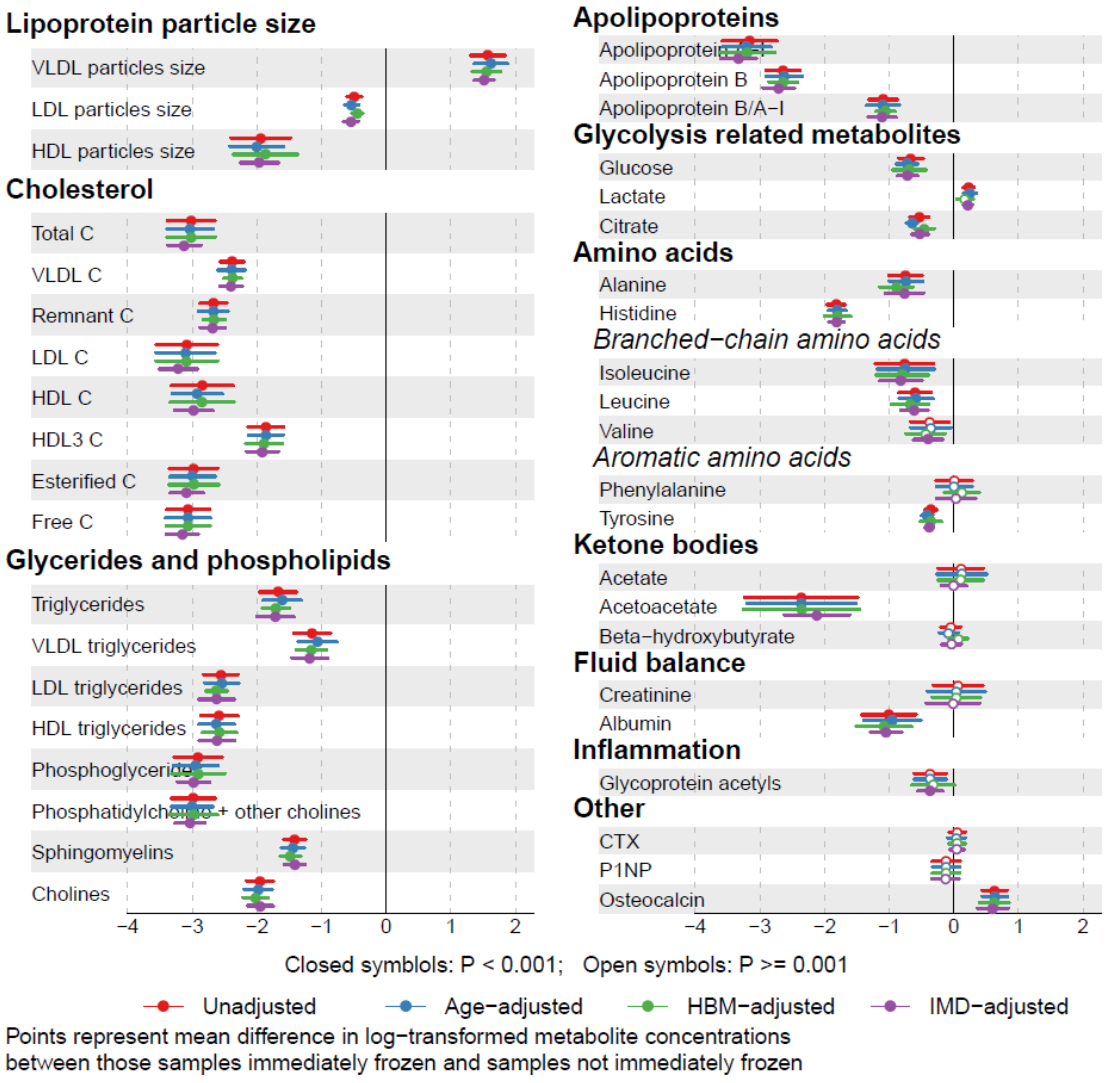

To limit the number of statistical tests and thus reduce the risk of chance findings, I initially analysed 23 metabolic traits, which included the amino acids, ketone bodies, glycolysis-related metabolites and one summary variable from

each lipid family (*e.g.* total triglycerides, total cholesterol). I aimed to perform further sub-group analyses if any associations were observed for the summary variables.

Comparing associations to previously published work

To check the reliability of the data, I compared associations with BMI, stratified by gender, to previously published results from adolescents (342), and differences in metabolic traits between those individuals ever taking statins and those individuals who had never taken a statin, to those previously published (451). Results were generally consistent with previously published data, despite a smaller sample size. A summary of these analyses is provided in Appendix 18.

8.2.3. Assessment of HBM, BMD and bone turnover

The definition of HBM is described in section 2.3.2, and the protocol for assessing TH, LS, and TB-BMD by DXA scanning is described in section 4.3. Non-fasted P1NP and total osteocalcin were measured as markers of bone formation and β-isomer of CTX-1 (β-CTX) was measured as a marker of bone resorption. Plasma was separated and frozen within 4 hours to −80°C and BTM concentrations were measured by electrochemiluminescence immunoassays (Roche Diagnostics), performed by Professor Bill Fraser and Dr Jonathan Tang at the University of East Anglia Medical School. Detection limits were 4.0, 0.6 and 0.01 μg/L for P1NP, osteocalcin and β-CTX, respectively. Reference ranges were supplied by UK Supra Regional Assay Service laboratory (reference range 0.1-0.5μg/L for β-CTX, 20-110μg/L for P1NP and 6.8-32.2μg/L for osteocalcin). Intra-assay coefficients of variation (CV), provided by Professor Fraser and Dr Tang, were <2%, <2% and <4%, for P1NP, osteocalcin and β-CTX, respectively. Inter-assay CVs were <3%, <5% and <5%, respectively.

8.2.4. OA outcome variables

OA sub-phenotypes were defined as described in the published papers based on baseline HBM analyses (226-228). The OA outcomes analysed are summarized in Table 23.

Table 23: OA outcome variables analysed in the metabolomics analysis in the HBM cohort and their derivation.

Variable	Description
Any hip osteophyte	Any superior acetabular, lateral femoral or medial femoral osteophyte grade ≥1
Any hip JSN	Any JSN grade ≥1
Any knee osteophyte	Any medial or lateral osteophyte grade ≥1
Any knee JSN	Any medial or lateral JSN grade ≥1
Any DIP osteophyte	Osteophyte grade ≥1 at the DIP joint
Any DIP JSN	JSN grade ≥1 at the DIP joint
Any CMC osteophyte	Osteophyte grade ≥1 at the CMC joint
Any CMC JSN	JSN grade ≥1 at the CMC joint

8.2.5. Statistical analysis

Many of the metabolic traits displayed a skewed distribution (Appendix 19). However, from previous experience working with metabolomic data, log transformation does not alter the conclusions drawn, compared to when a model with robust SEs is used (Figure 73), but can make the results more difficult to interpret. Some metabolic traits did not display a normal distribution when log transformed (I checked all other transformations using the Stata '*gladder*' command and these were unsuitable). Therefore, I used a robust SE model.

Figure 73: Comparison of robust SE and log-transformed methods of analysis for the association between HBM and the 23 metabolic traits analysed.

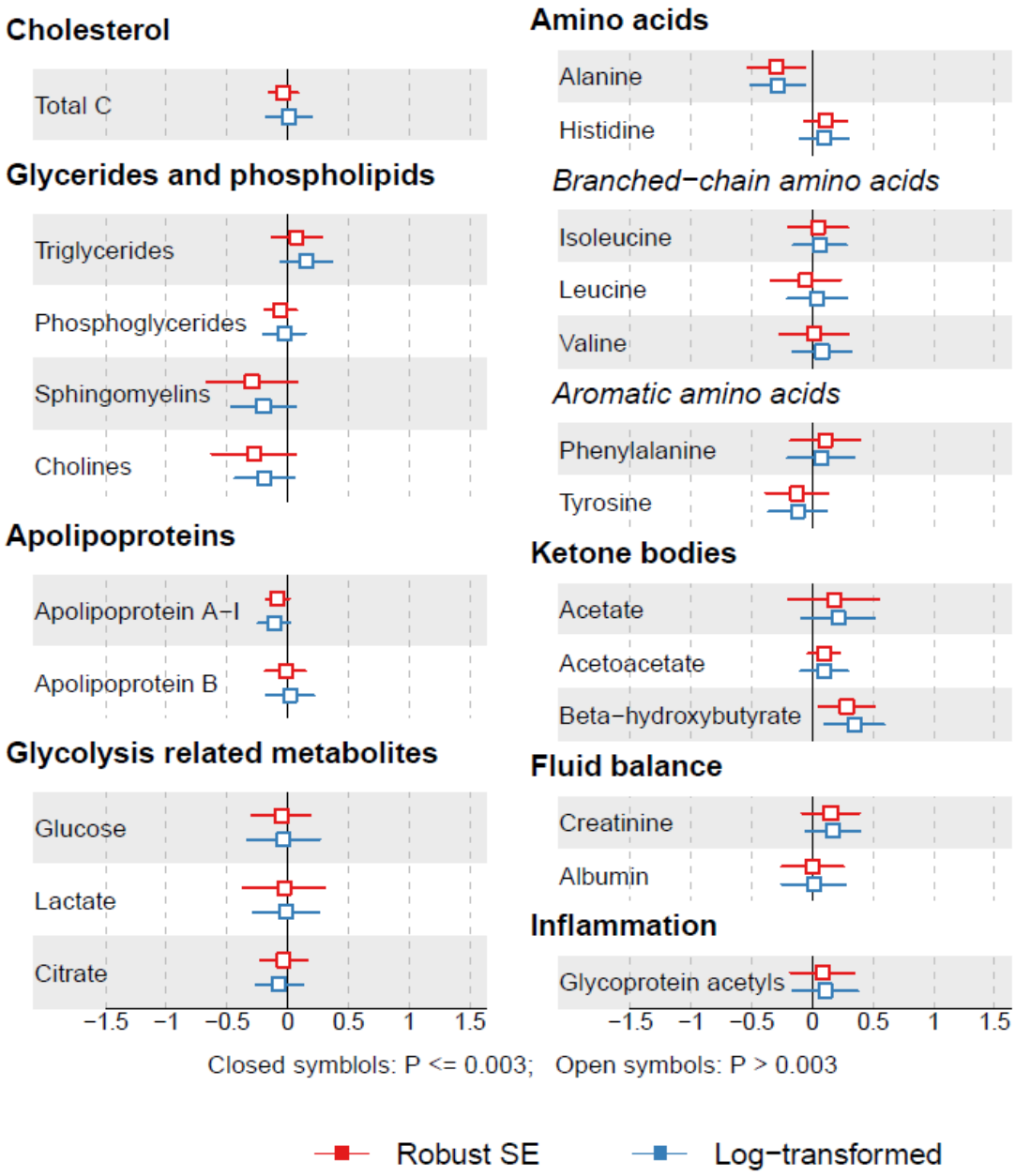

Points represent the mean difference in metabolic traits in SD units for the robust SE model and in SD units of the log transformed variable for the log transformed model. Adjusted for age and sex.

Although most metabolic traits were measured in units of mmol/L, the range of values varied between metabolic traits, for example concentrations of the amino acid tyrosine ranged from 0.03 to 0.12mmol/L, whereas the concentration of glucose ranged from 1.41 to 13.1mmol/L. Therefore, to present data in a way that can allow comparisons between metabolic traits, I performed initial analyses

with standardized metabolic traits. However, when comparing associations between populations, for example when comparing HBM and ALSPAC populations, as HBM is such an extreme and smaller population, I additionally analysed the metabolic traits in their original units.

Accounting for clustering

Methods for dealing with within-family clustering in the HBM population are discussed in section 5.1.2. Associations between continuous BMD/BTM variables and continuous metabolic traits were determined by GEE linear regression. For analyses of binary outcomes (*i.e.* OA sub-phenotype variables), analyses were performed using GEE logistic regression. Hip and knee OA analyses were performed on all available hip and knee x-rays, using GEE to account for within-person clustering rather than within-family. As only one hand radiograph was available per person, analyses of hand OA sub-phenotypes accounted for within-family clustering.

Correction for multiple testing

Although analyses were restricted to the 23 key metabolic traits, there was still a need to correct the significance threshold for multiple testing. As the metabolic traits assessed were highly correlated, I determined the significance threshold based on matrix spectral decomposition of a correlation matrix between the variables (452,453). The 23 metabolic traits generated 20 independent variables, so I set the *p*-value threshold at 0.05/20=0.003.

Determining models for analysis

Analyses were initially performed unadjusted. Age, sex, height, and weight were considered a priori confounders, so I performed further analyses using two additional models: model 2: adjusted for age, sex, and height and model 3: additionally adjusted for weight. Age was not linearly associated with some variables, so I categorized age into quintiles. Due to the large number of tests for multiple exposures/outcomes performed, I explored the need for adjustment for additional covariates such as menopause and use of glucocorticoids or

bisphosphonates for any metabolites associated with BMD, bone turnover or OA sub-phenotypes (Figure 74).

Sensitivity analyses

I excluded individuals with a metabolic trait concentration at least 7SD above or below the mean concentration. I excluded samples with any of the QC tags (rather than just setting particular metabolic traits as missing) provided by Nightingale Health (except low glutamine/high glutamate as glutamate was not analysed), outlined in section 8.2.2, in a separate analysis.

Figure 74: DAGs of hypothesized relationships between BMD/ bone turnover/OA sub-phenotypes, potential confounders, and metabolic traits.

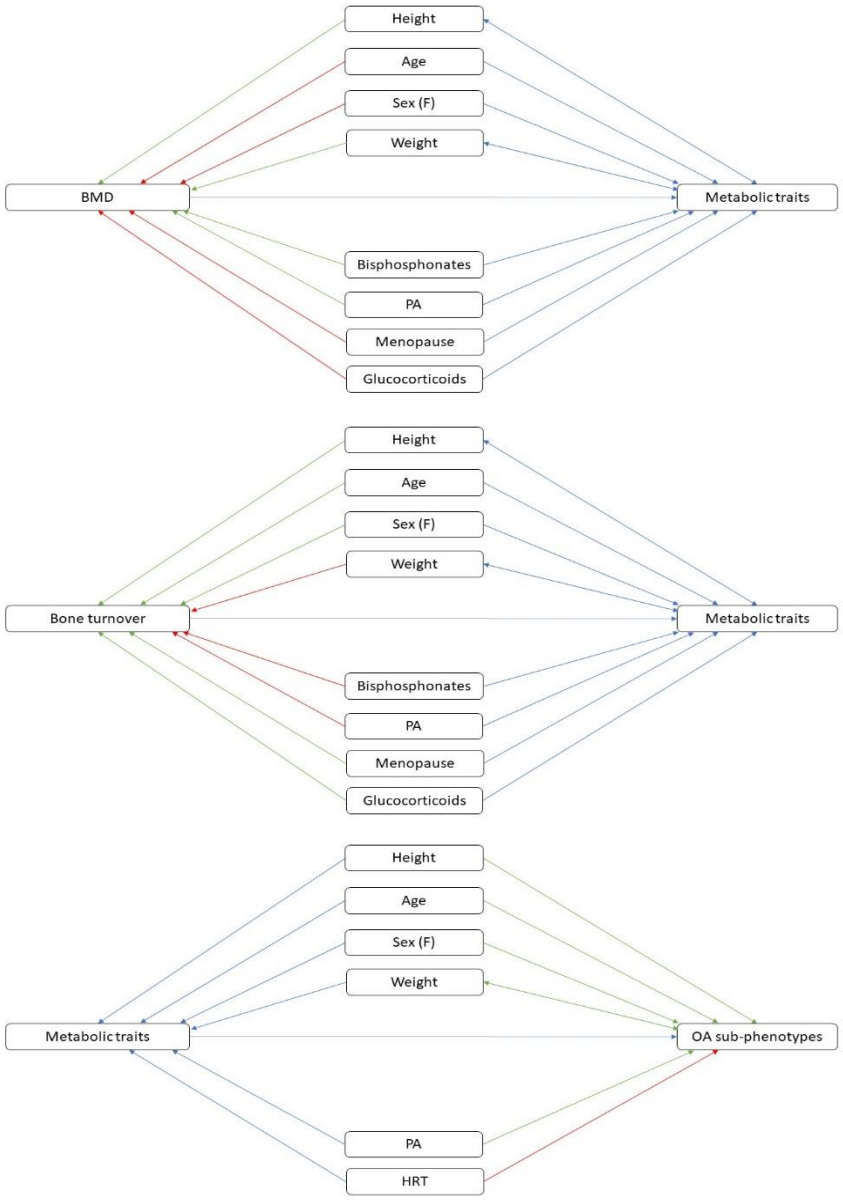

8.2.6. Determining the generalizability of observed associations

The Rotterdam study

I determined generalizability for analyses with BMD exposures and OA outcomes by replicating analyses for metabolic traits of interest in RS, described in section 5.2.2. Metabolomic profiling was performed on RS1 individuals who attended the fourth assessment, using the Nightingale health platform. Although the mean age of the RS population was slightly higher than the HBM population (75 (6) *vs* 59 (15) years), RS represents the largest population with detailed OA sub-phenotype data and metabolomic assessment in a population of male and female older adults. L1 and FN-BMD were assessed by DXA at the same outcome assessment clinic. Methods for performing X-rays, and assessment of radiographs for OA sub-phenotypes, have previously been described (232,454,455). I generated variables for any osteophyte and any JSN at the hip, knee, DIP and CMC joints of either hand/knee, as described for the HBM population (section 8.2.4). Associations between BMD variables (exposures) and metabolic traits (outcomes) were determined by linear regression and associations with OA outcomes were determined by logistic regression. Analyses were adjusted for age, sex, height, and weight.

ALSPAC

I assessed generalizability for the analyses of BTMs by replicating analyses for metabolic traits of interest in the ALSPAC populations, described in section 5.2.3. The ALSPAC mother's population was selected as it represents the largest population of adults with measurement of β-CTX and metabolic traits using the Nightingale health platform. The offspring population was also assessed to determine generalizability to a younger age range. In the ALSPAC populations, fasted β-CTX concentration was measured. Plasma was separated and frozen within 4 hours to −80°C and β-CTX concentration measured by

electrochemiluminescence immunoassay (Roche Diagnostics), with a detection limit of 0.01µg/L. Intra- and inter-assay CVs were <4% and <5%, respectively.

Analyses of ALSPAC populations were performed using linear regression. For the mother's cohort, the final model was adjusted for age, height, weight, menopausal status, and fasting time prior to sample collection (<8 or ≥8 hours). Height and weight were measured contemporaneous to blood sampling. To determine HRT use and use of other medications affecting bone turnover, ALSPAC women were asked if they were taking hormone replacement, and to list all current medications, from which I determined bisphosphonate and oral glucocorticoid use. Women were considered postmenopausal if they had not had a period in the last 12 months or if their periods had stopped due to hysterectomy, ablation/resection, chemotherapy, or other medical reasons (456). As only 14 mothers reported bisphosphonate use and 12 oral glucocorticoid use, I removed these mothers in a sensitivity analysis. For the offspring population, model 3 was adjusted for age, sex, height, weight, Tanner stage, and time of sample collection (AM or PM). Tanner pubertal stage was assessed by line drawings (457,458) using a paper questionnaire sent to all participants prior to clinic attendance.

8.3. Results

8.3.1. Descriptives of the HBM population included in these analyses

354 individuals from the HBM population had metabolomics analysis performed on their baseline blood samples. 229 (65%) had HBM, 231 (65%) were female and the mean age was 58.7 (15.1) years. Of these 354 individuals, 326 had their blood samples collected at a site with the ability to freeze the samples. A flowchart detailing the derivation of the sample for analyses is presented in Figure 75. A comparison of the individuals with metabolomic data included in these analyses, and those with metabolomic data but not included, is presented in Table 24. Of the 326 individuals, 320 had complete covariate data and were analysed. Descriptive statistics comparing those with and without HBM are presented in Appendix 20. Summary statistics for each of the 23 metabolic traits initially analysed are presented in Table 25.

Figure 75: Flowchart detailing the derivation of the HBM cohort metabolomics population.

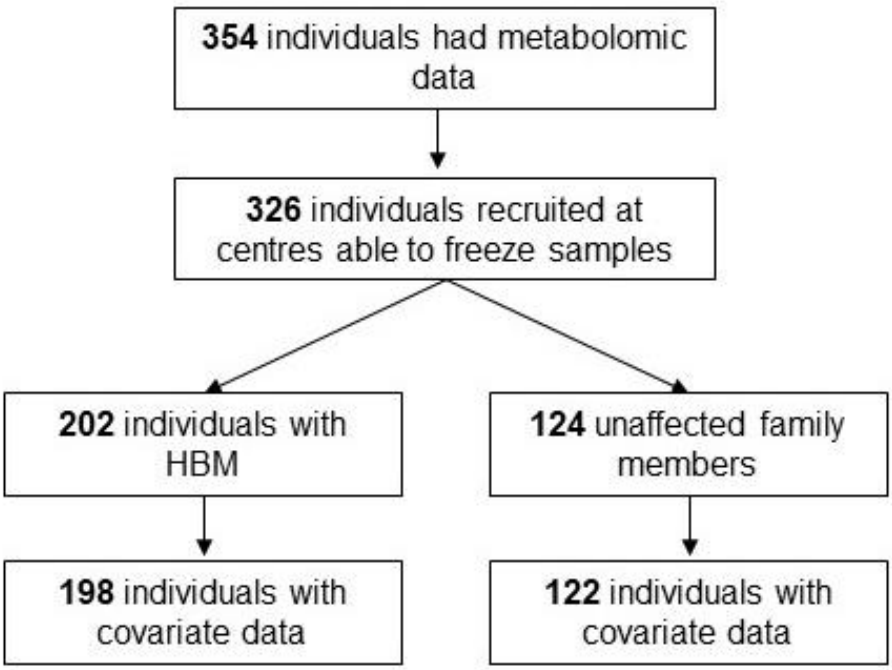

Table 24: Characteristics of HBM cohort included in the metabolomics analysis, those not included due to incorrect sample storage and those not included due to missing data.

	With metabolomic data and included N=320	**With metabolomic data but not included N=34**	**Without metabolomic data N=205**	***p* for difference**
		N (%)		
HBM	198 (62)	31 (91)	129 (63)	0.003
Female	206 (64)	25 (74)	137 (67)	0.525
Postmenopausal	154 (75)	12 (55)	100 (79)	0.045
Radiographic knee OA (KL≥2)	101 (33)	8 (29)	53 (33)	0.877
Radiographic hip OA (Croft ≥3)	71 (27)	7 (32)	31 (26)	0.865
Any joint replacement	35 (11)	4 (12)	16 (8)	0.464
History of HRT use	86 (45)	8 (40)	49 (44)	0.919
History of steroid use	66 (21)	9 (28)	50 (27)	0.219
History of bisphosphonate use	10 (3)	4 (14)	5 (3)	0.007
History of fracture	135 (42)	15 (44)	74 (37)	0.454
History of smoking	172 (54)	18 (60)	99 (54)	0.798
		Mean (SD)		
Age, years	59.1 (15.0)	54.7 (15.2)	59.1 (15.3)	0.270
Height, cm	168.7 (9.9)	167.8 (10.1)	168.0 (8.9)	0.623
Weight, kg	84.5 (17.0)	81.8 (14.2)	83.5 (17.8)	0.591
Total hip BMD Z-score	2.07 (1.61)	2.92 (2.02)	2.07 (1.64)	0.020
L1 BMD Z-score	2.53 (2.14)	3.50 (1.98)	2.80 (2.22)	0.033

p for difference from one-way ANOVA.

Table 25: Summary statistics for the 23 metabolic traits analysed in the HBM cohort.

Metabolic trait	N	Mean (SD)	Median (IQR)
Cholesterol			
Total cholesterol	320	0.610 (0.364)	0.497 (0.395, 0.722)
Glycerides and phospholipids			
Total triglycerides	320	0.671 (0.239)	0.606 (0.507, 0.777)
Phosphoglycerides	320	0.336 (0.173)	0.289 (0.235, 0.395)
Sphingomyelins	320	0.210 (0.114)	0.190 (0.167, 0.220)
Cholines	320	0.689 (0.408)	0.617 (0.528, 0.736)
Apolipoproteins			
Apolipoprotein-A1	320	0.546 (0.053)	0.540 (0.510, 0.577)
Apolipoprotein-B	320	0.299 (0.103)	0.279 (0.234, 0.337)
Glycolysis related metabolites			
Glucose	313	3.753 (1.333)	3.420 (3.090, 3.899)
Lactate	313	1.228 (0.515)	1.130 (0.944, 1.412)
Citrate	320	0.130 (0.023)	0.128 (0.115, 0.143)
Amino acids			
Alanine	320	0.316 (0.060)	0.314 (0.277, 0.349)
Histidine	320	0.025 (0.009)	0.024 (0.020, 0.028)
Isoleucine	320	0.045 (0.016)	0.042 (0.034, 0.053)
Leucine	320	0.067 (0.021)	0.064 (0.054, 0.075)
Valine	320	0.141 (0.041)	0.136 (0.115, 0.161)
Phenylalanine	302	0.061 (0.011)	0.059 (0.054, 0.066)
Tyrosine	320	0.051 (0.012)	0.049 (0.043, 0.057)
Ketone bodies			
Acetate	316	0.122 (0.080)	0.114 (0.101, 0.129)
Acetoacetate	319	0.011 (0.008)	0.009 (0.007, 0.013)
β-hydroxybutyrate	320	0.144 (0.067)	0.127 (0.107, 0.158)
Fluid balance			
Creatinine	315	0.060 (0.014)	0.058 (0.052, 0.065)
Albumin	320	0.079 (0.007)	0.078 (0.075, 0.082)
Inflammation			
Glycoprotein acetyls	320	1.308 (0.214)	1.291 (1.159, 1.444)

8.3.2. Associations with BMD variables

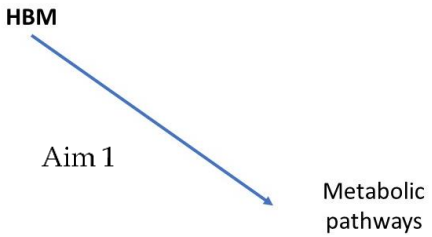

HBM status

In unadjusted analysis, there was some evidence for higher mean concentrations of citrate, phenylalanine and β-hydroxybutyrate in individuals with HBM, and lower mean concentrations of apolipoprotein-A1 and alanine (Figure 76).

However, only the associations with alanine and β-hydroxybutyrate met the corrected *p*-value threshold. After adjustment for potential covariates age, sex, height, and weight, HBM was still strongly associated alanine, with an effect size of -0.38SD ([95% CI -0.61,-0.16], *p*=0.001, effect size=difference in mean concentrations between individuals with and without HBM). Mean apolipoprotein-A1 concentration was lower in individuals with HBM (-0.10SD [-0.20,-3x10^{-3}], *p*=0.04), but this association was not robust to correction for multiple testing. There was evidence of an increased concentration of the ketone body β-hydroxybutyrate in HBM cases, with an effect size of 0.30SD (0.06,0.54), *p*=0.02. Full results are tabulated in Appendix 21.

Figure 76: Associations between HBM and the NMR-assessed metabolic traits.

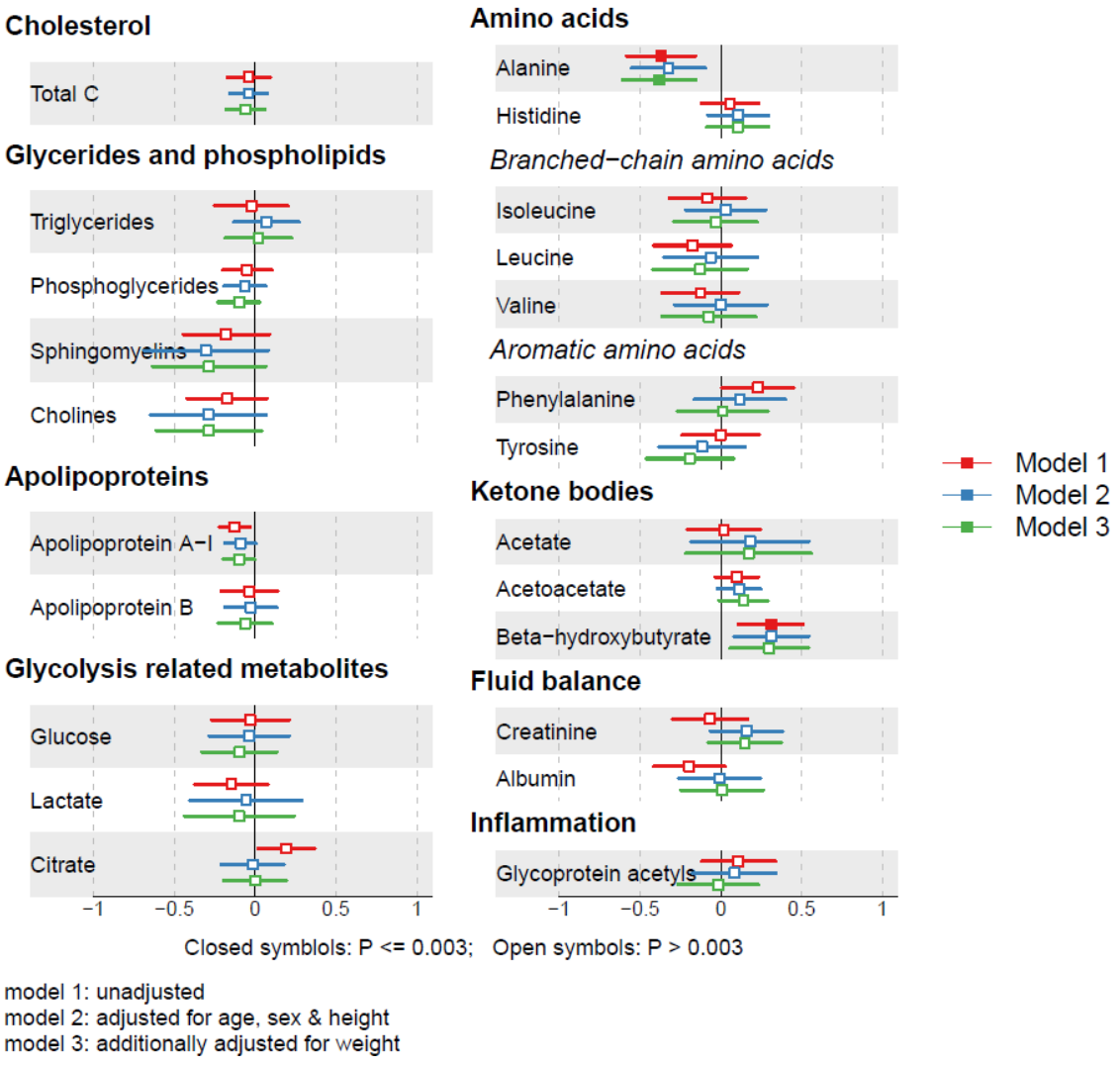

Points represent the SD difference in mean metabolic trait concentration between those with and without HBM. Horizontal bars represent 95%CIs.

Adjustment for additional potential covariates menopause, bisphosphonate use, and oral glucocorticoid use did not alter the strength of associations between HBM and apolipoprotein-A1, alanine or β-hydroxybutyrate (data not shown).

TB-BMD

In unadjusted analyses, TB-BMD appeared negatively associated with total cholines, citrate and tyrosine and positively associated with creatinine, but these associations did not meet the corrected *p*-value threshold (Figure 77). After adjustment for age, sex, height and weight, TB-BMD remained weakly negatively associated with cholines, with an SD increase in TB-BMD associated with 0.1SD lower total cholines (-0.19,-0.01), p=0.03. TB-BMD remained negatively associated with tyrosine concentration (-0.19 [-0.32,-0.07], p=0.003). Adjustment for menopause, bisphosphonate use, and oral glucocorticoid use did not alter these associations. Additional negative associations between TB-BMD and phosphoglycerides, alanine and leucine were observed, but were not robust to correction for multiple testing. Full results are tabulated in Appendix 22.

Figure 77: Associations between total body BMD and metabolic traits in the HBM cohort.

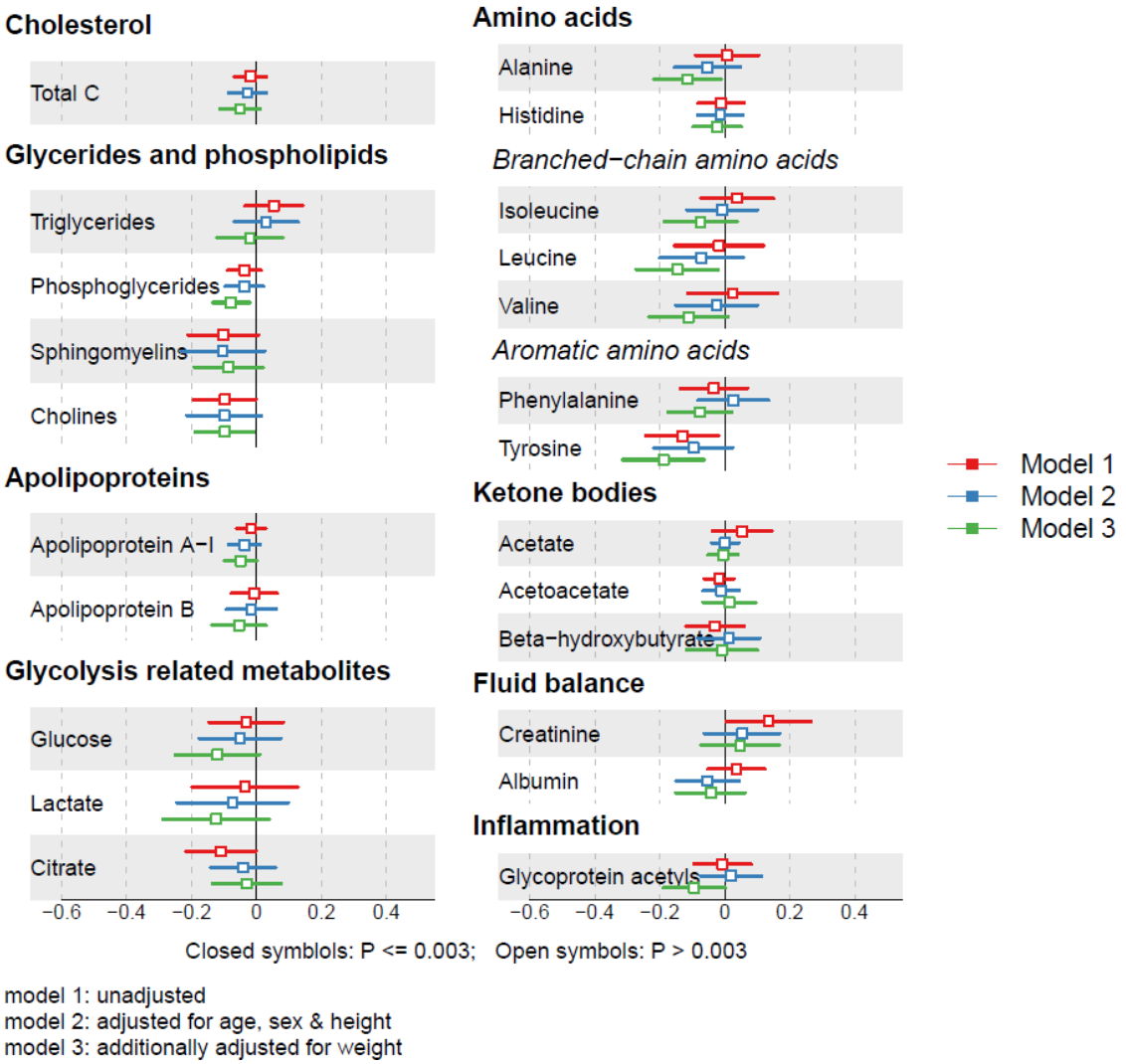

Points represent the SD increase in metabolic trait concentration per SD increase in TB-BMD. Horizontal bars represent 95% CIs.

L1-BMD

In unadjusted analyses, L1-BMD was inversely associated with alanine and positively associated with β-hydroxybutyrate, although neither association was robust to correction for multiple testing (Figure 78). After adjustment for age, sex, height, and weight, L1-BMD remained inversely associated with alanine (β=-0.17 [-0.26,-0.08], p=2x10^{-4}, β=SD change in alanine concentration per SD increase in L1-BMD). This association was robust to additional adjustment for

bisphosphonate use, glucocorticoid use, and menopausal status. Full results are tabulated in Appendix 23.

Figure 78: Associations between L1-BMD and metabolic traits in the HBM cohort.

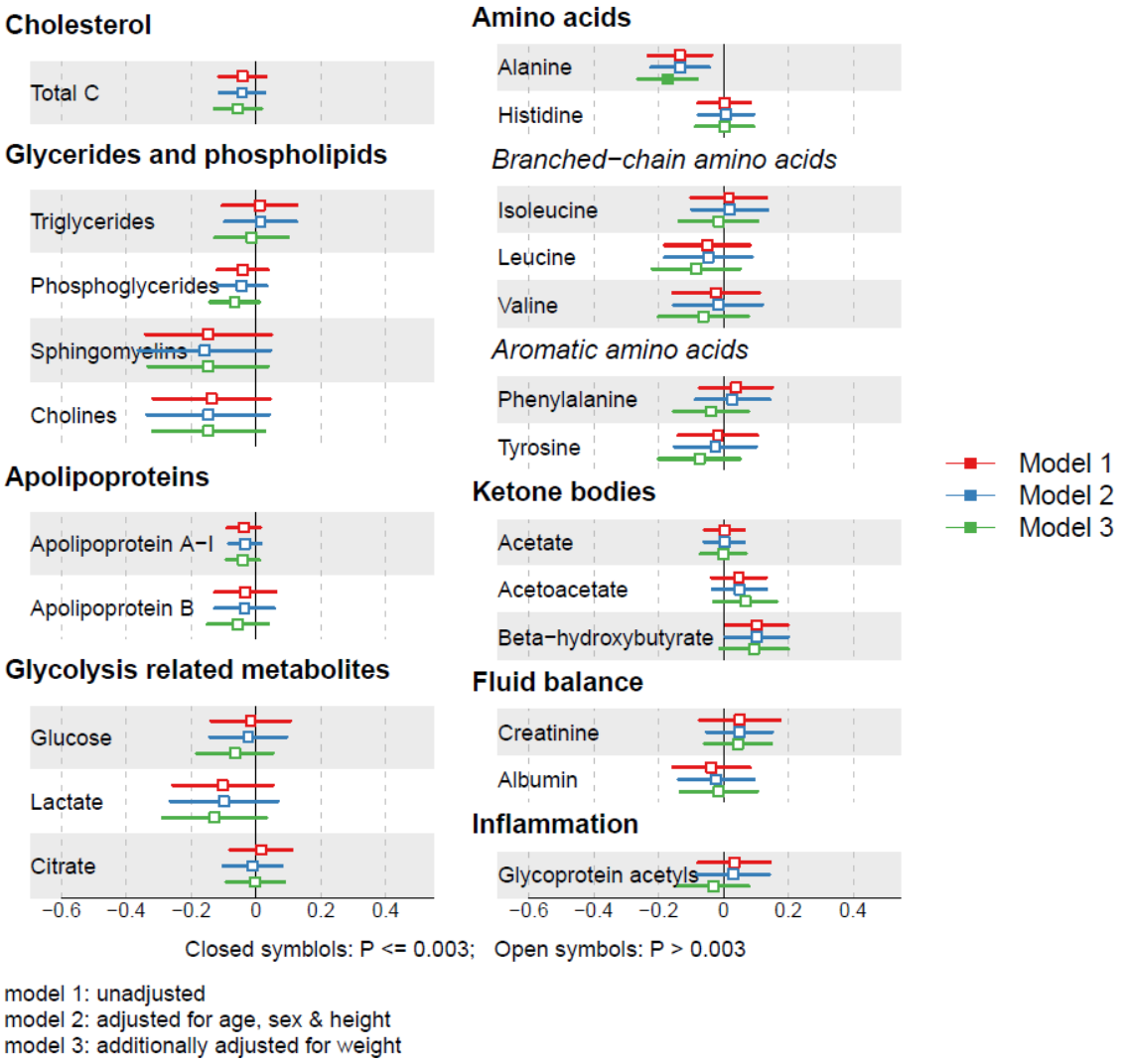

Points represent the SD increase in metabolic trait concentration per SD increase in L1-BMD. Horizontal bars represent 95% CIs.

Maximum TH-BMD

There was no strong evidence for an association between TH-BMD and any metabolic trait in unadjusted analyses (Figure 79). Negative associations with total cholesterol, phosphoglycerides, apolipoprotein-A1 and glucose were present only after adjustment for weight. None of these associations were robust

to correction for multiple testing. These could be evidence of potential collider bias, as weight might be a common effect of both HBM and increased blood glucose and total cholesterol. Full results are tabulated in Appendix 24.

Figure 79: Associations between maximal total hip BMD and metabolic traits in the HBM cohort.

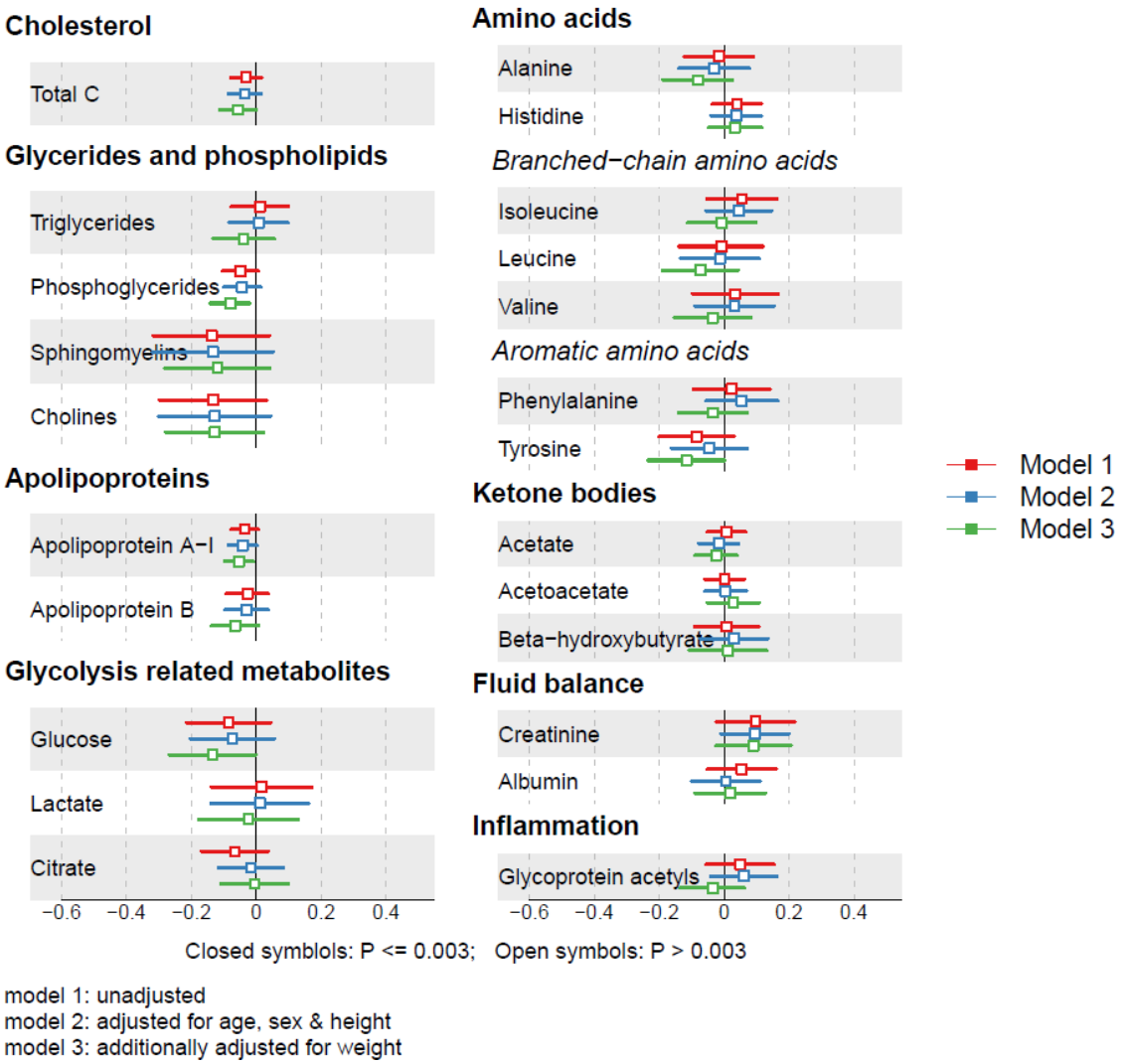

Points represent the SD increase in metabolic trait concentration per SD increase in TH-BMD. Horizontal bars represent 95% CIs.

Sensitivity analyses

The results of the sensitivity analyses are tabulated in Appendix 21-Appendix 24. When >7SD outliers were removed, CIs were narrowed for the association between L1-BMD and cholines, but the effect size was reduced -0.15SD (-

0.32,0.03) *vs* -0.06SD (-0.12,-3x10^{-3}). The same pattern was seen for the association between TB-BMD/TH-BMD and cholines when outliers were removed. When samples with quality control tags (low glucose, high lactate, abnormal macromolecule A, low protein content or high ethanol) were removed (N_{HBM}=3, $N_{no\ HBM}$=6), the associations of HBM and L1-BMD with alanine were partially attenuated (-0.38SD *vs* -0.26SD and -0.17SD *vs* -0.11SD, respectively). Removing the tagged samples widened the CIs for the association between TB-BMD and alanine and the null value was included (-0.08 [-0.19,0.03]). Evidence for associations between TB-BMD and phosphoglycerides, cholines, leucine and glycoprotein acetyls were weakened when tagged samples were removed (CIs just overlapped the null). The inverse association between HBM and apolipoprotein-A1 was attenuated by removal of tagged samples. Evidence for associations between TH-BMD and apolipoprotein-A1 and phosphoglycerides was also weakened by removing samples with QC tags.

8.3.3. Associations between metabolic traits and OA sub-phenotypes

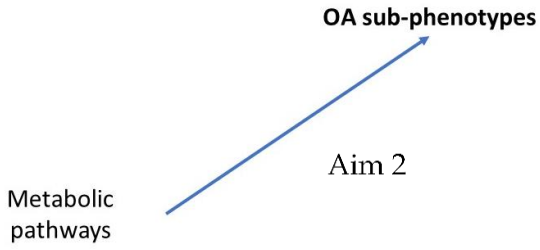

Hip Osteophytes

There was strong evidence for an increased odds of any hip osteophyte with increasing glucose concentration in unadjusted and age, sex, and height-adjusted analyses ($OR_{model\ 2}$=1.51 [1.16,1.98], p=0.002, Figure 80). Adjustment for weight did not attenuate the association, with an SD increase in glucose associated with 49% increased odds of hip osteophytes. There was some evidence for a decreased odds of hip osteophytes per SD increase in acetoacetate and an increased odds per SD increase in glycoprotein acetyls ($OR_{model\ 3}$=0.67 [0.47,0.96], p=0.03 and 1.29 [1.01,1.64], p=0.04, respectively).

Figure 80: Associations between metabolic traits and any hip osteophyte in the HBM cohort.

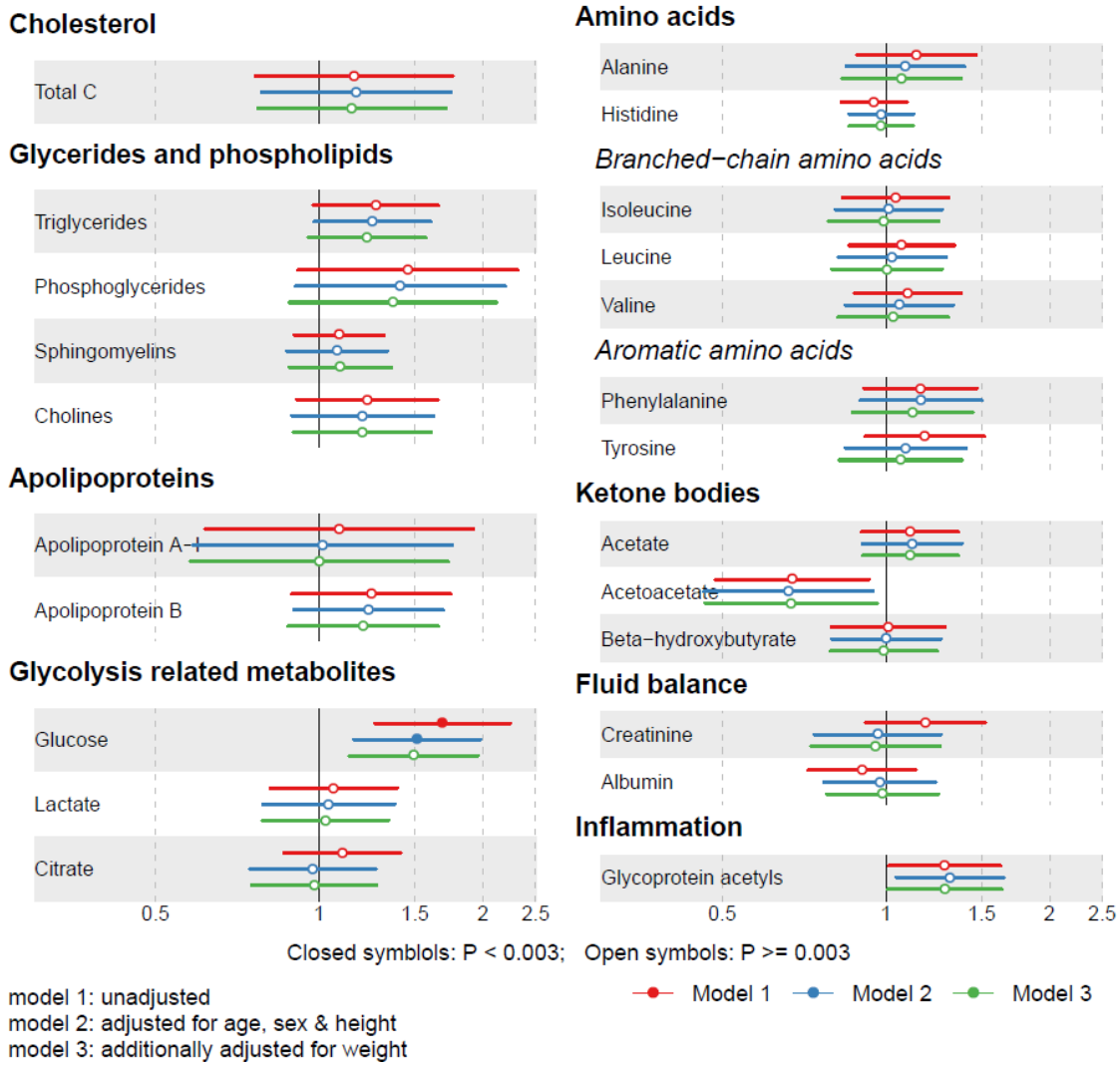

Points represent the OR for hip osteophytes per SD increase in metabolic trait concentration. Horizontal bars represent 95% CIs.

JSN

Evidence for associations between the metabolic traits and odds of hip JSN was very weak (Figure 81). The only metabolic traits where CIs did not overlap the null value were cholines ($OR_{model\ 3}$=1.23 [1.03,1.48], p=0.02) and creatinine ($OR_{model\ 3}$=0.72 [0.54,0.95], p=0.02).

Figure 81: Associations between standardized metabolic traits and hip JSN in the HBM cohort.

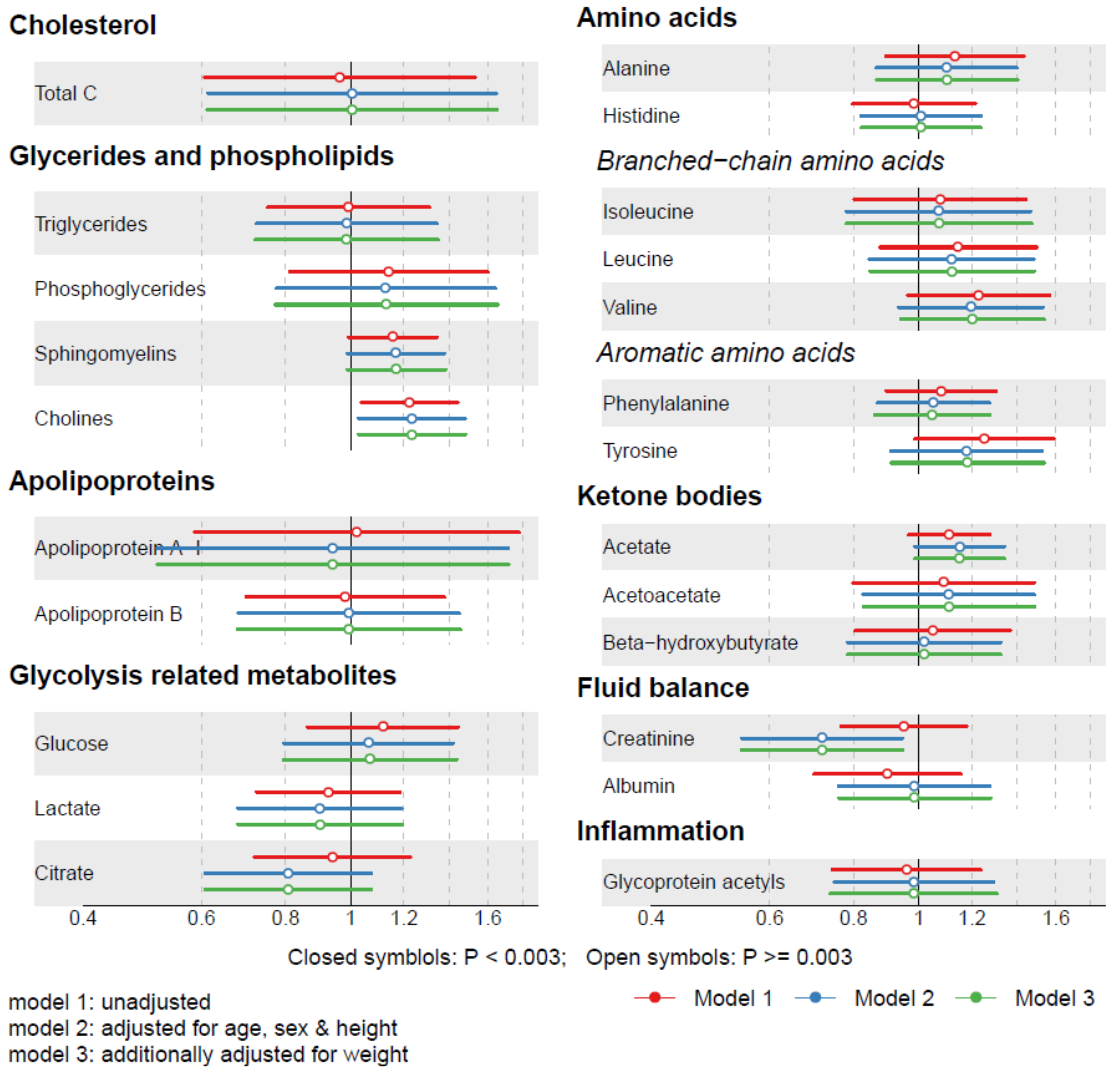

Points represent the OR for hip JSN per SD increase in metabolic trait concentration. Horizontal bars represent 95% CIs.

Knee

Osteophytes

I did not observe evidence for associations between any of the metabolic traits and any knee osteophyte (Figure 82). This was the same before and after adjustment for weight.

Figure 82: Associations between standardized metabolic traits and any knee osteophyte in the HBM cohort.

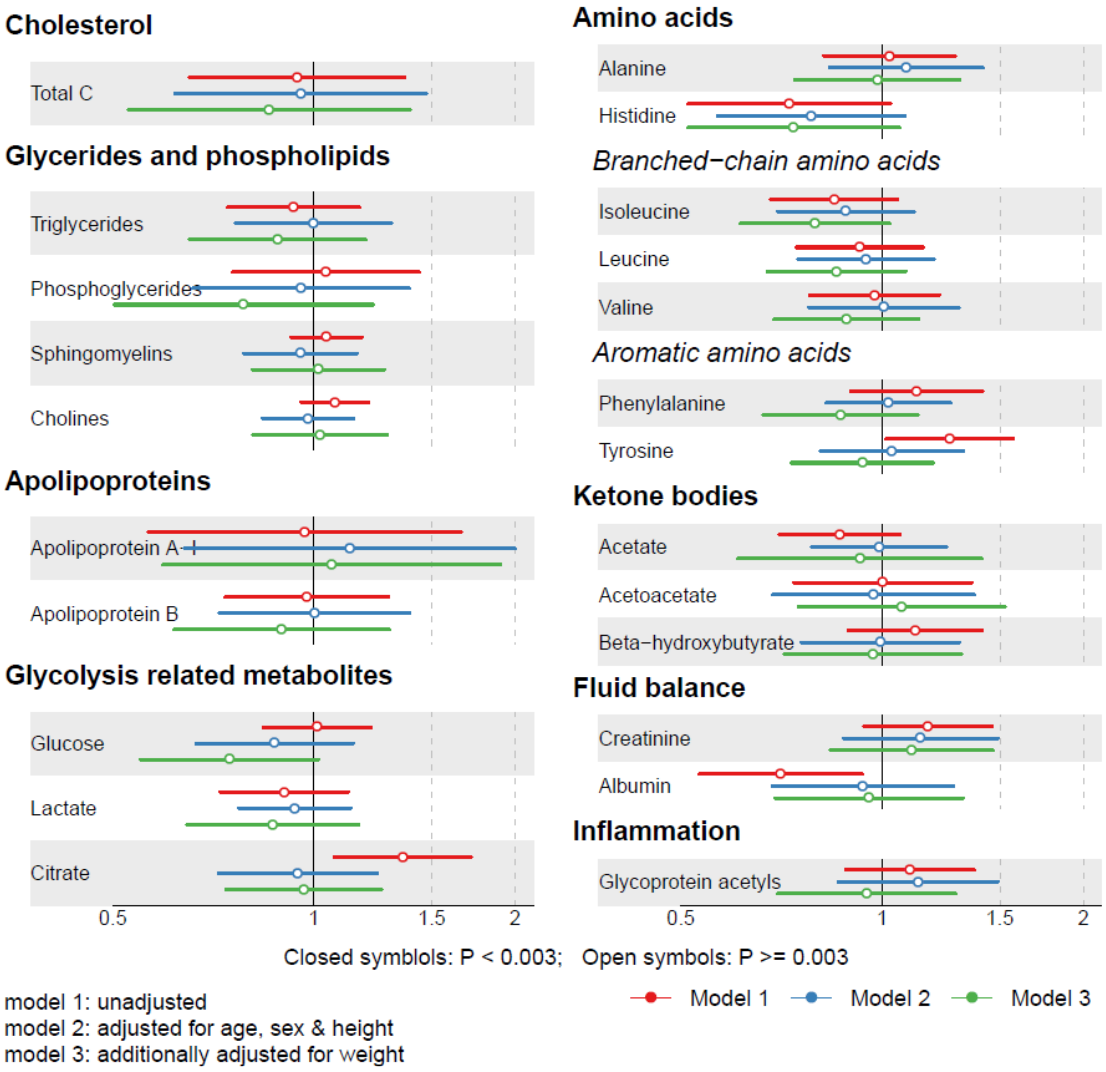

Points represent the OR for knee osteophytes per SD increase in metabolic trait concentration. Horizontal bars represent 95% CIs.

JSN

There was some evidence for an association between an SD increase in both sphingomyelins and cholines and a 20-30% increased odds of any knee JSN (p=0.03 and 0.01, respectively, Figure 83). I found some evidence that higher lactate concentration was associated with decreased odds of knee JSN ($OR_{model\ 3}$=0.57 [0.36,0.91], p=0.02. In unadjusted analyses, citrate was strongly associated with an increased odds of knee JSN, but the association was attenuated by

approximately 50% when adjusting for age, sex and height and CIs overlapped the null.

Figure 83: Associations between standardized metabolic traits and knee JSN in the HBM cohort.

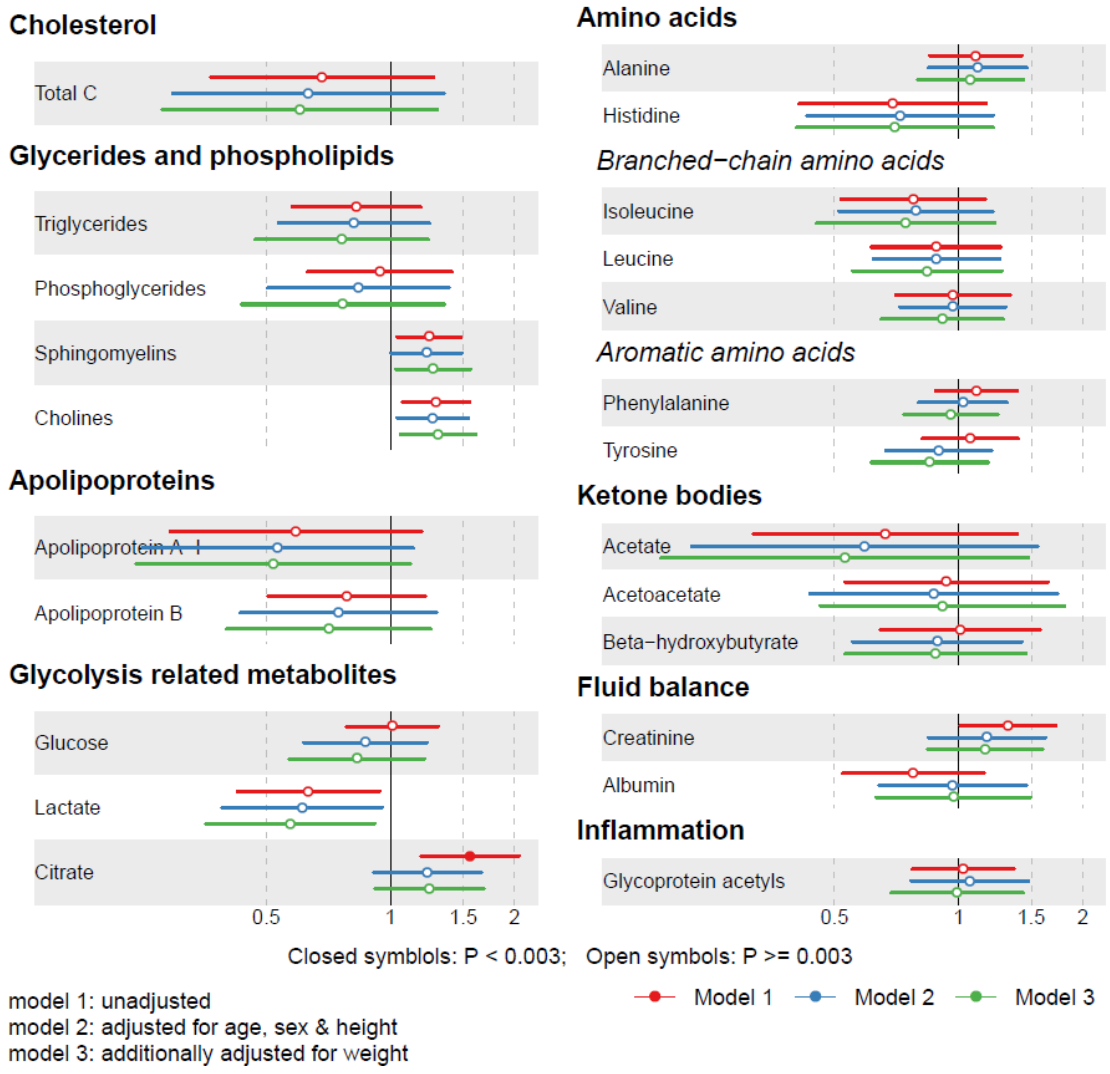

Points represent the OR for knee JSN per SD increase in metabolic trait concentration. Horizontal bars represent 95% CIs.

Hand

Osteophytes

Evidence for associations between metabolic traits and osteophytes at the DIP or CMC joints was weak, with the CIs overlapping the null when adjusted for age and sex, for all metabolic traits except lactate, for which there was some evidence

for a reduced odds of DIP osteophytes with increasing lactate concentration in all three models ($OR_{model\ 3}$=0.66 [0.49,0.89], p=0.006, Figure 84, Figure 85).

Figure 84: Associations between standardized metabolic traits and DIP osteophytes in the HBM cohort.

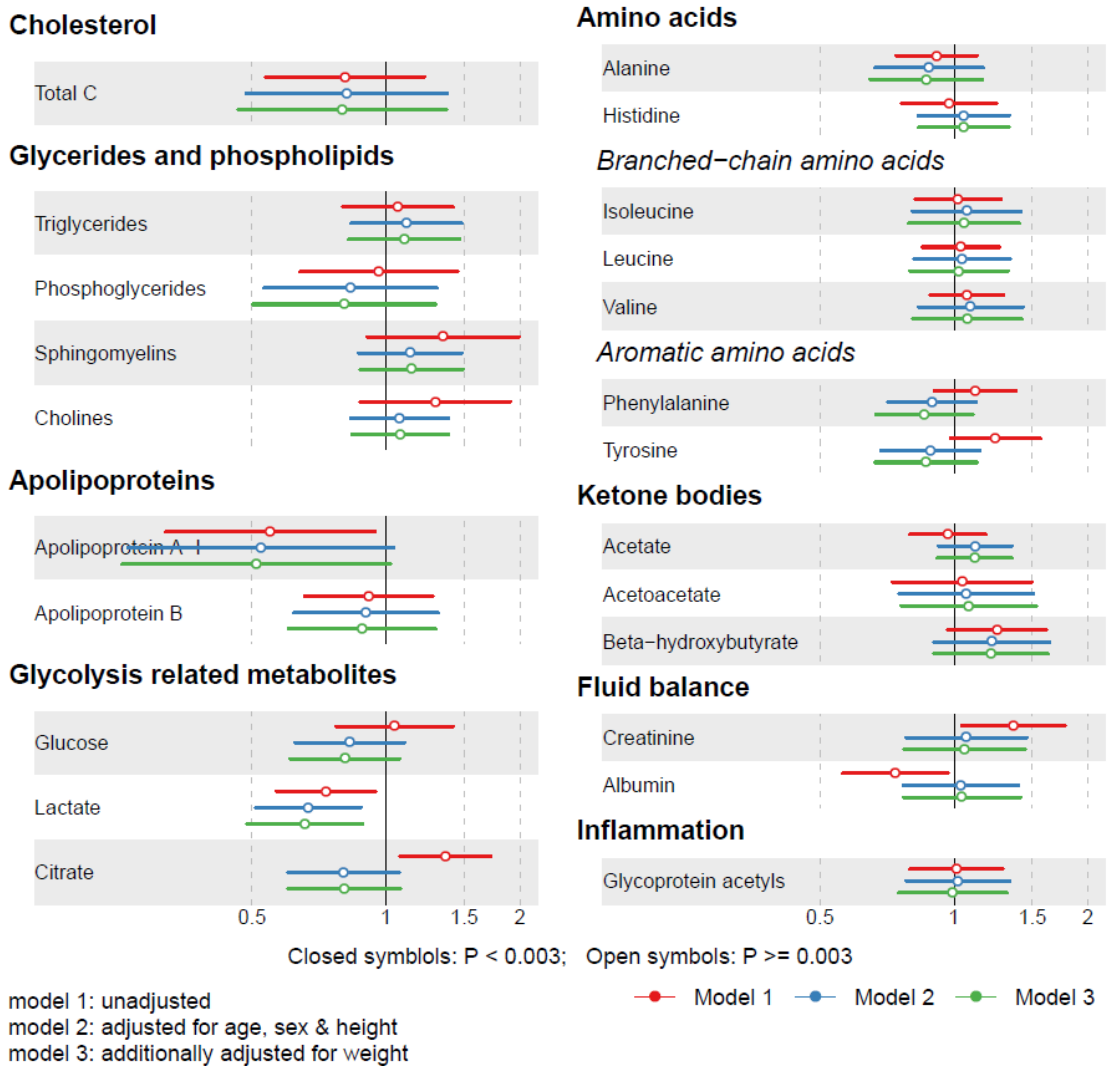

Points represent the OR for any DIP osteophyte per SD increase in metabolic trait concentration. Horizontal bars represent 95% CIs.

Figure 85: Associations between standardized metabolic traits and CMC osteophytes in the HBM cohort.

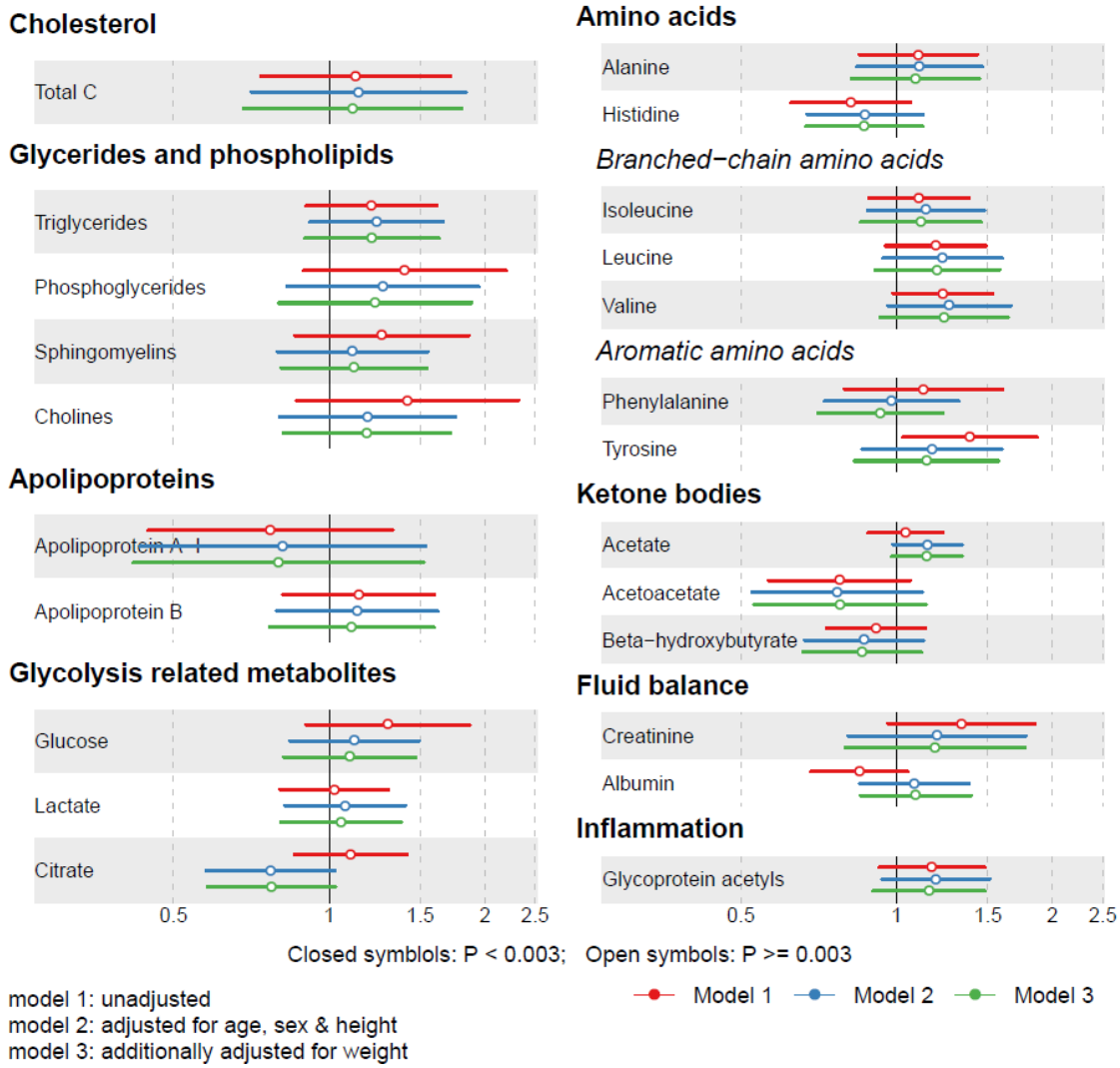

Points represent the OR for any CMC osteophyte per SD increase in metabolic trait concentration. Horizontal bars represent 95% CIs.

JSN

After adjustment for age and sex, there was evidence for a reduced odds of DIP JSN with increasing glucose and tyrosine concentrations ($OR_{model\ 3}$=0.65 [0.46,0.90] and 0.74 [0.58,0.94], respectively, p<0.02, Figure 86). Odds of CMC JSN, however, were higher with increasing total cholesterol and apoliprotein-A1 concentrations, although CIs were wide and the p-value was greater than the corrected threshold ($OR_{model\ 3}$=1.61 [1.08,2.40], p=0.02 and 1.86 [1.03,3.36], p=0.04, respectively, Figure 87).

Figure 86: Associations between standardized metabolic traits and DIP JSN in the HBM cohort.

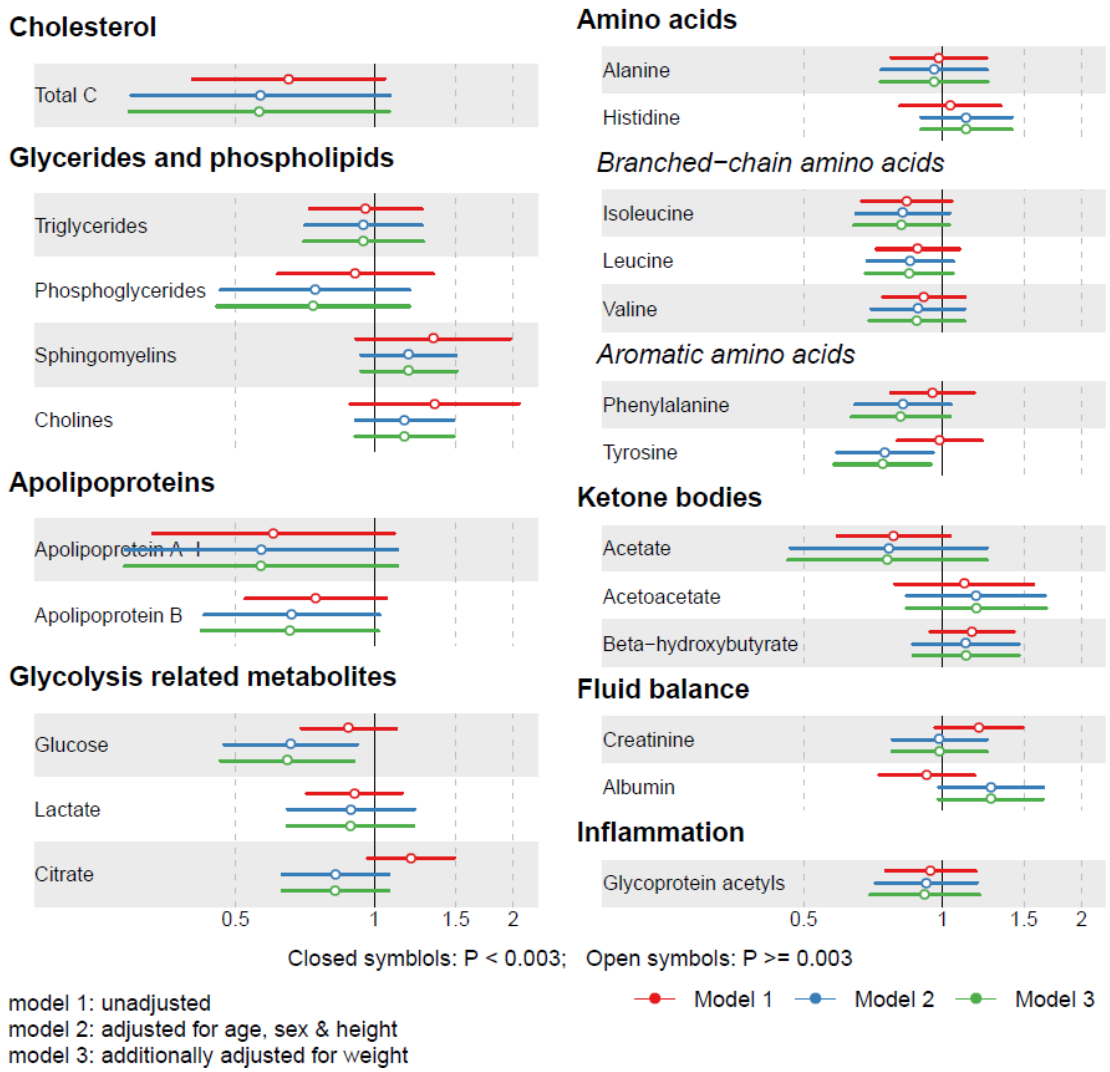

Points represent the OR for DIP JSN per SD increase in metabolic trait concentration. Horizontal bars represent 95% CIs.

Figure 87: Associations between standardized metabolic traits and CMC JSN in the HBM cohort.

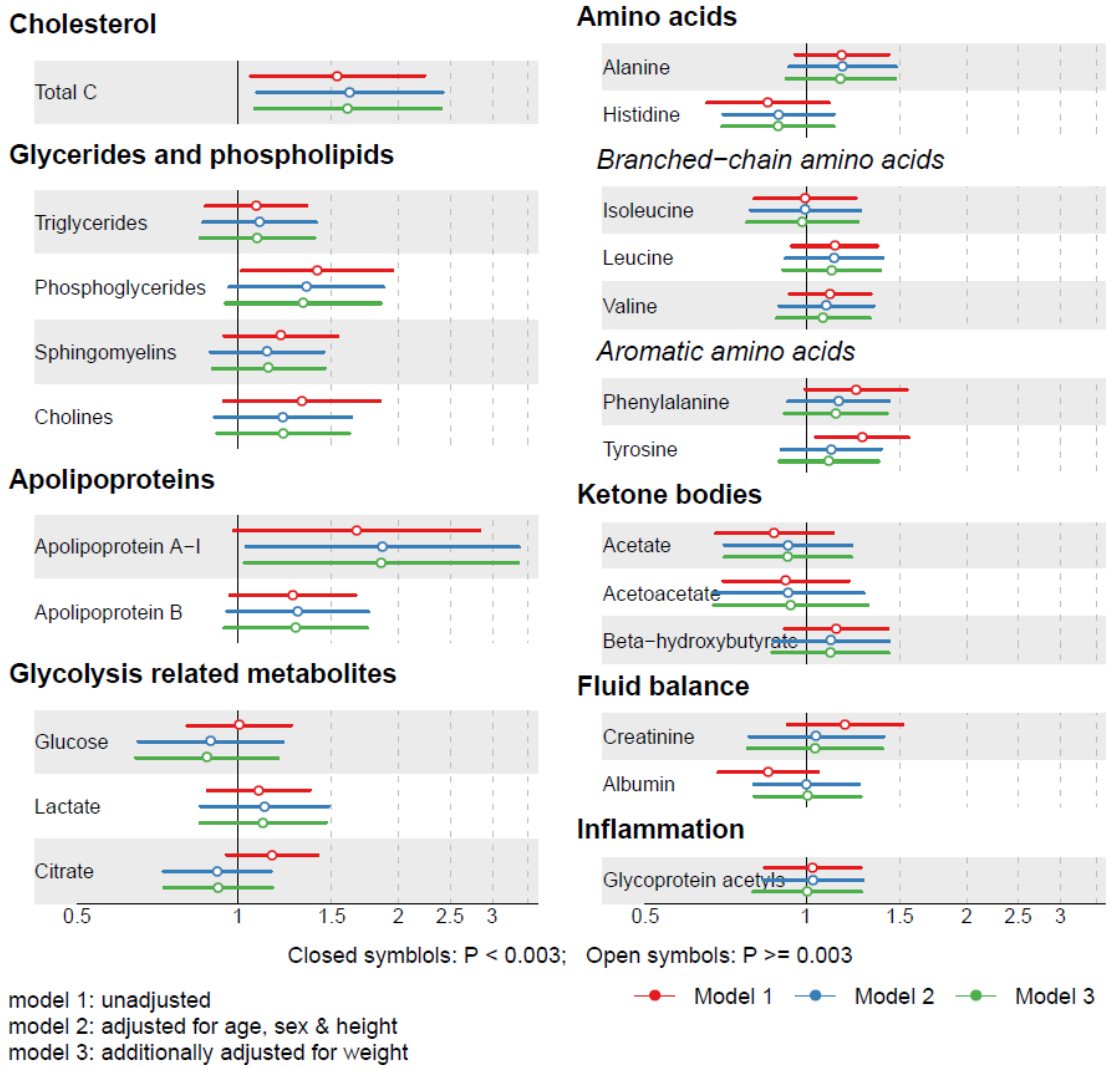

Points represent the OR for CMC JSN per SD increase in metabolic trait concentration. Horizontal bars represent 95% CIs.

Sensitivity analyses

Removing ≥7SD outliers weakened evidence for an association between acetoacetate and hip osteophytes, and attenuated associations between sphingomyelins/cholines and hip and knee JSN. An inverse association between acetate and hip JSN was apparent after the removal of outliers (full results provided in Appendix 25-Appendix 32).

8.3.4. Replication of BMD and OA associations in the general population

To determine the generalizability of any BMD or OA sub-phenotype-associated metabolic trait to the general population, I sought replication in a cohort sampled from the general population. The RS1 population had data for all radiographic sub-phenotypes and metabolomics data cross-sectionally for 2,801 individuals. As I did not identify any metabolic traits associated with BMD or OA sub-phenotypes at the Bonferroni-corrected *p*-value threshold, I attempted to replicate analyses for any metabolic traits associated with either TH/L1-BMD (as these were measured in the RS population) or any OA sub-phenotype at a suggestive *p*-value threshold (*i.e.* $p<0.05$) in the HBM cohort (Table 26).

Table 26: Summary of results of metabolomics analyses in the HBM cohort and the metabolic traits selected for replication.

Outcome	BMD				OA								Selected for Replication
	HBM	TB	L1	TH	Hip ost.	Hip JSN	Knee ost.	Knee JSN	DIP ost.	DIP JSN	CMC ost.	CMC JSN	
Acetoacetate					-								1
Acetate													0
Alanine	-		-										1
Albumin													0
Apolipoprotein A1													1
Apolipoprotein B													0
Beta hydroxybutyrate	+												Data not available
Citrate													0
Creatinine						-							1
Glucose					+					-			1
Glycoprotein acetyls					+								1
Histidine													0
Isoleucine													0
Lactate								-	-				1
Leucine													0
Phenylalanine													0
Total cholesterol													0
Triglycerides													0
Sphingomyelins													0
Cholines		-											Data not available
Phosphoglycerides													0
Tyrosine		-								-			1*
Valine													0

*'-' represents an inverse association identified at p<0.05, '+' represents a positive association at p<0.05. Blank boxes represent no identified associations or associations only identified after adjustment for weight. * TB-BMD data not available for replication.*

Descriptives of the study population

2,801 individuals from RS1 who attended the 4th outcome assessment (RS1-4) had metabolomic data. Descriptives of the RS1-4 population are presented in Table 27.

Table 27: Descriptives of the RS1-4 population with metabolomics data.

	Mean (SD)
Age (years)	75.0 (5.8)
Height (cm)	166.4 (9.2)
Weight (kg)	75.9 (13.2)
L1-BMD	0.998 (0.197)
Total hip BMD	1.109 (0.122)
	N (%)
Female	1,491 (57.9)
Hip osteophyte	1,599 (86.1)
Hip JSN	1,020 (54.9)
Knee osteophyte	1,215 (69.5)
Knee JSN	879 (50.3)
DIP osteophyte	1,635 (66.1)
DIP JSN	266 (10.8)
CMC osteophyte	1,132 (45.8)
CMC JSN	303 (12.3)

Osteophytes/ JSN represent an OARSI grade≥1.

The metabolic traits assessed in RS1 are summarised in Table 28.

Table 28: Summary of the metabolic traits assessed for associations with BMD or OA sub-phenotypes in the RS1-4 population.

Metabolic trait (mmol/l)	**N**	**Mean**	**SD**	**Median**	**LQ**	**UQ**
Glucose	2,801	4.817	1.180	4.506	4.208	4.983
Lactate	2,801	0.791	0.290	0.727	0.594	0.913
Alanine	2,801	0.293	0.069	0.285	0.244	0.331
Tyrosine	2,801	0.060	0.011	0.059	0.053	0.066
Acetoacetate	2,801	0.037	0.021	0.033	0.024	0.046
β-hydroxybutyrate	2,801	0.095	0.074	0.071	0.055	0.107
Creatinine	2,801	0.072	0.019	0.069	0.060	0.081
Glycoprotein acetyls	2,801	1.303	0.159	1.285	1.195	1.392

BMD

In unadjusted analyses, there was strong evidence for a positive association between both FN and L1-BMD and alanine, the opposite direction to that

observed in HBM (Table 29). The magnitudes of these associations were strengthened by adjustment for age, sex, and height. Additional adjustment for weight attenuated the association between FN-BMD and alanine by over 50% and CIs overlapped the null (β=-0.03 [-0.02,0.08], *p*=0.2). There was still some weak evidence for an association between L1-BMD and alanine, although the magnitude of the association was attenuated by approximately 50% (0.05 [0.01,0.09], *p*=0.02). In original units, this is equivalent to a 0.26mmol/L increase in alanine per 1g/cm^2 increase in L1-BMD (95%CI 0.04,0.48), compared to a 0.04mmol/L (0.02,0.07) decrease per 1g/cm^2 observed in the HBM population.

OA

Associations of glucose, acetoacetate and glycoprotein acetyls with any hip osteophyte, lactate with any knee JSN, lactate with any DIP osteophyte and glucose with any DIP JSN did not replicate in RS (Table 29). There was some evidence for a reduced odds of hip JSN with increasing creatinine concentration. This association was the same direction, but of weaker magnitude, to that observed in the HBM population (OR_{HBM} per 0.01mmol/L increase=0.76 [0.62,0.94] *vs* OR_{RS1}=0.91 [0.86,0.97]). There was weak evidence for a reduced odds of DIP JSN per SD increase in tyrosine concentration in RS. This was the same direction and of similar magnitude to the association observed in the HBM population (OR_{HBM} per 0.01mmol/L increase=0.78 [0.64,0.95] *vs* OR_{RS1}=0.86 [0.76,0.98]).

Table 29: Results of metabolomics replication analyses in the RS1-4 population and comparison with effect sizes in the HBM cohort.

			Model 1		Model 2		Model 3		HBM Model 3		
Exposure	**Outcome**	**N**	**β (95% CI)**	**p**	**β (95% CI)**	**p**	**β (95% CI)**	**p**	**N**	**β (95% CI)**	**p**
FN-BMD	Alanine	2,576	0.06 (0.02, 0.10)	0.002	0.08 (0.03, 0.12)	0.001	0.03 (-0.02, 0.08)	0.201	315	-0.08 (-0.19, 0.03)	0.153
L1-BMD	Alanine	2,576	0.07 (0.03, 0.11)	$4x10^{-4}$	0.10 (0.06, 0.14)	$4x10^{-6}$	0.05 (0.01, 0.09)	0.019	318	-0.17 (-0.26, -0.08)	$3x10^{-4}$
		N	**OR (95% CI)**	**p**	**OR (95% CI)**	**p**	**OR (95% CI)**	**p**		**OR (95% CI)**	**p**
Glucose	Hip osteophyte	1,823	0.99 (0.87, 1.13)	0.829	0.98 (0.87, 1.12)	0.740	0.99 (0.88, 1.15)	0.928	507	1.49 (1.14, 1.96)	0.004
Acetoacetate	Hip osteophyte	1,823	1.01 (0.89, 1.16)	0.884	0.97 (0.86, 1.11)	0.648	0.97 (0.85, 1.11)	0.634	519	0.67 (0.47, 0.96)	0.031
Glycoprotein acetyls	Hip osteophyte	1,823	0.92 (0.8, 1.05)	0.230	0.93 (0.81, 1.06)	0.252	0.94 (0.82, 1.07)	0.336	521	1.29 (1.01, 1.64)	0.042
Creatinine	Hip JSN	1,823	0.93 (0.85, 1.02)	0.138	0.85 (0.77, 0.95)	0.004	0.86 (0.77, 0.95)	0.005	511	0.72 (0.54, 0.95)	0.019
Lactate	Knee JSN	1,746	0.93 (0.85, 1.02)	0.141	0.95 (0,86, 1.04)	0.271	0.94 (0.85, 1.03)	0.185	588	0.57 (0.36, 0.91)	0.020
Lactate	DIP osteophyte	2,419	1.04 (0.95, 1.13)	0.423	1.06 (0.97, 1.15)	0.236	1.05 (0.96, 1.14)	0.333	312	0.66 (0.49, 0.89)	0.006
Glucose	DIP JSN	2,419	1.08 (0.96, 1.21)	0.176	1.09 (0.96, 1.22)	0.167	1.05 (0.92, 1.19)	0.408	312	0.65 (0.46, 0.90)	0.011
Tyrosine	DIP JSN	2,419	0.89 (0.77, 1.01)	0.079	0.89 (0.78, 1.02)	0.100	0.85 (0.74, 0.98)	0.025	319	0.74 (0.58, 0.94)	0.015

β represents the SD increase in metabolic trait concentration per SD increase in BMD. ORs are per SD increase in metabolic trait concentration. Model 1: unadjusted, model 2: adjusted for age, sex, and height, model 3: model 2 plus weight.

8.3.5. Metabolomics of bone turnover

Bone formation markers

P1NP

P1NP was not associated with any of the cholesterol, glyceride, phospholipid or apolipoprotein, ketone body, fluid balance or inflammation measures in any model (Figure 88). Weak evidence for a positive association with citrate was observed ($\beta_{model\ 3}$=0.11 [4x10^{-3},0.21], p=0.04). A positive association with alanine of magnitude 0.14SD (0.02,0.26) (model 3) was observed, but this was not robust to correction for multiple testing (p=0.03). Full results are tabulated in Appendix 33.

Figure 88: Associations between P1NP and metabolic traits in the HBM cohort.

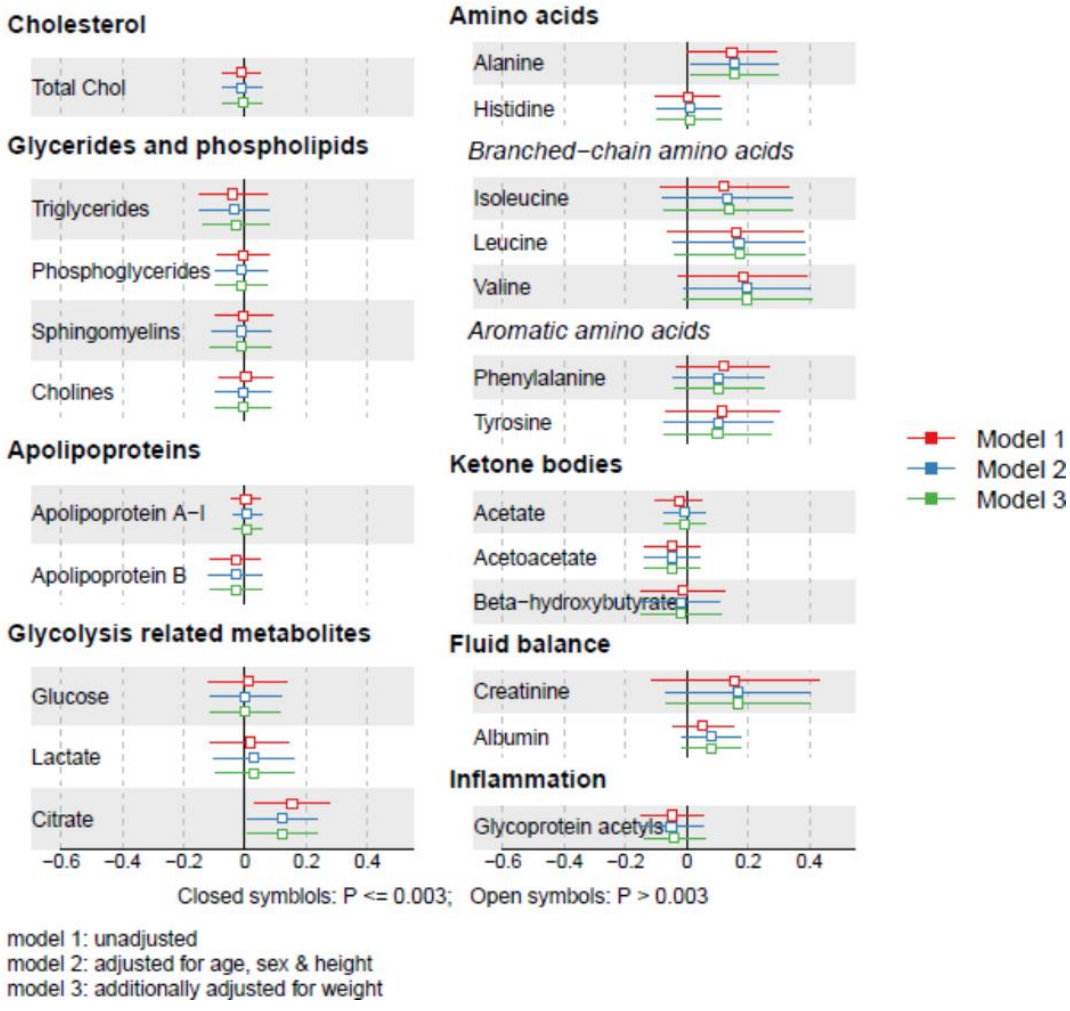

Points represent the SD increase in metabolic trait concentration per SD increase in P1NP. Horizontal bars represent 95% CIs.

Osteocalcin

There was some evidence for negative associations of osteocalcin with total triglycerides and lactate in all models, but these associations were not robust to correction for multiple testing (Figure 89). There was slightly stronger evidence of a positive association with citrate ($\beta_{model\ 3}$=0.14 [0.03,0.24], p=0.01), but this did not reach the corrected significance threshold in any model. After adjustment for all covariates, CIs for the association between osteocalcin and creatinine were narrower and no longer overlapped the null value (0.19 [$3x10^{-3}$,0.37], p=0.047). Full results are tabulated in Appendix 34.

Figure 89: Associations between plasma osteocalcin and metabolic traits in the HBM cohort.

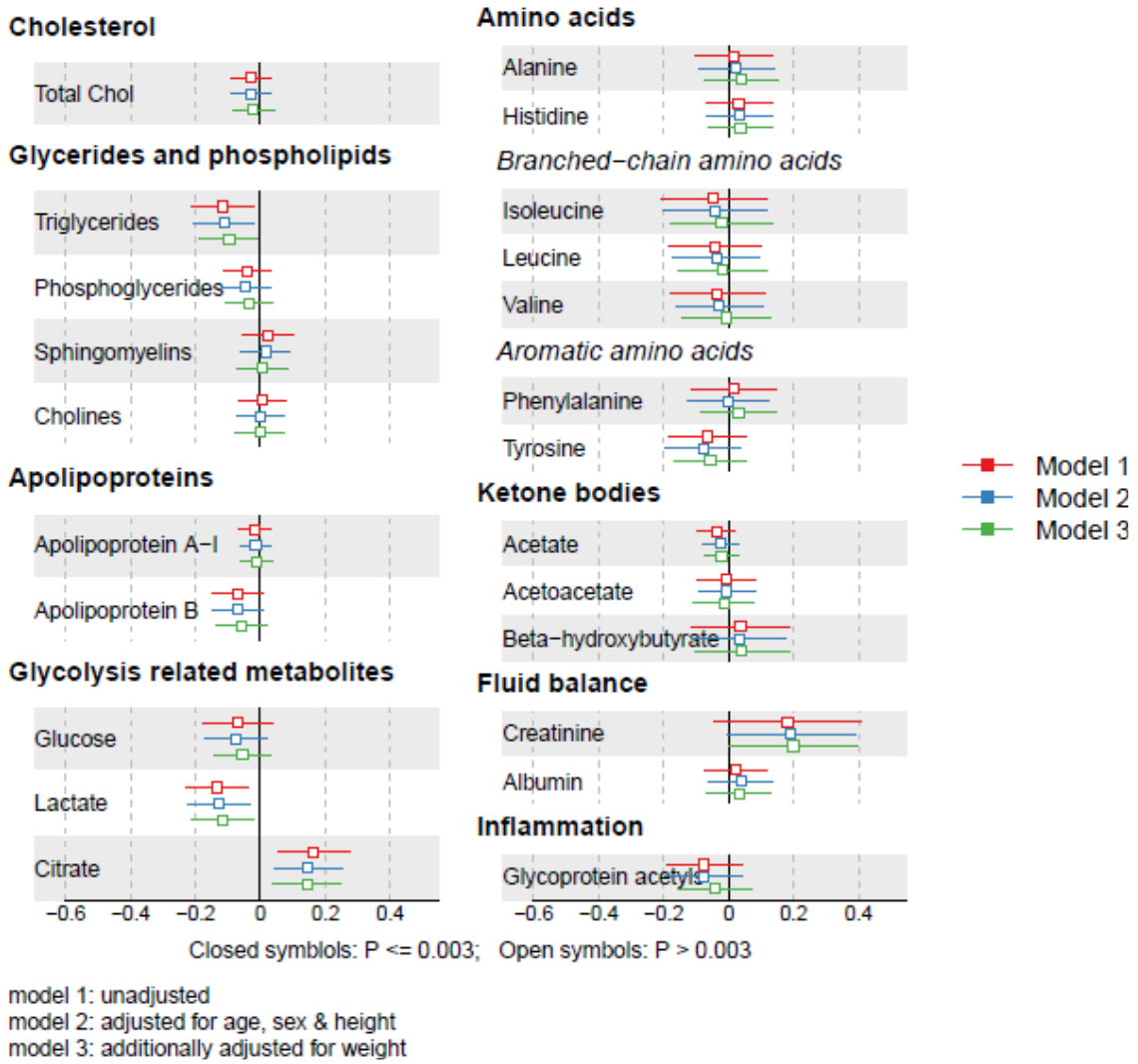

Points represent the SD increase in metabolic trait concentration per SD increase in osteocalcin. Horizontal bars represent 95% CIs.

Bone resorption

β-CTX

β-CTX was strongly inversely associated with triglycerides and positively associated with citrate in all models ($\beta_{model\ 3}$=-0.13 [-0.21,-0.05], p=0.002 and 0.19 [0.07,0.30], p=0.002, respectively) (Figure 90). There was weaker evidence for negative associations between β-CTX and phosphoglycerides, apolipoprotein-B and glucose, but these were of weak magnitude (magnitude ~-0.1SD, all p>0.003). Full results are tabulated in Appendix 35.

Figure 90: Associations between plasma β-CTX and metabolic traits in the HBM cohort.

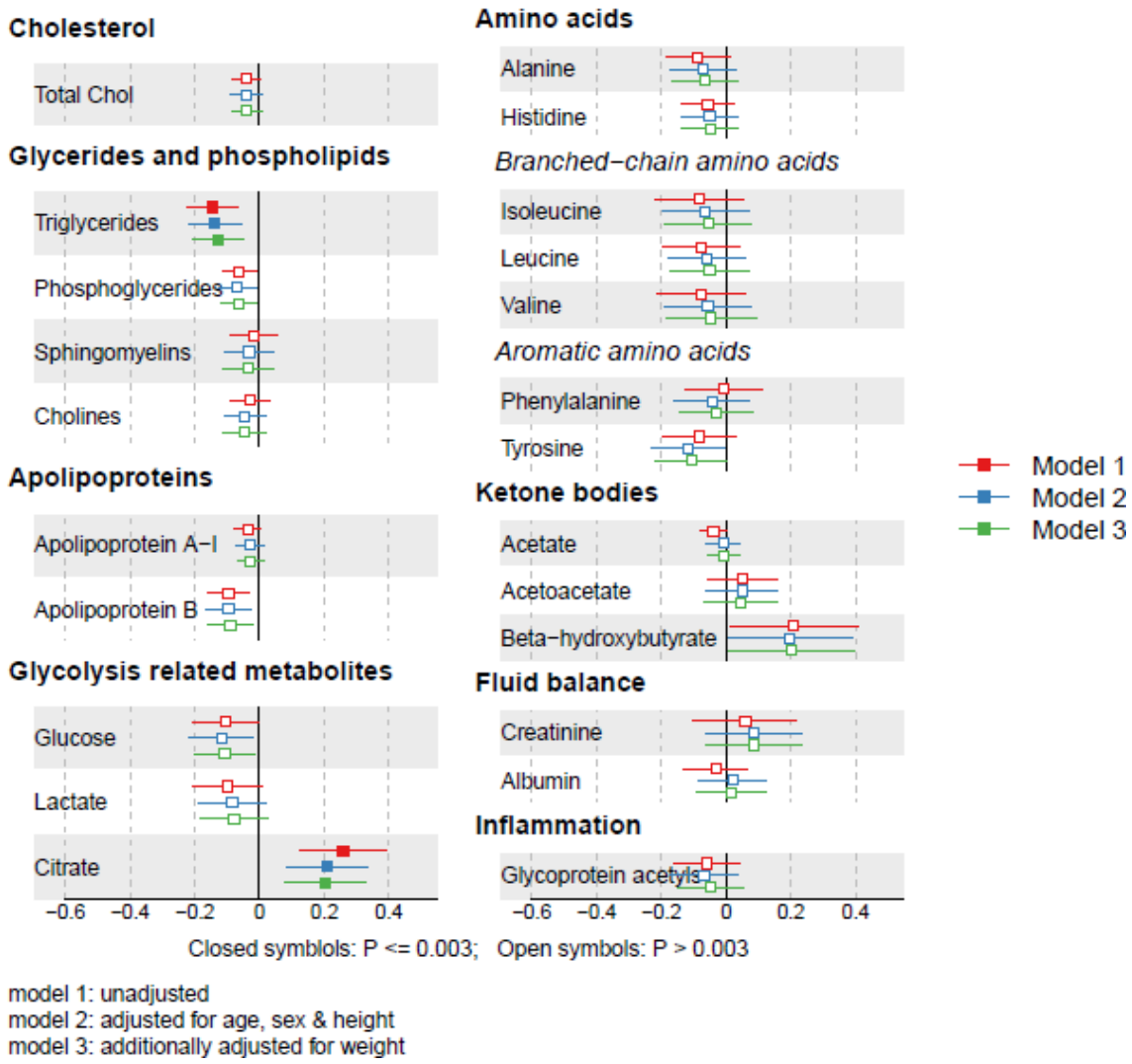

Points represent the SD increase in metabolic trait concentration per SD increase in β-CTX. Horizontal bars represent 95% CIs.

Adjustment for additional potential covariates menopause, bisphosphonate use, and oral glucocorticoid use did not attenuate the association between β-CTX and citrate (0.19 [0.07,0.30], p=0.001) or triglycerides (-0.15 [-0.23,-0.06], p=4x10^{-4}).

Determining differences in associations between HBM individuals and those with normal BMD

I next investigated differences in associations of β-CTX and citrate/triglycerides, between HBM individuals and the relatives without HBM, using stratified analyses and model 3. Mean citrate in the HBM cases was 0.132 (0.025)mmol/L

vs 0.127 (0.019)mmol/L in the relatives without HBM. Mean triglyceride concentrations were 0.672 (0.210)mmol/L and 0.670 (0.281)mmol/L, respectively. The sample size was small for each stratum (198 with HBM, 122 without), which led to wide CIs due to a lack of power. An interaction between HBM status and β-CTX was observed for citrate, but not for triglycerides (Figure 91, Figure 92). When combining all three BTMs in the same model, only β-CTX remained independently associated with citrate.

Figure 91: Association between β-CTX and citrate stratified by HBM status.

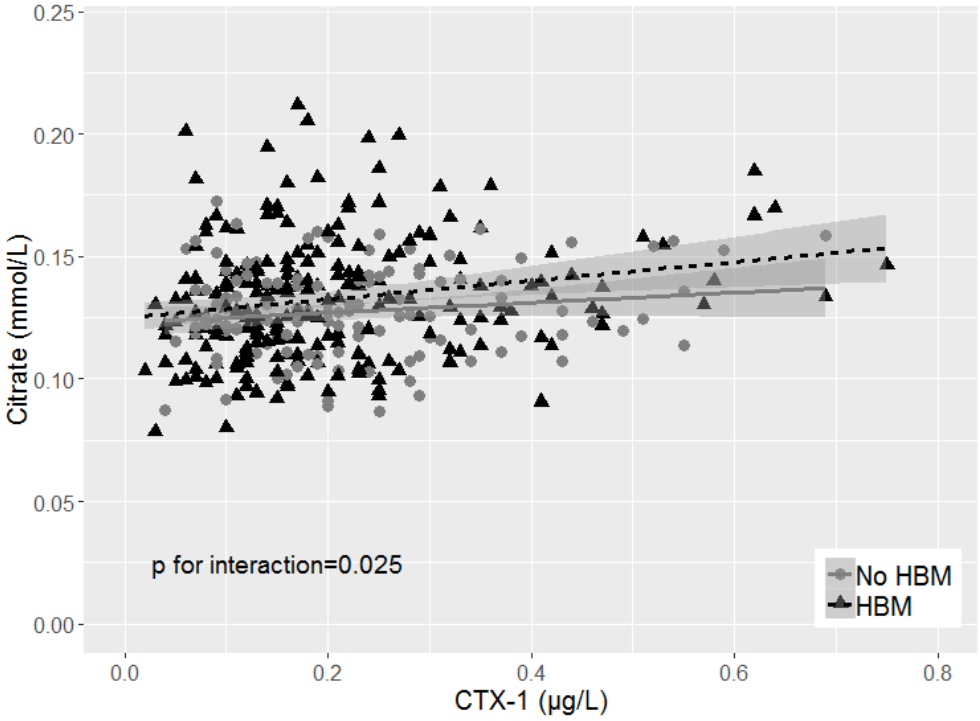

Figure 92: Associations between β-CTX and serum triglycerides, stratified by HBM status.

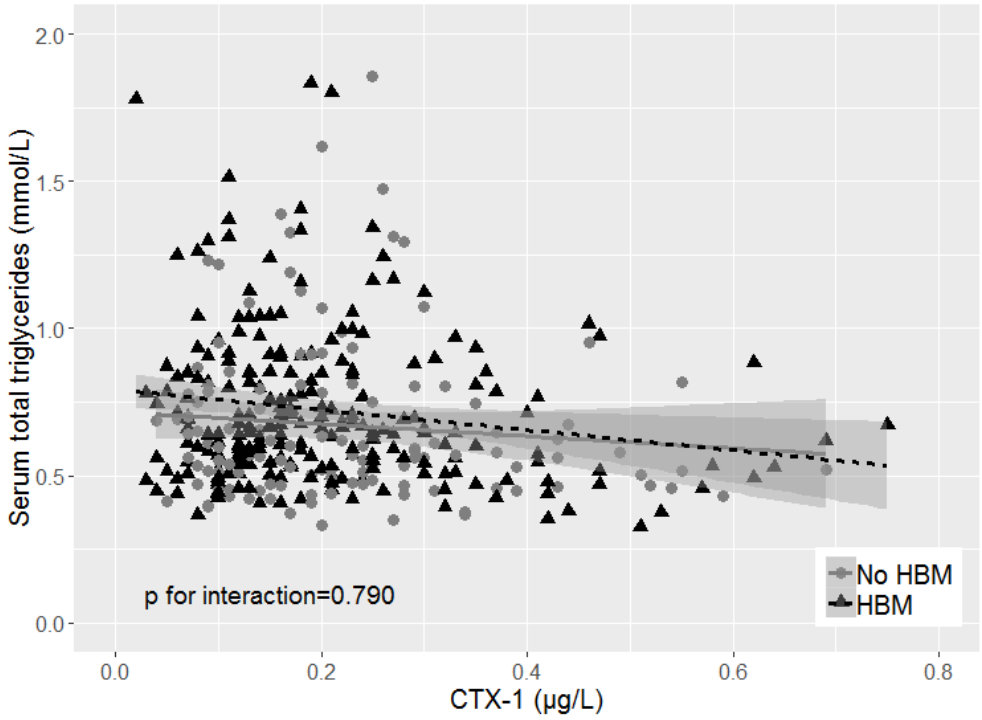

I performed additional analyses of the triglyceride sub-types; results are presented in Table 30. β-CTX was inversely associated with all triglyceride sub-variables (triglycerides in VLDL, LDL and HDL), particularly VLDL triglycerides. The association between osteocalcin and triglycerides appeared driven by VLDL. β-CTX was independently (of other BTMs) associated with total, VLDL and LDL triglycerides. After adjustment for other BTMs, there was weak evidence for positive relationships between P1NP and the triglyceride sub-types.

Table 30: Associations between BTMs and triglyceride subclass variables in individuals with HBM.

		Model 1		Model 2		Model 3		Model 4	
		β (95% CI)	***p*-value**	**β (95% CI)**	***p*-value**	**β (95% CI)**	***p*-value**	**β (95% CI)**	***p*-value**
β-CTX	**VLDL**	-0.15 (-0.23, -0.07)	$2.06x10^{-4}$	-0.14 (-0.23, -0.06)	0.001	-0.15 (-0.23, -0.07)	$4.09x10^{-4}$	-0.15 (-0.28, -0.01)	0.039
	LDL	-0.09 (-0.16, -0.03)	0.006	-0.08 (-0.16, -0.01)	0.027	-0.09 (-0.16, -0.02)	0.012	-0.13 (-0.25, -0.02)	0.023
	HDL	-0.10 (-0.17, -0.02)	0.008	-0.08 (-0.16, -0.01)	0.031	-0.09 (-0.16, -0.01)	0.018	-0.05 (-0.16, 0.06)	0.391
Osteocalcin	**VLDL**	-0.13 (-0.23, -0.04)	0.007	-0.13 (-0.22, -0.04)	0.006	-0.13 (-0.22, -0.04)	0.006	-0.12 (-0.27, 0.03)	0.126
	LDL	-0.04 (-0.17, 0.09)	0.533	-0.04 (-0.17, 0.10)	0.587	-0.04 (-0.16, 0.08)	0.532	-0.04 (-0.20, 0.11)	0.570
	HDL	-0.10 (-0.21, 0.01)	0.069	-0.10 (-0.21, 0.01)	0.085	-0.10 (-0.20, $3.48x10^{-3}$)	0.058	-0.10 (-0.23, 0.02)	0.105
P1NP	**VLDL**	-0.05 (-0.16, 0.05)	0.314	-0.05 (-0.16, 0.06)	0.370	-0.06 (-0.16, 0.05)	0.279	0.13 ($1.03x10^{-3}$, 0.25)	0.048
	LDL	0.04 (-0.08, 0.15)	0.550	0.04 (-0.08, 0.17)	0.502	0.04 (-0.08, 0.16)	0.532	0.14 (0.02, 0.26)	0.018
	HDL	-0.02 (-0.13, 0.08)	0.641	-0.02 (-0.13, 0.09)	0.764	-0.02 (-0.12, 0.08)	0.660	0.09 (0.01, 0.17)	0.035

β represents the increase in triglycerides in SD per SD increase in BTMs.

Model 1: unadjusted; model 2: adjusted for age and sex; model 3: model 2 plus height, weight, menopause, bisphosphonate, and oral glucocorticoid use; model 4: adjusted as per model 3 plus other BTMs.

Sensitivity analyses

Results of sensitivity analyses are provided in Appendix 33-Appendix 35. Removing 7SD outliers did not affect any of the associations between the BTMs and metabolic traits. Removing QC tagged samples did not affect any of the associations between β-CTX and the metabolic traits. There was some evidence for an inverse association between osteocalcin and apolipoprotein-B (-0.08 [-0.13,-0.02], p=0.01) after tagged samples were removed. Evidence for an association between P1NP and alanine was weakened slightly by removal of tagged samples (CIs overlapped zero).

8.3.6. Replication in the ALSPAC population

Descriptives of the study population

I aimed to assess whether bone resorption is similarly associated with citrate and triglycerides in peri-menopausal women with normal BMD (mean TH-BMD T-score +0.24 [1.6]) and adolescents, from the ALSPAC cohorts, in whom citrate and β-CTX had been contemporaneously measured. Derivation of the ALSPAC sample sizes is presented in Figure 93. Of 3,664 mothers with mean age 47.9 (4.4)years, 77% were pre-menopausal. Median β-CTX and mean citrate concentrations were 0.25 (0.18-0.35)µg/L and 0.09 (0.03)mmol/L, respectively. Of 2,492 adolescents, with mean age 15.4 (0.3)years, 53% were female. Median β-CTX and mean citrate concentrations were 0.94 (0.66-1.39)µg/L and 0.11 (0.02)mmol/L, respectively (Table 31).

Figure 93: Flowchart detailing the derivation of the ALSPAC maternal (left) and adolescent (right) populations contributing to this analysis.

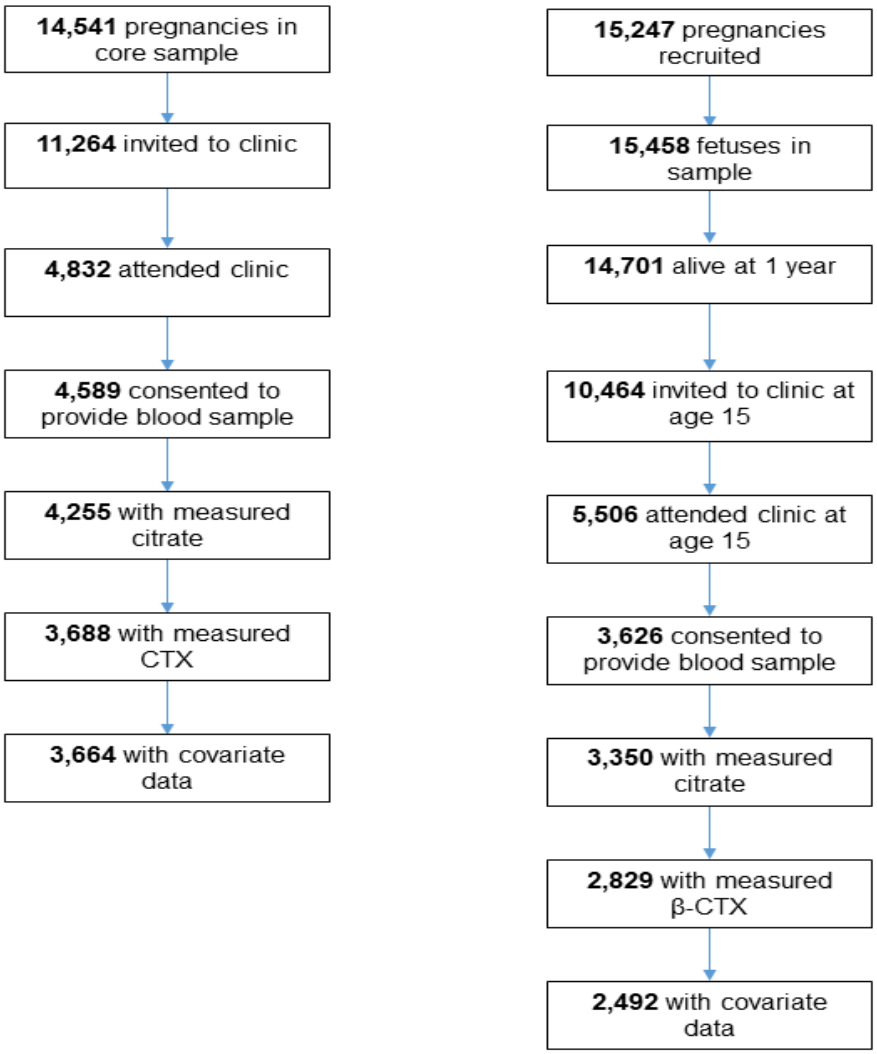

Table 31: Descriptives of the ALSPAC maternal and adolescent populations included in this analysis.

	Maternal N=3,664	**Adolescent N=2,492**
	Mean (SD)	
Age (years)	47.9 (4.4)	15.4 (0.3)
Height (cm)	164.1 (6.1)	169.6 (8.4)
Weight (kg)	71.2 (14.2)	61.9 (11.5)
BMI (kg/m^2)	26.4 (5.1)	21.5 (3.4)
TBFM (kg)	26.2 (9.7)	
TBLM (kg)	41.0 (4.7)	
TH-BMD (g/cm^2)	1.03 (0.14)	
TH-BMC (g)	32.1 (5.1)	
TBLH-BMD		1.035 (0.088)
Plasma citrate (mmol/L)	0.09 (0.03)	0.11 (0.02)
	Median (IQR)	
β-CTX (µg/L)	0.25 (0.18, 0.35)	0.94 (0.66, 1.39)
Total triglycerides (mmol/L)	0.92 (0.71, 1.23)	0.82 (0.69, 1.02)
Triglycerides in VLDL (mmol/L)	0.51 (0.35, 0.77)	0.51 (0.40, 0.67)
Triglycerides in LDL (mmol/L)	0.16 (0.13, 0.19)	0.12 (0.10, 0.14)
Triglycerides in HDL (mmol/L)	0.13 (0.11, 0.15)	0.10 (0.09, 0.11)
	N (%)	
Gender (Female)	3,664 (100.0)	1,308 (52.5)
Postmenopausal	849 (23.2)	
Oestrogen replacement use	158 (4.3)	
Tanner Stage[a]		
<Stage 5		1,261 (50.6)
Stage 5		1,231 (49.4)
Bisphosphonate use	14 (0.4)	
Oral glucocorticoid use	12 (0.3)	
Fasted <8 hours	673 (18.4)	
Time of sample collection (AM)		1,404 (56.3)
Alcohol consumption		
Less than once weekly	1,052 (43.0)	1,607 (76.0)
At least once weekly	1,394 (57.0)	509 (24.0)

[a]*Tanner stage below 5 represents an adolescent still going through puberty.*

Among ALSPAC mothers, a strong positive association was seen between β-CTX and citrate, robust to confounder adjustment (model 3, Table 32). This relationship was 60% lower than that seen in HBM individuals (fully adjusted β_{HBM}=0.05 [0.02,0.08] vs β_{ALSPAC}=0.02 [0.01,0.03], β=mmol/L increase in citrate per 1µg/L increase in β-CTX). The association between β-CTX and triglycerides also replicated in ALSPAC mothers (Table 32).

In adolescents, in analyses adjusted for age, sex, height, weight, Tanner stage and time of sample collection (model 3), a 1µg/L increase in β-CTX was associated

with a 0.022 (0.020,0.024) mmol/L increase in citrate (Table 32). The magnitude of the association between β-CTX and citrate in adolescents was less than 50% of that in HBM individuals. Inverse associations between β-CTX and total, LDL and HDL triglycerides were observed in the adolescent population (Table 32), but with a much smaller effect size than seen in the adult populations. After full adjustment (model 3), β-CTX remained positively related to total, LDL and HDL triglycerides.

Table 32: Associations between β-CTX and citrate and triglycerides in the ALSPAC maternal and adolescent populations.

		Model 1			Model 2			Model 3		
		β	**95% CI**	***p*-value**	**β**	**95% CI**	***p*-value**	**β**	**95% CI**	***p*-value**
Individuals with HBM N=198	**Citrate**	0.055	0.026, 0.083	1.89×10^{-4}	0.048	0.022, 0.075	2.95×10^{-4}	0.050	0.024, 0.076	1.71×10^{-4}
	Total TGs	-0.288	-0.445, -0.131	3.32×10^{-4}	-0.298	-0.465, -0.130	5.03×10^{-4}	-0.276	-0.434, -0.118	6.03×10^{-4}
	VLDL TGs	-0.239	-0.375, -0.102	0.001	-0.247	-0.392, -0.101	0.001	-0.228	-0.365, -0.090	0.001
	LDL TGs	-0.025	-0.041, -0.009	0.002	-0.026	-0.043, -0.009	0.002	-0.025	-0.041, -0.009	0.003
	HDL TGs	-0.009	-0.016, -0.002	0.013	-0.009	-0.016, -0.002	0.015	-0.008	-0.015, -0.001	0.027
Maternal population N=3,664	**Citrate**	0.026	0.020, 0.032	1.28×10^{-16}	0.022	0.016, 0.028	5.10×10^{-12}	0.020	0.013, 0.026	1.95×10^{-9}
	Total TGs	-0.414	-0.530, -0.298	3.31×10^{-12}	-0.502	-0.624, -0.380	1.17×10^{-15}	-0.354	-0.471, -0.237	3.03×10^{-9}
	VLDL TGs	-0.356	-0.453, -0.259	8.33×10^{-13}	-0.409	-0.512, -0.307	7.28×10^{-15}	-0.274	-0.372, -0.176	4.00×10^{-8}
	LDL TGs	-0.017	-0.030, -0.005	0.008	-0.035	-0.049, -0.022	1.95×10^{-7}	-0.030	-0.043, -0.016	1.60×10^{-5}
	HDL TGs	-0.026	-0.034, -0.018	3.43×10^{-11}	-0.035	-0.043, -0.027	1.76×10^{-17}	-0.032	-0.040, -0.024	4.86×10^{-14}
Adolescent population N=2,492	**Citrate**	0.018	0.016, 0.019	4.39×10^{-106}	0.023	0.021, 0.025	1.06×10^{-93}	0.022	0.020, 0.024	2.10×10^{-74}
	Total TGs	-0.024	-0.047, -0.002	0.034	-0.010	-0.043, 0.022	0.535	0.041	0.007, 0.076	0.019
	VLDL TGs	-0.001	-0.020, 0.018	0.919	-0.021	-0.050, 0.007	0.141	0.028	-0.002, 0.058	0.068
	LDL TGs	-0.012	-0.015, -0.009	3.61×10^{-13}	0.007	0.003, 0.011	3.16×10^{-4}	0.007	0.003, 0.012	0.001
	HDL TGs	-0.005	-0.006, -0.003	7.48×10^{-11}	0.001	-0.001, 0.003	0.465	0.002	2.93×10^{-4}, 0.005	0.026

β represents the change in citrate or triglycerides in mmol/L per 1µg/L increase in β-CTX.

Model 1: unadjusted; model 2: adjusted for age (and sex in the adolescent and HBM populations); model 3: adjusted for age, height, weight, menopause, less than 8 hours of fasting in the maternal population and age, sex, height, weight, Tanner stage and time of sample collection in the adolescent population. Model 3 adjusted for age, sex, height, weight, menopause, bisphosphonate, and oral glucocorticoid use for the HBM population. TGs=triglycerides.

8.4. Discussion

8.4.1. BMD, bone turnover and metabolic traits

Summary of findings

In this chapter, I have provided evidence for a positive association between β-CTX and plasma citrate, and consistent but weaker associations between osteocalcin/P1NP and citrate. Furthermore, β-CTX and osteocalcin both demonstrated inverse associations with plasma triglycerides in individuals with unexplained HBM, despite adjustment for a range of confounders. Associations between the bone resorption marker, β-CTX, and citrate and total plasma triglycerides were independent of the two bone formation markers, osteocalcin and P1NP. This positive association between β-CTX and citrate was further observed in peri-menopausal women and adolescents from ALSPAC (Table 33). I also found evidence for associations between HBM/L1-BMD and reduced serum alanine, but the opposite direction of effect was observed in the general population (Table 33).

Table 33: Summary of key findings of this chapter.

								Replicated	
Outcome	**L1-BMD**	**Hip ost.**	**Hip JSN**	**Knee JSN**	**DIP ost.**	**DIP JSN**	**B-CTX**	**RS**	**ALSPAC**
Acetoacetate		-						0	
Alanine	-							1[a]	
Citrate							+		1
Creatinine			-					1	
Glucose		+				-		0	
Glycoprotein acetyls		+						0	
Lactate				-	-			0	
Triglycerides							-		1[b]
Tyrosine						-		1	

[a]*Opposite direction of effect observed.* [b]*Opposite direction of effect observed in ALSPAC adolescents.*

Citrate

Citrate is synthesized in mitochondria from acetyl-CoA and oxaloacetate during the Krebs cycle, where most remains, regulating energy production (459,460). Hence, soft tissue cellular metabolism is not considered a major source of plasma citrate (460). Approximately 80% of citrate is stored in bone and 2% of bone content is citrate (461). Citrate, found between hydrated layers of bone mineral and which binds to the surface of apatite crystals, is thought to prevent formation of larger crystals, thereby maintaining bone structural properties (462,463). Human osteoblasts can produce citrate; it is hypothesized that citrate is incorporated into bone directly from osteoblast secretion, and that, as bone is resorbed and both bone collagen and mineral are degraded, citrate is released into the circulation generating the major source of plasma citrate (464). This concurs with the positive relationships I observed between citrate and both age and bone resorption, and an inverse association recently identified between β-CTX and citrate in a smaller sample from the ALSPAC adolescent population (434). Due to its suggested association with bone mineral, plasma citrate may provide information on turnover of bone mineral during bone resorption.

Stronger citrate-β-CTX associations in the context of HBM compared with individuals with normal BMD may simply reflect the greater quantity of bone in the HBM skeleton and therefore a greater source of citrate. It has been previously shown that HBM individuals have increased cortical volumetric BMD measured by pQCT, possibly due to reduced bone turnover allowing more time for secondary mineralization (200). Alternatively, the mineral platelets may be structured differently in HBM, contributing to increased bone strength (200), which may result in citrate being released more readily during bone resorption.

Triglycerides

The inverse association between β-CTX and triglycerides in the adult HBM and peri-menopausal populations is consistent with previous findings from the European Male Ageing Study; mean β-CTX concentrations were lower in male individuals with serum triglyceride concentrations above 150mg/dL,

independent of other components of the metabolic syndrome such as hyperglycaemia (465). As I observed, increased osteocalcin has been associated with reduced triglycerides in adults (465,466). The metabolic impact of osteocalcin has further been demonstrated in animal studies, where osteocalcin-deficient mice display a distinct metabolic phenotype with greater accumulation of fat mass and higher serum triglyceride levels (202). In my analyses, the inverse association between osteocalcin and triglycerides was not independent of β-CTX. It is important to note that I determined associations between *total* osteocalcin and serum triglycerides, rather than the *uncarboxylated* form proposed to be metabolically active (202). Yet, the finding that β-CTX, rather than osteocalcin, was independently associated with triglycerides raises the possibility that β-CTX influences triglycerides via a separate pathway from osteocalcin. As this analysis is cross-sectional, I am unable to determine if higher β-CTX causes decreased triglyceride levels or vice versa, yet a recent analysis did not find evidence of a causal pathway between triglycerides and BMD after accounting for pleiotropy, consistent with the lack of any causal effect of triglycerides on bone turnover (467).

In adolescents, I observed the opposite direction of effect between β-CTX and triglycerides: β-CTX was positively related to triglycerides after adjustment for weight. This is unlikely to be explained by collider bias as weight is unlikely to be a common outcome in this analysis. One possible explanation is that during adolescence, increased bone resorption likely reflects bone modelling during growth rather than bone remodelling, as indicated by the positive association between β-CTX and periosteal circumference previously reported in this adolescent population (468). Pubertal growth may increase both bone modelling and fat storage concurrently, with higher associated plasma triglyceride levels. Whilst in mature adults, bone remodelling predominates and hence the direction of association reverses.

Alanine

Alanine is a non-essential amino acid, widely used for protein synthesis, and forms a source of energy in muscles (469). Alanine is released into the circulation by the breakdown of muscle tissue (for example during prolonged periods of fasting) and is taken up by the liver to be used as a substrate in gluconeogenesis (470). An analysis of dietary protein intake in female participants from TwinsUK observed a positive relationship between alanine intake and forearm and LS-BMD, but not FN-BMD (471). *In vitro* studies suggest that alanine is able to stimulate insulin secretion, promoting osteoblast differentiation, hence leading to increased bone formation (471). This is consistent with the positive relationship between L1-BMD and alanine observed in the RS1 population and the weak but positive association between P1NP and alanine in the HBM population, but inconsistent with the inverse association between HBM and alanine. The discrepancy in observed relationships could reflect systematic, unmeasured differences in fasting time prior to sample collection (*i.e.* HBM cases may have been more likely to eat closer to the time of sample collection), increased alanine metabolism by the liver in individuals with HBM or reduced muscle breakdown in HBM individuals (HBM females have been previously shown to have a greater LM than their non-HBM relatives (201)). The magnitude of the association between HBM and alanine was weakened by removing samples with QC tags, including low glucose, which reflects glucose metabolism to pyruvate due to incorrect sample storage. This occurs via a pathway involving alanine. However, associations were still present after removing these samples and therefore this is unlikely to explain the inverse relationship with HBM.

8.4.2. Metabolic traits and OA sub-phenotypes

I did not find evidence for associations between any of the BMD or BTM-associated metabolic traits and OA sub-phenotypes. However, I did observe weak evidence for associations between three metabolic traits (creatinine, tyrosine and apolipoprotein-A1) and OA sub-phenotypes, with a consistent direction of effect in both the HBM and RS1 populations (Table 33). None of

these metabolic traits were BCAAs or histidine, the ratio of which has previously been related to OA risk (447,448). None of the associations met the Bonferroni-corrected *p*-value threshold in either population; I therefore cannot rule out the possibility that these are chance findings.

8.4.3. Strengths of this research

As far as I am aware, this is the first study to determine the metabolic profiles of bone turnover and OA sub-phenotypes. Additional strengths include the unique HBM population, allowing me to determine differences in metabolic traits between those with and without HBM, plus the ability to evaluate generalizability of findings in large population-based cohorts. All cohorts had detailed phenotypic data which allowed adjustment for a range of potential confounders. The metabolomics platform used is highly reproducible (395), allowing comparison between populations.

8.4.4. Limitations of this research

The major limitation of this work is the possible degradation of the HBM samples, leading to reduced reliability of metabolic trait measurements. HBM study samples had been stored at -80°C for up to ten years before metabolomics analysis; however, previous studies suggest that long-term storage is unlikely to significantly affect citrate measurements (472). The effect of different storage conditions and freeze-thaw cycles on metabolic trait concentrations may affect lipids, alanine and glucose (473); reassuringly the association between β-CTX and plasma triglycerides replicated with a similar effect size in the ALSPAC maternal cohort, but this could explain the inconsistency in direction of effect for alanine between the HBM and RS populations. As HBM index cases were recruited before their relatives, the samples were stored for longer, allowing more time for sample degradation. However, this is unlikely to explain the inverse relationship between HBM and alanine as multiple freeze-thaw cycles are likely to increase, rather than decrease, alanine concentration (473). Concentrations of most metabolic traits assessed for replication in RS1 were similar between the HBM

and RS1 populations, although concentrations for most metabolic traits were slightly lower in the HBM population. Mean concentration of total cholesterol was almost eight times lower in the HBM population compared to the RS1 population and therefore no conclusions can be made on the relationship between total cholesterol and BMD, BTMs or OA sub-phenotypes in the HBM population.

Although I hypothesized that metabolic traits would be on the causal pathway between BMD/bone turnover and OA, this cross-sectional study is unable to examine directions of causality. BTM measurements provide a measurement of current bone turnover at the time of assessment only. BTMs are affected by fasting time, with β-CTX levels increasing with fasting (474). A weaker association was observed between β-CTX and citrate in those ALSPAC mothers with shorter fasts. The samples collected from the HBM population were not collected when fasting.

8.4.5. Future work

The aim of this chapter was to identify metabolic traits which mediate the relationship between BMD and OA. I did not identify any metabolic traits associated with both BMD and OA, so did not perform mediation analyses. One could conclude that metabolic pathways do not mediate the relationship between BMD and OA. Although a metabolic effect of bone turnover has been observed in animal studies (202), MR studies in children do not provide evidence for a causal effect of BMD on BMI (401), suggesting that bone turnover may not have a metabolic effect in humans. In Chapter 9, I will perform MR to determine the causal effect of BMD on BMI in adults. Lack of evidence for associations of metabolic traits with BMD and OA could alternatively be due to the issues with the sample degradation in the HBM population. Additionally, it may be that metabolic traits may not mediate the relationship between BMD and OA in a population with extreme elevations in BMD, but there may be metabolic pathways mediating this relationship in the general population. Replication of

the full analysis (rather than just metabolic traits of interest) is required to confirm that there are no metabolic traits associated with both BMD and OA.

To determine if circulating citrate levels truly represent bone turnover, analyses are required to determine change in circulating citrate levels in response to osteoporosis treatments, for example by determining changes in circulating citrate levels during bisphosphonate treatment. This chapter provides limited data as to how β-CTX relates to citrate and triglycerides in adult men, or adults with low bone mass, so further analyses are required in these populations. Further analyses are required to determine the direction of association between alanine and LS-BMD in other population-based cohorts and cohorts with low BMD. MR could be performed to determine causality for metabolic traits associated with BMD, BTMs or OA, for example to determine if dietary alanine intake has a causal effect on BMD.

8.4.6. Conclusions

As none of the identified metabolic traits were associated with both bone and OA phenotypes, I was unable to perform the mediation analyses originally planned. However, in this chapter, I have provided strong evidence for a relationship between bone turnover and circulating citrate, which was stronger in the HBM population compared to the general population, providing novel hypotheses about differences in the structure of bone mineral between individuals with and without HBM. Given that citrate binds to apatite nanocrystals (462), one could hypothesize that circulating citrate may reflect breakdown of bone mineral. Further studies are justified to explore whether plasma citrate concentration is altered by factors known to modulate bone resorption, such as bisphosphonates, to determine the direction of causality and whether measuring circulating citrate could have clinical utility.

CHAPTER 9. USING GENETICS TO DETERMINE THE CAUSAL ROLE OF BONE IN OSTEOARTHRITIS

9.1. Background and aims

As discussed in Chapter 3,Chapter 6 and Chapter 7, several large population-based studies have identified positive relationships between BMD and OA of the hip (208-211,412) and knee (209,212-215,217,396-398). Furthermore, the fact that HBM individuals have an increased odds of radiographic OA at these joints (226,227), is highly suggestive of a causal effect of BMD on OA, due to the temporal relationship between HBM development and OA onset. As discussed in section 1.2.5, BMI is a risk factor for OA. Although BMI explained approximately 50% of the association between HBM and knee OA, the association persisted (227), suggesting that BMD influences OA via BMI-independent pathways.

A positive relationship between BMD and BMI is well-established. The skeleton adapts to the increased load placed upon it by a higher BMI, reducing fracture risk. Therefore, a causal pathway between BMI and BMD is widely accepted. However, a causal pathway between BMD and BMI is plausible, via the metabolic effects of bone turnover (Chapter 2, Chapter 8). However, analyses of a population of children suggested that there is no causal pathway between FN- or LS-BMD and BMI (401), although this finding is yet to be replicated in an adult population.

Recent MR analyses have determined a causal role of both BMI and BMD on risk of hip and knee OA (139,261,441). MR estimates for the relationship between BMD and OA may be biased by relationships of the instrument to a confounder of the BMD-OA relationship, *i.e.* BMI, as BMD SNPs may be related to BMI due to the strong correlation between these two phenotypes. Funck-Brentano *et al* tried to eliminate this bias by removing any SNPs nominally associated with BMI from their analyses (261). On the other hand, Hackinger *et al* identified a genetic correlation between LS-BMD and OA (137), which suggests shared biological pathways contribute to both BMD and OA development. If this is the case, one would expect to see bidirectional causal relationships between BMD and OA.

However, another potential explanation for the genetic correlation could be the presence of spinal osteophytes artefactually elevating LS-BMD.
I hypothesize that there will be bidirectional relationships between BMD and BMI, BMD and OA and BMI and OA (Figure 94) and therefore aim to test these relationships using MR. I will perform both 1S and 2SMR, to determine reliability of estimates, using the largest possible data sources to increase power. I then aim to use formal MVMR methods, to determine the direct (*i.e.* unconfounded) causal pathways between these variables, and latent causal variable (LCV) analysis to determine if BMD has a causal effect on OA, independent of shared genetic aetiology.

Figure 94: Hypothesized relationships between BMD, BMI, and OA.

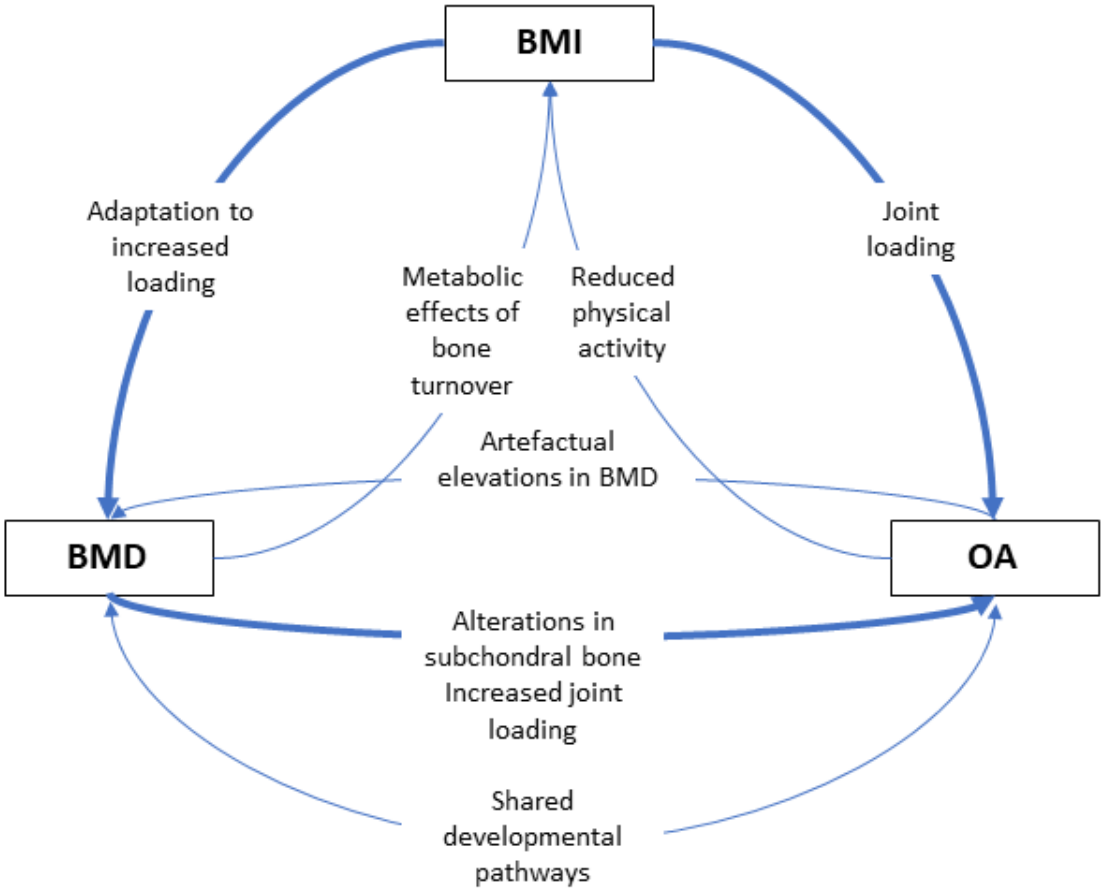

Thicker arrows represent stronger hypothesized relationships.

In addition to determining the BMI-independent causal role of BMD on hip and knee OA, I will examine the causal role of BMD in the individual radiographic

OA sub-phenotypes, and whether BMD is specifically causally related to the bony sub-phenotypes (*i.e.* osteophytes and subchondral sclerosis) rather than JSN. Therefore, my final aim of this chapter is to determine the relationship between PRS for eBMD and radiographic hip and knee OA sub-phenotypes, using individual-level data from the RS population. I am unable to perform formal 1SMR in RS as I do not have access to BMD data for the full sample. However, PRS analysis allows the determination of a causal effect, without quantification of magnitude of effect.

9.2. Methods

9.2.1. Bidirectional and multivariable MR analyses

Data sources

GEFOS

The Genetic Factors for Osteoporosis (GEFOS) consortium was a collaboration of 17 discovery cohorts (n=32,961) from North America, Europe, East Asia, and Australia and 34 replication populations (n=50,933) to identify genetic variants associated with FN-BMD and LS-BMD (204). Full methodology has been published elsewhere (204). This analysis represents the largest GWAS to-date of FN-BMD and therefore FN-BMD genome-wide significant loci from this analysis were selected to instrument eBMD in UK Biobank in 1SMR (as an instrument for eBMD not generated in UK Biobank does not exist). More recently, the GEFOS consortium has performed a GWAS of eBMD in 426,824 individuals from UK Biobank (386). Summary statistics from this GWAS were used for 2SMR.

GIANT

BMI summary statistics for 2SMR were taken from the GWAS meta-analysis performed by the Genetic Investigation of Anthropometric Traits (GIANT) consortium. This meta-analysis was performed in two stages: stage one including 80 BMI GWAS (n=234,069) and stage two including an additional 34 GWAS (n=88,137) (475). This represents the largest BMI GWAS which does not include the UK Biobank population and I could therefore use the summary statistics for 2SMR with UK Biobank-derived outcome statistics. 77 SNPs were associated with BMI at genome-wide significance in the mixed-sex European populations, of which 63 represented independent loci. These SNPs also instrumented BMI in 1SMR.

GO

The Genetics of Osteoarthritis (GO) consortium is a collaboration of cohorts aiming to identify novel genetic variants for OA. The most recent published GO GWAS meta-analysed UK Biobank and arcOGEN (77,052 cases, 378,169 controls) (141). ArcOGEN is a population of UK-based Europeans with clinically diagnosed knee and/or hip OA (131). More recently, the GO consortium has expanded to include additional cohorts and the total sample size is now >800,000 from 13 international cohorts, with full details of cohort specific GWAS published elsewhere (476). This has allowed the largest GWAS meta-analysis for OA, excluding UK Biobank individuals, to be performed, generating summary statistics to be used for 2SMR when the SNP-exposure summary statistics have been generated in the UKBB population. (*i.e.* eBMD).

A summary of all MR analyses performed in this chapter is presented in Table 34.

Table 34: Summary of all MR analyses performed.

	Exposure		Outcome	
		Source		Source
1S	eBMD	Individual-level eBMD in UKBB I:FN-BMD SNPs from GEFOS (204)	Knee OA	Individual-level HD knee OA status in UKBB
2S	eBMD	Summary statistics from GEFOS UKBB eBMD GWAS N=426,824 (386)	Knee OA	Summary statistics from GO consortium GWAS based on radiographic, clinical evaluation, joint replacement, self-reported or HD knee OA, excluding UKBB N=44,001 ca, 301,541 co (476)
1S	eBMD	Individual-level eBMD in UKBB I:FN-BMD SNPs from GEFOS	Hip OA	Individual-level HD hip OA status in UKBB
2S	eBMD	Summary statistics from GEFOS UKBB eBMD GWAS N=426,824	Hip OA	Summary statistics from GO consortium GWAS based on radiographic, clinical evaluation, joint replacement, self-reported or HD hip OA, excluding UKBB N=25,237 ca, 272,284 co
1S	eBMD	Individual-level eBMD in UKBB I:FN-BMD SNPs from GEFOS	BMI	Individual-level BMI data in UKBB
2S	eBMD	Summary statistics from GEFOS UKBB eBMD GWAS N=426,824	BMI	Summary statistics from GIANT European BMI GWAS N=339,224 (475)
1S	BMI	Individual-level BMI data in UKBB I: BMI SNPs from GIANT	Knee OA	Individual-level HD knee OA status in UKBB
2S	BMI	Summary statistics from GIANT European BMI GWAS N=339,224	Knee OA	Summary statistics from UKBB and arcOGEN GWAS HD knee OA N=24,955 ca, 378,169 co (141)
1S	BMI	Individual-level BMI data in UKBB I: BMI SNPs from GIANT	Hip OA	Individual-level HD hip OA status in UKBB
2S	BMI	Summary statistics from GIANT European BMI GWAS N=339,224	Hip OA	Summary statistics from UKBB and arcOGEN GWAS of HD hip OA N=15,704 ca, 378,169 co
1S	BMI	Individual-level BMI data in UKBB I: BMI SNPs from GIANT	eBMD	Individual-level eBMD data in UKBB

2S	BMI	Summary statistics from GIANT European BMI GWAS N=339,224	eBMD	Summary statistics from GEFOS UKBB eBMD GWAS N=426,824
1S	Knee OA	Individual-level data on HD knee OA in UKBB I: knee OA SNPs from the GO consortium meta-analysis (excluding UKBB)	eBMD	Individual-level eBMD data in UKBB
2S	Knee OA	Summary statistics from GO consortium GWAS of knee OA, excluding UKBB N=44,001 ca, 301,541 co	eBMD	Summary statistics from GEFOS UKBB eBMD GWAS N=426,824
1S	Knee OA	Individual-level data on HD knee OA in UKBB I: knee OA SNPs from the GO consortium meta-analysis (excluding UKBB)	BMI	Individual-level BMI data in UKBB
2S	Knee OA	Summary statistics from UKBB and arcOGEN GWAS of HD knee OA N=24,955 ca, 378,169 co	BMI	Summary statistics from GIANT European BMI GWAS N=339,224
1S	Hip OA	Individual-level data on HD hip OA in UKBB I: hip OA SNPs from the GO consortium meta-analysis (excluding UKBB)	eBMD	Individual-level eBMD data in UKBB
2S	Hip OA	Summary statistics from GO consortium GWAS of hip OA, excluding UKBB N=25,237 ca, 272,284 co	eBMD	Summary statistics from GEFOS UKBB eBMD GWAS N=426,824
1S	Hip OA	Individual-level data on HD hip OA in UKBB I: hip OA SNPs from the GO consortium meta-analysis (excluding UKBB)	BMI	Individual-level BMI data in UKBB
2S	Hip OA	Summary statistics from UKBB and arcOGEN GWAS of HD hip OA N=15,704 ca, 378,169 co	BMI	Summary statistics from GIANT European BMI GWAS N=339,224

I: instrumented by; ca: cases; co: controls.

1SMR analyses

1SMR, as described in section 5.3.3, was performed in the UK Biobank population, which is described in detail in section 5.2.1. Analyses were restricted to individuals of white British ethnicity.

eBMD assessment

BMD was estimated by ultrasound measurement of the calcaneus using a Sahara Clinical Bone Sonometer, from a combination of speed of sound (SOS) and broadband ultrasound attenuation (BUA) (477). As described by Morris *et al*, men with an eBMD measurement $\leq$0.18 or $\geq$1.06g/cm^2 were excluded, whilst women with a value $\leq$0.12 or $\geq$1.025g/cm^2 were excluded (386).

Hospital-diagnosed OA ascertainment

Hospital-diagnosed hip and knee OA were determined from hospital episode statistics (HES) data (478), using International Statistical Classification of Diseases and Related Health Problems (ICD) 9/10 codes previously reported (Table 35) (141). Those with arthropathies at other joints and inflammatory polyarthropathies were excluded from the control population. A complete list of exclusion codes for controls is presented in Appendix 36.

Physical activity assessment

Total weekly metabolic equivalent task (MET) minutes were calculated based on IPAQ responses (section 4.2), completed via touchscreen questionnaire at the assessment clinic.

Table 35: ICD codes used to identify cases of hospital-diagnosed hip and knee OA in UK Biobank.

Joint	Code		Description
	ICD10	**ICD9**	
Hip	M16		"Coxarthrosis"
	M160		"Primary coxarthrosis, bilateral"
	M161		"Other primary coxarthrosis"
	M169		"Coxarthrosis, unspecified"
	M1905		"Primary arthrosis of other joints (pelvic region and thigh)"
	M1995		"Arthrosis, unspecified (pelvis region and thigh)"
		71535	"Osteoarthrosis, localized, primary or secondary, pelvic region and thigh"
		71515	"Osteoarthrosis, localized, primary, pelvic region and thigh"
Knee	M17		"Gonarthrosis"
	M170		"Primary gonarthrosis, bilateral"
	M171		"Other primary gonarthrosis"
	M179		"Gonarthrosis, unspecified"
	M1906		"Primary arthrosis of other joints (lower leg)"
	M1996		"Arthrosis, unspecified (lower leg)"
		71536	"Osteoarthrosis, localized, primary or secondary, lower leg"
		71516	"Osteoarthrosis, localized, primary, lower leg"

Statistical analysis

1SMR was performed using the instrumental-variable regression ('*ivreg*') function of the AER package (372). Exposures were instrumented by an unweighted PRS, generated as the sum of the dosage for exposure-increasing alleles (data sources provided in Table 34). Analyses were adjusted for sex, genotyping chip and 10 PCs. Continuous exposures (eBMD/BMI) were standardized prior to analysis. Effect estimates for binary outcomes (hip/knee OA) represent risk differences. I therefore performed additional two stage regression, first regressing the instruments on the exposure, generating predicted values of the exposure, then regressing the predicted values of the exposure on the binary outcomes using a logistic regression model. This gave an estimate of the OR per SD increase in the exposure, allowing comparison with 2SMR estimates, although the SEs for this estimate are likely to be underestimated (479).

2SMR analyses

2SMR was performed as described in section 5.3.3. SNP-exposure and SNP-outcome summary statistics are presented in Appendix 37-Appendix 42. Steiger filtering was performed to exclude SNPs which explained a greater proportion of the variance in the outcome than the exposure variable (480). SNP-specific r^2 were estimated from the sample size and *p*-value using the '*get_r_from_pn'* function for linear variables, and using the log OR, effect allele frequency and case prevalence and the '*get_r_from_lor'* function for binary traits. Seven eBMD SNPs were excluded due to a larger r^2 for hip OA, four eBMD SNPs for knee OA and two for BMI. Two BMI SNPs explained a greater proportion of variance in hip OA risk, one for knee OA risk and 15 explained a greater proportion of the variance in eBMD. One knee OA SNP was excluded due to a greater r^2 for eBMD. All Steiger filtered SNPs are listed in Appendix 37-Appendix 42.

Sensitivity analyses

A summary of how the MR assumptions, outlined in section 5.3.3, were tested is provided in Figure 95.

Figure 95: Summary of how the assumptions of MR were tested.

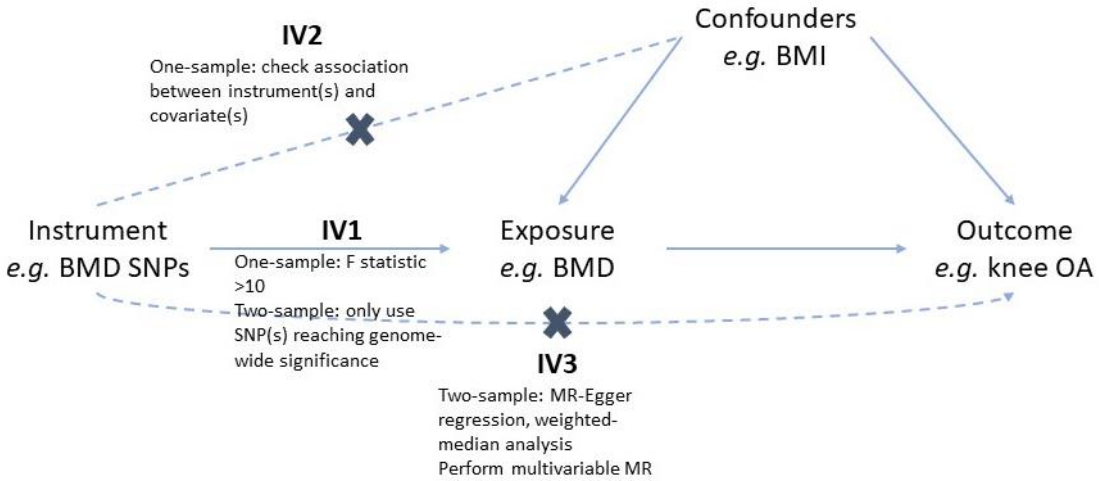

MVMR

As I hypothesized that BMI is a confounder of the BMD-OA relationship (*i.e.* a common causes of both phenotypes), I determined the independent effect of BMD on OA outcomes by performing 1SMVMR, including PRS for both BMI and BMD as instruments, as described in section 5.3.3. Analyses were adjusted for sex, genotyping chip and 10 PCs.

Latent Causal Variable model

The LCV model, developed by O'Connor and Price, estimates the causal effect of one trait on another trait when the two traits are genetically correlated (481). The genetic correlation between the two traits is modelled as a latent variable, and the genetic correlation between the latent variable and each trait is assessed (481). A perfect genetic correlation between the latent variable and one of the traits suggests a fully genetically causal effect of that trait on the other trait (481). If the trait has a partial causal effect on the (outcome) trait of interest (*i.e.* the genetic correlation between the latent variable and the (exposure) trait is less than 1), partial causality can be estimated using the genetic causality proportion (GCP), with a value of 0 representing no causal effect and a value closer to 1 representing a stronger causal effect (481). Although this method is unable to determine bidirectional relationships between traits, as I hypothesized that any observed causal effect of OA on BMD is likely to reflect shared genetic aetiology, rather than a true causal effect of OA on BMD, I deemed this method appropriate.

Three datasets were required to run this model: genome-wide summary statistics for SNP-BMD associations, genome-wide summary statistics for SNP-OA associations and LD scores. The LD scores were generated from the 1,000 Genomes European population and were download from https://data.broadinstitute.org/alkesgroup/LDSCORE/ (eur_w_ld_chr.tar.bz). To maximise sample size for the OA summary statistics, whilst limiting to a fully European population, I aimed to use OA GWAS summary statistics generated from UK Biobank. I could not use the eBMD summary statistics for the SNP-

exposure relationships due to the large sample overlap, and thus used the GEFOS European FN/LS-BMD GWAS summary statistics (which are adjusted for weight) (482). I therefore performed GWAS of both hospital-diagnosed hip and knee OA, adjusting for weight, within UK Biobank. GWAS was performed as described in section 5.3.2 and the published protocol (358). 410,052 individuals were included in the GWAS of knee OA and 400,516 in the GWAS of hip OA. QQplots are provided in Figure 96.

I removed the MHC region (Chr6, 28.5-33.5Mb) from both sets of summary statistics, as well as SNPs with a MAF<0.05, as recommended by the authors (481). Analyses were restricted to SNPs present in both datasets. Alleles were harmonized so that the beta corresponded to the same effect allele. Betas were then transformed by dividing by their SE. Analyses were performed using the 'RunLCV.R' script provided by the authors (https://github.com/lukejoconnor/LCV).

Figure 96: QQplots of p-values from weight-adjusted GWAS of hospital-diagnosed hip OA (a) and hospital-diagnosed knee OA (b) in UK Biobank.

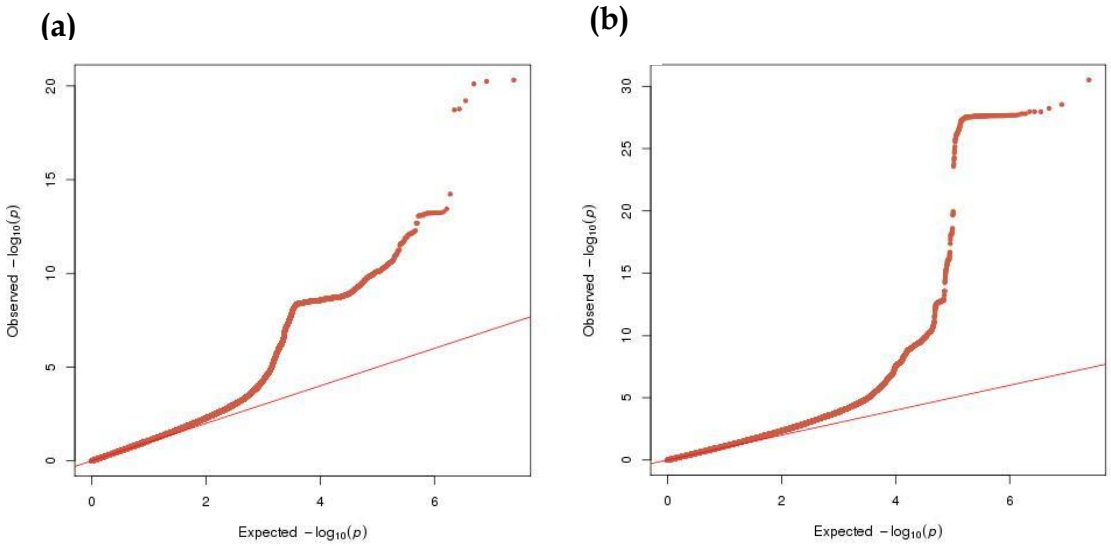

λ_{hip}=1.05, λ_{knee}=1.09.

9.2.2. BMD PRS

Selection of genetic variants

Genetic variants were selected from the largest GWAS of BMD to date, the Morris eBMD GWAS (386). Non-autosomal SNPs were excluded.

Study population

These analyses were performed in the RS population, outlined in section 5.2.2.

Generation of PRS

Dosages for eBMD SNPs were extracted from VCF files of HRC version1.1-imputed genotype data using the vcftools software (483), with the '*– recode –recode-INFO-all*' option. This was performed separately for each chromosome and for each cohort. The '*vcf-concat*' command was then used to combine all SNPs across the 22 chromosomes into one file. '*vcf-query*' was used to extract the dosage from the 'info' column.

Dosage data for the extracted SNPs were then imported into R. As vcftools extracts dosage based on the alternative allele, the dosage was converted to the dosage for the reference allele by subtracting the dosage from two, unless the reference allele was the BMD-decreasing allele, in which case the dosage of the alternative allele was used. The dosage was then multiplied by the beta for the BMD-increasing allele from the GWAS (386). Scores were generated using the '*rowSums()*' command on the weighted BMD-increasing allele dosage. PRS were generated using independent SNPs identified by clumping, using the TwoSampleMR '*clump_data*' function. This was 362 SNPs, of which eight had a MAF<0.001, an imputation info score<0.8 or an HWE *p*-value<$1x10^{-6}$ and were excluded.

Outcome measures

Outcome measures assessed in RS, and their derivation, are presented in Table 36.

Table 36: Summary of OA outcomes analysed in the Rotterdam study population.

Prevalent	Hip osteophyte score	Sum of inferior and superior femoral and acetabular osteophyte grades across the left and right hips
	Hip JSN score	Sum of left and right semi-quantitative hip JSN grades
	Hip subchondral sclerosis	Subchondral sclerosis observed at either hip (binary)
	Knee osteophyte score	Sum of osteophyte grades across the medial and lateral, tibial and femoral regions, across both knees
	Knee JSN score	Sum of medial and lateral grades across both knees
	Knee subchondral sclerosis	Subchondral sclerosis observed at either knee (binary)
Progressive	Change in summed knee osteophyte score Change in summed knee JSN score	Follow-up scores were calculated as above for prevalent scores and the baseline score subtracted from the score at follow-up (RS1-3 for knees)

Covariates

PRS analyses in the RS population were adjusted for age at baseline, sex and 10 PCs. For analyses of progressive OA sub-phenotypes, follow-up time was included as a covariate.

Statistical analysis

In each RS cohort, PRS were normally distributed (Figure 97). Summed osteophyte and JSN scores were analysed as continuous outcomes, despite being skewed (Figure 98, Figure 99), using linear regression models. Analyses were performed separately in each cohort. Results for the three cohorts were then meta-analysed using a weighted fixed effects model and the R '*metafor*' package.

Figure 97: Histograms of the eBMD PRS in RS1, RS2 and RS3.

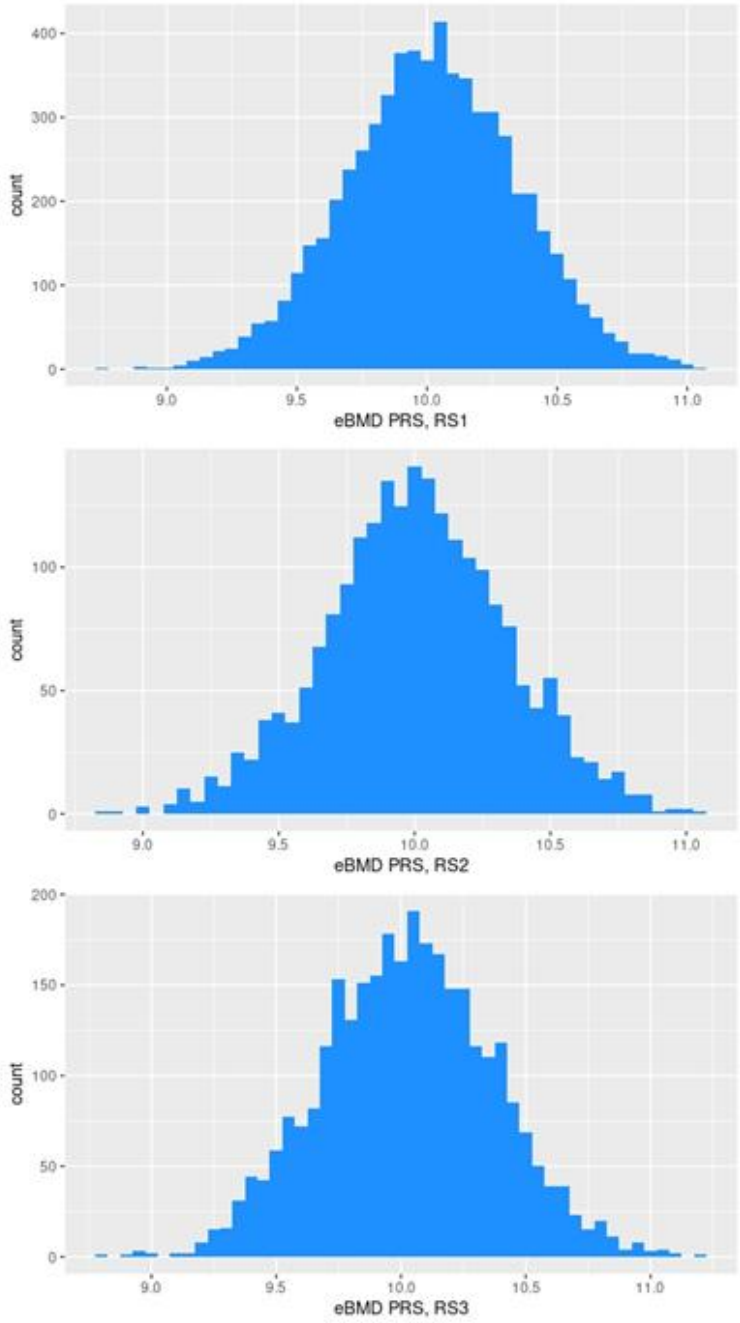

Figure 98: Histograms of prevalent OA variables in the three Rotterdam study cohorts.

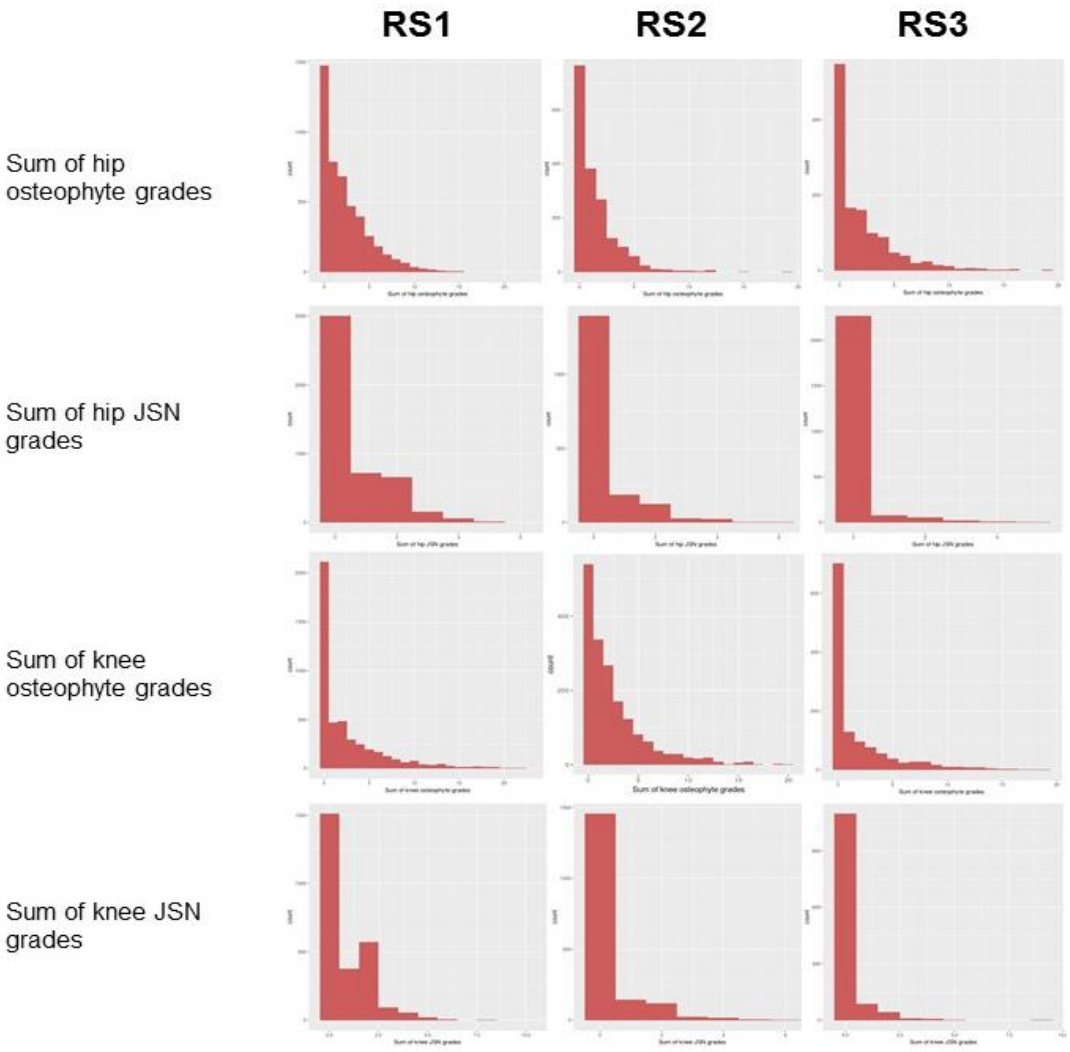

Figure 99: Histograms of change in knee OA sub-phenotypes in the RS1 cohort.

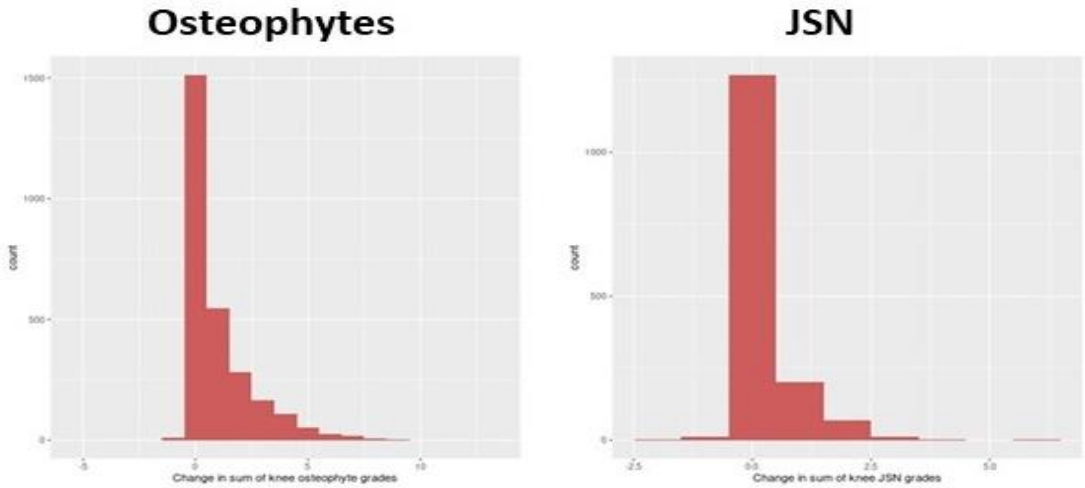

9.3. Results

9.3.1. MR analyses to determine causal pathways between BMD, BMI, and OA

MR analyses of bidirectional causal pathways between BMD and OA

In 1SMR, eBMD was causally related to both hip and knee OA, with an SD increase in eBMD related to a 0.8% (0.1,1.4) increased probability of having hip OA and 1.7% (0.9,2.5) increased probability of having knee OA (Table 37). This was equal to approximately 28% increased odds for hip OA and 40% increased odds for knee. The F-statistic confirmed sufficient instrument strength (F>3000). However, the BMD risk score was related to BMI, violating the second assumption of MR (Table 38).

Table 37: Results of 1S univariable and MVMR in UK Biobank.

					Two-stage least-squares regression		Two-stage linear-logistic regression	
	Exposure	**Outcome**	**F-statistic**	**N**	**estimate (95% CI)**	***p*-value**	**OR (95% CI)**	***p*-value**
UVMR	eBMD	Hip OA	3,390	190,408	0.008 (0.001, 0.014)[rd]	0.016	1.28 (1.05, 1.57)	0.016
	eBMD	Knee OA	3,483	194,638	0.017 (0.009, 0.025)[rd]	$3x10^{-5}$	1.40 (1.20, 1.63)	$3x10^{-5}$
	BMI	Hip OA	4,201	333,828	0.015 (0.010, 0.021)[rd]	$6x10^{-8}$	1.60 (1.35, 1.91)	$7x10^{-8}$
	BMI	Knee OA	4,446	341,686	0.036 (0.029, 0.043)[rd]	$<2x10^{-16}$	2.01 (1.76, 2.29)	$<2x10^{-16}$
	BMI	eBMD	2,952	218,700	0.073 (0.037, 0.109)[sd]	$6x10^{-5}$		
	Hip OA	eBMD	107	190,408	1.10 (0.36, 1.84)[sd]	0.003		
	Hip OA	BMI	197	333,828	0.54 (0.01, 1.07)[sd]	0.048		
	Knee OA	eBMD	49	194,638	4.16 (2.74, 5.57)[sd]	$8x10^{-9}$		
	Knee OA	BMI	87	341,686	8.44 (6.65, 10.23)[sd]	$<2x10^{-16}$		
MVMR	eBMD	Hip OA	275	190,175	0.007 (0.001, 0.013)[rd]	0.027	1.26 (1.03, 1.54)	0.027
	BMI	Hip OA	211	190,175	0.013 (0.006, 0.020)[rd]	$6x10^{-4}$	1.49 (1.19, 1.87)	$5x10^{-4}$
	eBMD	Knee OA	275	194,404	0.015 (0.008, 0.023)[rd]	$1x10^{-4}$	1.36 (1.16, 1.59)	$1x10^{-4}$
	BMI	Knee OA	211	194,404	0.034 (0.025, 0.043)[rd]	$3x10^{-13}$	1.93 (1.62, 2.30)	$3x10^{-13}$
	Hip OA	eBMD	7.5	190,175	1.12 (0.35, 1.89)[sd]	0.004		
	BMI	eBMD	43	190,175	0.084 (0.040, 0.128)[sd]	$2x10^{-4}$		
	Knee OA	eBMD	1.2	194,404	5.76 (2.62, 8.89)[sd]	$3x10^{-4}$		
	BMI	eBMD	1.4	194,404	-0.195 (-0.392, 0.001)[sd]	0.052		

[sd]estimate represents the SD increase in outcome per unit increase in exposure. Estimates for binary exposures represent the SD increase in outcome per doubling in risk of exposure. [rd]Estimates for binary outcomes represent the risk difference per SD increase in exposure. ORs are per SD increase in exposure.

Table 38: Associations between the four 1SMR PRS instruments and potential confounders in UK Biobank.

	Score			
	BMD	**BMI**	**Hip OA**	**Knee OA**
Age, years	$-3x10^{-3}$ (-0.01, $3x10^{-3}$)	$-5x10^{-3}$ (-0.01, $4x10^{-4}$)	0.01 (-0.01, 0.02)	$5x10^{-4}$ (-0.02, 0.02)
Height, cm	0.03 (0.02, 0.04)	0.01 ($-7x10^{-5}$, 0.01)	-0.01 (-0.03, $1x10^{-3}$)	-0.15 (-0.17, -0.13)
Weight, kg	0.04 (0.03, 0.06)	0.32 (0.31, 0.33)	$-2x10^{-3}$ (-0.03, 0.02)	0.33 (0.29, 0.37)
BMI, kg/m^2	0.01 ($2x10^{-3}$, 0.01)	*0.11 (0.11, 0.11)*	$4x10^{-3}$ ($-4x10^{-3}$, 0.01)	0.16 (0.15, 0.18)
eBMD, g/cm^2	*0.004 (0.004, 0.004)*	$2x10^{-4}$ ($1x10^{-4}$, $3x10^{-4}$)	$5x10^{-4}$ ($2x10^{-4}$, 0.001)	$2x10^{-3}$ ($2x10^{-3}$, $3x10^{-3}$)
Hip OA	1.01 (1.00, 1.01)	1.01 (1.01, 1.02)	*1.07 (1.06, 1.08)*	1.02 (1.00, 1.04)
Knee OA	1.01 (1.00, 1.01)	1.02 (1.01, 1.02)	1.05 (1.02, 1.08)	*1.06 (1.05, 1.07)*
Physical Activity, total weekly MET-minutes	-2.82 (-7.56, 1.93)	2.77 (--1.30, 6.84)	-0.39 (-11, 10)	-0.48 (-16, 15)
HRT use, ever	1.00 (1.00, 1.00)	1.00 (1.00, 1.00)	1.00 (1.00, 1.01)	1.00 (0.99, 1.01)

Estimates for continuous covariates represent the per-allele unit increase (e.g. a value of 0.03 for height represents a per-allele increase in height of 0.03cm). Estimates for binary variables represent the per-allele OR. Estimates in italics represent the association between the PRS and the variable that the PRS instruments.

In 2SMR, IVW provided evidence for a causal effect of eBMD on hip OA (OR per SD increase=1.09 [1.03,1.16]), which was relatively consistent (in magnitude) across the three MR methods (Figure 100). Leave-one-out analysis did not suggest that any individual SNP was driving this relationship (Appendix 43). Excluding two SNPs more strongly related to BMI than eBMD did not alter results (Table 39). Evidence for a causal effect on knee OA was weaker (OR_{IVW}=1.04 [1.00,1.09]), but did not appear to be driven by a particular SNP (Appendix 43). When restricting to 10 SNPs also associated with FN-BMD with genome-wide significance ($p \leq 5x10^{-8}$) in GEFOS, the magnitude of effect was stronger for hip OA (OR_{IVW}=1.40 [1.12,1.74]), but this effect estimate was less consistent with the MR-Egger and weighted median estimates (Table 39, Figure 101). Evidence for a causal effect on knee OA, however, was more consistent (in magnitude) across the three methods (OR_{IVW}=1.21 [1.01,1.44], Figure 102).

Figure 100: Comparison of results of two-sample MR across the three methods.

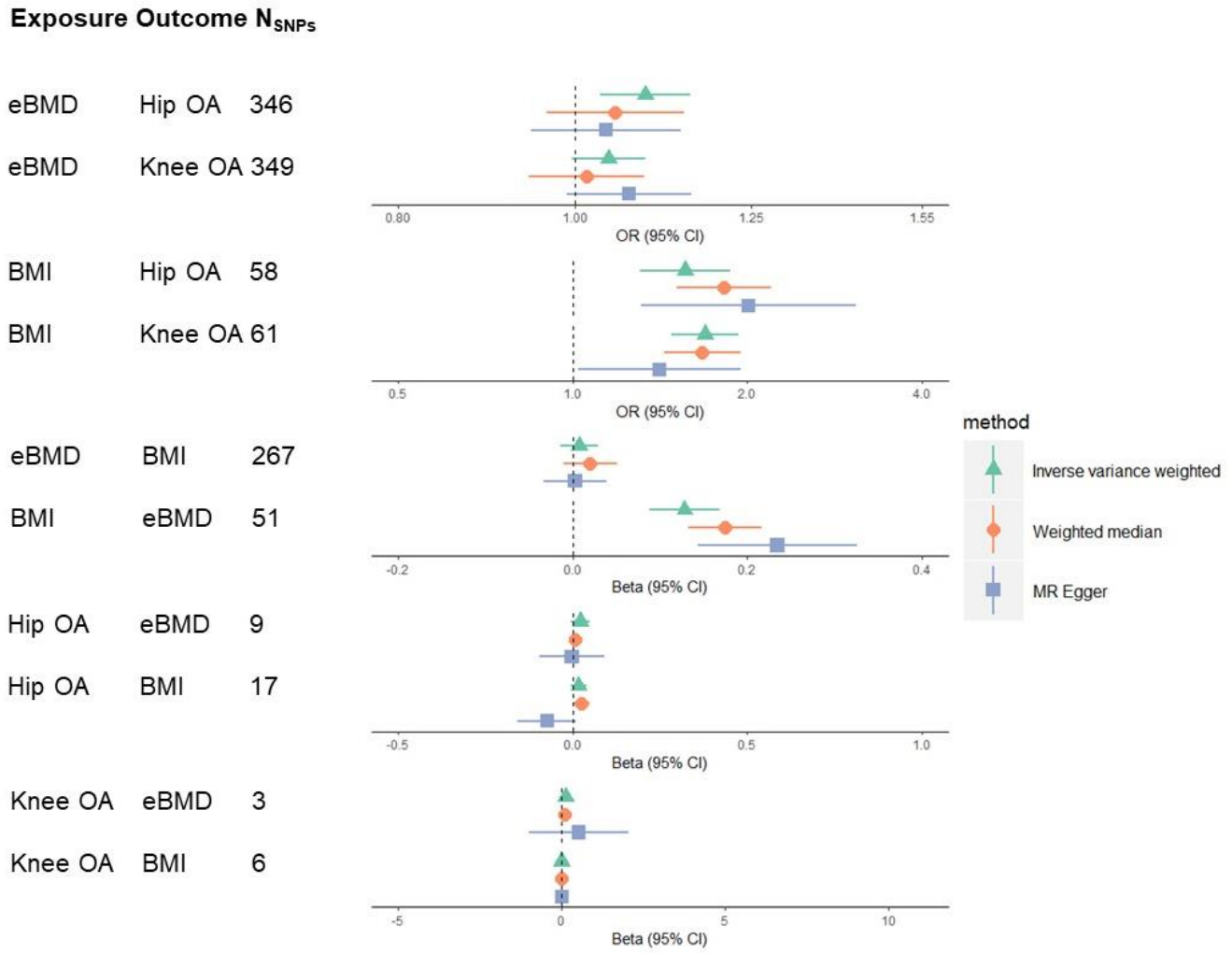

Table 39: Full two-sample MR results.

				IVW		MR-Egger				Weighted median	
Exposure	**Steiger filtered SNPs**	**N SNPs[a]**	**Outcome**	**estimate (95% CI)**	***p*-value**	**estimate (95% CI)**	***p*-value**	**Intercept**	***p*-value**	**estimate (95% CI)**	***p*-value**
eBMD	7	346	Hip OA	1.09 (1.03,1.16)	0.002	1.04 (0.95,1.14)	0.416	1.00 (1.00,1.01)	0.178	1.05 (0.97,1.15)	0.236
Excluding BMI Steiger filtered SNPs	2	344	Hip OA	1.09 (1.03,1.16)	0.002	1.04 (0.94,1.14)	0.450	1.00 (1.00,1.01)	0.156	1.05 (0.96,1.15)	0.264
Restricted to SNPs associated with FN-BMD at genome-wide significance	0	10	Hip OA	1.40 (1.12,1.74)	0.002	0.89 (0.37,2.10)	0.789	1.03 (0.98,1.07)	0.313	1.22 (0.98,1.52)	0.068
eBMD	4	349	Knee OA	1.04 (1.00,1.09)	0.068	1.07 (0.99,1.16)	0.086	1.00 (1.00,1.00)	0.554	1.02 (0.94,1.10)	0.691
Excluding BMI Steiger filtered SNPs	2	347	Knee OA	1.04 (1.00,1.09)	0.067	1.07 (0.99,1.16)	0.090	1.00 (1.00,1.00)	0.479	1.02 (0.94,1.09)	0.687
Restricted to SNPs associated with FN-BMD at genome-wide significance	0	10	Knee OA	1.21 (1.01,1.44)	0.034	1.15 (0.54,2.41)	0.730	1.00 (0.96,1.04)	0.886	1.26 (1.07,1.49)	0.006
eBMD	2	267	BMI	0.01 (0.01,0.03)	0.472	$3x10^{-3}$ (-0.03,0.04)	0.877	$2x10^{-4}$ ($-9x10^{-4}$, $1x10^{-3}$)	0.737	0.02 (-0.01,0.05)	0.209
Excluding hip and knee OA Steiger filtered SNPs	9	258	BMI	$3x10^{-3}$ (-0.02,0.02)	0.771	$5x10^{-3}$ (-0.03,0.04)	0.802	$-6x10^{-5}$ ($-1x10^{-3}$, $1x10^{-3}$)	0.919	0.02 (-0.01,0.05)	0.231
BMI	4	58	Hip OA	1.56 (1.31,1.87)	$8x10^{-7}$	2.01 (1.31,3.08)	0.002	0.99 (0.98,1.00)	0.208	1.83 (1.50,2.21)	$1x10^{-9}$
Excluding eBMD Steiger filtered SNPs	8	50	Hip OA	1.46 (1.26,1.71)	$1x10^{-6}$	2.01 (1.41,2.84)	$3x10^{-4}$	0.99 (0.98,1.00)	0.056	1.74 (1.44,2.11)	$1x10^{-8}$
BMI	1	61	Knee OA	1.69 (1.48,1.93)	$1x10^{-14}$	1.41 (1.02,1.95)	0.040	1.01 (1.00,1.02)	0.228	1.67 (1.44,1.95)	$2x10^{-11}$
Excluding eBMD Steiger filtered SNPs	10	51	Knee OA	1.61 (1.42,1.84)	$1x10^{-12}$	1.40 (1.03,1.90)	0.037	1.00 (1.00,1.01)	0.317	1.67 (1.43,1.96)	$3x10^{-10}$
BMI	11	51	eBMD	0.13 (0.09,0.17)	$7x10^{-10}$	0.23 (0.14,0.33)	$7x10^{-6}$	-0.01 (-0.01,	0.035	0.17 (0.14,0.21)	$8x10^{-19}$

Excluding hip and knee OA Steiger filtered SNPs	3	48	eBMD	0.13 (0.09,0.17)	$1x10^{-9}$	0.24 (0.15,0.33)	$9x10^{-6}$	$-4x10^{-4}$) $-4x10^{-3}$ (-0.01,$-1x10^{-3}$)	0.016	0.18 (0.14,0.22)	$2x10^{-19}$
Hip OA	0	9	eBMD	0.02 (-0.01,0.05)	0.117	$-1x10^{-3}$ (-0.09,0.09)	0.976	$2x10^{-3}$ (-0.01,0.01)	0.622	0.01 (-0.01,0.03)	0.396
Hip OA	0	17	BMI	0.02 ($-5x10^{-3}$, 0.04)	0.120	-0.07 (-0.16,0.01)	0.110	0.01 ($9x10^{-4}$,0.02)	0.046	0.02 ($7x10^{-4}$,0.05)	0.044
excluding rs12209223[b]	0	16	BMI	0.03 (0.01,0.04)	0.009	-0.03 (-0.11,0.06)	0.548	$5x10^{-3}$ ($-3x10^{-3}$,0.01)	0.242	0.03 ($4x10^{-3}$,0.05)	0.023
Knee OA	1	3	eBMD	0.13 (0.03,0.23)	0.010	0.53 (-0.99,2.06)	0.617	-0.03 (-0.12,0.07)	0.696	0.10 (0.06,0.14)	$5x10^{-6}$
Knee OA	0	6	BMI	$1x10^{-4}$ (-0.03,0.03)	0.995	0.02 (-0.15,0.19)	0.842	$-1x10^{-3}$ (-0.01,0.01)	0.839	$5x10^{-3}$ (-0.03,0.04)	0.821

[a]*Number of SNPs after Steiger filtering.* [b]*The rs12209223 OA-risk increasing allele was identified in a GWAS of height, with the same allele associated with an increased height.*

Effect sizes for binary exposures represents the SD increase per doubling in OA risk. Effect sizes for BMD and BMI analyses represent the SD increase in outcome per SD increase in exposure.

Figure 101: Plot of two-sample MR results for the causal effect of eBMD on hip OA, restricted to 10 SNPs also associated with FN-BMD at genome-wide significance.

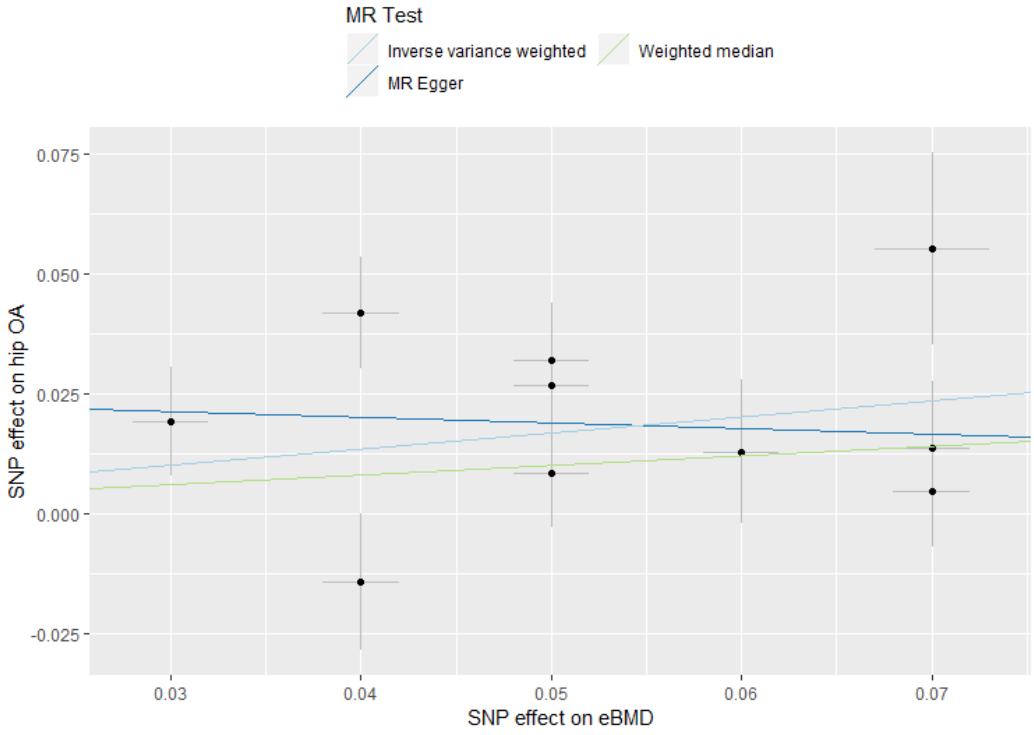

Figure 102: Plot of two-sample MR results for the causal effect of eBMD on knee OA, restricted to 10 SNPs also associated with FN-BMD at genome-wide significance.

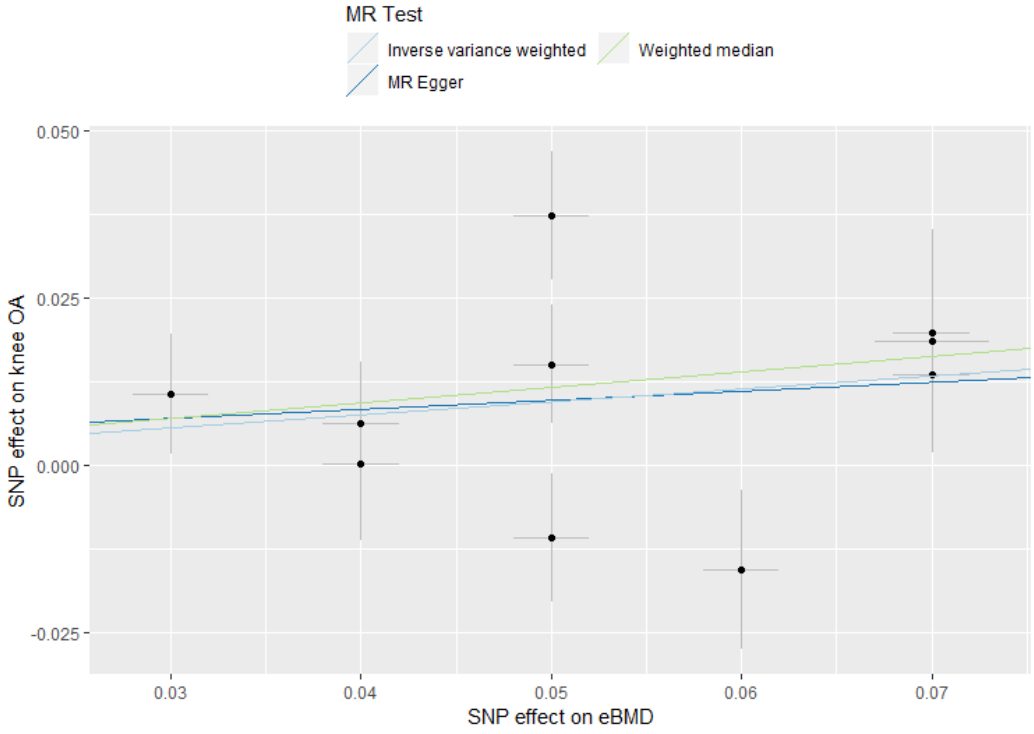

There was evidence for a causal pathway between hip OA and higher eBMD in 1SMR (SD increase per doubling in odds of hip OA=1.10 [0.36,1.84]) (Table 37), but not 2SMR (Figure 100). Evidence for a causal effect of knee OA on eBMD was provided by 1SMR (β=4.15 [2.74,5.56]) and 2SMR (β=0.13 [0.03,0.23]), with a positive effect observed for all three 2SMR methods, albeit of weak magnitude, with wide CIs overlapping the null for the MR-Egger regression (Figure 100). The leave-one-out analysis identified a stronger positive effect when removing rs143384, a 5' UTR variant in *GDF5* (Appendix 43). The knee, but not hip OA, PRS was related to BMI, potentially invalidating IV2 (Table 38). The other two knee OA SNPs are an intronic variant in *FTO* and an intergenic variant mapped to *TMEM18*, suggesting that the observed causal effect of knee OA on eBMD was mediated by a pleiotropic effect on BMI.

Using MR to determine bidirectional relationships with BMI

1SMR provided evidence that BMI has a strong causal effect on hip and knee OA, with an SD increase in BMI associated with a 1.5% (1.0,2.1) increased risk of hip, and 3.6% (2.9,4.3) increased risk of knee, OA (Table 37). 2SMR suggested that BMI is causally related to hip and knee OA, with an SD increase in BMI related to a 56 (31,87)% increased odds of hip, and a 69 (48,93)% increased odds of knee, OA. These results were consistent across the three 2SMR methods, apart from the causal effect of BMI on knee OA estimated by MR-Egger, which was approximately 30% weaker, albeit in the same direction (Figure 100). Leave-one-out analysis did not identify any individual SNPs driving this effect (Appendix 43).

There was strong evidence from 1SMR that the causal pathway between BMI and knee OA was bidirectional, with weaker evidence for hip OA (Table 37). Additional adjustment for total weekly PA did not attenuate these relationships (data not shown). 2SMR, however, provided inconsistent evidence for a causal effect of hip OA on BMI and did not provide evidence for a causal pathway from knee OA to BMI (Figure 100*)*. The leave-one-out analysis suggested that the removal of rs12209223 had a particularly strong effect on the observed 2SMR

results for the effect of hip OA on BMI (Appendix 43). The A allele, associated with an increased risk of hip OA, has been associated with height with genome-wide significance (484). I therefore repeated the 2SMR of hip OA on BMI, excluding this SNP. There was evidence for a causal effect of BMI on hip OA (SD increase in BMI per doubling in odds of hip OA=0.03 [0.01,0.04]), with results still inconsistent between the IVW/weighted median estimates and the MR-Egger estimate (Table 39).

I could not perform bidirectional 1SMR for BMD-BMI as the FN-BMD SNPs were taken from a GWAS adjusted for weight, which meant the SNPs may be inversely related to weight, but 2SMR, using summary statistics from a GWAS not adjusted for weight, did not identify a causal effect of eBMD on BMI *(*Figure 100*)*. There was robust evidence for a causal effect of BMI on eBMD in 1SMR, with an SD increase in BMI causing a 0.07 (0.04,0.11) SD increase in eBMD (Table 37). This estimate was similar to that from 2SMR, for which the effect size was consistent across methods. The MR-Egger intercept revealed weak evidence of horizontal pleiotropy (Figure 100, Table 39), although the MR-Egger estimate was stronger than the IVW estimate, suggesting that the pleiotropic effect was weakening the causal effect estimate. The leave-one-out analysis did not identify any outlying SNPs (Appendix 43).

Using MVMR to determine the BMI-independent causal effect of eBMD on OA

Overall, 1SMR and 2SMR provided consistent evidence that BMI is a confounder of the relationship between BMD and hip/knee OA. I therefore used 1SMVMR to examine the causal effect of eBMD on OA, accounting for shared relationships with BMI. Following adjustment for BMI, eBMD was found to be an independent causal risk factor for both hip and knee OA (risk difference=0.007 [0.001,0.013] and 0.015 [0.008,0.023], respectively, Table 37). This was equivalent of 26% and 36% increased odds per SD increase in BMD, respectively, and similar in magnitude to that observed in MR analyses not accounting for BMI. BMI was a much stronger risk factor, compared to BMD, for both hip and knee OA (Table

37). SW conditional F-statistics were >200 for both instruments, suggesting that these results are not biased by weak instruments.

I aimed to determine the BMI-independent effect of OA on BMD. MVMR provided evidence for a BMI-independent causal effect of OA on eBMD (β_{hip}=1.12 [0.35,1.89] and β_{knee}=5.76 [2.62,8.89], Table 37). The causal effect of BMI on BMD was independent of hip OA (β=0.08 [0.04,0.13]). However, when conditioning on knee OA, an inverse effect of BMI on BMD was observed (β=-0.20 [-0.39,1x10^{-3}]). However, of note, these results are vulnerable to weak instrument bias as conditional F statistics were 7.5 and 1.2 for hip and knee OA, respectively.

Summary of findings from bidirectional MR

A full summary of all MR analyses is presented in Figure 103. Overall, MR provided evidence for causal pathways from BMI to BMD, hip, and knee OA. MR did not provide evidence for a causal effect of eBMD on BMI. There was strong evidence for a causal effect of BMD on both hip and knee OA in 1SMR, although the magnitude of effect was much weaker for 2SMR. There was evidence for a causal pathway from knee OA to eBMD, but evidence was less consistent for a causal effect of hip OA on eBMD.

Figure 103: Summary of results of MR analyses for hip OA (left) and knee OA (right).

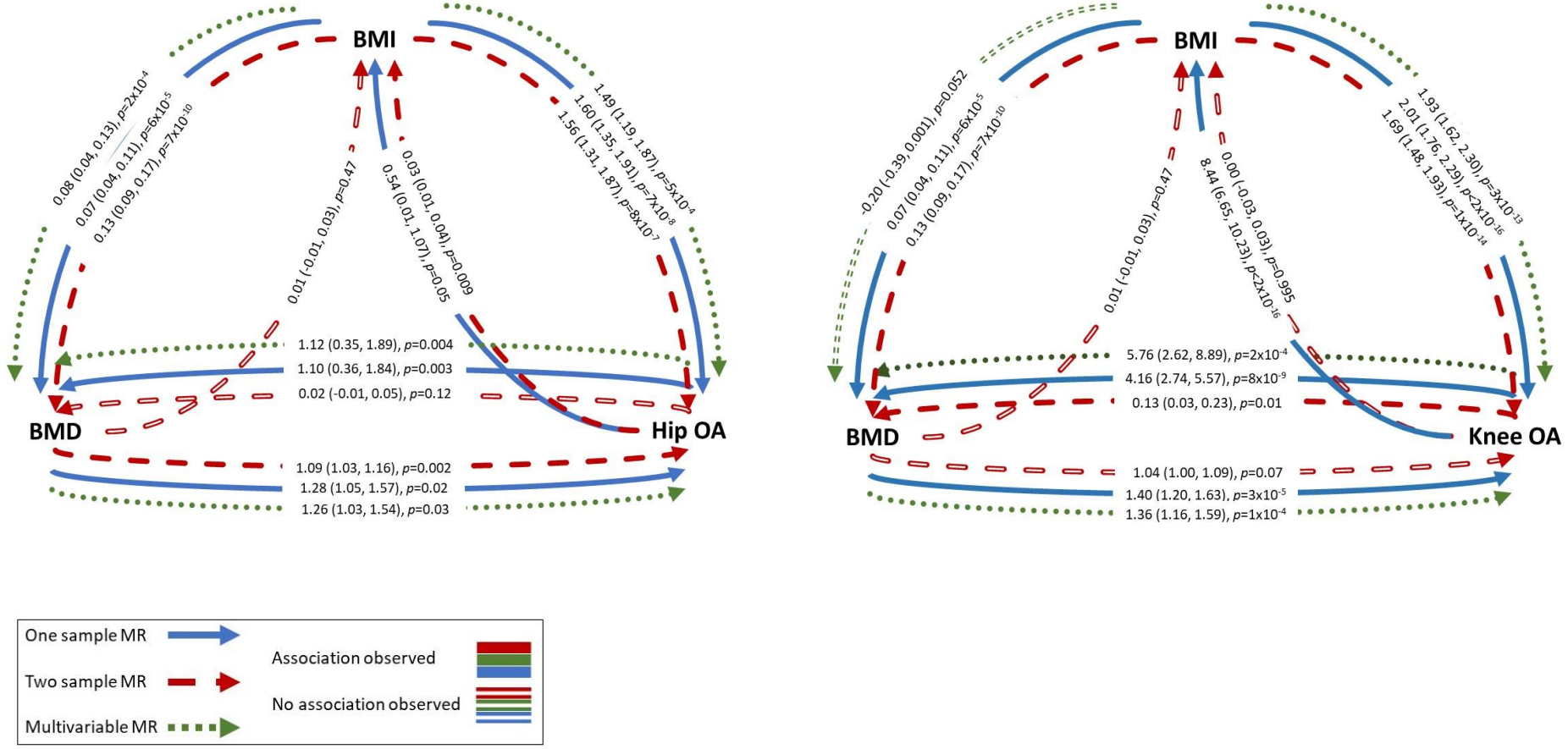

Effect estimates represent the SD increase in outcome per SD increase in exposure for BMD-BMI and BMD-BMI analyses, the OR per SD increase in exposure for BMI-OA and BMD-OA analyses and the SD increase in BMD or BMI per 1 unit increase in the log odds of OA.

Using LCV analyses to determine the true causal effect of BMD on OA

To determine if shared underlying genetic aetiology fully explains the observed causal effect of BMD on OA, I performed LCV modelling using weight-adjusted summary statistics for both FN/LS-BMD and hip/knee OA. LCV analyses identified evidence for genetic correlations between BMD (both FN and LS) and OA at both the hip and knee, ranging from rho=0.16 for the correlation between FN-BMD and hospital-diagnosed hip OA, to rho=0.23 for the genetic correlation between LS-BMD and hip OA (Table 40). There was evidence for a partial causal effect of BMD at both sites on OA at both sites, independent of genetic correlation and weight, with the largest magnitude of causal effect observed for FN-BMD and knee OA, with a genetic causality proportion of 0.64.

Table 40: Results of latent causal variable modelling of the genetic correlation between FN/ LS-BMD and hip/knee OA, as well as the estimate of the genetic causality proportion.

Trait 1	Trait 2	Rho (SE)	GCP (SE)	*p*-value
FN-BMD	Hospital-diagnosed hip OA	0.16 (0.02)	0.56 (0.07)	$3x10^{-20}$
	Hospital-diagnosed knee OA	0.19 (0.07)	0.64 (0.21)	$1x10^{-7}$
LS-BMD	Hospital-diagnosed hip OA	0.23 (0.08)	0.57 (0.21)	0.002
	Hospital-diagnosed knee OA	0.20 (0.07)	0.59 (0.25)	0.003

Rho represents the genetic correlation between the two traits, estimated by LD score regression. The GCP is an estimate of the genetic component of trait 1 which is causal for trait 2. A value closer to 1 represents stronger causality of trait 1 on trait 2. A negative value represents the proportion of the genetic component for trait 2 that is causal for trait 1 (481).

9.3.2. Using PRS to determine the role of bone in radiographic OA sub-phenotype prevalence and progression

There was no strong evidence of relationships between the PRS and prevalent hip or knee OA sub-phenotypes in RS (Table 41). Follow-up OA sub-phenotype data was only available for the RS1 population, limiting the sample size for progression analyses. However, there was some evidence of a positive relationship between the eBMD PRS and both change in summed knee osteophytes and summed knee JSN (Table 41).

Table 41: Associations between eBMD PRS and radiographic OA sub-phenotypes in the Rotterdam study cohorts.

			Unadjusted			**Adjusted**		
	Outcome	**N**	**β**	**95% CI**	***p***	**B**	**95% CI**	***p***
Prevalent	Hip JSN score	8,773	0.032	-0.015,0.080	0.180	0.030	-0.016,0.077	0.204
	Hip osteophyte score	7,594	-0.023	-0.191,0.146	0.792	-0.040	-0.204,0.124	0.636
	Hip subchondral sclerosis	7,156	1.161	0.975,1.384	0.094	1.168	0.980,1.393	0.083
	Knee JSN score	5,635	0.059	-0.011,0.128	0.099	0.064	-0.005,0.133	0.071
	Knee osteophyte score	7,524	0.172	-0.066,0.410	0.157	0.183	-0.052,0.418	0.126
	Knee subchondral sclerosis	5,233	1.046	0.781,1.400	0.762	1.047	0.777,1.411	0.764
Progressive	Change in knee JSN score	1,549	0.110	0.015,0.205	0.024	0.109	0.014,0.204	0.024
	Change in knee osteophyte score	2,717	0.193	0.015,0.371	0.034	0.190	0.014,0.367	0.035

Betas represent the unit increase in outcome per unit increase in PRS for (change in) summed scores or the OR per unit increase in PRS for subchondral sclerosis.

9.4. Discussion

9.4.1. Summary of findings

In this chapter, I have found strong evidence for a causal effect of BMD on hip and knee OA using 1SMR, which was relatively consistent with 2SMR. MVMR confirmed that the effect of BMD on OA is independent of BMI. These results also suggest that there is a bidirectional causal effect between OA and eBMD. I have confirmed strong causal effects of BMI on eBMD, hip and knee OA, with no causal effect of eBMD on BMI. The observed causal effect of BMI on eBMD in this adult population is consistent with a previous analysis of a paediatric population (mean age 10), where a causal effect of BMI on FN-BMD was observed (401). As seen in this current analysis, Kemp *et al* found no evidence for a causal effect of BMD on BMI (401). The strong causal effect of BMI on both hip and knee OA corroborates previous MR analyses (139,261,441).

9.4.2. Context of this work

I observed a causal effect of BMD, measured from heel ultrasound scans, on hip and knee OA, consistent with previous MR analyses which identified a causal effect of FN and LS-BMD on hip and knee OA (139,261). This suggests that BMD has a causal effect on OA, regardless of the site or method of measurement. However, the magnitude of effect of eBMD on OA was larger in 2SMR restricted to SNPs associated with FN-BMD. There are two potential explanations for a stronger effect of BMD on OA when restricting to FN-BMD loci. The first is that FN-BMD is measured by DXA, which is a more specific measure of BMD than the estimates generated from heel ultrasound. Heel ultrasound measures may be influenced by factors such as FM, which could lead to the inclusion of instruments not specific to BMD, increasing heterogeneity of the individual-SNP Wald ratios in 2SMR. An alternative explanation is that a large proportion of bone at the FN is cortical, whereas bone at the heel is predominantly trabecular (485,486). Increased cortical BMD could correlate with increased density or

thickness of the subchondral bone plate, creating greater pressure on the underlying cartilage.

I have found some evidence for reverse causality in the relationship between eBMD and OA. The positive direction of effect is as expected from artefactual elevation, rather than loss of bone mass due to reduced PA. However, as I do not expect BMD measurements at the heel to be artefactually elevated by features of OA, the observed causal effect of OA on eBMD in 1SMR may reflect biological pleiotropy (*i.e.* the same underlying biological pathways may be contributing to both phenotypes). As discussed in section 3.3.2, consistent with shared biological mechanisms contributing to both BMD and OA, Hackinger *et al* identified a genetic correlation between LS-BMD (but not FN) and OA (137) and identified a novel locus in *SMAD3* from the cross-phenotype meta-analysis of OA and LS-BMD (137). SMAD3 is part of the TGFβ signalling pathway, which regulates osteoblast differentiation. Evidence for a role of this pathway in OA pathogenesis in discussed in section 3.3.2. As discussed in section 3.3.2, other pathways with roles in both BMD development and OA aetiology include the Wnt and BMP signalling pathways. However, it should be noted that the knee OA PRS was also related to BMI, suggesting a pleiotropic effect of the instrument on BMI could also explain the observed causal effect of knee OA on eBMD.

I did find stronger, more consistent, evidence for an effect of eBMD on OA, as opposed to vice versa. This could reflect the stronger instrument for eBMD, but the LCV analyses using the full set of summary statistics provided further evidence for a causal pathway between BMD and OA, independent of genetic correlation (and confounding by weight). Overall, this suggests that bone may still have a direct effect on OA, for example via increased joint loading, or structural differences in the subchondral bone, which have been linked to progression of JSN (405). The sub-phenotype analyses in RS were inconclusive, although evidence for relationships between the eBMD PRS and change in knee scores (both osteophytes and JSN) was stronger than evidence for associations with prevalent scores, providing further evidence for a role of BMD in knee OA progression, including JSN progression and osteophyte development (discussed

in Chapter 6). This finding suggests that BMD may be an ongoing factor in the pathogenesis of OA, rather than its initiation.

9.4.3. Strengths of this work

I have utilised the largest datasets possible to maximize the power to detect causal effects. I have ensured that there is no overlap between the exposure and outcome populations. I have utilised the availability of individual-level data in UKBB to perform 1SMR to strengthen evidence, as well as radiographic sub-phenotype data to investigate the association between higher genetically predicted eBMD and OA sub-phenotypes.

9.4.4. Limitations

I was unable to use eBMD instruments for 1SMR, as they were identified in the same population used for analyses; reassuringly F-statistics suggested that the FN-BMD instrument was of reasonable strength. The OA outcomes for 1SMR were based on hospital-diagnosis; it is unclear how hospital diagnosis relates to radiographic features of OA, such as JSN, which are commonly used as clinical trial outcomes. Using a severe phenotype as the outcome means reduced power in GWAS, as the phenotype is rare and a composite of structural features and pain, leading to fewer genome-wide significant loci and a greater chance of weak-instrument bias (as highlighted by the much smaller F-statistics for the OA instruments). The OA outcomes from the GO consortium included a range of definitions of hip and knee OA, including hospital diagnosis, radiographic evidence, and self-reported OA definitions. Heterogeneity in phenotype, reflecting a combination of pain and structural symptoms, reduces the power to detect loci in GWAS. The ORs from 1SMR are estimates and SEs are likely underestimated (479), therefore caution should be taken when interpreting CIs. There may be additional risk factors related to the genetic variants which I did not include in the MVMR model. Most individuals included were of white European ancestry, limiting generalizability to other ethnicities. PRS analysis using FN or LS-BMD loci could not be performed in RS as it is part of GEFOS.

9.4.5. Future work

The results of this work provide evidence for both a causal role of BMD on hip and knee OA, and shared underlying biology contributing to both phenotypes. In Chapter 10, I will investigate the contribution of biological pathways (*e.g.* Wnt signalling, TGFβ signalling) to both BMD and OA risk. I will select pathways involved in both bone formation and bone resorption and compare the contribution of variation in these pathways to both eBMD and OA risk. To perform formal MR analyses of the BMI-independent causal effect of BMD on OA sub-phenotypes and their progression, GWAS summary statistics are required for these sub-phenotypes. This was beyond the scope of this PhD, but LCV analyses to determine if there is a causal effect of BMD on particular OA sub-phenotypes, independent of genetic correlation, would make an important contribution to our knowledge of the role of bone in OA pathogenesis.

9.4.6. Conclusions

I have found evidence for a BMI-independent causal effect of BMD on hip and knee OA, and some evidence for a bidirectional causal effect which I hypothesize to reflect shared underlying genetic aetiology. I have confirmed strong causal effects of BMI/BMD on hip and knee OA. Further analyses are required to determine the shared pathways contributing to both BMD and OA, and to determine the mechanisms by which higher BMD causes OA.

CHAPTER 10. THE ROLE OF BONE PATHWAYS IN OSTEOARTHRITIS PATHOGENESIS

10.1. Background and aims

As discussed in sections 1.2.2 and 3.2, bone turnover is involved in OA pathogenesis via subchondral bone remodelling. A role of the Wnt and TGFβ signalling pathways in OA pathogenesis is widely accepted (section 3.3.2), but it is currently unclear to what extent these pathways contribute to OA risk, and whether the role of these pathways is direct (via their role in chondrocyte differentiation) or mediated by their role in bone formation. The first aim of this chapter is to use UK Biobank data to determine the contribution of genetic variation in the Wnt (and specifically canonical Wnt) and TGFβ superfamily signalling pathways, as well as a pathway specific to osteoclast differentiation, to variation in OA phenotypes. I aim to determine the specific contribution of the OPG-RANK-RANKL system, which, as discussed in section 2.1, is responsible for regulating bone resorption by osteoclasts and is the drug target for Denosumab. I aim to compare the variance in OA and in eBMD explained by these pathways and determine if the variance in OA explained by these pathways is altered by conditioning on eBMD (Aim 1, Figure 104). If the variance explained is unchanged by conditioning on eBMD, this would suggest that the effect of these pathways on OA risk is direct, for example mediated by an effect on chondrocytes and thus JSN (left pathway, Aim 1, Figure 104). However, if the variance explained is reduced when conditioning on eBMD, this would suggest the effect is mediated by bone (right pathway, Aim 1, Figure 104). Subsequently, I aim to use RS data to determine the contribution of genetic variation in these pathways to osteophyte and JSN severity (Aim 1, Figure 104).

Figure 104: Diagrams summarising the key aims of this chapter.

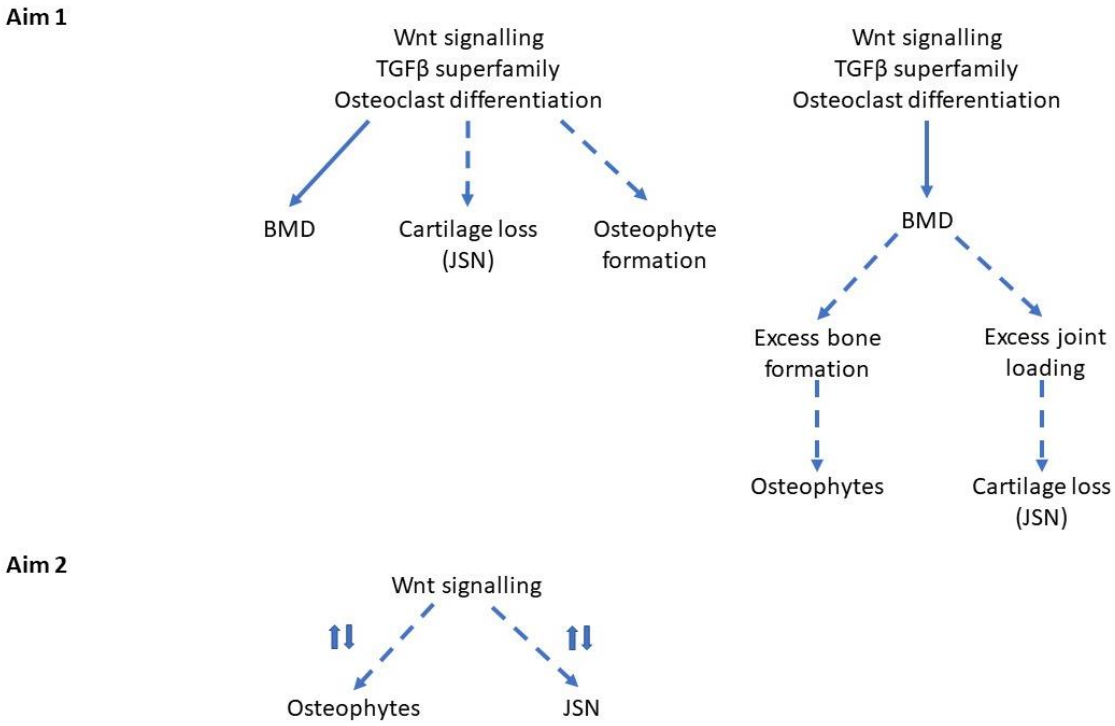

Arrows represent causal pathways, with dashed arrows representing hypothesized causal pathways.

Although the pathway analyses outlined above will be performed to determine the contribution of variation in these pathways to OA risk and severity of radiographic OA sub-phenotypes, these analyses will not provide information on whether overactivation or inhibition of signalling via these pathways contributes to OA pathogenesis. One method to determine this is to measure a key inhibitor of a pathway and determine the relationship of levels of the inhibitor with OA. The Wnt inhibitor sclerostin has been measured in the HBM population. Previous analyses have shown that individuals with HBM have elevated plasma sclerostin levels, which may reflect the greater number of osteocytes present, as indicated by a positive causal effect of BMD on plasma sclerostin concentration in a subsequent MR analysis (487,488). As discussed in section 3.3.2, Wnt antagonists such as sclerostin may have a role in OA pathogenesis. However, there have been few studies investigating the association between circulating sclerostin and OA, and these have used small populations of patients undergoing

TJR and healthy controls, thus not investigating individual sub-phenotypes (489,490). These studies have conflicting findings, with one finding little evidence of an association between OA and serum sclerostin (490), and the other finding reduced sclerostin levels in those with a higher radiographic severity of OA (489). Therefore, the second aim of this chapter is to determine cross-sectional associations between plasma sclerostin and OA sub-phenotypes (osteophytes, JSN, subchondral sclerosis and chondrocalcinosis) at the hip, knee, and hand in the HBM population (Aim 2, Figure 104).

10.2. Methods

10.2.1. Contributions of genetic variation in bone pathways to OA risk

Study population

Analyses with hospital-diagnosed OA outcomes were performed in the UK Biobank population (section 5.2.1), that had data for eBMD and at least one hospital-diagnosed OA variable. Analyses with radiographic OA outcomes were performed using baseline data for the three RS populations.

Outcomes

Derivation of hospital-diagnosed OA variables in UK Biobank and measurement of eBMD, as well as radiographic OA variables in RS, are described in Chapter 9. Radiographic OA sub-phenotypes were binarised based on the presence of any osteophyte or any JSN at each joint (*i.e.* summed score $\geq$1). ICD codes used to derive hospital-diagnosed hand OA are presented in Table 42 (261).

Table 42: ICD codes used to identify cases of hospital-diagnosed hand OA in UK Biobank.

Joint	Code		Description
	ICD10	**ICD9**	
Hand	M151		"Heberden nodes (with arthropathy)"
	M152		"Bouchard nodes (with arthropathy)"
	M154		"Erosive (osteo)arthrosis"
	M180		"Primary arthrosis of first carpometacarpal joints, bilateral"
	M181		"Other primary arthrosis of first carpometacarpal joint"
	M189		"Arthrosis of the first carpometacarpal joint, unspecified"
	M1904		"Primary arthrosis of other joints (hand)"
	M1994		"Arthrosis, unspecified (hand)"
		71534	"Osteoarthrosis, localized, primary or secondary, hand"
		71514	"Osteoarthrosis, localized, primary, hand"

GWAS

GWAS of eBMD and hospital-diagnosed OA in UK Biobank

To generate SNP-outcome effect estimates to calculate pathway-specific r^2, I performed GWAS of eBMD and hospital-diagnosed hip, knee, and hand OA in UK Biobank, restricting the OA GWAS to those with eBMD data, so that the sample size was the same when adjusting for eBMD, ensuring that any change in effect size for a SNP was not due to sample size differences. 12,321,875 SNPs were analysed with sample sizes ranging from 222,952 for hand OA to 241,487 for eBMD (all white Europeans). Pre-GWAS QC of genetic data is described in section 5.3.1. GWAS were performed as described in section 5.3.2. Conditional GWAS were performed for OA at each joint, adjusting for eBMD. QQplots to assess population stratification are presented in Figure 105 and Figure 106, and Miami plots comparing unadjusted with eBMD-adjusted analyses are presented in Appendix 44.

Figure 105: QQplots from GWAS of hospital-diagnosed hand (top), hip (middle) and knee (bottom) OA in UK Biobank, with and without adjustment for eBMD.

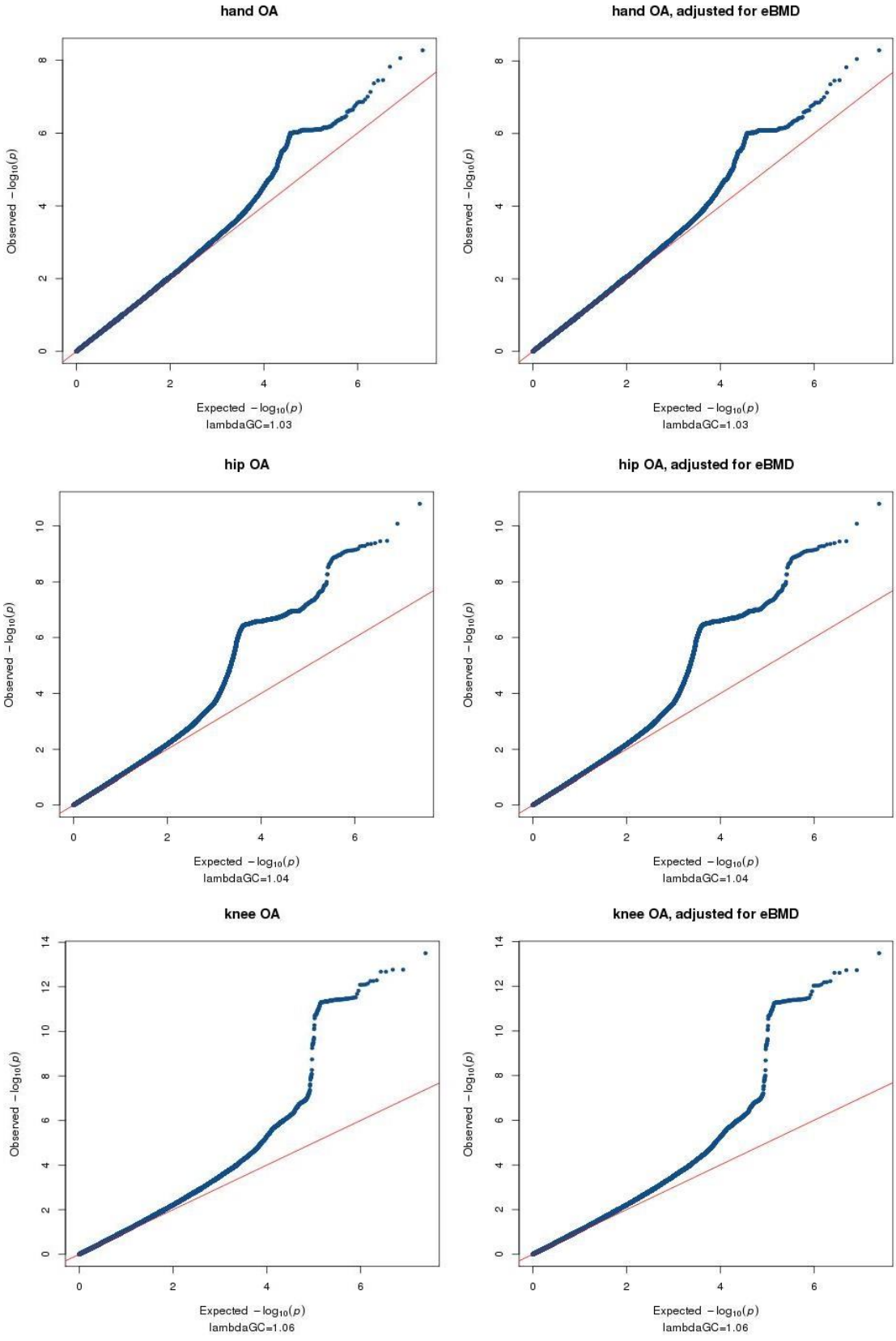

Figure 106: QQplot from GWAS of eBMD in UK Biobank, restricted to individuals with data for hospital-diagnosed OA in at least one joint.

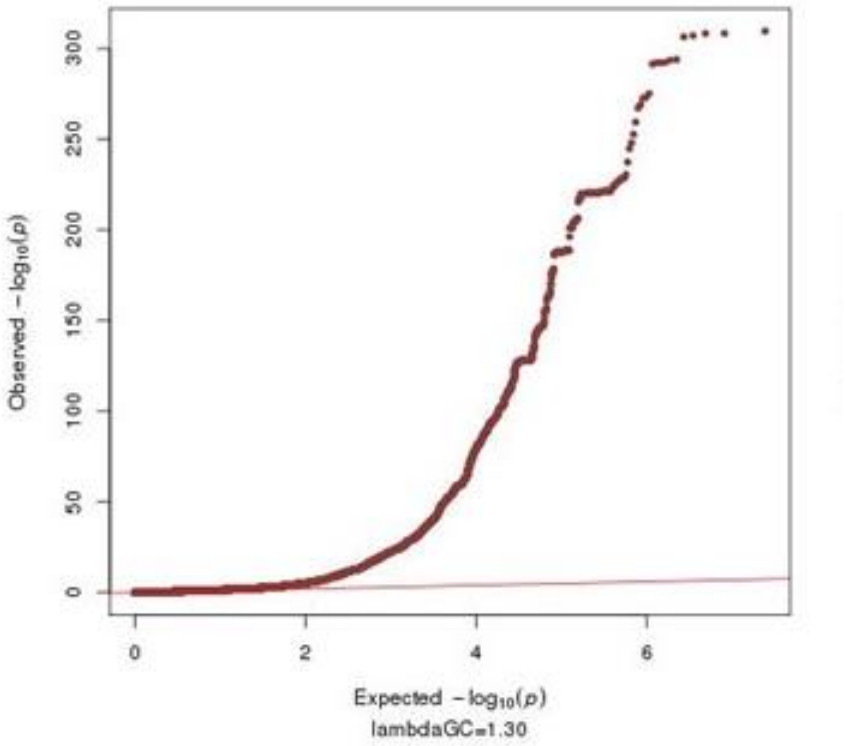

GWAS of OA sub-phenotypes in RS

To extract estimates for the effect of pathway-annotated SNPs on osteophytes and JSN at each joint, GWAS in the three RS cohorts were performed as described in section 5.3.2. Post-GWAS QC was performed using '*EasyQC*' software (version 9.2): SNPs with a MAF<0.05, duplicate IDs, mismatched alleles compared to the reference HRCv1.1 dataset (downloaded from https://www.uni-regensburg.de/medizin/epidemiologie-praeventivmedizin/genetische-epidemiologie/software/) or with an allele frequency difference >0.2 from the reference dataset were excluded. Meta-analyses were then performed, for 5,282,396 SNPs common to all three populations, as described in section 5.3.2. QQplots for all analyses, after meta-analysis, are provided in Figure 107. QQplots for each population are provided in Appendix 45.

Figure 107: QQplots for the GWAS meta-analysis of each radiographic OA sub-phenotype in the total Rotterdam study population.

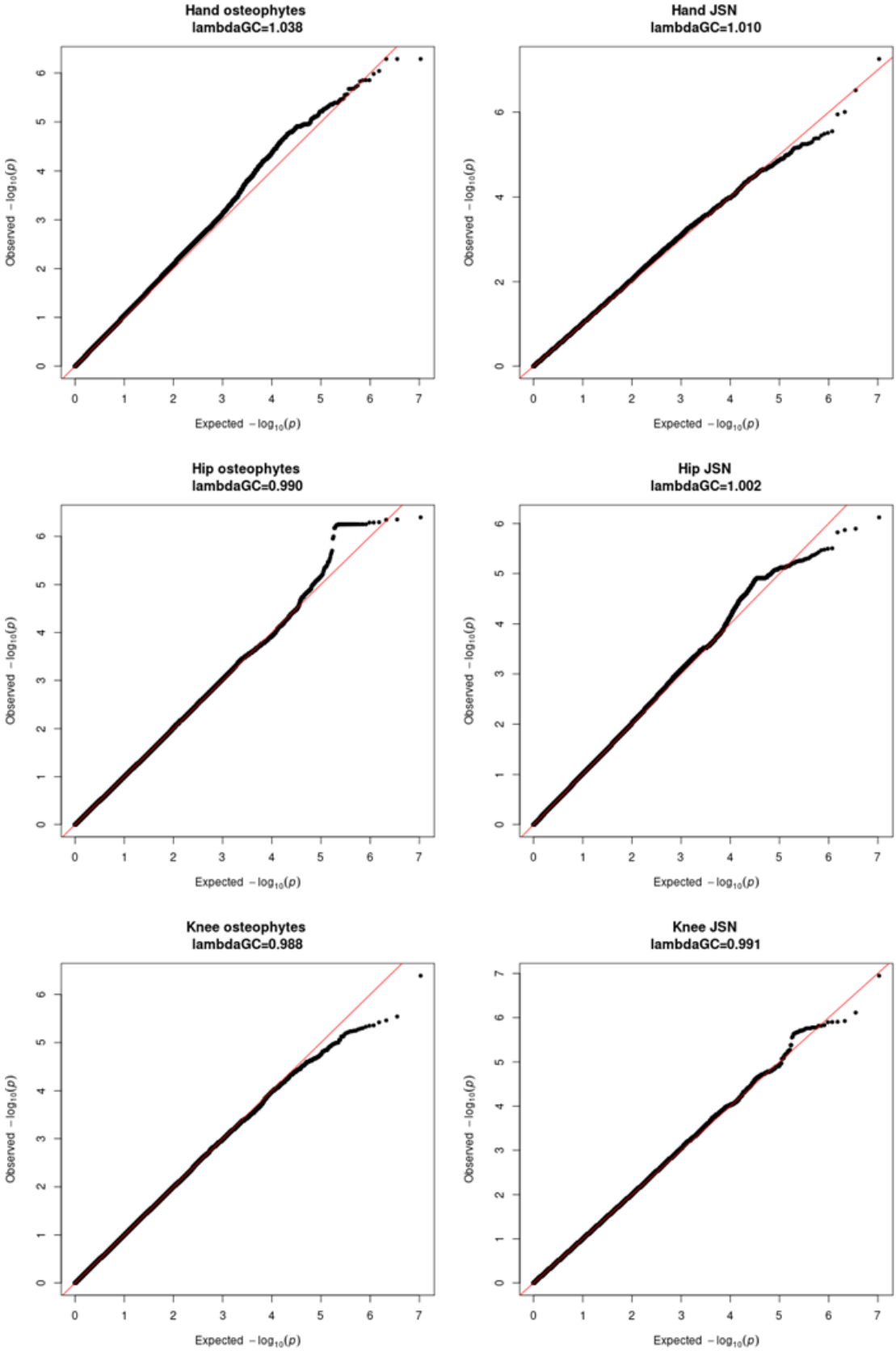

Extracting pathway-specific variants

To ensure only independent loci were included to calculate pathway-specific r^2, I used LD pruning to generate a list of independent SNPs within the UK Biobank cleaned genotype data (QC procedure described in section 5.3.1). This allowed SNP r^2 estimates to be summed across a pathway without having to account for LD between variants. For RS, I performed pruning on the SNPs included in the meta-analysis, using the largest population (RS1). Pruning was performed using the Plink '*indep-pairwise*' function, with a window size of 50kb, a step size of five and an r^2 threshold of 0.2.

I downloaded the latest version of the relevant Kegg pathways for homo sapiens (Figure 108-Figure 110) (491). I extracted a list of all genes from the Kegg pathway and then downloaded the genome position for each gene from NCBI gene (https://www.ncbi.nlm.nih.gov/gene/), using the 'hg19' assembly. I used two approaches to determine pathway-specific variants: one based on all SNPs within 20kb upstream and downstream of all genes (location-based) and one based on all *cis*-eQTLs (<1Mb from the gene) associated with expression of pathway genes in blood, identified by the eQTLGen Consortium (492) (expression-based). For the expression-based approach, I wrote R code to search for all genes in the pathway in the file downloaded from eQTLGen ('*2019-12-11-cis-eQTLsFDR0.05-ProbeLevel-CohortInfoRemoved-BonferroniAdded (1).txt.gz*', downloaded 15th May 2020). To check for genes that were missed due to alternative gene names, I downloaded the Ensembl IDs for genes not discovered in the file and searched for those. This did not identify any additional SNPs.

Once I had generated the list of pathway-specific variants, I filtered these on the list of independent loci generated by LD pruning, and calculated the SNP-specific r^2 estimates for the filtered variants in R. Non-biallelic SNPs in UK Biobank were excluded.

Figure 108: KEGG pathway map used to generate a list of genes involved in overall Wnt signalling and canonical Wnt signalling.

Image removed for copyright purposes

Downloaded from https://www.kegg.jp/kegg-bin/highlight_pathway?scale=1.0&map=hsa04310&keyword=wnt. The grey dashed line represents the nucleus.

Figure 109: KEGG pathway used to identify genes in the osteoclast differentiation pathway.

Downloaded from https://www.kegg.jp/kegg-bin/highlight_pathway?scale=1.0&map=hsa04380&keyword=osteoclast.

Figure 110: KEGG pathway map used to generate TGFβ and BMP pathway-specific gene lists.

A gene was annotated to the BMP-specific pathway if signalling was via the BMP receptors, as highlighted in blue. A gene was annotated to TGFβ-specific signalling if it was involved in signalling by TGFβ, Activin or Nodal receptors, as highlighted in yellow. Genes such as ERK and SMAD6/7 were annotated to both BMP- and TGFβ-specific signalling. Downloaded from: https://www.kegg.jp/kegg-bin/highlight_pathway?scale=1.0&map=hsa04350&keyword=tgfb.

Calculation of pathway-specific r^2

The proportion of the variance explained by each SNP was calculated as the variance explained by an individual SNP ($2\beta^2EAF(1-EAF)$), divided by the total phenotypic variance, as described in section 5.3.5. For eBMD, the total phenotypic variance was the SD of eBMD in the GWAS population, squared. For OA variables, the total phenotypic variance was estimated using the equation provided on page 160. The proportion of variance explained by each SNP was then summed across the pathway to generate the pathway r^2.

10.2.2. The relationship between circulating sclerostin and OA sub-phenotypes

Measurement of plasma sclerostin

Plasma sclerostin concentrations in the HBM population were assessed from blood samples, collected at baseline, by ELISA immunoassay by Professor Bill Fraser and Dr Jonathan Tang. Individuals whose samples were collected at a site without the correct storage facilities to immediately freeze the samples were excluded from these analyses. Intra- and inter-assay CVs, provided by Professor Fraser and Dr Tang, were <5% and <13%, respectively.

Radiographic sub-phenotype outcomes

I used baseline binary variables for any osteophyte and any JSN of grade $\geq$1, at each joint, as described in section 8.2.4. Subchondral sclerosis and chondrocalcinosis of the hip and knee were assessed as present or absent. OA was defined as a KL grade $\geq$2 at the knee and a Croft score $\geq$3 at the hip.

Statistical analysis

Person-level analyses were performed, using GEE logistic regression, to determine the association between plasma sclerostin (standardized) and binary OA sub-phenotype variables, accounting for within-family clustering. Analyses were initially performed unadjusted (model 1), before adjusting for age and sex

(model 2) and then additionally height and weight (model 3). Finally, P1NP was added to model 3 to determine if observed associations were independent of current levels of osteoblast activity. Measurement of P1NP is described in section 8.2.3. As I analysed 12 prevalent outcome variables, I performed Bonferroni correction to give a significance threshold of 0.004, to investigate the potential role of chance observations. I additionally adjusted for creatinine in a sensitivity analysis, to determine if renal function explained results.

Association of sclerostin loci with OA phenotypes

Two loci were associated with plasma sclerostin levels at genome-wide significance in a recent meta-analysis of 10,584 individuals (488). The association of these two SNPs with OA at the hand, hip and knee was assessed in the latest GO meta-analysis (section 9.2.1). Summary statistics for the two SNPs were provided by Dr Lorraine Southam, Helmholtz University, with permission of the GO steering committee. I performed IVW to generate an estimate of the causal effect of plasma sclerostin on OA at each site, although with only two SNPs I was unable to perform additional analyses such as MR-Egger to determine if results may be biased by horizontal pleiotropy.

10.3. Results

10.3.1. Contribution of variation in bone pathways to OA risk

Descriptive characteristics of the UK Biobank population included in these analyses are presented in Table 43.

Table 43: Descriptive characteristics of the UK Biobank population analysed.

	N (%)
Female	135,874 (54.4)
Hospital-diagnosed OA	
Hand	1,623 (0.7)
Hip	7,519 (3.2)
Knee	13,005 (5.4)
	Mean (SD)
eBMD (g/cm^2)	0.540 (0.124)
Age (years)	56.3 (8.0)

Table 44 presents the variance in each outcome (columns) for each pathway (rows) using the two annotation methods. The total variance explained by all SNPs, annotated to any of the pathways by location, was 22% for eBMD, 16% for hand OA, 17% for hip OA and 16% for knee OA. Variance explained by all eQTLs across the pathways was 15% for eBMD and 6% for OA at all joints. The number of SNPs annotated to each pathway varied, mainly due to the number of genes annotated to each pathway: only three genes were annotated to OPG-RANK-RANKL whereas 139 genes contributed to the Wnt signalling pathway. Estimates for pathways with many annotated genes were therefore higher than those with few annotated genes. Therefore, it was unsurprising that the largest r^2 for all phenotypes was for the Wnt signalling pathway (location-based r^2=0.075, 0.064, 0.066 and 0.065 for eBMD, hand, hip, and knee OA, respectively). eBMD had higher r^2 values than OA at any site, across all pathways and both methods, suggesting that these pathways explain a greater proportion of variance in eBMD compared to OA risk. Using the location-based approach, BMP signalling explained more variance in eBMD than canonical Wnt signalling, despite fewer

annotated SNPs (0.060 *vs* 0.048). This pattern was not seen for the OA phenotypes. As expected, the r^2 for eBMD and the OPG-RANK-RANKL pathway, specific to bone resorption, was twice that of the OA phenotypes (0.004 *vs* 0.002). Of the three OA phenotypes, the total r^2 was slightly higher for hip, compared to hand and knee OA, although differences between sites were small for all pathways.

Table 44: Variance in eBMD and hospital-diagnosed OA in UK Biobank explained by each of the biological pathways.

		eBMD N=241,487	**Hand OA N=222,952**	**Hip OA N=228,761**	**Knee OA N=233,944**
Location-Based	Wnt N_{SNPs}=14,521	0.075	0.064	0.066	0.065
	Canonical Wnt N_{SNPs}=9,364	0.048	0.041	0.042	0.042
	TGFβ N_{SNPs}=7,353	0.047	0.034	0.034	0.034
	BMP N_{SNPs}=7,550	0.060	0.035	0.035	0.034
	Osteoclast differentiation N_{SNPs}=7,876	0.044	0.034	0.036	0.036
	OPG-RANK-RANKL N_{SNPs}=339	0.004	0.002	0.002	0.002
	All N_{SNPs}=36,270	0.220	0.162	0.166	0.164
Expression-Based	Wnt N_{SNPs}=5,025	0.085	0.022	0.024	0.024
	Canonical Wnt N_{SNPs}=2,975	0.070	0.013	0.014	0.014
	TGFβ N_{SNPs}=2,186	0.021	0.010	0.011	0.012
	BMP N_{SNPs}=2,419	0.026	0.012	0.011	0.012
	Osteoclast differentiation N_{SNPs}=4,916	0.038	0.024	0.022	0.026
	All N_{SNPs}=12,318	0.150	0.058	0.058	0.062

When calculating pathway-specific r^2 based on blood eQTLs for genes in each pathway, despite fewer SNPs than using the location-based approach, the variance in eBMD explained by the Wnt signalling pathway was greater (8.5% *vs* 7.5%, Table 44). This pattern was not seen for OA. The r^2 for the osteoclast differentiation pathway was similar for eBMD despite 38% fewer SNPs (location-

based r^2=0.044, expression-based r^2=0.038). The largest r^2 for hand and knee OA were seen for eQTLs annotated to the osteoclast differentiation pathway (0.024 and 0.026, respectively), and for hip OA the largest contributor was the Wnt signalling pathway (0.024). r^2 values were similar across OA at the three joints.

The contribution of variation in genetic pathways mediated by BMD

I next aimed to determine if adjustment for eBMD changed the variance in OA risk explained by each pathway, to determine if the contribution of each pathway to OA risk was mediated by BMD or represented a direct effect on OA risk. I used summary statistics from a GWAS for each OA phenotype adjusted for eBMD. As the SE of the SNP-outcome effect could be increased or decreased by adjustment for a covariate, and yet the total phenotypic variance would be the same, I calculated the denominator for the OA outcomes using SEs and betas from unadjusted analyses. If eBMD mediates the effect of a pathway on OA risk, one would expect the betas to decrease in magnitude upon adjustment and therefore the estimated r^2 would decrease. However, adjustment for eBMD made no difference to the variance in OA risk explained by each pathway (Figure 111), suggesting that variance in OA risk explained by these pathways is not mediated by eBMD.

Figure 111: Comparison of r^2 values for each OA phenotype, with and without adjustment for eBMD, in UK Biobank.

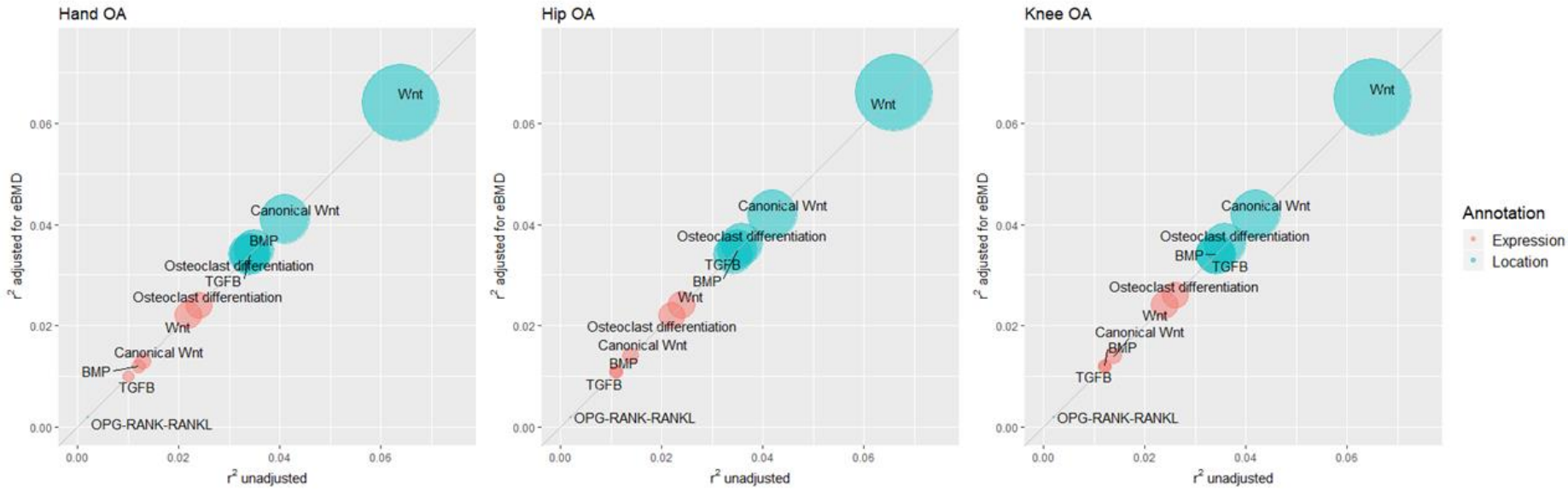

Point sizes are proportional to the number of annotated SNPs.

10.3.2. Contribution of variation in bone pathways to OA sub-phenotypes

I next aimed to determine if the variation explained by these pathways differs between osteophytes and JSN, to determine the role of these pathways in the pathogenic processes of OA. Descriptive characteristics of the RS population, with complete data for both sub-phenotypes at least one joint and included in the GWAS meta-analysis, are presented in Table 45.

Table 45: Descriptive characteristics of the Rotterdam Study population analysed.

		Mean (SD)
Age		64.7 (9.1)
		N (%)
Female		5,621 (57.3)
Hand		
	Any osteophyte	6,708 (77.2)
	Any JSN	1,598 (18.4)
Hip		
	Any osteophyte	4,739 (63.7)
	Any JSN	2,052 (27.6)
Knee		
	Any osteophyte	3,263 (57.8)
	Any JSN	1,600 (28.3)

Table 46 displays the r^2 estimates for each sub-phenotype, at each joint, in the total RS population. Sample sizes were much smaller in RS than UK Biobank analyses, which appears to have caused inflated beta estimates and thus r^2 estimates, as evidenced by the ~0.2 greater summed r^2 for knee sub-phenotypes compared to hip/hand sub-phenotypes, where the sample size was smaller by 2,000-3,000 individuals. Results are therefore not comparable to those presented in section 10.3.1, or between joints. There was no consistent pattern, across joints, of a particular pathway explaining more variance in osteophytes *vs* JSN or vice versa.

Table 46: Comparison of r^2 values for each radiographic OA sub-phenotype in the Rotterdam Study population.

		Hip N=7,441		Knee N=5,644		Hand N=8,687	
		Osteophytes	**JSN**	**Osteophytes**	**JSN**	**Osteophytes**	**JSN**
Location-Based	Wnt N_{SNPs}=1,942	0.251	0.277	0.359	0.335	0.227	0.247
	Canonical Wnt N_{SNPs}=1,091	0.136	0.165	0.207	0.187	0.127	0.140
	TGFβ N_{SNPs}=620	0.095	0.089	0.097	0.115	0.068	0.080
	BMP N_{SNPs}=672	0.100	0.089	0.116	0.120	0.081	0.082
	Osteoclast differentiation N_{SNPs}=1,320	0.188	0.175	0.233	0.244	0.153	0.152
	OPG-RANK-RANKL N_{SNPs}=30	0.003	0.005	0.003	0.004	0.004	0.003
	All pathway SNPs N_{SNPs}=4,032	0.552	0.556	0.718	0.723	0.434	0.496
Expression-Based	Wnt N_{SNPs}=1,714	0.203	0.261	0.324	0.299	0.209	0.234
	Canonical Wnt N_{SNPs}=1,048	0.115	0.157	0.199	0.184	0.129	0.136
	TGFβ N_{SNPs}=848	0.113	0.121	0.171	0.155	0.093	0.110
	BMP N_{SNPs}=843	0.135	0.100	0.177	0.182	0.100	0.111
	Osteoclast differentiation N_{SNPs}=1,803	0.236	0.232	0.334	0.307	0.223	0.219
	All pathway eQTLs N_{SNPs}=4,248	0.566	0.602	0.781	0.784	0.520	0.549

10.3.3. The role of sclerostin in OA

I next utilised the availability of measured plasma sclerostin in the HBM population to determine if circulating levels of this Wnt inhibitor are related to radiographic OA sub-phenotypes (Aim 2, Figure 104).

Participant characteristics

In the HBM population, 362 individuals had at least one hip, knee, or hand radiograph, plus measured plasma sclerostin and covariate data. 64% had HBM. Descriptive characteristics of these 362 individuals are presented in Table 47. The mean plasma sclerostin concentration was 83.2 (41.1) pmol/L (standard range 0-80pmol/L).

Table 47: Characteristics of the HBM study population analysed.

		N (%)
High Bone Mass		232 (64)
Sex (Female)		239 (66)
Hand	DIP osteophyte	217 (60)
	DIP JSN	146 (41)
	CMC osteophyte	231 (64)
	CMC JSN	159 (44)
Knee	Osteophyte	115 (34)
	Subchondral sclerosis	13 (4)
	JSN	63 (19)
	Chondrocalcinosis	28 (9)
	OA (KL$\geq$2)	117 (35)
Hip	Osteophyte	227 (77)
	Subchondral sclerosis	12 (4)
	JSN	92 (31)
	Bilateral JSN	32 (11)
	Chondrocalcinosis	19 (7)
	OA (Croft $\geq$3)	78 (27)
		Mean (SD)
Age (years)		59.6 (14.7)
Plasma sclerostin (pmol/L)		83.2 (41.1)
Height (cm)		168.7 (9.7)
Weight (kg)		84.4(16.7)

Cross-sectional associations between plasma sclerostin and OA sub-phenotypes

In unadjusted analyses, higher plasma sclerostin was positively associated with OA at the hip and knee, presence of osteophytes of any severity in the DIP, CMC, knee, and hip, as well as any JSN at the knee, and any chondrocalcinosis at the knee and hip. The strongest associations were observed for the hand osteophyte variables (OR_{DIP}=1.59 [1.25,2.03] and OR_{CMC}=1.62 [1.24,2.12], OR per SD increase in plasma sclerostin (Figure 112)). Associations of plasma sclerostin with hip OA, osteophytes and chondrocalcinosis, and knee chondrocalcinosis, were not robust to correction for multiple testing. After adjustment for age and sex, the associations between plasma sclerostin and hip OA, hand and hip osteophytes, and hip and knee chondrocalcinosis were attenuated by over 50%, with CIs overlapping one. CIs for the association between plasma sclerostin and OA and osteophytes in the knee joint just overlapped one, but this was further attenuated in model 3. However, a strong inverse association between plasma sclerostin and CMC JSN became apparent in model 2 (OR=0.68 [0.53,0.87]), which persisted after adjustment for height, weight and P1NP. Adjustment for maximum TH-BMD (instead of P1NP) did not alter results, nor did adjustment for creatinine (data not shown).

In summary, these observational analyses provide evidence for a reduced odds of JSN at the CMC joint with increasing plasma sclerostin, but there was no evidence for a relationship with JSN at the hip or knee. This was the opposite direction of effect compared to osteophytes at the hip or knee, where there was very weak evidence (CIs overlapping one) for an increased odds of osteophytes with increasing plasma sclerostin.

Figure 112: Cross-sectional associations between plasma sclerostin and OA-sub-phenotypes of the hip, knee, and hand in the HBM cohort.

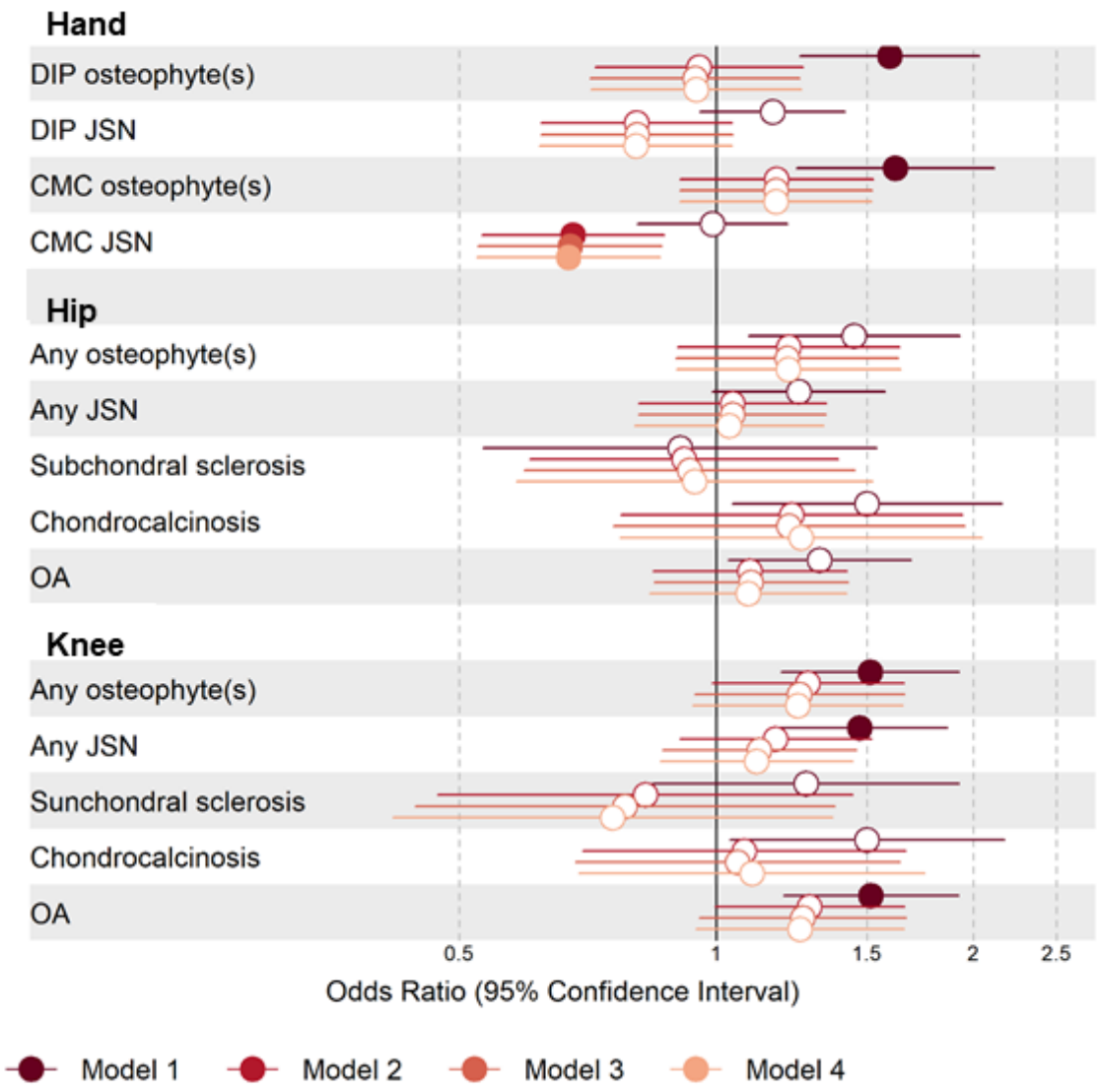

Points represent ORs per SD increase in plasma sclerostin concentration. Horizontal bars represent 95% CIs. N=361 for hand OA variables, 334 for knee variables, 294 for hip variables.

Associations between sclerostin loci and OA phenotypes

Having observed strong evidence for an inverse relationship between plasma sclerostin and thumb JSN in observational analyses, I next aimed to determine if sclerostin loci were associated with a reduced odds of thumb OA, to try and determine if cross-sectional relationships reflected a causal pathway. There was evidence for a protective association between the rs215226 A allele and hand OA

in the GO consortium (OR=0.97 [0.95,1.00], p=0.033). This allele was also associated with higher plasma sclerostin levels. Effect sizes were consistent between thumb and finger OA (OR_{thumb}=0.97 [0.93,1.00], p=0.033 and OR_{finger}=0.97 [0.94,1.00], p=0.086). There was some evidence of a weak protective effect of the rs215226 A allele on knee OA (0.99 [0.97,1.00], p=0.044). There was no evidence for an association between the rs215226 loci and hip OA risk, or between the rs7241221 loci and OA (Table 48). IVW estimates were consistent with a potential protective effect of sclerostin against hand OA, although CIs were wide.

Table 48: Summary statistics for the two sclerostin loci from the largest GO consortium meta-analysis to date, and results of MR analysis.

SNP	OA								Serum sclerostin			
	Phenotype	**EA**	**NEA**	**EAF**	**Cases**	**Controls**	**OR**	**95% CI**	***P***	**EAF**	**B**	**SE**	***p***
rs215226		A	G	0.591	21,208	285,124	0.974	0.951,0.998	0.033	0.597	0.205	0.014	$5x10^{-49}$
rs7241221	Hand OA	G	A	0.775	21,208	285,124	1.002	0.974,1.031	0.910	0.772	0.109	0.017	$4x10^{-11}$
IVW meta-analysis							0.901	0.809,1.003	0.056				
rs215226		A	G	0.585	10,818	255,841	0.970	0.936,1.004	0.086				
rs7241221	Finger OA	G	A	0.768	10,818	255,841	0.997	0.958,1.038	0.902				
IVW meta-analysis							0.880	0.753,1.028	0.108				
rs215226		A	G	0.589	10,559	236,671	0.965	0.933,0.997	0.033				
rs7241221	Thumb OA	G	A	0.771	10,559	236,671	1.004	0.966,1.044	0.832				
IVW meta-analysis							0.870	0.742,1.019	0.084				
rs215226		A	G	0.597	36,523	317,638	0.995	0.977,1.013	0.562				
rs7241221	Hip OA	G	A	0.779	36,523	317,638	0.994	0.974,1.016	0.617				
IVW meta-analysis							0.970	0.896,1.052	0.464				
rs215226		A	G	0.598	63,502	335,819	0.986	0.972,1.000	0.044				
rs7241221	Knee OA	G	A	0.782	63,502	335,819	1.003	0.986,1.019	0.741				
IVW meta-analysis							0.947	0.882,1.016	0.126				

10.4. Discussion

In this chapter, I have estimated the variance explained in OA phenotypes by key pathways in bone regulation and determined that the effect of genetic variation in these pathways on hospital-diagnosed OA risk is unchanged when using summary statistics from GWAS adjusted for eBMD, suggesting that these pathways have a direct effect on OA development. Furthermore, I have identified evidence for a reduced odds of thumb JSN with increasing plasma sclerostin in the HBM population, further suggesting a role of inhibition of the Wnt signalling pathway in OA pathogenesis.

10.4.1. Pathway analyses

The variance explained in eBMD was consistently higher across all pathways compared to each hospital-diagnosed OA phenotype. One potential explanation is that the OA phenotype represents a combination of pain and structural progression. I hypothesize that the pathways analysed contribute to OA pathogenesis via structural progression, overall reducing the magnitude of effect of the pathway-specific SNPs on OA, reducing the r^2 estimate. The difference in r^2 between eBMD and hospital-diagnosed OA was greater when pathway-specific variants were identified by their effect on gene expression (*i.e.* eQTLs), compared to location. This suggests that circulating levels of factors expressed by pathway-specific genes have a stronger role in maintaining eBMD rather than joint homeostasis, particularly for the Wnt signalling pathway. However, it should be noted that the phenotypic variance represents variance in actual measured eBMD but variance in risk for OA, which may limit comparability.

The total proportion of variance explained by all pathways, when SNPs were selected based on location, was slightly higher for hip, compared to knee, OA. This is consistent with the greater heritability estimates for hip, compared to knee, OA discussed in section 1.2.5. Knee OA is thought be more strongly influenced by risk factors with a modifiable component, such as obesity, than hip

OA (10). When SNPs were selected based on location, Wnt signalling made the greatest contribution to variation in OA risk at all three joints. However, when selecting SNPs based on eQTL effects, osteoclast differentiation contributed a similar proportion to Wnt signalling. This suggests that genes contributing to osteoclast differentiation are more highly expressed in the blood than genes contributing to Wnt signalling. This is likely explained by the fact that these cells share a common precursor with macrophages, and these precursors circulate in the blood (493). As discussed in section 2.1.1, M-CSF, a component of the osteoclast differentiation pathway, contributes to the proliferation, differentiation, and survival of several cells from the monocyte lineage (161). This highlights a limitation of selecting SNPs purely based on their regulation of gene expression in one tissue, if comparing cell-specific pathways.

Despite a similar number of annotated SNPs, the variance in eBMD explained by the BMP-specific pathway was greater than the TGFβ-specific pathway, suggesting that the BMP-specific pathway is a greater contributor to variation in BMD. A novel variant in *SMAD9* was identified through whole exome sequencing in the HBM study (205). The *SMAD9* mutation identified in the HBM study was predicted to reduce the inhibitory activity of SMAD9 on BMP signalling, providing evidence for a key role of the BMP signalling pathway in determining bone mass (205). Further evidence for a stronger role of the BMP-specific pathway is that more of the loci identified in the recent eBMD GWAS were annotated to BMP genes, compared to TGFβ genes (386).

The lack of attenuation of proportion of variance explained in hospital-diagnosed OA by the osteoclast-specific pathways when conditioning on eBMD suggests that osteoclasts have a direct role in joint homeostasis, as well as bone remodelling. This is consistent with previous *in vitro* evidence that peripheral blood mononuclear cells (PBMCs) from OA patients showed enhanced differentiation into osteoclasts compared to PBMCs from individuals without OA (494). The relationship between bone turnover and OA is discussed in detail in section 3.2; however, as discussed previously, most studies are based on the

relationship of *systemic* bone turnover, which may not reflect bone remodelling at the local joint level. As discussed in section 1.2.2, subchondral bone remodelling is a key pathogenic feature of OA (18). Consistent with a key role of osteoclasts in subchondral bone remodelling, a cross-sectional analysis found that women with symptoms of knee OA, taking the bisphosphonate alendronate which inhibits osteoclasts, had less subchondral bone attrition, compared to women with symptoms not taking alendronate (495). It is possible that osteoclasts contribute to the early stages of OA pathogenesis, as rats treated with alendronate showed reduced subchondral bone loss and osteophyte formation, but still developed subchondral sclerosis (496). A comparison of r^2 values for osteoclast differentiation between OA incidence and progression would be a method of testing this hypothesis. In addition to a role of osteoclasts in subchondral bone remodelling, *in vitro* evidence suggests that osteoclasts are able to degrade both calcified and non-calcified cartilage, via the action of Cathepsin-K and MMPs (497). As discussed in section 3.3.2, Cathepsin-K, mainly expressed by osteoclasts, is able to cleave type II collagen (301) and *in vitro* studies suggest that Cathepsin-K is able to activate MMP9 secreted by osteoclasts (498).

Due to the large, unfeasible estimates of the r^2 generated for the sub-phenotype analyses (*i.e.* sum of variance explained >40% for all sub-phenotypes), I am unable to draw any conclusions for the proportion of variance in OA sub-phenotypes explained by these pathways. It is possible that the equation for estimating the r^2 from effect estimates and SEs is only suitable when the sample size is large enough that SNPs not associated with the outcome have negligible beta estimates. However, it should be noted that the variance explained would be expected to be larger for a more specific phenotype, such as osteophytes or JSN, compared to a composite phenotype such as hospital-diagnosed OA.

10.4.2. Wnt antagonism and OA

Observational analyses in the HBM population suggest that reduced Wnt antagonism may be a factor in thumb OA pathogenesis. Although the population is enriched by individuals with elevated plasma sclerostin levels and a higher

prevalence of OA, the association between plasma sclerostin and OA in the HBM population is unlikely to be explained by collider bias, as elevated BMD is more likely to be a common cause, rather than a common outcome. It is currently unclear whether circulating sclerostin correlates with joint level expression, or whether circulating sclerostin can have a direct effect on the joint. Circulating sclerostin is thought to be predominantly produced by osteocytes and the elevated circulating sclerostin levels in HBM individuals is evidence supporting this hypothesis (487). It is therefore unlikely that osteocyte-derived sclerostin levels mediate the relationship between high BMD and OA risk, as one would expect to see a positive relationship between circulating sclerostin and OA. As the opposite direction of effect was observed, it is possible that serum sclerostin is a marker of joint level sclerostin expression and pleiotropic effects of the Wnt signalling pathway on BMD and OA. Results of the lookup of the two genome-wide significant loci in the thumb OA GWAS agree with a protective effect of sclerostin, with the allele associated with increased sclerostin at the *B4GALNT3* locus associated with a reduced odds of thumb OA at nominal significance (p<0.05). However, there was no evidence for an association between the *GALNT1* locus and thumb OA. *B4GALNT3* encodes a galatosaminyltransferase, responsible for glycosylation of target molecules; it has been hypothesized that this enzyme may modify sclerostin, protecting it from degradation (488).

Consistent with differential effects of sclerostin on cartilage *vs* bone, Chan *et al* measured reduced SOST expression in the subchondral bone adjacent to the area of meniscectomy in two animal models of OA, but increased expression in cartilage (278). This pattern was confirmed in human cartilage samples from OA patients (278). *In vitro* analyses suggested that SOST downregulated MMP/ADAMTS production and inhibited GAG release from cartilage samples in response to IL-1α stimulation, indicating a mechanism by which sclerostin may reduce cartilage degradation in response to initial joint damage (278). In a *SOST* knockout mouse model, higher expression of catabolic enzymes, as well as markers of chondrocyte hypertrophy, were observed, providing further evidence for a role of sclerostin in protecting against cartilage degeneration (277). Studies

of human OA joints found that sclerostin expression in the subchondral bone was inversely related to severity of cartilage degeneration (281), and in a mouse knockout model, a greater subchondral bone mass, but no cartilage abnormality, was observed (279), suggesting that the protective role of sclerostin against JSN is mediated by reduced subchondral density.

Evidence for an inverse relationship between serum sclerostin and thumb JSN, as well as previous evidence that FRZB may be protective against cartilage loss (499), and the evidence that canonical Wnt signalling can inhibit chondrocyte differentiation and hypertrophy (500), overall suggests that targeting the Wnt signalling pathway may be an effective strategy for OA therapies. However, this would have to be at a joint level, through intra-articular injection, to avoid side effects such as decreased BMD. Any therapeutic targeting this pathway should retain a balance between Wnt signalling and inhibition, as chondrocyte-specific inhibition of β-catenin signalling led to cartilage loss in a mouse model (501) and *SOST* overexpressing mice had enhanced cartilage loss compared to wildtype mice (280). A phase-2a RCT of intra-articular injection of a small-molecule Wnt inhibitor, Lorecivivint, showed promising results, in terms of reducing pain and maintaining mJSW in the knee of individuals with unilateral knee OA (502). *In vivo* and *in vitro* studies suggest that this molecule inhibits two intranuclear kinases, independent of β-catenin, inhibiting expression of Wnt pathway genes, leading to chondrogenesis and inhibition of IL-1β-induced MMP expression and pro-inflammatory cytokine production (503). Further trials are required to determine whether intra-articular injections of Wnt inhibitors are beneficial for other joints.

10.4.3. Strengths

This represents the first analysis aimed at quantifying the variance in BMD and OA explained by key bone pathways, and at determining the relationship between plasma sclerostin and OA sub-phenotypes. I used detailed pathway maps from a publicly available database to extract all genes currently annotated to these pathways and two different methods to identify genetic variants linked

to these genes. LD pruning restricted analyses to the same independent loci across phenotypes for comparability and allowed a pathway-specific r^2 to be simply calculated by summing SNP r^2 estimates.

10.4.4. Limitations

The BOLT-LMM model used for GWAS of binary traits in UK Biobank may overestimate SNP-outcome effects and underestimate *p*-values for rare variants when the outcome is a binary trait with a case proportion <10% (359), which was the case for the GWAS of hospital-diagnosed OA outcomes. Simulations suggest that the knee and hip OA GWAS, with case proportions >3%, may have an inflated type-1 error rate for genome-wide significant loci only (359), but only one SNP, used to calculate the r^2 for knee OA, reached genome-wide significance. For the rarer hand OA phenotype, any SNP with a MAF<0.01 may have an inflated test statistic (359), but as SNPs with a lower MAF contribute less to the total numerator, it is unlikely that these SNPs would have largely overinflated the r^2 estimate.

For some pathways, there were differences in variance explained between the eQTL-based and position-based approaches. This in part can be explained by the fact that there were often fewer eQTLs within 1Mb than SNPs within 20Kb of the gene, particularly in UK Biobank where lower frequency variants were retained. Selecting SNPs purely based on an association with expression of a gene excludes variants that may have other functions in gene regulation, such as missense and alternative splicing variants. Conversely, for eBMD, despite eQTLs only including a third of the number of SNPs compared to selection based on location, the r^2 was larger and similar for the Wnt and osteoclast differentiation pathways, respectively. The range from which *cis*-eQTLs were selected was larger than when I selected based on position, suggesting that limiting to 20Kb upstream or downstream of the gene is too conservative. A 1Mb threshold was used to determine *cis* from *trans* eQTLs (492), but including all SNPs within this threshold may include eQTLs for non-pathway genes. Therefore, time-permitting, these analyses should be repeated using multiple thresholds for the

location-based approach, comparing the r^2 generated to that generated using eQTLs. This pattern was not observed for hospital-diagnosed OA, though, suggesting that the additional *cis*-eQTLs selected are annotated to genes that play a more important role in eBMD variation than OA risk. Alternatively, an eQTL can be associated with expression of multiple genes and it is possible that the higher r^2 reflects the inclusion of an eQTL for a key gene from another pathway. In future, until more data are available for regulatory functions for all SNPs, a combination of SNPs within a certain distance upstream/downstream of a gene plus all eQTLs (*cis* and *trans*) would be the most comprehensive way to select all variants linked to a pathway. It would be useful to exclude eQTLs annotated to multiple genes in sensitivity analyses.

The eQTLGen eQTLs are loci associated with expression of genes in blood, rather than specific tissues. As the pathways analysed have been selected based on their role in bone and joint development, they may not be expressed in blood, meaning that eQTLs were not available for certain genes in the pathway which may have a key role in OA pathogenesis (*e.g. SOST*). This was particularly noticeable for the OPG-RANK-RANKL system. It is unclear if gene expression levels for these pathway genes would correlate with expression levels in the blood and therefore eQTLs representing bone and joint-level expression of genes in the pathway would be desirable for future analyses, to determine how much variation in tissue-specific expression of genes in these pathways contributes to BMD/OA. I was unable to determine the interaction between pathways and whether interactions may increase the variance explained. There is evidence for interactions between these pathways, for example the BMP2 regulation of canonical Wnt signalling discussed in section 3.3.2.

The fact that the beta estimates for hospital-diagnosed OA did not change after adjustment for eBMD could just reflect a lack of association between the SNPs and eBMD, rather than a lack of mediation of effect by eBMD. Alternatively, it could reflect such small effect sizes on the risk difference scale that attenuation was negligible (*e.g.* the maximum unadjusted β for knee OA was 0.0559 and the

maximum adjusted β was 0.0565). The lack of attenuation could be explained by the fact that I was only able to adjust for eBMD, rather than FN-BMD, which, as discussed in Chapter 9, has a stronger effect on OA risk. DXA assessment is currently underway in a subset of UK Biobank, which will allow these analyses to be repeated adjusting for FN-BMD.

A lack of CIs around the r^2 estimate means that it is unclear how precise the r^2 estimates are. This makes it difficult to draw any conclusions about differences between phenotypes when estimates are very close. To determine precision of these estimates, one would have to perform data simulations and generate CIs by bootstrapping, which was beyond the scope of this PhD.

Finally, the sclerostin analyses were cross-sectional and, as there are currently only two SNPs to instrument plasma sclerostin, MR analyses were underpowered to determine if this represents a causal protective effect, or whether this relationship could be explained by unmeasured confounding. The HBM study represents the only population (that I am aware of) to have data for OA sub-phenotypes and plasma sclerostin measurements, limiting generalizability.

10.4.5. Future directions

Although these results suggest that the effect of variation in these pathways on OA risk is not mediated by BMD, there is still a possibility that the effect could be mediated by other bone parameters, such as bone shape. As described in section 1.2.5, alterations in the shape of the hip, such as cam-type deformities, are a key risk factor for hip OA. However, phenotypes such as hip shape have not yet been derived in the UK Biobank population and I was therefore unable to determine the contribution of hip shape to the variation in hip OA explained by these pathways, but this analysis could be performed in the future.

The advantage of the individual SNP r^2 analysis was not having to pick a reference allele or allele weighting which I would have had to with PRS. However, new methods are being developed through the software '*PRSice*'

(https://www.prsice.info/quick_start_prset/), which generate a pathway-specific PRS based on GWAS summary statistics for the trait of interest. It will therefore be interesting to generate pathway specific PRS, using summary statistics for both BMD and OA from a separate population to determine the reference allele. I could then determine the variance explained in eBMD and OA sub-phenotypes in UK Biobank by these PRS and whether these estimates are comparable to the estimates from the individual SNPs.

Measurement of plasma sclerostin is currently underway in all OAI individuals who provided blood samples at baseline. This will allow replication of the observational analyses for the relationship between circulating sclerostin and each OA sub-phenotype. As longitudinal data are available for the OAI cohort, I will be able to determine if circulating sclerostin is associated with incidence and/or progression of OA sub-phenotypes. OAI sclerostin measurements will contribute to an updated GWAS meta-analysis of plasma sclerostin, which should have more power to detect additional loci for plasma sclerostin, increasing the strength of the instrument for MR studies.

Finally, when the relevant data is available to perform GWAS of OA progression, I could repeat the r^2 analyses. This will allow the determination of whether the contribution of variation in the bone pathways differs between prevalent and progressive disease, potentially providing further information on the role of these pathways in OA pathogenesis.

10.4.6. Conclusions

In this chapter, I have determined the contribution of key bone pathways to OA at the hip, knee, and hand, and that the variance explained in OA by each pathway is not explained by eBMD, suggesting that these pathways contribute to OA pathogenesis directly, rather than via BMD. I have determined a potential role of Wnt inhibition in protecting against hand OA, although further analyses are required to replicate the association and to determine if this represents a true causal effect.

CHAPTER 11. THE ROLE OF IGF-1 IN OSTEOARTHRITIS PATHOGENESIS

11.1. Background and aims

Insulin-like growth factor-1 (IGF-1) is a hormone involved in skeletal growth and development (504). Most circulating IGF-1 is produced by the liver in response to growth hormone stimulation (504). IGF-1 can also be produced by specific tissues, including chondrocytes (504,505). *In vitro* studies of animal cartilage have suggested that IGF-1 is able to stimulate proteoglycan synthesis (506), upregulate type II collagen expression and downregulate MMP13 expression (507), all of which suggests that IGF-1 may be *protective* against cartilage degeneration. However, the observation that *IGF1* is expressed by osteoblasts and osteoclasts, but not osteocytes, in human osteophyte tissue, suggests a role of IGF-1 in osteophyte formation (508).

Epidemiological evidence of an association between circulating IGF-1 and OA is currently inconclusive (509), with the largest population-based study so far identifying a *positive* association between IGF-1 concentration and bilateral knee OA (510). Consistent with a positive association between circulating IGF-1 and OA risk, individuals with acromegaly (a disorder of excess growth hormone production) are at an increased risk of developing secondary OA (509). In contrast, polymorphisms in the *IGF1* gene, associated with lower IGF-1 levels, have been linked to a higher prevalence of OA (366,367).

In this chapter, I will utilise the large-scale availability of data for serum IGF-1 in the UK Biobank population, to determine the association between IGF-1 and hospital-diagnosed OA at the hand, hip, and knee. I aim to determine if adjustment for eBMD attenuates any relationship, as BMD may be a mediator of the effect of IGF-1 on OA, due to its role in regulating osteoblastogenesis (511). A lack of attenuation by adjustment for eBMD suggests a direct influence of IGF-1 on the joint, highlighting another pathway contributing to the shared aetiology of BMD and OA. I will also determine if adjustment for BMI alters the relationship between IGF-1 and OA, as an inverse relationship between IGF-1 and BMI has been observed (512), which could reflect the key role of the IGF-1 axis in growth (504) or regulating adiposity (513).

Secondly, I aim to use MR to determine the causal effect of circulating IGF-1 on OA at each joint. The MR analyses will use IGF-1-associated SNPs identified in the Cohorts for Heart and Aging Research in Genetic Epidemiology (CHARGE) meta-analysis, which also performed a GWAS of IGF binding protein-3 (IGF-BP3) (514). IGF-BP3 binds to circulating IGF-1, regulating the bioavailability of IGF-1 (504). Out of eight IGF-1-associated SNPs, three were also associated with IGF-BP3 levels. Finally, I will use MVMR to determine if any observed causal effects occur independently of BMI.

11.2. Methods

11.2.1. Study population

UK Biobank

The UK Biobank population is described in section 5.2.1. 421,527 individuals had complete data for the observational analyses. Observational analyses were not restricted on ethnicity. After exclusion of related individuals, individuals of non-white European ancestry, and sex-mismatches, 332,059 (79%) had genetic data and were included in MR analyses. Figure 113 details the derivation of these sample sizes.

Figure 113: Flowchart detailing sample size derivation for the observational and MR UK Biobank populations.

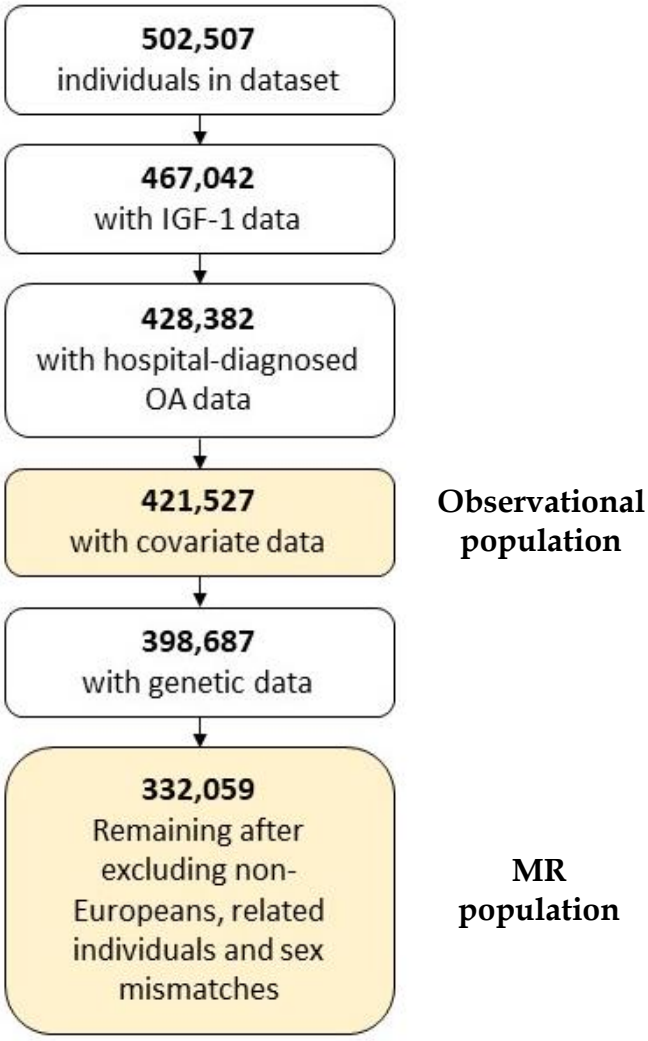

11.2.2. IGF-1 assessment

Serum IGF-1 was assessed in UK Biobank at baseline using the Liaison XL chemiluminescent immunoassay (Diasorin Ltd). Biomarker data were downloaded in April 2019. Average within-laboratory coefficients of variation were 6.0% for low, 5.3% for medium and 6.2% for high concentrations (515). QC procedures have been published previously (516).

11.2.3. Outcomes

Hospital-diagnosed hip, knee and hand OA were determined from HES data using ICD codes previously reported for hip and knee (141) and hand (261) OA, as described in sections 9.2 and 10.2.1.

11.2.4. Covariates

Age, sex, BMI, ethnicity, HRT use and PA were hypothesized confounders of the association between IGF-1 and OA. Ethnic background was ascertained by touchscreen questionnaire at the initial assessment centre and was categorised as White, Mixed (White and Black Caribbean, White and Black African, White, and Asian or any other Mixed background), Asian or Asian British, Black or Black British, Chinese or other ethnic group. HRT use (ever used) was ascertained by touchscreen questionnaire.

11.2.5. Statistical analysis

Observational

Serum IGF-1 concentration was positively skewed by a few outliers (Figure 114) and therefore I log-transformed IGF-1 for observational analyses, as this appeared to improve the distribution (Figure 115). Associations between log-transformed IGF-1 concentration and binary OA outcomes were determined using multivariable logistic regression. Analyses were performed using four models: [1] unadjusted; [2] adjusting for age and sex, [3] additionally adjusting for ethnicity and HRT and [4] additional adjustment for BMI. Coefficients were

transformed by the natural logarithm of two to generate an OR per doubling in IGF-1 concentration. Additional analyses were performed stratified by sex to determine sex-specific effects. I performed sensitivity analyses excluding individuals with hospital-diagnosed acromegaly (ICD10 code E220, ICD9 code 2530) or with an arthropathy related to an endocrine disorder (ICD10 code M145, ICD9 code 7130) (N=94). Individuals for whom serum IGF-1 was measured from an aliquot other than the first aliquot (N=43,728) were also removed as a sensitivity analysis, as sample dilution issues have been reported by UK Biobank and the dilution increases with increasing aliquot (516).

Figure 114: Histogram of IGF-1 concentration in UK Biobank.

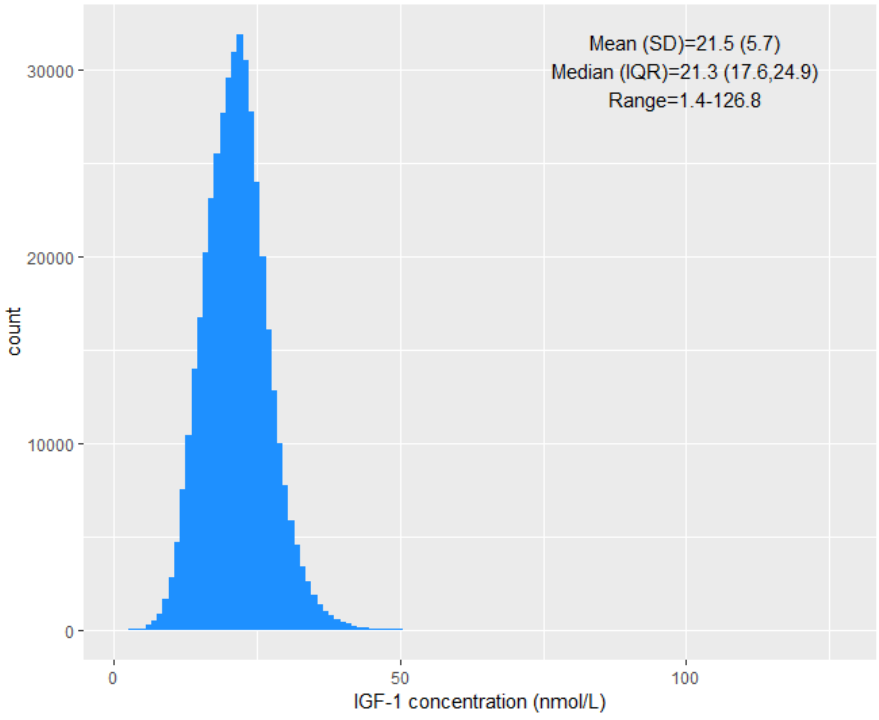

Figure 115: Histogram of log-transformed IGF-1 concentration in UK Biobank.

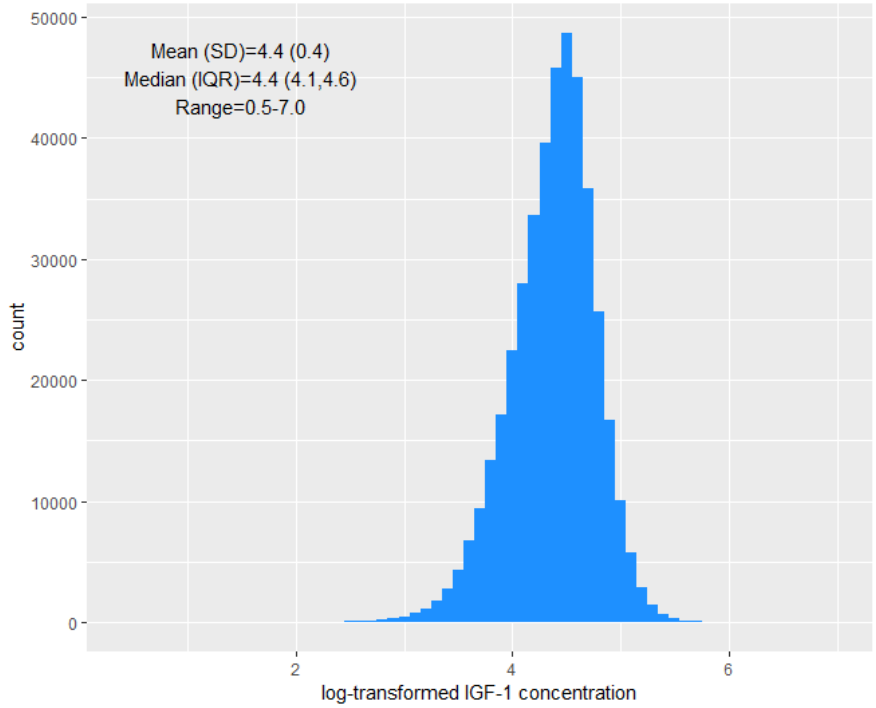

Causal inference

Genotyping and imputation

Genotyping and imputation in UK Biobank are described in section 5.3.1.

IGF-1 instrument selection

The eight SNPs, associated with IGF-1 at genome-wide significance from the CHARGE meta-analysis, were used to instrument IGF-1 (514). These SNPs, and their associations with IGF-1 and hand, hip and knee OA in UK Biobank are presented in Table 49. SNP-exposure summary data for 2SMR were extracted from the Teumer *et al* meta-analysis (514). Two of these SNPs were also associated with IGF-BP3 levels and another one was identified from a bivariate analysis of IGF-1 and IGF-BP3. The CHARGE study employed a sample-size weighted Z-score based meta-analysis to manage assay heterogeneity across cohorts, which does not generate a beta or SE (514). Hence betas and SEs, provided by the CHARGE consortium, were estimated from *p*-values using the measure of Visscher *et al* (517).

Table 49: IGF-1 instruments and their associations with IGF-1 and hip and knee OA in UK Biobank.

SNP	EA	IGF-1			Hip OA			Knee OA			Hand OA		
		Beta	**SE**	***P***	**OR**	**SE**	***p***	**OR**	**SE**	***p***	**OR**	**SE**	***P***
rs1065656*	G	0.050	0.003	$4x10^{-84}$	0.987	0.015	0.392	1.019	0.012	0.116	1.000	0.033	0.996
rs2153960	A	0.048	0.003	$6x10^{-76}$	1.025	0.016	0.125	1.023	0.013	0.061	1.010	0.034	0.774
rs509035	A	0.054	0.003	$5x10^{-102}$	0.998	0.015	0.897	1.011	0.012	0.342	0.999	0.033	0.981
rs646776*	T	-0.029	0.003	$3x10^{-25}$	0.939	0.016	$2x10^{-4}$	0.992	0.013	0.543	1.051	0.039	0.181
rs700753*	G	0.113	0.002	$<1x10^{-300}$	0.982	0.015	0.234	0.984	0.011	0.155	0.987	0.032	0.687
rs780093	C	0.060	0.002	$1x10^{-135}$	1.041	0.016	0.007	1.021	0.012	0.066	0.967	0.030	0.280
rs934073	G	0.035	0.003	$4x10^{-43}$	1.011	0.016	0.471	1.000	0.012	0.988	1.017	0.034	0.608
rs978458	C	-0.074	0.003	$6x10^{-172}$	0.953	0.015	0.003	0.983	0.012	0.180	0.991	0.034	0.794
IGF-1 PRS[a]		0.058	0.001	$<1x10^{-300}$	1.018	0.006	0.001	1.010	0.004	0.019	0.993	0.012	0.539

Associations adjusted for sex, genotyping chip and 10 PCs. Betas represent the per-effect allele increase in standardized IGF-1.

**SNPs also associated with IGF-BP3 in the CHARGE meta-analysis (514). [a]Sum of IGF-1-increasing alleles for the eight SNPs.*

Statistical analysis

1SMR

1SMR was performed as described in section 5.3.3. Analyses were performed using the individual SNPs as instruments and then using an unweighted PRS to instrument IGF-1. Analyses were adjusted for sex, genotyping chip and 10 PCs. IGF-1, not log-transformed to aid interpretation, was standardized prior to analysis. The assumptions of MR are outlined in section 5.3.3 and Figure 116 summarizes how these assumptions were tested. To limit potential horizontal pleiotropy, I repeated analyses, firstly excluding the SNPs also associated with IGF-BP3 at genome-wide significance (rs700753, rs646776, rs1065656) and secondly using just the intronic *IGF1* SNP (rs978458) as the instrument. Power calculations for 1SMR were performed using mRnd (http://cnsgenomics.com/shiny/mRnd/) (518). Power estimates are presented in Table 50.

Table 50: Power estimates for 1SMR analyses in the UK Biobank MR population.

	Power		
	Total population (N=332,092)	**Female population (N=178,719)**	**Male population (N=153,373)**
Hand OA (K=0.007)[a]			
OR=0.95	0.06	0.06	0.05
OR=0.90	0.08	0.07	0.06
OR=0.80	0.16	0.13	0.08
OR=0.70	0.30	0.24	0.12
OR=0.60	0.48	0.39	0.17
Hip OA (K=0.03)			
OR=1.05	0.08	0.06	0.06
OR=1.10	0.17	0.11	0.10
OR=1.20	0.50	0.30	0.26
OR=1.30	0.83	0.57	0.51
OR=1.40	0.97	0.82	0.75
Knee OA (K=0.05)			
OR=1.05	0.10	0.07	0.05
OR=1.10	0.24	0.15	0.14
OR=1.20	0.70	0.45	0.39
OR=1.30	0.96	0.78	0.72
OR=1.40	1.00	0.95	0.92

All power calculations estimated based on an R^2_{xz} (i.e. the proportion of variance in the exposure explained by the instrument) of 0.01 and a type-1 error rate of 0.05.

K=proportion of cases within the MR population. [a]K=0.010 for females and 0.004 for males.

Figure 116: Assumptions of MR and how they were tested in both one-sample and two-sample MR analyses of the causal effect of IGF-1 on OA.

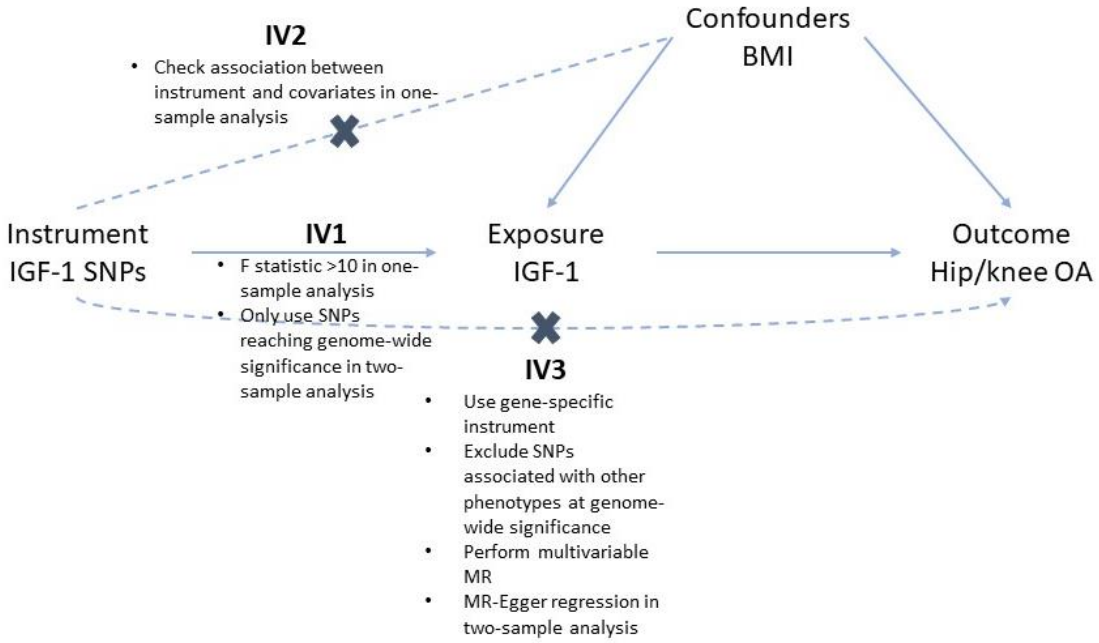

2SMR

Methodology for 2SMR is described in section 5.3.3. SNP-exposure summary statistics were extracted from the CHARGE meta-analysis (Appendix 46) (514). To provide estimates of the SNP-outcome association, hip and knee OA summary statistics for the IGF-1 SNPs were extracted from the GWAS meta-analysis of UK Biobank and arcOGEN (Appendix 46) (141). For hand OA, I performed a GWAS of hospital-diagnosed hand OA in UK Biobank, using methods described in sections 5.3.2 and 10.2.1, and extracted the IGF-1 SNPs from the summary statistics (Appendix 46). Steiger filtering did not identify any SNPs explaining a greater proportion of variation in OA compared to IGF-1. Cochran's Q statistic was calculated as a measure of potential pleiotropy.

Multivariable MR

To determine the BMI-independent causal effect of IGF-1 on OA, I performed 1SMVMR. Methodology for MVMR is described in section 5.3.3. An unweighted BMI PRS was generated as described in section 9.2.1 (475). Associations of the BMI SNPs with BMI in UK Biobank are presented in Appendix 47. MVMR was also performed with height (instead of BMI) as a covariate, instrumented by height SNPs (Appendix 48) from the GIANT meta-analysis of 253,288 individuals (484). In MVMR, SW conditional F-statistics were calculated for IGF-1 and BMI to determine conditional instrument strength (377).

Factorial MR

To determine the additive effects of BMI and IGF-1 on OA risk, the MR population was stratified based on whether the PRS for IGF-1 was above/equal to or below the median. The same was performed for BMI PRS. The population was then categorised into four groups: 1) those below the median for IGF-1 PRS and below the median for BMI PRS; 2) those above/equal to the median for IGF-1 PRS and those below the median for BMI PRS; 3) those below the median for IGF-1 PRS and those above the median for BMI and 4) those above the median for both IGF-1 and BMI PRS. Logistic regression analyses were then performed with PRS category as the exposure and OA variables as the outcome, adjusting for sex, genotyping chip and 10 PCs.

11.3. Results

11.3.1. Descriptives of the study population

The mean age of the observational and MR populations was 56.4 (SD 8.1) and 56.5 (8.0) years, respectively, and 54% were female (Table 51). The mean IGF-1 concentration was 21.5 (6) nmol/L for both populations. Of the observational population, 3.1% had hospital-diagnosed hip, 5.4% had hospital-diagnosed knee, and 0.7% had hospital-diagnosed hand, OA. Proportions for the MR population were 3.2%, 5.4%, and 0.7%, respectively.

Table 51: Descriptive characteristics of the UK Biobank population included in the observational and MR analyses.

	Observational population (N=421,527)		**MR population (N=332,059)**	
	Mean	**SD**	**Mean**	**SD**
Age (years)	56.4	8.1	56.5	8.0
Height (cm)	168.6	9.2	168.9	9.2
Weight (kg)	77.9	15.8	78.0	15.8
BMI (kg/m^2)	27.3	4.7	27.3	4.7
IGF-1 (nmol/L)[a]	21.3	17.6, 24.9	21.3	17.6, 24.9
	N	**%**	**N**	**%**
Female	227,738	54.0	178,699	53.8
HRT use	84,341	37.0	67,181	37.6
Ethnicity				
White	401,844	95.3	332,059	100
Black/ Black British	6,500	1.5		
Asian/ Asian British	6,489	1.5		
Chinese	1,335	0.3		
Mixed	1,619	0.4		
Other	3,740	0.9		
Hospital-diagnosed OA				
Hip	12,425	3.1	9,951	3.2
Knee	22,278	5.4	17,338	5.4
Hand	2,727	0.7	2,165	0.7

[a]*Values represent the median and IQR.*

11.3.2. Observational results

In unadjusted analyses, increasing IGF-1 concentration was associated with lower odds of hip, knee, and hand OA (Table 52), with the largest effect seen for

hand OA (OR per doubling in IGF-1=0.61 [0.57,0.65], p=2x10^{-58}). Adjustment for age and sex reduced the strength of all associations, but there was still evidence for a protective effect of IGF-1 on all outcomes. However, IGF-1 was strongly inversely associated with BMI in the UK Biobank population, with an SD higher IGF-1 concentration associated with a 0.13SD lower BMI. Further adjustment for ethnicity and HRT use did not alter observed associations. When I added BMI to the model, there was still evidence of a protective effect of IGF-1 on hand OA, albeit of weaker magnitude (OR=0.87 [0.82,0.93], p=4x10^{-5}). The association with knee OA was fully attenuated by adjustment for BMI. I observed some evidence for an increased odds of hospital-diagnosed hip OA, based on results from model 4 (OR=1.04 [1.01,1.07], p=0.014), and evidence of an interaction between log-transformed IGF-1 and BMI on odds of hip OA, with a stronger magnitude of effect of IGF-1 on hip OA with increasing BMI (OR for interaction term=1.02 [1.01,1.03], p=2x10^{-6}, representing the increase in effect of IGF-1 on hip OA per 1kg/m^2 increase in BMI). The addition of eBMD to model 4, in a subset of 222,386 individuals with eBMD data, did not attenuate the relationship with hip OA (OR=1.06 [1.02,1.11], p=0.008).

Table 52: Results from observational analyses of associations between IGF-1 and hospital-diagnosed OA in UK Biobank.

	Hip OA (N=398,965)			**Knee OA (N=408,872)**			**Hand OA (N=389,308)**		
Model	**OR**	**95% CI**	***P***	**OR**	**95% CI**	***P***	**OR**	**95% CI**	***p***
1	0.71	0.69, 0.74	6x10^{-108}	0.68	0.66, 0.69	2x10^{-250}	0.61	0.57, 0.65	1x10^{-58}
2	0.94	0.91, 0.97	3x10^{-4}	0.80	0.78, 0.82	7x10^{-74}	0.80	0.75, 0.86	6x10^{-11}
3	0.94	0.91, 0.97	4x10^{-4}	0.81	0.80, 0.83	2x10^{-64}	0.82	0.77, 0.88	3x10^{-9}
4	1.04	1.01, 1.07	0.014	0.99	0.96, 1.01	0.223	0.87	0.82, 0.93	4x10^{-5}

When I stratified BMI-adjusted analyses by sex, the association between IGF-1 and hip OA was only present in the female population (OR$_F$=1.07 [1.03,1.12] *vs* OR$_M$=1.00 [0.95,1.05]). The inverse association between IGF-1 and hand OA was present, with a similar magnitude, in both sexes. Restricting analyses to 377,602 individuals whose IGF-1 was measured from the first aliquot did not alter conclusions drawn. Observational results were the same when individuals with

hospital-diagnosed acromegaly or endocrine-related arthropathies were removed (Table 53).

Table 53: Observational associations between IGF-1 and hospital-diagnosed OA in UK Biobank, after removing individuals with acromegaly or endocrine-related arthropathies.

	Hip OA (N=398,928)			Knee OA (N=408,832)			Hand OA (N=389,282)		
Model	**OR**	**95% CI**	***P***	**OR**	**95% CI**	***P***	**OR**	**95% CI**	***p***
1	0.71	0.69, 0.73	$5x10^{-110}$	0.68	0.66, 0.69	$4x10^{-252}$	0.61	0.57, 0.65	$2x10^{-58}$
2	0.94	0.91, 0.97	$1x10^{-4}$	0.80	0.78, 0.82	$8x10^{-75}$	0.80	0.75, 0.86	$6x10^{-11}$
3	0.94	0.91, 0.97	$1x10^{-4}$	0.81	0.79, 0.83	$2x10^{-65}$	0.82	0.77, 0.88	$3x10^{-9}$
4	1.04	1.00, 1.07	0.025	0.98	0.96, 1.01	0.185	0.87	0.82, 0.93	$4x10^{-5}$

11.3.3. MR results

In 1SMR, using individual IGF-1-associated SNPs as instruments, I found evidence for an increased odds of hip OA with increasing IGF-1 concentration (OR per SD increase in IGF-1=1.20 [1.01,1.43], p=0.033, Table 54). Combining genotypes for the eight SNPs in a PRS strengthened the instrument (F-statistic: 3774 *vs* 563) and the evidence for a causal effect of IGF-1 on hip OA (OR=1.35 [1.13,1.63], p=0.001, Table 54, Figure 117). An effect of IGF-1 on knee OA was also observed when using the IGF-1 PRS instrument (OR=1.19 [1.03,1.37], p=0.019, Figure 117). Although I found no evidence of a causal effect of IGF-1 on hand OA, these analyses were likely underpowered due to the rarity of hospital-diagnosed hand OA (Table 50). Evidence for a causal effect of IGF-1 on hip and knee OA was stronger when excluding the three SNPs also associated with IGF-BP3 at genome-wide significance (OR_{hip}=1.57 [1.21,2.02], p=0.001 and OR_{knee}=1.30 [1.07,1.58], p=0.008, Table 54). The Sargan statistic was reduced from 30.5 (p<0.001) to 4.4 (p=0.35), suggesting that results were less biased by pleiotropy when excluding IGF-BP3 SNPs. The causal effect of IGF-1 also persisted when I restricted the instrument to the single intronic *IGF1* SNP, although CIs were wider (OR_{hip}=1.93 [1.25,2.97], p=0.003 and OR_{knee}=1.26 [0.90,1.76], p=0.179). When stratifying by sex, there was stronger evidence for an effect of IGF-1 on hip OA in females than males (OR_F=1.42 [1.12,1.80] *vs* OR_M=1.27 [0.94,1.71], Figure 118),

although analysis in males had lower power (Table 50).

Table 54: Results of 1SMR of the causal role of circulating IGF-1 on hospital-diagnosed OA in UK Biobank.

	Individual SNPs (all 8 SNPs)		**Allele score**		**Allele score (excluding IGF-BP3 SNPs)**		***IGF1* SNP only**	
	OR (CI)	***p***	**OR (CI)**	***p***	**OR (CI)**	***p***	**OR (CI)**	***p***
Hand (N=306, 748)	0.90 (0.63, 1.29)	0.564	0.88 (0.60, 1.31)	0.539	0.99 (0.57, 1.70)	0.958	1.13 (0.45, 2.87)	0.795
Hip (N=314, 499)	1.20 (1.01, 1.43)	0.033	1.35 (1.13, 1.63)	0.001	1.57 (1.21, 2.02)	0.001	1.93 (1.25, 2.97)	0.003
Knee (N=321, 930)	1.11 (0.97, 1.26)	0.129	1.19 (1.03, 1.37)	0.019	1.30 (1.07, 1.58)	0.008	1.26 (0.90, 1.76)	0.179

When determining the causal relationship using 2SMR, although CIs widened, effect sizes were similar (Figure 117), with findings consistent with a positive effect of IGF-1 on hip OA (OR=1.26 [0.99,1.61], p=0.065). Weighted median analyses further suggested a positive effect of IGF-1 on OA risk, but estimates were much weaker, with CIs overlapping the null (Figure 119). The MR-Egger estimate differed in direction of effect (Figure 119), suggesting horizontal pleiotropy (OR=0.61 [0.29,1.30], p=0.25, intercept p-value=0.1). Cochran's Q value also suggested pleiotropy (Q=19.6, p=0.007). Further evidence for pleiotropy was supported by the stronger evidence for a causal effect when rs700753 and rs10655656 were removed in leave-one-out analysis (Figure 120); these two SNPs were also associated with IGF-BP3. When removing these SNPs, the causal effect estimate for IGF-1 became stronger (OR=1.49 [1.21,1.83], p=1x10^{-4}) and consistent in direction with the MR-Egger estimate (OR=5.88 [0.70,49], p=0.2, p for intercept=0.3, Figure 121). Cochran's Q was also reduced when these three SNPs were removed (Q_{hip}=4.4, p=0.35). The effect of IGF-1 on hip OA was even stronger when restricting to the single intronic *IGF1* SNP (OR=1.92 [1.22,3.03], p=0.005).

Figure 117: Comparison of observational and MR results for the association between IGF-1 and hospital-diagnosed OA.

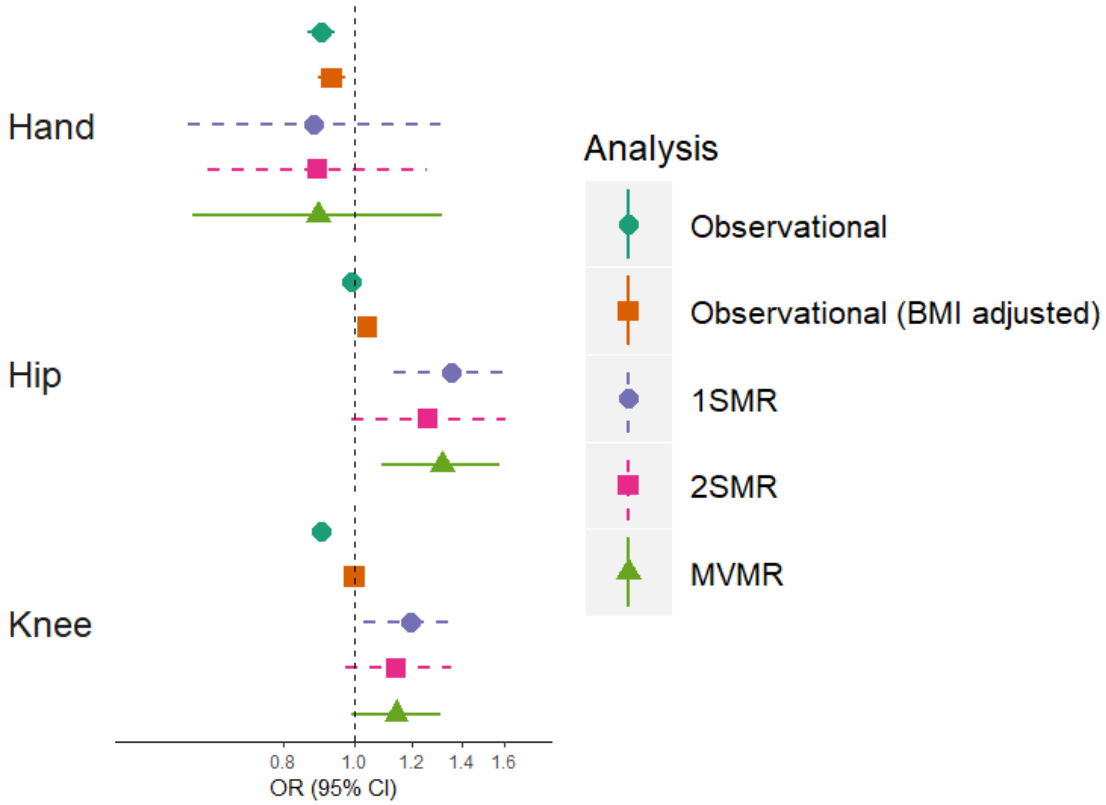

The observational results without adjustment for BMI represent the results for model 3.

Figure 118: Observational and one-sample MR results for hip OA in UK Biobank, stratified by sex.

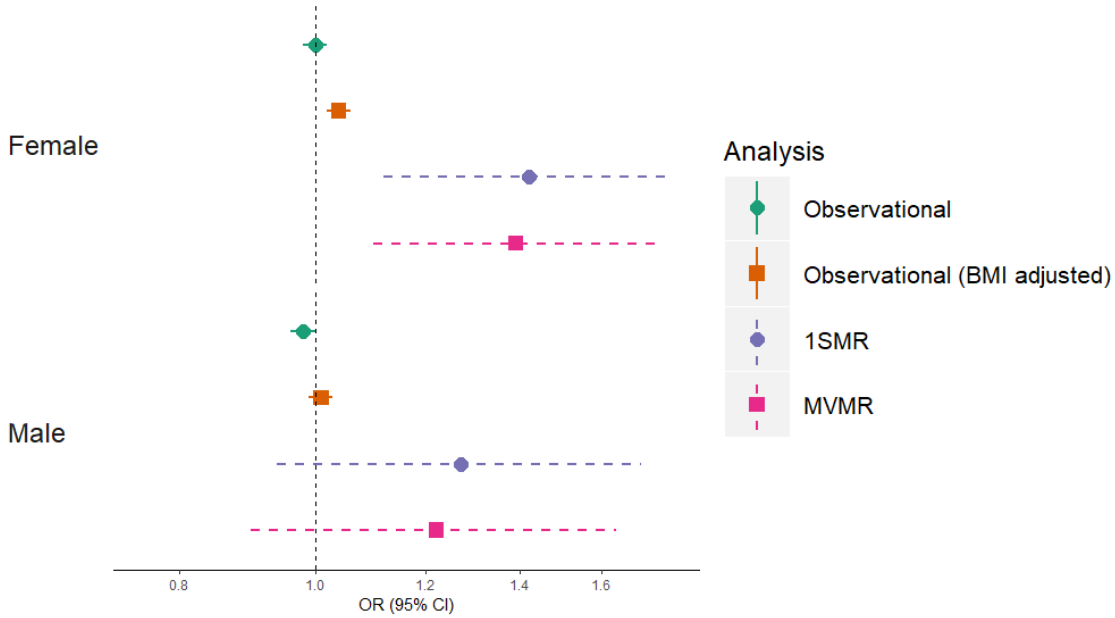

Points represent the OR per SD increase in IGF-1 concentration. Horizontal bars represent 95% CIs. Observational results=model 3.

Figure 119: Comparison of IVW, weighted median and MR-Egger estimates for the causal effect of IGF-1 on hospital-diagnosed OA, using all eight IGF-1-associated SNPs.

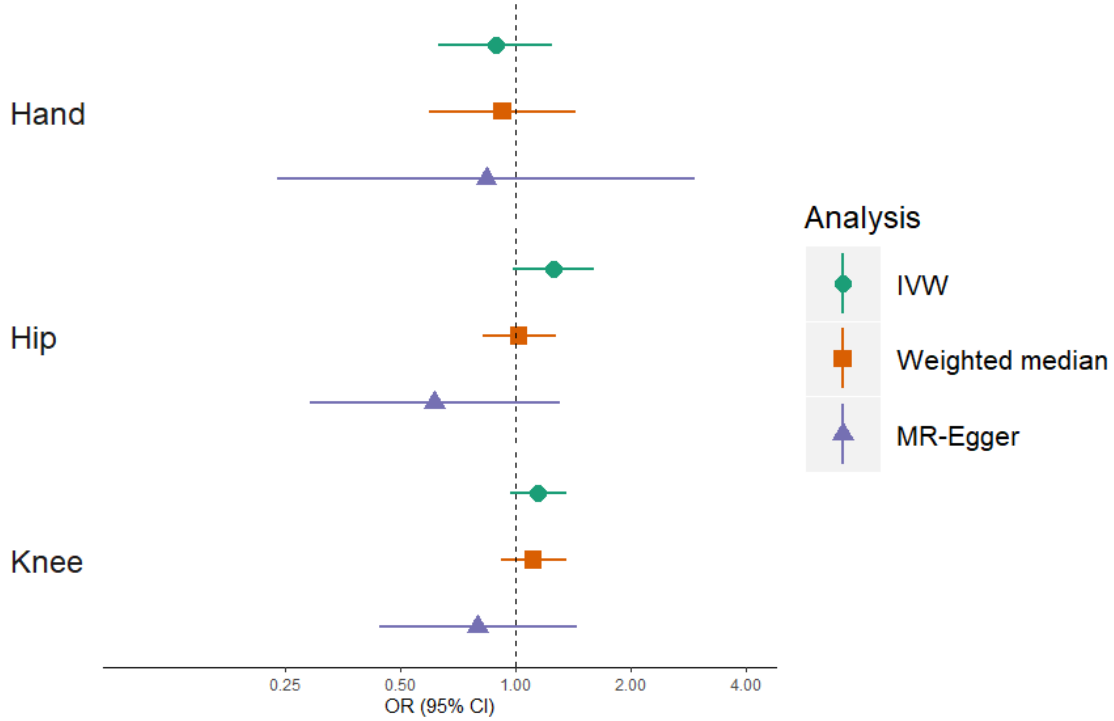

Points represent the OR per SD increase in IGF-1 concentration. Horizontal bars represent 95% CIs.

Figure 120: Results of leave-one-out analysis for the causal effect of IGF-1 on hip OA.

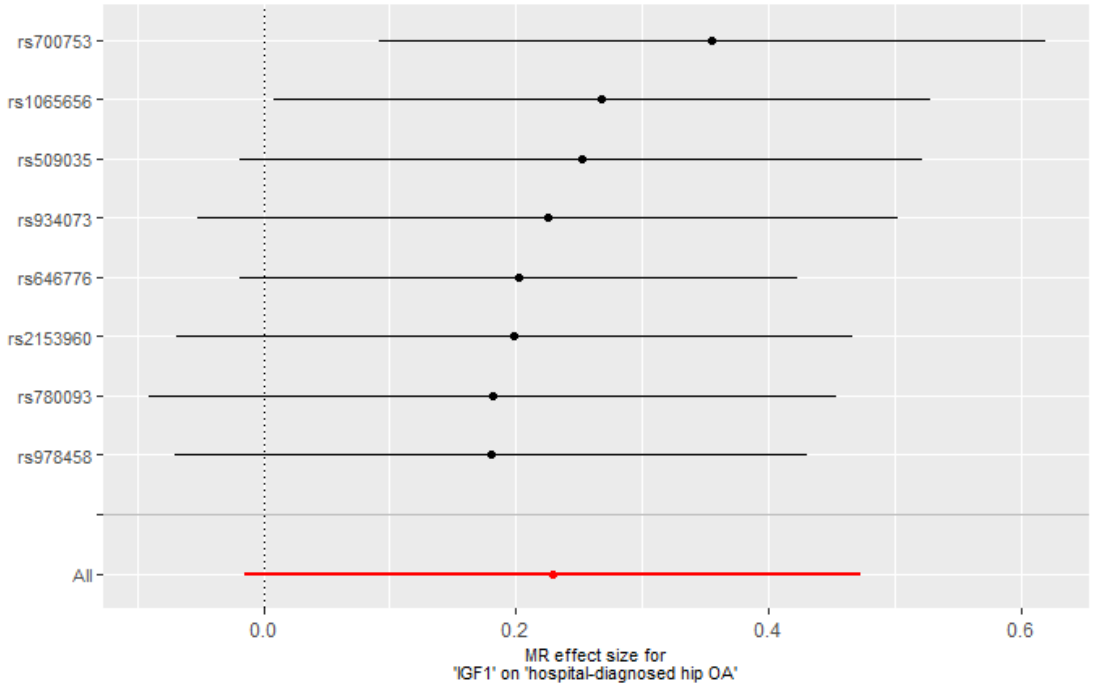

Figure 121: Results from two-sample MR analysis of IGF-1 on hospital-diagnosed hip OA, restricted to the five SNPs not associated with IGF-BP3 at genome-wide significance.

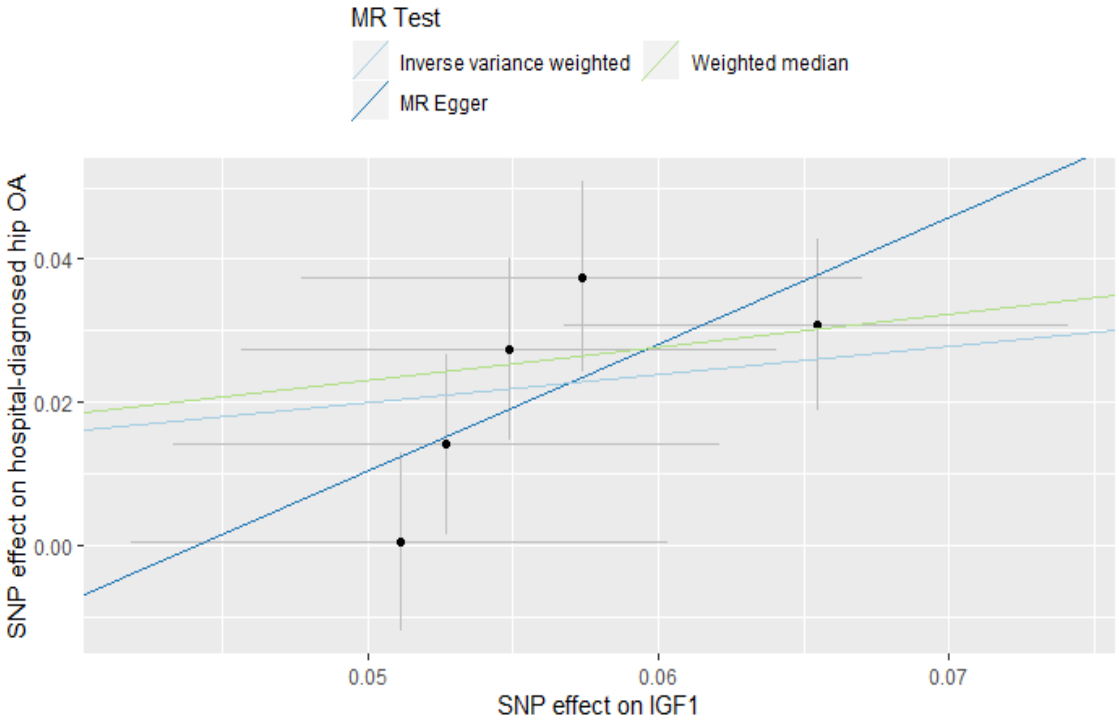

Evidence for a causal effect of IGF-1 on knee OA was weak in 2SMR using all eight SNPs, and inconsistent in direction between the IVW and MR-Egger estimates (Figure 119). The rs700753 SNP appeared to have a large effect on the estimates (Figure 122), and after excluding this SNP and the other two SNPs associated with IGF-BP3 at genome-wide significance, there was stronger evidence for a causal effect from IVW analysis (OR=1.33 [1.10,1.60], p=0.003) which was consistent in direction with the MR-Egger estimate (OR=2.09 [0.21,21], p=0.6, Figure 123). Evidence for heterogeneity was also weaker (Q reduced from 14.9, p=0.038 to 5.9, p=0.206, MR-Egger intercept p-value=0.7). There was no evidence for a causal effect of IGF-1 on hospital-diagnosed hand OA in 2SMR (Figure 119). There was equally no evidence for a causal effect of IGF-BP3 on hip or knee OA using 2SMR, but some evidence for a protective effect of IGF-BP3 on hand OA (Table 55). 1SMR was not possible as IGF-BP3 has not been measured in UK Biobank.

Figure 122: Results of leave-one-out analysis for the causal effect of IGF-1 on knee OA.

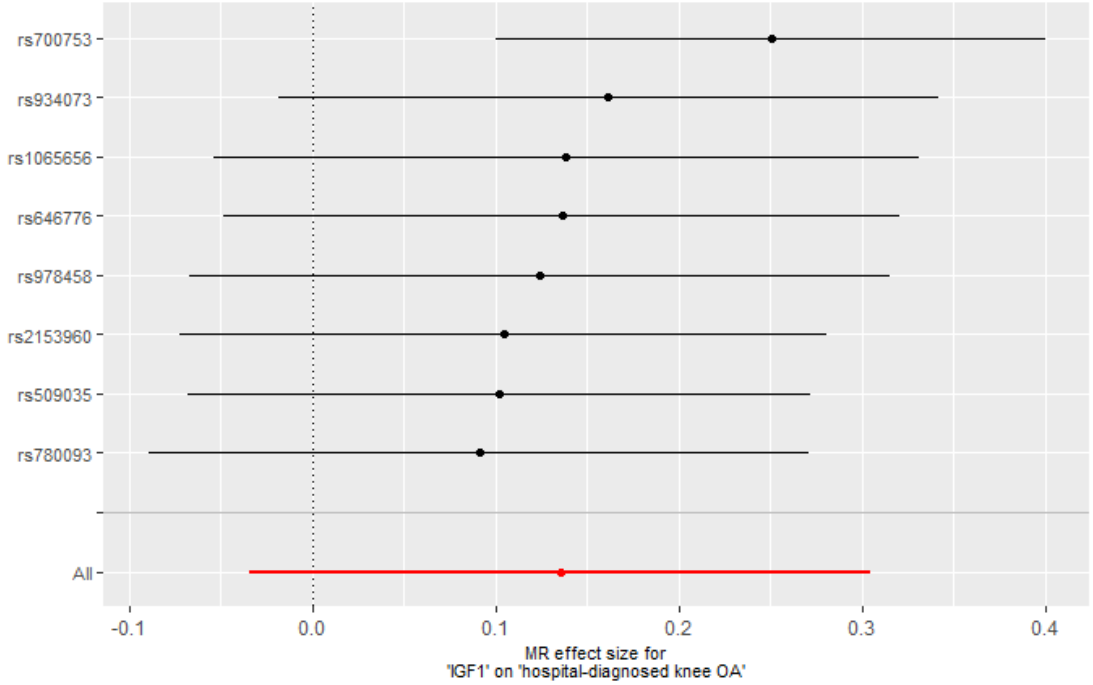

Figure 123: Results from two-sample MR analysis of IGF-1 on hospital-diagnosed knee OA, restricted to the five SNPs not associated with IGF-BP3 at genome-wide significance.

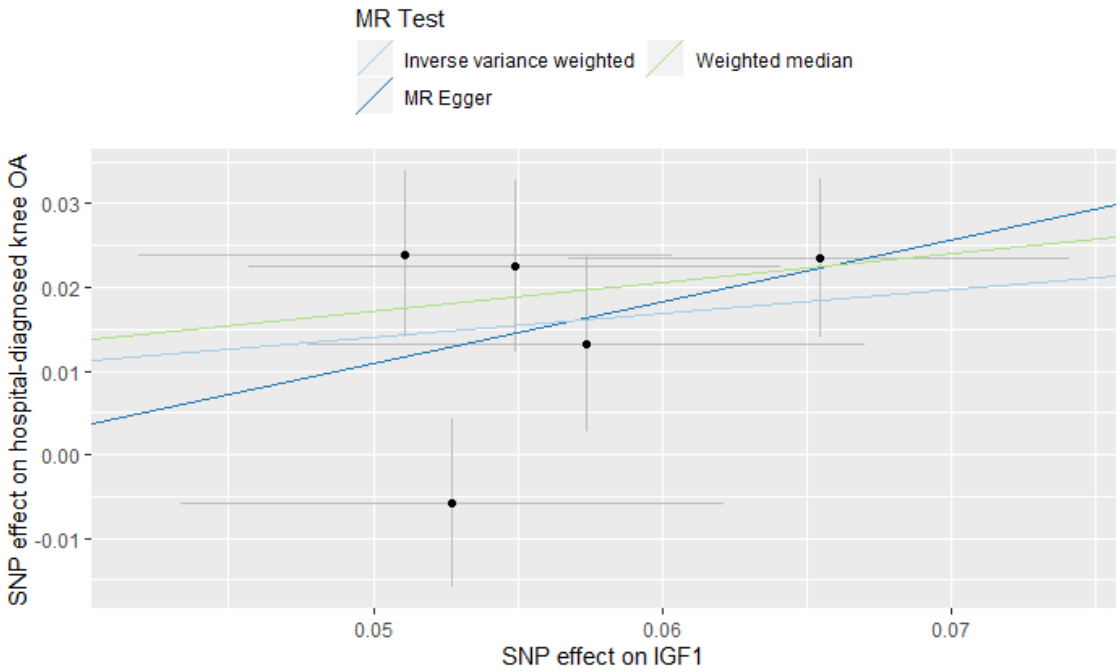

Table 55: Two-sample MR results for the causal effect of IGF-BP3 on hospital-diagnosed OA outcomes.

		IVW			Weighted median			MR-Egger		
		OR	**95% CI**	***p***	**OR**	**95% CI**	***p***	**OR**	**95% CI**	***P***
All SNPs (N_{SNPs}=5)	Hand	0.88	0.75, 1.02	0.090	0.82	0.69, 0.97	0.021	0.72	0.52, 0.99	0.136
	Hip	1.00	0.90, 1.10	0.965	1.01	0.94, 1.08	0.808	1.15	0.99, 1.33	0.156
	Knee	0.97	0.92, 1.02	0.284	0.97	0.92, 1.03	0.297	0.98	0.88, 1.10	0.799
Excluding IGF-1 SNPs (N_{SNPs}=2)	Hand	0.85	0.64, 1.13	0.272						
	Hip	1.03	0.95, 1.11	0.491						
	Knee	0.97	0.91, 1.03	0.375						

When checking the assumptions of 1SMR, I found evidence for an association between the IGF-1 PRS and both BMI and HRT use (Table 56), violating the assumption that an instrument is independent of confounders of the exposure-outcome relationship (IV2). Despite a strong inverse relationship between BMI and measured IGF-1, the association between the IGF-1 PRS and BMI was positive. I performed additional 1SMR, adjusting for HRT use, which did not attenuate the association between IGF-1 and hip OA (data not shown).

Table 56: Associations between the IGF-1 PRS and potential mediators/confounders of the IGF-1-OA relationship in UK Biobank.

Covariate	Beta	95% CI	*p*
Age (years)	-1.08×10^{-4}	-0.001, 0.001	0.787
Male	-0.004	-0.017, 0.009	0.537
BMI (kg/m^2)	0.017	0.008, 0.025	1×10^{-4}
HRT (ever used)	0.008	0.003, 0.014	0.002
Age at menopause	-0.002	$-0.004, 3.89 \times 10^{-4}$	0.104
eBMD	-0.021	-0.082, 0.041	0.512

Beta represents the unit increase in PRS per one-year increase in age and age at menopause or the difference between sexes. For BMI, beta represents the unit increase in BMI per unit increase in PRS. For HRT, beta represents the log odds of ever taking HRT per unit increase in PRS. Adjusted for sex, genotyping chip and 10 PCs.

I hypothesized that BMI could mediate the effect of IGF-1 on hip OA; therefore, I performed MVMR to determine the causal effect of IGF-1 on hospital-diagnosed OA, independent of BMI.

I used the IGF-1 and BMI PRS' as instruments and found evidence for an independent causal pathway between IGF-1 and hip OA (OR=1.32 [1.09,1.58], p=0.004), with weaker evidence for a causal effect on knee OA (OR=1.14 [0.99,1.31], p=0.078, Figure 117). Evidence for a causal effect of IGF-1 on both hip and knee OA was stronger after excluding the IGF-BP3 SNPs (OR_{hip}=1.49 [1.16,1.93] and OR_{knee}=1.22 [1.00,1.48]). The effect sizes for the causal role of IGF-1 on hip and knee OA were unchanged when performing MVMR with height instead of BMI (Table 57). Like univariable MR, when stratifying by sex, a stronger effect of IGF-1 on hip OA was seen in females (OR_F=1.39 [1.10,1.76] *vs* OR_M=1.21 [0.90,1.63], Figure 118).

Table 57: One-sample results and multivariable MR results for the causal effect of IGF-1 on OA in UK Biobank.

	Univariable MR			**MVMR: IGF-1 and BMI**					
	Genetically predicted IGF-1			**Genetically predicted IGF-1**			**Genetically predicted BMI**		
	risk difference	**95% CI**	***p***	**risk difference**	**95% CI**	***p***	**risk difference**	**95% CI**	***p***
Hand OA	-0.001	-0.004, 0.002	0.534	-0.001	-0.004, 0.002	0.554	-0.001	-0.003, 0.002	0.601
Hip OA	0.009	0.004, 0.015	0.001	0.009	0.003, 0.014	0.003	0.015	0.010, 0.021	<0.001
Knee OA	0.009	0.001, 0.016	0.019	0.006	-0.001, 0.014	0.081	0.035	0.029, 0.042	<0.001
				MVMR: IGF-1 and height					
	Genetically predicted IGF-1			**Genetically predicted IGF-1**			**Genetically predicted height**		
Hand OA	-0.001	-0.004, 0.002	0.534	-0.001	-0.004, 0.002	0.542	$-3x10^{-5}$	-0.002, 0.001	0.968
Hip OA	0.009	0.004, 0.015	0.001	0.009	0.003, 0.015	0.002	0.001	-0.002, 0.005	0.344
Knee OA	0.009	0.001, 0.016	0.019	0.008	0.001, 0.015	0.029	0.003	-0.001, 0.007	0.106

Risk differences are per SD increase in IGF-1.

11.3.4. Factorial MR to determine the additive effect of high IGF-1 and high BMI

I next performed factorial MR to identify any additive effect of IGF-1 and BMI on OA. Those with a BMI and IGF-1 PRS above the median had the greatest odds of hip OA (OR=1.12 [1.06,1.18], p=1x10^{-4}), compared to those with scores below the median (Figure 124), suggesting an additive effect of higher serum IGF-1 and higher BMI on hip OA risk. No difference in the odds of knee OA was apparent between those with a high BMI PRS and low IGF-1 PRS *vs.* those with a high IGF-1 PRS and high BMI PRS (Figure 124), suggesting that IGF-1 may not contribute to knee OA risk. Results were similar when stratified by sex (Figure 125).

Figure 124: Factorial MR analyses of the interaction between IGF-1 and BMI on hip and knee OA risk in UK Biobank.

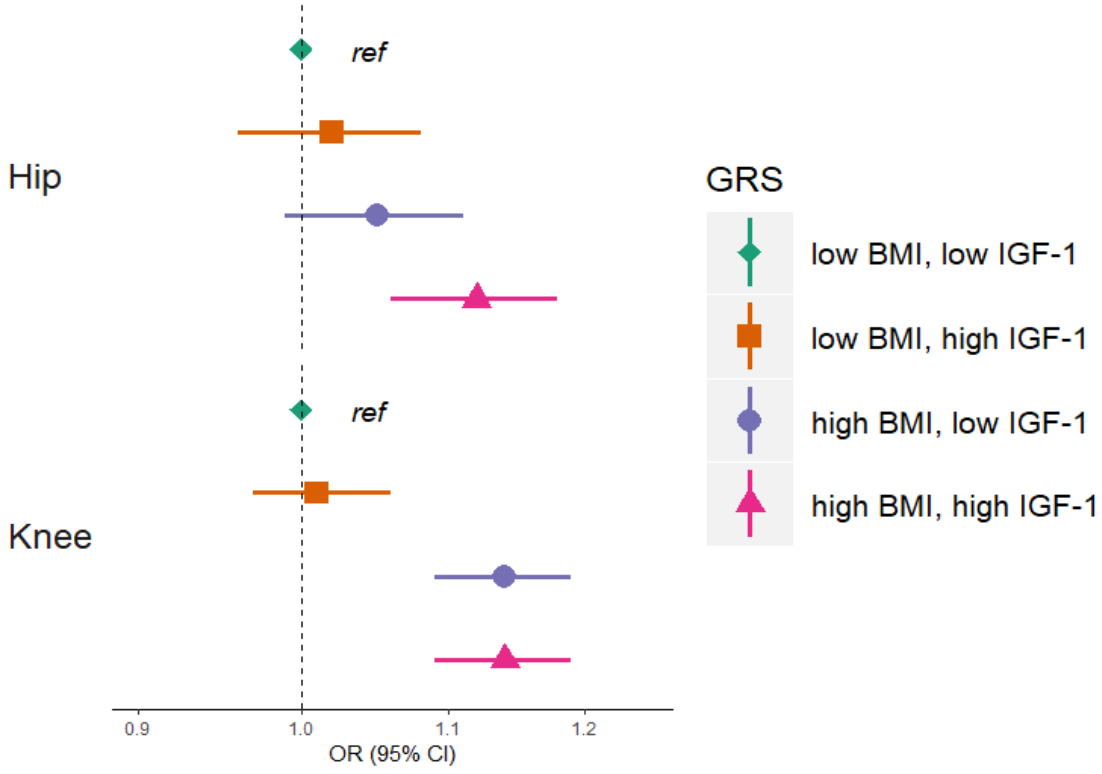

Points represent the OR for individuals in each BMI/IGF-1 PRS category compared to those with a BMI PRS below the median and an IGF-1 PRS below the median (reference category). Horizontal bars represent 95% CIs.

Figure 125: Factorial MR analyses of the interaction between IGF-1 and BMI on hip and knee OA risk in UK Biobank, stratified by sex.

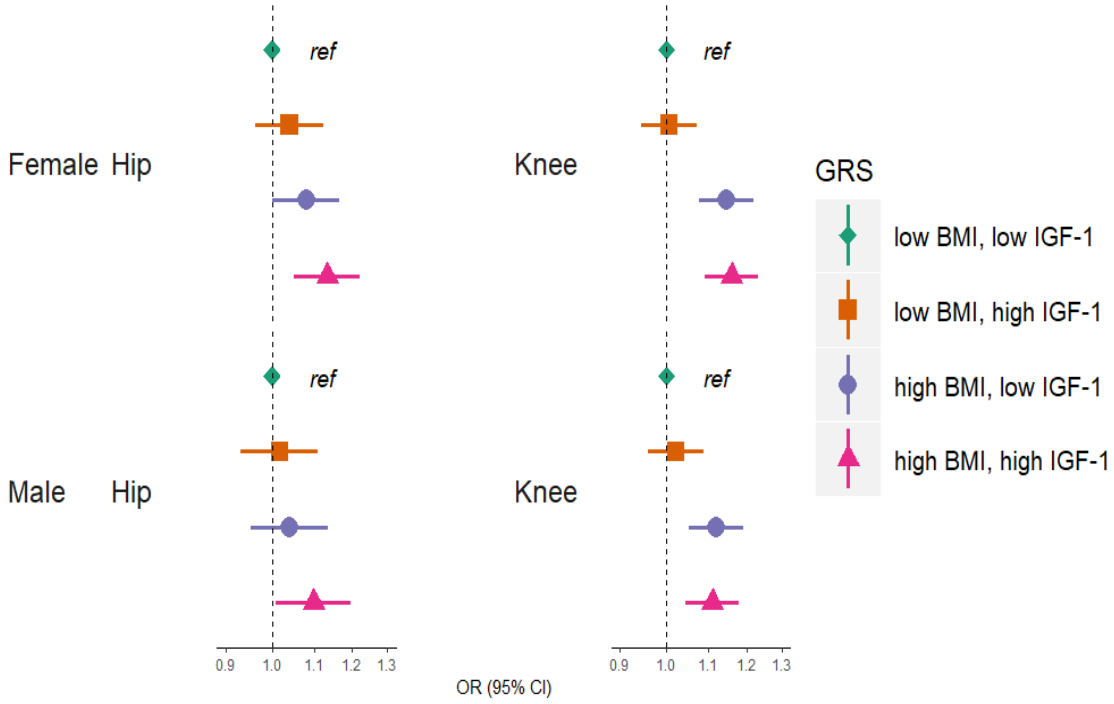

11.4. Discussion

11.4.1. Summary of findings

I have found evidence for a causal effect of higher circulating IGF-1 on the risk of hospital-diagnosed hip OA in a large population of white European adults. This effect is independent of BMI. Both observational and MR analyses suggest that the effect of IGF-1 on hip OA is greater in those with a higher BMI, suggesting BMI modifies the effect of IGF-1 on hip OA. I detected evidence for a causal role of IGF-1 as a risk factor for knee OA, though this was weaker than that for hip OA.

11.4.2. Context of this research

This is the first study to use MR to determine the causal relationships between IGF-1 and OA at the hand, hip, or knee. Two prior studies have identified a positive relationship between a microsatellite polymorphism in the *IGF1* promoter and radiographic hip OA (519,520). This polymorphism was related to lower serum IGF-1 concentrations in a subset of 50 individuals (521), but the authors could not conclude that the SNP was the causal variant, or in LD with a variant causing OA (520).

The lack of observational evidence for an association between IGF-1 and knee OA is consistent with a previous case-control study (Framingham Osteoarthritis Study) of both incident and progressive radiographic knee OA (522), and a cross-sectional analyses in the Baltimore Longitudinal Study of Aging (523). Lloyd *et al* identified a positive association between IGF-1 and radiographic knee OA in Chingford women, but only for severe, bilateral knee OA (510). The phenotype of hospital-diagnosed OA in this analysis is likely to reflect more severe radiographic or clinically apparent (*i.e.* painful) OA. UK Biobank lacks data on whether cases had bilateral or unilateral disease, which may contribute to the inconsistency in findings. Furthermore, Lloyd *et al* found weak evidence for increased serum IGF-1 in individuals with radiographic DIP OA (510), which

contrasts with the protective association between IGF-1 and hand OA observed. Although the age-standardized prevalence of radiographic hand OA was 27% in the US Framingham population (524), UK hospital-diagnosis was much rarer, likely due to the lack of surgical management options for hand OA, so that individuals are unlikely to be referred to secondary care for assessment, meaning the MR analyses of hand OA were underpowered to confirm or refute the reported effect.

Consistent with a role of the IGF-1/IGF-BP axis on hip OA risk, a GWAS of hip OA identified two loci near *IGFBP3* associated with a decreased odds of hip OA and decreased circulating IGF-BP3 (not IGF-1) (525). *In vivo* functional studies suggest *IGFBP3* overexpression in cartilage from patients with knee OA results in decreased aggrecan and increased MMP-13 expression (525). The two OA-associated SNPs near *IGFBP3* were not instruments in my analyses, nor in LD with any of the instruments used. The 2SMR analyses did not suggest a causal effect of circulating IGF-BP3 on hip OA risk.

The lack of consistency between the observational and MR results may reflect the difference in exposures; for observational analyses, the exposure was current measured IGF-1 levels, whereas for MR analyses, the exposure was genetically predicted IGF-1 levels (371). Different relationships of measured IGF-1 and the IGF-1 PRS with BMI may be explained by a negative feedback loop, whereby higher IGF-1 levels throughout the lifecourse lead to a higher body mass which, over a sustained period of time, may reduce IGF-1 production by the liver (512). However, the BMI PRS was not associated with current IGF-1 levels ($\beta=3x10^{-4}$ [95%CI: $-4x10^{-3}$, $4x10^{-3}$]). I therefore hypothesize that higher IGF-1 throughout the life-course may drive the progression of OA, and the MVMR analyses suggest that this effect is not mediated by BMI. One potential pathway is via increased BMD, a reported risk factor for hip OA (207). IGF-1 contributes to skeletal development and increases BMD by promoting MSC differentiation into osteoblasts (511). However, adjustment for eBMD did not attenuate the observational relationship between IGF-1 and hip OA. An alternative explanation is that higher IGF-1 during development may lead to alterations in

hip shape. IGF-1 is important for endochondral bone formation (526) and several genes linked to endochondral bone formation were identified in a recent GWAS meta-analysis of hip shape (527). Variation in hip shape is associated with hip OA (section 1.2.5). As I observed a stronger effect of IGF-1 on hip OA in females, I further hypothesize that IGF-1 levels could lower circulating oestrogen levels, leading to increased OA risk, as oestrogen may be protective against OA (528). However, the IGF-1 PRS was not related to menopausal age (data not shown). Another potential explanation for the differences between the observational and MR results could be additional unmeasured confounding, biasing the observational analyses (371). The potential for confounders to strongly bias observational results is highlighted by the difference in direction of effect observed for hip OA, before and after adjustment for BMI. As long as the instrument used for MR analysis meets the three key assumptions of MR, the MR estimate is not biased by confounding (367) and therefore I can have more confidence in the estimates generated by MR.

11.4.3. Strengths of this work

A major strength of this analysis is the availability of data for IGF-1 concentration and hospital diagnosis of OA for over 400,000 individuals, making this the most well-powered study to determine the observational relationship between IGF-1 and OA. I also had genotype data for over 300,000 individuals, which meant I had 80% power to detect a causal OR of at least 1.28. The availability of genetic data meant that I was able to perform 1SMVMR analysis to determine if there is a BMI-independent causal effect of IGF-1 on hip OA.

11.4.4. Methodological issues and limitations

The outcome was hospital-diagnosed OA, which is likely to represent a more extreme and progressive OA phenotype. Although I excluded controls with other diagnosed arthropathies, there may still be controls with radiographic or clinical features of OA which have not been diagnosed, although this is likely to bias the results towards the null. Sex-stratified and hand OA analyses had low power,

meaning I am unable to draw conclusions from these analyses. I am unable to determine if the effect of IGF-1 is independent of IGF-BPs, as IGF-BPs have not been measured in UKBB. The summary statistics for the SNP-IGF-1 associations for 2SMR were estimated from *p*-values and therefore betas may not accurately reflect the true SNP-exposure association. However, these effect estimates were not used for 1SMR, which generated consistent results. I did not generate the BMI instrument from the largest GWAS of BMI, as a large proportion of individuals included in this meta-analysis were from UK Biobank and I was concerned about overestimating causal effect estimates due to 'winner's-curse bias' (529,530). Dichotomizing the population based on their PRS may not be the most efficient method for performing factorial MR (531). I therefore cannot rule out a possible unobserved interaction between IGF-1 and BMI on knee OA risk. The MR analyses were restricted to those of white European ancestry, limiting the generalizability to other ethnicities. The overall UKBB population is also predominantly white British, with a higher prevalence of homeowners and non-smokers, with a lower BMI and fewer self-reported health concerns than the general population (532), again limiting the generalizability of the observational results. There is also the possibility that 'survivor bias' may explain the associations observed; if higher IGF-1 levels are related to a lower mortality risk, those with higher IGF-1 levels will be surviving long enough to develop chronic diseases, such as OA. However, evidence suggests that IGF-1 levels are not related to all-cause mortality (533,534). The UK Biobank population is limited by latent population structure (geographical variation in allele frequencies) even after restricting to white European individuals and adjusting for PCs and assessment centre (535), which may confound the relationship between IGF-1 and hospital-diagnosed hip OA.

11.4.5. Future work

Further MR analyses are required to determine if IGF-1 is related to radiographic features of OA, and their progression, in a large cohort of individuals from the general population. This will help uncover the mechanism by which IGF-1 causes

hip/knee OA; previous studies have identified *IGF1* gene expression in osteoblasts and osteoclasts from human osteophyte tissue, suggesting that the role of IGF-1 in OA pathogenesis is via osteophyte formation (508). Unfortunately, to the best of my knowledge, total serum IGF-1 has not been measured in a large cohort with radiographic data, such as RS, and therefore I was unable to determine the relationship between IGF-1 and radiographic OA sub-phenotypes. It also remains to be determined whether circulating IGF-1 concentrations correlate with tissue-specific levels.

As discussed earlier, the stronger effect estimates for MR, compared to observational analyses, suggests that lifetime exposure to higher IGF-1 levels has a greater effect on hip and knee OA risk compared to IGF-1 levels measured at a single timepoint in adulthood. However, an RCT is required to determine if interventions to reduce IGF-1 levels in older adults reduces the incidence and progression of hip and knee OA, as earlier interventions could interfere with growth and skeletal development.

Finally, as discussed earlier, IGF-1 may affect hip OA risk through alterations in hip morphology. It is therefore important to determine the relationship between IGF-1 levels and hip shape in a cohort of individuals without OA (*e.g.* an adolescent cohort).

11.4.6. Conclusions

I have identified robust evidence that higher concentrations of serum IGF-1 are a causal risk factor for hip OA in a large UK population, with some evidence for a causal role in knee OA, and no evidence for an association with hand OA. MVMR analyses suggest that this causal role is independent of BMI, consistent with the observational analyses for hip, but not knee, OA. Further study is required to determine the mechanism underlying this relationship.

CHAPTER 12. DISCUSSION

In this chapter, I will summarise the key results and how these add to the current knowledge of OA pathogenesis, and my hypotheses for biological mechanisms in OA. I will then discuss the next steps and translational potential of this work.

12.1. Summary of key findings and further hypotheses

12.1.1. HBM is associated with radiographic hip and knee OA sub-phenotype progression

The overall aim of this PhD was to determine the role of bone in the pathogenesis of OA. This could be separated into five key aims, as summarized in Figure 19, Page 99. Prior to this work, higher BMD was an established risk factor for prevalent OA of the hip and knee, with sparse and inconclusive evidence for a role of BMD in hip and knee OA progression (discussed in section 3.1). The major limitation of these previous analyses has been the categorization of OA progression based on change in overall KL grade, which, as discussed in Chapter 6, mainly reflects incident JSN at the knee. My first key aim was therefore to determine the role of BMD in hip and knee OA progression, including progression of the radiographic sub-phenotypes, by analysing a unique population with extreme elevations in BMD, and their relatives without HBM.

In Chapter 6 and Chapter 7, I provide evidence that HBM is related to worsening (*i.e.* the combined incidence and/or progression) of both knee and hip osteophytes and JSN, independent of TBFM. Based on the previous observations of cross-sectional relationships between HBM and knee/hip OA representing relationships with osteophytes, rather than JSN (226-228), and the observation that HBM individuals have more enthesophytes than individuals without HBM (402), it was hypothesized that HBM individuals have a propensity to form more bone (207). This hypothesis, in combination with the observation that individuals with atrophic hip OA have lower BMD and an increased fracture risk (454), suggests that HBM individuals are more likely to develop hypertrophic OA but are not at an increased risk of cartilage loss. However, the observed associations

between HBM and worsening of JSN at both the hip and knee refutes this hypothesis and suggests that HBM individuals experience cartilage degeneration after osteophyte formation. The relationship with worsening of osteophytes was stronger than the relationship with JSN, which could reflect either the greater variability of osteophyte scoring, or the hypothesized 'bone-forming' phenotype of HBM (402). The fact that at an association between HBM and worsening of JSN was observed though is an interesting finding as there is limited evidence to suggest that BMD is a risk factor for incident/progressive JSN. Observed associations were stronger at the knee, compared to the hip, which could reflect the slightly larger sample size for the knee OA analyses (as individuals under the age of 40 were included), or a greater role of BMD in knee OA pathogenesis. As I treated my outcome as a continuous variable and my analyses were therefore not restricted to individuals with OA at baseline, my analyses were less likely to be biased by collider bias. The fact that I observed the opposite direction of effect from the previous knee OA studies, which were case-only analyses, suggests that collider bias is the explanation for the previously observed protective effect (229,233).

Published analyses of the role of BMD in hip/knee OA progression have mainly been limited to large cohorts, allowing sufficient numbers to perform analyses of individuals with OA at baseline (229,232,233,235). Although these analyses are longitudinal, with BMD measurement preceding follow-up, the possibility that BMD is artefactually elevated (*i.e.* by spinal osteophytes or buttressing of osteophytes at the hip) cannot be ruled out. HBM individuals have been specifically selected based on generalized BMD elevations, and baseline DXA scans were inspected to rule out artefactual elevations by features of OA (197). HBM is genetically determined, by either an over-representation of polygenic variants associated with BMD (203), or rare monogenic variants (196,205). Therefore, a true temporal relationship can be inferred, suggestive of a causal pathway between HBM and OA progression.

HBM was additionally associated with severity of OA symptoms at both the hip and knee, with a stronger magnitude of effect at the knee. Symptoms were only assessed cross-sectionally, so I could not draw any conclusions about progression of symptoms. The HBM relationship with symptoms at the knee was explained by severity of osteophytes at follow-up, whereas the severity of pain at the hip was independent of severity of radiographic features. JSN severity did not attenuate the relationship between HBM and knee symptoms by the same magnitude as osteophytes, suggesting that osteophytes are a greater contributor to pain at the knee. It has been hypothesized that osteophyte formation is an attempt to stabilize the joint, protecting from further damage (19). However, evidence suggesting a strong contribution of osteophytes to OA symptoms in HBM individuals suggests that osteophytosis may be a pathogenic, rather than protective, feature.

Possible explanations for an observational association between HBM and OA sub-phenotype incidence/progression include a true causal pathway, reverse causality, unmeasured confounding bias, or shared developmental pathways (*i.e.* shared genetic aetiology). The temporal relationship between HBM and OA development means reverse causality is an unlikely explanation. Additional analyses to determine a true causal pathway from shared genetic aetiology are described in sections 12.1.3-12.1.5.

12.1.2. Metabolomics analysis in the HBM population did not identify any metabolic mediators of the HBM-OA relationship

A causal effect of HBM on OA could be mediated by metabolic consequences of the HBM phenotype. As HBM is related to elevated FM, which is hypothesized to be a consequence of genetically-determined HBM and low bone turnover (201), I hypothesized that metabolic traits may mediate the HBM-OA relationship, reflecting altered metabolic regulation in HBM individuals by reduced osteocalcin. In Chapter 8, I therefore performed metabolomics analyses

to identify metabolic traits associated with both HBM/BMD/bone turnover and OA sub-phenotypes, with the aim of then determining whether these metabolic traits mediate the relationship between HBM and OA, ultimately identifying metabolic pathways which may be involved in OA pathogenesis in HBM individuals, and thus potential druggable targets. However, possibly due to sample degradation resulting from long-term storage of blood samples (discussed in section 12.2.2), no metabolic traits were identified that were associated with both HBM/BMD/BTMs and OA variables.

However, albeit not related to OA pathogenesis, I did identify a strong relationship between bone resorption (assessed by current CTX-1 levels) and circulating citrate. This relationship was independent of bone formation markers and replicated in two cohorts sampled from the general population (a cohort of mixed-sex adolescents and a cohort of adult women). The relationship was stronger in HBM individuals than either general population cohort or relatives without HBM. The presence of citrate in bone has already been established, with a hypothesized role in regulating the structure of bone mineral (460,462,463). The fact that citrate was, albeit cross-sectionally, associated with current levels of bone resorption in three populations, of different age and gender composition, is consistent with the knowledge that bone is a major source of plasma citrate (460). This represents the first analysis to compare associations between bone resorption levels and plasma citrate between individuals with high BMD and those with normal BMD. A stronger relationship between bone resorption and citrate in HBM individuals could reflect prolonged secondary mineralization in HBM individuals (200), with more mineral associated with more citrate, or could reflect differences in bone mineral structure in HBM, allowing citrate to be more readily released into the circulation. I therefore hypothesize that citrate could be a specific marker of turnover of bone mineral. Further analyses are required to determine the response of circulating citrate to interventions aimed at reducing bone resorption, such as bisphosphonates, to further test this hypothesis.

12.1.3. Evidence for a BMI-independent causal effect of BMD on hip and knee OA

BMI is perhaps the strongest confounder of any relationship between HBM and worsening features of OA, via increased joint loading, or increased adiposity increasing adipokine production which may be detrimental to the joint (84,85). In Chapter 9, I investigated the causal role of BMD on OA at the hip and knee, extending previous analyses (139,261) by using multivariable MR, and I found evidence for a causal role of BMD on hip and knee OA, independent of BMI. Bidirectional MR analyses confirmed that BMI is a confounder (*i.e.* common cause of both BMD and hip/knee OA). The fact that a causal effect of eBMD on BMI was not observed, in addition to no evidence for a relationship between plasma osteocalcin and total cholesterol and only weak evidence for inverse relationships between osteocalcin and serum triglycerides and glucose in the metabolomics analysis (section 12.1.2), suggests that the endocrine effect of osteocalcin observed in mice (202) may not translate to humans. However, methodological issues with the metabolomics data restricts the conclusions that can be made from these data.

MR provided some, yet inconclusive, evidence for a causal effect of OA on BMD, representing the first MR analysis to examine this direction of causality. Possible explanations for a true causal effect of OA on BMD include artefactual elevation, although this was unlikely to be the case for eBMD, or reduced PA due to pain, but this would have led to a detrimental effect on BMD. I hypothesized that weak evidence for causal effects of OA on BMD was an artefact of the shared underlying biological pathways (such as Wnt and TGFβ signalling, discussed in section 3.3.2) and I employed the latent causal variable methodology to determine the genetic correlation of BMD and OA, as well as the proportion of genetic effect on BMD causal for OA. For this analysis, I used summary statistics from BMD and OA GWAS adjusted for weight, to take account of confounding. This analysis provided evidence for a genetic correlation between FN/LS-BMD

and hip/knee OA reflecting the shared genetic aetiology (section 12.1.4), as well as a causal effect of BMD on OA.

12.1.4. Key pathways in bone metabolism appear to contribute independently to OA risk

I hypothesized that the genetic correlation between BMD and OA was explained by the contribution of key bone and cartilage regulatory pathways to both phenotypes. Prior to this work, it was known that key pathways involved in osteoblast and osteoclast function, such as the Wnt signalling pathway, have a role in OA pathogenesis, but the exact contribution of these pathways had not been quantified. In Chapter 10, I attempted to quantify the contribution of genetic variation in key pathways to OA risk in Chapter 10. I selected three key pathways in bone development and metabolism which have been implicated in the pathogenesis of OA, namely Wnt signalling, the TGFβ superfamily and the osteoclast differentiation pathway, as discussed in section 3.3.2. I used GWAS summary statistics to estimate SNP-specific r^2 for all independent SNPs annotated to each pathway, either by their location within ±20kb of a pathway gene, or by an association with gene expression in blood. These analyses suggested that the contribution of genetic variation in these pathways is similar between OA at the hand, hip, and knee, but lower than the contribution to eBMD variation. Adjustment for eBMD did not affect r^2 estimates, suggesting that these pathways have a direct role in OA pathogenesis. When identifying pathway-specific variants based on genetic location, the Wnt signalling pathway was the greatest contributor to variation in OA risk, whereas when selecting pathway-specific variants based on effect on gene expression in the blood, the osteoclast differentiation pathway explained a similar proportion of the variance in OA risk to that explained by Wnt signalling.

Additionally, in Chapter 10, I determined cross-sectional associations between plasma sclerostin and radiographic OA sub-phenotypes in the HBM population, identifying strong evidence for a reduced odds of JSN at the thumb joint with

increasing plasma sclerostin concentration, which was not explained by adjustment for age, sex, height, weight, or current levels of bone formation. I further determined the relationship between the two known loci for plasma sclerostin levels (488) and OA at the thumb base, with evidence suggesting that the observed cross-sectional relationship may reflect a causal effect of plasma sclerostin on reduced odds of thumb OA, although there was heterogeneity in estimates between the two SNPs. This adds to the body of evidence suggesting a protective role of Wnt inhibition in OA pathogenesis (536).

12.1.5. Circulating IGF-1 is a risk factor for hip and knee OA

IGF-1 regulates skeletal growth, and serum levels are related to periosteal expansion and BMD (511). Mechanisms of action include regulation of osteoblastogenesis, as well as regulation of chondrocyte differentiation and hypertrophy at the growth plate (511). Due to the role in both osteoblast and chondrocyte regulation, in Chapter 11, I aimed to clarify the role of IGF-1 in OA pathogenesis by determining the association between serum IGF-1 and hospital-diagnosed OA at the hand, hip and knee in the UK Biobank population. Several observational analyses of the relationship between IGF-1 and OA have been performed, using much smaller sample sizes, and have generated conflicting results (509). Possible explanations for these conflicting results include phenotype heterogeneity, the lack of adjustment for key covariates such as BMI, or measurement of current IGF-1 levels which may not reflect IGF-1 levels throughout the lifecoure. I therefore utilised genetic loci related to IGF-1 levels to perform MR to determine the effect of genetically predicted IGF-1 on OA risk, as well as levels assessed at one timepoint in UK Biobank.

In the observational analyses, prior to adjustment for BMI, IGF-1 levels appeared inversely related to hospital-diagnosed OA at the three joints. For hand OA, this relationship persisted after adjustment for BMI, whereas the association with knee OA was attenuated, and IGF-1 became positively related to hip OA. Although measured IGF-1 was inversely related to BMI, genetically predicted

IGF-1 was positively related to BMI, suggesting that IGF-1 has differing relationships with BMI at different stages of the lifecourse. Subsequent MR analyses, including MVMR accounting for BMI, provided evidence for a causal effect of higher serum IGF-1 on hip OA, with weaker evidence for knee OA, and no evidence for a causal effect on hand OA, suggesting that higher IGF-1 levels throughout the lifecourse are involved in the pathogenesis of hip and knee OA. This study represented the largest analysis of observational relationships between IGF-1 and OA, and the first MR study to quantify the causal effect of IGF-1 on OA, independent of confounding and reverse causality. I did not observe attenuation of results when adjusting for eBMD, suggesting that BMD does not contribute to this relationship, thus meaning the IGF-1 axis could be another source of shared biology between BMD and OA.

12.1.6. Hypothesized mechanisms

Figure 126 summarizes the results discussed in sections 12.1.1-12.1.5 and my hypotheses for mechanisms behind the relationship between HBM and worsening of radiographic features of OA.

Figure 126: Summary of hypotheses to explain the relationship between HBM and prevalent and progressive OA.

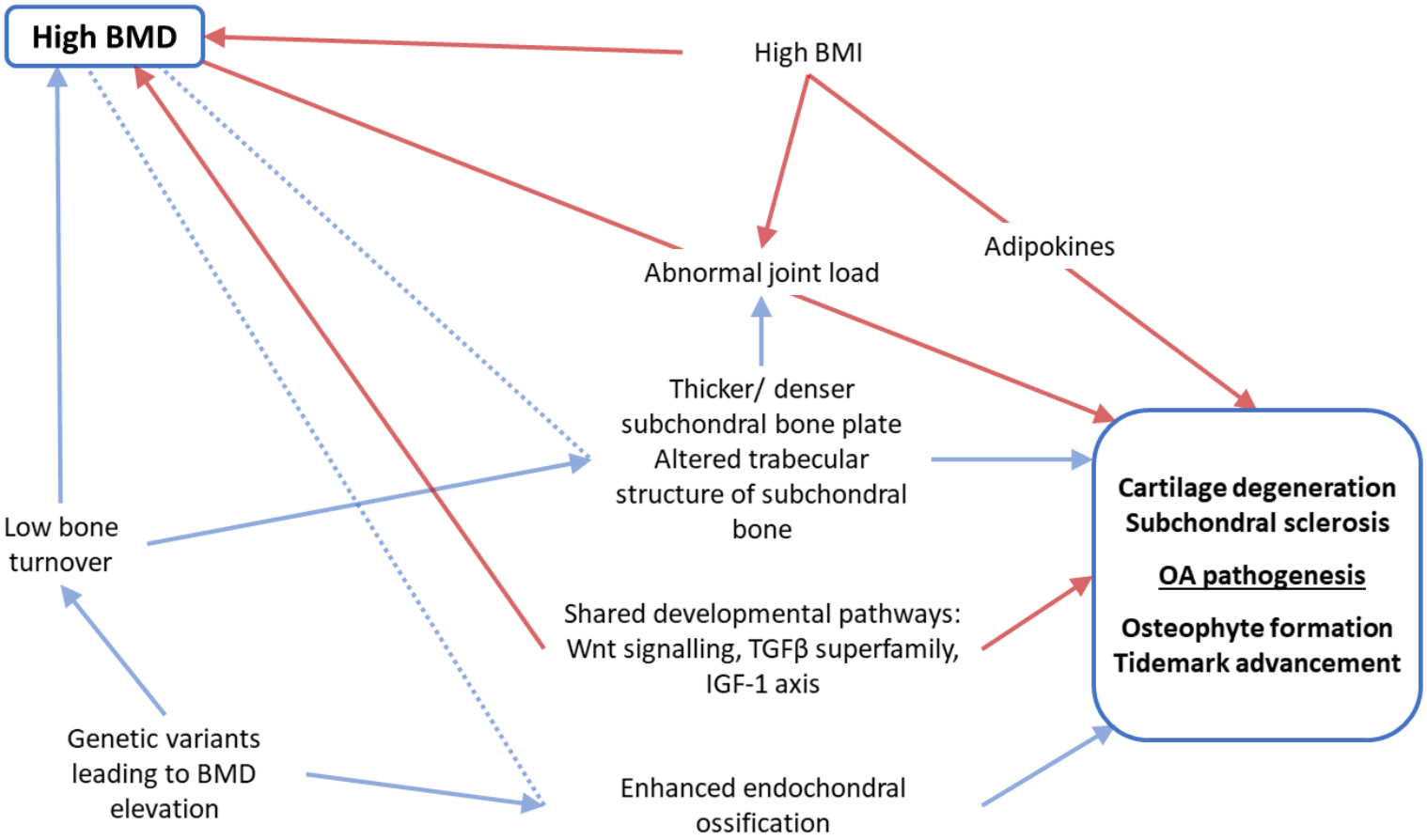

Dotted lines represent correlations rather than hypothesized causal pathways. Red arrows represent evidence provided by the results of this thesis.

As well as the hypothesized direct effect of altered joint biomechanics due to increased loading by high BMD, a true causal pathway between high BMD and worsening OA sub-phenotypes could be explained by low bone turnover (201), which may contribute to a denser subchondral bone, creating greater pressure on the cartilage. However, although denser subchondral bone with lower bone turnover may contribute to subsequent disease progression, these features are not believed to initiate the disease process (18). Structure of the underlying subchondral trabecular bone could be altered in HBM individuals, as increased trabecular density at both the tibia and radius has been observed (200). Trabecular bone integrity of subchondral bone, with thinning of vertical, but thickening of horizontal, trabeculae has been linked to JSN progression, suggesting a role of trabecular bone in cartilage loss (537). Another analysis suggested that higher trabecular number and thickness plus reduced trabecular separation is linked to medial JSN progression (326), which would explain the relationship between HBM and development of JSN over eight years.

In addition to the Wnt signalling, TGFβ superfamily and osteoclast differentiation pathways and the IGF-1 axis, enhanced endochondral ossification could contribute to osteophyte formation and OA pathogenesis in HBM individuals, and to shared genetic aetiology. In a recent GWAS of TH/L1-BMD in HBM individuals and individuals with low bone mass, two established BMD loci annotated to genes involved in endochondral ossification (*MEF2C* and *SOX6*) were identified (203). Endochondral ossification occurs in developing osteophytes (406). Re-establishment of endochondral ossification at the tidemark can lead to formation of additional tidemarks, advancing the area of calcified cartilage and reducing the articular cartilage (18), which could explain the relationship between HBM and development of JSN.

12.2. Main strengths and limitations

Analysis-specific strengths and limitations are discussed in the relevant results chapter. In this section, I will summarise the key strengths and limitations of the overall thesis.

12.2.1. Strengths

The major strength of the work presented in this thesis is the range of methods used, analysing the most appropriate data source for each research question. Although the HBM population was small, it allowed the study of differences in radiographic OA sub-phenotypes in individuals with extremely elevated BMD, against their family members with normal or low BMD. The fact that HBM is likely to have a predominantly genetic aetiology allows inferences about the temporal relationship between HBM and OA to be made, so results are unlikely to be explained by reverse causality. The availability of OA sub-phenotype data for a larger sample size in the RS population allowed replication of analyses in the general population and allowed some genetic analyses of OA sub-phenotypes. The availability of genotype data for over 400,000 individuals in UK Biobank allowed well-powered genetic analyses for causal inference.

12.2.2. Limitations

The two key limitations of this work are loss-to-follow-up in the HBM population, reducing power and potentially biasing results for the progression analyses, as well as the lack of radiographic measures in UK Biobank.

As referrals for DXA scans are normally due to conditions or medications related to older age, the HBM population at baseline was relatively old, so after 10 years there was a large drop-out due to death or ill health (only 58% of individuals recruited at the relevant sites were able to be followed-up, including 57% of those aged over 40 years at baseline). Fortunately, the proportion of individuals with HBM did not differ between those with or without follow-up data, suggesting that there was no greater proportion of loss-to-follow-up in HBM individuals.

However, there is also the concern that HBM individuals were more engaged with the study at baseline than their relatives without HBM, meaning that those with HBM still alive were more likely to participate in follow-up, regardless of health, whereas individuals without HBM were more likely to participate in follow-up if they were healthy and more altruistic, leading to a healthy-selection bias in the relative population, which could potentially cause spurious associations between HBM and worsening OA. Perhaps of some concern was the fact that, out of the follow-up population, relatives without HBM were more highly educated than HBM individuals, although adjustment for education did not alter conclusions. As well as possible selection bias, loss-to-follow-up led to very small sample sizes for the analyses of change in OA sub-phenotypes. Analyses of binary variables were underpowered (power <80%), generating CIs overlapping the null.

The hospital-diagnosed OA phenotypes assessed in UK Biobank are unlikely to be comparable to radiographic OA definitions (based on KL/Croft score), as presentation to primary care and referral to secondary care likely reflects factors such as pain and referral practices, with radiographic evidence often being used to confirm a diagnosis upon presentation to secondary care. Therefore, hospital-diagnosed OA is likely to reflect a severe, painful phenotype. Hospital-diagnosed hand OA was the least common phenotype in UK Biobank, whereas, as discussed in section 1.2.4, prevalence estimates for radiographic hand OA in any joint of the hand are higher than those for radiographic hip or knee OA (37-39). This is likely to reflect the lack of surgical procedures for hand OA, meaning GPs will be less likely to refer a hand OA patient to secondary care, compared to a hip or knee OA patient. Hospital-diagnosed OA phenotypes are therefore less useful when trying to identify mechanisms driving the structural progression of OA, and thus drug targets to reduce progression. Analyses of BMD in UK Biobank were also limited to BMD estimated from a combination of speed of sound and broadband ultrasound attenuation at the heel. The estimated correlation between DXA-assessed BMD and ultrasound-assessed eBMD is 0.42-0.61 (538) and there is

a moderate genetic correlation between eBMD and FN-BMD (positive) and fracture risk (negative) (477). However, as discussed in Chapter 9, the composition of cortical *vs* trabecular bone differs between the hip and the heel, and these two different types of bone may have different roles in OA pathogenesis.

12.3. Future work

12.3.1. Examining the relationship between plasma sclerostin and OA sub-phenotypes in OAI

I have found strong cross-sectional evidence for an association between plasma sclerostin and reduced odds of thumb JSN. However, this association requires replication in the general population. As discussed in section 10.4.5, sclerostin measurements are underway in OAI, which could be used to replicate analyses of cross-sectional associations between plasma sclerostin and OA sub-phenotypes and perform longitudinal analyses of incident and progressive sub-phenotypes. The OAI population will be included in an updated GWAS meta-analysis of plasma sclerostin, which will hopefully be better powered to detect additional loci. If additional SNPs for sclerostin are identified, the MR analyses could be repeated with a stronger instrument, again increasing power.

12.3.2. Additional MR analyses to further assess pleiotropy

I have provided evidence for a BMI-independent causal effect of BMD on OA, although I have also found evidence for a direct effect of key pathways in bone development on OA risk. To further examine the pathways contributing to pleiotropy in the MR analyses of BMD on OA, I could annotate the Morris eBMD SNPs to the biological pathways analysed in Chapter 10, via their annotated gene. These annotations could be used to perform MR of eBMD on OA and determine if effect estimates differ across biological pathways. Evidence for directional pleiotropy (*i.e.* a value much greater than zero for the average SNP

effect on OA risk, not mediated by BMD) for specific pathways will be further evidence that these pathways have a direct effect on OA. Restricting to eBMD instruments not annotated to these pleiotropic pathways may give a pleiotropy-robust estimate of the causal effect of BMD on OA.

The low power of the MR-Egger method meant that CIs were very wide for analyses with few SNPs, limiting interpretability. Additionally, given the evidence for a direct effect of key bone pathways in OA pathogenesis generated in Chapter 10, and the inconsistency in results between the IVW, weighted median and MR-Egger methods for the causal effect of eBMD on knee OA (section 9.3.1), further analyses are required to determine the pleiotropy-independent causal effect of BMD on OA. Since performing the analyses presented in this thesis, additional MR methods have been developed to generate pleiotropy-robust estimates of the causal effect in MR (539). These include methods to identify and remove, or downweight, outlier SNPs (539). If all SNPs are valid IVs, one would expect the Wald ratio estimate to be consistent across SNPs (539). However, if a SNP is associated with the outcome via a pathway not including the exposure (*i.e.* horizontal pleiotropy), and is thus an invalid instrument, the Wald ratio will differ from the estimates provided by valid instruments (539). MR pleiotropy residual sum and outlier (MR-PRESSO) is an example of a method which has recently been developed to identify and remove outliers, which identifies outliers by comparing the residuals for each SNP from the regression line to the expected residual when there is no horizontal pleiotropy (540).

12.3.3. Additional pathways to consider

I selected key signalling pathways in bone development for the pathway analyses, as there is evidence for a role of these pathways in OA pathogenesis, and the biology of these pathways is well understood. However, other key pathways remain which should be investigated in the future. As I hypothesize that enhanced endochondral ossification contributes to osteophyte formation in

individuals with HBM, repeating pathway analyses with genes linked to endochondral ossification, and comparing variance explained between the OA sub-phenotypes, would be an important extension to this analysis. Other pathways identified based on the Morris annotated genes (386), such as adipogenesis, could likewise be investigated. Furthermore, to extend the analysis of the role of osteoclast pathways in OA pathogenesis, and determine if osteoclast pathways do have a direct role in OA pathogenesis or whether this is mediated by bone turnover, one could perform a GWAS of CTX-1 to identify genetic variants associated with bone resorption. These variants could then be used in an MR analysis of the causal effect of bone resorption on prevalent and progressive OA, using methods described in section 12.2.2 to identify pleiotropy (*i.e.* an effect of the variants on OA not mediated by bone resorption).

12.3.4. Bone shape

This work has focused on the role of bone mass in the pathogenesis of OA and has not focused on the role of bone shape. As discussed in Chapter 1, cam deformities of the hip are a risk factor for OA. More recently, associations between three OA loci and subtle variations in hip shape, such as a wider upper femur, were identified, suggesting a contribution of subtle variations in hip shape in the general population to OA pathogenesis (541). At the knee, relationships between the ratio of medial femoral to tibial subchondral surface area and incident symptoms have been observed (542). Analyses of the role of bone shape in OA pathogenesis were beyond the scope of this PhD.

12.3.5. Radiographic phenotyping in UK Biobank

Looking further ahead, the full data release from the UK Biobank imaging study is expected in 2022. This imaging study aims to recruit 100,000 individuals from the original population for various scans, including hip and knee DXA (343). This will allow the largest possible GWAS of DXA-assessed BMD to be performed (without adjustment for weight), which can be used to determine if FN-BMD does have a stronger causal effect on OA than eBMD. Knee and hip DXA scans

could be used to assess osteophytes and JSN in UK Biobank, as long as this method is validated against grading from radiographs, and automated due to the scale of the task. This will remove the limitation of only having a severe, clinical measure of OA, and will allow most analyses performed in this thesis to be repeated with either a larger sample size or with more specific phenotypes. This will be particularly useful for repeating the pathway analyses to determine the variance explained in each OA sub-phenotype, as this larger sample size should generate more accurate estimates of the proportion of variance explained.

12.4. Translational potential

This work has highlighted the potential to target bone pathways to reduce structural progression of OA. The contribution of the Wnt signalling pathway to variance in OA risk, as well as the observed inverse relationship between sclerostin and thumb JSN, reiterates the potential benefit of Wnt inhibition in reducing structural OA progression (536). However, any treatment for OA must be balanced with the potential adverse impact on BMD and fracture risk, particularly in those more vulnerable to fracture, as the osteoporosis treatment Romosozumab aims to reduce, rather than increase, sclerostin levels (543). As the effect of IGF-1 on OA was of low magnitude and likely to reflect an effect across the lifecourse, targeting the IGF-1 axis is unlikely to be beneficial due to the key role of IGF-1 in skeletal growth and development (504).

Targeting osteoclast pathways may be the best option, as reducing osteoclast function could lead to both BMD increases and reduced OA progression, as highlighted by the promising results for the RCT of the Cathepsin-K inhibitor, MIV-711, discussed in section 3.3.2. However, further analyses are required to determine the exact mechanism by which osteoclast differentiation contributes to OA, and whether this pathway contributes specifically to disease incidence or progression, as this will affect timing of any intervention. Also, development of the Cathepsin-K inhibitor, Odanacatib, developed as an osteoporosis treatment, has been abandoned by the sponsor due to the observation of an increased risk of

cardiovascular events in those taking the drug (544), suggesting that targeting Cathepsin-K may lead to adverse effects on other systems. Alternatively, targeting pathways involved in endochondral ossification may be beneficial in reducing osteophyte formation and thus pain.

It will be important to test any potential treatment in groups with different sub-phenotypes of OA and in those with progressive *vs* non-progressive disease. For example, when patients from the trial of risedronate were stratified by progressors and non-progressors, as defined by change in mJSW, lower subchondral trabecular bone loss at the knee in those taking the highest dose of risedronate was observed in the progression group only (545), suggesting that bisphosphonates may only be effective in individuals with progressive disease, consistent with the theory that subchondral bone turnover is a key feature in the pathogenesis of early-stage disease (18). As the ultimate aim of OA drug trials is to reduce progression in those who already have the disease, interventions targeting risk factors for disease progression rather than incidence will have the greatest benefit for OA patients. Further genetic analyses of OA progression would be beneficial to identify genetic loci associated with disease progression, which could inform development of drugs to specifically reduce progression in those who already have the disease, the ultimate aim of OA drug trials.

Circulating citrate levels may have translational potential as an additional biomarker of bone resorption, should levels be shown to be responsive to therapies known to reduce bone turnover. As citrate may reflect release of inorganic bone mineral into the circulation, measurement of citrate in osteoporosis may provide further information on the resorption process, in addition to CTX-1 which reflects breakdown of the organic phase of the bone matrix.

12.5. Conclusions

In this thesis, I have identified a strong positive relationship between HBM and change in osteophytes and JSN at both the hip and knee, over an average of eight

years. I have confirmed a BMI-independent causal role of BMD on OA risk and provided evidence that this is not fully explained by the shared underlying biological pathways contributing to both BMD and OA. It remains to be determined if the association between BMD and hip/knee OA sub-phenotype progression represents a BMI-independent causal effect, although adjustment for TBFM did not attenuate the relationships between HBM and hip/knee OA sub-phenotype progression.

I have attempted to quantify the role of key bone pathways in variance in OA risk, with results suggesting that the Wnt signalling, TGFβ superfamily and osteoclast differentiation pathways have a direct role in OA pathogenesis. I have provided evidence for a role of the Wnt inhibitor sclerostin in reducing odds of OA specifically at the thumb. This result requires replication in a cohort generalizable to the general population and further analyses to determine causality. Finally, I have provided evidence that circulating levels of IGF-1 are a risk factor for both hip and knee OA. Further work is required to determine if intervening on IGF-1 levels in later life reduces OA risk.

Overall, this work has furthered our knowledge of the role of bone in OA pathogenesis, highlighting BMD as a potential interventional target to reduce structural progression, as well as highlighting specific pathways for further analyses to determine their exact role in pathogenesis (*e.g.* the IGF-1 axis, osteoclast differentiation), which can potentially be translated to novel druggable targets in the future.

REFERENCES

1. Drake RL, Vogl AW, Mitchell AWM. The Body. Gray's Anatomy for students. Third ed. Philadelphia, US: Churchill Livingstone; 2015.
2. Tarafder S, Lee CH. Chapter 14 - Synovial Joint: In Situ Regeneration of Osteochondral and Fibrocartilaginous Tissues by Homing of Endogenous Cells. In: Lee SJ, Yoo JJ, Atala A, editors. In Situ Tissue Regeneration. Boston: Academic Press; 2016. p. 253-73.
3. Poole AR. The Normal Synovial Joint. 2010 [cited 18/02/2014]. In: The OARSI Primer [Internet]. http://primer.oarsi.org/, [cited 18/02/2014].
4. Tamer TM. Hyaluronan and synovial joint: function, distribution and healing. Interdiscip Toxicol. 2013;6(3):111-25.
5. Li G, Yin J, Gao J, Cheng TS, Pavlos NJ, Zhang C, et al. Subchondral bone in osteoarthritis: insight into risk factors and microstructural changes. Arthritis Res Ther. 2013;15(6):223.
6. Willmott H. Trauma and Orthopaedics at a Glance: John Wiley & Sons, Ltd.; 2016.
7. Hunter DJ, Felson DT. Osteoarthritis. BMJ. 2006;332(7542):639.
8. Kraus VB, Blanco FJ, Englund M, Karsdal MA, Lohmander LS. Call for standardized definitions of osteoarthritis and risk stratification for clinical trials and clinical use. Osteoarthr Cartil. 2015;23(8):1233-41.
9. Hochberg MC, Gravallese EM, Silman AJ, Smolen JS, Weinblatt ME, Weisman MH. Rheumatology. Seventh ed. Philadelphia, PA: Elsevier; 2018.
10. Hunter DJ, Bierma-Zeinstra S. Osteoarthritis. Lancet. 2019;393(10182):1745-59.
11. Glyn-Jones S, Palmer AJ, Agricola R, Price AJ, Vincent TL, Weinans H, et al. Osteoarthritis. Lancet. 2015;386(9991):376-87.
12. Akkiraju H, Nohe A. Role of Chondrocytes in Cartilage Formation, Progression of Osteoarthritis and Cartilage Regeneration. J Dev Biol. 2015;3(4):177-92.
13. Mobasheri A, Batt M. An update on the pathophysiology of osteoarthritis. Ann Phys Rehabil Med. 2016;59(5-6):333-9.
14. Man GS, Mologhianu G. Osteoarthritis pathogenesis - a complex process that involves the entire joint. J Med Life. 2014;7(1):37-41.
15. Anandarajah AP. Pathogenesis of Osteoarthritis. In: Bagchi D, Moriyama H, Raychaudhuri S, editors. Arthritis Pathophysiology, prevention, and therapeutics. Florida, US: Taylor and Francis Group; 2011.
16. Lambova SN, Muller-Ladner U. Osteoarthritis - Current Insights in Pathogenesis, Diagnosis and Treatment. Curr Rheumatol Rev. 2018;14(2):91-7.
17. Dreier R. Hypertrophic differentiation of chondrocytes in osteoarthritis: the developmental aspect of degenerative joint disorders. Arthritis Res Ther. 2010;12(5):216.
18. Burr DB, Gallant MA. Bone remodelling in osteoarthritis. Nat Rev Rheumatol. 2012;8(11):665-73.

19. Donell S. Subchondral bone remodelling in osteoarthritis. EFORT Open Rev. 2019;4(6):221-9.
20. Scanzello CR, Goldring SR. The role of synovitis in osteoarthritis pathogenesis. Bone. 2012;51(2):249-57.
21. Robinson WH, Lepus CM, Wang Q, Raghu H, Mao R, Lindstrom TM, et al. Low-grade inflammation as a key mediator of the pathogenesis of osteoarthritis. Nat Rev Rheumatol. 2016;12(10):580-92.
22. Clunie GW, N.; Nikiphorou, E.; Jadon, D. Oxford Handbook of Rheumatology. Fourth ed. New York, United States of America: Oxford University Press; 2018.
23. Altman R, Alarcón G, Appelrouth D, Bloch D, Borenstein D, Brandt K, et al. The American College of Rheumatology criteria for the classification and reporting of osteoarthritis of the hand. Arthritis Rheum. 1990;33(11):1601-10.
24. Altman R, Alarcón G, Appelrouth D, Bloch D, Borenstein D, Brandt K, et al. The American College of Rheumatology criteria for the classification and reporting of osteoarthritis of the hip. Arthritis Rheum. 1991;34(5):505-14.
25. Altman R, Asch E, Bloch D, Bole G, Borenstein D, Brandt K, et al. Development of criteria for the classification and reporting of osteoarthritis. Classification of osteoarthritis of the knee. Diagnostic and Therapeutic Criteria Committee of the American Rheumatism Association. Arthritis Rheum. 1986;29(8):1039-49.
26. Al-Sukaini A, Azam M, Samanta A. Rheumatology A Clinical Handbook. Banbury, Oxfordshire, UK: Scion Publishing Limited; 2014.
27. Buckland-Wright C. Review of the anatomical and radiological differences between fluoroscopic and non-fluoroscopic positioning of osteoarthritic knees. Osteoarthr Cartil. 2006;14 Suppl A:A19-31.
28. Kloppenburg M, Kwok W-Y. Hand osteoarthritis—a heterogeneous disorder. Nat Rev Rheumatol. 2012;8(1):22-31.
29. Altman RD, Gold GE. Atlas of individual radiographic features in osteoarthritis, revised. Osteoarthr Cartil. 2007;15 Suppl A:A1-56.
30. Kellgren JH, Lawrence JS. Radiological assessment of osteo-arthrosis. Ann Rheum Dis. 1957;16(4):494-502.
31. Kohn MD, Sassoon AA, Fernando ND. Classifications in Brief: Kellgren-Lawrence Classification of Osteoarthritis. Clin Orthop Relat Res. 2016;474(8):1886-93.
32. Schiphof D, Boers M, Bierma-Zeinstra SM. Differences in descriptions of Kellgren and Lawrence grades of knee osteoarthritis. Ann Rheum Dis. 2008;67(7):1034-6.
33. Burnett S, Cooper C, Spector T. A radiographic atlas of osteoarthritis. London: Springer Verlag; 1994.
34. Cross M, Smith E, Hoy D, Nolte S, Ackerman I, Fransen M, et al. The global burden of hip and knee osteoarthritis: estimates from the global burden of disease 2010 study. Ann Rheum Dis. 2014;73(7):1323-30.
35. Lawrence RC, Felson DT, Helmick CG, Arnold LM, Choi H, Deyo RA, et al. Estimates of the prevalence of arthritis and other rheumatic conditions in the United States: Part II. Arthritis Rheum. 2008;58(1):26-35.

36. Hawker GA. Osteoarthritis is a serious disease. Clin Exp Rheumatol. 2019;37 Suppl 120(5):3-6.
37. Kim C, Linsenmeyer KD, Vlad SC, Guermazi A, Clancy MM, Niu J, et al. Prevalence of Radiographic and Symptomatic Hip Osteoarthritis in an Urban United States Community: The Framingham Osteoarthritis Study. Arthritis Rheumatol. 2014;66(11):3013-7.
38. Felson DT, Naimark A, Anderson J, Kazis L, Castelli W, Meenan RF. The prevalence of knee osteoarthritis in the elderly. The Framingham Osteoarthritis Study. Arthritis Rheum. 1987;30(8):914-8.
39. Dahaghin S, Bierma-Zeinstra SM, Ginai AZ, Pols HA, Hazes JM, Koes BW. Prevalence and pattern of radiographic hand osteoarthritis and association with pain and disability (the Rotterdam study). Ann Rheum Dis. 2005;64(5):682-7.
40. Haugen IK, Englund M, Aliabadi P, Niu J, Clancy M, Kvien TK, et al. Prevalence, incidence and progression of hand osteoarthritis in the general population: the Framingham Osteoarthritis Study. Ann Rheum Dis. 2011;70(9):1581-6.
41. Johnson VL, Hunter DJ. The epidemiology of osteoarthritis. Best Pract Res Clin Rheumatol. 2014;28(1):5-15.
42. Neogi T, Zhang Y. Epidemiology of osteoarthritis. Rheum Dis Clin North Am. 2013;39(1):1-19.
43. O'Neill TW, McCabe PS, McBeth J. Update on the epidemiology, risk factors and disease outcomes of osteoarthritis. Best Pract Res Clin Rheumatol. 2018;32(2):312-26.
44. Dagenais S, Garbedian S, Wai EK. Systematic review of the prevalence of radiographic primary hip osteoarthritis. Clin Orthop Relat Res. 2009;467(3):623-37.
45. Kerkhof HJ, Meulenbelt I, Akune T, Arden NK, Aromaa A, Bierma-Zeinstra SM, et al. Recommendations for standardization and phenotype definitions in genetic studies of osteoarthritis: the TREAT-OA consortium. Osteoarthr Cartil. 2011;19(3):254-64.
46. Jordan JM, Helmick CG, Renner JB, Luta G, Dragomir AD, Woodard J, et al. Prevalence of Hip Symptoms and Radiographic and Symptomatic Hip Osteoarthritis in African Americans and Caucasians: The Johnston County Osteoarthritis Project. J Rheumatol. 2009;36(4):809.
47. Jordan JM, Helmick CG, Renner JB, Luta G, Dragomir AD, Woodard J, et al. Prevalence of knee symptoms and radiographic and symptomatic knee osteoarthritis in African Americans and Caucasians: the Johnston County Osteoarthritis Project. J Rheumatol. 2007;34(1):172-80.
48. Zhang Y, Xu L, Nevitt MC, Niu J, Goggins JP, Aliabadi P, et al. Lower prevalence of hand osteoarthritis among Chinese subjects in Beijing compared with white subjects in the United States: The Beijing Osteoarthritis Study. Arthritis Rheum. 2003;48(4):1034-40.
49. Nevitt MC, Xu L, Zhang Y, Lui L-Y, Yu W, Lane NE, et al. Very low prevalence of hip osteoarthritis among Chinese elderly in Beijing, China, compared with whites in the United States: The Beijing osteoarthritis study. Arthritis Rheum. 2002;46(7):1773-9.

50. Zhang Y, Xu L, Nevitt MC, Aliabadi P, Yu W, Qin M, et al. Comparison of the prevalence of knee osteoarthritis between the elderly Chinese population in Beijing and whites in the United States: The Beijing osteoarthritis study. Arthritis Rheum. 2001;44(9):2065-71.
51. Felson DT, Zhang Y, Hannan MT, Naimark A, Weissman BN, Aliabadi P, et al. The incidence and natural history of knee osteoarthritis in the elderly, the framingham osteoarthritis study. Arthritis Rheum. 1995;38(10):1500-5.
52. Leyland KM, Hart DJ, Javaid MK, Judge A, Kiran A, Soni A, et al. The natural history of radiographic knee osteoarthritis: A fourteen-year population-based cohort study. Arthritis Rheum. 2012;64(7):2243-51.
53. Oliveria SA, Felson DT, Reed JI, Cirillo PA, Walker AM. Incidence of symptomatic hand, hip, and knee osteoarthritis among patients in a health maintenance organization. Arthritis Rheum. 1995;38(8):1134-41.
54. Kopec JA, Rahman MM, Berthelot JM, Le Petit C, Aghajanian J, Sayre EC, et al. Descriptive epidemiology of osteoarthritis in British Columbia, Canada. J Rheumatol. 2007;34(2):386-93.
55. Sun J, Gooch K, Svenson LW, Bell NR, Frank C. Estimating osteoarthritis incidence from population-based administrative health care databases. Ann Epidemiol. 2007;17(1):51-6.
56. Prieto-Alhambra D, Judge A, Javaid MK, Cooper C, Diez-Perez A, Arden NK. Incidence and risk factors for clinically diagnosed knee, hip and hand osteoarthritis: influences of age, gender and osteoarthritis affecting other joints. Ann Rheum Dis. 2014;73(9):1659-64.
57. Yu D, Peat G, Bedson J, Jordan KP. Annual consultation incidence of osteoarthritis estimated from population-based health care data in England. Rheumatology. 2015;54(11):2051-60.
58. Chen A, Gupte C, Akhtar K, Smith P, Cobb J. The Global Economic Cost of Osteoarthritis: How the UK Compares. Arthritis. 2012;2012:698709.
59. Gupta S, Hawker GA, Laporte A, Croxford R, Coyte PC. The economic burden of disabling hip and knee osteoarthritis (OA) from the perspective of individuals living with this condition. Rheumatology. 2005;44(12):1531-7.
60. March LM, Bachmeier CJ. Economics of osteoarthritis: a global perspective. Baillieres Clin Rheumatol. 1997;11(4):817-34.
61. Murray CJL, Lopez AD, World Health O, World B, Harvard School of Public H. The Global burden of disease : a comprehensive assessment of mortality and disability from diseases, injuries, and risk factors in 1990 and projected to 2020 : summary / edited by Christopher J. L. Murray, Alan D. Lopez. Geneva: World Health Organization; 1996.
62. Vos T, Abajobir AA, Abate KH, Abbafati C, Abbas KM, Abd-Allah F, et al. Global, regional, and national incidence, prevalence, and years lived with disability for 328 diseases and injuries for 195 countries, 1990-2016: a systematic analysis for the Global Burden of Disease Study 2016. Lancet. 2017;390(10100):1211-59.
63. Woolf AD, Pfleger B. Burden of major musculoskeletal conditions. Bull World Health Organ. 2003;81(9):646-56.
64. Vincent TL, Watt FE. Osteoarthritis. Medicine. 2018;46(3):187-95.

65. Srikanth VK, Fryer JL, Zhai G, Winzenberg TM, Hosmer D, Jones G. A meta-analysis of sex differences prevalence, incidence and severity of osteoarthritis. Osteoarthr Cartil. 2005;13(9):769-81.
66. Cirillo DJ, Wallace RB, Wu L, Yood RA. Effect of hormone therapy on risk of hip and knee joint replacement in the Women's Health Initiative. Arthritis Rheum. 2006;54(10):3194-204.
67. Zhai G, Cicuttini F, Srikanth V, Cooley H, Ding C, Jones G. Factors associated with hip cartilage volume measured by magnetic resonance imaging: The Tasmanian Older Adult Cohort Study. Arthritis Rheum. 2005;52(4):1069-76.
68. Cicuttini F, Forbes A, Morris K, Darling S, Bailey M, Stuckey S. Gender differences in knee cartilage volume as measured by magnetic resonance imaging. Osteoarthr Cartil. 1999;7(3):265-71.
69. Jones G, Glisson M, Hynes K, Cicuttini F. Sex and site differences in cartilage development: a possible explanation for variations in knee osteoarthritis in later life. Arthritis Rheum. 2000;43(11):2543-9.
70. Ding C, Cicuttini F, Scott F, Glisson M, Jones G. Sex differences in knee cartilage volume in adults: role of body and bone size, age and physical activity. Rheumatology. 2003;42(11):1317-23.
71. Palazzo C, Nguyen C, Lefevre-Colau M-M, Rannou F, Poiraudeau S. Risk factors and burden of osteoarthritis. Ann Phys Rehabil Med. 2016;59(3):134-8.
72. MacGregor AJ, Antoniades L, Matson M, Andrew T, Spector TD. The genetic contribution to radiographic hip osteoarthritis in women: results of a classic twin study. Arthritis Rheum. 2000;43(11):2410-6.
73. Spector TD, Cicuttini F, Baker J, Loughlin J, Hart D. Genetic influences on osteoarthritis in women: a twin study. BMJ. 1996;312(7036):940-3.
74. Zhai G, Stankovich J, Ding C, Scott F, Cicuttini F, Jones G. The genetic contribution to muscle strength, knee pain, cartilage volume, bone size, and radiographic osteoarthritis: a sibpair study. Arthritis Rheum. 2004;50(3):805-10.
75. Neame RL, Muir K, Doherty S, Doherty M. Genetic risk of knee osteoarthritis: a sibling study. Ann Rheum Dis. 2004;63(9):1022-7.
76. Allen KD. Racial and ethnic disparities in osteoarthritis phenotypes. Curr Opin Rheumatol. 2010;22(5):528-32.
77. Blagojevic M, Jinks C, Jeffery A, Jordan KP. Risk factors for onset of osteoarthritis of the knee in older adults: a systematic review and meta-analysis. Osteoarthr Cartil. 2010;18(1):24-33.
78. Zheng H, Chen C. Body mass index and risk of knee osteoarthritis: systematic review and meta-analysis of prospective studies. BMJ Open. 2015;5(12):e007568.
79. Holliday KL, McWilliams DF, Maciewicz RA, Muir KR, Zhang W, Doherty M. Lifetime body mass index, other anthropometric measures of obesity and risk of knee or hip osteoarthritis in the GOAL case-control study. Osteoarthr Cartil. 2011;19(1):37-43.
80. Christensen R, Bartels EM, Astrup A, Bliddal H. Effect of weight reduction in obese patients diagnosed with knee osteoarthritis: a systematic review and meta-analysis. Ann Rheum Dis. 2007;66(4):433-9.

81. Flugsrud GB, Nordsletten L, Espehaug B, Havelin LI, Meyer HE. Risk factors for total hip replacement due to primary osteoarthritis: a cohort study in 50,034 persons. Arthritis Rheum. 2002;46(3):675-82.
82. Flugsrud GB, Nordsletten L, Espehaug B, Havelin LI, Engeland A, Meyer HE. The impact of body mass index on later total hip arthroplasty for primary osteoarthritis: a cohort study in 1.2 million persons. Arthritis Rheum. 2006;54(3):802-7.
83. Jiang L, Xie X, Wang Y, Wang Y, Lu Y, Tian T, et al. Body mass index and hand osteoarthritis susceptibility: an updated meta-analysis. Int J Rheum Dis. 2016;19(12):1244-54.
84. Xie C, Chen Q. Adipokines: New Therapeutic Target for Osteoarthritis? Curr Rheumatol Rep. 2019;21(12):71.
85. Urban H, Little CB. The role of fat and inflammation in the pathogenesis and management of osteoarthritis. Rheumatology. 2018;57(suppl_4):iv10-iv21.
86. Messina OD, Vidal Wilman M, Vidal Neira LF. Nutrition, osteoarthritis and cartilage metabolism. Aging Clin Exp Res. 2019;31(6):807-13.
87. Thomas S, Browne H, Mobasheri A, Rayman MP. What is the evidence for a role for diet and nutrition in osteoarthritis? Rheumatology. 2018;57(suppl_4):iv61-iv74.
88. Thomas S, Browne H, Mobasheri A, Rayman MP. What is the evidence for a role for diet and nutrition in osteoarthritis? Rheumatology. 2018;57(suppl_4):iv61-iv74.
89. Urquhart DM, Tobing JFL, Hanna FS, Berry P, Wluka AE, Ding C, et al. What Is the Effect of Physical Activity on the Knee Joint? A Systematic Review. Med Sci Sports Exerc. 2011;43(3).
90. Regnaux JP, Lefevre-Colau MM, Trinquart L, Nguyen C, Boutron I, Brosseau L, et al. High-intensity versus low-intensity physical activity or exercise in people with hip or knee osteoarthritis. Cochrane Database Syst Rev. 2015(10):Cd010203.
91. Kraus VB, Sprow K, Powell KE, Buchner D, Bloodgood B, Piercy K, et al. Effects of Physical Activity in Knee and Hip Osteoarthritis: A Systematic Umbrella Review. Med Sci Sports Exerc. 2019;51(6).
92. Yucesoy B, Charles LE, Baker B, Burchfiel CM. Occupational and genetic risk factors for osteoarthritis: a review. Work. 2015;50(2):261-73.
93. Dulay GS, Cooper C, Dennison EM. Knee pain, knee injury, knee osteoarthritis & work. Best Pract Res Clin Rheumatol. 2015;29(3):454-61.
94. Andersen S, Thygesen LC, Davidsen M, Helweg-Larsen K. Cumulative years in occupation and the risk of hip or knee osteoarthritis in men and women: a register-based follow-up study. Occup Environ Med. 2012;69(5):325-30.
95. Schram B, Orr R, Pope R, Canetti E, Knapik J. Risk factors for development of lower limb osteoarthritis in physically demanding occupations: A narrative umbrella review. J Occup Health. 2019;62(1).
96. Kellgren JH, Lawrence JS. Rheumatism in miners. II. X-ray study. Br J Ind Med. 1952;9(3):197-207.

97. Kwon S, Kim W, Yang S, Choi KH. Influence of the type of occupation on osteoarthritis of the knee in men: The Korean National Health and Nutrition Examination Survey 2010-2012. J Occup Health. 2019;61(1):54-62.
98. Litwic A, Edwards MH, Dennison EM, Cooper C. Epidemiology and burden of osteoarthritis. Br Med Bull. 2013;105:185-99.
99. Hui M, Doherty M, Zhang W. Does smoking protect against osteoarthritis? Meta-analysis of observational studies. Ann Rheum Dis. 2011;70(7):1231.
100. Silverwood V, Blagojevic-Bucknall M, Jinks C, Jordan JL, Protheroe J, Jordan KP. Current evidence on risk factors for knee osteoarthritis in older adults: a systematic review and meta-analysis. Osteoarthr Cartil. 2015;23(4):507-15.
101. Kong L, Wang L, Meng F, Cao J, Shen Y. Association between smoking and risk of knee osteoarthritis: a systematic review and meta-analysis. Osteoarthr Cartil. 2017;25(6):809-16.
102. Felson DT, Zhang Y. Smoking and osteoarthritis: a review of the evidence and its implications. Osteoarthr Cartil. 2015;23(3):331-3.
103. Englund M. The role of biomechanics in the initiation and progression of OA of the knee. Best Pract Res Clin Rheumatol. 2010;24(1):39-46.
104. Egloff C, Hügle T, Valderrabano V. Biomechanics and pathomechanisms of osteoarthritis. Swiss Med Wkly. 2012;142:w13583.
105. von Porat A, Roos EM, Roos H. High prevalence of osteoarthritis 14 years after an anterior cruciate ligament tear in male soccer players: a study of radiographic and patient relevant outcomes. Ann Rheum Dis. 2004;63(3):269-73.
106. Englund M, Roos EM, Lohmander LS. Impact of type of meniscal tear on radiographic and symptomatic knee osteoarthritis: a sixteen-year followup of meniscectomy with matched controls. Arthritis Rheum. 2003;48(8):2178-87.
107. Muthuri SG, McWilliams DF, Doherty M, Zhang W. History of knee injuries and knee osteoarthritis: a meta-analysis of observational studies. Osteoarthr Cartil. 2011;19(11):1286-93.
108. Bastick AN, Belo JN, Runhaar J, Bierma-Zeinstra SM. What Are the Prognostic Factors for Radiographic Progression of Knee Osteoarthritis? A Meta-analysis. Clin Orthop Relat Res. 2015;473(9):2969-89.
109. Wilkinson JM, Zeggini E. The Genetic Epidemiology of Joint Shape and the Development of Osteoarthritis. Calcif Tissue Int. 2020.
110. Faber BG, Frysz M, Tobias JH. Unpicking observational relationships between hip shape and osteoarthritis: hype or hope? Curr Opin Rheumatol. 2020;32(1):110-8.
111. Nelson AE. The importance of hip shape in predicting hip osteoarthritis. Current treatment options in rheumatology. 2018;4(2):214-22.
112. Saberi Hosnijeh F, Zuiderwijk ME, Versteeg M, Smeele HT, Hofman A, Uitterlinden AG, et al. Cam Deformity and Acetabular Dysplasia as Risk Factors for Hip Osteoarthritis. Arthritis Rheumatol. 2017;69(1):86-93.
113. Thomas GER, Palmer AJR, Andrade AJ, Pollard TCB, Fary C, Singh PJ, et al. Diagnosis and management of femoroacetabular impingement. Br J Gen Pract. 2013;63(612):e513.

114. Tanamas S, Hanna FS, Cicuttini FM, Wluka AE, Berry P, Urquhart DM. Does knee malalignment increase the risk of development and progression of knee osteoarthritis? A systematic review. Arthritis Rheum. 2009;61(4):459-67.
115. Felson DT, Niu J, Gross KD, Englund M, Sharma L, Cooke TD, et al. Valgus malalignment is a risk factor for lateral knee osteoarthritis incidence and progression: findings from the Multicenter Osteoarthritis Study and the Osteoarthritis Initiative. Arthritis Rheum. 2013;65(2):355-62.
116. Brouwer GM, van Tol AW, Bergink AP, Belo JN, Bernsen RM, Reijman M, et al. Association between valgus and varus alignment and the development and progression of radiographic osteoarthritis of the knee. Arthritis Rheum. 2007;56(4):1204-11.
117. Runhaar J, van Middelkoop M, Reijman M, Vroegindeweij D, Oei EH, Bierma-Zeinstra SM. Malalignment: a possible target for prevention of incident knee osteoarthritis in overweight and obese women. Rheumatology. 2014;53(9):1618-24.
118. Sharma L, Song J, Dunlop D, Felson D, Lewis CE, Segal N, et al. Varus and valgus alignment and incident and progressive knee osteoarthritis. Ann Rheum Dis. 2010;69(11):1940-5.
119. Miyamoto Y, Mabuchi A, Shi D, Kubo T, Takatori Y, Saito S, et al. A functional polymorphism in the 5′ UTR of GDF5 is associated with susceptibility to osteoarthritis. Nat Genet. 2007;39(4):529-33.
120. Francis-West PH, Parish J, Lee K, Archer CW. BMP/GDF-signalling interactions during synovial joint development. Cell Tissue Res. 1999;296(1):111-9.
121. Valdes AM, Spector TD, Doherty S, Wheeler M, Hart DJ, Doherty M. Association of the DVWA and GDF5 polymorphisms with osteoarthritis in UK populations. Ann Rheum Dis. 2009;68(12):1916.
122. Evangelou E, Chapman K, Meulenbelt I, Karassa FB, Loughlin J, Carr A, et al. Large-scale analysis of association between GDF5 and FRZB variants and osteoarthritis of the hip, knee, and hand. Arthritis Rheum. 2009;60(6):1710-21.
123. Valdes AM, Evangelou E, Kerkhof HJ, Tamm A, Doherty SA, Kisand K, et al. The GDF5 rs143383 polymorphism is associated with osteoarthritis of the knee with genome-wide statistical significance. Ann Rheum Dis. 2011;70(5):873-5.
124. Valdes AM, Loughlin J, Timms KM, van Meurs JJB, Southam L, Wilson SG, et al. Genome-wide association scan identifies a prostaglandin-endoperoxide synthase 2 variant involved in risk of knee osteoarthritis. Am J Hum Genet. 2008;82(6):1231-40.
125. Zhai G, van Meurs JB, Livshits G, Meulenbelt I, Valdes AM, Soranzo N, et al. A genome-wide association study suggests that a locus within the ataxin 2 binding protein 1 gene is associated with hand osteoarthritis: the Treat-OA consortium. J Med Genet. 2009;46(9):614-6.
126. Kerkhof HJ, Lories RJ, Meulenbelt I, Jonsdottir I, Valdes AM, Arp P, et al. A genome-wide association study identifies an osteoarthritis susceptibility locus on chromosome 7q22. Arthritis Rheum. 2010;62(2):499-510.
127. Nakajima M, Takahashi A, Kou I, Rodriguez-Fontenla C, Gomez-Reino JJ, Furuichi T, et al. New sequence variants in HLA class II/III region associated

with susceptibility to knee osteoarthritis identified by genome-wide association study. PLoS One. 2010;5(3):e9723.
128. Evangelou E, Valdes AM, Kerkhof HJ, Styrkarsdottir U, Zhu Y, Meulenbelt I, et al. Meta-analysis of genome-wide association studies confirms a susceptibility locus for knee osteoarthritis on chromosome 7q22. Ann Rheum Dis. 2011;70(2):349-55.
129. Panoutsopoulou K, Southam L, Elliott KS, Wrayner N, Zhai G, Beazley C, et al. Insights into the genetic architecture of osteoarthritis from stage 1 of the arcOGEN study. Ann Rheum Dis. 2011;70(5):864-7.
130. Day-Williams AG, Southam L, Panoutsopoulou K, Rayner NW, Esko T, Estrada K, et al. A variant in MCF2L is associated with osteoarthritis. Am J Hum Genet. 2011;89(3):446-50.
131. Zeggini E, Panoutsopoulou K, Southam L, Rayner NW, Day-Williams AG, Lopes MC, et al. Identification of new susceptibility loci for osteoarthritis (arcOGEN): a genome-wide association study. Lancet. 2012;380(9844):815-23.
132. Evangelou E, Kerkhof HJ, Styrkarsdottir U, Ntzani EE, Bos SD, Esko T, et al. A meta-analysis of genome-wide association studies identifies novel variants associated with osteoarthritis of the hip. Ann Rheum Dis. 2014;73(12):2130-6.
133. Styrkarsdottir U, Thorleifsson G, Helgadottir HT, Bomer N, Metrustry S, Bierma-Zeinstra S, et al. Severe osteoarthritis of the hand associates with common variants within the ALDH1A2 gene and with rare variants at 1p31. Nat Genet. 2014;46(5):498-502.
134. Yau MS, Yerges-Armstrong LM, Liu Y, Lewis CE, Duggan DJ, Renner JB, et al. Genome-Wide Association Study of Radiographic Knee Osteoarthritis in North American Caucasians. Arthritis Rheumatol. 2017;69(2):343-51.
135. Styrkarsdottir U, Helgason H, Sigurdsson A, Norddahl GL, Agustsdottir AB, Reynard LN, et al. Whole-genome sequencing identifies rare genotypes in COMP and CHADL associated with high risk of hip osteoarthritis. Nat Genet. 2017;49(5):801-5.
136. Liu Y, Yau MS, Yerges-Armstrong LM, Duggan DJ, Renner JB, Hochberg MC, et al. Genetic Determinants of Radiographic Knee Osteoarthritis in African Americans. J Rheumatol. 2017.
137. Hackinger S, Trajanoska K, Styrkarsdottir U, Zengini E, Steinberg J, Ritchie GRS, et al. Evaluation of shared genetic aetiology between osteoarthritis and bone mineral density identifies SMAD3 as a novel osteoarthritis risk locus. Hum Mol Genet. 2017;26(19):3850-8.
138. Casalone E, Tachmazidou I, Zengini E, Hatzikotoulas K, Hackinger S, Suveges D, et al. A novel variant in GLIS3 is associated with osteoarthritis. Ann Rheum Dis. 2018.
139. Zengini E, Hatzikotoulas K, Tachmazidou I, Steinberg J, Hartwig FP, Southam L, et al. Genome-wide analyses using UK Biobank data provide insights into the genetic architecture of osteoarthritis. Nat Genet. 2018;50(4):549-58.
140. Styrkarsdottir U, Lund SH, Thorleifsson G, Zink F, Stefansson OA, Sigurdsson JK, et al. Meta-analysis of Icelandic and UK data sets identifies missense variants in SMO, IL11, COL11A1 and 13 more new loci associated with osteoarthritis. Nat Genet. 2018.

141. Tachmazidou I, Hatzikotoulas K, Southam L, Esparza-Gordillo J, Haberland V, Zheng J, et al. Identification of new therapeutic targets for osteoarthritis through genome-wide analyses of UK Biobank data. Nat Genet. 2019;51(2):230-6.
142. den Hollander W, Boer CG, Hart DJ, Yau MS, Ramos YFM, Metrustry S, et al. Genome-wide association and functional studies identify a role for matrix Gla protein in osteoarthritis of the hand. Ann Rheum Dis. 2017;76(12):2046-53.
143. Esbrit P, Herrera S, Portal-Núñez S, Nogués X, Díez-Pérez A. Parathyroid Hormone-Related Protein Analogs as Osteoporosis Therapies. Calcif Tissue Int. 2016;98(4):359-69.
144. Wray N, Visscher PM. Estimating Trait Heritability. Nature Education. 2008;1(1):29.
145. Liu JM, Zhao HY, Ning G, Chen Y, Zhang LZ, Sun LH, et al. IGF-1 as an early marker for low bone mass or osteoporosis in premenopausal and postmenopausal women. J Bone Miner Metab. 2008;26(2):159-64.
146. Castano-Betancourt MC, Evans DS, Ramos YF, Boer CG, Metrustry S, Liu Y, et al. Novel Genetic Variants for Cartilage Thickness and Hip Osteoarthritis. PLoS Genet. 2016;12(10):e1006260.
147. Castano Betancourt MC, Cailotto F, Kerkhof HJ, Cornelis FM, Doherty SA, Hart DJ, et al. Genome-wide association and functional studies identify the DOT1L gene to be involved in cartilage thickness and hip osteoarthritis. Proc Natl Acad Sci U S A. 2012;109(21):8218-23.
148. Cibrian Uhalte E, Wilkinson JM, Southam L, Zeggini E. Pathways to understanding the genomic aetiology of osteoarthritis. Hum Mol Genet. 2017;26(R2):R193-r201.
149. Skarp S, Kamarainen OP, Wei GH, Jakkula E, Kiviranta I, Kroger H, et al. Whole exome sequencing in Finnish families identifies new candidate genes for osteoarthritis. PLoS One. 2018;13(8):e0203313.
150. Beswick AD, Wylde V, Gooberman-Hill R, Blom A, Dieppe P. What proportion of patients report long-term pain after total hip or knee replacement for osteoarthritis? A systematic review of prospective studies in unselected patients. BMJ Open. 2012;2(1):e000435.
151. Watt FE, Hamid B, Garriga C, Judge A, Hrusecka R, Custers RJH, et al. The molecular profile of synovial fluid changes upon joint distraction and is associated with clinical response in knee osteoarthritis. Osteoarthr Cartil. 2020;28(3):324-33.
152. Jansen MP, Boymans T, Custers RJH, Van Geenen RCI, Van Heerwaarden RJ, Huizinga MR, et al. Knee Joint Distraction as Treatment for Osteoarthritis Results in Clinical and Structural Benefit: A Systematic Review and Meta-Analysis of the Limited Number of Studies and Patients Available. Cartilage. 2020:1947603520942945.
153. Takahashi T, Baboolal TG, Lamb J, Hamilton TW, Pandit HG. Is Knee Joint Distraction a Viable Treatment Option for Knee OA?-A Literature Review and Meta-Analysis. J Knee Surg. 2019;32(8):788-95.
154. Goh EL, Lou WCN, Chidambaram S, Ma S. The role of joint distraction in the treatment of knee osteoarthritis: a systematic review and quantitative analysis. Orthop Res Rev. 2019;11:79-92.

155. Burr DB. Chapter 1 - Bone Morphology and Organization. In: Burr DB, Allen MR, editors. Basic and Applied Bone Biology (Second Edition): Academic Press; 2019. p. 3-26.
156. Carter DR, Beaupré GS. Skeletal Tissue Histomorphology and Mechanics. Skeletal Function and Form: Mechanobiology of Skeletal Development, Aging, and Regeneration. Cambridge: Cambridge University Press; 2000. p. 31-52.
157. Boskey AL, Robey PG. The Composition of Bone. Primer on the Metabolic Bone Diseases and Disorders of Mineral Metabolism. 2018:84-92.
158. Bradley EW, Westendorf JJ, van Wijnen AJ, Dudakovic A. Osteoblasts. Primer on the Metabolic Bone Diseases and Disorders of Mineral Metabolism. 2018:31-7.
159. Bonewald LF. Osteocytes. Primer on the Metabolic Bone Diseases and Disorders of Mineral Metabolism. 2018:38-45.
160. Karner CM, Hilton MJ. Endochondral Ossification. Primer on the Metabolic Bone Diseases and Disorders of Mineral Metabolism. 2018:12-9.
161. Takayanagi H. Osteoclast Biology and Bone Resorption. Primer on the Metabolic Bone Diseases and Disorders of Mineral Metabolism. 2018:46-53.
162. Yasuda Y, Kaleta J, Brömme D. The role of cathepsins in osteoporosis and arthritis: Rationale for the design of new therapeutics. Adv Drug Deliv Rev. 2005;57(7):973-93.
163. Stone JA, McCrea JB, Witter R, Zajic S, Stoch SA. Clinical and translational pharmacology of the cathepsin K inhibitor odanacatib studied for osteoporosis. Br J Clin Pharmacol. 2019;85(6):1072-83.
164. Burr DB, Bellido T, White KE. Bone structure and function. In: Hochberg MC, Silman A, Smolen J, Weinblatt ME, Weisman M, editors. Rheumatology. 1. Sixth ed: Elsevier 2015. p. 42-55.
165. Bou-Gharios G, de Crombrugghe B. Type I Collagen Structure, Synthesis and Regulation. In: Bilezikian JP, Raisz LG, Martin TJ, editors. Principles of Bone Biology. 1. Third ed: Elsevier; 2008. p. 285-318.
166. Currey JD. Bones : structure and mechanics. Second ed. Princeton, N.J. : Princeton University Press; 2006.
167. Bilezikian JP, Raisz LG, Rodan GA. Principles of bone biology. Second ed. San Diego: Academic Press; 2002.
168. Alvarez J, Horton J, Sohn P, Serra R. The perichondrium plays an important role in mediating the effects of TGF-beta1 on endochondral bone formation. Dev Dyn. 2001;221(3):311-21.
169. de Gorter DJJ, Sánchez-Duffhues G, ten Dijke P. Signal Transduction Cascades Controlling Osteoblast Differentiation. Primer on the Metabolic Bone Diseases and Disorders of Mineral Metabolism. 2018:54-9.
170. A. Zhong Z, Ethen NJ, Williams BO. Recent Developments in Understanding the Role of Wnt Signaling in Skeletal Development and Disease. Primer on the Metabolic Bone Diseases and Disorders of Mineral Metabolism. 2018:68-74.
171. Lories RJ, Corr M, Lane NE. To Wnt or not to Wnt: the bone and joint health dilemma. Nat Rev Rheumatol. 2013;9(6):328-39.

172. Wu M, Chen G, Li Y-P. TGF-β and BMP signaling in osteoblast, skeletal development, and bone formation, homeostasis and disease. Bone Res. 2016;4:16009-.
173. MacFarlane EG, Haupt J, Dietz HC, Shore EM. TGF-β Family Signaling in Connective Tissue and Skeletal Diseases. Cold Spring Harb Perspect Biol. 2017;9(11).
174. Shi C, Mishina Y. The TGF-β Superfamily in Bone Formation and Maintenance. Primer on the Metabolic Bone Diseases and Disorders of Mineral Metabolism. 2018:60-7.
175. Zhai G, Doré J, Rahman P. TGF-β signal transduction pathways and osteoarthritis. Rheumatol Int. 2015;35(8):1283-92.
176. Wysolmerski JJ. Parathyroid Hormone-Related Protein: An Update. J Clin Endocrinol Metab. 2012;97(9):2947-56.
177. Isales CM, Seeman E. Menopause and Age-related Bone Loss. Primer on the Metabolic Bone Diseases and Disorders of Mineral Metabolism. 2018:155-61.
178. Kenkre JS, Bassett J. The bone remodelling cycle. Ann Clin Biochem. 2018;55(3):308-27.
179. Allen MR, Burr DB. Chapter 5 - Bone Growth, Modeling, and Remodeling. In: Burr DB, Allen MR, editors. Basic and Applied Bone Biology (Second Edition): Academic Press; 2019. p. 85-100.
180. Rucci N. Molecular biology of bone remodelling. Clin Cases Miner Bone Metab. 2008;5(1):49-56.
181. Szulc P, Bauer DC, Eastell R. Biochemical Markers of Bone Turnover in Osteoporosis. Primer on the Metabolic Bone Diseases and Disorders of Mineral Metabolism. 2018:293-301.
182. de la Piedra C, Calero JA, Traba ML, Asensio MD, Argente J, Muñoz MT. Urinary α and β C-Telopeptides of Collagen I: Clinical Implications in Bone Remodeling in Patients with Anorexia Nervosa. Osteoporos Int. 1999;10(6):480-6.
183. Njeh CF, Fuerst T, Hans D, Blake GM, Genant HK. Radiation exposure in bone mineral density assessment. Appl Radiat Isot. 1999;50(1):215-36.
184. Lewiecki EM, Miller PD, Watts NB. Standard Techniques of Bone Mass Measurement in Adults. Primer on the Metabolic Bone Diseases and Disorders of Mineral Metabolism. 2018:252-9.
185. World Health O. Assessment of fracture risk and its application to screening for postmenopausal osteoporosis : report of a WHO study group [meeting held in Rome from 22 to 25 June 1992]. Geneva: World Health Organization; 1994.
186. McClung MR, Miller PD, Papapoulos SE. Osteoporosis. Primer on the Metabolic Bone Diseases and Disorders of Mineral Metabolism. 2018:393-7.
187. Harvey NC, Curtis EM, Dennison EM, Cooper C. The Epidemiology of Osteoporotic Fractures. Primer on the Metabolic Bone Diseases and Disorders of Mineral Metabolism. 2018:398-404.
188. Giusti A, Papapoulos SE. Bisphosphonates for Postmenopausal Osteoporosis. Primer on the Metabolic Bone Diseases and Disorders of Mineral Metabolism. 2018:545-52.

189. Costa AG, Lewiecki EM, Bilezikian JP. Denosumab. Primer on the Metabolic Bone Diseases and Disorders of Mineral Metabolism. 2018:553-8.
190. Cosman F, Greenspan SL. Parathyroid Hormone and Abaloparatide Treatment for Osteoporosis. Primer on the Metabolic Bone Diseases and Disorders of Mineral Metabolism. 2018:559-66.
191. Silva BC, Bilezikian JP. Parathyroid hormone: anabolic and catabolic actions on the skeleton. Curr Opin Pharmacol. 2015;22:41-50.
192. McClung MR. Future Therapies. Primer on the Metabolic Bone Diseases and Disorders of Mineral Metabolism. 2018:603-9.
193. Gregson CL, Hardcastle SA, Cooper C, Tobias JH. Friend or foe: high bone mineral density on routine bone density scanning, a review of causes and management. Rheumatology. 2013;52(6):968-85.
194. Gelb BD, Shi G-P, Chapman HA, Desnick RJ. Pycnodysostosis, a Lysosomal Disease Caused by Cathepsin K Deficiency. Science. 1996;273(5279):1236.
195. Leupin O, Piters E, Halleux C, Hu S, Kramer I, Morvan F, et al. Bone overgrowth-associated mutations in the LRP4 gene impair sclerostin facilitator function. J Biol Chem. 2011;286(22):19489-500.
196. Gregson CL, Wheeler L, Hardcastle SA, Appleton LH, Addison KA, Brugmans M, et al. Mutations in Known Monogenic High Bone Mass Loci Only Explain a Small Proportion of High Bone Mass Cases. J Bone Miner Res. 2016;31(3):640-9.
197. Gregson CL, Steel SA, O'Rourke KP, Allan K, Ayuk J, Bhalla A, et al. 'Sink or swim': an evaluation of the clinical characteristics of individuals with high bone mass. Osteoporosis Int. 2012;23(2):643-54.
198. Gregson CL, Steel S, Yoshida K, Reid M, Tobias JH. An Investigation into the Impact of Osteoarthritic Changes on Bone Mineral Density Measurements in Patients with High Bone Mass. American Society for Bone Mineral Research; Montreal, Canada2008.
199. Little RD, Carulli JP, Del Mastro RG, Dupuis J, Osborne M, Folz C, et al. A mutation in the LDL receptor-related protein 5 gene results in the autosomal dominant high-bone-mass trait. Am J Hum Genet. 2002;70(1):11-9.
200. Gregson CL, Sayers A, Lazar V, Steel S, Dennison EM, Cooper C, et al. The high bone mass phenotype is characterised by a combined cortical and trabecular bone phenotype: findings from a pQCT case-control study. Bone. 2013;52(1):380-8.
201. Gregson CL, Paggiosi MA, Crabtree N, Steel SA, McCloskey E, Duncan EL, et al. Analysis of body composition in individuals with high bone mass reveals a marked increase in fat mass in women but not men. J Clin Endocrinol Metab. 2013;98(2):818-28.
202. Lee NK, Sowa H, Hinoi E, Ferron M, Ahn JD, Confavreux C, et al. Endocrine regulation of energy metabolism by the skeleton. Cell. 2007;130(3):456-69.
203. Gregson CL, Newell F, Leo PJ, Clark GR, Paternoster L, Marshall M, et al. Genome-wide association study of extreme high bone mass: Contribution of common genetic variation to extreme BMD phenotypes and potential novel BMD-associated genes. Bone. 2018;114:62-71.

204. Estrada K, Styrkarsdottir U, Evangelou E, Hsu YH, Duncan EL, Ntzani EE, et al. Genome-wide meta-analysis identifies 56 bone mineral density loci and reveals 14 loci associated with risk of fracture. Nat Genet. 2012;44(5):491-501.
205. Gregson CL, Bergen DJM, Leo P, Sessions RB, Wheeler L, Hartley A, et al. A Rare Mutation in SMAD9 Associated With High Bone Mass Identifies the SMAD-Dependent BMP Signaling Pathway as a Potential Anabolic Target for Osteoporosis. J Bone Miner Res. 2020;35(1):92-105.
206. Foss MV, Byers PD. Bone density, osteoarthrosis of the hip, and fracture of the upper end of the femur. Ann Rheum Dis. 1972;31(4):259-64.
207. Hardcastle SA, Dieppe P, Gregson CL, Davey Smith G, Tobias JH. Osteoarthritis and bone mineral density: are strong bones bad for joints? BoneKEy Rep. 2015;4:624.
208. Nevitt MC, Lane NE, Scott JC, Hochberg MC, Pressman AR, Genant HK, et al. Radiographic osteoarthritis of the hip and bone mineral density. The Study of Osteoporotic Fractures Research Group. Arthritis Rheum. 1995;38(7):907-16.
209. Burger H, van Daele PL, Odding E, Valkenburg HA, Hofman A, Grobbee DE, et al. Association of radiographically evident osteoarthritis with higher bone mineral density and increased bone loss with age. The Rotterdam Study. Arthritis Rheum. 1996;39(1):81-6.
210. Chaganti RK, Parimi N, Lang T, Orwoll E, Stefanick ML, Nevitt M, et al. Bone mineral density and prevalent osteoarthritis of the hip in older men for the Osteoporotic Fractures in Men (MrOS) Study Group. Osteoporos Int. 2010;21(8):1307-16.
211. Antoniades L, MacGregor AJ, Matson M, Spector TD. A cotwin control study of the relationship between hip osteoarthritis and bone mineral density. Arthritis Rheum. 2000;43(7):1450-5.
212. Hannan MT, Anderson JJ, Zhang Y, Levy D, Felson DT. Bone mineral density and knee osteoarthritis in elderly men and women. The Framingham Study. Arthritis Rheum. 1993;36(12):1671-80.
213. Hart DJ, Mootoosamy I, Doyle DV, Spector TD. The relationship between osteoarthritis and osteoporosis in the general population: the Chingford Study. Ann Rheum Dis. 1994;53(3):158-62.
214. Sowers M, Lachance L, Jamadar D, Hochberg MC, Hollis B, Crutchfield M, et al. The associations of bone mineral density and bone turnover markers with osteoarthritis of the hand and knee in pre- and perimenopausal women. Arthritis Rheum. 1999;42(3):483-9.
215. Lee S, Kim TN, Kim SH. Knee osteoarthritis is associated with increased prevalence of vertebral fractures despite high systemic bone mineral density: a cross-sectional study in an Asian population. Mod Rheumatol. 2014;24(1):172-81.
216. Wen L, Shin MH, Kang JH, Yim YR, Kim JE, Lee JW, et al. The relationships between bone mineral density and radiographic features of hand or knee osteoarthritis in older adults: data from the Dong-gu Study. Rheumatology. 2016;55(3):495-503.
217. Sowers MF, Hochberg M, Crabbe JP, Muhich A, Crutchfield M, Updike S. Association of bone mineral density and sex hormone levels with osteoarthritis

of the hand and knee in premenopausal women. Am J Epidemiol. 1996;143(1):38-47.
218. Arokoski JP, Arokoski MH, Jurvelin JS, Helminen HJ, Niemitukia LH, Kroger H. Increased bone mineral content and bone size in the femoral neck of men with hip osteoarthritis. Ann Rheum Dis. 2002;61(2):145-50.
219. Iwamoto J, Takeda T, Ichimura S. Forearm bone mineral density in postmenopausal women with osteoarthritis of the knee. J Orthop Sci. 2002;7(1):19-25.
220. Glowacki J, Tuteja M, Hurwitz S, Thornhill TS, Leboff MS. Discordance in femoral neck bone density in subjects with unilateral hip osteoarthritis. J Clin Densitom. 2010;13(1):24-8.
221. Goerres GW, Hauselmann HJ, Seifert B, Michel BA, Uebelhart D. Patients with knee osteoarthritis have lower total hip bone mineral density in the symptomatic leg than in the contralateral hip. J Clin Densitom. 2005;8(4):484-7.
222. Karlsson MK, Magnusson H, Coster MC, Vonschewelov T, Karlsson C, Rosengren BE. Patients with hip osteoarthritis have a phenotype with high bone mass and low lean body mass. Clin Orthop Relat Res. 2014;472(4):1224-9.
223. Karlsson MK, Magnusson H, von Schewelov T, Coster M, Karlsson C, Rosengren BE. Patients with Osteoarthritis in all Three Knee Compartments and Patients with Medial Knee Osteoarthritis Have a Phenotype with High Bone Mass and High Fat Mass but Proportionally Low Lean Mass. Open Orthop J. 2014;8:390-6.
224. Karlsson MK, Magnusson H, Coster M, Karlsson C, Rosengren BE. Patients with knee osteoarthritis have a phenotype with higher bone mass, higher fat mass, and lower lean body mass. Clin Orthop Relat Res. 2015;473(1):258-64.
225. von Schewelov T, Magnusson H, Coster M, Karlsson C, Rosengren BE. Osteoarthritis of the Distal Interphalangeal and First Carpometacarpal Joints is Associated with High Bone Mass in Women and Small Bone Size and Low Lean Mass in Men. Open Orthop J. 2015;9:399-404.
226. Hardcastle SA, Dieppe P, Gregson CL, Hunter D, Thomas GE, Arden NK, et al. Prevalence of radiographic hip osteoarthritis is increased in high bone mass. Osteoarthr Cartil. 2014;22(8):1120-8.
227. Hardcastle SA, Dieppe P, Gregson CL, Arden NK, Spector TD, Hart DJ, et al. Individuals with high bone mass have an increased prevalence of radiographic knee osteoarthritis. Bone. 2015;71:171-9.
228. Gregson CL, Hardcastle SA, Murphy A, Faber B, Fraser WD, Williams M, et al. High Bone Mass is associated with bone-forming features of osteoarthritis in non-weight bearing joints independent of body mass index. Bone. 2017;97:306-13.
229. Zhang Y, Hannan MT, Chaisson CE, McAlindon TE, Evans SR, Aliabadi P, et al. Bone mineral density and risk of incident and progressive radiographic knee osteoarthritis in women: the Framingham Study. J Rheumatol. 2000;27(4):1032-7.
230. Hochberg MC, Lethbridge-Cejku M, Tobin JD. Bone mineral density and osteoarthritis: data from the Baltimore Longitudinal Study of Aging. Osteoarthr Cartil. 2004;12 Suppl A:S45-8.

231. Barbour KE, Murphy LB, Helmick CG, Hootman JM, Renner JB, Jordan JM. Bone Mineral Density and the Risk of Hip and Knee Osteoarthritis: The Johnston County Osteoarthritis Project. Arthritis Care Res. 2017;69(12):1863-70.
232. Bergink AP, Uitterlinden AG, Van Leeuwen JP, Hofman A, Verhaar JA, Pols HA. Bone mineral density and vertebral fracture history are associated with incident and progressive radiographic knee osteoarthritis in elderly men and women: the Rotterdam Study. Bone. 2005;37(4):446-56.
233. Hart DJ, Cronin C, Daniels M, Worthy T, Doyle DV, Spector TD. The relationship of bone density and fracture to incident and progressive radiographic osteoarthritis of the knee: the Chingford Study. Arthritis Rheum. 2002;46(1):92-9.
234. Nevitt MC, Zhang Y, Javaid MK, Neogi T, Curtis JR, Niu J, et al. High systemic bone mineral density increases the risk of incident knee OA and joint space narrowing, but not radiographic progression of existing knee OA: the MOST study. Ann Rheum Dis. 2010;69(1):163-8.
235. Bergink AP, Rivadeneira F, Bierma-Zeinstra SM, Carola Zillikens M, Arfan Ikram M, Uitterlinden AG, et al. Are bone mineral density and fractures related to the incidence and progression of radiographic osteoarthritis of the knee, hip and hand in elderly men and women? the rotterdam study. Arthritis Rheumatol. 2018.
236. Paternoster L, Tilling K, Davey Smith G. Genetic epidemiology and Mendelian randomization for informing disease therapeutics: Conceptual and methodological challenges. PLoS Genet. 2017;13(10):e1006944.
237. National Joint Registry for England, Wales, Northern Ireland and the Isle of Man 16th Annual Report. 2019.
238. Pelletier JP, Cooper C, Peterfy C, Reginster JY, Brandi ML, Bruyère O, et al. What is the predictive value of MRI for the occurrence of knee replacement surgery in knee osteoarthritis? Ann Rheum Dis. 2013;72(10):1594.
239. Hardcastle SA, Gregson CL, Deere KC, Smith GD, Dieppe P, Tobias JH. High bone mass is associated with an increased prevalence of joint replacement: a case-control study. Rheumatology. 2013;52(6):1042-51.
240. Cai G, Otahal P, Cicuttini F, Wu F, Munugoda IP, Jones G, et al. The association of subchondral and systemic bone mineral density with osteoarthritis-related joint replacements in older adults. Osteoarthr Cartil. 2020.
241. Peel NF, Barrington NA, Blumsohn A, Colwell A, Hannon R, Eastell R. Bone mineral density and bone turnover in spinal osteoarthrosis. Ann Rheum Dis. 1995;54(11):867-71.
242. Garnero P, Piperno M, Gineyts E, Christgau S, Delmas PD, Vignon E. Cross sectional evaluation of biochemical markers of bone, cartilage, and synovial tissue metabolism in patients with knee osteoarthritis: relations with disease activity and joint damage. Ann Rheum Dis. 2001;60(6):619-26.
243. Stewart A, Black A, Robins SP, Reid DM. Bone density and bone turnover in patients with osteoarthritis and osteoporosis. J Rheumatol. 1999;26(3):622-6.
244. Bettica P, Cline G, Hart DJ, Meyer J, Spector TD. Evidence for increased bone resorption in patients with progressive knee osteoarthritis: longitudinal results from the Chingford study. Arthritis Rheum. 2002;46(12):3178-84.

245. Jordan KM, Syddall HE, Garnero P, Gineyts E, Dennison EM, Sayer AA, et al. Urinary CTX-II and glucosyl-galactosyl-pyridinoline are associated with the presence and severity of radiographic knee osteoarthritis in men. Ann Rheum Dis. 2006;65(7):871-7.
246. Hunter DJ, Hart D, Snieder H, Bettica P, Swaminathan R, Spector TD. Evidence of altered bone turnover, vitamin D and calcium regulation with knee osteoarthritis in female twins. Rheumatology. 2003;42(11):1311-6.
247. Min S, Wang C, Lu W, Xu Z, Shi D, Chen D, et al. Serum levels of the bone turnover markers dickkopf-1, osteoprotegerin, and TNF-alpha in knee osteoarthritis patients. Clin Rheumatol. 2017.
248. Dieppe P, Cushnaghan J, Young P, Kirwan J. Prediction of the progression of joint space narrowing in osteoarthritis of the knee by bone scintigraphy. Ann Rheum Dis. 1993;52(8):557-63.
249. McCarthy C, Cushnaghan J, Dieppe P. The predictive role of scintigraphy in radiographic osteoarthritis of the hand. Osteoarthr Cartil. 1994;2(1):25-8.
250. Nwosu LN, Allen M, Wyatt L, Huebner JL, Chapman V, Walsh DA, et al. Pain prediction by serum biomarkers of bone turnover in people with knee osteoarthritis: an observational study of TRAcP5b and cathepsin K in OA. Osteoarthr Cartil. 2017;25(6):858-65.
251. Bruyere O, Delferriere D, Roux C, Wark JD, Spector T, Devogelaer JP, et al. Effects of strontium ranelate on spinal osteoarthritis progression. Ann Rheum Dis. 2008;67(3):335-9.
252. Alexandersen P, Karsdal MA, Byrjalsen I, Christiansen C. Strontium ranelate effect in postmenopausal women with different clinical levels of osteoarthritis. Climacteric. 2011;14(2):236-43.
253. Cooper C, Reginster J-Y, Chapurlat R, Christiansen C, Genant H, Bellamy N, et al. Efficacy and safety of oral strontium ranelate for the treatment of knee osteoarthritis: rationale and design of randomised, double-blind, placebo-controlled trial. Curr Med Res Opin. 2012;28(2):231-9.
254. Reginster J-Y, Beaudart C, Neuprez A, Bruyère O. Strontium ranelate in the treatment of knee osteoarthritis: new insights and emerging clinical evidence. Ther Adv Musculoskelet Dis. 2013;5(5):268-76.
255. Bruyère O, Reginster J-Y, Bellamy N, Chapurlat R, Richette P, Cooper C, et al. Clinically meaningful effect of strontium ranelate on symptoms in knee osteoarthritis: a responder analysis. Rheumatology. 2014;53(8):1457-64.
256. Pelletier J-P, Roubille C, Raynauld J-P, Abram F, Dorais M, Delorme P, et al. Disease-modifying effect of strontium ranelate in a subset of patients from the Phase III knee osteoarthritis study SEKOIA using quantitative MRI: reduction in bone marrow lesions protects against cartilage loss. Ann Rheum Dis. 2015;74(2):422-9.
257. Tenti S, Cheleschi S, Guidelli GM, Galeazzi M, Fioravanti A. What about strontium ranelate in osteoarthritis? Doubts and securities. Mod Rheumatol. 2014;24(6):881-4.
258. Spector TD, Conaghan PG, Buckland-Wright JC, Garnero P, Cline GA, Beary JF, et al. Effect of risedronate on joint structure and symptoms of knee

osteoarthritis: results of the BRISK randomized, controlled trial [ISRCTN01928173]. Arthritis Res Ther. 2005;7(3):R625-R33.
259. Bingham CO, 3rd, Buckland-Wright JC, Garnero P, Cohen SB, Dougados M, Adami S, et al. Risedronate decreases biochemical markers of cartilage degradation but does not decrease symptoms or slow radiographic progression in patients with medial compartment osteoarthritis of the knee: results of the two-year multinational knee osteoarthritis structural arthritis study. Arthritis Rheum. 2006;54(11):3494-507.
260. Garnero P, Aronstein WS, Cohen SB, Conaghan PG, Cline GA, Christiansen C, et al. Relationships between biochemical markers of bone and cartilage degradation with radiological progression in patients with knee osteoarthritis receiving risedronate: the Knee Osteoarthritis Structural Arthritis randomized clinical trial. Osteoarthr Cartil. 2008;16(6):660-6.
261. Funck-Brentano T, Nethander M, Movérare-Skrtic S, Richette P, Ohlsson C. Causal Factors for Knee, Hip, and Hand Osteoarthritis: A Mendelian Randomization Study in the UK Biobank. Arthritis Rheumatol. 2019;71(10):1634-41.
262. Yerges-Armstrong LM, Yau MS, Liu Y, Krishnan S, Renner JB, Eaton CB, et al. Association analysis of BMD-associated SNPs with knee osteoarthritis. J Bone Miner Res. 2014;29(6):1373-9.
263. Luyten FP, Tylzanowski P, Lories RJ. Wnt signaling and osteoarthritis. Bone. 2009;44(4):522-7.
264. Corr M. Wnt-beta-catenin signaling in the pathogenesis of osteoarthritis. Nat Clin Pract Rheumatol. 2008;4(10):550-6.
265. Wang Y, Fan X, Xing L, Tian F. Wnt signaling: a promising target for osteoarthritis therapy. Cell communication and signaling : CCS. 2019;17(1):97.
266. Loughlin J, Dowling B, Chapman K, Marcelline L, Mustafa Z, Southam L, et al. Functional variants within the secreted frizzled-related protein 3 gene are associated with hip osteoarthritis in females. Proc Natl Acad Sci U S A. 2004;101(26):9757-62.
267. Lane NE, Lian K, Nevitt MC, Zmuda JM, Lui L, Li J, et al. Frizzled-related protein variants are risk factors for hip osteoarthritis. Arthritis Rheum. 2006;54(4):1246-54.
268. Min JL, Meulenbelt I, Riyazi N, Kloppenburg M, Houwing-Duistermaat JJ, Seymour AB, et al. Association of the Frizzled-related protein gene with symptomatic osteoarthritis at multiple sites. Arthritis Rheum. 2005;52(4):1077-80.
269. Leijten JC, Bos SD, Landman EB, Georgi N, Jahr H, Meulenbelt I, et al. GREM1, FRZB and DKK1 mRNA levels correlate with osteoarthritis and are regulated by osteoarthritis-associated factors. Arthritis Res Ther. 2013;15(5):R126.
270. van den Bosch MH, Blom AB, van de Loo FA, Koenders MI, Lafeber FP, van den Berg WB, et al. Brief Report: Induction of Matrix Metalloproteinase Expression by Synovial Wnt Signaling and Association With Disease Progression in Early Symptomatic Osteoarthritis. Arthritis Rheumatol. 2017;69(10):1978-83.
271. Monteagudo S, Cornelis FMF, Aznar-Lopez C, Yibmantasiri P, Guns LA, Carmeliet P, et al. DOT1L safeguards cartilage homeostasis and protects against osteoarthritis. Nat Commun. 2017;8:15889.

272. Evangelou E, Valdes AM, Castano-Betancourt MC, Doherty M, Doherty S, Esko T, et al. The DOT1L rs12982744 polymorphism is associated with osteoarthritis of the hip with genome-wide statistical significance in males. Ann Rheum Dis. 2013;72(7):1264-5.
273. Weng LH, Wang CJ, Ko JY, Sun YC, Wang FS. Control of Dkk-1 ameliorates chondrocyte apoptosis, cartilage destruction, and subchondral bone deterioration in osteoarthritic knees. Arthritis Rheum. 2010;62(5):1393-402.
274. Oh H, Chun C-H, Chun J-S. Dkk-1 expression in chondrocytes inhibits experimental osteoarthritic cartilage destruction in mice. Arthritis Rheum. 2012;64(8):2568-78.
275. Funck-Brentano T, Bouaziz W, Marty C, Geoffroy V, Hay E, Cohen-Solal M. Dkk-1-mediated inhibition of Wnt signaling in bone ameliorates osteoarthritis in mice. Arthritis Rheumatol. 2014;66(11):3028-39.
276. Zarei A, Hulley PA, Sabokbar A, Javaid MK. Co-expression of DKK-1 and Sclerostin in Subchondral Bone of the Proximal Femoral Heads from Osteoarthritic Hips. Calcif Tissue Int. 2017;100(6):609-18.
277. Bouaziz W, Funck-Brentano T, Lin H, Marty C, Ea HK, Hay E, et al. Loss of sclerostin promotes osteoarthritis in mice via beta-catenin-dependent and -independent Wnt pathways. Arthritis Res Ther. 2015;17:24.
278. Chan BY, Fuller ES, Russell AK, Smith SM, Smith MM, Jackson MT, et al. Increased chondrocyte sclerostin may protect against cartilage degradation in osteoarthritis. Osteoarthr Cartil. 2011;19(7):874-85.
279. Roudier M, Li X, Niu QT, Pacheco E, Pretorius JK, Graham K, et al. Sclerostin is expressed in articular cartilage but loss or inhibition does not affect cartilage remodeling during aging or following mechanical injury. Arthritis Rheum. 2013;65(3):721-31.
280. Zhou S, Ge Y, Li Y, Bao Z, Yao C, Teng H, et al. Accelerated development of instability-induced osteoarthritis in transgenic mice overexpressing SOST. Int J Clin Exp Pathol. 2017;10(11):10830-40.
281. Wu L, Guo H, Sun K, Zhao X, Ma T, Jin Q. Sclerostin expression in the subchondral bone of patients with knee osteoarthritis. Int J Mol Med. 2016;38(5):1395-402.
282. Abed E, Couchourel D, Delalandre A, Duval N, Pelletier JP, Martel-Pelletier J, et al. Low sirtuin 1 levels in human osteoarthritis subchondral osteoblasts lead to abnormal sclerostin expression which decreases Wnt/beta-catenin activity. Bone. 2014;59:28-36.
283. Blom AB, Brockbank SM, van Lent PL, van Beuningen HM, Geurts J, Takahashi N, et al. Involvement of the Wnt signaling pathway in experimental and human osteoarthritis: prominent role of Wnt-induced signaling protein 1. Arthritis Rheum. 2009;60(2):501-12.
284. Nalesso G, Thomas BL, Sherwood JC, Yu J, Addimanda O, Eldridge SE, et al. WNT16 antagonises excessive canonical WNT activation and protects cartilage in osteoarthritis. Ann Rheum Dis. 2017;76(1):218-26.
285. Törnqvist AE, Grahnemo L, Nilsson KH, Funck-Brentano T, Ohlsson C, Movérare-Skrtic S. Wnt16 Overexpression in Osteoblasts Increases the

Subchondral Bone Mass but has no Impact on Osteoarthritis in Young Adult Female Mice. Calcif Tissue Int. 2020.
286. Lodewyckx L, Luyten FP, Lories RJ. Genetic deletion of low-density lipoprotein receptor-related protein 5 increases cartilage degradation in instability-induced osteoarthritis. Rheumatology. 2012;51(11):1973-8.
287. Shin Y, Huh YH, Kim K, Kim S, Park KH, Koh J-T, et al. Low-density lipoprotein receptor–related protein 5 governs Wnt-mediated osteoarthritic cartilage destruction. Arthritis Res Ther. 2014;16(1):R37.
288. Valdes AM, Hart DJ, Jones KA, Surdulescu G, Swarbrick P, Doyle DV, et al. Association study of candidate genes for the prevalence and progression of knee osteoarthritis. Arthritis Rheum. 2004;50(8):2497-507.
289. Yamada Y, Okuizumi H, Miyauchi A, Takagi Y, Ikeda K, Harada A. Association of transforming growth factor beta1 genotype with spinal osteophytosis in Japanese women. Arthritis Rheum. 2000;43(2):452-60.
290. Aref-Eshghi E, Liu M, Harper PE, Doré J, Martin G, Furey A, et al. Overexpression of MMP13 in human osteoarthritic cartilage is associated with the SMAD-independent TGF-β signalling pathway. Arthritis Res Ther. 2015;17(1):264.
291. Leijten JC, Emons J, Sticht C, van Gool S, Decker E, Uitterlinden A, et al. Gremlin 1, frizzled-related protein, and Dkk-1 are key regulators of human articular cartilage homeostasis. Arthritis Rheum. 2012;64(10):3302-12.
292. Yang X, Chen L, Xu X, Li C, Huang C, Deng CX. TGF-beta/Smad3 signals repress chondrocyte hypertrophic differentiation and are required for maintaining articular cartilage. J Cell Biol. 2001;153(1):35-46.
293. Wang Q, Tan QY, Xu W, Qi HB, Chen D, Zhou S, et al. Cartilage-specific deletion of Alk5 gene results in a progressive osteoarthritis-like phenotype in mice. Osteoarthr Cartil. 2017;25(11):1868-79.
294. Shen J, Li J, Wang B, Jin H, Wang M, Zhang Y, et al. Deletion of the transforming growth factor β receptor type II gene in articular chondrocytes leads to a progressive osteoarthritis-like phenotype in mice. Arthritis Rheum. 2013;65(12):3107-19.
295. Wu Q, Kim K-O, Sampson ER, Chen D, Awad H, O'Brien T, et al. Induction of an osteoarthritis-like phenotype and degradation of phosphorylated Smad3 by Smurf2 in transgenic mice. Arthritis Rheum. 2008;58(10):3132-44.
296. Chen R, Mian M, Fu M, Zhao JY, Yang L, Li Y, et al. Attenuation of the progression of articular cartilage degeneration by inhibition of TGF-β1 signaling in a mouse model of osteoarthritis. Am J Pathol. 2015;185(11):2875-85.
297. Guermazi A, Kalsi G, Niu J, Crema MD, Copeland RO, Orlando A, et al. Structural effects of intra-articular TGF-β1 in moderate to advanced knee osteoarthritis: MRI-based assessment in a randomized controlled trial. BMC Musculoskelet Disord. 2017;18(1):461.
298. Scharstuhl A, Glansbeek HL, van Beuningen HM, Vitters EL, van der Kraan PM, van den Berg WB. Inhibition of endogenous TGF-beta during experimental osteoarthritis prevents osteophyte formation and impairs cartilage repair. J Immunol. 2002;169(1):507-14.

299. Zhao W, Wang T, Luo Q, Chen Y, Leung VY, Wen C, et al. Cartilage degeneration and excessive subchondral bone formation in spontaneous osteoarthritis involves altered TGF-β signaling. J Orthop Res. 2016;34(5):763-70.
300. Papathanasiou I, Malizos KN, Tsezou A. Bone morphogenetic protein-2-induced Wnt/β-catenin signaling pathway activation through enhanced low-density-lipoprotein receptor-related protein 5 catabolic activity contributes to hypertrophy in osteoarthritic chondrocytes. Arthritis Res Ther. 2012;14(2):R82.
301. Kafienah W, Brömme D, Buttle DJ, Croucher LJ, Hollander AP. Human cathepsin K cleaves native type I and II collagens at the N-terminal end of the triple helix. Biochem J. 1998;331(3):727-32.
302. Konttinen YT, Mandelin J, Li TF, Salo J, Lassus J, Liljeström M, et al. Acidic cysteine endoproteinase cathepsin K in the degeneration of the superficial articular hyaline cartilage in osteoarthritis. Arthritis Rheum. 2002;46(4):953-60.
303. Kozawa E, Cheng XW, Urakawa H, Arai E, Yamada Y, Kitamura S, et al. Increased expression and activation of cathepsin K in human osteoarthritic cartilage and synovial tissues. J Orthop Res. 2016;34(1):127-34.
304. Kozawa E, Nishida Y, Cheng XW, Urakawa H, Arai E, Futamura N, et al. Osteoarthritic change is delayed in a Ctsk-knockout mouse model of osteoarthritis. Arthritis Rheum. 2012;64(2):454-64.
305. Conaghan PG, Bowes MA, Kingsbury SR, Brett A, Guillard G, Rizoska B, et al. Disease-Modifying Effects of a Novel Cathepsin K Inhibitor in Osteoarthritis: A Randomized, Placebo-Controlled Study. Ann Intern Med. 2019.
306. Lawlor DA, Bedford C, Taylor M, Ebrahim S. Agreement between measured and self-reported weight in older women. Results from the British Women's Heart and Health Study. Age Ageing. 2002;31(3):169-74.
307. Adamson J, Lawlor DA, Ebrahim S. Chronic diseases, locomotor activity limitation and social participation in older women: cross sectional survey of British Women's Heart and Health Study. Age Ageing. 2004;33(3):293-8.
308. Kim LG, Adamson J, Ebrahim S. Influence of life-style choices on locomotor disability, arthritis and cardiovascular disease in older women: prospective cohort study. Age Ageing. 2013;42(6):696-701.
309. Nuesch E, Pablo P, Dale CE, Prieto-Merino D, Kumari M, Bowling A, et al. Incident disability in older adults: prediction models based on two British prospective cohort studies. Age Ageing. 2015;44(2):275-82.
310. Bellamy N, Buchanan WW, Goldsmith CH, Campbell J, Stitt LW. Validation study of WOMAC: a health status instrument for measuring clinically important patient relevant outcomes to antirheumatic drug therapy in patients with osteoarthritis of the hip or knee. J Rheumatol. 1988;15(12):1833-40.
311. Whitehouse SL, Lingard EA, Katz JN, Learmonth ID. Development and testing of a reduced WOMAC function scale. J Bone Joint Surg Br. 2003;85(5):706-11.
312. Yang KG, Raijmakers NJ, Verbout AJ, Dhert WJ, Saris DB. Validation of the short-form WOMAC function scale for the evaluation of osteoarthritis of the knee. J Bone Joint Surg Br. 2007;89(1):50-6.

313. Syddall HE, Aihie Sayer A, Dennison EM, Martin HJ, Barker DJ, Cooper C. Cohort profile: the Hertfordshire cohort study. Int J Epidemiol. 2005;34(6):1234-42.
314. van der Pas S, Castell MV, Cooper C, Denkinger M, Dennison EM, Edwards MH, et al. European project on osteoarthritis: design of a six-cohort study on the personal and societal burden of osteoarthritis in an older European population. BMC Musculoskelet Disord. 2013;14:138.
315. Kanis JA, Johansson H, Harvey NC, McCloskey EV. A brief history of FRAX. Arch Osteoporos. 2018;13(1):118-.
316. Deere KC, Hannam K, Coulson J, Ireland A, McPhee JS, Moss C, et al. Quantifying Habitual Levels of Physical Activity According to Impact in Older People: Accelerometry Protocol for the VIBE Study. J Aging Phys Act. 2016;24(2):290-5.
317. Devlin NJ, Krabbe PF. The development of new research methods for the valuation of EQ-5D-5L. The European journal of health economics : HEPAC : health economics in prevention and care. 2013;14 Suppl 1:S1-3.
318. Janssen MF, Pickard AS, Golicki D, Gudex C, Niewada M, Scalone L, et al. Measurement properties of the EQ-5D-5L compared to the EQ-5D-3L across eight patient groups: a multi-country study. Qual Life Res. 2013;22(7):1717-27.
319. Craig CL, Marshall AL, Sjostrom M, Bauman AE, Booth ML, Ainsworth BE, et al. International physical activity questionnaire: 12-country reliability and validity. Med Sci Sports Exerc. 2003;35(8):1381-95.
320. Wylde V, Lenguerrand E, Gooberman-Hill R, Beswick AD, Marques E, Noble S, et al. Effect of local anaesthetic infiltration on chronic postsurgical pain after total hip and knee replacement: the APEX randomised controlled trials. Pain. 2015;156(6):1161-70.
321. Dewey CR, Hawkins NS. The relationship between the treatment of cough during early infancy and maternal education level, age and number of other children in the household. ALSPAC Study Team. Avon Longitudinal Study of Pregnancy and Childhood. Child Care Health Dev. 1998;24(3):217-27.
322. van Hout B, Janssen MF, Feng YS, Kohlmann T, Busschbach J, Golicki D, et al. Interim scoring for the EQ-5D-5L: mapping the EQ-5D-5L to EQ-5D-3L value sets. Value Health. 2012;15(5):708-15.
323. Gregson CL. The epidemiology of high bone mass [PhD thesis]: Bristol; 2011.
324. Shepherd JA, Fan B, Lu Y, Wu XP, Wacker WK, Ergun DL, et al. A multinational study to develop universal standardization of whole-body bone density and composition using GE Healthcare Lunar and Hologic DXA systems. J Bone Miner Res. 2012;27(10):2208-16.
325. Genant HK. Universal standardization for dual X-ray absorptiometry: patient and phantom cross-calibration results. J Bone Miner Res. 1995;10(6):997-8.
326. Standardization of proximal femur bone mineral density (BMD) measurements by DXA. International Committee for Standards in Bone Measurement. Bone. 1997;21(4):369-70.
327. Hui SL, Gao S, Zhou XH, Johnston CC, Jr., Lu Y, Gluer CC, et al. Universal standardization of bone density measurements: a method with optimal

properties for calibration among several instruments. J Bone Miner Res. 1997;12(9):1463-70.
328. Fan B, Lu Y, Genant H, Fuerst T, Shepherd J. Does standardized BMD still remove differences between Hologic and GE-Lunar state-of-the-art DXA systems? Osteoporos Int. 2010;21(7):1227-36.
329. Hardcastle SA. Characterisation of osteoarthritis phenotype in a unique multi-centre cohort of individuals with extremely high bone mass [PhD thesis]: Bristol; 2015.
330. Kirkwood BR, Sterne JAC. Essential medical statistics. Second ed. Malden, Mass.: Blackwell Science; 2003.
331. Altman DG, Bland JM. Measurement in Medicine: The Analysis of Method Comparison Studies. J Royal Stat Soc. 1983;32(3):307-17.
332. Schneider CA, Rasband WS, Eliceiri KW. NIH Image to ImageJ: 25 years of image analysis. Nature methods. 2012;9(7):671-5.
333. Landis JR, Koch GG. The measurement of observer agreement for categorical data. Biometrics. 1977;33(1):159-74.
334. Croft P, Cooper C, Wickham C, Coggon D. Defining osteoarthritis of the hip for epidemiologic studies. Am J Epidemiol. 1990;132(3):514-22.
335. White H. A Heteroskedasticity-Consistent Covariance Matrix Estimator and a Direct Test for Heteroskedasticity. Econometrica. 1980;48(4):817-38.
336. Huber PJ, editor The behavior of maximum likelihood estimates under nonstandard conditions. Proceedings of the Fifth Berkeley Symposium on Mathematical Statistics and Probability, Volume 1: Statistics; 1967 1967; Berkeley, Calif.: University of California Press.
337. Tobin J. Estimation of Relationships for Limited Dependent Variables. Econometrica. 1958;26(1):24-36.
338. McDonald JF, Moffitt RA. The Uses of Tobit Analysis. Rev Econ Stat. 1980;62(2):318-21.
339. McBee M. Modeling Outcomes With Floor or Ceiling Effects: An Introduction to the Tobit Model. Gift Child Q. 2010;54(4):314-20.
340. Leckie G. Introduction to Multilevel Modelling Using MLwiN. Personal Communication2020.
341. Sudlow C, Gallacher J, Allen N, Beral V, Burton P, Danesh J, et al. UK Biobank: An Open Access Resource for Identifying the Causes of a Wide Range of Complex Diseases of Middle and Old Age. PLoS Med. 2015;12(3):e1001779.
342. Würtz P, Wang Q, Kangas AJ, Richmond RC, Skarp J, Tiainen M, et al. Metabolic signatures of adiposity in young adults: Mendelian randomization analysis and effects of weight change. PLoS Med. 2014;11(12):e1001765-e.
343. Allen NE, Sudlow C, Peakman T, Collins R. UK biobank data: come and get it. Sci Transl Med. 2014;6(224):224ed4.
344. Ikram MA, Brusselle GGO, Murad SD, van Duijn CM, Franco OH, Goedegebure A, et al. The Rotterdam Study: 2018 update on objectives, design and main results. Eur J Epidemiol. 2017;32(9):807-50.
345. Hofman A, Grobbee DE, de Jong PT, van den Ouweland FA. Determinants of disease and disability in the elderly: the Rotterdam Elderly Study. Eur J Epidemiol. 1991;7(4):403-22.

346. Boyd A, Golding J, Macleod J, Lawlor DA, Fraser A, Henderson J, et al. Cohort Profile: the 'children of the 90s'--the index offspring of the Avon Longitudinal Study of Parents and Children. Int J Epidemiol. 2013;42(1):111-27.
347. Fraser A, Macdonald-Wallis C, Tilling K, Boyd A, Golding J, Davey Smith G, et al. Cohort Profile: the Avon Longitudinal Study of Parents and Children: ALSPAC mothers cohort. Int J Epidemiol. 2013;42(1):97-110.
348. Northstone K, Lewcock M, Groom A, Boyd A, Macleod J, Timpson N, et al. The Avon Longitudinal Study of Parents and Children (ALSPAC): an update on the enrolled sample of index children in 2019. Wellcome Open Res. 2019;4:51-.
349. Bycroft C, Freeman C, Petkova D, Band G, Elliott LT, Sharp K, et al. The UK Biobank resource with deep phenotyping and genomic data. Nature. 2018;562(7726):203-9.
350. Mitchell R, Hemani G, Dudding T, Corbin L, Harrison S, Paternoster L. UK Biobank Genetic Data: MRC-IEU Quality Control, version 2 2019.
351. Huang J, Howie B, McCarthy S, Memari Y, Walter K, Min JL, et al. Improved imputation of low-frequency and rare variants using the UK10K haplotype reference panel. Nat Commun. 2015;6:8111.
352. Howie B, Marchini J, Stephens M. Genotype imputation with thousands of genomes. G3 (Bethesda). 2011;1(6):457-70.
353. Manichaikul A, Mychaleckyj JC, Rich SS, Daly K, Sale M, Chen WM. Robust relationship inference in genome-wide association studies. Bioinformatics. 2010;26(22):2867-73.
354. Suri P, Palmer MR, Tsepilov YA, Freidin MB, Boer CG, Yau MS, et al. Genome-wide meta-analysis of 158,000 individuals of European ancestry identifies three loci associated with chronic back pain. PLoS Genet. 2018;14(9):e1007601-e.
355. Tam V, Patel N, Turcotte M, Bossé Y, Paré G, Meyre D. Benefits and limitations of genome-wide association studies. Nat Rev Genet. 2019;20(8):467-84.
356. Bush WS, Moore JH. Chapter 11: Genome-wide association studies. PLoS Comput Biol. 2012;8(12):e1002822-e.
357. Loh P-R, Tucker G, Bulik-Sullivan BK, Vilhjálmsson BJ, Finucane HK, Salem RM, et al. Efficient Bayesian mixed-model analysis increases association power in large cohorts. Nat Genet. 2015;47(3):284-90.
358. Mitchell R, Elsworth B, Raistrick CA, Paternoster L, Hemani G, Gaunt TR. MRC IEU UK Biobank GWAS pipeline version 2.2019.
359. Loh P-R, Kichaev G, Gazal S, Schoech AP, Price AL. Mixed-model association for biobank-scale datasets. Nat Genet. 2018;50(7):906-8.
360. Price AL, Patterson NJ, Plenge RM, Weinblatt ME, Shadick NA, Reich D. Principal components analysis corrects for stratification in genome-wide association studies. Nat Genet. 2006;38(8):904-9.
361. Winkler TW, Day FR, Croteau-Chonka DC, Wood AR, Locke AE, Mägi R, et al. Quality control and conduct of genome-wide association meta-analyses. Nat Protoc. 2014;9(5):1192-212.
362. Loh PR. BOLT-LMM v2.3.4 User Manual 2019 [Available from: https://data.broadinstitute.org/alkesgroup/BOLT-LMM/downloads/BOLT-LMM_v2.3.4_manual.pdf.

363. Devlin B, Roeder K. Genomic Control for Association Studies. Biometrics. 1999;55(4):997-1004.
364. Smith JGJG. Genome-Wide Association Study in Humans. Cardiovascular Genomics. 2009;573:231.
365. Turner SD. qqman: an R package for visualizing GWAS results using Q-Q and manhattan plots. bioRxiv. 2014:005165.
366. Smith GD, Ebrahim S. 'Mendelian randomization': can genetic epidemiology contribute to understanding environmental determinants of disease? Int J Epidemiol. 2003;32(1):1-22.
367. Lawlor DA, Harbord RM, Sterne JA, Timpson N, Davey Smith G. Mendelian randomization: using genes as instruments for making causal inferences in epidemiology. Stat Med. 2008;27(8):1133-63.
368. Smith GD, Ebrahim S. Mendelian randomization: prospects, potentials, and limitations. Int J Epidemiol. 2004;33(1):30-42.
369. Zheng J, Baird D, Borges MC, Bowden J, Hemani G, Haycock P, et al. Recent Developments in Mendelian Randomization Studies. Current epidemiology reports. 2017;4(4):330-45.
370. Hemani G, Bowden J, Davey Smith G. Evaluating the potential role of pleiotropy in Mendelian randomization studies. Hum Mol Genet. 2018;27(R2):R195-r208.
371. Davies NM, Holmes MV, Davey Smith G. Reading Mendelian randomisation studies: a guide, glossary, and checklist for clinicians. BMJ. 2018;362:k601.
372. Kleiber C, Zeileis A. AER: Applied Econometrics with R. R package version 1.2-7. 2019.
373. Baum CF, Schaffer ME, Stillman S. IVREG2: Stata module for extended instrumental variables/2SLS and GMM estimation. Statistical Software Components: Boston College Department of Economics; 2002.
374. Burgess S, Thompson SG, Collaboration CCG. Avoiding bias from weak instruments in Mendelian randomization studies. Int J Epidemiol. 2011;40(3):755-64.
375. Staiger D, Stock JH. Instrumental Variables Regression with Weak Instruments. Econometrica. 1997;65(3):557-86
376. Sargan JD. The estimation of economic relationships using instrumental variables. Econometrica. 1958;26(3):393-415.
377. Sanderson E, Davey Smith G, Windmeijer F, Bowden J. An examination of multivariable Mendelian randomization in the single-sample and two-sample summary data settings. Int J Epidemiol. 2019;48(3):713-27.
378. Davey Smith G, Hemani G. Mendelian randomization: genetic anchors for causal inference in epidemiological studies. Hum Mol Genet. 2014;23(R1):R89-98.
379. Burgess S, Butterworth A, Thompson SG. Mendelian randomization analysis with multiple genetic variants using summarized data. Genet Epidemiol. 2013;37(7):658-65.
380. Hemani G, Zheng J, Elsworth B, Wade KH, Haberland V, Baird D, et al. The MR-Base platform supports systematic causal inference across the human phenome. Elife. 2018;7.

381. Bowden J, Davey Smith G, Burgess S. Mendelian randomization with invalid instruments: effect estimation and bias detection through Egger regression. Int J Epidemiol. 2015;44(2):512-25.
382. Bowden J, Del Greco MF, Minelli C, Davey Smith G, Sheehan N, Thompson J. A framework for the investigation of pleiotropy in two-sample summary data Mendelian randomization. Stat Med. 2017;36(11):1783-802.
383. Bowden J, Davey Smith G, Haycock PC, Burgess S. Consistent Estimation in Mendelian Randomization with Some Invalid Instruments Using a Weighted Median Estimator. Genet Epidemiol. 2016;40(4):304-14.
384. Sanderson E, Windmeijer F. A weak instrument test in linear IV models with multiple endogenous variables. Journal of econometrics. 2016;190(2):212-21.
385. Purcell SM, Wray NR, Stone JL, Visscher PM, O'Donovan MC, Sullivan PF, et al. Common polygenic variation contributes to risk of schizophrenia and bipolar disorder. Nature. 2009;460(7256):748-52.
386. Morris JA, Kemp JP, Youlten SE, Laurent L, Logan JG, Chai RC, et al. An atlas of genetic influences on osteoporosis in humans and mice. Nat Genet. 2019;51:258–66.
387. Shim H, Chasman DI, Smith JD, Mora S, Ridker PM, Nickerson DA, et al. A Multivariate Genome-Wide Association Analysis of 10 LDL Subfractions, and Their Response to Statin Treatment, in 1868 Caucasians. PLoS One. 2015;10(4):e0120758.
388. Zhai G, Randell EW, Rahman P. Metabolomics of osteoarthritis: emerging novel markers and their potential clinical utility. Rheumatology. 2018.
389. Soininen P, Kangas AJ, Wurtz P, Suna T, Ala-Korpela M. Quantitative serum nuclear magnetic resonance metabolomics in cardiovascular epidemiology and genetics. Circ Cardiovasc Genet. 2015;8(1):192-206.
390. Rankin NJ, Preiss D, Welsh P, Burgess KEV, Nelson SM, Lawlor DA, et al. The emergence of proton nuclear magnetic resonance metabolomics in the cardiovascular arena as viewed from a clinical perspective. Atherosclerosis. 2014;237(1):287-300.
391. Wishart DS, Tzur D, Knox C, Eisner R, Guo AC, Young N, et al. HMDB: the Human Metabolome Database. Nucleic Acids Res. 2007;35(Database issue):D521-D6.
392. Soininen P, Kangas AJ, Wurtz P, Tukiainen T, Tynkkynen T, Laatikainen R, et al. High-throughput serum NMR metabonomics for cost-effective holistic studies on systemic metabolism. Analyst. 2009;134(9):1781-5.
393. Inouye M, Kettunen J, Soininen P, Silander K, Ripatti S, Kumpula LS, et al. Metabonomic, transcriptomic, and genomic variation of a population cohort. Mol Syst Biol. 2010;6:441.
394. Kujala UM, Makinen VP, Heinonen I, Soininen P, Kangas AJ, Leskinen TH, et al. Long-term leisure-time physical activity and serum metabolome. Circulation. 2013;127(3):340-8.
395. Wurtz P, Kangas AJ, Soininen P, Lawlor DA, Davey Smith G, Ala-Korpela M. Quantitative Serum Nuclear Magnetic Resonance Metabolomics in Large-Scale Epidemiology: A Primer on -Omic Technologies. Am J Epidemiol. 2017;186(9):1084-96.

396. Kim YH, Lee JS, Park JH. Association between bone mineral density and knee osteoarthritis in Koreans: the Fourth and Fifth Korea National Health and Nutrition Examination Surveys. Osteoarthr Cartil. 2018;26(11):1511-7.
397. Lethbridge-Cejku M, Tobin JD, Scott WW, Jr., Reichle R, Roy TA, Plato CC, et al. Axial and hip bone mineral density and radiographic changes of osteoarthritis of the knee: data from the Baltimore Longitudinal Study of Aging. J Rheumatol. 1996;23(11):1943-7.
398. Hochberg MC, Lethbridge-Cejku M, Scott WW, Jr., Reichle R, Plato CC, Tobin JD. Upper extremity bone mass and osteoarthritis of the knees: data from the Baltimore Longitudinal Study of Aging. J Bone Miner Res. 1995;10(3):432-8.
399. Berry PA, Maciewicz RA, Cicuttini FM, Jones MD, Hellawell CJ, Wluka AE. Markers of bone formation and resorption identify subgroups of patients with clinical knee osteoarthritis who have reduced rates of cartilage loss. J Rheumatol. 2010;37(6):1252-9.
400. Parsons C, Judge A, Leyland K, Bruyere O, Petit Dop F, Chapurlat R, et al. Novel approach to estimate Osteoarthritis progression - use of the reliable change index in the evaluation of joint space loss. Arthritis Care Res. 2018;71(2):300-7.
401. Kemp JP, Sayers A, Smith GD, Tobias JH, Evans DM. Using Mendelian randomization to investigate a possible causal relationship between adiposity and increased bone mineral density at different skeletal sites in children. Int J Epidemiol. 2016;45(5):1560-72.
402. Hardcastle SA, Dieppe P, Gregson CL, Arden NK, Spector TD, Hart DJ, et al. Osteophytes, Enthesophytes, and High Bone Mass A Bone-Forming Triad With Potential Relevance in Osteoarthritis. Arthritis Rheumatol. 2014;66(9):2429-39.
403. van Meurs JB. Osteoarthritis year in review 2016: genetics, genomics and epigenetics. Osteoarthr Cartil. 2017;25(2):181-9.
404. Peacock M, Turner CH, Econs MJ, Foroud T. Genetics of Osteoporosis. Endocr Rev. 2002;23(3):303-26.
405. Lo GH, Schneider E, Driban JB, Price LL, Hunter DJ, Eaton CB, et al. Periarticular bone predicts knee osteoarthritis progression: Data from the Osteoarthritis Initiative. Semin Arthritis Rheum. 2018;48(2):155-61.
406. Ruiz-Heiland G, Horn A, Zerr P, Hofstetter W, Baum W, Stock M, et al. Blockade of the hedgehog pathway inhibits osteophyte formation in arthritis. Ann Rheum Dis. 2012;71(3):400-7.
407. Lee JY, Harvey WF, Price LL, Paulus JK, Dawson-Hughes B, McAlindon TE. Relationship of bone mineral density to progression of knee osteoarthritis. Arthritis Rheum. 2013;65(6):1541-6.
408. Fedak KM, Bernal A, Capshaw ZA, Gross S. Applying the Bradford Hill criteria in the 21st century: how data integration has changed causal inference in molecular epidemiology. Emerg Themes Epidemiol. 2015;12:14-.
409. Cicuttini FM, Baker J, Hart DJ, Spector TD. Association of pain with radiological changes in different compartments and views of the knee joint. Osteoarthr Cartil. 1996;4(2):143-7.

410. Neogi T, Felson D, Niu J, Nevitt M, Lewis CE, Aliabadi P, et al. Association between radiographic features of knee osteoarthritis and pain: results from two cohort studies. BMJ. 2009;339:b2844.
411. Edwards MH, Paccou J, Ward KA, Jameson KA, Moss C, Woolston J, et al. The relationship of bone properties using high resolution peripheral quantitative computed tomography to radiographic components of hip osteoarthritis. Osteoarthr Cartil. 2017;25(9):1478-83.
412. Cooper C, Cook PL, Osmond C, Fisher L, Cawley MI. Osteoarthritis of the hip and osteoporosis of the proximal femur. Ann Rheum Dis. 1991;50(8):540-2.
413. Hochberg MC. Do risk factors for incident hip osteoarthritis (OA) differ from those for progression of hip OA? J Rheumatol Suppl. 2004;70:6-9.
414. Wesseling J, Bierma-Zeinstra SM, Kloppenburg M, Meijer R, Bijlsma JW. Worsening of pain and function over 5 years in individuals with 'early' OA is related to structural damage: data from the Osteoarthritis Initiative and CHECK (Cohort Hip & Cohort Knee) study. Ann Rheum Dis. 2015;74(2):347-53.
415. Kim C, Nevitt MC, Niu J, Clancy MM, Lane NE, Link TM, et al. Association of hip pain with radiographic evidence of hip osteoarthritis: diagnostic test study. BMJ. 2015;351:h5983.
416. Nieuwenhuijse MJ, Nelissen RG. Hip pain and radiographic signs of osteoarthritis. BMJ. 2015;351:h6262.
417. Javaid MK, Lane NE, Mackey DC, Lui LY, Arden NK, Beck TJ, et al. Changes in proximal femoral mineral geometry precede the onset of radiographic hip osteoarthritis: The study of osteoporotic fractures. Arthritis Rheum. 2009;60(7):2028-36.
418. Patel A, Baird D, Hardcastle S, Gregory J, Aspenden R, Faber B, et al. Do alterations in hip shape explain the increased risk of hip osteoarthritis in individuals with high bone mass? [Conference abstract]. In press 2016.
419. Nicholls AS, Kiran A, Pollard TC, Hart DJ, Arden CP, Spector T, et al. The association between hip morphology parameters and nineteen-year risk of end-stage osteoarthritis of the hip: a nested case-control study. Arthritis Rheum. 2011;63(11):3392-400.
420. Agricola R, Waarsing JH, Arden NK, Carr AJ, Bierma-Zeinstra SM, Thomas GE, et al. Cam impingement of the hip: a risk factor for hip osteoarthritis. Nat Rev Rheumatol. 2013;9(10):630-4.
421. Alberti KG, Eckel RH, Grundy SM, Zimmet PZ, Cleeman JI, Donato KA, et al. Harmonizing the metabolic syndrome: a joint interim statement of the International Diabetes Federation Task Force on Epidemiology and Prevention; National Heart, Lung, and Blood Institute; American Heart Association; World Heart Federation; International Atherosclerosis Society; and International Association for the Study of Obesity. Circulation. 2009;120(16):1640-5.
422. Esposito K, Chiodini P, Capuano A, Colao A, Giugliano D. Fracture risk and bone mineral density in metabolic syndrome: a meta-analysis. J Clin Endocrinol Metab. 2013;98(8):3306-14.
423. Wong SK, Chin KY, Suhaimi FH, Ahmad F, Ima-Nirwana S. The Relationship between Metabolic Syndrome and Osteoporosis: A Review. Nutrients. 2016;8(6).

424. Zhou J, Zhang Q, Yuan X, Wang J, Li C, Sheng H, et al. Association between metabolic syndrome and osteoporosis: A meta-analysis. Bone. 2013;57(1):30-5.
425. Muka T, Trajanoska K, Kiefte-de Jong JC, Oei L, Uitterlinden AG, Hofman A, et al. The Association between Metabolic Syndrome, Bone Mineral Density, Hip Bone Geometry and Fracture Risk: The Rotterdam Study. PLoS One. 2015;10(6):e0129116.
426. Zheng J, Brion MJ, Kemp JP, Warrington NM, Borges MC, Hemani G, et al. The Effect of Plasma Lipids and Lipid-Lowering Interventions on Bone Mineral Density: A Mendelian Randomization Study. J Bone Miner Res. 2020.
427. Leeming DJ, Alexandersen P, Karsdal MA, Qvist P, Schaller S, Tanko LB. An update on biomarkers of bone turnover and their utility in biomedical research and clinical practice. Eur J Clin Pharmacol. 2006;62(10):781-92.
428. Vasikaran S, Eastell R, Bruyere O, Foldes AJ, Garnero P, Griesmacher A, et al. Markers of bone turnover for the prediction of fracture risk and monitoring of osteoporosis treatment: a need for international reference standards. Osteoporos Int. 2011;22(2):391-420.
429. Henriksen K, Christiansen C, Karsdal MA. Role of biochemical markers in the management of osteoporosis. Climacteric. 2015;18 Suppl 2:10-8.
430. Kindblom JM, Ohlsson C, Ljunggren O, Karlsson MK, Tivesten A, Smith U, et al. Plasma osteocalcin is inversely related to fat mass and plasma glucose in elderly Swedish men. J Bone Miner Res. 2009;24(5):785-91.
431. Wei J, Karsenty G. An overview of the metabolic functions of osteocalcin. Rev Endocr Metab Disord. 2015;16(2):93-8.
432. Qi H, Bao J, An G, Ouyang G, Zhang P, Wang C, et al. Association between the metabolome and bone mineral density in pre- and post-menopausal Chinese women using GC-MS. Mol Biosyst. 2016;12(7):2265-75.
433. Miyamoto T, Hirayama A, Sato Y, Koboyashi T, Katsuyama E, Kanagawa H, et al. A serum metabolomics-based profile in low bone mineral density postmenopausal women. Bone. 2017;95:1-4.
434. Kemp JP, Sayers A, Fraser WD, Davey Smith G, Ala-Korpela M, Evans DM, et al. A Metabolic Screen in Adolescents Reveals an Association Between Circulating Citrate and Cortical Bone Mineral Density. J Bone Miner Res. 2019:e3697.
435. Zhao Q, Shen H, Su KJ, Zhang JG, Tian Q, Zhao LJ, et al. Metabolomic profiles associated with bone mineral density in US Caucasian women. Nutr Metab. 2018;15:57.
436. Wang J, Yan D, Zhao A, Hou X, Zheng X, Chen P, et al. Discovery of potential biomarkers for osteoporosis using LC-MS/MS metabolomic methods. Osteoporos Int. 2019;30(7):1491-9.
437. Miyamoto T, Hirayama A, Sato Y, Koboyashi T, Katsuyama E, Kanagawa H, et al. Metabolomics-based profiles predictive of low bone mass in menopausal women. Bone Rep. 2018;9:11-8.
438. Moayyeri A, Cheung CL, Tan KC, Morris JA, Cerani A, Mohney RP, et al. Metabolomic Pathways to Osteoporosis in Middle-Aged Women: A Genome-Metabolome-Wide Mendelian Randomization Study. J Bone Miner Res. 2018;33(4):643-50.

439. Li S, Felson DT. What is the evidence to support the association between metabolic syndrome and osteoarthritis? - A systematic review. Arthritis Care Res. 2018.
440. Sanchez-Santos MT, Judge A, Gulati M, Spector TD, Hart DJ, Newton JL, et al. Association of metabolic syndrome with knee and hand osteoarthritis: A community-based study of women. Semin Arthritis Rheum. 2018.
441. Hindy G, Akesson KE, Melander O, Aragam KG, Haas ME, Nilsson PM, et al. Cardiometabolic polygenic risk scores and osteoarthritis outcomes: a Mendelian randomization study from the Malm Diet and Cancer Study and the UK Biobank. Arthritis Rheumatol. 2019.
442. Mickiewicz B, Kelly JJ, Ludwig TE, Weljie AM, Wiley JP, Schmidt TA, et al. Metabolic analysis of knee synovial fluid as a potential diagnostic approach for osteoarthritis. J Orthop Res. 2015;33(11):1631-8.
443. Zhang WD, Likhodii S, Zhang YH, Aref-Eshghi E, Harper PE, Randell E, et al. Classification of Osteoarthritis Phenotypes By Metabolomics Analysis. Arthritis Rheumatol. 2014;66:S564-S5.
444. Williamson MP, Humm G, Crisp AJ. 1H nuclear magnetic resonance investigation of synovial fluid components in osteoarthritis, rheumatoid arthritis and traumatic effusions. Br J Rheumatol. 1989;28(1):23-7.
445. Carlson AK, Rawle RA, Wallace CW, Brooks EG, Adams E, Greenwood MC, et al. Characterization of synovial fluid metabolomic phenotypes of cartilage morphological changes associated with osteoarthritis. Osteoarthr Cartil. 2019;27(8):1174-84.
446. Xu Z, Chen T, Luo J, Ding S, Gao S, Zhang J. Cartilaginous Metabolomic Study Reveals Potential Mechanisms of Osteophyte Formation in Osteoarthritis. J Proteome Res. 2017;16(4):1425-35.
447. Zhai G, Wang-Sattler R, Hart DJ, Arden NK, Hakim AJ, Illig T, et al. Serum branched-chain amino acid to histidine ratio: a novel metabolomic biomarker of knee osteoarthritis. Ann Rheum Dis. 2010;69(6):1227-31.
448. Zhang WD, Sun G, Aitken D, Likhodii S, Liu M, Martin G, et al. Lysophosphatidylcholines to phosphatidylcholines ratio predicts advanced knee osteoarthritis. Rheumatology. 2016;55(9):1566-74.
449. Zhang W, Sun G, Likhodii S, Liu M, Aref-Eshghi E, Harper PE, et al. Metabolomic analysis of human plasma reveals that arginine is depleted in knee osteoarthritis patients. Osteoarthr Cartil. 2016;24(5):827-34.
450. NightingaleHealth. Result file description. Personal Communication2017.
451. Wurtz P, Wang Q, Soininen P, Kangas AJ, Fatemifar G, Tynkkynen T, et al. Metabolomic Profiling of Statin Use and Genetic Inhibition of HMG-CoA Reductase. J Am Coll Cardiol. 2016;67(10):1200-10.
452. Cheverud JM. A simple correction for multiple comparisons in interval mapping genome scans. Heredity. 2001;87(Pt 1):52-8.
453. Nyholt DR. A simple correction for multiple testing for single-nucleotide polymorphisms in linkage disequilibrium with each other. Am J Hum Genet. 2004;74(4):765-9.
454. Castano-Betancourt MC, Rivadeneira F, Bierma-Zeinstra S, Kerkhof HJ, Hofman A, Uitterlinden AG, et al. Bone parameters across different types of hip

osteoarthritis and their relationship to osteoporotic fracture risk. Arthritis Rheum. 2013;65(3):693-700.
455. Kerkhof HJ, Bierma-Zeinstra SM, Arden NK, Metrustry S, Castano-Betancourt M, Hart DJ, et al. Prediction model for knee osteoarthritis incidence, including clinical, genetic and biochemical risk factors. Ann Rheum Dis. 2014;73(12):2116-21.
456. Wang Q, Ferreira DLS, Nelson SM, Sattar N, Ala-Korpela M, Lawlor DA. Metabolic characterization of menopause: cross-sectional and longitudinal evidence. BMC Med. 2018;16(1):17.
457. Marshall WA, Tanner JM. Variations in pattern of pubertal changes in girls. Arch Dis Child. 1969;44(235):291-303.
458. Marshall WA, Tanner JM. Variations in the pattern of pubertal changes in boys. Arch Dis Child. 1970;45(239):13-23.
459. Iacobazzi V, Infantino V. Citrate--new functions for an old metabolite. Biol Chem. 2014;395(4):387-99.
460. Costello LC, Franklin RB. Plasma Citrate Homeostasis: How It Is Regulated; And Its Physiological and Clinical Implications. An Important, But Neglected, Relationship in Medicine. HSOA journal of human endocrinology. 2016;1(1).
461. Costello LC, Franklin RB, Reynolds MA, Chellaiah M. The Important Role of Osteoblasts and Citrate Production in Bone Formation: "Osteoblast Citration" as a New Concept for an Old Relationship. The Open bone journal. 2012;4.
462. Hu YY, Rawal A, Schmidt-Rohr K. Strongly bound citrate stabilizes the apatite nanocrystals in bone. Proc Natl Acad Sci U S A. 2010;107(52):22425-9.
463. Davies E, Muller KH, Wong WC, Pickard CJ, Reid DG, Skepper JN, et al. Citrate bridges between mineral platelets in bone. Proc Natl Acad Sci U S A. 2014;111(14):E1354-63.
464. Franklin RB, Chellaiah M, Zou J, Reynolds MA, Costello LC. Evidence that Osteoblasts are Specialized Citrate-producing Cells that Provide the Citrate for Incorporation into the Structure of Bone. The Open bone journal. 2014;6:1-7.
465. Laurent MR, Cook MJ, Gielen E, Ward KA, Antonio L, Adams JE, et al. Lower bone turnover and relative bone deficits in men with metabolic syndrome: a matter of insulin sensitivity? The European Male Ageing Study. Osteoporos Int. 2016;27(11):3227-37.
466. Fernandez-Real JM, Izquierdo M, Ortega F, Gorostiaga E, Gomez-Ambrosi J, Moreno-Navarrete JM, et al. The relationship of serum osteocalcin concentration to insulin secretion, sensitivity, and disposal with hypocaloric diet and resistance training. J Clin Endocrinol Metab. 2009;94(1):237-45.
467. Li GH, Cheung CL, Au PC, Tan KC, Wong IC, Sham PC. Positive effects of low LDL-C and statins on bone mineral density: an integrated epidemiological observation analysis and Mendelian randomization study. Int J Epidemiol. 2019.
468. Kemp JP, Sayers A, Paternoster L, Evans DM, Deere K, St Pourcain B, et al. Does bone resorption stimulate periosteal expansion? A cross-sectional analysis of beta-C-telopeptides of type I collagen (CTX), genetic markers of the RANKL pathway, and periosteal circumference as measured by pQCT. J Bone Miner Res. 2014;29(4):1015-24.

469. National Center for Biotechnology Information. PubChem Database. Alanine, CID=602. [Available from: https://pubchem.ncbi.nlm.nih.gov/compound/Alanine.
470. Felig P. The glucose-alanine cycle. Metabolism. 1973;22(2):179-207.
471. Jennings A, MacGregor A, Spector T, Cassidy A. Amino Acid Intakes Are Associated With Bone Mineral Density and Prevalence of Low Bone Mass in Women: Evidence From Discordant Monozygotic Twins. J Bone Miner Res. 2016;31(2):326-35.
472. Haid M, Muschet C, Wahl S, Romisch-Margl W, Prehn C, Moller G, et al. Long-Term Stability of Human Plasma Metabolites during Storage at -80 degrees C. J Proteome Res. 2018;17(1):203-11.
473. Pinto J, Domingues MR, Galhano E, Pita C, Almeida Mdo C, Carreira IM, et al. Human plasma stability during handling and storage: impact on NMR metabolomics. Analyst. 2014;139(5):1168-77.
474. Clowes JA, Hannon RA, Yap TS, Hoyle NR, Blumsohn A, Eastell R. Effect of feeding on bone turnover markers and its impact on biological variability of measurements. Bone. 2002;30(6):886-90.
475. Locke AE, Kahali B, Berndt SI, Justice AE, Pers TH, Day FR, et al. Genetic studies of body mass index yield new insights for obesity biology. Nature. 2015;518(7538):197-206.
476. Boer CG, Hatzikotoulas K, Southam L, GOConsortium, Zeggini E. Deciphering osteoarthritis genetics across 826,690 individuals from 9 global populations. *manuscript in preparation*.
477. Kemp JP, Morris JA, Medina-Gomez C, Forgetta V, Warrington NM, Youlten SE, et al. Identification of 153 new loci associated with heel bone mineral density and functional involvement of GPC6 in osteoporosis. Nat Genet. 2017;49(10):1468-75.
478. NHSDigital. Hospital Episode Statistics (HES) [updated 26/3/2019. Available from: https://digital.nhs.uk/data-and-information/data-tools-and-services/data-services/hospital-episode-statistics.
479. Burgess S, Small DS, Thompson SG. A review of instrumental variable estimators for Mendelian randomization. Stat Methods Med Res. 2017;26(5):2333-55.
480. Hemani G, Tilling K, Davey Smith G. Orienting the causal relationship between imprecisely measured traits using GWAS summary data. PLoS Genet. 2017;13(11):e1007081.
481. O'Connor LJ, Price AL. Distinguishing genetic correlation from causation across 52 diseases and complex traits. Nat Genet. 2018;50(12):1728-34.
482. Zheng HF, Forgetta V, Hsu YH, Estrada K, Rosello-Diez A, Leo PJ, et al. Whole-genome sequencing identifies EN1 as a determinant of bone density and fracture. Nature. 2015;526(7571):112-7.
483. Danecek P, Auton A, Abecasis G, Albers CA, Banks E, DePristo MA, et al. The variant call format and VCFtools. Bioinformatics. 2011;27(15):2156-8.
484. Wood AR, Esko T, Yang J, Vedantam S, Pers TH, Gustafsson S, et al. Defining the role of common variation in the genomic and biological architecture of adult human height. Nat Genet. 2014;46(11):1173-86.

485. Wasnich R, Davis J, Ross P, Vogel J. Effect of thiazide on rates of bone mineral loss: a longitudinal study. BMJ. 1990;301(6764):1303-5.
486. Crilly RG, Cox L. A comparison of bone density and bone morphology between patients presenting with hip fractures, spinal fractures or a combination of the two. BMC Musculoskelet Disord. 2013;14:68-.
487. Gregson CL, Poole KE, McCloskey EV, Duncan EL, Rittweger J, Fraser WD, et al. Elevated circulating Sclerostin concentrations in individuals with high bone mass, with and without LRP5 mutations. J Clin Endocrinol Metab. 2014;99(8):2897-907.
488. Zheng J, Maerz W, Gergei I, Kleber M, Drechsler C, Wanner C, et al. Mendelian Randomization Analysis Reveals a Causal Influence of Circulating Sclerostin Levels on Bone Mineral Density and Fractures. J Bone Miner Res. 2019;34(10):1824-36.
489. Mabey T, Honsawek S, Tanavalee A, Wilairatana V, Yuktanandana P, Saetan N, et al. Plasma and synovial fluid sclerostin are inversely associated with radiographic severity of knee osteoarthritis. Clin Biochem. 2014;47(7-8):547-51.
490. Theologis T, Efstathopoulos N, Nikolaou V, Charikopoulos I, Papapavlos I, Kokkoris P, et al. Association between serum and synovial fluid Dickkopf-1 levels with radiographic severity in primary knee osteoarthritis patients. Clin Rheumatol. 2017;36(8):1865-72.
491. Kanehisa M, Goto S. KEGG: kyoto encyclopedia of genes and genomes. Nucleic Acids Res. 2000;28(1):27-30.
492. Võsa U, Claringbould A, Westra H-J, Bonder MJ, Deelen P, Zeng B, et al. Unraveling the polygenic architecture of complex traits using blood eQTL metaanalysis. bioRxiv. 2018:447367.
493. Zhou Y, Deng HW, Shen H. Circulating monocytes: an appropriate model for bone-related study. Osteoporos Int. 2015;26(11):2561-72.
494. Durand M, Komarova SV, Bhargava A, Trebec-Reynolds DP, Li K, Fiorino C, et al. Monocytes from patients with osteoarthritis display increased osteoclastogenesis and bone resorption: The In Vitro Osteoclast Differentiation in Arthritis study. Arthritis Rheum. 2013;65(1):148-58.
495. Carbone LD, Nevitt MC, Wildy K, Barrow KD, Harris F, Felson D, et al. The relationship of antiresorptive drug use to structural findings and symptoms of knee osteoarthritis. Arthritis Rheum. 2004;50(11):3516-25.
496. Siebelt M, Waarsing JH, Groen HC, Müller C, Koelewijn SJ, de Blois E, et al. Inhibited osteoclastic bone resorption through alendronate treatment in rats reduces severe osteoarthritis progression. Bone. 2014;66:163-70.
497. Löfvall H, Newbould H, Karsdal MA, Dziegiel MH, Richter J, Henriksen K, et al. Osteoclasts degrade bone and cartilage knee joint compartments through different resorption processes. Arthritis Res Ther. 2018;20(1):67.
498. Christensen J, Shastri VP. Matrix-metalloproteinase-9 is cleaved and activated by cathepsin K. BMC Res Notes. 2015;8:322.
499. Lories RJ, Peeters J, Bakker A, Tylzanowski P, Derese I, Schrooten J, et al. Articular cartilage and biomechanical properties of the long bones in Frzb-knockout mice. Arthritis Rheum. 2007;56(12):4095-103.

500. Day TF, Guo X, Garrett-Beal L, Yang Y. Wnt/beta-catenin signaling in mesenchymal progenitors controls osteoblast and chondrocyte differentiation during vertebrate skeletogenesis. Dev Cell. 2005;8(5):739-50.
501. Zhu M, Chen M, Zuscik M, Wu Q, Wang Y-J, Rosier RN, et al. Inhibition of beta-catenin signaling in articular chondrocytes results in articular cartilage destruction. Arthritis Rheum. 2008;58(7):2053-64.
502. Yazici Y, McAlindon TE, Gibofsky A, Lane NE, Clauw D, Jones M, et al. Lorecivivint, a Novel Intra-articular CLK/DYRK1A Inhibitor and Wnt Pathway Modulator for Treatment of Knee Osteoarthritis: A Phase 2 Randomized Trial. Arthritis Rheumatol. 2020.
503. Deshmukh V, O'Green AL, Bossard C, Seo T, Lamangan L, Ibanez M, et al. Modulation of the Wnt pathway through inhibition of CLK2 and DYRK1A by lorecivivint as a novel, potentially disease-modifying approach for knee osteoarthritis treatment. Osteoarthr Cartil. 2019;27(9):1347-60.
504. Laron Z. Insulin-like growth factor 1 (IGF-1): a growth hormone. Mol Pathol. 2001;54(5):311-6.
505. Nilsson A, Isgaard J, Lindahl A, Dahlstrom A, Skottner A, Isaksson OG. Regulation by growth hormone of number of chondrocytes containing IGF-I in rat growth plate. Science. 1986;233(4763):571-4.
506. McQuillan DJ, Handley CJ, Campbell MA, Bolis S, Milway VE, Herington AC. Stimulation of proteoglycan biosynthesis by serum and insulin-like growth factor-I in cultured bovine articular cartilage. Biochem J. 1986;240(2):423-30.
507. Zhang M, Zhou Q, Liang QQ, Li CG, Holz JD, Tang D, et al. IGF-1 regulation of type II collagen and MMP-13 expression in rat endplate chondrocytes via distinct signaling pathways. Osteoarthr Cartil. 2009;17(1):100-6.
508. Middleton J, Arnott N, Walsh S, Beresford J. Osteoblasts and osteoclasts in adult human osteophyte tissue express the mRNAs for insulin-like growth factors I and II and the type 1 IGF receptor. Bone. 1995;16(3):287-93.
509. Claessen KM, Ramautar SR, Pereira AM, Smit JW, Biermasz NR, Kloppenburg M. Relationship between insulin-like growth factor-1 and radiographic disease in patients with primary osteoarthritis: a systematic review. Osteoarthr Cartil. 2012;20(2):79-86.
510. Lloyd ME, Hart DJ, Nandra D, McAlindon TE, Wheeler M, Doyle DV, et al. Relation between insulin-like growth factor-I concentrations, osteoarthritis, bone density, and fractures in the general population: the Chingford study. Ann Rheum Dis. 1996;55(12):870-4.
511. Yakar S, Werner H, Rosen CJ. Insulin-like growth factors: actions on the skeleton. J Mol Endocrinol. 2018;61(1):T115-t37.
512. Faupel-Badger JM, Berrigan D, Ballard-Barbash R, Potischman N. Anthropometric correlates of insulin-like growth factor 1 (IGF-1) and IGF binding protein-3 (IGFBP-3) levels by race/ethnicity and gender. Ann Epidemiol. 2009;19(12):841-9.
513. Berryman DE, Glad CA, List EO, Johannsson G. The GH/IGF-1 axis in obesity: pathophysiology and therapeutic considerations. Nat Rev Endocrinol. 2013;9(6):346-56.

514. Teumer A, Qi Q, Nethander M, Aschard H, Bandinelli S, Beekman M, et al. Genomewide meta-analysis identifies loci associated with IGF-I and IGFBP-3 levels with impact on age-related traits. Aging Cell. 2016;15(5):811-24.
515. Fry D, Almond R, Moffat S, Gordon M, Singh P. UK Biobank Biomarker Project: Companion Document to Accompany Serum Biomarker Data Version 1.0. 2019.
516. UKBiobank. Biomarker assay quality procedures: approaches used to minimise systematic and random errors (and the wider epidemiological implications). 2019 02 April 2019.
517. Rietveld CA, Medland SE, Derringer J, Yang J, Esko T, Martin NW, et al. GWAS of 126,559 Individuals Identifies Genetic Variants Associated with Educational Attainment. Science. 2013;340(6139):1467.
518. Brion MJ, Shakhbazov K, Visscher PM. Calculating statistical power in Mendelian randomization studies. Int J Epidemiol. 2013;42(5):1497-501.
519. Meulenbelt I, Bijkerk C, Miedema HS, Breedveld FC, Hofman A, Valkenburg HA, et al. A genetic association study of the IGF-1 gene and radiological osteoarthritis in a population-based cohort study (the Rotterdam Study). Ann Rheum Dis. 1998;57(6):371-4.
520. Zhai G, Rivadeneira F, Houwing-Duistermaat JJ, Meulenbelt I, Bijkerk C, Hofman A, et al. Insulin-like growth factor I gene promoter polymorphism, collagen type II alpha1 (COL2A1) gene, and the prevalence of radiographic osteoarthritis: the Rotterdam Study. Ann Rheum Dis. 2004;63(5):544-8.
521. Vaessen N, Heutink P, Janssen JA, Witteman JC, Testers L, Hofman A, et al. A polymorphism in the gene for IGF-I: functional properties and risk for type 2 diabetes and myocardial infarction. Diabetes. 2001;50(3):637-42.
522. Fraenkel L, Zhang Y, Trippel SB, McAlindon TE, LaValley MP, Assif A, et al. Longitudinal analysis of the relationship between serum insulin-like growth factor-I and radiographic knee osteoarthritis. Osteoarthr Cartil. 1998;6(5):362-7.
523. Hochberg MC, Lethbridge-Cejku M, Scott WW, Jr., Reichle R, Plato CC, Tobin JD. Serum levels of insulin-like growth factor in subjects with osteoarthritis of the knee. Data from the Baltimore Longitudinal Study of Aging. Arthritis Rheum. 1994;37(8):1177-80.
524. Zhang Y, Jordan JM. Epidemiology of osteoarthritis. Clin Geriatr Med. 2010;26(3):355-69.
525. Evans DS, Cailotto F, Parimi N, Valdes AM, Castano-Betancourt MC, Liu Y, et al. Genome-wide association and functional studies identify a role for IGFBP3 in hip osteoarthritis. Ann Rheum Dis. 2015;74(10):1861-7.
526. Guntur AR, Rosen CJ. IGF-1 regulation of key signaling pathways in bone. BoneKey Rep. 2013;2:437.
527. Baird DA, Evans DS, Kamanu FK, Gregory JS, Saunders FR, Giuraniuc CV, et al. Identification of novel loci associated with hip shape: a meta-analysis of genome-wide association studies. J Bone Miner Res. 2018.
528. Felson DT, Lawrence Rc Fau - Dieppe PA, Dieppe Pa Fau - Hirsch R, Hirsch R Fau - Helmick CG, Helmick Cg Fau - Jordan JM, Jordan Jm Fau - Kington RS, et al. Osteoarthritis: new insights. Part 1: the disease and its risk factors. (0003-4819 (Print)).

529. Yengo L, Sidorenko J, Kemper KE, Zheng Z, Wood AR, Weedon MN, et al. Meta-analysis of genome-wide association studies for height and body mass index in ~700000 individuals of European ancestry. Hum Mol Genet. 2018;27(20):3641-9.
530. Haycock PC, Burgess S, Wade KH, Bowden J, Relton C, Davey Smith G. Best (but oft-forgotten) practices: the design, analysis, and interpretation of Mendelian randomization studies. Am J Clin Nutr. 2016;103(4):965-78.
531. Rees JMB, Foley CN, Burgess S. Factorial Mendelian randomization: using genetic variants to assess interactions. Int J Epidemiol. 2020;49(4):1147-58.
532. Fry A, Littlejohns TJ, Sudlow C, Doherty N, Adamska L, Sprosen T, et al. Comparison of Sociodemographic and Health-Related Characteristics of UK Biobank Participants With Those of the General Population. Am J Epidemiol. 2017;186(9):1026-34.
533. Laughlin GA, Barrett-Connor E, Criqui MH, Kritz-Silverstein D. The prospective association of serum insulin-like growth factor I (IGF-I) and IGF-binding protein-1 levels with all cause and cardiovascular disease mortality in older adults: the Rancho Bernardo Study. J Clin Endocrinol Metab. 2004;89(1):114-20.
534. Saydah S, Graubard B, Ballard-Barbash R, Berrigan D. Insulin-like growth factors and subsequent risk of mortality in the United States. Am J Epidemiol. 2007;166(5):518-26.
535. Haworth S, Mitchell R, Corbin L, Wade KH, Dudding T, Budu-Aggrey A, et al. Apparent latent structure within the UK Biobank sample has implications for epidemiological analysis. Nat Commun. 2019;10(1):333.
536. Lories RJ, Monteagudo S. Review Article: Is Wnt Signaling an Attractive Target for the Treatment of Osteoarthritis? Rheumatol Ther. 2020.
537. Kraus VB, Feng S, Wang SC, White S, Ainslie M, Le Graverand MPH, et al. Subchondral Bone Trabecular Integrity Predicts and Changes Concurrently With Radiographic and Magnetic Resonance Imaging-Determined Knee Osteoarthritis Progression. Arthritis Rheum. 2013;65(7):1812-21.
538. Gonnelli S, Cepollaro C, Gennari L, Montagnani A, Caffarelli C, Merlotti D, et al. Quantitative ultrasound and dual-energy X-ray absorptiometry in the prediction of fragility fracture in men. Osteoporos Int. 2005;16(8):963-8.
539. Slob EAW, Burgess S. A comparison of robust Mendelian randomization methods using summary data. Genet Epidemiol. 2020;44(4):313-29.
540. Verbanck M, Chen C-Y, Neale B, Do R. Detection of widespread horizontal pleiotropy in causal relationships inferred from Mendelian randomization between complex traits and diseases. Nat Genet. 2018;50(5):693-8.
541. Baird DA, Paternoster L, Gregory JS, Faber BG, Saunders FR, Giuraniuc CV, et al. Investigation of the relationship between susceptibility loci for hip osteoarthritis and DXA-derived hip shape in a population based cohort of peri-menopausal women. Arthritis Rheumatol. 2018;70(12):1984-93.
542. Everhart JS, Siston RA, Flanigan DC. Tibiofemoral subchondral surface ratio (SSR) is a predictor of osteoarthritis symptoms and radiographic progression: data from the Osteoarthritis Initiative (OAI). Osteoarthr Cartil. 2014;22(6):771-8.

543. McClung MR, Grauer A, Boonen S, Bolognese MA, Brown JP, Diez-Perez A, et al. Romosozumab in postmenopausal women with low bone mineral density. N Engl J Med. 2014;370(5):412-20.
544. McClung MR, O'Donoghue ML, Papapoulos SE, Bone H, Langdahl B, Saag KG, et al. Odanacatib for the treatment of postmenopausal osteoporosis: results of the LOFT multicentre, randomised, double-blind, placebo-controlled trial and LOFT Extension study. Lancet Diabetes Endocrinol. 2019;7(12):899-911.
545. Buckland-Wright JC, Messent EA, Bingham CO, 3rd, Ward RJ, Tonkin C. A 2 yr longitudinal radiographic study examining the effect of a bisphosphonate (risedronate) upon subchondral bone loss in osteoarthritic knee patients. Rheumatology. 2007;46(2):257-64.

APPENDICES

Appendix 1: Manuscript generated from the results of the analysis of the relationship between HBM and knee OA progression, published in Osteoarthritis and Cartilage.

Osteoarthritis and Cartilage 28 (2020) 1180–1190

Osteoarthritis and Cartilage

OARSI OSTEOARTHRITIS RESEARCH SOCIETY INTERNATIONAL

Individuals with high bone mass have increased progression of radiographic and clinical features of knee osteoarthritis

A. Hartley †‡*, S.A. Hardcastle †§, L. Paternoster ‡, E. McCloskey ‖¶#, K.E.S. Poole ††, M.K. Javaid ‡‡, M. Aye §§, K. Moss ‖‖, R. Granell ‡, J. Gregory ¶¶, M. Williams ##, J.H. Tobias †‡, C.L. Gregson †

† Musculoskeletal Research Unit, Translational Health Sciences, Bristol Medical School, University of Bristol, Bristol, UK
‡ MRC Integrative Epidemiology Unit, Population Health Sciences, Bristol Medical School, University of Bristol, Bristol, UK
§ Royal National Hospital for Rheumatic Diseases, Royal United Hospitals Bath NHS Foundation Trust, Bath, UK
‖ Academic Unit of Bone Metabolism, Department of Oncology and Metabolism, The Mellanby Centre for Bone Research, University of Sheffield, Sheffield, UK
¶ Centre for Metabolic Diseases, University of Sheffield Medical School, Sheffield, UK
# Centre for Integrated Research Into Musculoskeletal Ageing, University of Sheffield Medical School, Sheffield, UK
†† Cambridge NIHR Biomedical Research Centre and the Wellcome Trust Clinical Research Facility, Cambridge
‡‡ Nuffield Department of Orthopaedics, Rheumatology and Musculoskeletal Sciences, University of Oxford, Oxford, UK
§§ Department of Diabetes, Endocrinology and Metabolism, Hull and East Yorkshire Hospitals NHS Trust, Hull, UK
‖‖ Centre for Rheumatology, St George's Hospital, St George's Healthcare NHS Trust, London, UK
¶¶ Institute of Medical Science, School of Medicine, University of Aberdeen, Aberdeen, UK
Department of Radiology, Southmead Hospital, North Bristol NHS Trust, Bristol UK

ARTICLE INFO

Article history:
Received 24 September 2019
Accepted 26 March 2020

Keywords:
Osteoarthritis
Progression
High bone mass
BMD
WOMAC
Health-related quality of life

SUMMARY

Objective: High bone mass (HBM) is associated with an increased prevalence of radiographic knee OA (kOA), characterized by osteophytosis. We aimed to determine if progression of radiographic kOA, and its sub-phenotypes, is increased in HBM and whether observed changes are clinically relevant.
Design: A cohort with and without HBM (L1 and/or total hip bone mineral density Z-score≥+3.2) had knee radiographs collected at baseline and 8-year follow-up. Sub-phenotypes were graded using the OARSI atlas. Medial/lateral tibial/femoral osteophyte and medial/lateral joint space narrowing (JSN) grades were summed and Δosteophytes, ΔJSN derived. Pain, function and stiffness were quantified using the WOMAC questionnaire. Associations between HBM status and sub-phenotype progression were determined using multivariable linear/poisson regression, adjusting for age, sex, height, baseline sub-phenotype grade, menopause, education and total body fat mass (TBFM). Generalized estimating equations accounted for individual-level clustering.
Results: 169 individuals had repeated radiographs, providing 330 knee images; 63% had HBM, 73% were female, mean (SD) age was 58 (12) years. Whilst HBM was not clearly associated with overall Kellgren–Lawrence measured progression (RR = 1.55 [0.56,4.32]), HBM was positively associated with both Δosteophytes and ΔJSN individually (adjusted mean differences between individuals with and without HBM 0.45 [0.01,0.89] and 0.15 [0.01,0.29], respectively). HBM individuals had higher WOMAC knee pain scores (β = 7.42 [1.17,13.66]), largely explained by adjustment for osteophyte score (58% attenuated) rather than JSN (30% attenuated) or TBFM (16% attenuated). The same pattern was observed for symptomatic stiffness and functional limitation.
Conclusions: HBM is associated with osteophyte progression, which appears to contribute to increased reported pain, stiffness and functional loss.

Introduction

The relationship between bone mineral density (BMD) and osteoarthritis (OA) has been of interest for almost 50 years, since

* Address correspondence and reprint requests to: A. Hartley, Musculoskeletal Research Unit, Translational Health Sciences, Bristol Medical School, University of Bristol, Bristol, UK
E-mail address: ah14433@bristol.ac.uk (A. Hartley).

https://doi.org/10.1016/j.joca.2020.03.020
1063-4584/

the observation that femoral heads removed during surgical repair of hip fracture were mostly unaffected by OA, indicating a potential inverse association between osteoporosis and OA[1]. Since then, several large population-based studies assessing the relationship between BMD and *prevalent* and/or *incident* radiographic knee OA (kOA, usually defined as a Kellgren–Lawrence (KL) grade≥2) have suggested that higher BMD is a risk factor for both[2–8]. Fewer studies have assessed individual radiographic sub-phenotypes of knee OA (kOA) (e.g., osteophytes and joint space narrowing [JSN]), although in the Framingham population prevalent osteophytosis, rather than JSN, was associated with higher BMD[2] and in the Chingford study hip BMD was related to incident knee osteophytes[9].

Evidence for an association between BMD and radiographic kOA *progression* has been less consistent. Zhang *et al.* found evidence for a lower odds of kOA progression with higher BMD quartile in the Framingham cohort[6], whereas Hart *et al.* found lower hip BMD in women with progressive joint space narrowing (JSN) from the Chingford study[9]. An analysis from the Rotterdam study suggested that higher lumbar spine BMD (LS-BMD) is associated with an increased odds of kOA and osteophyte progression[10]; however, this was refuted by analyses from the multicentre osteoarthritis study and the Johnston county osteoarthritis project (JoCo)[11,12]. Consistent with a protective effect of BMD on risk of kOA progression, strontium ranelate, an osteoporosis treatment reported to increase bone formation and decrease bone resorption, reduced knee cartilage loss (assessed by JSN) and western Ontario and McMaster universities OA index (WOMAC) pain score compared to placebo[13].

A novel approach to investigate the 'BMD-progressive kOA' relationship is to examine a population with generalized high BMD, as the causal direction between BMD and kOA can be inferred due to the temporal relationship[1]. The UK-based High Bone Mass (HBM) study is a multi-centred study of individuals with unexplained (i.e., not by disorders known to artefactually elevate BMD) generalized high BMD and their unaffected relatives[14]. Previous analyses have identified an increased odds of prevalent radiographic kOA in individuals with HBM, with an increased odds of osteophytes, but not JSN[15]. Although previous analyses identified increased fat mass in HBM individuals[16] and adiposity as a risk factor for kOA[17], body mass index (BMI) adjustment only partly explained the relationship between HBM and kOA[15]. The prevalence of joint replacement and non-steroidal anti-inflammatory drug use were also higher in individuals with HBM, suggestive of increased OA progression[18]. We hence aimed to establish the relationship between HBM and radiographic kOA progression, particularly osteophyte progression. We further aimed to determine whether individuals with HBM have more clinical kOA symptoms and to what extent this is explained by radiographic OA sub-phenotypes.

Methods

The high bone mass study

Participants were recruited as part of the UK-based HBM study. Index cases were initially identified by screening Dual energy X-ray absorptiometry (DXA) databases for T and/or Z-scores≥+4. All DXA images were inspected by trained clinicians in order to exclude scans with artefactual elevation of DXA BMD (e.g., degenerative disease, OA, surgical/malignant artefacts). Full details of DXA database screening and participant recruitment have been published[14]. Index cases passed on invitations to first-degree relatives and spouses/partners who underwent the same assessments. Participants who were aged <18, pregnant, or unable to give written informed consent were excluded. In first-degree relatives, HBM was defined as summed L1 plus TH Z-score≥+3.2. HBM in spouses was defined as per index cases. In addition to greater BMD, peripheral quantitative computed tomography analyses have identified a larger periosteal circumference and evidence of a greater bone volume[19]. Recruitment ran between 2005 and 2010. In total, 437 individuals were recruited from the eight centres participating in follow-up, of which 274 (63%) had HBM. 254 (58%) alive and consenting participants were followed up between 2017 and 2018; 217 (85%) completed a postal questionnaire and 174 (69%) attended for follow-up knee radiographs (Supplementary Fig. 1).

Written informed consent was obtained in line with the declaration of Helsinki[20]. The study was approved by the Bath Multicentre Research Ethics Committee (REC reference 05/Q2001/78) and each local NHS REC. Follow-up data collection was approved by the Central Bristol REC and NHS Health Research Authority.

BMD assessment

DXA scans were performed of the TH and LS at baseline and, after 8 years follow-up, of the TH, LS and total body (TB) using standard protocols at each assessment centre. 169/174 (97%) participants re-attended their original assessment centre, limiting measurement error due to differential procedures. DXA scans were performed on Hologic scanners in Bath, Bristol, Oxford, Sheffield and St George's and General Electric Lunar scanners in Cambridge and Hull. Known differences in calibration exist between Hologic and Lunar[21,22]. We limited systematic bias by converting TH and LS-BMD measures to standardized BMD (sBMD)[22,23]. All images were visually inspected for positioning errors (missing body mass coded none/unilateral/bilateral) and metal artefacts (coded none/rings/large jewellery or joint replacement).

Assessment of osteoarthritis

Radiographic

Standing anteroposterior (AP), fully-extended, knee X-rays were performed at baseline and follow-up using standard protocols at each centre. To limit observer bias, all radiographs were pooled for analysis, with the reader blinded to HBM status, demographics and timepoint. Radiographs were graded for semi-quantitative OA sub-phenotypes (osteophytes/JSN, graded 0–3) and binary subchondral sclerosis using the OA Research Society International (OARSI) atlas[24]. Overall OA was graded using KL[25]. The presence/absence of chondrocalcinosis was also assessed. Variables generated by KL grading and the OARSI atlas are summarised in Table I, along with derived progression variables. Radiographs were inspected for poor image quality, rotation and/or tilt. Radiographs were viewed in open source imageJ software[26]; minimal medial joint space width (mJSW) and maximum tibial plateau width were quantitatively measured using a custom-designed macro (JG). All readings were performed by one assessor (AH) after focussed radiological training with a musculoskeletal radiologist (MW) and a rheumatologist (SAH). A random selection of 72 knees (20%) were regraded to determine intra-rater reliability and graded by a second reader (SAH) to determine inter-rater reliability. Weighted intra-rater kappa statistics for KL grade, all osteophyte and JSN variables, and unweighted kappa for chondrocalcinosis were >0.85. The intra-rater reliability kappa for subchondral sclerosis was 0.55, representing moderate agreement[27]. Inter-rater weighted kappas for KL grade and all osteophyte grades were >0.8. Medial and lateral JSN and chondrocalcinosis kappas were all >0.65. The inter-rater kappa for any subchondral sclerosis was 0.47. Intraclass correlation coefficients for intra- and inter-rater reliability of quantitative measures (mJSW, maximal tibial plateau width) were ≥0.99.

Continuous measures of mJSW at the two timepoints were used to calculate a Reliable Change Index (RCI), which determines if the

Variable	Grading	Variable used in analysis
Osteoarthritis (KL grade)	0–4	Progressive OA: KL grade ≥2 at baseline and an increase in grade at follow-up Incident OA: KL grade <2 at baseline and ≥2 at follow-up
Osteophytes		
Medial femoral	0–3	Osteophyte progression: Sum of all semi-quantitative osteophyte grades at follow-up − sum at baseline
Lateral femoral	0–3	
Medial tibial	0–3	
Lateral tibial	0–3	
JSN		
Medial	0–3	JSN progression: Sum of both semi-quantitative JSN grades at follow-up − sum at baseline
Lateral	0–3	
Subchondral sclerosis		
Medial	0, 1	Incident sclerosis: no sclerosis (medial or lateral) at baseline and any sclerosis at follow-up
Lateral	0, 1	
Chondrocalcinosis	0, 1	Incident chondrocalcinosis: no chondrocalcinosis at baseline and chondrocalcinosis at follow-up
mJSW	continuous	Change in mJSW: mJSW at follow-up − mJSW at baseline Reliable change in mJSW: Reliable change index ≤ −1.96

Abbreviations: OARSI: osteoarthritis research society international; KL: Kellgren–Lawrence; JSN: joint space narrowing; mJSW: medial minimal joint space width.

Table I Variables generated by Kellgren–Lawrence grading and the OARSI atlas and variables derived for analysis

Osteoarthritis and Cartilage

change in mJSW is meaningful over and above measurement error. Methodology for RCI calculation has been published elsewhere[28]:

$$RCI = \frac{mJSW_2 - mJSW_1}{\sqrt{(\sigma_1^2 + \sigma_2^2 - 2\sigma_2 r(mJSW_1, mJSW_2))}}$$

The RCI is a Z-score and therefore a level exceeding 1.96 is used to denote a 'true' change over and above measurement error. A binary variable for reliable change in mJSW was therefore generated for those with an RCI ≤ −1.96.

Clinical

Knee pain, stiffness and limitation of function were assessed by postal questionnaire at 8-year follow-up. To limit non-response bias, the questionnaire was resent if not returned within 3 weeks. If still unreturned after a further 2 weeks, a reminder telephone call was made. The WOMAC questionnaire was included in this postal questionnaire; the short version function scale was used to limit participant burden[29,30]. The pain subscale (five questions), stiffness (two questions) and function (seven questions), each had five possible responses (none, mild, moderate, severe, extreme) scored 0–4, respectively. Missing values for pain or function questions were mean-imputed if a participant was missing one question on the pain scale and ≤3 on the function scale. Average scores were calculated for each subscale and scaled to give a score ranging from 0 to 100, with 0 representing no pain, stiffness or limitation of function[31]. Health-related quality of life (HR-QoL) was determined using the EuroQol EQ-5D questionnaire[32]. Responses to the five questions were converted to index values using the crosswalk index value calculator and UK value set[33]. If an individual was missing a response for any domain, an index value was not calculated.

Covariate data

At baseline, structured interview and clinical examination determined participant characteristics including age, menopausal status and standing height. Highest educational attainment (as a marker of socioeconomic status [SES]), determined by follow-up questionnaire, was categorised as up to GCSE/O-Level (or equivalent), A-Level (or equivalent) and degree level or above. TB fat mass (TBFM) was assessed by TB DXA scans.

Statistical analysis

Associations between HBM status and binary OA incidence and progression variables were determined by multivariable poisson regression, to generate an estimate of the risk ratio[34], using generalized estimating equations (GEE) to account for clustering in knee radiographs per person. Associations with continuous osteophyte and JSN progression variables were determined by multivariable GEE linear regression with robust standard errors to account for any non-normal distributions in outcome variables. Betas from analysis of continuous variables represent the difference in mean outcome between those with and without HBM (e.g., a beta of one for Δosteophyte represents a 1-point greater increase in summed osteophyte score). Osteophyte and/or JSN scores of 0 at baseline were included in analyses. Analyses were initially performed unadjusted (model 1), then adjusted for age and sex (and baseline sub-phenotype score for continuous outcomes) (model 2), then additionally adjusting for height, menopause and education (model 3). Our previous analyses have identified that HBM is associated with increased TBFM, with evidence suggesting this is a consequence rather than a cause of HBM[16]. Therefore, adiposity is predicted to be on the causal pathway in these analyses, hence a possible mediating effect was determined by additional adjustment for TBFM in model 4. All analyses were restricted to individuals with complete data for model 4. Statistical analysis was performed in Stata version 15 (Statacorp, USA) and R version 3.5.1. In line with the recommendation of the American Statistical Association, we base our interpretation of the results on the size of associations and their confidence intervals (CIs), rather than *P*-values[35].

Sensitivity analyses

Joints with knee replacements (TKR) were excluded; however, as TKR were likely performed due to severe OA, analyses of progressive OA were repeated assuming knees with KL ≥ 2 and TKR at follow-up had progressive OA. Those with a baseline KL score<2 and TKR at follow-up were coded as both incident and progressive OA cases. A person-level analysis, using variables for OA progression in either knee or the highest value of the two knees for osteophyte/JSN scores was performed. Individuals reporting a 'cartilage operation' (12 knees), knee lavage/washout/arthroscopy (16 knees) or a steroid injection (9 knees) by questionnaire were removed. A model adjusting for metal artefacts on DXA scans, and analyses removing individuals with positioning errors leading to under-measurement of TBFM by DXA (10 knees) were performed. We further adjusted for maximum tibial plateau width to determine whether BMD, rather than bone size, explained any associations observed. Finally, to check conclusions were valid despite skewed continuous outcomes, all linear analyses were repeated using a Poisson model.

Results

Characteristics of the study population

Baseline and follow-up radiographs were available from 169 individuals, 63% of whom had HBM. Mean follow-up time was 8.3 years (SD 1.0), which did not differ between individuals with and

	All $N = 169$	HBM Individuals $N = 107$	Non-HBM Relatives $N = 62$	*P* value for difference
N (%)				
Female gender	124 (73.3)	90 (84.1)	34 (54.8)	7.22×10^{-5}
Postmenopausal at baseline	85 (68.5)	67 (74.4)	18 (52.9)	0.037
Menopause transition during follow-up	13 (10.8)*	7 (8.1)	6 (17.7)	0.131
History of ERT use†	55 (45.5)†	44 (50.0)	11 (33.3)	0.151
History of smoking‡	81 (50.6)	49 (49.0)	32 (53.3)	0.596
Alcohol consumption‖				0.037
Never	15 (9.0)	7 (6.7)	8 (12.9)	
Monthly or less	60 (35.9)	46 (43.8)	14 (22.6)	
Weekly	49 (29.3)	29 (27.6)	20 (32.3)	
Daily/most days	43 (25.8)	23 (21.9)	20 (32.3)	
Physical activity at baseline				0.453
low	19 (11.6)§	11 (10.8)	8 (12.9)	
Medium	58 (35.4)	33 (32.4)	25 (40.3)	
High	87 (53.0)	58 (56.9)	29 (46.8)	
Education‖				0.061
Up to GCSE/O level	67 (41.4)	50 (48.1)	17 (29.3)	
A level or equivalent	37 (22.8)	22 (21.2)	15 (25.9)	
Degree or equivalent	58 (35.8)	32 (30.8)	26 (44.8)	
Mean (SD)				
Age at baseline, years	57.7 (12.3)	58.4 (12.6)	56.4 (11.7)	0.303
Age at follow-up, years	65.9 (12.4)	66.7 (12.7)	64.7 (11.8)	0.312
Height at baseline, cm	167.7 (9.2)	166.5 (8.0)	169.8 (10.6)	0.036
Weight at baseline, kg	82.6 (17.6)	84.1 (17.6)	80.0 (17.4)	0.146
BMI at baseline (kg/m^2)	29.4 (5.9)	30.4 (6.2)	27.7 (5.0)	0.003
TBFM (kg)¶	32.1 (10.9)	33.2 (11.3)	30.0 (10.0)	0.076
Baseline TH Z-Score	2.03 (1.50)	2.96 (0.95)	0.46 (0.80)	8.55×10^{-39}
Baseline TH-BMD, g/cm^2 #	1.15 (0.19)	1.25 (0.14)	0.97 (0.13)	1.03×10^{-26}
Change in TH-BMD, % per year#	−0.31 (0.92)	−0.44 (0.94)	−0.09 (0.84)	0.020
Baseline L1 Z-Score	2.47 (1.96)	3.64 (1.25)	0.44 (1.14)	4.20×10^{-37}
Baseline L1-BMD, g/cm^2**	1.26 (0.22)	1.38 (0.15)	1.06 (0.14)	1.39×10^{-29}
Change in L1-BMD, % per year**	0.02 (1.19)	0.02 (1.24)	0.02 (1.09)	0.994
Follow-up time, years	8.3 (1.0)	8.3 (0.7)	8.2 (1.3)	0.871

Abbreviations: ERT: estrogen replacement therapy; BMI: body mass index; TBFM: total body fat mass; BMD: bone mineral density; TH: total hip; L1: 1st lumbar vertebra.

* $N = 120$ (86 HBM, 34 relatives).
† Past or present (assessed at follow-up).
‡ $N = 112$ (81 HBM, 31 relatives) c: $N = 121$ (88 HBM, 33 relatives).
§ $N = 164$ (102 HBM).
‖ $N = 162$ (104 HBM, 58 relatives).
¶ Assessed at follow-up.
\# $N = 166$ (104 HBM).
** $N = 167$ (105 HBM).

Table II Characteristics of the study population

	All knees		HBM knees		Non-HBM knees	
	Total N	N (%)	Total N	N (%)	Total N	N (%)
OA (KL ≥ 2)						
Baseline	330	94 (28.48)	209	72 (34.45)	121	22 (18.18)**
Follow-up	312	129 (41.35)	194	97 (50.00)	118	32 (27.12)***
Incident	232	55 (23.71)	135	41 (30.37)	97	14 (14.43)**
Progressive	80	24 (30.00)	59	19 (32.20)	21	5 (23.81)
Knee replacement						
Baseline	337	7 (2.08)	214	5 (2.34)	123	2 (1.63)
Follow-up	337	25 (7.42)	214	20 (9.35)	123	5 (4.07)
Incident	330	18 (5.45)	209	15 (7.18)	121	3 (2.48)
Subchondral sclerosis						
Baseline	330	6 (1.82)	209	4 (1.91)	121	2 (1.65)
Follow-up	312	19 (6.09)	194	11 (5.67)	118	8 (6.78)
Incident	310	17 (5.48)	193	10 (5.18)	117	7 (5.98)
Chondrocalcinosis						
Baseline	330	18 (5.45)	209	11 (5.26)	121	7 (5.79)
Follow-up	312	39 (12.50)	194	26 (13.40)	118	13 (11.02)
Incident	297	26 (8.75)	186	20 (10.75)	111	6 (5.41)
Reliable change in mJSW (RCI ≤ −1.96)	299	16 (5.4)	189	14 (7.41)	110	2 (1.82)*
Osteophyte score						
Baseline	330		209		121**	
0		236 (71.52)		137 (65.55)		99 (81.82)
1–4		79 (23.94)		59 (28.23)		20 (16.53)
≥5		15 (4.55)		13 (6.22)		2 (1.65)
Follow-up	312		194		118***	
0		183 (58.65)		97 (50.00)		86 (72.88)
1–4		97 (31.09)		69 (35.57)		28 (23.73)
≥5		32 (10.26)		28 (14.43)		4 (3.39)
Delta	312		194		118***	
<1		211 (67.63)		115 (59.28)		96 (81.36)
1		33 (10.58)		25 (12.89)		8 (6.78)
>1		68 (21.79)		54 (27.84)		14 (11.86)
JSN score						
Baseline	330		209		121	
0		283 (85.76)		177 (84.69)		106 (87.60)
1–2		43 (13.03)		29 (13.88)		14 (11.57)
≥3		4 (1.21)		3 (1.44)		1 (0.83)
Follow-up	312		194		118	
0		244 (78.21)		146 (75.26)		98 (83.05)
1–2		59 (18.91)		40 (20.62)		19 (16.10)
≥3		9 (2.88)		8 (4.12)		1 (0.85)
Delta	312		194		118*	
<1		267 (85.58)		162 (83.51)		105 (88.98)
1		35 (11.22)		22 (11.34)		13 (11.02)
>1		10 (3.21)		10 (5.15)		0 (0.00)
	Total N	**Median (IQR)**	**Total N**	**Median (IQR)**	**Total N**	**Median (IQR)**
WOMAC at follow-up						
Pain	154	5 (0, 30)	100	12.5 (0, 40)	54	0 (0, 10)***[a]
Stiffness	153	12.5 (0, 37.5)	99	25 (0, 50)	54	0 (0, 25)**[a]
Function	153	3.6 (0, 28.6)	99	10.7 (0, 39.3)	54	0 (0, 17.9)**[a]
	Total N	**Mean (SD)**	**Total N**	**Mean (SD)**	**Total N**	**Mean (SD)**
mJSW						
Baseline	328	4.98 (1.17)	209	5.02 (1.18)	119	4.92 (1.14)
Follow-up	300	4.84 (1.39)	188	4.89 (1.53)	112	4.76 (1.11)
Delta	298	−0.206 (1.15)	188	−0.241 (1.27)	110	−0.144 (0.90)

*: $P < 0.05$; **: $P < 0.01$, ***: $P < 0.001$.
a: P values for skewed outcomes were generated from a Mann-Witney U test.
Abbreviations: HBM: high bone mass; KL: Kellgren–Lawrence; JSN: joint space narrowing; RCI: reliable change index; mJSW: medial minimal joint space width.

Table III Prevalence of radiographic and clinical OA sub-phenotypes in the study population

Osteoarthritis and Cartilage

without HBM (Table II). Those with follow-up data were more commonly female, premenopausal and physically active and less likely to smoke and have diabetes than individuals not followed-up, although the proportion of females in the baseline and follow-up populations was similar (65 vs 73%, respectively) (Supplementary Table 1). No differential loss-to-follow-up between HBM cases and their relatives was evident; the baseline prevalence of kOA, kOA sub-phenotypes, and TKR were similar in those with and without follow-up radiographs.

As expected, based on baseline observations, individuals with HBM were more commonly female (84% vs 55%), postmenopausal (74% vs 53%) with greater baseline BMD (mean TH-BMD 1.25 vs 0.97 g/cm^2) and BMI (30.4 vs 27.7 kg/m^2) than individuals without HBM (Table II). Overall, changes in TH and LS-BMD over 8 years were minimal; more marked declines in TH-BMD in HBM individuals (−0.44 vs −0.09% per year) were explained by older age of HBM cases in regression analyses.

HBM and the incidence and progression of OA overall

The prevalence of radiographic kOA (KL ≥ 2) was higher at both baseline and follow-up in individuals with HBM compared with those with normal BMD (34 vs 18% at baseline, 50 vs 27% at follow-up, Table III). After adjustment (model 4) a weak trend was seen towards more incident (relative risk [RR] = 1.71 [0.88.3.33]) and progressive (RR = 1.55 [0.56.4.32]) kOA in HBM individuals, but CIs were wide. Combining incident and progressive OA as a single variable, we observed increased risk of incident/progressive OA in individuals with HBM (OR = 1.76 [1.03.3.02]).

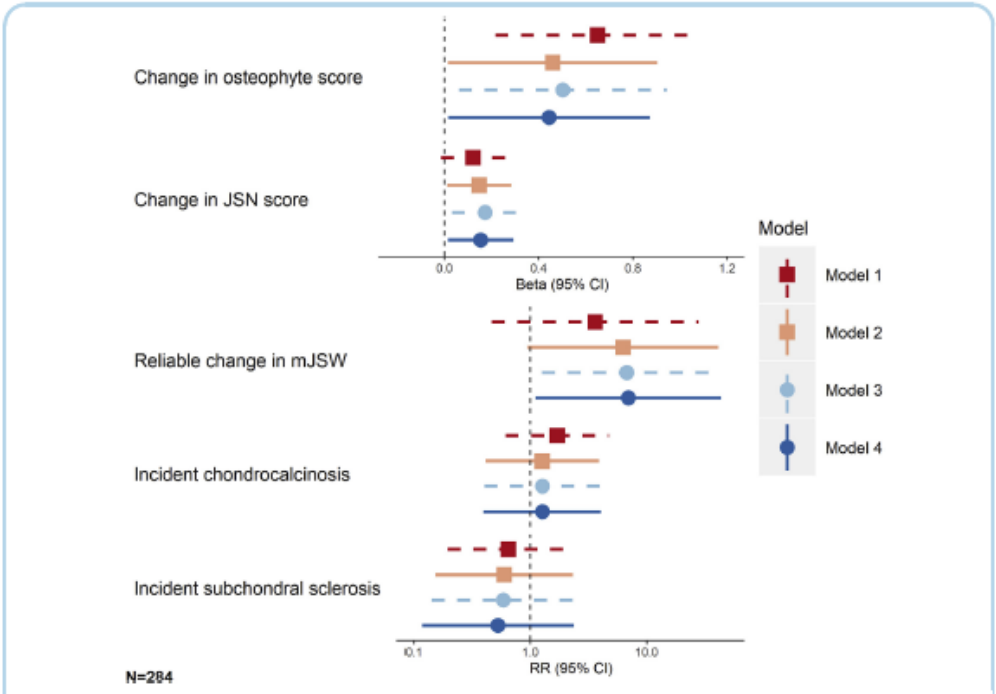

Fig. 1 Associations between HBM status and incident and progressive OA sub-phenotypes. Points for continuous outcomes represent the difference in mean outcome between individuals with and without HBM (For example, a beta of for Δosteophyte would represent a one point greater increase in summed osteophyte score, which is the equivalent of the appearance of one additional osteophyte over 8 years or the increase in size of an osteophyte already present). Points for binary outcomes represent the risk ratio for individuals with HBM compared to their relatives with normal BMD. Model 1: unadjusted, Model 2: adjusted for age and sex (plus baseline score for continuous outcomes), Model 3: adjusted for age, sex, height, SES and menopause (plus baseline score for continuous outcomes), Model 4: Model three plus TBFM. $N_{mJSW} = 278$; $N_{chondrocalcinosis} = 274$; $N_{subchondral\ sclerosis} = 287$. Abbreviations: JSN: joint space narrowing; mJSW: medial minimal joint space width.

HBM and the incidence and progression of OA sub-phenotypes

Individuals with HBM had greater osteophyte development (Δosteophyte: change in summed osteophyte score since baseline, reflecting incidence and/or progression) than individuals without HBM (unadjusted mean difference = 0.65 [0.22.1.08],P = 0.003, Fig. 1). Adjustment for age, sex, baseline osteophyte score, menopause, SES, height and TBFM explained approximately one-third of this relationship (fully-adjusted mean difference = 0.44 [0.02.0.87],P = 0.041). Furthermore, a strong association between *baseline* TH-BMD and osteophyte development was observed (β = 0.28 [0.05.0.51],P=0.019, β represents the change in Δosteophyte score per SD increase in TH-BMD). No association between *change* in TH-BMD and osteophyte development was evident (Supplementary Fig. 2).

Development of JSN was more common in individuals with HBM, independent of TBFM, but this association (mean difference = 0.16 [0.02.0.29],P = 0.028) was less pronounced than that seen for osteophyte development. When JSN development was measured using reliable change in mJSW, HBM individuals had an increased risk of 'true' JSN, independent of TBFM (RR = 6.94 [1.10.43.6],P = 0.039), although CIs were wide reflecting the rarity of this outcome. Whilst *baseline* TH-BMD was associated with increased risk of reliable change in mJSW (fully-adjusted RR = 2.59 [1.29.5.19],P=0.007), *change* in TH-BMD between baseline and follow-up was not (Supplementary Fig. 2). *At both baseline and follow-up, the prevalence of chondrocalcinosis and subchondral sclerosis were similar in those with and without HBM* (Supplementary Table 2), *as was the incidence of both* (Fig. 1).

HBM and clinical features of OA

Before adjustment (model 1), individuals with HBM had approximately 10-point higher WOMAC scores (β_{pain} = 11.2 [5.4,17.0], $\beta_{stiffness}$ = 11.0[4.5,17.5] and $\beta_{function}$ = 9.7[4.8,14.7], all $P < 0.001$), compared to relatives with normal BMD. In analyses adjusted for age, sex, height, menopause and SES (model 3), these associations persisted with mean differences in WOMAC scores all > 6.5/100 (Fig. 2). Further adjustment for TBFM or JSN score attenuated these associations by approximately 20%, whereas adjustment for follow-up osteophyte score attenuated these associations by > 50%. The same pattern was observed for HR-QoL, with HBM individuals having a lower HR-QoL compared to relatives

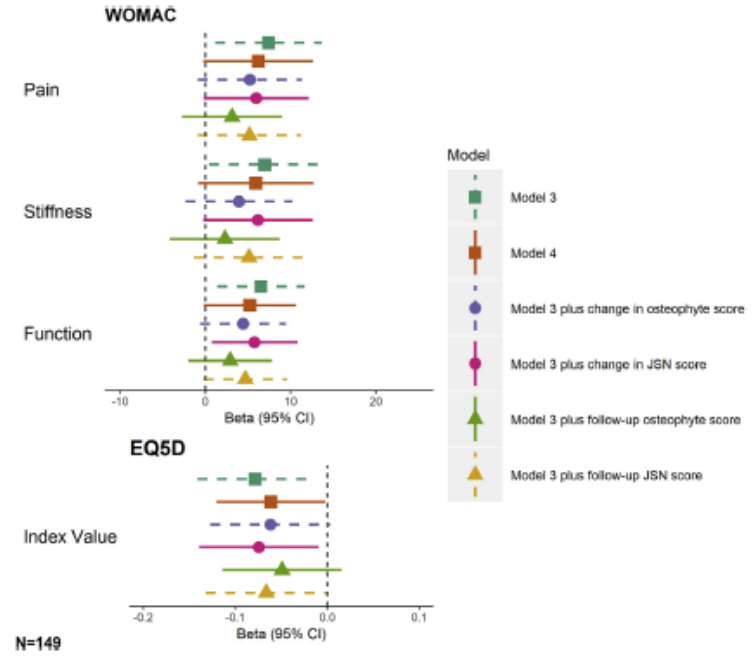

Fig. 2 Associations between HBM status and WOMAC pain, stiffness and function subscale scores and health-related quality of life. Points represent the mean difference in WOMAC scores between individuals with HBM and relatives/spouses without HBM. Person-level analysis, accounting for clustering in families. Follow-up osteophyte and JSN score is the highest of the two knees. Model 1: unadjusted, Model 3: adjusted for age, sex, height, SES and menopause. $N_{stiffness/function}$ = 148.

without HBM ($\beta_{model\ 3} = -0.07[-0.13,-3.90x10^{-3}]$), with further adjustment for osteophyte scores attenuating this association by a greater proportion than TBFM or JSN adjustment (Fig. 2).

Investigating dose–response relationships between BMD and OA outcomes

Baseline TH-BMD Z-score was categorized into quartiles in both the HBM and non-HBM populations. Osteophyte development increased with increasing TH-BMD quartile in the HBM population (p for trend=0.043), until quartile 4, where mean Δosteophyte score appeared to plateau; no such relationship was seen in the non-HBM group [Fig. 3(A)]. No evidence of a dose–response relationship between TH-BMD and ΔJSN was detected [Fig. 3(B)]. A clear dose–response relationship between TH-BMD and WOMAC pain scores was observed in individuals with HBM (p for trend<0.001) but not the non-HBM group [Fig. 3(C)].

Sensitivity analyses

Findings were consistent when analyses were performed at a person-level, although CIs widened. Including ten additional knees with baseline OA and incident TKR strengthened the magnitude of the association between HBM and OA progression (fully-adjusted RR = 1.99 [0.87.4.54]), but CIs were still wide as only 86 individuals had OA at baseline (i.e., could progress). Including three knees, with KL < 2 at baseline and TKR at follow-up, as incident OA weakened evidence for an association between HBM and incident OA (RR = 1.53 [0.82.2.87]). Excluding five individuals who attended a different study site for their follow-up radiographs did not alter findings, nor did adjustment for metal artefacts or removal of individuals with DXA positioning errors. Excluding knees of individuals self-reporting a prior cartilage operation or knee washout/lavage/arthroscopy marginally strengthened the association between HBM and Δosteophytes, but otherwise conclusions were unchanged (Supplementary Fig. 3). Additional adjustment for maximum tibial plateau width did not attenuate the association between HBM and osteophyte development. Repeating analyses using a Poisson regression model did not alter conclusions drawn.

Discussion

This study is the first to evaluate progression of sub-phenotypes of kOA in a population with HBM. Both initial appearance and subsequent growth of osteophytes are increased in individuals with HBM compared to those with normal BMD. Furthermore, we have shown that HBM individuals suffer a greater burden of clinical symptoms of kOA (pain, stiffness and functional limitation), with poorer HR-QoL, with symptoms largely explained by adjustment for osteophytosis severity. Our results are consistent with the one general population study which identified a positive relationship between LS-BMD and knee osteophyte progression[10].

The relationship between high BMI and kOA is widely acknowledged[17,36]. HBM is characterised by increased TBFM[16], with development of HBM likely preceding fat mass accumulation due to its genetic origin[37]. TBFM could mediate the association between HBM and OA progression through increased joint loading or other metabolic pathways. However, the associations we observed between HBM and greater osteophyte development were independent of TBFM. This finding is consistent with one earlier population-based study of North American women in whom those with low BMD and low BMI had the lowest KL grades, those with high BMD and high BMI had the highest KL grades, and those with

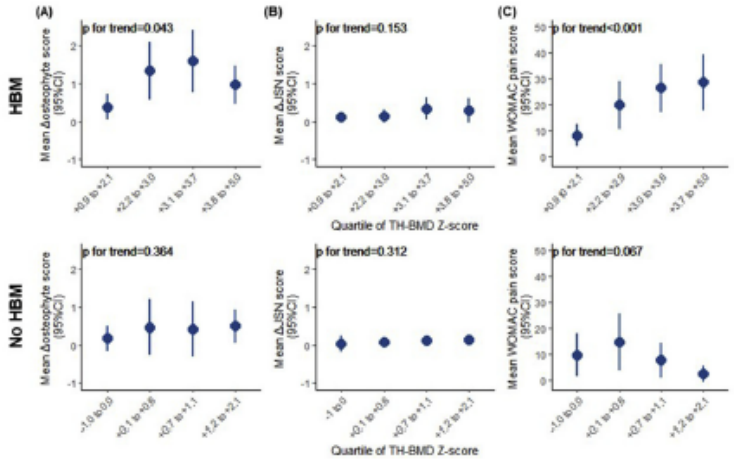

Fig. 3 Association between quartiles of total hip BMD Z-score and (A) change in osteophyte score (B) change in JSN score and (C) WOMAC pain scores in individuals with HBM (top) and relatives without HBM (bottom). Results for mean osteophyte scores are based on GEE-linear regression accounting for two knees per individual. Abbreviations: TH-BMD: total hip bone mineral density.

low BMI and high BMD had similar KL grades to those with high BMI and low BMD, suggesting that the underlying biological pathway leading to increased osteophyte development in individuals with higher BMD is independent of adiposity[3].

Our previous analyses of this HBM population identified an increased presence of enthesophytes, reflecting their 'bone-forming' phenotype[38]. Increased osteophyte development over 8 years provides further evidence for this phenotype. As both BMD and kOA are highly heritable[39,40], one potential explanation for this 'bone-forming' phenotype is pleiotropy, whereby the same genetic variants contribute to both phenotypes: genetic analyses in the Osteoarthritis Initiative and JoCo populations identified a positive association between four BMD-associated genetic single nucleotide polymorphisms (SNPs) and kOA[41]. Such pleiotropy could reflect a causal pathway between BMD and kOA, supported by a recent mendelian randomisation (MR) study[42], or shared underlying biological pathways contributing to both phenotypes. Individuals with HBM have an over-representation of common BMD-associated variants, including those which annotate to bone-forming pathways, e.g. Wnt signalling[37], also linked to OA[43]. Although, a more recent genome-wide analysis did not find evidence for a genetic correlation between FN-BMD and kOA[44]. Differences in subchondral bone texture may explain the positive, albeit weaker, association between HBM and JSN progression[1]. Higher trabecular number and thickness plus reduced trabecular separation in subchondral bone have been linked to medial JSN progression[45]. Individuals with HBM have increased trabecular density at both the tibia and radius[19]; it is currently unknown whether HBM individuals have altered subchondral trabecular bone texture predictive of JSN progression.

In contrast to our analysis, Zhang *et al.* found that risk of kOA progression declined with increasing BMD in the Framingham cohort[6]. One possible explanation for this disparity is that authors defined kOA progression as change in KL score in those with prevalent kOA at baseline. To have KL $\geq$ 2, an individual must present with osteophytes and to increase KL grade, JSN must occur[25]. Therefore, progression from KL = 2 to KL = 3 relies solely on incident JSN, not worsening of osteophyte grade. Using an increased KL grade to define progression is also vulnerable to bias due to a ceiling effect, as those with a KL grade of four at baseline cannot progress. Another potential explanation for the observed inverse association in the Framingham study is 'collider bias', as analyses were restricted to those with kOA at baseline (i.e., case only), thereby potentially inducing a negative correlation between BMD and any other variable that influences incident OA. If any such variable is also associated with progression and is not appropriately controlled for in the analysis, a 'backdoor pathway' from high BMD to kOA progression can be induced. This can manifest as a negative association, when in fact there is none, or even a true positive association[46].

Our finding that individuals with HBM suffer increased clinical symptoms of OA, independent of TBFM, is consistent with a recent MR analysis which identified a causal relationship between FN-BMD and hospital-diagnosed kOA, even after excluding BMI-associated SNPs from the instrument[42]. OA is frequently diagnosed clinically due to symptoms, such as pain, rather than by radiography[47] and therefore hospital-diagnosed kOA is likely to reflect symptomatic OA, confirmed by radiographic changes. One Bradford–Hill criterion supporting causal inference is a dose–response relationship[48]; we found increased WOMAC pain scores with increasing TH-BMD quartiles in HBM individuals. The observation that adjustment for osteophyte severity at follow-up attenuated the association between HBM and pain to a greater extent than adjustment for JSN is consistent with the findings of Cicuttini *et al.*, who observed that the odds of ever having knee pain was increased in middle-aged women with osteophytes compared to those without osteophytes, and this association was stronger than the association between knee JSN and knee pain[49]. However, Neogi *et al.* found that JSN, rather than osteophytes, was more strongly related to knee pain in individuals with knees discordant for pain[50].

Strengths and limitations

The HBM study constitutes a large cohort of individuals with relatively rare, unexplained, generalized HBM[14]. Detailed data were collected at baseline and follow-up allowing for adjustment for potential confounders. We analysed change in OA sub-phenotypes separately as well as using KL score, which allowed us to detect the strong relationship with osteophyte development and the weaker relationship with change in JSN. We analysed change in osteophytes and JSN as continuous measures, increasing statistical power to detect associations, and reducing the possibility of a ceiling effect by increasing the range of possible values from 0 to 6 for JSN and 0–12 for osteophytes. However, this study has some limitations. The method of identifying individuals from NHS DXA databases ascertained an older population such that a relatively large proportion were unable to be followed-up due to death or poor health. X-rays and DXA scans were performed using standard protocols at each centre but were not cross-calibrated. Sample size restrictions meant we could not evaluate change in osteophyte score in individuals with osteophytes at baseline (progression) separately from those with no osteophytes at baseline (incidence). A small number of individuals (0.3%) had a baseline summed osteophyte score of at least 10, almost the maximum score, meaning progression of summed score was limited. All those with a score $\geq$10 at baseline were HBM cases, meaning the relationship between HBM and osteophyte progression may have been underestimated due to a possible ceiling effect. Baseline and follow-up radiographs were not read paired and we did observe a few negative scores for change in osteophytes (<4%) and change in JSN (<2%), which were included in analyses. Removing these values as 'measurement error' could have biased results as there is likely to be the same proportion of measurement error overinflating change, for which we would not be able to account. Reassuringly, the small proportion with negative values did not differ between HBM and relatives. Radiographic grading of OA sub-phenotypes is subjective, which we limited using an established atlas[24], and our intra-rater and inter-rater reliability were substantial for all variables except subchondral sclerosis[27]. WOMAC scores were only collected at follow-up and therefore we were not able to assess change in symptoms. Finally, as this is an extreme population with a female majority, generalizability is limited.

Conclusions

We have found evidence that individuals with HBM have increased osteophyte development over 8 years, independent of fat mass, and a greater number and/or size of osteophytes is associated with greater pain, stiffness and functional limitation and reduced HR-QoL. Future analyses are planned to determine the underlying biological pathways leading to this increased osteophyte development. It is hoped that understanding of such pathways will offer opportunities to identify targets for therapies aimed at reducing the clinical symptoms of OA.

Contributions

Conception and design: JHT and CLG. Analysis and interpretation of the data: AH, JHT, CLG. Drafting of the article: AH and CLG. Critical revision of the article for important intellectual content: all authors. Final approval of the article: all authors. Provision of study materials or patients: EM, MW, MKJ, KESP, MA, KM, TA, JHT. Statistical

expertise: LP, RG, JHT, CLG. Obtaining of funding: EM, MKJ, KESP, JHT, CLG. Technical support: SAH, MW, JG, JVM. Collection and assembly of data: AH, SAH, EM, MW, MKJ, KESP, MA, KM, TA, JHT, CLG. AH and CLG will serve as guarantors for the contents of this paper.

Conflict of interest

The authors have no competing interests to disclose.

Funding sources

The HBM study was supported by The Wellcome Trust (080280/Z/06/Z), the National Institute for Health Research Clinical Research Network (portfolio no. 5163) and Versus Arthritis (ref 20,000). AH is funded by the Wellcome Trust (grant ref 20378/Z/16/Z). Follow-up imaging at the Hull site was funded by OSPREY (OSteoPorosis Research in East Yorkshire). AH, LP, JHT and CLG work in, or are affiliated with, a University of Bristol and MRC funded unit (MC_UU_00,011/1).

Acknowledgements

We would like to thank all our HBM study participants and the staff at the University of Bristol and our collaborating centres: Addenbrooke's Wellcome Trust Clinical Research Facility, NIHR Bone Biomedical Research Unit in Sheffield, the Centre for Metabolic Bone Disease in Hull, Southmead Hospital in Bristol, Nuffield Orthopaedic Centre in Oxford, the Royal National Hospital for Rheumatic Diseases in Bath and St George's Hospital in London. We would grateful to Joyce van Meurs for thevaluable comments on this manuscript.

Supplementary data

Supplementary data to this article can be found online at https://doi.org/10.1016/j.joca.2020.03.020.

References

1. Hardcastle SA, Dieppe P, Gregson CL, Davey Smith G, Tobias JH. Osteoarthritis and bone mineral density: are strong bones bad for joints? BoneKEy Rep 2015;4:624.
2. Hannan MT, Anderson JJ, Zhang Y, Levy D, Felson DT. Bone mineral density and knee osteoarthritis in elderly men and women. The Framingham Study. Arthritis Rheum 1993;36(12):1671–80.
3. Sowers MF, Hochberg M, Crabbe JP, Muhich A, Crutchfield M, Updike S. Association of bone mineral density and sex hormone levels with osteoarthritis of the hand and knee in premenopausal women. Am J Epidemiol 1996;143(1):38–47.
4. Burger H, van Daele PL, Odding E, Valkenburg HA, Hofman A, Grobbee DE, *et al*. Association of radiographically evident osteoarthritis with higher bone mineral density and increased bone loss with age. The Rotterdam Study. Arthritis Rheum 1996;39(1):81–6.
5. Sowers M, Lachance L, Jamadar D, Hochberg MC, Hollis B, Crutchfield M, *et al*. The associations of bone mineral density and bone turnover markers with osteoarthritis of the hand and knee in pre- and perimenopausal women. Arthritis Rheum 1999;42(3):483–9.
6. Zhang Y, Hannan MT, Chaisson CE, McAlindon TE, Evans SR, Aliabadi P, *et al*. Bone mineral density and risk of incident and progressive radiographic knee osteoarthritis in women: the Framingham Study. J Rheumatol 2000;27(4):1032–7.
7. Hochberg MC, Lethbridge-Cejku M, Tobin JD. Bone mineral density and osteoarthritis: data from the baltimore longitudinal study of aging. Osteoarthritis Cartilage 2004;12(Suppl A):S45–8.
8. Bergink AP, Rivadeneira F, Bierma-Zeinstra SM, Carola Zillikens M, Arfan Ikram M, Uitterlinden AG, *et al*. Are Bone Mineral Density and Fractures Related to the Incidence and Progression of Radiographic Osteoarthritis of the Knee, Hip and Hand in Elderly Men and Women? the Rotterdam Study. Hoboken, NJ): Arthritis & rheumatology; 2018.
9. Hart DJ, Cronin C, Daniels M, Worthy T, Doyle DV, Spector TD. The relationship of bone density and fracture to incident and progressive radiographic osteoarthritis of the knee: the Chingford Study. Arthritis Rheum 2002;46(1):92–9.
10. Bergink AP, Uitterlinden AG, Van Leeuwen JP, Hofman A, Verhaar JA, Pols HA. Bone mineral density and vertebral fracture history are associated with incident and progressive radiographic knee osteoarthritis in elderly men and women: the Rotterdam Study. Bone 2005;37(4):446–56.
11. Nevitt MC, Zhang Y, Javaid MK, Neogi T, Curtis JR, Niu J, *et al*. High systemic bone mineral density increases the risk of incident knee OA and joint space narrowing, but not radiographic progression of existing knee OA: the MOST study. Ann Rheum Dis 2010;69(1):163–8.
12. Barbour KE, Murphy LB, Helmick CG, Hootman JM, Renner JB, Jordan JM. Bone mineral density and the risk of hip and knee osteoarthritis: the Johnston county osteoarthritis project. Arthritis Care Res 2017;69(12):1863–70.
13. Reginster JY, Badurski J, Bellamy N, Bensen W, Chapurlat R, Chevalier X, *et al*. Efficacy and safety of strontium ranelate in the treatment of knee osteoarthritis: results of a double-blind, randomised placebo-controlled trial. Ann Rheum Dis 2013;72(2):179–86.
14. Gregson CL, Steel SA, O'Rourke KP, Allan K, Ayuk J, Bhalla A, *et al*. Sink or swim': an evaluation of the clinical characteristics of individuals with high bone mass. Osteoporos Int 2012;23(2):643–54.
15. Hardcastle SA, Dieppe P, Gregson CL, Arden NK, Spector TD, Hart DJ, *et al*. Individuals with high bone mass have an increased prevalence of radiographic knee osteoarthritis. Bone 2015;71:171–9.
16. Gregson CL, Paggiosi MA, Crabtree N, Steel SA, McCloskey E, Duncan EL, *et al*. Analysis of body composition in individuals with high bone mass reveals a marked increase in fat mass in women but not men. J Clin Endocrinol Metabol 2013;98(2):818–28.
17. Silverwood V, Blagojevic-Bucknall M, Jinks C, Jordan JL, Protheroe J, Jordan KP. Current evidence on risk factors for knee osteoarthritis in older adults: a systematic review and meta-analysis. Osteoarthritis Cartilage 2015;23(4):507–15.
18. Hardcastle SA, Gregson CL, Deere KC, Smith GD, Dieppe P, Tobias JH. High bone mass is associated with an increased prevalence of joint replacement: a case-control study. Rheumatology 2013;52(6):1042–51.
19. Gregson CL, Sayers A, Lazar V, Steel S, Dennison EM, Cooper C, *et al*. The high bone mass phenotype is characterised by a combined cortical and trabecular bone phenotype: findings from a pQCT case-control study. Bone 2013;52(1):380–8.
20. World medical association declaration of helsinki ethical principles for medical research involving human subjects. JAMA, J Am Med Assoc 2013;310(20):2191–4.
21. Shepherd JA, Fan B, Lu Y, Wu XP, Wacker WK, Ergun DL, *et al*. A multinational study to develop universal standardization of whole-body bone density and composition using GE Healthcare Lunar and Hologic DXA systems. J Bone Miner Res : Off J Am Soc Bone Miner Res 2012;27(10):2208–16.

22. Fan B, Lu Y, Genant H, Fuerst T, Shepherd J. Does standardized BMD still remove differences between Hologic and GE-Lunar state-of-the-art DXA systems? Osteoporos Int : J established Result Coop between Eur Found Osteoporos National Osteoporos Found USA 2010;21(7):1227–36.
23. Hanson J. Standardization of femur BMD. J Bone Miner Res : Off J Am Soc Bone Miner Res 1997;12(8):1316–7.
24. Altman RD, Gold GE. Atlas of individual radiographic features in osteoarthritis, revised. Osteoarthritis Cartilage 2007;15(Suppl A):A1–A56.
25. Kellgren JH, Lawrence JS. Radiological assessment of osteo-arthrosis. Ann Rheum Dis 1957;16(4):494–502.
26. Schneider CA, Rasband WS, Eliceiri KW. NIH Image to ImageJ: 25 years of image analysis. Nat Methods 2012;9(7):671–5.
27. Landis JR, Koch GG. The measurement of observer agreement for categorical data. Biometrics 1977;33(1):159–74.
28. Parsons C, Judge A, Leyland K, Bruyere O, Petit Dop F, Chapurlat R, *et al*. Novel approach to estimate Osteoarthritis progression - use of the reliable change index in the evaluation of joint space loss. Arthritis Care Res 2018;71(2):300–7.
29. Whitehouse SL, Lingard EA, Katz JN, Learmonth ID. Development and testing of a reduced WOMAC function scale. J Bone Jt Surg Br 2003;85(5):706–11.
30. Bellamy N, Buchanan WW, Goldsmith CH, Campbell J, Stitt LW. Validation study of WOMAC: a health status instrument for measuring clinically important patient relevant outcomes to antirheumatic drug therapy in patients with osteoarthritis of the hip or knee. J Rheumatol 1988;15(12):1833–40.
31. Wylde V, Lenguerrand E, Gooberman-Hill R, Beswick AD, Marques E, Noble S, *et al*. Effect of local anaesthetic infiltration on chronic postsurgical pain after total hip and knee replacement: the APEX randomised controlled trials. Pain 2015;156(6):1161–70.
32. Herdman M, Gudex C, Lloyd A, Janssen M, Kind P, Parkin D, *et al*. Development and preliminary testing of the new five-level version of EQ-5D (EQ-5D-5L). Qual Life Res : Inter J Qual life Aspect Treat, Care Rehabil 2011;20(10):1727–36.
33. van Hout B, Janssen MF, Feng YS, Kohlmann T, Busschbach J, Golicki D, *et al*. Interim scoring for the EQ-5D-5L: mapping the EQ-5D-5L to EQ-5D-3L value sets. Value Health : J Inter Soc Pharmacoeconomics Outcomes Res 2012;15(5):708–15.
34. McNutt L-A, Wu C, Xue X, Hafner JP. Estimating the relative risk in cohort studies and clinical trials of common outcomes. Am J Epidemiol 2003;157(10):940–3.
35. Wasserstein RL, Lazar NA. The ASA statement on p-values: context, process, and purpose. Am Statistician 2016;70(2):129–33.
36. Zheng H, Chen C. Body mass index and risk of knee osteoarthritis: systematic review and meta-analysis of prospective studies. BMJ open 2015;5(12), e007568.
37. Gregson CL, Newell F, Leo PJ, Clark GR, Paternoster L, Marshall M, *et al*. Genome-wide association study of extreme high bone mass: contribution of common genetic variation to extreme BMD phenotypes and potential novel BMD-associated genes. Bone 2018;114:62–71.
38. Hardcastle SA, Dieppe P, Gregson CL, Arden NK, Spector TD, Hart DJ, *et al*. Osteophytes, enthesophytes, and high bone mass A bone-forming triad with potential relevance in osteoarthritis. Arthritis & Rheumatology. 2014;66(9):2429–39.
39. van Meurs JB. Osteoarthritis year in review 2016: genetics, genomics and epigenetics. Osteoarthritis Cartilage 2017;25(2):181–9.
40. Peacock M, Turner CH, Econs MJ, Foroud T. Genetics of osteoporosis. Endocr Rev 2002;23(3):303–26.
41. Yerges-Armstrong LM, Yau MS, Liu Y, Krishnan S, Renner JB, Eaton CB, *et al*. Association analysis of BMD-associated SNPs with knee osteoarthritis. J Bone Miner Res : the official journal of the American Society for Bone and Mineral Research 2014;29(6):1373–9.
42. Funck-Brentano T, Nethander M, Moverare-Skrtic S, Richette P, Ohlsson C. Causal Factors for Knee, Hip and Hand Osteoarthritis: A Mendelian Randomization Study in the UK Biobank. Arthritis Rheumatol (Hoboken, NJ) 2019;71(10):1634–41.
43. Usami Y, Gunawardena AT, Iwamoto M, Enomoto-Iwamoto M. Wnt signaling in cartilage development and diseases: lessons from animal studies. Laboratory investigation; a journal of technical methods and pathology 2016;96(2):186–96.
44. Hackinger S, Trajanoska K, Styrkarsdottir U, Zengini E, Steinberg J, Ritchie GRS, *et al*. Evaluation of shared genetic aetiology between osteoarthritis and bone mineral density identifies SMAD3 as a novel osteoarthritis risk locus. Hum Mol Genet 2017;26(19):3850–8.
45. Lo GH, Schneider E, Driban JB, Price LL, Hunter DJ, Eaton CB, *et al*. Periarticular Bone Predicts Knee Osteoarthritis Progression: Data from the Osteoarthritis Initiative 2018. 1532-866X (Electronic)).
46. Paternoster L, Tilling K, Davey Smith G. Genetic epidemiology and Mendelian randomization for informing disease therapeutics: conceptual and methodological challenges. PLoS Genet 2017;13(10), e1006944.
47. Hunter DJ, Bierma-Zeinstra S. Osteoarthritis. Lancet (London, England) 2019;393(10182):1745–59.
48. Fedak KM, Bernal A, Capshaw ZA, Gross S. Applying the Bradford Hill criteria in the 21st century: how data integration has changed causal inference in molecular epidemiology. Emerg Themes Epidemiol 2015;12:14.
49. Cicuttini FM, Baker J, Hart DJ, Spector TD. Association of pain with radiological changes in different compartments and views of the knee joint. Osteoarthritis Cartilage 1996;4(2):143–7.
50. Neogi T, Felson D, Niu J, Nevitt M, Lewis CE, Aliabadi P, *et al*. Association between radiographic features of knee osteoarthritis and pain: results from two cohort studies. BMJ (Clinical research ed) 2009;339:b2844.

Appendix 2: Manuscript generated from the results of the analysis of the relationship between HBM and hip OA progression, published in Arthritis Research and Therapy.

Hartley et al. Arthritis Research & Therapy (2021) 23:4
https://doi.org/10.1186/s13075-020-02371-0

Arthritis Research & Therapy

RESEARCH ARTICLE Open Access

Increased development of radiographic hip osteoarthritis in individuals with high bone mass: a prospective cohort study

April Hartley[1,2*], Sarah A. Hardcastle[1,3], Monika Frysz[1,2], Jon Parkinson[4], Lavinia Paternoster[2], Eugene McCloskey[5,6,7], Kenneth E. S. Poole[8], Muhammad K. Javaid[9], Mo Aye[10], Katie Moss[11], Martin Williams[12], Jon H. Tobias[1,2] and Celia L. Gregson[1]

Abstract

Background: Individuals with high bone mass (HBM) have a greater odds of prevalent radiographic hip osteoarthritis (OA), reflecting an association with bone-forming OA sub-phenotypes (e.g. osteophytosis, subchondral sclerosis). As the role of bone mineral density (BMD) in hip OA progression is unclear, we aimed to determine if individuals with HBM have increased incidence and/or progression of bone-forming OA sub-phenotypes.

Methods: We analysed an adult cohort with and without HBM (L1 and/or total hip BMD *Z*-score $\geq +3.2$) with pelvic radiographs collected at baseline and 8-year follow-up. Sub-phenotypes were graded using the OARSI atlas. Superior/inferior acetabular/femoral osteophyte and medial/superior joint space narrowing (JSN) grades were summed and Δosteophyte and ΔJSN derived. Pain and functional limitations were quantified using the WOMAC questionnaire. Associations between HBM status and change in OA sub-phenotypes were determined using multivariable linear/logistic regression, adjusting for age, sex, height, total body fat mass, follow-up time and baseline sub-phenotype grade. Generalised estimating equations accounted for individual-level clustering.

Results: Of 136 individuals, 62% had HBM at baseline, 72% were female and mean (SD) age was 59 (10) years. HBM was positively associated with both Δosteophytes and ΔJSN (adjusted mean grade differences between individuals with and without HBM $\beta_{osteophyte} = 0.30$ [0.01, 0.58], $p = 0.019$ and $\beta_{JSN} = 0.10$ [0.01, 0.18], $p = 0.019$). Incident subchondral sclerosis was rare. HBM individuals had higher WOMAC hip functional limitation scores ($\beta = 8.3$ [0.7, 15.98], $p = 0.032$).

Conclusions: HBM is associated with the worsening of hip osteophytes and JSN over an average of 8 years, as well as increased hip pain and functional limitation.

Keywords: Hip osteoarthritis, Progression, High bone mass, BMD, WOMAC

* Correspondence: april.hartley@bristol.ac.uk
[1]Musculoskeletal Research Unit, Translational Health Sciences, Bristol Medical School, University of Bristol, Bristol, UK
[2]MRC Integrative Epidemiology Unit, Population Health Sciences, Bristol Medical School, University of Bristol, Bristol, UK
Full list of author information is available at the end of the article

Introduction

Osteoarthritis (OA) of the hip is highly prevalent, affecting approximately 1% of the worldwide population, significantly contributing to global disability [1]. Currently, no disease-modifying medications are available; therapy consists of pain management until severity warrants a total hip replacement (THR). Detection of risk factors for hip OA progression offers an opportunity to identify potential targets for the development of therapeutic interventions.

Higher bone mineral density (BMD) has been associated with *prevalent* hip OA in several case-control [2, 3] and population-based studies [4–7]. However, such analyses are complicated as BMD is often measured at the hip and therefore it is hard to determine whether increased BMD is a cause, or feature, of hip OA [4–6, 8]. In men with discordant hip OA, Arokoski et al. found femoral neck (FN)-BMD to be 4% higher in the more severely affected hip, reflecting increased FN volume (measured by MRI) [9]. This may reflect a process known as buttressing, whereby osteophytes extend across the FN to artefactually increase measured BMD [10]. However, Chaganti et al. identified a relationship between total hip (TH) cortical volumetric BMD (vBMD, measurement of which it not artefactually increased by bone size) and hip OA in 3886 men in the Study of Osteoporotic Fractures in Men (MrOS) [5]. Moreover, lumbar spine (LS)-BMD can be artefactually elevated by the presence of spinal osteophytes, a feature of spinal OA [4–6]. However, Nevitt et al. found that the relationship between LS-BMD and severe hip OA persisted despite adjustment for spinal osteophytes [4]. Furthermore, they found a relationship between calcaneal BMD and hip OA in over 4000 women from the Study of Osteoporotic Fractures (SOF), although of lower magnitude than seen for TH-BMD [4].

More recently, in a unique population of individuals with high bone mass (HBM), Hardcastle et al. reported those with HBM to have an increased odds of hip OA, reflecting a greater odds of osteophytosis but not joint space narrowing (JSN) [10]. HBM in index cases was defined as a TH or LS-BMD *Z*-score of at least + 3.2, with a *Z*-score of at least + 1.2 at the other site, identifying a generalised high BMD phenotype [11]. Genetic analysis of HBM individuals suggests that the HBM phenotype is at least in part determined by the polygenic inheritance of multiple BMD-associated loci [12]; thus, the temporal relationship is suggestive of a causal pathway between generalised high BMD and prevalent hip OA.

Fewer longitudinal analyses have addressed the relationship between BMD and the *incidence* and/or *progression* of hip OA. In the Johnston County OA project (JoCo) studying 928 older adults over median 6.5 years, although BMD did not predict incident radiographic hip OA, it was inversely associated with incident *symptomatic* radiographic hip OA [13]. Furthermore, Bergink et al. identified an increased odds of both hip OA incidence and progression in those in the highest quartile of FN-BMD compared to the lowest quartile [14], whilst Hochberg et al. identified a dose-response relationship between both forearm and FN-BMD and the incidence of hip OA in SOF [15].

We aimed to determine the role of high BMD in hip OA by examining whether HBM individuals also have an increased odds of hip OA *incidence* and/or *progression*, using 8-year follow-up data collected in this unique cohort. We further aimed to determine the relationship between HBM and clinical features of OA, namely pain and functional limitations.

Methods

The high bone mass study

Participants were recruited as part of the UK-based HBM study. Index cases were initially identified by screening routine clinical National Health Service (NHS) dual-energy X-ray absorptiometry (DXA) databases (254,736 DXA scans from seven UK hospitals) for individuals who had had *T* and/or *Z*-scores $\geq +4$. All 1290 DXA images were inspected by trained clinicians to exclude scans with artefactual elevations of DXA BMD (e.g. degenerative disease, OA, surgical/malignant artefacts). Full details of DXA database screening and participant recruitment have been published [11]. Generalised HBM was defined as a L1 or TH-BMD *Z*-score $\geq +3.2$ with a *Z*-score $\geq +1.2$ at the other skeletal site. A + 3.2 threshold was consistent with the only published precedent for identifying HBM using DXA [16] and most appropriately differentiated generalised HBM from artefact [11]. The use of *Z*-score, rather than *T*-score, limited age bias [11]. Index cases passed on invitations to first-degree relatives and spouses/partners who underwent the same assessments. HBM in spouses was defined as per index cases. In first-degree relatives, HBM was defined as summed L1 plus TH *Z*-score $\geq +3.2$, as this identified relatives with BMD overlapping the index case BMD distribution [11]. Participants who were aged < 18, pregnant or unable to give written informed consent were excluded. Baseline recruitment of 363 adults (237 [65%] with HBM) ran between 2005 and 2010 across seven NHS centres (which participated in follow-up). Two hundred seven (57%) were alive and contactable in 2016; 149 (72%) of whom completed a postal questionnaire and attended for follow-up hip radiographs between 2017 and 2018 (Fig. 1).

Assessment of BMD

DXA scans were performed of the TH and LS at baseline and, after 8 years follow-up, of the TH, LS and total

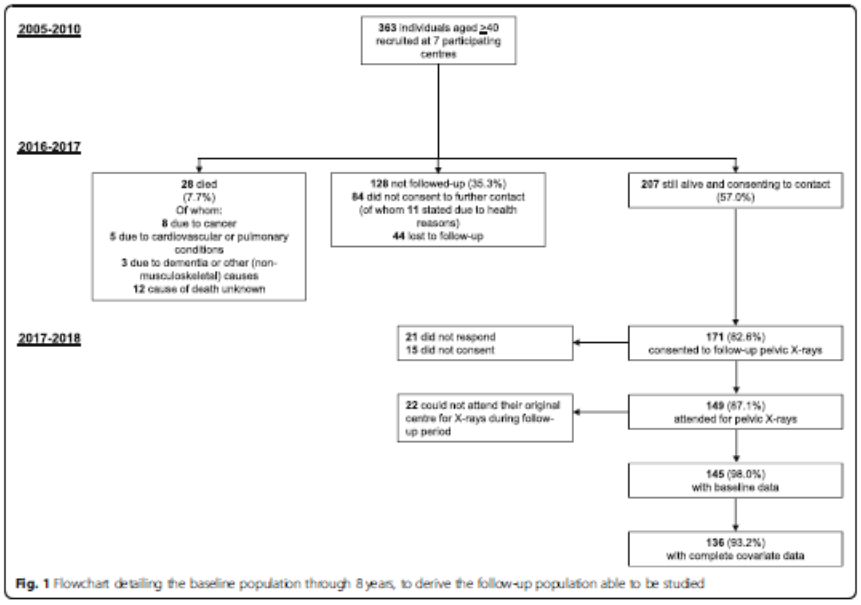

Fig. 1 Flowchart detailing the baseline population through 8 years, to derive the follow-up population able to be studied

body (TB) using standard protocols at each assessment centre. All but five (97%) participants re-attended their original centre, limiting measurement error due to differential procedures. DXA scans were performed on Hologic scanners in Bath, Bristol, Sheffield and St George's London and GE Lunar scanners in Cambridge and Hull. Known differences in calibration exist between Hologic and Lunar [17, 18]. We limited systematic bias by converting TH and LS-BMD measures to standardised BMD (sBMD) [18, 19]. All images were visually inspected for positioning and metal artefacts (e.g. hip prosthesis).

Assessment of radiographic OA

Standing anteroposterior (AP) pelvic X-rays were performed at baseline and follow-up using standard protocols at each centre. To limit observer bias, all radiographs were pooled for analysis, with the reader blinded to HBM status, demographics and timepoint. Radiographs were graded for semi-quantitative OA sub-

Table 1 Variables generated by Croft scoring and the OARSI atlas, with additional derived variables

Variable	Grading	Variable used in the analysis
Osteoarthritis (Croft score)	0–5	Progressive OA: Croft score ≥ 3 at baseline and an increase in score at follow-up Incident OA: Croft score < 3 at baseline and ≥ 3 at follow-up
Osteophytes		Change in osteophyte score: sum of all semi-quantitative osteophyte grades at follow-up minus their sum at baseline
Superior femoral	0–3	
inferior femoral	0–3	
Superior acetabular	0–3	
inferior acetabular	0, 1	
JSN		Change in JSN score: sum of both superior and medial semi-quantitative JSN grades at follow-up minus this sum at baseline
Superior	0–3	
Medial	0–3	

Abbreviations: OARSI Osteoarthritis Research Society International, *JSN* joint space narrowing, *mJSW* medial minimal joint space width

phenotypes (osteophytes and JSN, graded 0–3) and subchondral sclerosis (graded as present or absent) using the OARSI atlas [20]. The presence or absence of subchondral cysts was also evaluated. Overall OA was graded using Croft scoring [21]. Generated and derived progression variables are summarised in Table 1. Radiographs, viewed in open source ImageJ software [22], were inspected for poor image quality, rotation and/or tilt. All readings were performed by one assessor (AH) after focussed radiological training with a musculoskeletal radiologist (MW) and rheumatologist (SAH). A random selection of 72 hips (20%) were regraded to determine intra-rater reliability and graded by a second reader (SAH) to determine inter-rater reliability.

Assessment of clinical OA

Hip pain and limitation of function were assessed by postal questionnaire at 8-year follow-up. To limit non-response bias, the questionnaire was resent if not returned within 3 weeks. If still unreturned after a further 2 weeks, a reminder telephone call was made. The postal questionnaire included the short version WOMAC function scale [23, 24], which limited participant burden. The pain subscale (five questions relating to pain walking on a flat surface, ascending/descending stairs, at night, sitting or lying and standing upright) and function (seven questions relating to difficulty ascending stairs, rising from sitting, walking on flat, getting in/out of a car, putting on socks/stockings, rising from bed and sitting) each had five possible responses (none, mild, moderate, severe, extreme) scored 0–4, respectively. Missing values for pain or function questions were mean-imputed if a participant was missing one question on the pain scale and ≤ 3 on the function scale. Average scores were calculated for each subscale and scaled to give a score ranging from 0 to 100, with 0 representing no pain or functional limitation [25].

Covariate data

At baseline, structured interviews and clinical examination determined participant characteristics including age and standing height. Total body fat mass (TBFM) was assessed by TB DXA scan. Baseline menopausal status, alcohol consumption and history of hormone replacement therapy (HRT) use and smoking were determined by researcher-administered questionnaires. Baseline physical activity levels were determined using the International Physical Activity Questionnaire sent by post [26–28]. Menopausal status, history of smoking and highest educational status were determined by postal questionnaire at follow-up.

Statistical analysis

Associations between HBM status and OA incidence were determined by multivariable logistic regression. We included all hips to increase sample size and thus statistical power, using generalised estimating equations (GEE), which account for correlation between hips from the same individual and produce unbiased estimates in analyses of clustered data [29]. This analysis was restricted to hips with a Croft score < 3 at baseline.

Associations concerning change in osteophytes and JSN (continuous variables) were determined by multivariable GEE linear regression with robust standard errors to account for any non-normal distributions in outcome variables [30, 31]. Betas from analysis of continuous variables represent the difference in mean outcome between those with and without HBM (e.g. a beta of 1 for change in osteophyte score represents a 1-point greater increase in osteophyte score in HBM individuals). Osteophyte and/or JSN scores of 0 at baseline were included in analyses of change in osteophytes and JSN, optimising sample size. Analyses were initially performed unadjusted (model 1) and then adjusted for age, sex and time between radiographs (and baseline sub-phenotype score for continuous outcomes) (model 2). Our previous analyses found HBM to be associated with increased TBFM, with evidence suggesting this is a consequence rather than a cause of HBM [32]. Therefore, adiposity, hypothesised to be on the causal pathway in these analyses, was adjusted for as TBFM in model 3 along with height, to investigate a possible mediating effect of adiposity. Analyses were restricted to individuals with complete data for model 3. Statistical analysis was performed in Stata version 15 (Statacorp, USA) and R version 3.5.1.

Sensitivity analyses

Joints with THR were excluded from the main analyses; however, as THR may have been performed due to severe OA, those with a baseline Croft score < 3 and THR at follow-up were coded as incident OA cases, if they had stated that their THR was performed due to 'arthritis' ($n = 4$). Two individuals without OA at baseline, who had a THR at follow-up due to fracture, were coded as having no incident OA. A person-level analysis, using the sum of the osteophyte and the sum of the JSN scores for the two hips, used GEE to account for correlation within families. Incident OA in person-level analyses represents incident OA in either hip. A model adjusting for metal artefacts on DXA images, analyses removing individuals with DXA positioning errors potentially leading to under-measurement of TBFM (10 hips) and analyses removing individuals who visited a different study site for follow-up (10 hips) were all performed. To check that associations between HBM and change in OA sub-

phenotypes were not explained by bone size, we performed an additional analysis adjusting for the FN area (measured at follow-up). Finally, to check if conclusions were valid despite skewed continuous outcomes, all linear analyses were repeated using a Poisson model.

Results

Characteristics of the study population

Follow-up radiographic and covariate data were available for 136 individuals, with 62% having HBM (index cases or relatives with HBM). The proportion of individuals with HBM did not differ between the populations with and without follow-up data. Those with follow-up data were younger, were less likely to have had hip OA at baseline, to have ever smoked, to be postmenopausal, but were more physically active (Supplementary Table 1). Mean follow-up time for those with complete data was 8.2 (SD 1.0) years and did not differ between those with and without HBM (Table 2). HBM cases were more commonly female (85 vs 50%), with a trend towards a higher proportion of postmenopausal women. HBM individuals had greater baseline BMD (mean TH-BMD 1.24 vs 0.98 g/cm^2), BMI (29.8 vs 27.5 kg/m^2) and TBFM (33.0 vs 29.1 kg) than individuals without HBM (Table 2), consistent with previous observations in this population [11, 32]. Physical activity levels did not differ between HBM individuals and those without HBM.

Repeatability of radiographic OA variables

Weighted intra-rater kappa statistics for the Croft score and all osteophyte (except inferior acetabular) were > 0.7. The intra-rater reliability kappa for inferior acetabular osteophytes was 0.49, for medial JSN was 0.66 and for superior JSN was 0.49. AH observed no acetabular sclerosis or subchondral cysts. Intra-rater reliability for femoral sclerosis was perfect. Inter-rater weighted kappas for the Croft score and all osteophyte grades (except inferior acetabular) were > 0.6, representing substantial agreement [33]. The inter-rater kappa for inferior acetabular osteophytes was 0.38, with kappas of 0.48 for medial JSN and 0.39 for superior JSN. There was disagreement on the one observed case of femoral sclerosis and the one case of subchondral cysts, so these variables were excluded from analyses.

Table 2 Characteristics of the study population, constituting individuals with and without HBM, who were followed up at 8 years

	All, *N* = 136	HBM, *N* = 86	Relatives without HBM, *N* = 50	*p* value for difference
		***N* (%)**		
Female gender	98 (72.1)	73 (84.9)	25 (50.0)	< 0.001
Postmenopausal[b]	75 (76.5)	59 (80.8)	16 (64.0)	0.087
Menopause transition during the follow-up period	11 (11.2)	6 (8.2)	5 (20.0)	0.177
History of HRT use[f]	49 (50.0)	39 (53.4)	10 (40.0)	0.508
History of smoking[f]	66 (48.9)	42 (49.4)	24 (48.0)	0.874
Physical activity category[b]				
Low	14 (10.7)	9 (11.0)	5 (10.2)	
Medium	46 (35.1)	26 (31.7)	20 (40.8)	0.567
High	71 (54.2)	47 (57.3)	24 (49.0)	
Education category[f]				
Up to GCSE/O level	55 (42.0)	42 (50.0)	13 (27.7)	
A level or equivalent	26 (19.9)	17 (20.2)	9 (19.2)	0.019
Degree or equivalent	50 (38.2)	25 (29.8)	25 (53.2)	
		Mean (SD)		
Age, years[b]	59.2 (10.2)	60.2 (9.9)	57.5 (10.6)	0.136
Height, cm[b]	167.8 (9.6)	166.1 (8.4)	170.8 (10.8)	0.005
Weight, kg[b]	81.5 (17.0)	82.1 (16.0)	80.6 (18.7)	0.619
BMI (kg/m^2)[b]	28.9 (5.5)	29.8 (5.6)	27.5 (5.1)	0.017
TBFM (kg)[f]	31.6 (10.6)	33.0 (10.9)	29.1 (9.5)	0.035
TH-BMD, g/cm^2 [b]	1.143 (0.182)	1.242 (0.129)	0.976 (0.131)	< 0.001
L1-BMD, g/cm^2 [b]	1.255 (0.215)	1.377 (0.149)	1.049 (0.141)	< 0.001
Follow-up time, years	8.2 (1.0)	8.2 (0.7)	8.2 (1.4)	0.817

Abbreviations: *HBM* high bone mass, *HRT* hormone replacement therapy, *BMI* body mass index, *TBFM* total body fat mass, *TH-BMD* total hip bone mineral density
[b] Assessed at baseline
[f] Assessed as follow-up

Table 3 Prevalence of radiographic and clinical sub-phenotypes of OA in the study population, stratified by HBM status

	All hips		HBM hips		Non-HBM hips	
	Total *N*	***N* (%) with sub-phenotype**	**Total *N***	***N* (%) with sub-phenotype**	**Total *N***	***N* (%) with sub-phenotype**
OA (Croft ≥ 3)						
Baseline	285	22 (7.7)	179	13 (7.3)	106	9 (8.5)
Follow-up	275	33 (12.0)	173	24 (13.9)	102	9 (8.8)
Incident	257	18 (7.0)	162	15 (9.3)	95	3 (3.2)
Progressive	18	5 (27.8)	11	2 (18.2)	7	3 (42.9)
Hip replacement (identified on radiograph)						
Baseline	290	5 (1.7)	184	5 (2.7)	106	0
Follow-up	290	15 (5.2)	184	11 (6.0)	106	4 (3.8)
Incident	285	10 (3.5)	179	6 (3.4)	106	4 (3.8)
Osteophyte score						
Baseline	285		179		106	
0		203 (71.2)		126 (70.4)		77 (72.6)
1–4		75 (26.3)		50 (27.9)		25 (23.6)
≥ 5		7 (2.5)		5 (2.8)		4 (3.8)
Follow-up	275		173		102	
0		161 (58.6)		94 (54.3)		67 (65.7)
1–4		105 (38.2)		73 (42.2)		32 (31.4)
≥ 5		9 (3.3)		6 (3.5)		3 (2.9)
Delta	275		173		102	
< 1		201 (73.1)		121 (69.9)		80 (78.4)
1		48 (17.5)		32 (18.5)		16 (15.7)
> 1		26 (9.5)		20 (11.6)		6 (5.9)
JSN score						
Baseline	285		179		106	
0		253 (88.8)		160 (89.4)		93 (87.7)
1–2		27 (9.5)		16 (8.9)		11 (10.4)
≥ 3		5 (1.8)		3 (1.7)		2 (1.9)
Follow-up	275		173		102	
0		241 (87.6)		149 (86.1)		92 (90.2)
1–2		28 (10.2)		20 (11.6)		8 (7.8)
≥ 3		6 (2.2)		4 (2.3)		2 (2.0)
Delta	275		173		102	
< 1		261 (94.9)		161 (93.1)		100 (98.0)
1		12 (4.4)		10 (5.8)		2 (2.0)
> 1		2 (0.7)		2 (1.2)		0 (0.0)
	All individuals		**HBM individuals**		**Relatives without HBM**	
	Total *N*	**Median (IQR)**	**Total *N***	**Median (IQR)**	**Total *N***	**Median (IQR)**
WOMAC at follow-up						
Pain	145	0 (0, 25)	92	10 (0, 35)	53	0 (0, 15)
Function	145	3.6 (0, 25)	92	10.7 (0, 30.4)	53	0 (0, 14.3)
	Total *N*	***N* (%)**	**Total *N***	***N* (%)**	**Total *N***	***N* (%)**
Hip replacement (self-reported)	145	16 (11.0)	92	13 (14.1)	53	3 (5.7)

Abbreviations: HBM high bone mass, *OA* osteoarthritis, *JSN* joint space narrowing, *WOMAC* Western Ontario and McMaster Universities Osteoarthritis Index

HBM and the incidence and progression of overall hip OA

Radiographic hip OA was observed in 7.7% of all 290 hips at baseline and 12.0% at follow-up (Table 3). Of the 257 OA-free hips at baseline, 7.0% developed OA. There was no clear evidence that HBM was associated with an increased risk of overall incident OA measured by Croft score, before (model 1, OR = 2.54 [95%CI 0.66, 9.71], Fig. 2) or after adjustment for age, sex and follow-up time (model 2, 1.65 [0.41, 6.70]). Due to the low baseline prevalence of overall OA defined as Croft score ≥ 3 (i.e. the presence of osteophytes *and* JSN), we were unable to analyse OA progression. Using Croft score ≥ 1 to define OA at baseline, 82 hips had potential to progress, of which 16 had a higher Croft score at follow-up than baseline (12 with HBM). However, no clear association between HBM and overall OA progression was observed (model 3, OR 4.14 [0.81, 21.3], Fig. 2). When combining incident and progressive OA to generate a variable for any incident or progressive hip OA, HBM was still not clearly associated with the overall change in hip OA severity (model 3, OR 1.72 [0.58, 5.11]).

Combined incidence and progression of radiographic hip OA sub-phenotypes

Of the total population, 28.8% hips had at least one osteophyte at baseline, rising to 41.5% at follow-up (Table 3). JSN was much less prevalent at baseline and follow-up (11.3% and 12.4%, respectively). In unadjusted analyses, we found evidence that individuals with HBM experienced greater changes in both osteophyte and JSN scores than individuals without HBM ($\beta_{osteophyte} = 0.30$ [0.05, 0.54], $p = 0.019$ and $\beta_{JSN} = 0.09$ [0.01, 0.16], $p = 0.019$, β reflects the difference in the mean change in osteophyte/JSN score between those with and without HBM). These associations persisted after adjustment for age, sex, follow-up time, baseline score, height and TBFM (model 3) (Fig. 2).

HBM and clinical features of hip OA

HBM was associated with 12-point [95% CI 5, 18] higher WOMAC pain scores and 13-point [7, 19] higher function scores in unadjusted analyses. Adjustment for age, sex, height and TBFM attenuated these relationships by

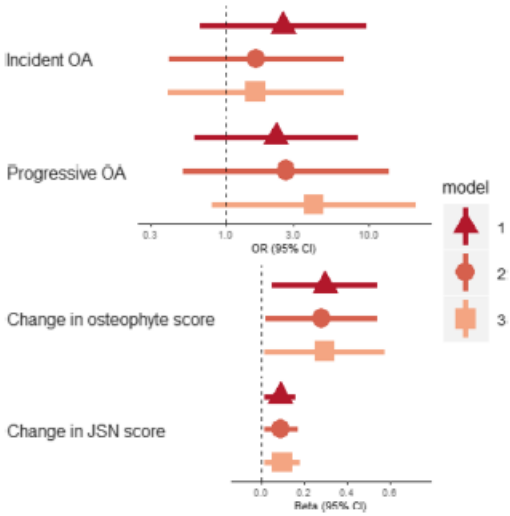

Fig. 2 Associations between HBM and incident and progressive OA and change in OA sub-phenotypes. Points for continuous outcomes represent the difference in mean outcome between individuals with and without HBM (for example, a beta of 1 for change in osteophyte score would represent a 1-point greater increase in summed osteophyte score, which is the equivalent of the appearance of one additional osteophyte over 8 years or the increase in the size of an osteophyte already present). Points for binary outcomes represent the odds ratio for individuals with HBM compared to their relatives with normal BMD. Model 1: unadjusted; model 2: adjusted for age, sex and follow-up time (plus baseline score for continuous outcomes); model 3: adjusted for age, sex, follow-up time, height and TBFM (plus baseline score for continuous outcomes). $N_{incident\ OA} = 248$; $N_{continuous\ outcomes} = 263$. *Abbreviation*: *JSN* joint space narrowing

approximately one-third to one-half (β_{pain} = 6.4 [− 1.4, 14.2], p = 0.105 and $\beta_{function}$ = 8.3 [0.7, 15.8], p = 0.032, β represents the difference in mean WOMAC score between those with and without HBM). Further adjustment for osteophyte or JSN score at follow-up did not appear to explain these relationships (Fig. 3). There was some weak evidence supporting an increased odds of self-reported hip replacement in individuals with HBM who completed the follow-up questionnaire, compared to those without HBM (age, sex, height and TBFM-adjusted OR = 4.27 [0.94, 19.5], p = 0.061, N = 148).

Sensitivity analyses

Including six individuals with an incident THR and a Croft score < 3 at baseline in the analysis of incident OA did not alter conclusions drawn. Neither did removing 10 hips from individuals who visited a different study site for follow-up radiographs, removing hips from individuals with DXA positioning errors, nor additional adjustment for TB DXA artefact. Conclusions were unchanged when performing a person-level analysis accounting for within-family clustering, although CIs were wider due to the reduced sample size (Supplementary Figure 1). Additional adjustment for the FN area (as a measure of bone size) marginally attenuated effect estimates ($\beta_{osteophyte}$ = 0.26 [0.01, 0.52] to 0.21 [− 0.02, 0.44] and β_{JSN} = 0.08 [0.01, 0.16] to 0.07 [4.74×10^{-3}, 0.13]). Conclusions were unchanged when using a Poisson model, although the association between HBM and change in JSN score was stronger than the association with change in osteophyte score; however, it should be noted that these analyses may be biased by the need to recode negative values as zero.

Discussion

We have found evidence for increased osteophyte development (i.e. incidence and/or progression) and JSN at the hip, over an average of 8 years in individuals with HBM, compared to their relatives without HBM. Radiographic JSN is thought to indirectly reflect cartilage loss [34]. Furthermore, individuals with HBM have more hip pain and limitation of function in their daily activities, which adds further evidence for increased OA severity in this population. Low statistical power limited our ability to draw strong conclusions about the relationship between HBM and overall incident OA, based on the Croft score.

Few studies have determined the association between BMD and hip OA incidence or progression. Bergink et al. observed a relationship between FN-BMD and both hip OA incidence and progression in the Rotterdam study population [14]. We have extended these findings by determining the relationship between high BMD and the incidence and/or progression of individual radiographic sub-phenotypes. Barbour et al. identified weak evidence for worsening osteophytes with increasing BMD in JoCo, but no evidence for a relationship with

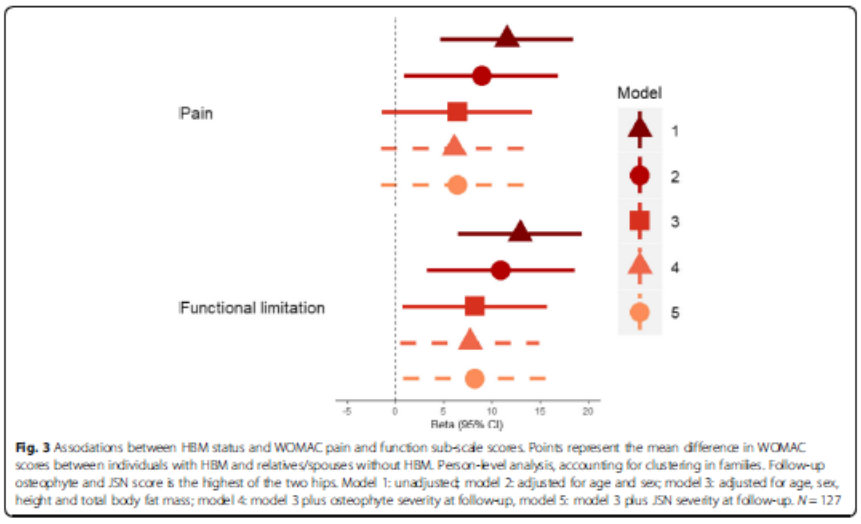

Fig. 3 Associations between HBM status and WOMAC pain and function sub-scale scores. Points represent the mean difference in WOMAC scores between individuals with HBM and relatives/spouses without HBM. Person-level analysis, accounting for clustering in families. Follow-up osteophyte and JSN score is the highest of the two hips. Model 1: unadjusted; model 2: adjusted for age and sex; model 3: adjusted for age, sex, height and total body fat mass; model 4: model 3 plus osteophyte severity at follow-up, model 5: model 3 plus JSN severity at follow-up. N = 127

JSN progression [13], which is inconsistent with our observed (albeit weak) relationship between HBM and change in JSN score. Hochberg et al. identified a dose-response relationship between BMD and subsequent incidence of OA in SOF [15]. However, this relationship was no longer present when defining incidence based on JSN alone. In our analyses, whilst we did not observe strong evidence for an association between HBM and incident hip OA, possibly due to low numbers, the direction of effect was consistent with previous findings.

Our observed relationship between HBM and hip pain is consistent with studies of population-based cohorts, which have identified an increased BMD in those reporting hip pain [4]. The severity of OA sub-phenotypes did not appear to explain the relationship between HBM and hip pain or functional limitations, suggesting that HBM individuals have an increased risk of clinical OA independent of radiographic severity. The WOMAC questionnaire measures pain over the past 48 h, which may explain why radiographic OA severity did not explain current pain, as pain could increase during stages of rapid OA progression not captured by radiographs [35]. An analysis of the Framingham and OA Initiative populations found that fewer than 25% of individuals with radiographic hip OA reported hip pain, and fewer than 20% reporting hip pain had radiographic hip OA [36]. It is possible that increased pain and functional limitation in the HBM population could reflect other conditions of the hip, such as bursitis [37] or features of a mild skeletal dysplasia, or inflammation not detected on the radiograph.

Increased TBFM in the HBM population [32] did not appear to explain the relationship between HBM and change in radiographic OA sub-phenotypes. Adjustment for the FN area, as a measure of bone size, only explained a small proportion of the relationship. Unfortunately, we do not have measures of FN width, a reported risk factor for hip OA progression [38]. It is plausible that HBM individuals would have greater FN width due to greater bone mass meaning measures of FN area may not equate to FN width in this population. Another factor which may mediate the relationship between HBM and development of hip OA sub-phenotypes is differences in hip shape. HBM individuals more commonly have features of cam-type deformity (i.e. larger femoral head size and reduced sphericity) compared to their relatives without HBM [39]. Evidence suggests that cam-type deformities are a risk factor for end-stage hip OA and hence potentially for hip OA progression [40, 41].

Although HBM is likely to be caused by the polygenic inheritance of multiple BMD loci [12], or the monogenic inheritance of rare variants [42], indicating that HBM precedes OA development, we cannot rule out the possibility that biological pleiotropy, rather than a causal effect, explains our results. We have previously identified an increased prevalence of pelvic enthesophytes in the HBM population, leading to the hypothesis that HBM individuals may have a genetic predisposition to form extra bone [43]. We observed a stronger effect size for the relationship between HBM and change in hip osteophyte score, than we did for that between HBM and change in hip JSN score, which further suggests a 'bone-forming' phenotype in this population. Further evidence for pleiotropy was provided by Hackinger et al. who found weak evidence for a genetic correlation between hip OA and LS-BMD, but not hip OA and FN-BMD [44]. By performing a cross-phenotype meta-analysis between overall OA and LS-BMD, the authors identified novel loci in the *SMAD3* gene [44]. SMAD3 is part of the transforming growth factor β (TGFβ) signalling pathway, regulating osteoblast differentiation and thus bone formation. The first discovered hip OA locus, growth differentiation factor-5 (*GDF5*), is a ligand for this pathway [45], suggesting that this pathway contributes to both BMD and hip OA.

Strengths and limitations

The HBM study constitutes the largest population of individuals with extreme, unexplained, generalised HBM [11]. We analysed change in OA sub-phenotypes separately, which allowed us to detect the stronger relationship with osteophyte development compared to change in JSN. We analysed change in osteophytes and JSN as continuous measures, increasing statistical power to detect associations and reducing the possibility of a ceiling effect by increasing the range of possible values from 0 to 6 for JSN and 0 to 10 for osteophytes and eliminating the possibility of selection bias in a case-only analysis.

The method of identifying individuals from NHS DXA databases ascertained a predominantly female and older population such that a relatively large proportion were unable to be followed up after 8 years, due to death or poor health. Hence, there was a lower baseline prevalence of radiographic hip OA in the population able to be followed up, meaning we had limited power to assess hip OA incidence and progression based on the overall Croft score. The baseline cross-sectional study was powered to determine if the odds of OA differed between HBM individuals and their relatives with an expected recruitment of 200 cases and 200 controls [10]. However, loss-to-follow-up over 8 years reduced our sample size and a retrospective power calculation for the analyses presented here showed that we had approximately 65% power to detect the change in osteophyte and JSN scores reported here and lower power to detect a difference in proportion of incident hip OA between HBM individuals and their non-HBM relatives. Radiographs and DXA scans were performed using standard protocols at each

centre but were not standardised across centres. However, as 97% of individuals re-attended the same centre for follow-up, this is unlikely to affect our measures for *change* in radiographic features. Furthermore, measuring change in sub-phenotype variables did not separate hip OA sub-phenotype progression from incidence since these results had to be pooled to optimise sample size. As baseline and follow-up radiographs were not read as pairs, we did observe a few negative scores for change in osteophytes (8%) and change in JSN (1.5%), which were included in analyses, because removing these values as 'measurement error' would have biased results as there was likely to have been the same proportion of measurement error overinflating change, for which we would not have been able to account (hence the reasoning for not basing conclusions on the Poisson analysis). Radiographic grading of OA sub-phenotypes is subjective, which we limited using an established atlas [20], although our intra-rater and inter-rater reliability were low for a few variables, attenuating the conclusions we can draw from this analysis. As the reader was blinded to timepoint, it is unlikely that radiographic features were systematically under-graded at baseline and over-graded at follow-up, meaning measurement error is unlikely to explain our results. WOMAC scores were only collected at follow-up, and therefore, we cannot draw conclusions about the relationship between HBM and symptomatic OA *progression*. Finally, as HBM individuals represent a rare and extreme tail of the BMD distribution, findings may not be generalisable to the wider population.

Conclusions

We have found evidence for associations between HBM and worsening of radiographic sub-phenotypes of hip OA over 8 years. We further provide evidence for greater symptoms of OA in HBM individuals. These associations are independent of the elevated fat mass observed in HBM individuals. Further genetic analyses are planned to determine the BMI-independent causal role of BMD in hip OA progression and to identify the underlying biological pathways explaining these associations.

Supplementary Information

The online version contains supplementary material available at https://doi.org/10.1186/s13075-020-02371-0.

Additional file 1: Supplementary Table 1. Baseline characteristics for those with and without follow-up data, **Supplementary Figure 1**. associations between HBM and incident OA and incident and progressive OA sub-phenotypes in person-level analyses.

Abbreviations

AP: Anteroposterior; BMD: Bone mineral density; BMI: Body mass index; CIs: Confidence intervals; DXA: Dual-energy X-ray absorptiometry; FN: Femoral neck; GEE: Generalised estimating equations; HBM: High bone mass; JoCo: Johnston County Osteoarthritis Project; JSN: Joint space narrowing; LS: Lumbar spine; MrOS: Study of Osteoporotic Fractures in Men; OA: Osteoarthritis; REC: Research Ethics Committee; sBMD: Standardised bone mineral density; SOF: Study of Osteoporotic Fractures; TB: Total body; TBFM: Total body fat mass; TH: Total hip; THR: Total hip replacement; vBMD: Volumetric bone mineral density

Acknowledgements

We would like to thank all our HBM study participants and the staff at the University of Bristol and our collaborating centres: Addenbrooke's Wellcome Trust Clinical Research Facility, NIHR Bone Biomedical Research Unit in Sheffield, the Centre for Metabolic Bone Disease in Hull, Southmead Hospital in Bristol, Nuffield Orthopaedic Centre in Oxford, the Royal National Hospital for Rheumatic Diseases in Bath and St George's Hospital in London.

Authors' contributions

Conceptualization: JHT and CLG. Methodology: AH, SAH, JHT and CLG. Software: JP. Formal analysis: AH, JHT and CLG. Investigation: AH, SAH, MF, EM, KESP, MKJ, MA, KM, MW, JHT and CLG. Writing of the original draft: AH, JT and CLG. Writing, review and editing: all authors. The authors read and approved the final manuscript.

Funding

The HBM study was supported by The Wellcome Trust (080280/Z/06/Z), the National Institute for Health Research Clinical Research Network (portfolio no. 5163) and Versus Arthritis (ref 20000). AH is funded by the Wellcome Trust (grant ref. 203788/Z/16/Z). Follow-up imaging at the Hull site was funded by OSPREY (OSteoPorosis Research in East Yorkshire). AH, LP, JHT and CLG work in, or are affiliated with, a University of Bristol and MRC funded unit (MC_UU_00011/1).

Availability of data and materials

The datasets during and/or analysed during the current study available from the corresponding author on reasonable request.

Ethics approval and consent to participate

Written informed consent was obtained in line with the Declaration of Helsinki [46]. The study was approved by the Bath Multi-centre Research Ethics Committee (REC reference 05/Q2001/78) and each local NHS REC. Follow-up data collection was approved by the Central Bristol REC and NHS Health Research Authority.

Consent for publication

Not applicable.

Competing interests

The authors have no competing interests to disclose.

Author details

[1]Musculoskeletal Research Unit, Translational Health Sciences, Bristol Medical School, University of Bristol, Bristol, UK. [2]MRC Integrative Epidemiology Unit, Population Health Sciences, Bristol Medical School, University of Bristol, Bristol, UK. [3]Royal National Hospital for Rheumatic Diseases, Royal United Hospitals Bath NHS Foundation Trust, Bath, UK. [4]Division of Informatics, Imaging & Data Sciences, Faculty of Medical and Human Sciences, University of Manchester, Manchester, UK. [5]Academic Unit of Bone Metabolism, Department of Oncology and Metabolism, The Mellanby Centre For Bone Research, University of Sheffield, Sheffield, UK. [6]Centre for Metabolic Diseases, University of Sheffield Medical School, Sheffield, UK. [7]Centre for Integrated Research into Musculoskeletal Ageing, University of Sheffield Medical School, Sheffield, UK. [8]Cambridge NIHR Biomedical Research Centre and the Wellcome Trust Clinical Research Facility, Cambridge, UK. [9]Nuffield Department of Orthopaedics, Rheumatology and Musculoskeletal Sciences, University of Oxford, Oxford, UK. [10]Department of Diabetes, Endocrinology and Metabolism, Hull and East Yorkshire Hospitals NHS Trust, Hull, UK. [11]Centre for Rheumatology, St George's Hospital, St George's Healthcare NHS Trust, London, UK. [12]Department of Radiology, Southmead Hospital, North Bristol NHS Trust, Bristol, UK.

Received: 20 August 2020 Accepted: 9 November 2020
Published online: 06 January 2021

References

1. Cross M, Smith E, Hoy D, Nolte S, Ackerman I, Fransen M, et al. The global burden of hip and knee osteoarthritis: estimates from the global burden of disease 2010 study. Ann Rheum Dis. 2014;73(7):1323–30.
2. Stewart A, Black A, Robins SP, Reid DM. Bone density and bone turnover in patients with osteoarthritis and osteoporosis. J Rheumatol. 1999;26(3):622–6.
3. Glowacki J, Tuteja M, Hurwitz S, Thornhill TS, Leboff MS. Discordance in femoral neck bone density in subjects with unilateral hip osteoarthritis. J Clin Densitom. 2010;13(1):24–8.
4. Nevitt MC, Lane NE, Scott JC, Hochberg MC, Pressman AR, Genant HK, et al. Radiographic osteoarthritis of the hip and bone mineral density. The Study of Osteoporotic Fractures Research Group. Arthritis Rheum. 1995;38(7):907–16.
5. Chaganti RK, Parimi N, Lang T, Orwoll E, Stefanick ML, Nevitt M, et al. Bone mineral density and prevalent osteoarthritis of the hip in older men for the Osteoporotic Fractures in Men (MrOS) Study Group. Osteoporos Int. 2010;21(8):1307–16.
6. Antoniades L, MacGregor AJ, Matson M, Spector TD. A cotwin control study of the relationship between hip osteoarthritis and bone mineral density. Arthritis Rheum. 2000;43(7):1450–5.
7. Edwards MH, Paccou J, Ward KA, Jameson KA, Moss C, Woolston J, et al. The relationship of bone properties using high resolution peripheral quantitative computed tomography to radiographic components of hip osteoarthritis. Osteoarthritis Cartilage. 2017;25(9):1478–83.
8. Burger H, van Daele PL, Odding E, Valkenburg HA, Hofman A, Grobbee DE, et al. Association of radiographically evident osteoarthritis with higher bone mineral density and increased bone loss with age. Rotterdam Stud Arthritis Rheum. 1996;39(1):81–6.
9. Arokoski JP, Arokoski MH, Jurvelin JS, Helminen HJ, Niemitukia LH, Kroger H. Increased bone mineral content and bone size in the femoral neck of men with hip osteoarthritis. Ann Rheum Dis. 2002;61(2):145–50.
10. Hardcastle SA, Dieppe P, Gregson CL, Hunter D, Thomas GE, Arden NK, et al. Prevalence of radiographic hip osteoarthritis is increased in high bone mass. Osteoarthr Cartil. 2014;22(8):1120–8.
11. Gregson CL, Steel SA, O'Rourke KP, Allan K, Ayuk J, Bhalla A, et al. 'Sink or swim': an evaluation of the clinical characteristics of individuals with high bone mass. Osteoporosis Int. 2012;23(2):643–54.
12. Gregson CL, Newell F, Leo PJ, Clark GR, Paternoster L, Marshall M, et al. Genome-wide association study of extreme high bone mass: contribution of common genetic variation to extreme BMD phenotypes and potential novel BMD-associated genes. Bone. 2018;114:62–71.
13. Barbour KE, Murphy LB, Helmick CG, Hootman JM, Renner JB, Jordan JM. Bone mineral density and the risk of hip and knee osteoarthritis: the Johnston county osteoarthritis project. Arthritis Care Res. 2017;69(12):1868–70.
14. Bergink AP, Rivadeneira F, Bierma-Zeinstra SM, Carola Zillikens M, Arfan Ikram M, Uitterlinden AG, et al. Are bone mineral density and fractures related to the incidence and progression of radiographic osteoarthritis of the knee, hip and hand in elderly men and women? The Rotterdam study. Arthritis Rheumatol. 2018;71(3):361–9.
15. Hochberg MC. Do risk factors for incident hip osteoarthritis (OA) differ from those for progression of hip OA? J Rheumatol Suppl. 2004;70:6–9.
16. Little RD, Carulli JP, Del Mastro RG, Dupuis J, Osborne M, Folz C, et al. A mutation in the LDL receptor-related protein 5 gene results in the autosomal dominant high-bone-mass trait. Am J Hum Genet. 2002;70(1):11–9.
17. Shepherd JA, Fan B, Lu Y, Wu XP, Wacker WK, Ergun DL, et al. A multinational study to develop universal standardization of whole-body bone density and composition using GE Healthcare lunar and Hologic DXA systems. J Bone Miner Res. 2012;27(10):2208–16.
18. Fan B, Lu Y, Genant H, Fuerst T, Shepherd J. Does standardized BMD still remove differences between Hologic and GE-Lunar state-of-the-art DXA systems? Osteoporos Int. 2010;21(7):1227–36.
19. Hanson J. Standardization of femur BMD. J Bone Miner Res. 1997;12(8):1316–7.
20. Altman RD, Gold GE. Atlas of individual radiographic features in osteoarthritis, revised. Osteoarthritis Cartilage. 2007;15(Suppl A):A1–56.
21. Croft P, Cooper C, Wickham C, Coggon D. Defining osteoarthritis of the hip for epidemiologic studies. Am J Epidemiol. 1990;132(3):514–22.
22. Schneider CA, Rasband WS, Eliceiri KW. NIH Image to ImageJ: 25 years of image analysis. Nat Methods. 2012;9(7):671–5.
23. Whitehouse SL, Lingard EA, Katz JN, Learmonth ID. Development and testing of a reduced WOMAC function scale. J Bone Joint Surg Br. 2003;85(5):706–11.
24. Bellamy N, Buchanan WW, Goldsmith CH, Campbell J, Stitt LW. Validation study of WOMAC: a health status instrument for measuring clinically important patient relevant outcomes to antirheumatic drug therapy in patients with osteoarthritis of the hip or knee. J Rheumatol. 1988;15(12):1833–40.
25. Wylde V, Lenguerrand E, Gooberman-Hill R, Beswick AD, Marques E, Noble S, et al. Effect of local anaesthetic infiltration on chronic postsurgical pain after total hip and knee replacement: the APEX randomised controlled trials. Pain. 2015;156(6):1161–70.
26. Craig CL, Marshall AL, Sjostrom M, Bauman AE, Booth ML, Ainsworth BE, et al. International physical activity questionnaire: 12-country reliability and validity. Med Sci Sports Exerc. 2003;35(8):1381–95.
27. Hagstromer M, Oja P, Sjostrom M. The International Physical Activity Questionnaire (IPAQ): a study of concurrent and construct validity. Public Health Nutr. 2006;9(6):755–62.
28. Hallal PC, Victora CG. Reliability and validity of the International Physical Activity Questionnaire (IPAQ). Med Sci Sports Exerc. 2004;36(3):556.
29. Ballinger GA. Using generalized estimating equations for longitudinal data analysis. Organ Res Methods. 2004;7(2):127–50.
30. Huber PJ, editor The behavior of maximum likelihood estimates under nonstandard conditions. Proceedings of the Fifth Berkeley Symposium on Mathematical Statistics and Probability, volume 1: statistics; 1967 1967; Berkeley, Calif: University of California Press.
31. White H. A heteroskedasticity-consistent covariance matrix estimator and a direct test for heteroskedasticity. Econometrica. 1980;48(4):817–38.
32. Gregson CL, Paggiosi MA, Crabtree N, Steel SA, McCloskey E, Duncan EL, et al. Analysis of body composition in individuals with high bone mass reveals a marked increase in fat mass in women but not men. J Clin Endocrinol Metab. 2013;98(2):818–28.
33. Landis JR, Koch GG. The measurement of observer agreement for categorical data. Biometrics. 1977;33(1):159–74.
34. Guermazi A, Hunter DJ, Roemer FW. Plain radiography and magnetic resonance imaging diagnostics in osteoarthritis: validated staging and scoring. J Bone Joint Surg Am. 2009;91(Suppl 1):54–62.
35. Wesseling J, Bierma-Zeinstra SMA, Kloppenburg M, Meijer R, Bijlsma JWJ. Worsening of pain and function over 5 years in individuals with 'early' OA is related to structural damage: data from the Osteoarthritis Initiative and CHECK (Cohort Hip & Cohort Knee) study. Ann Rheum Dis. 2015;74(2):347.
36. Kim C, Nevitt MC, Niu J, Clancy MM, Lane NE, Link TM, et al. Association of hip pain with radiographic evidence of hip osteoarthritis: diagnostic test study. BMJ. 2015;351:h5983.
37. Nieuwenhuijse MJ, Nelissen RG. Hip pain and radiographic signs of osteoarthritis. BMJ. 2015;351:h6262.
38. Javaid MK, Lane NE, Mackey DC, Lui LY, Arden NK, Beck TJ, et al. Changes in proximal femoral mineral geometry precede the onset of radiographic hip osteoarthritis: the study of osteoporotic fractures. Arthritis Rheum. 2009;60(7):2028–36.
39. Patel A, Baird D, Hardcastle S, Gregory J, Aspenden R, Faber B, et al. Do alterations in hip shape explain the increased risk of hip osteoarthritis in individuals with high bone mass? [Conference abstract]. Bone research society annual meeting 2016; Liverpool, UK. 2016.
40. Nicholls AS, Kiran A, Pollard TCB, Hart DJ, Arden CPA, Spector T, et al. The association between hip morphology parameters and nineteen-year risk of end-stage osteoarthritis of the hip: a nested case–control study. Arthritis Rheumatism. 2011;63(11):3392–400.
41. Agricola R, Heijboer MP, Bierma-Zeinstra SM, Verhaar JA, Weinans H, Waarsing JH. Cam impingement causes osteoarthritis of the hip: a nationwide prospective cohort study (CHECK). Ann Rheum Dis. 2013;72(6):918–23.
42. Gregson CL, Bergen DJM, Leo P, Sessions RB, Wheeler L, Hartley A, et al. A rare mutation in SMAD9 associated with high bone mass identifies the SMAD-dependent BMP signaling pathway as a potential anabolic target for osteoporosis. J Bone Miner Res. 2020;35(1):92–105.
43. Hardcastle SA, Dieppe P, Gregson CL, Arden NK, Spector TD, Hart DJ, et al. Osteophytes, enthesophytes, and high bone mass a bone-forming triad with potential relevance in osteoarthritis. Arthritis Rheumatol. 2014;66(9):2429–39.

44. Hackinger S, Trajanoska K, Styrkarsdottir U, Zengini E, Steinberg J, Ritchie GRS, et al. Evaluation of shared genetic aetiology between osteoarthritis and bone mineral density identifies SMAD3 as a novel osteoarthritis risk locus. Hum Mol Genet. 2017;26(19):3850–8.
45. Cibrian Uhalte E, Wilkinson JM, Southam L, Zeggini E. Pathways to understanding the genomic aetiology of osteoarthritis. Hum Mol Genet. 2017;26(R2):R198–r201.
46. World Medical Association Declaration of Helsinki ethical principles for medical research involving human subjects. J Am Med Assoc. 2013;310(20):2191–4.

Publisher's Note

Appendix 3: Manuscript based on results of metabolomics of bone turnover, published in Clinical Endocrinology.

Received: 14 August 2019 | Revised: 22 October 2019 | Accepted: 26 October 2019
DOI: 10.1111/cen.14119

ORIGINAL ARTICLE

WILEY

Metabolomics analysis in adults with high bone mass identifies a relationship between bone resorption and circulating citrate which replicates in the general population

April Hartley[1,2,3] | Lavinia Paternoster[1,2] | David M. Evans[1,2,4] | William D. Fraser[5] | Jonathan Tang[5] | Debbie A. Lawlor[1,2,6] | Jon H. Tobias[1,3] | Celia L. Gregson[3]

[1]Medical Research Council Integrative Epidemiology Unit, Population Health Sciences, Bristol Medical School, University of Bristol, Bristol, UK

[2]Population Health Sciences, Bristol Medical School, Bristol University, Bristol, UK

[3]Musculoskeletal Research Unit, Translation Health Sciences, Bristol Medical School, University of Bristol, Bristol, UK

[4]Translational Research Institute, The University of Queensland Diamantina Institute, Brisbane, Qld, Australia

[5]Department of Medicine, Norwich Medical School, University of East Anglia, Norwich, UK

[6]National Institute for Health Research Bristol Biomedical Research Centre, Bristol, UK

Correspondence
April Hartley, Musculoskeletal Research Unit, Learning and Research Building, Southmead Hospital, Bristol, BS10 5NB, UK.
Email: april.hartley@bristol.ac.uk

Funding Information
The HBM study was supported by The Wellcome Trust and the National Institute for Health Research Clinical Research Network (portfolio no. 5163). AH is funded by the Wellcome Trust (grant ref 20378/Z/16/Z). Initial HBM data collection was funded by a Wellcome Trust Clinical Research Training Fellowship for CLG (grant ref 080280/Z/06/Z). CLG is currently funded by a Clinician Scientist Fellowship from Versus Arthritis (grant ref 20000). The UK Medical Research Council and Wellcome (grant ref 102215/2/13/2) and the University of Bristol provide core support for ALSPAC. Bone and metabolite measurements in ALSPAC mothers were funded by the British Heart Foundation (grant ref SP/07/008/24066), Wellcome Trust (grant ref WT092830M), the UK

Abstract

Objective: Bone turnover, which regulates bone mass, may exert metabolic consequences, particularly on markers of glucose metabolism and adiposity. To better understand these relationships, we examined cross-sectional associations between bone turnover markers (BTMs) and metabolic traits.

Design: β-C-terminal telopeptide of type-I collagen (β-CTX), procollagen type-1 amino-terminal propeptide (P1NP) and osteocalcin were assessed by electrochemiluminescence immunoassays. Metabolic traits, including lipids and glycolysis-related metabolites, were measured using nuclear magnetic resonance spectroscopy. Associations of BTMs with metabolic traits were assessed using Generalized Estimating Equation linear regression, accounting for within-family correlation, adjusting for potential confounders (age, sex, height, weight, menopause, bisphosphonate and oral glucocorticoid use).

Patients: 198 adults with high bone mass (HBM, BMD Z-score>+3.2), mean [SD] age 61.6 [13.7] years; 77% female.

Results: Of 23 summary metabolic traits, citrate was positively related to all BTMs: adjusted $\beta_{\beta\text{-CTX}} = 0.050$ (95% CI 0.024, 0.076), $P = 1.71 \times 10^{-4}$, $\beta_{\text{osteocalcin}} = 6.54 \times 10^{-4}$ (1.87×10^{-4}, 0.001), $P = .006$ and $\beta_{\text{P1NP}} = 2.40 \times 10^{-4}$ (6.49×10^{-5}, 4.14×10^{-4}), $P = .007$ (β = increase in citrate (mmol/L) per 1 μg/L BTM increase). Inverse relationships of β-CTX (β = −0.276 [−0.434, −0.118], $P = 6.03 \times 10^{-4}$) and osteocalcin (−0.004 [−0.007, −0.001], $P = .020$) with triglycerides were also identified. We explored the generalizability of these associations in 3664 perimenopausal women (age 47.9 [4.4] years) from a UK family cohort. We confirmed a positive, albeit lower magnitude, association between β-CTX and citrate (adjusted $\beta_{\text{women}} = 0.020$ [0.013, 0.026], $P = 1.95 \times 10^{-9}$) and an inverse association of similar magnitude between β-CTX and triglycerides (β = −0.354 [−0.471, −0.237], $P = 3.03 \times 10^{-9}$).

Conclusions: Bone resorption is positively related to circulating citrate and inversely related to triglycerides. Further studies are justified to determine whether plasma citrate or triglyceride concentrations are altered by factors known to modulate bone resorption, such as bisphosphonates.

Medical Research Council (grant ref G1001357) and UK National Institute for Health Research (grant ref NF-SI-0611-10196). Teen Focus 3 was funded by the Wellcome Trust and MRC (grant ref 076467/Z/05/Z). Metabolomics analysis of the ALSPAC adolescent cohort was funded by the MRC (grant ref MC_UU_12013/1). AH, LP, DE, DAL, JHT work in, or are affiliated with, a University of Bristol and MRC funded unit (MC_UU_00011/1-6).

KEYWORDS
ALSPAC, bone turnover, citrate, high bone mass, metabolomics, triglycerides

1 | INTRODUCTION

Bone is increasingly recognized to play a role in regulating energy metabolism. Osteocalcin is a measure of osteoblast function and thus bone formation.[1-5] Osteocalcin-deficient mice have increased blood glucose, reduced insulin levels and an increase in fat mass compared to wild-type mice.[4] In human populations, osteocalcin has been inversely associated with fat mass and blood glucose levels.[5,6]

As osteocalcin is an abundant protein in the bone matrix, it can also be used as a marker of bone turnover, the combined process of bone formation and bone resorption.[1,2] When resorption exceeds formation, age-related bone loss occurs (potentially leading to osteoporosis).[1] In clinical practice, bone turnover is commonly measured by N-terminal propeptide of type 1 procollagen (P1NP, a collagen product of bone formation) and beta collagen type 1 cross-linked C-telopeptide (β-CTX, a collagen product of bone resorption); the latter particularly being used to monitor response to osteoporosis treatments.[1-5] Bone turnover markers (BTMs), which reflect metabolism of type 1 collagen,[1,2,7] may also aid identification of individuals at risk of fracture.[1,2]

We recently gained understanding of the 'bone turnover – metabolic phenotype' by investigating a rare and extreme population with high bone mass (HBM). We previously found HBM to be a sporadic finding of generalized raised bone mineral density (BMD) on dual-energy X-ray absorptiometry (DXA) scanning, with a prevalence of 0.18% among a UK DXA-scanned adult population, characterized by a largely asymptomatic mild skeletal dysplasia.[8] Compared with relatives with normal BMD, HBM individuals have lower bone turnover, including reduced osteocalcin levels, with increased fat mass in women.[9]

We therefore aimed to understand the relationships between bone turnover and metabolic markers by examining cross-sectional associations between BTMs and a series of metabolic traits measured using a high-throughput proton nuclear magnetic resonance spectroscopy (NMR) platform, in HBM individuals. We hypothesized that the predominant associations observed would be between BTMs and metabolic markers of fat metabolism. Furthermore, we aimed to assess the generalizability of any bone turnover-associated metabolic traits, by examining whether similar relationships exist in unselected individuals of differing age groups from the general population.

2 | METHODS

2.1 | High bone mass (HBM) population

The HBM study is a UK-based multicentred observational study of adults with unexplained HBM. At four of our larger centres, 788 cases of unexplained HBM were identified by screening NHS dual X-ray absorptiometry (DXA) databases (n = 219 088 DXA images). Full details of DXA database screening and participant recruitment have previously been reported.[8] In brief, HBM was defined as a) L1 Z-score of ≥+3.2 plus total hip Z-score of ≥+1.2 or b) total hip Z-score ≥+3.2 plus L1 Z-score of ≥+1.2. Cases with significant osteoarthritis and/or other causes of raised BMD were excluded (eg surgical metalwork, Paget's disease, metastases). Index cases were asked to pass on study invitations to their first-degree relatives and spouse/partner(s). Relatives/spouses with HBM were in turn asked to pass on study invitations to their first-degree relatives and spouses. First-degree relatives and spouses were recruited, in whom HBM status was defined as L1 Z plus total hip Z-scores of ≥+3.2. Family controls comprised unaffected relatives and spouses (Figure S1). All participants (214 with HBM and 126 family controls without HBM) were clinically assessed by one doctor using a standardized structured history and examination questionnaire, after which nonfasted phlebotomy was performed. Written informed consent was obtained from all participants in line with the Declaration of Helsinki.[10] Recruitment ran from July 2005 to April 2010. Participants were excluded if they were under 18 years old, pregnant or unable to provide written informed consent for any reason. The study was approved by the Bath Multi-centre Research Ethics Committee (REC reference 05/Q2001/78) and at each local NHS REC.

2.2 | Avon longitudinal study of parents and children (ALSPAC)

ALSPAC is a long-standing prospective cohort study of 14 541 pregnancies with expected delivery dates between 01/04/1991 and 31/12/1992, in Southwest England.[11,12] Of these pregnancies, 14 676 foetuses resulted in 14 062 live births, with 13 988 children alive at 1 year. When the oldest children were aged approximately

7 years, an attempt was made to augment the initial sample, resulting in 811 additional children being enrolled. We analysed data collected from the mothers (first clinic session December 2008-July 2011) and offspring when aged 15 years (third clinic). A total of 11 264 (77.5%) mothers were invited, of whom 4832 attended (42.9%). A total of 10 464 (71.2%) offspring were invited, of whom 5506 (52.6%) attended (Figure S2). The study website details all available data through a fully searchable data dictionary: http://www.bristol.ac.uk/alspac/researchers/our-data/. Ethical approval was obtained from the ALSPAC Ethics and Law committee and the local Research Ethics Committees.

2.3 | Assessment of bone turnover markers

In the HBM population, nonfasted P1NP and total osteocalcin were measured as markers of bone formation and β-CTX was measured as a marker of bone resorption. In ALSPAC populations, fasted β-CTX concentration was measured. In all, plasma was separated and frozen within 4 hours to −80°C and BTM concentrations were measured by electrochemiluminescence immunoassays (Roche Diagnostics), with detection limits of 4.0, 0.6 and 0.01 μg/L for P1NP, osteocalcin and β-CTX, respectively. Reference ranges were supplied by UK Supra Regional Assay Service laboratory (reference range 0.1-0.5 μg/L for β-CTX, 20-110 μg/L for P1NP and 6.8-32.2 μg/L for osteocalcin). All inter- and intra-assay coefficients of variation were <6%.

2.4 | Nuclear magnetic resonance (NMR) metabolic profiling

Plasma metabolic profiling was performed using a targeted high-throughput proton NMR platform, which measures absolute concentrations of over 150 metabolic traits, including 14 lipoprotein subclasses, lipids, glycolysis-related metabolites, amino acids, ketone bodies and biomarkers of fluid balance and inflammation.[20,22] The protocol has been published elsewhere.[15-16] To reduce the number of statistical tests performed, we specifically focused analyses on the total measures for (nonfasted) lipids, glycerides and phospholipids, apolipoproteins (rather than their subfactions), in addition to all amino acids, ketone bodies, markers of fluid balance and inflammation and low molecular weight metabolites, including glycolysis-related metabolites. This totalled 23 measures (summarized in Table S1).

2.5 | Covariates

In the HBM population, researcher-administered questionnaires quantified bisphosphonate and glucocorticoid use, tobacco and alcohol consumption, menopausal history and use of oestrogen replacement in women. ALSPAC offspring pubertal stage was assessed by Tanner line drawings,[17,18] using a paper questionnaire sent to all participants prior to clinic attendance. ALSPAC women were asked if they were taking hormone replacement, and to list all current medications, from which bisphosphonate and oral glucocorticoid use was determined. Maternal alcohol consumption was ascertained as part of a postal questionnaire sent in 2010. Women were considered postmenopausal if they had not had a period in the last 12 months or if their periods had stopped due to hysterectomy, ablation/ resection, chemotherapy or other medical reasons.[19] Height and weight were measured contemporaneous to blood sampling.

2.6 | Statistical analysis

Histograms of exposure and outcome variables were visually inspected to identify skewed variables. Descriptive statistics were summarized as mean with standard deviations (SD) (or median [interquartile range, IQR] for skewed variables) and counts (percentages). Associations between BTMs and metabolic traits were assessed by multivariable linear regression, with standardized variables to allow comparisons between metabolic traits. Robust standard errors (SEs), which remain unbiased if data are skewed, and confidence intervals (CIs) were estimated. Repeating all analyses log-transforming outcome variables did not alter our findings, and therefore, original units with robust SEs are presented.

To account for intrafamily clustering, associations between BTMs and metabolic traits were determined using generalized estimating equation (GEE) linear regression. Analyses were initially performed unadjusted (model 1), then adjusted for the a priori confounders age and sex (model 2) and finally also adjusted for additional confounders height, weight, menopausal status, bisphosphonate and glucocorticoid use (model 3). All BTMs were then added to model 3 (model 4). We tested for interaction between β-CTX concentration and HBM status using model 3. Due to the number of tests performed in our initial metabolite screen (23 outcomes), we adjusted our P value threshold of significance to account for multiple testing (α threshold $0.05/23 = 0.002$).

Analyses of ALSPAC populations also used standard multivariable linear regression with robust SEs. For the mother's cohort, model 3 was adjusted for age, height, weight, menopausal status and fasting time prior to sample collection (<8 or ≥8 hours). As only 14 mothers reported bisphosphonate use and 12 oral glucocorticoid use, we removed these mothers in a sensitivity analysis. For the offspring population, model 3 was adjusted for age, sex, height, weight, Tanner stage and time of sample collection (AM or PM). All adjusted analyses, including in the HBM population, were performed with the metabolic traits in their original units to allow comparison between populations. All analyses were performed in Stata version 13 (Statacorp), and figures were generated using R version 3.5.1.

3 | RESULTS

3.1 | Characteristics of the HBM population

The 198 HBM individuals had mean (SD) age 62 (14) years, BMI 30.5 (5.8) kg/m², and 77% were female. Median (IQR) BTM concentrations were as follows: β-CTX 0.17 (0.12-0.25) μg/L, P1NP 32.0 (23.0-44.0) μg/L and osteocalcin 16.6 (13.1-21.2) μg/L (Table S2).

3.2 | Unadjusted analysis of metabolic traits and bone turnover in individuals with HBM

Of 23 metabolic traits, plasma citrate was positively related to all three BTMs ($\beta_{\beta\text{-CTX}}$ = 0.31 [0.15, 0.48], $P = 1.89 \times 10^{-4}$, β_{P1NP} = 0.19 [0.03, 0.35], P = .017 and $\beta_{Osteocalcin}$ = 0.22 [0.07, 0.38], P = .006, β represents the SD increase in citrate per SD increase in BTM) (Figure 1), but only the β-CTX-citrate association met our corrected P value threshold (Table 1 shows results where β represents the mmol/L increase in citrate per 1 μg/L increase in BTM). Mean (SD) citrate concentration was 0.13 (0.03) mmol/L and increased by quintile of β-CTX (Figure 2A). Both β-CTX and osteocalcin were inversely associated with triglycerides (standardized β = −0.16 [−0.25, −0.07], $P = 3.32 \times 10^{-4}$, β = −0.13 [−0.23, −0.03], P = .009 respectively), whilst P1NP was not. Nominal inverse associations between all three BTMs and phosphoglycerides, P1NP and cholines, β-CTX and apolipoprotein B, β-CTX/ osteocalcin and glucose, osteocalcin and lactate, β-CTX and alanine, with a positive association between β-CTX and β-hydroxybutyrate, were detected ($0.002 < P \leq .05$).

3.3 | Adjusted analysis of metabolic traits and bone turnover in individuals with HBM

As citrate was most strongly related to bone turnover, it was prioritized for further analysis. The associations between citrate and all three BTMs were unchanged by adjustment for confounders (Table 1). When combining all three BTMs in model 4, only β-CTX remained independently associated with citrate, with similar effect sizes as seen before adjustment ($\beta_{model\ 1}$ = 0.06 [0.03, 0.08], $P = 1.89 \times 10^{-4}$ and $\beta_{model\ 4}$ = 0.05 [0.01, 0.10], P = .019, β represents the unit increase in citrate in mmol/L per 1 μg/L increase in β-CTX).

β-CTX-triglyceride and osteocalcin-triglyceride associations were also robust to covariate adjustment (Table 1). β-CTX was inversely associated with all triglyceride subvariables (triglycerides in VLDL, LDL and HDL), particularly VLDL triglycerides (Table S3). The association between osteocalcin and triglycerides appeared driven

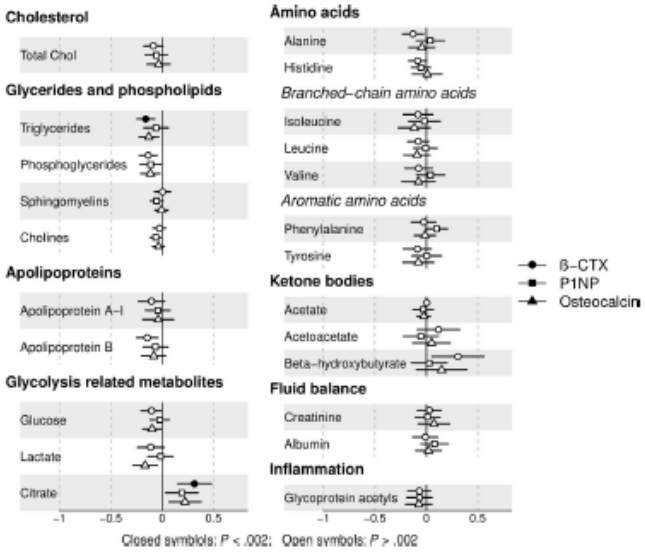

FIGURE 1 Unadjusted associations between bone turnover markers and metabolic traits for all individuals with HBM. Points represent the SD increase in metabolic trait per SD increase in bone turnover marker. Horizontal lines represent 95% confidence intervals. Results are presented in SD units for comparison between metabolic traits. N ranges from 186 to 198 depending on metabolite. Abbreviations: β-CTX: collagen type 1 cross-linked C-telopeptide; P1NP: N-terminal propeptide of type 1 procollagen. Total C: total cholesterol

TABLE 1 Multivariable associations between bone turnover markers and citrate/triglycerides in individuals with HBM

N = 198	Model 1		Model 2		Model 3		Model 4	
	β (95% CI)	*P* value	β (95% CI)	*P* value	β (95% CI)	*P* value	β (95% CI)	*P* value
Citrate								
β-CTX	0.055 (0.026, 0.083)	1.89×10^{-4}	0.048 (0.022, 0.075)	2.95×10^{-4}	0.050 (0.024, 0.076)	1.71×10^{-4}	0.054 (0.009, 0.098)	.019
P1NP	2.36×10^{-4} (4.21×10^{-5}, 4.30×10^{-4})	.017	2.35×10^{-4} (5.13×10^{-5}, 4.18×10^{-4})	.012	2.40×10^{-4} (6.49×10^{-5}, 4.14×10^{-4})	.007	-3.60×10^{-5} (-2.88×10^{-4}, 2.16×10^{-4})	.779
Osteocalcin	6.90×10^{-4} (2.03×10^{-4}, 0.001)	.006	6.61×10^{-4} (1.76×10^{-4}, 0.001)	.008	6.54×10^{-4} (1.87×10^{-4}, 0.001)	.006	1.84×10^{-6} (-6.98×10^{-4}, 7.01×10^{-4})	.996
Triglycerides								
β-CTX	−0.288 (−0.445, −0.131)	3.32×10^{-4}	−0.298 (−0.465, −0.130)	5.03×10^{-4}	−0.276 (−0.434, −0.118)	6.03×10^{-4}	−0.377 (−0.628, −0.125)	.003
P1NP	−0.001 (−0.002, 0.001)	.327	−0.001 (−0.002, 0.001)	.332	−0.001 (−0.002, 0.001)	.277	−0.002 (−0.013, 0.034)	.516
Osteocalcin	−0.004 (−0.007, −0.001)	.009	−0.004 (−0.007, −0.001)	.010	−0.004 (−0.007, −0.001)	.020	0.002 (-3.27×10^{-4}, 0.004)	.104

Note: β represents the increase in citrate/triglycerides in mmol/L per 1 μg/L increase in bone turnover marker. Model 1: unadjusted; Model 2: adjusted for age and sex; Model 3: adjusted for age, sex, height, weight, menopause, bisphosphonate and oral glucocorticoid use; Model 4: Adjusted as per model 3 plus other bone turnover markers.

Abbreviations: β-CTX, collagen type 1 cross-linked C-telopeptide; P1NP, N-terminal propeptide of type 1 procollagen.

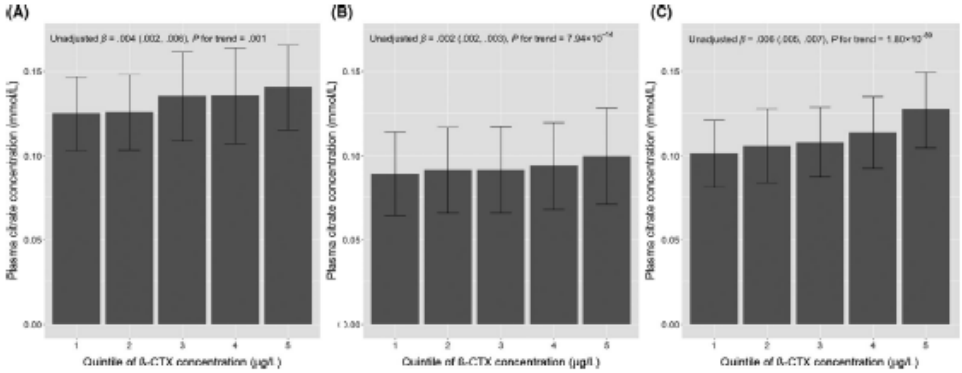

FIGURE 2 Mean citrate concentrations by quintiles of β-CTX in the (A) high bone mass, (B) ALSPAC mothers and (C) ALSPAC offspring populations. β represents the increase in citrate in mmol/L per increase in β-CTX quintile from unadjusted analyses. Abbreviations: β-CTX, collagen type 1 cross-linked C-telopeptide

by VLDL. As seen with citrate, when combining all BTMs in the same model, only β-CTX was independently associated with total, VLDL and LDL triglycerides, and osteocalcin was independently associated with HDL triglycerides (Table 1, Table S3). Triglycerides were not related to citrate (age- and sex-adjusted standardized β = −0.038 [−0.191, 0.114]).

3.4 | Generalizability of the association between β-CTX and metabolic traits

We aimed to assess whether bone resorption is similarly associated with citrate in different populations: perimenopausal women with normal BMD (mean [SD] total hip T-score + 0.24 [1.6]) and

TABLE 2 associations between β-CTX and citrate and triglycerides in the ALSPAC maternal and adolescent populations

	Model 1			Model 2			Model 3		
	β	95% CI	*P* value	β	95% CI	*P* value	β	95% CI	*P* value
Maternal population N = 3664									
Citrate	0.026	0.020, 0.032	1.28×10^{-16}	0.022	0.016, 0.028	5.10×10^{-12}	0.020	0.013, 0.026	1.95×10^{-9}
Total TGs	−0.414	−0.530, −0.298	3.31×10^{-12}	−0.502	−0.624, −0.380	1.17×10^{-15}	−0.354	−0.471, −0.237	3.03×10^{-9}
VLDL TGs	−0.356	−0.453, −0.259	8.33×10^{-13}	−0.409	−0.512, −0.307	7.28×10^{-15}	−0.274	−0.372, −0.176	4.00×10^{-8}
LDL TGs	−0.017	−0.030, −0.005	.008	−0.035	−0.049, −0.022	1.95×10^{-7}	−0.030	−0.043, −0.016	1.60×10^{-5}
HDL TGs	−0.026	−0.034, −0.018	3.43×10^{-11}	−0.035	−0.043, −0.027	1.76×10^{-12}	−0.032	−0.040, −0.024	4.86×10^{-14}
Adolescent population N = 2492									
Citrate	0.018	0.016, 0.019	4.39×10^{-106}	0.023	0.021, 0.025	1.06×10^{-93}	0.022	0.020, 0.024	2.10×10^{-74}
Total TGs	−0.024	−0.047, −0.002	.034	−0.010	−0.043, 0.022	.535	0.041	0.007, 0.076	.019
VLDL TGs	−0.001	−0.020, 0.018	.919	−0.021	−0.050, 0.007	.141	0.028	−0.002, 0.058	.068
LDL TGs	−0.012	−0.015, −0.009	3.61×10^{-13}	0.007	0.003, 0.011	3.16×10^{-4}	0.007	0.003, 0.012	.001
HDL TGs	−0.005	−0.006, −0.003	7.48×10^{-11}	0.001	−0.001, 0.003	.465	0.002	2.93×10^{-4}, 0.005	.026

Note: β represents the change in citrate or triglycerides in mmol/L per 1 μg/L increase in β-CTX. Model 1: unadjusted; Model 2: adjusted for age; Model 3: adjusted for age, height, weight, menopause, <8 h of fasting in the maternal population and age, sex, height, weight, Tanner stage and time of sample collection in the adolescent population.

adolescents from the ALSPAC cohorts, in whom citrate and β-CTX (but not P1NP or osteocalcin) had been contemporaneously measured. Of 3664 mothers with mean age 47.9 (4.4) years, 77% were premenopausal. Median β-CTX and mean citrate concentrations were 0.25 (0.18-0.35) μg/L and 0.09 (0.03) mmol/L, respectively. Of 2492 adolescents, with mean age 15.4 (0.3) years, 53% were female. Median β-CTX and the mean citrate concentrations were 0.94 (0.66-1.39) μg/L and 0.11 (0.02) mmol/L, respectively (Table S4).

Among ALSPAC mothers, a strong positive association was seen between β-CTX and citrate (mean citrate concentrations increased by quintile of β-CTX; Figure 2B), robust to confounder adjustment (model 3; Table 2). The magnitude of the relationship was less marked than that seen in the HBM population (fully adjusted β_{HBM} = 0.050 [0.024, 0.076] vs $\beta_{mothers}$ = 0.020 [0.013, 0.026], β = mmol/L increase in citrate per 1 μg/L increase in β-CTX). The association between β-CTX and triglycerides also replicated in ALSPAC mothers (Table 2).

In adolescents, β-CTX quintile was strongly related to citrate (Figure 2C). In adjusted analyses (model 3), a 1 μg/L increase in β-CTX was associated with a 0.022 (0.020, 0.024) mmol/L increase in citrate, $P = 2.10 \times 10^{-74}$ (Table 2). The magnitude of the association between β-CTX and citrate in adolescents was less than that seen in the HBM population. Inverse associations between β-CTX and total, LDL and HDL triglycerides were also observed in the adolescent population (Table 2), but with a much smaller effect size than seen in the adult populations. After full adjustment (model 3), β-CTX remained positively related to total, LDL and HDL triglycerides. Triglycerides were inversely related to citrate in both ALSPAC populations (fully adjusted $\beta_{mothers}$ = −0.059 [−0.090, −0.028] and $\beta_{adolescents}$ = −0.095 [−0.135, −0.055], β represents the SD increase in triglycerides per SD increase in citrate). However, adjustment for triglycerides did not attenuate the relationship between β-CTX and citrate in either population.

3.5 | Associations between β-CTX and citrate by HBM status

Whilst strong associations were observed between β-CTX and citrate in all three study populations (HBM individuals, ALSPAC mothers, ALSPAC children), beta coefficients were greater in HBM individuals. To confirm that relationships between β-CTX and citrate are relatively strong in HBM cases, we tested for an interaction between β-CTX concentration and citrate according to HBM status, by combining individuals with HBM with their family controls with normal BMD (n = 122, Figure S1). These family controls were younger than the HBM individuals (mean 55.0 vs 61.6 years), less commonly female (44% vs 77%), taller (mean 171.7 vs 166.9 cm) and had lower BMD (mean TH-BMD Z-score 0.53 vs 3.02). Median β-CTX and mean citrate concentrations in the family controls were 0.20 (0.11, 0.28) and 0.13 (0.03) mmol/L, respectively. There was strong evidence for a lower age and sex-adjusted mean β-CTX concentration in HBM cases compared to their relatives and weak evidence for a higher mean citrate concentration (mean differences = −0.047 [−0.078,

−0.016] μg/L and 0.005 [−2.76 × 10^{-4}, 0.010] mmol/L for β-CTX and citrate, respectively). After adjustment (model 3), no association was seen between β-CTX and citrate in these family controls; however, the sample size was small (n = 122) and confidence intervals wide (β = 0.002[−0.02, 0.03], *P* = .9). A likelihood ratio test confirmed a difference in the association between β-CTX and citrate according to HBM status (*P* = .02; Figure 3).

3.6 | Sensitivity analyses

Adjusting for alcohol and creatinine levels in all populations and excluding ALSPAC mothers reporting bisphosphonates or glucocorticoid use did not change conclusions. The association between β-CTX and citrate was similar in pre- and postmenopausal ALSPAC mothers (*P* for interaction = .3), and between those fasting <8 vs ≥8 hours before sample collection (*P* for interaction = .8).

4 | DISCUSSION

We report a positive association between β-CTX and plasma citrate, and consistent but weaker associations between osteocalcin/ P1NP and citrate. Furthermore, β-CTX and osteocalcin both demonstrated inverse associations with plasma triglycerides in individuals with unexplained HBM, despite adjustment for a range of confounders. Associations between the bone resorption marker, β-CTX, and citrate and total plasma triglycerides were independent of the two bone formation markers, osteocalcin and P1NP. This positive association between β-CTX and citrate was further observed in perimenopausal women and adolescents from the ALSPAC population-based cohort.

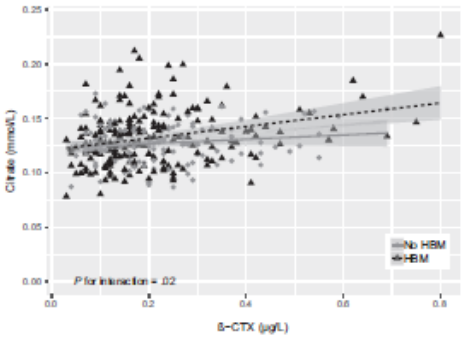

FIGURE 3 Associations between β-CTX and citrate in individuals with HBM and family members with normal BMD. N_{HBM} = 198 and $N_{Relatives}$ = 122. Regression lines represent the unadjusted associations between β-CTX and citrate (β_{HBM} = 0.055 [0.026, 0.083] and $\beta_{No\ HBM}$ = 0.022 [−0.003, 0.046] where β represents the increase in mmol/L of citrate per 1 μg/L increase in β-CTX. After adjusting for age, sex, height, weight, menopause, bisphosphonate use and oral glucocorticoid use (model 3), β-CTX was still associated with citrate in individuals with HBM (0.050 [95% CI 0.024, 0.076], *P* = 1.71 × 10^{-4}) but no association was seen in relatives with normal BMD (8.03 × 10^{-4} [−0.024, 0.026], *P* = .95)

Citrate is synthesized in mitochondria from acetyl-CoA and oxaloacetate during the Krebs cycle, where most remains, regulating energy production.[20,21] Hence, soft tissue cellular metabolism is not considered a major source of plasma citrate.[21] Approximately 80% of citrate is stored in bone and 2% of bone content is citrate.[22] Citrate, found between hydrated layers of bone mineral and which binds to the surface of apatite crystals, is thought to prevent formation of larger crystals and thereby maintain bone structural properties.[23,24] Human osteoblasts can produce citrate; it is hypothesized that citrate is incorporated into bone directly from osteoblast secretion, and that, as bone is resorbed and both bone collagen and mineral are degraded, citrate is released into the circulation generating the major source of plasma citrate.[25] This concurs with the positive relationships we observed between citrate and both age and bone resorption and an inverse association recently identified between β-CTX and citrate in a smaller sample from the ALSPAC adolescent population.[26] Due to its suggested association with bone mineral, we hypothesize that plasma citrate may provide information on turnover of bone mineral during bone resorption.

Stronger citrate-β-CTX associations in the context of HBM compared with individuals with normal BMD may simply reflect the greater quantity of bone in the HBM skeleton and therefore a greater source of citrate. We have previously shown that HBM individuals have increased cortical volumetric BMD measured by pQCT, possibly due to reduced bone turnover allowing more time for secondary mineralization.[27] Alternatively, the mineral platelets may be structured differently in HBM, contributing to increased bone strength,[27] which may result in citrate being released more readily during bone resorption.

The inverse association between β-CTX and triglycerides in the adult HBM and perimenopausal populations is consistent with previous findings from the European Male Ageing Study (EMAS); mean β-CTX concentrations were lower in male individuals with serum triglyceride concentrations above 150 mg/dL, independent of other components of the metabolic syndrome such as hyperglycaemia.[28] As we observed, increased osteocalcin has also been associated with reduced triglycerides in adults.[28,29] The metabolic impact of osteocalcin has further been demonstrated in animal studies, where osteocalcin-deficient mice display a distinct metabolic phenotype with greater accumulation of fat mass and higher serum triglyceride levels.[4] In our analyses, the inverse association between osteocalcin and triglycerides was not independent of β-CTX. It is important to note that we determined associations between *total* osteocalcin and serum triglycerides, rather than the *uncarboxylated* form proposed to be metabolically active.[4] Yet, our finding that β-CTX, rather than osteocalcin, was independently associated with triglycerides raises the possibility that β-CTX influences triglycerides via a separate pathway from osteocalcin. As this analysis is cross-sectional, we are unable to determine whether increased β-CTX causes decreased triglyceride levels or vice versa, yet a recent analysis did not find

evidence of a causal pathway between triglycerides and BMD after accounting for pleiotropy, consistent with the lack of any causal effect of triglycerides on bone turnover.[50]

In adolescents, we observed the opposite direction of effect between β-CTX and triglycerides, after adjustment for covariates: β-CTX was positively related to triglycerides after adjustment for weight. One possible explanation is that during adolescence, increased bone resorption likely reflects bone modelling during growth rather than bone remodelling, as indicated by the positive association between β-CTX and periosteal circumference previously reported in this adolescent population.[51] Pubertal growth may increase both bone modelling and fat storage concurrently, with higher associated plasma triglyceride levels. Whilst in mature adults, bone remodelling predominates, and hence, the direction of association reverses.

4.1 | Strengths and limitations

Strengths include the unique HBM population plus the ability to evaluate generalizability of findings in large population-based cohorts of perimenopausal women and adolescents. All cohorts had detailed phenotypic data which allowed for models to be adjusted for a range of potential confounders. The metabolomics platform used is highly reproducible and allows efficient quantification of a larger number of biomarkers at scale.[52]

Nevertheless, this cross-sectional study is unable to examine directions of causality. HBM study samples had been stored at −80°C for up to 10 years before metabolomics analysis; however, previous studies suggest that long-term storage is unlikely to significantly affect citrate measurements.[53] The effect of different storage conditions and freeze-thaw cycles on metabolic trait concentrations may affect lipids, alanine and glucose [54]; reassuringly our association between β-CTX and plasma triglycerides replicated with a similar effect size in the ALSPAC maternal cohort. Citrate has established dietary sources which may explain the clear positive association with fasting duration. β-CTX is also affected by fasting time, with β-CTX levels increasing with fasting.[55] A weaker association was observed between β-CTX and citrate in those ALSPAC mothers with shorter fasts. The samples collected from the HBM population were not collected when fasting. As the HBM population is predominantly female, we wanted to replicate our analysis in a female population. The ALSPAC maternal cohort is predominantly perimenopausal compared to the HBM population which is mainly postmenopausal; however, as far as we are aware, the ALSPAC maternal population is the largest available cohort of women with measured β-CTX and citrate. Finally, our study provides limited data as to how β-CTX relates to citrate and triglycerides in adult men, or adults with low bone mass, in whom further analyses are required.

5 | CONCLUSIONS

We have identified that plasma citrate is positively associated with β-CTX in two separate adult populations. Given that citrate binds to apatite nanocrystals,[25] we hypothesize that circulating citrate may reflect breakdown of bone mineral. Further studies are justified to explore whether plasma citrate concentration is altered by factors known to modulate bone resorption, such as bisphosphonates, to determine the direction of causality.

ACKNOWLEDGEMENTS

We would like to thank all our HBM study participants and the staff at our collaborating centres: the Wellcome Trust Clinical Research Facility in Birmingham, Cambridge National Institute for Health Research (NIHR) Biomedical Research Centre and Addenbrooke's Wellcome Trust Clinical Research Facility, NIHR Bone Biomedical Research Unit in Sheffield, and the Centre for Metabolic Bone Disease in Hull. We are extremely grateful to all the families who took part in the ALSPAC study, the midwives for their help in recruiting them and the whole ALSPAC team, which includes interviewers, computer and laboratory technicians, clerical workers, research scientists, volunteers, managers, receptionists and nurses.

CONFLICT OF INTEREST

DAL has received support in the last 10 years from the UK Medical Research Council, National Institute of Health Research, British Heart Foundation, Diabetes UK, Wellcome Trust, the European Research Council, US National Institute of Health and from Roche Diagnostics and Medtronic Ltd for research unrelated to that presented here. WDF has received consultancy fees from Siemens, Becton Dickinson and Roche.

ORCID

April Hartley https://orcid.org/0000-0003-4932-1588
Jonathan Tang https://orcid.org/0000-0001-6305-6333

DATA AVAILABILITY STATEMENT

The HBM data that support the findings of this study are available on request from the corresponding author. The data are not publicly available due to privacy or ethical restrictions. ALSPAC data access is through a system of managed open access. The ALSPAC access policy details how data can be accessed by researchers: http://www.bristol.ac.uk/media-library/sites/alspac/documents/researchers/data-access/ALSPAC_Access_Policy.pdf.

REFERENCES

1. Leeming DJ, Alexandersen P, Karsdal MA, Qvist P, Schaller S, Tankó LB. An update on biomarkers of bone turnover and their utility in biomedical research and clinical practice. *Eur J Clin Pharmacol*. 2006;62(10):781-792.
2. Vasikaran S, Eastell R, Bruyère O, et al. Markers of bone turnover for the prediction of fracture risk and monitoring of osteoporosis treatment: a need for international reference standards. *Osteoporos Int*. 2011;22(2):391-420.
3. Henriksen K, Christiansen C, Karsdal MA. Role of biochemical markers in the management of osteoporosis. *Climacteric*. 2015;18(Suppl 2):10-18.
4. Lee NK, Sowa H, Hinoi E, et al. Endocrine regulation of energy metabolism by the skeleton. *Cell*. 2007;130(3):456-469.

5. Kindblom JM, Ohlsson C, Ljunggren Ö, et al. Plasma osteocalcin is inversely related to fat mass and plasma glucose in elderly Swedish men. *J Bone Miner Res*. 2009;24(5):785-791.
6. Wei J, Karsenty G. An overview of the metabolic functions of osteocalcin. *Rev Endocr Metab Disord*. 2015;16(2):93-98.
7. Karsdal MA, Henriksen K, Leeming DJ, et al. Biochemical markers and the FDA Critical Path: how biomarkers may contribute to the understanding of pathophysiology and provide unique and necessary tools for drug development. *Biomarkers*. 2009;14(3):181-202.
8. Gregson CL, Steel SA, O'Rourke KP, et al. 'Sink or swim': an evaluation of the clinical characteristics of individuals with high bone mass. *Osteoporosis Int*. 2012;23(2):643-654.
9. Gregson CL, Paggiosi MA, Crabtree N, et al. Analysis of body composition in individuals with high bone mass reveals a marked increase in fat mass in women but not men. *J Clin Endocrinol Metab*. 2013;98(2):818-828.
10. World medical association declaration of Helsinki ethical principles for medical research involving human subjects. *JAMA*. 2013;310(20):2191-2194.
11. Fraser A, Macdonald-Wallis C, Tilling K, et al. Cohort profile: the Avon longitudinal study of parents and children: ALSPAC mothers cohort. *Int J Epidemiol*. 2013;42(1):97-110.
12. Boyd A, Golding J, Macleod J, et al. Cohort profile: the 'children of the 90s'–the index offspring of the Avon longitudinal study of parents and children. *Int J Epidemiol*. 2013;42(1):111-127.
13. Soininen P, Kangas AJ, Würtz P, et al. High-throughput serum NMR metabonomics for cost-effective holistic studies on systemic metabolism. *Analyst*. 2009;134(9):1781-1785.
14. Soininen P, Kangas AJ, Würtz P, Suna T, Ala-Korpela M. Quantitative serum nuclear magnetic resonance metabolomics in cardiovascular epidemiology and genetics. *Circ Cardiovasc Genet*. 2015;8(1):192-206.
15. Kujala UM, Mäkinen VP, Heinonen I, et al. Long-term leisure-time physical activity and serum metabolome. *Circulation*. 2013;127(3):340-348.
16. Inouye M, Kettunen J, Soininen P, et al. Metabonomic, transcriptomic, and genomic variation of a population cohort. *Mol Syst Biol*. 2010;6:441.
17. Marshall WA, Tanner JM. Variations in pattern of pubertal changes in girls. *Arch Dis Child*. 1969;44(235):291-303.
18. Marshall WA, Tanner JM. Variations in the pattern of pubertal changes in boys. *Arch Dis Child*. 1970;45(239):13-23.
19. Wang Q, Ferreira DLS, Nelson SM, Sattar N, Ala-Korpela M, Lawlor DA. Metabolic characterization of menopause: cross-sectional and longitudinal evidence. *BMC Med*. 2018;16(1):17.
20. Iacobazzi V, Infantino V. Citrate–new functions for an old metabolite. *Biol Chem*. 2014;395(4):387-399.
21. Costello LC, Franklin RB. Plasma citrate homeostasis: how it is regulated; and its physiological and clinical implications. An important, but neglected, relationship in medicine. *HSOA J Hum Endocrinol*. 2016;1(1). https://doi.org/10.24966/HE-9640/100005
22. Costello LC, Franklin RB, Reynolds MA, Chellaiah M. The important role of osteoblasts and citrate production in bone formation: "Osteoblast Citration" as a new concept for an old relationship. *Open Bone J*. 2012;4:22425-22429.
23. Hu YY, Rawal A, Schmidt-Rohr K. Strongly bound citrate stabilizes the apatite nanocrystals in bone. *Proc Natl Acad Sci USA*. 2010;107(52):22425-22429.
24. Davies E, Muller KH, Wong WC, et al. Citrate bridges between mineral platelets in bone. *Proc Natl Acad Sci USA*. 2014;111(14):E1354-E1363.
25. Franklin RB, Chellaiah M, Zou J, et al. Evidence that osteoblasts are specialized citrate-producing cells that provide the citrate for incorporation into the structure of bone. *Open Bone J*. 2014;6:1-7.
26. Kemp JP, Sayers A, Fraser WD, et al. A metabolic screen in adolescents reveals an association between circulating citrate and cortical bone mineral density. *J Bone Miner Res*. 2019;34:1306–1313.
27. Gregson CL, Sayers A, Lazar V, et al. The high bone mass phenotype is characterised by a combined cortical and trabecular bone phenotype: findings from a pQCT case-control study. *Bone*. 2013;52(1):380-388.
28. Laurent MR, Cook MJ, Gielen E, et al. Lower bone turnover and relative bone deficits in men with metabolic syndrome: a matter of insulin sensitivity? The European male ageing study. *Osteoporos Int*. 2016;27(11):3227-3237.
29. Fernández-Real JM, Izquierdo M, Ortega F, et al. The relationship of serum osteocalcin concentration to insulin secretion, sensitivity, and disposal with hypocaloric diet and resistance training. *J Clin Endocrinol Metab*. 2009;94(1):237-245.
30. Li GH, Cheung CL, Au PC, Tan KC, Wong IC, Sham PC. Positive effects of low LDL-C and statins on bone mineral density: an integrated epidemiological observation analysis and Mendelian randomization study. *Int J Epidemiol*. 2019. https://doi.org/10.1093/ije/dyz145
31. Kemp JP, Sayers A, Paternoster L, et al. Does bone resorption stimulate periosteal expansion? A cross-sectional analysis of beta-C-telopeptides of type I collagen (CTX), genetic markers of the RANKL pathway, and periosteal circumference as measured by pQCT. *J Bone Miner Res*. 2014;29(4):1015-1024.
32. Würtz P, Kangas AJ, Soininen P, Lawlor DA, Davey Smith G, Ala-Korpela M. Quantitative serum nuclear magnetic resonance metabolomics in large-scale epidemiology: a primer on -omic technologies. *Am J Epidemiol*. 2017;186(9):1084-1096.
33. Haid M, Muschet C, Wahl S, et al. Long-term stability of human plasma metabolites during storage at -80 degrees C. *J Proteome Res*. 2018;17(1):203-211.
34. Pinto J, Domingues MRM, Galhano E, et al. Human plasma stability during handling and storage: impact on NMR metabolomics. *Analyst*. 2014;139(5):1168-1177.
35. Clowes JA, Hannon RA, Yap TS, Hoyle NR, Blumsohn A, Eastell R. Effect of feeding on bone turnover markers and its impact on biological variability of measurements. *Bone*. 2002;30(6):886-890.

SUPPORTING INFORMATION

Additional supporting information may be found online in the Supporting Information section.

How to cite this article: Hartley A, Paternoster L, Evans DM, et al. Metabolomics analysis in adults with high bone mass identifies a relationship between bone resorption and circulating citrate which replicates in the general population. *Clin Endocrinol (Oxf)*. 2019;00:1–9. https://doi.org/10.1111/cen.14119

Appendix 4: Manuscript based on results of Mendelian randomization of IGF-1 and hospital-diagnosed OA, published in Rheumatology.

RHEUMATOLOGY

Rheumatology 2020;0:1–11
doi:10.1093/rheumatology/keaa597

Original Article

Mendelian randomization provides evidence for a causal effect of higher serum IGF-1 concentration on risk of hip and knee osteoarthritis

April Hartley [1,2], Eleanor Sanderson [1], Lavinia Paternoster[1], Alexander Teumer [3], Robert C. Kaplan[4], Jon H. Tobias[1,2] and Celia L. Gregson [2]

Abstract

Objectives. How insulin-like growth factor-1 (IGF-1) is related to OA is not well understood. We determined relationships between IGF-1 and hospital-diagnosed hand, hip and knee OA in UK Biobank, using Mendelian randomization (MR) to determine causality.

Methods. Serum IGF-1 was assessed by chemiluminescent immunoassay. OA was determined using Hospital Episode Statistics. One-sample MR (1SMR) was performed using two-stage least-squares regression, with an unweighted IGF-1 genetic risk score as an instrument. Multivariable MR included BMI as an additional exposure (instrumented by BMI genetic risk score). MR analyses were adjusted for sex, genotyping chip and principal components. We then performed two-sample MR (2SMR) using summary statistics from Cohorts for Heart and Aging Research in Genetic Epidemiology (CHARGE) (IGF-1, $N = 30\,884$) and the recent genome-wide association study meta-analysis ($N = 455\,221$) of UK Biobank and Arthritis Research UK OA Genetics (arcOGEN).

Results. A total of 332 092 adults in UK Biobank had complete data. Their mean (s.d.) age was 56.5 (8.0) years and 54% were female. IGF-1 was observationally related to a reduced odds of hand OA [odds ratio per doubling = 0.87 (95% CI 0.82, 0.93)], and an increased odds of hip OA [1.04 (1.01, 1.07)], but was unrelated to knee OA [0.99 (0.96, 1.01)]. Using 1SMR, we found strong evidence for an increased risk of hip [odds ratio per s.d. increase = 1.57 (1.21, 2.01)] and knee [1.30 (1.07, 1.58)] OA with increasing IGF-1 concentration. By contrast, we found no evidence for a causal effect of IGF-1 concentration on hand OA [0.98 (0.57, 1.70)]. Results were consistent when estimated using 2SMR and in multivariable MR analyses accounting for BMI.

Conclusion. We have found evidence that increased serum IGF-1 is causally related to higher risk of hip and knee OA.

Key words: OA, UK Biobank, insulin-like growth factor-1, Mendelian randomization, BMI

Rheumatology key messages

- Genetically determined serum insulin-like growth factor-1 is related to an increased risk of hip and knee OA.
- A high genetic risk for increased insulin-like growth factor-1 and BMI confers the highest risk for hip OA.
- Overall, results suggest a causal role of serum insulin-like growth factor-1 in hip and knee OA.

[1]MRC Integrative Epidemiology Unit, Population Health Sciences, [2]Musculoskeletal Research Unit, Translational Health Sciences, Bristol Medical School, University of Bristol, Bristol, UK, [3]Institute for Community Medicine, University Medicine Greifswald, Greifswald, Germany and [4]Department of Epidemiology and Public Health, Albert Einstein College of Medicine, New York, NY, USA

Submitted 24 February 2020; accepted 12 August 2020

Correspondence to: April Hartley, Musculoskeletal Research Unit, Learning and Research Building Level 1, Southmead Hospital, Bristol BS10 5NB, UK.
E-mail: april.hartley@bristol.ac.uk

Introduction

OA is highly prevalent, with an estimated 3.8% of the worldwide population affected by knee and 0.9% by hip OA [1]. Currently there are no disease-modifying drugs available; therapy consists of pain management and, when severe, joint replacement, with an estimated cost greater than £850 million in the UK for primary knee and hip replacement [2].

CLINICAL SCIENCE

Insulin-like growth factor-1 (IGF-1) is a hormone regulating skeletal growth and development [3]. Most circulating IGF-1 is produced by the liver in response to growth hormone stimulation [3], whilst some is produced by specific tissues, e.g. chondrocytes [3, 4]. *In vitro* studies of animal cartilage suggest that IGF-1 can stimulate proteoglycan synthesis [5], upregulate type 2 collagen and downregulate MMP-13 expression [6], all of which imply that IGF-1 may be protective against cartilage degeneration (and hence OA). Epidemiological evidence supporting an IGF-1–OA association has been inconclusive [7], with the largest cross-sectional study ($N = 761$) identifying a positive association between IGF-1 concentration and bilateral knee OA [8]. A positive association between IGF-1 and OA risk is further supported by findings from individuals with acromegaly (a disorder of excess growth hormone production), who have increased OA risk [7]. Conversely, polymorphisms in the *IGF-1* promoter region, associated with lower IGF-1 levels, have been linked to higher OA prevalence [9, 10]. BMI is a strong risk factor for OA [11] and is inversely related to IGF-1 [12]; BMI may therefore mediate any inverse association between IGF-1 and OA.

Mendelian randomization (MR) enables causal inference in epidemiology. MR uses genetic variants, robustly associated with an exposure, as an instrument for the exposure, to determine the causal relationship with an outcome [13]. As genetic variants are randomly assigned at conception and cannot be changed, the genetic instrument(s) is generally independent of confounders of the exposure–outcome relationship and unaffected by reverse causality [13]. Frequently, the instrument(s) may be related to the outcome via a causal pathway not mediated by the exposure (i.e. horizontal pleiotropy), violating a key assumption of MR [13]. Hence, multivariable MR (MVMR) methods have been developed to estimate the direct causal effect of the exposure on the outcome when the instrument(s) may affect the outcome through another related exposure, provided the related exposure is included in the model, along with valid instruments for each exposure [14].

We aimed to utilize the large-scale availability of data for serum IGF-1 in the UK Biobank population to firstly determine the observational associations between IGF-1 and hospital-diagnosed OA at the hand, hip and knee, and then to use MR to determine the causal effect of circulating IGF-1 on OA at each joint. After this, we aimed to use MVMR to determine whether any observed causal effects are independent of BMI.

Methods

Observational analysis

UK Biobank population

UK Biobank is a UK-wide population of ~500 000 people, aged 38–73 years, recruited during 2006–10 [15]. Participants provided a range of information (e.g. demographics, health status) via questionnaires and interviews; anthropometric measures and blood samples were collected (data available at: www.ukbiobank.ac.uk). A detailed description of the study design, participants and quality control (QC) methods is published elsewhere [15]. UK Biobank received ethical approval from the Research Ethics Committee (REC reference 11/NW/0382).

Measurement of serum IGF-1

Serum IGF-1 was measured at baseline using the Liaison XL chemiluminescent immunoassay, Diasorin Ltd (Dartford, UK) (data downloaded April 2019). Average within-laboratory coefficients of variation were 6.0% for low, 5.3% for medium and 6.2% for high concentrations [16]. QC procedures have been published [17].

Determination of hospital-diagnosed OA

Hand, hip and knee OA were determined from Hospital Episode Statistics [18] using the International Statistical Classification of Diseases and Related Health Problems (ICD) 9/10 codes previously reported for hand [19], hip and knee [20] OA (data downloaded January 2019). Inclusion (cases) and exclusion (controls) codes (to exclude controls with OA in other joints and inflammatory polyarthropathies) are listed in supplementary Table S1A and B, available at *Rheumatology* online, respectively.

Covariates

BMI was determined from measured height and weight at the assessment clinic [weight (kg)/height (m)^2]. Ethnic background (Supplementary Methods, available at *Rheumatology* online) and oestrogen replacement therapy (ERT) use were ascertained by touchscreen questionnaire.

Statistical analysis

Positively skewed serum IGF-1 concentrations were log-transformed, and associations with binary OA outcomes determined using multivariable logistic regression. Analyses were performed in four stages: (i) unadjusted; (ii) adjusting for age and sex; (iii) additionally adjusting for ethnicity and ERT use; and (iv) additional adjustment for BMI. Coefficients were transformed by ln(2) to generate an odds ratio (OR) per doubling in IGF-1 concentration. Results are presented as OR per s.d. increase in IGF-1 in figures to allow comparison with MR estimates. Additional stratified analyses determined gender-specific associations. We did not correct our *P*-value threshold for multiple testing as our three outcomes are highly correlated. We performed sensitivity analyses excluding individuals with acromegaly (ICD10 code E220, ICD9 code 2530), endocrine-related arthropathy (M145, 7130) ($N = 94$) and individuals for whom serum IGF-1 was measured from an aliquot other than the first aliquot ($N = 43728$), as sample dilution issues have been reported by UK Biobank and the dilution increases with increasing aliquot [17].

Causal inference using MR

Genotyping and imputation

Pre-imputation QC, phasing, imputation and QC filtering are described elsewhere [21, 22] and summarized in Supplementary Methods, available at *Rheumatology* online.

One-sample MR

Eight independent single nucleotide polymorphisms (SNPs) associated with IGF-1 at genome-wide significance, in the Cohorts for Heart and Aging Research in Genetic Epidemiology (CHARGE) meta-analysis, instrumented IGF-1 [23] (Table 1). Two of these SNPs were also associated with IGF-BP3 levels and one was identified from a bivariate analysis of IGF-1 and IGF-BP3. Analyses were performed using the individual SNPs (in the same analysis) and then an unweighted genetic risk score (GRS, generated by summing IGF-1-increasing allele dosage). One-sample (1SMR) analyses were adjusted for sex, genotyping chip and 10 principal components (PCs) (to account for population stratification, i.e. minor allele frequency variation due to ancestral differences). IGF-1 was standardized prior to analysis. Two-stage least-squares regression was performed using the 'ivreg2' package in Stata (StataCorp, College Station, Texas US) [24], which provides an estimate of the risk difference for a binary outcome. We generated an estimate of the OR per s.d. increase in IGF-1 by first regressing the instruments on IGF-1, generating predicted values of IGF-1, and then regressing these predicted values on the binary outcomes using logistic regression. The standard errors (SEs) for the OR estimate can be underestimated [25], but conclusions were the same when using the two-stage least-squares model (supplementary Table S2, available at *Rheumatology* online), therefore we present the OR estimates. A summary of the assumptions of MR, and how we tested these, is presented in Fig. 1. Power calculations for one-sample MR were performed using mRnd (http://cnsgenomics.com/shiny/mRnd/) [28] (supplementary Table S3, available at *Rheumatology* online).

Two-sample MR

SNP-exposure summary data were extracted from the CHARGE meta-analysis [23]. The study employed a sample-size weighted Z-score based meta-analysis due to assay heterogeneity across cohorts, hence betas and SEs could not be generated [23]. Betas were estimated from *P*-values [from the IGF-1 genome-wide association study (GWAS)] using the method of Rietveld *et al.* [29]. Summary statistics are shown in supplementary Table S4, available at *Rheumatology* online. To provide estimates of the SNP–outcome association, summary statistics for the IGF-1 SNPs were extracted from the largest GWAS meta-analysis of hip and knee OA to date, from UK Biobank and Arthritis Research UK OA Genetics (arcOGEN; a population with severe OA) [20]. Estimates for hand OA were generated by our own GWAS of hospital-diagnosed hand OA in UK Biobank, adjusting for sex, genotyping chip and 10 PCs, using a linear mixed model within the software '*BOLT*' [30], as described in the published protocol [31]. Steiger filtering was performed to identify SNPs explaining a greater proportion of variance in OA sub-phenotypes compared with IGF-1 [32]. No SNPs were identified for exclusion. Summary statistics are presented in supplementary Table S4, available at *Rheumatology* online. Causal effects were estimated using inverse-variance weighted regression, performed using the TwoSampleMR R package [33]. MR-Egger regression was also performed to estimate possible bias due to directional pleiotropy, i.e. to provide valid causal estimates even if one of the key assumptions of MR was invalidated (Fig. 1). MR-Egger does not constrain the intercept of the regression line between the SNP–exposure and the SNP–outcome estimates at 0, and thus produces a valid estimate if the correlation between the direct SNP–outcome effect (i.e.

TABLE 1 Associations of IGF-1 instruments for one-sample analyses with IGF-1 and OA in UK Biobank

SNP	EA	IGF-1			Hip OA			Knee OA		
		Beta	SE	*P*	OR	SE	*P*	OR	SE	*P*
rs1065656*	G	0.050	0.003	4×10^{-84}	0.987	0.015	0.392	1.019	0.012	0.116
rs2153960	A	0.048	0.003	6×10^{-78}	1.025	0.016	0.125	1.023	0.013	0.061
rs509035	A	0.054	0.003	5×10^{-102}	0.998	0.015	0.897	1.011	0.012	0.342
rs646776*	T	−0.029	0.003	3×10^{-25}	0.939	0.016	2×10^{-4}	0.992	0.013	0.543
rs700753*	G	0.113	0.002	$<1 \times 10^{-300}$	0.982	0.015	0.234	0.984	0.011	0.155
rs780093	C	0.060	0.002	1×10^{-135}	1.041	0.016	0.007	1.021	0.012	0.066
rs934073	G	0.035	0.003	4×10^{-43}	1.011	0.016	0.471	1.000	0.012	0.988
rs978458	C	−0.074	0.003	6×10^{-172}	0.953	0.015	0.003	0.983	0.012	0.180
IGF-1 GRS		0.058	0.001	$<1 \times 10^{-300}$	1.018	0.006	0.001	1.010	0.004	0.019

Adjusted for sex, genotyping chip and 10 principal components. Betas represent the per-effect allele increase in standardized IGF-1. *SNPs also associated with IGF-BP3 in the CHARGE meta-analysis [23]. IGF-1: insulin-like growth factor-1; EA: effect allele; NEA: alternative allele; EAF: effect allele frequency; OR: odds ratio; SE: standard error; GRS: genetic risk score; CHARGE: Cohorts for Heart and Aging Research in Genetic Epidemiology.

FIG. 1 The assumptions of MR and how we tested these assumptions in our analyses

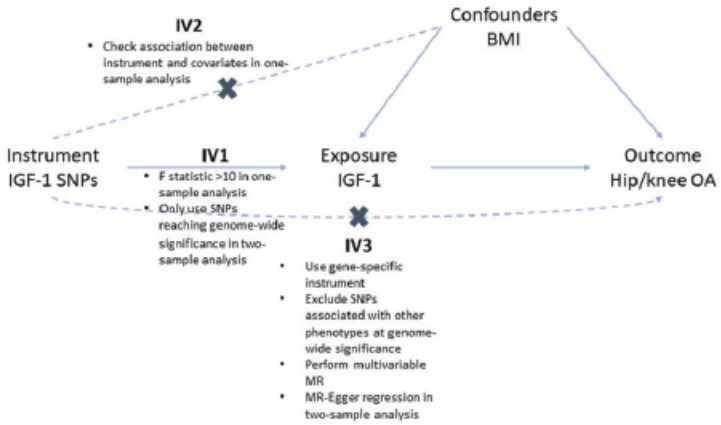

For an MR effect estimate to be valid, the instrument(s) must satisfy three key assumptions [26]: IV1 [the instrument(s) must be robustly associated with the exposure]; IV2 [the instrument(s) must not be associated with any confounders of the exposure–outcome relationship]; and IV3 [the instruments(s) can only be associated with the outcome via the exposure and not via a different biological pathway independent of the exposure (i.e. horizontal pleiotropy)]. In one-sample analyses, IV1 was tested by calculating the F-statistic, which is a measure of instrument strength. A cut-off of $\geq$10 is used to determine sufficient instrument strength [13]. IV2 was tested by determining the association between the instruments and potential confounders of the exposure–outcome relationship. The Sargan statistic was used to detect evidence of potential pleiotropy; this statistic is a measure of variation in the outcome the instrument explains, independent of the exposure variable [14]. To limit potential horizontal pleiotropy, we repeated analyses excluding the SNPs also associated with IGF-BP3 at genome-wide significance (rs700753, rs646776, rs1065656) and using just the intronic IGF-1 SNP (rs978458) as the instrument. In 2S analyses, to satisfy IV1, we ensured that all instruments were robustly associated with the exposure by only including SNPs associated with the exposure at genome-wide significance. To address IV3, MR-Egger regression was performed to generate an estimate of horizontal pleiotropy. Cochran's Q statistic was also calculated as a measure of potential pleiotropy. Weighted median regression was performed to determine the robustness of IVW estimates as weighted median estimates are valid even if up to 50% of the SNPs are not valid instruments [27]. To limit potential horizontal pleiotropy, we repeated analyses excluding the SNPs also associated with IGF-BP3. In MVMR, Sanderson-Windmeijer (S-W) conditional F-statistics were calculated for IGF-1 and BMI to determine conditional instrument strength [14]. MR: Mendelian randomization; SNP: single nucleotide polymorphism; IGF-1: insulin-like growth factor-1; IVW: inverse variance weighted.

the effect of a SNP on the outcome not mediated by the exposure) (IV3, Fig. 1) and the SNP-exposure effect (IV1, Fig. 1) is 0 [34]. The drawback of the method is the reduced statistical power. A summary of additional two-sample (2SMR) analyses, testing the assumptions of MR, is presented in Fig. 1.

Multivariable MR

We conducted one-sample MVMR to determine the BMI-independent causal effect of IGF-1 on OA. An unweighted BMI GRS was generated using the 63 independent SNPs (after linkage disequilibrium clumping with an r^2 threshold of 0.001) from the Genetic Investigation of Anthropometric Traits (GIANT) consortium GWAS of the European sex-combined population [35] (supplementary Table S5, available at *Rheumatology* online, details the SNPs and their association with BMI in UK Biobank). Analyses were performed as for 1SMR, with the inclusion of BMI and the BMI risk score in the two-stage least-squares regression model. MVMR was also performed with height (instead of BMI) as a covariate (supplementary Tables S2 and Table S6, available at *Rheumatology* online).

Factorial MR

Factorial MR was used to determine whether there is an effect of high IGF-1 on OA risk, over and above the effect of high BMI. The MR population was stratified by the median for IGF-1 GRS and for BMI GRS and then categorized as those: (i) below the median for IGF-1

GRS and BMI GRS; (ii) above/equal to the median for IGF-1 GRS and below the median for BMI GRS; (iii) below the median for IGF-1 GRS and above the median for BMI; and (iv) above the median for both IGF-1 and BMI GRS. Logistic regression analysed GRS category (exposure) and OA variables (outcomes) adjusting for sex, genotyping chip and 10 PCs.

Results

Participant characteristics

In total, 421 527 individuals had complete data for observational analyses, of whom 332 059 (79%) had genetic data and were included in MR analyses (supplementary Fig. S1, available at *Rheumatology* online, details sample derivation). The mean (s.d.) ages of the observational and MR populations were 56.4 (8.1) and 56.5 (8.0) years, respectively. In both populations 54% were female, mean BMI was 27.3 (4.7) kg/m^2 and IGF-1 concentration 21.5 (6) nmol/l (Table 2). In the observational population, 3.1% had hospital-diagnosed hip OA, 5.4% knee OA and 0.7% hand OA; respective proportions for the MR population were 3.2, 5.4 and 0.7%.

Evidence from the observational data

In unadjusted analyses, increasing IGF-1 concentration was associated with lower odds of hand, hip and knee OA (Table 3), with the strongest association seen for hand OA [OR per doubling = 0.61 (95% CI 0.57, 0.65), $P = 1.5 \times 10^{-58}$]. Adjustment for age and sex reduced the strength of all associations, although evidence remained for a protective association of IGF-1 on all three OA outcomes. Further adjustment for ethnicity and ERT use did not alter observed associations. However, IGF-1 was strongly inversely associated with BMI in the UK Biobank population, with an s.d. increase in IGF-1 associated with a 0.13 s.d. decrease in BMI. When BMI was added to the model, only evidence suggesting a protective association of IGF-1 on hand OA [OR = 0.87 (0.82, 0.93), $P = 4.2 \times 10^{-5}$] remained. Whilst the association between IGF-1 and knee OA was fully attenuated by BMI adjustment, some evidence emerged for an increased odds of hip OA [OR = 1.04 (1.01, 1.07), $P = 0.014$]. There was evidence of an interaction between log-transformed IGF-1 and BMI [OR for interaction term = 1.02 (1.01, 1.03), $P = 2 \times 10^{-5}$].

When BMI-adjusted analyses were stratified by sex, the association between IGF-1 and hip OA was only seen in females [$OR_F = 1.07$ (1.03, 1.12) *vs* $OR_M = 1.00$ (0.95, 1.05), supplementary Fig. S2, available at *Rheumatology* online]. The inverse association between IGF-1 and hand OA was seen with a similar magnitude in both sexes. Restricting analyses to 377 602 individuals whose IGF-1 was measured from their first aliquot did not alter conclusions drawn, nor did removing those with acromegaly, endocrine-related arthropathies or restricting to the MR population.

Evidence from MR analyses

In 1SMR analyses, using individual IGF-1-associated SNPs as instruments, we found evidence for an increased odds of hip OA with increasing IGF-1 concentration [OR per s.d. increase in IGF-1 = 1.20 (1.01, 1.43),

TABLE 2 Characteristics of the observational and MR study populations derived from the UK Biobank population

	Observational population ($N = 421\,527$)		MR sub-population ($N = 332\,059$)	
	Mean	s.d.	Mean	s.d.
Age, years	56.4	8.1	56.5	8.0
Height, cm	168.6	9.2	168.9	9.2
Weight, kg	77.9	15.8	78.0	15.8
BMI, kg/m^2	27.3	4.7	27.3	4.7
IGF-1, nmol/l[a]	21.3	17.6, 24.9	21.3	17.6, 24.9
	N	%	*N*	%
Female	227 738	54.0	178 699	53.8
ERT use	84 341	37.0	67 181	37.6
Ethnicity				
White	401 844	95.3		
Black/Black British	6500	1.5		
Asian/Asian British	6489	1.5		
Chinese	1335	0.3		
Mixed	1619	0.4		
Other	3740	0.9		
Hospital-diagnosed OA				
Hip	12 425	3.1	9951	3.2
Knee	22 278	5.4	17 338	5.4
Hand	2727	0.7	2165	0.7

[a]Values represent median and interquartile range. ERT: oestrogen replacement therapy; MR: Mendelian randomization.

TABLE 3 Observational associations between serum IGF-1 and hospital-diagnosed hip, knee and hand OA

	Hip OA (N = 398 965)			Knee OA (N = 408 872)			Hand OA (N = 389 308)		
Model	OR	95% CI	P	OR	95% CI	P	OR	95% CI	P
Unadjusted	0.71	0.69, 0.74	6.10×10^{-108}	0.68	0.66, 0.69	2.47×10^{-250}	0.61	0.57, 0.65	1.45×10^{-58}
Adjusted for age and sex	0.94	0.91, 0.97	3.31×10^{-4}	0.80	0.78, 0.82	6.98×10^{-74}	0.80	0.75, 0.86	5.59×10^{-11}
Adjust for age, ethnicity, ERT	0.94	0.91, 0.97	3.59×10^{-4}	0.81	0.80, 0.83	1.63×10^{-64}	0.82	0.77, 0.88	2.96×10^{-9}
Adjusted for age, ethnicity, ERT, BMI	1.04	1.01, 1.07	0.014	0.99	0.96, 1.01	0.223	0.87	0.82, 0.93	4.21×10^{-5}

ORs are per doubling in IGF-1 concentration. IGF-1: insulin-like growth factor-1; OR: odds ratio; ERT: oestrogen replacement therapy.

FIG. 2 Comparison of observational and MR estimates of the effect of IGF-1 on hand, hip and knee OA

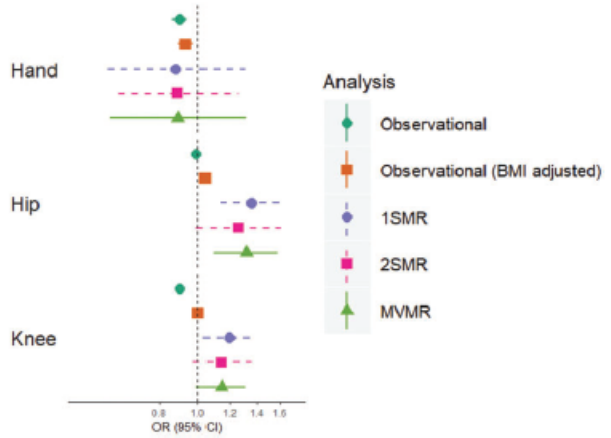

Points represent odds ratios for OA per standard deviation increase in IGF-1 concentration. Horizontal bars represent 95% CIs. Observational analyses adjusted for age, sex, ERT, ethnicity and BMI. MR analyses adjusted for sex, genotyping chip and 10 principal components. OR: odds ratio; 1SMR: one-sample Mendelian randomization; 2SMR: two-sample Mendelian randomization; MVMR: multivariable Mendelian randomization; MR: Mendelian randomization; IGF-1: insulin-like growth factor-1; ERT: oestrogen replacement therapy.

$P = 0.033$]. Combining genotypes for the eight SNPs in a GRS strengthened the instrument (F-statistic: 3774 *vs* 563) and the evidence for a causal effect of IGF-1 on hip OA [OR = 1.35 (1.13, 1.63), $P = 0.001$, Fig. 2]. An effect of IGF-1 on knee OA was also observed when using the IGF-1 GRS instrument [OR = 1.19 (1.03, 1.37), $P = 0.019$]. Although we found no evidence of a causal effect of IGF-1 on hand OA [OR = 0.88 (0.60, 1.31), $P = 0.539$], these analyses were likely underpowered due to the rarity of hospital-diagnosed hand OA (supplementary Table S3, available at *Rheumatology* online). Evidence for a causal effect of IGF-1 on hip and knee OA was stronger when excluding the three SNPs also associated with IGF-BP3 levels [$OR_{Hip} = 1.57$ (1.21, 2.02), $P = 0.001$ and $OR_{Knee} = 1.30$ (1.07, 1.58), $P = 0.008$, supplementary Table S7, available at *Rheumatology* online]. The Sargan statistic was reduced from 30.5 ($P < 0.001$) to 4.4 ($P = 0.35$), suggesting that results were less biased by pleiotropy when excluding IGF-BP3 SNPs. Effects persisted when restricting to the

single intronic *IGF-1* SNP [OR_{hip} = 1.93 (1.25, 2.97), P = 0.003 and OR_{knee} = 1.26 (0.90, 1.76), P = 0.179]. When stratifying by sex, stronger evidence for an effect of IGF-1 on hip OA was seen in females (supplementary Fig. S2, available at *Rheumatology* online), although analysis in males had lower power due to smaller sample size (supplementary Table S3, available at *Rheumatology* online). When checking the assumptions of 1SMR, we found evidence for an association between the IGF-1 GRS and both BMI and ERT use (supplementary Table S8, available at *Rheumatology* online), violating assumption IV2 (Fig. 1). Despite a strong inverse relationship between BMI and measured IGF-1, the association between the IGF-1 GRS and BMI was positive. We repeated 1SMR, adjusting for ERT use, which did not attenuate the association between IGF-1 and hip OA.

When determining the causal relationship using 2SMR, although CIs widened, effect sizes were similar (Fig. 2), with findings consistent with a positive effect of IGF-1 on hip OA [OR = 1.26 (0.99, 1.61), P = 0.065]. The MR-Egger estimate differed in direction of effect (supplementary Figs S3 and S4, available at *Rheumatology* online), suggesting horizontal pleiotropy may explain the observed association (Cochran's Q = 19.6, P = 0.007). Further evidence for a potential pleiotropic effect was supported by two outlying SNPs (supplementary Fig. S4, available at *Rheumatology* online), rs646776 and rs700753; both were associated with IGF-BP3. When removing all three SNPs associated with IGF-BP3, the causal effect estimate for IGF-1 strengthened [OR = 1.49 (1.21, 1.83), $P = 1 \times 10^{-4}$] and was consistent in direction with the MR-Egger estimate [OR = 5.88 (0.70, 49.13), P = 0.200, P for intercept = 0.292, supplementary Table S7, available at *Rheumatology* online]. Cochran's Q was also reduced (Q_{hip} = 4.4, P = 0.354 and Q_{knee} = 5.9, P = 0.206). We found no evidence of a causal effect of IGF-BP3 on hip or knee OA risk, but some evidence for a protective effect of IGF-BP3 on hand OA (supplementary Table S9, available at *Rheumatology* online). The effect of IGF-1 on hip OA was even stronger when restricting to the single intronic *IGF1* SNP [OR = 1.92 (1.22, 3.03), P = 0.005].

We postulated that BMI could mediate the effect of IGF-1 on hip OA; therefore, we performed MVMR to determine the causal effect of IGF-1 on hospital-diagnosed OA, independent of BMI. We found evidence for a BMI-independent causal pathway between IGF-1 and hip OA [OR = 1.32 (1.09, 1.58), P = 0.004], with weaker evidence for a causal effect on knee OA [OR = 1.14 (0.99, 1.31), P = 0.078, Fig. 2]. Evidence for a causal effect of IGF-1 on both hip and knee OA was stronger after excluding the IGF-BP3 SNPs (supplementary Table S7, available at *Rheumatology* online). The effect sizes for the causal role of IGF-1 on hip and knee OA were unchanged when performing MVMR with height instead of BMI (supplementary Table S2, available at *Rheumatology* online). Like univariable MR, a stronger effect of IGF-1 on hip OA was seen in females than males (supplementary Fig. S2, available at *Rheumatology* online), although this could be due to the smaller sample size of the male population.

We next performed factorial MR to identify any additive effect of IGF-1 and BMI on OA. Those with a BMI and IGF-1 GRS above the median had the greatest odds of hip OA [OR = 1.12 (1.06, 1.18), $P = 1 \times 10^{-4}$] compared with those with scores below the median (Fig. 3), suggesting an additive effect of higher serum IGF-1 and higher BMI on hip OA risk. No difference in the odds of knee OA was apparent between those with a high BMI GRS and low IGF-1 GRS *vs* those with a high IGF-1 GRS and high BMI GRS (Fig. 3). Results were similar when stratified by sex (supplementary Fig. S5, available at *Rheumatology* online).

In summary, our observational analyses provide evidence for a protective effect of higher serum IGF-1 on hand OA but an increased odds of hip OA after adjustment for BMI. An increased odds of hip OA is consistent with the MR analyses, which provided evidence for a causal effect of IGF-1 on hip and knee OA. Observational and factorial MR analyses both provided evidence for an interaction between high serum IGF-1 and high BMI on hip OA risk.

Discussion

We have found evidence for a causal effect of higher circulating IGF-1 on the risk of hospital-diagnosed hip OA in a large population-based cohort of white European adults. This effect is independent of BMI. Both observational and MR analyses suggested that the effect of IGF-1 on hip OA is greater in those with a higher BMI, suggesting BMI modifies the effect of IGF-1 on hip OA. We detected evidence for a causal role of IGF-1 as a risk factor for knee OA, though this was weaker than that for hip OA. To the best of our knowledge, this is the first study to use MR to determine the causal relationships between IGF-1 and OA at the hand, hip or knee. Two prior studies have identified a positive relationship between a microsatellite polymorphism in the *IGF-1* promoter and radiographic hip OA [9, 10]. However, this polymorphism was also related to lower serum IGF-1 concentrations in a subset of 50 individuals [36], but the authors could not conclude that the SNP was the causal variant, or in linkage disequilibrium with a variant causing OA [10].

The lack of observational evidence for an association between IGF-1 and knee OA is consistent with a previous case–control study (Framingham Osteoarthritis Study) of both incident and progressive radiographic knee OA [37], and a cross-sectional analysis in the Baltimore Longitudinal Study of Aging [38]. Lloyd *et al.* [8] identified a positive association between IGF-1 and radiographic knee OA in the Chingford population, but only for severe and bilateral knee OA. Our phenotype of hospital-diagnosed OA is likely to reflect more severe radiographic or more clinically apparent (i.e. painful) OA. We lacked data on whether cases had bilateral or unilateral disease, which may contribute to the inconsistency

FIG. 3 Factorial MR analysis of the interaction between IGF-1 and BMI on hip and knee OA risk

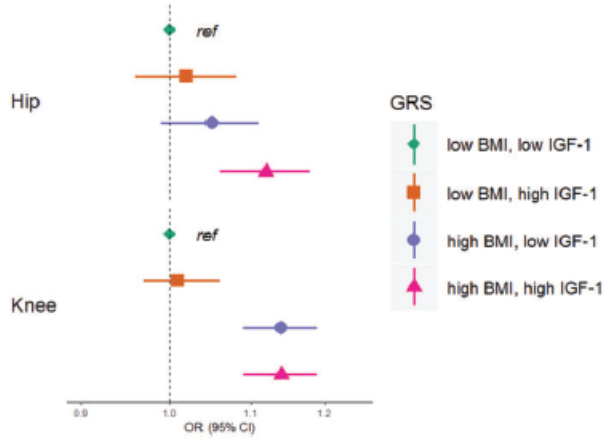

Points represent the odds ratio for individuals in each BMI/IGF-1 GRS category compared with those with a BMI risk score below the median and an IGF-1 score below the median (reference category). Horizontal bars represent 95% CIs. Analyses adjusted for sex, genotyping chip and 10 principal components. MR: Mendelian randomization; IGF-1: insulin-like growth factor-1; GRS: genetic risk score.

in findings. Furthermore, Lloyd *et al.* [8] found weak evidence for increased serum IGF-1 in individuals with radiographic DIP joint OA, which contrasts with the protective association between IGF-1 and hand OA that we observed. Although the age-standardized prevalence of radiographic hand OA was 27% in the US Framingham population [39], UK hospital-diagnosis was much rarer, likely due to the lack of surgical management options for hand OA, meaning our MR analyses of hand OA were underpowered to confirm or refute the reported effect.

Consistent with a role of the IGF-1/IGF-BP axis on hip OA risk, a GWAS of hip OA identified two loci near *IGF-BP3* [40] where SNPs were associated with a decreased odds of hip OA and decreased circulating IGF-BP3 (not IGF-1) [40]. *In vivo* functional studies suggest that IGF-BP3 overexpression in cartilage from patients with knee OA results in decreased aggrecan and increased MMP-13 expression, two markers of cartilage degradation [40]. The two OA-associated SNPs near *IGF-BP3* were not instruments in our analyses, nor in linkage disequilibrium with any of the SNPs used in our instrument. Our two-sample MR analyses did not suggest a causal effect of circulating IGF-BP3 on hip OA risk.

The lack of consistency between our observational and MR results may reflect the difference in exposures; for observational analyses, the exposure was current measured IGF-1 levels whereas for MR analyses, the exposure was genetically predicted IGF-1 levels [41]. Different relationships of measured IGF-1 and the IGF-1 GRS with BMI may be explained by a negative feedback loop, whereby higher IGF-1 levels throughout the life-course lead to a higher body mass, which, over a sustained period of time, may reduce IGF-1 production by the liver [12]. However, the BMI GRS was not associated with current IGF-1 levels [$\beta = 3.12 \times 10^{-4}$ (95% CI −0.004, 0.004)]. We therefore hypothesize that higher IGF-1 throughout the life-course may drive the progression of OA, and our MVMR analyses suggest that this effect is not mediated by BMI. One potential pathway is via increased bone mineral density (BMD), a reported risk factor for hip OA [42]. IGF-1 contributes to skeletal development and increases BMD by promoting mesenchymal stem cell differentiation into osteoblasts [43]. However, adjustment for BMD did not attenuate our observational relationship between IGF-1 and hip OA (data not shown). An alternative explanation is that increased IGF-1 during development may lead to alterations in hip shape. IGF-1 is important for endochondral bone formation [44] and several genes linked to endochondral bone formation were identified in a recent GWAS meta-analysis of hip shape [45]. Variation in hip shape is associated with hip OA [46]. A cohort with IGF-1 and hip shape measured prior to OA onset (i.e. an adolescent cohort) is needed to better understand this relationship. As we observed a stronger effect of IGF-1 on hip OA in females, we further hypothesized that IGF-1 levels could lower circulating oestrogen levels, leading to increased

OA risk, as oestrogen may be protective against OA [47]. However, the IGF-1 GRS was not related to menopausal age. Another potential explanation for the differences between the observational and MR results could be additional unmeasured confounding, biasing the observational analyses [41]. The potential for confounders to strongly bias observational results is highlighted by the difference in direction of effect observed for hip OA, before and after adjustment for BMI. As long as the instrument used for MR analysis meets the three key assumptions of MR (highlighted in Fig. 1), the MR estimate is not biased by confounding [13] and therefore we have more confidence in our estimates generated by MR.

A major strength of this analysis is the availability of extensive data for both IGF-1 concentrations and hospital diagnosed OA for >400 000 individuals, making this the most well-powered study to determine the observational relationship between IGF-1 and OA, to date. Furthermore, we had genotype data available for >300 000 individuals, providing 80% power to detect a causal OR of >1.28. The availability of these genetic data enabled us to perform one-sample MVMR analysis to determine the true causal effect of IGF-1 on hip OA, independent of BMI. However, we acknowledge limitations within these analyses. Although we excluded controls with other diagnosed arthropathies, some may still have had undiagnosed OA, although this would likely bias results towards the null. Our sex-stratified and hand OA analyses had low power, meaning we are unable to draw robust conclusions. The effect sizes of the summary statistics for the SNP–IGF-1 associations, used for two-sample MR analyses, were approximated as an s.d. unit change in IGF-1 from the corresponding *P*-values, direction of association, sample size and allele frequency [29]. However, these effect estimates were not used for 1SMR, which generated consistent results. We chose not to generate our BMI instrument from the largest GWAS of BMI, as a large proportion of individuals included in this meta-analysis were from UK Biobank and we were concerned about overestimating causal effect estimates due to 'Winner's-curse bias' [48, 49]. We acknowledge that dichotomizing the population based on their GRS may not be the most efficient method for performing factorial MR and we cannot rule out a possible unobserved interaction between IGF-1 and BMI on knee OA risk. Recently, an alternative method was proposed for greater power in factorial MR analyses, using the complete set of instruments and their interactions [50]. The overall UK Biobank population is predominantly white British, with a higher prevalence of home-owners and non-smokers, a lower BMI and fewer self-reported health concerns than the general population [51], and MR analyses were restricted to those of white European ancestry, limiting generalizability. 'Survivor bias' may explain associations observed; if higher IGF-1 levels are related to a lower mortality risk, those with higher IGF-1 levels will be surviving long enough to develop chronic diseases such as OA. However, IGF-1 levels appear independent of all-cause mortality [52]. The UK Biobank population is limited by latent population structure even after restricting to white Europeans and adjusting for PCs [53], which may confound the relationship between IGF-1 and hospital-diagnosed hip OA. The discrepancy between observational and MR analyses most likely reflects unmeasured confounding, highlighting the utility of MR.

We identified robust evidence that higher concentrations of serum IGF-1 are a causal risk factor for hip OA in a very large UK population, with some evidence for a causal role in knee OA, and no evidence for an association with hand OA. Our MVMR analyses suggest that this causal role is independent of BMI, consistent with our observational analyses for hip, but not knee, OA. Further study is justified to determine the mechanism underlying this relationship.

Acknowledgements

This research has been conducted using the UK Biobank Resource under Application Number 17295. A.H. is funded by the Wellcome Trust (grant ref. 20378/Z/16/Z). C.L.G. was funded by Versus Arthritis (grant ref. 20000). Support for the IGF-1 GWAS meta-analysis (A.T., R.C.K.) was provided by the National Institute of Aging (grant ref. 1R01AG031890) and the National Heart, Lung and Blood Institute (grant ref. R01HL075516, 2R01HL105756). A.H., E.S., L.P., J.H.T. and C.L.G. work in, or are affiliated with, a University of Bristol and MRC funded unit (MC_UU_00011/1).

Data availability

UK Biobank data is available through a procedure described at https://www.ukbiobank.ac.uk/principles-of-access/. Hip and knee OA GWAS summary statistics are publicly available at https://www.ebi.ac.uk/gwas/.

Funding: No specific funding was received from any funding bodies in the public, commercial or not-for-profit sectors to carry out the work described in this manuscript.

Disclosure statement: The authors have declared no conflicts of interest.

Supplementary data

Supplementary data are available at *Rheumatology* online.

References

1 Cross M, Smith E, Hoy D *et al*. The global burden of hip and knee osteoarthritis: estimates from the global burden of disease 2010 study. Ann Rheum Dis 2014;73:1323–30.

2 Chen A, Gupte C, Akhtar K, Smith P, Cobb J. The global economic cost of osteoarthritis: how the UK compares. Arthritis 2012;2012:1–6.

3 Laron Z. Insulin-like growth factor 1 (IGF-1): a growth hormone. 2001;54:311–6.

4 Nilsson A, Isgaard J, Lindahl A *et al.* Regulation by growth hormone of number of chondrocytes containing IGF-I in rat growth plate. Science 1986;233:571–4.

5 McQuillan DJ, Handley CJ, Campbell MA *et al.* Stimulation of proteoglycan biosynthesis by serum and insulin-like growth factor-I in cultured bovine articular cartilage. Biochem J 1986;240:423–30.

6 Zhang M, Zhou Q, Liang QQ *et al.* IGF-1 regulation of type II collagen and MMP-13 expression in rat endplate chondrocytes via distinct signaling pathways. Osteoarthritis Cartilage 2009;17:100–6.

7 Claessen KM, Ramautar SR, Pereira AM *et al.* Relationship between insulin-like growth factor-1 and radiographic disease in patients with primary osteoarthritis: a systematic review. Osteoarthritis Cartilage 2012; 20:79–86.

8 Lloyd ME, Hart DJ, Nandra D *et al.* Relation between insulin-like growth factor-I concentrations, osteoarthritis, bone density, and fractures in the general population: the Chingford study. Ann Rheum Dis 1996;55:870–4.

9 Meulenbelt I, Bijkerk C, Miedema HS *et al.* A genetic association study of the IGF-1 gene and radiological osteoarthritis in a population-based cohort study (the Rotterdam Study). Ann Rheum Dis 1998;57:371–4.

10 Zhai G, Rivadeneira F, Houwing-Duistermaat JJ *et al.* Insulin-like growth factor I gene promoter polymorphism, collagen type II alpha1 (COL2A1) gene, and the prevalence of radiographic osteoarthritis: the Rotterdam Study. Ann Rheum Dis 2004;63:544–8.

11 Zengini E, Hatzikotoulas K, Tachmazidou I *et al.* Genome-wide analyses using UK Biobank data provide insights into the genetic architecture of osteoarthritis. Nat Genet 2018;50:549–58.

12 Faupel-Badger JM, Berrigan D, Ballard-Barbash R, Potischman N. Anthropometric correlates of insulin-like growth factor 1 (IGF-1) and IGF binding protein-3 (IGFBP-3) levels by race/ethnicity and gender. Ann Epidemiol 2009;19:841–9.

13 Lawlor DA, Harbord RM, Sterne JA, Timpson N, Davey Smith G. Mendelian randomization: using genes as instruments for making causal inferences in epidemiology. Stat Med 2008;27:1133–63.

14 Sanderson E, Davey Smith G, Windmeijer F, Bowden J. An examination of multivariable Mendelian randomization in the single-sample and two-sample summary data settings. Int J Epidemiol 2019;48:713–27.

15 Allen NE, Sudlow C, Peakman T, Collins R; on behalf of UK Biobank. UK biobank data: come and get it. Sci Transl Med 2014;6:224ed4.

16 Fry D. Almond R. Moffat S. Gordon M. Singh P. UK Biobank Biomarker Project: companion document to accompany serum biomarker data version 1.0. 2019. Available from: https://biobank.ndph.ox.ac.uk/showcase/showcase/docs/serum_biochemistry.pdf.

17 UK Biobank. Biomarker assay quality procedures: approaches used to minimise systematic and random errors (and the wider epidemiological implications). 2019. Available from: http://biobank.ctsu.ox.ac.uk/crystal/crystal/docs/biomarker_issues.pdf.

18 NHS Digital. Hospital Episode Statistics (HES). Available from: https://digital.nhs.uk/data-and-information/data-tools-and-services/data-services/hospital-episode-statistics (26 March 2019, date last edited).

19 Funck-Brentano T, Nethander M, Movérare-Skrtic S, Richette P, Ohlsson C. Causal factors for knee, hip and hand osteoarthritis: a Mendelian randomization study in the UK Biobank. Arthritis Rheumatol 2019;71:1634–41.

20 Tachmazidou I, Hatzikotoulas K, Southam L *et al.* Identification of new therapeutic targets for osteoarthritis through genome-wide analyses of UK Biobank data. Nat Genet 2019;51:230–6.

21 Bycroft C, Freeman C, Petkova D *et al.* The UK Biobank resource with deep phenotyping and genomic data. Nature 2018;562:203–9.

22 Mitchell R, Hemani G, Dudding T *et al.* UK Biobank genetic data: MRC-IEU quality control, version 2 2019. Available from: https://data.bris.ac.uk/datasets/1ovaau5sxunp2cv8rcy88688w/UK%20Biobank%20Genetic%20Data_MRC%20IEU%20Quality%20Control%20version%202.pdf

23 Teumer A, Qi Q, Nethander M, Aschard H *et al.* Genomewide meta-analysis identifies loci associated with IGF-I and IGFBP-3 levels with impact on age-related traits. Aging Cell 2016;15:811–24.

24 Baum CF, Schaffer ME, Stillman S. IVREG2: stata module for extended instrumental variables/2SLS and GMM estimation. Statistical Software Components: Boston College Department of Economics, 2002.

25 Burgess S, Small DS, Thompson SG. A review of instrumental variable estimators for Mendelian randomization. Stat Methods Med Res 2017;26:2333–55.

26 Zheng J, Baird D, Borges MC *et al.* Recent developments in Mendelian randomization studies. Curr Epidemiol Rep 2017;4:330–45.

27 Bowden J, Davey Smith G, Haycock PC, Burgess S. Consistent estimation in Mendelian randomization with some invalid instruments using a weighted median estimator. Genet Epidemiol 2016;40:304–14.

28 Brion MJ, Shakhbazov K, Visscher PM. Calculating statistical power in Mendelian randomization studies. Int J Epidemiol 2013;42:1497–501.

29 Rietveld CA, Medland SE, Derringer J *et al.* GWAS of 126,559 individuals identifies genetic variants associated with educational attainment. Science 2013;340:1467–71.

30 Loh P-R, Kichaev G, Gazal S, Schoech AP, Price AL. Mixed-model association for biobank-scale datasets. Nat Genet 2018;50:906–8.

31 Mitchell R, Elsworth B, Raistrick CA *et al.* MRC IEU UK Biobank GWAS Pipeline Version 2. 2019. Available from:

https://data.bris.ac.uk/datasets/pnoat8cxo0u52p6ynfaekeigi/MRC%20IEU%20UK%20Biobank%20GWAS%20pipeline%20version%202.pdf

32 Hemani G, Tilling K, Davey Smith G. Orienting the causal relationship between imprecisely measured traits using GWAS summary data. PLoS Genet 2017;13:e1007081.

33 Hemani G, Zheng J, Elsworth B *et al.* The MR-Base platform supports systematic causal inference across the human phenome. eLife 2018;7:e34408.

34 Bowden J, Davey Smith G, Burgess S. Mendelian randomization with invalid instruments: effect estimation and bias detection through Egger regression. Int J Epidemiol 2015;44:512–25.

35 Locke AE, Kahali B, Berndt SI *et al.* Genetic studies of body mass index yield new insights for obesity biology. Nature 2015;518:197–206.

36 Vaessen N, Heutink P, Janssen JA *et al.* A polymorphism in the gene for IGF-I: functional properties and risk for type 2 diabetes and myocardial infarction. Diabetes 2001;50:637–42.

37 Fraenkel L, Zhang Y, Trippel SB *et al.* Longitudinal analysis of the relationship between serum insulin-like growth factor-I and radiographic knee osteoarthritis. Osteoarthritis Cartilage 1998;6:382–7.

38 Hochberg MC, Lethbridge-Cejku M, Scott WW Jr *et al.* Serum levels of insulin-like growth factor in subjects with osteoarthritis of the knee. Data from the Baltimore Longitudinal Study of Aging. Arthritis Rheum 1994;37:1177–80.

39 Zhang Y, Jordan JM. Epidemiology of osteoarthritis. Clin Geriatr Med 2010;26:355–69.

40 Evans DS, Cailotto F, Parimi N *et al.* Genome-wide association and functional studies identify a role for IGFBP3 in hip osteoarthritis. Ann Rheum Dis 2015;74:1861–7.

41 Davies NM, Holmes MV D, Smith G. Reading Mendelian randomisation studies: a guide, glossary, and checklist for clinicians. BMJ 2018;362:k601.

42 Hardcastle SA, Dieppe P, Gregson CL, Davey Smith G, Tobias JH. Osteoarthritis and bone mineral density: are strong bones bad for joints? Bonekey Rep 2015;4:624.

43 Yakar S, Werner H, Rosen CJ. Insulin-like growth factors: actions on the skeleton. J Mol Endocrinol 2018;61:T115–37.

44 Guntur AR, Rosen CJ. IGF-1 regulation of key signaling pathways in bone. Bonekey Rep 2013;2:437.

45 Baird DA, Evans DS, Kamanu FK *et al.* Identification of novel loci associated with hip shape: a meta-analysis of genome-wide association studies. J Bone Miner Res 2019;34:241–51.

46 Faber BG, Baird D, Gregson CL *et al.* DXA-derived hip shape is related to osteoarthritis: findings from in the MrOS cohort. Osteoarthritis Cartilage 2017;25:2031–8.

47 Felson DT, Lawrence RC, Dieppe PA *et al.* Osteoarthritis: new insights. Part 1: the disease and its risk factors. Ann Intern Med 2000;133:635–46.

48 Yengo L, Sidorenko J, Kemper KE, *et al.* Meta-analysis of genome-wide association studies for height and body mass index in ~700000 individuals of European ancestry. Hum Mol Genet 2018;27:3641–9.

49 Haycock PC, Burgess S, Wade KH *et al.* Best (but oft-forgotten) practices: the design, analysis, and interpretation of Mendelian randomization studies. Am J Clin Nutr 2016;103:965–78.

50 Rees JMB, Foley CN, Burgess S. Factorial Mendelian randomization: using genetic variants to assess interactions. Int J Epidemiol 2019; doi: 10.1093/ije/dyz161.

51 Fry A, Littlejohns TJ, Sudlow C *et al.* Comparison of sociodemographic and health-related characteristics of UK biobank participants with those of the general population. Am J Epidemiol 2017;186:1026–34.

52 Saydah S, Graubard B, Ballard-Barbash R, Berrigan D. Insulin-like growth factors and subsequent risk of mortality in the United States. Am J Epidemiol 2007;166:518–26.

53 Haworth S, Mitchell R, Corbin L *et al.* Apparent latent structure within the UK Biobank sample has implications for epidemiological analysis. Nat Commun 2019;10:333.

Appendix 5: Abstract based on results of multivariable MR analyses, accepted for poster presentation at the OARSI annual meeting, 2020.

significant difference (P<0.05) between the effective rate of the experimental group and that of the control group. All indicators of KOOS were improved, with the significant differences in symptom score, sports score and entertainment ability score, and the life quality reladsvblmadmted to the knee (P < 0.05). The levels of serumIL-1β,TNF-α were all decreased in the experimental group, with a significant difference in the degree of IL-1β decrease (P<0.05).

Conclusions: Qufengzhitong Capsule is effective in the treatment of chronic knee osteoarthritis and its mechanism may be related to the regulation of the expression of serum IL-1β and TNF-α of patients with chronic knee osteoarthritis.

596

USING MULTIVARIABLE MENDELIAN RANDOMIZATION TO ESTIMATE THE BMI-INDEPENDENT CAUSAL EFFECT OF BONE MINERAL DENSITY ON OSTEOARTHRITIS

A. Hartley [1], E. Sanderson [1], R. Granell [1], L. Paternoster [1], J. Zheng [1], L. Southam [2], E. Zeggini [2], C.L. Gregson [1], J.H. Tobias [1]. [1] *Univ. of Bristol, Bristol, United Kingdom;* [2] *Helmholtz Zentrum Munchen, Neuherberg, Germany*

Purpose: Observational analyses have suggested that high Bone Mineral Density (BMD) is a risk factor for hip and knee osteoarthritis (OA), but it is unclear whether this represents a causal effect of BMD on OA or shared underlying biological pathways (genetic pleiotropy). It is also unclear whether these relationships are independent of the confounding effect of body mass index (BMI). Mendelian randomisation (MR) uses genetic variants robustly associated with an exposure to determine the causal effect of an exposure and an outcome, independent of confounding and reverse causality. We therefore performed two-sample (2S), one-sample (1S), and multivariable (MV)MR analyses to uncover the causal pathways between BMD, BMI and OA.

Methods: Single nucleotide polymorphisms (SNPs) associated with BMD estimated from heel ultrasound (eBMD) in the latest genome wide association study (GWAS) in UK Biobank were used to instrument BMD. BMI was instrumented by SNPs from the largest Genetic Investigation of Anthropometric Traits (GIANT) consortium GWAS not including UK Biobank. Hip and knee OA were instrumented by SNPs identified from a meta-analysis of Genetics of Osteoarthritis (GO) consortium cohorts (excluding UK Biobank). Independent SNPs associated with the exposure at genome-wide significance were included as instruments. 362 SNPs were used to instrument eBMD, 69 for BMI, 10 for hip and 4 for knee OA. MR estimates were generated using inverse-variance weighting (IVW) fixed effects meta-analysis. MR-Egger regression was used to identify potential horizontal pleiotropy. 2SMR analyses were performed with the MR-Base R package. 1SMR analyses were performed using individual-level data from UK Biobank. Unweighted allele scores were generated for each exposure. A BMD allele score was generated using 43 independent femoral neck (FN) BMD SNPs identified by the Genetics of Osteoporosis (GEFOS) consortium. Two stage least squares regression was performed using the allele score as the instrument and adjusting for age, sex and 10 principal components (population stratification). 1S MVMR was performed, including both BMD and BMI and allele scores associated with them as instruments in the same model, to determine if there is a causal pathway from BMD to OA, independent of BMI.

Results: In 2SMR analyses, there was strong evidence for a causal effect of eBMD on hip OA (OR per SD increase in eBMD=1.09 [1.03,1.16], p=0.002) but weaker evidence for a causal effect on knee OA (OR=1.04 [1.00,1.09], p=0.07). Directions of effect were consistent when using MR-Egger analysis. Effect sizes were stronger, for both outcomes, when restricting to 10 SNPs also associated with FN BMD (GEFOS) at genome-wide significance ($p<5x10^{-8}$). Results suggested that the causal pathway between eBMD and knee OA was bidirectional, with evidence for a causal effect of knee OA on eBMD (β=0.13 [0.03,0.23], p=0.01, β represents the SD increase in BMD per doubling in OA risk). We did not find evidence for a causal effect of eBMD on BMI. BMI was strongly causally related to hip/knee OA and eBMD (OR=1.51 [1.28,1.78], OR=1.64 [1.44,1.86] and β=0.10 [0.06,0.15], respectively, all $p<10^{-5}$), with consistent results when using the pleiotropy-robust MR-Egger method. Results were generally consistent using 1SMR, although there was additional evidence for causal effects of hip OA on eBMD and of hip and knee OA on BMI. MVMR analyses identified a BMI-independent causal pathway between eBMD and hip and knee OA (risk difference per SD increase in BMD=0.007 [0.001,0.013], p=0.03 and 0.015 [0.007,0.023], $p=10^{-4}$, respectively).

Conclusions: These Results demonstrate that previously observed relationships between higher BMD and OA partly reflect confounding by BMI. In addition, there is evidence of an independent causal effect of eBMD on OA, however this relationship appears to be bi-directional, suggesting that shared biological pathways contribute to both traits.

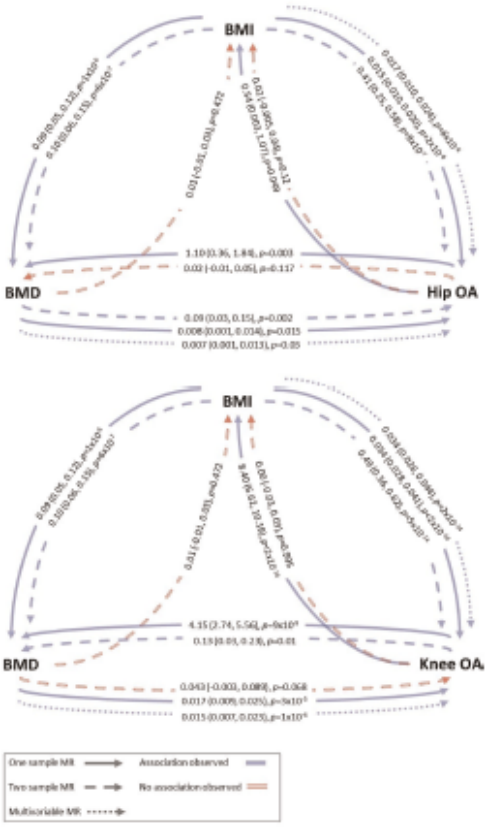

Summary of results from all MR analyses

Estimates represent the SD increase in BMI per SD increase in BMD and vice versa. For analyses with continuous exposures (BMI/BMD) and binary outcomes (hip/knee OA), 1S/MV estimates represent the risk difference per SD increase in exposure and 2S estimates represent the increase in log odds per SD increase in exposure. Estimates from analyses with OA as the exposure represent the SD increase in outcome per doubling in OA risk.

597

INCIDENCE AND PROGRESSION OF ANKLE OSTEOARTHRITIS: THE JOHNSTON COUNTY OSTEOARTHRITIS PROJECT

A. Jaleel, C. Alvarez, J.B. Renner, Y.M. Golightly, A.E. Nelson. *Univ. of North Carolina at Chapel Hill, Chapel Hill, NC, USA*

Purpose: Osteoarthritis involving the ankles has been relatively understudied. We have previously demonstrated associations of older age, obesity, and prior injury with prevalent radiographic ankle OA (rAOA) in a community-based cohort (Lateef 2017), but little is known

Appendix 6: Abstract based on IGF-1 results, accepted for oral presentation at the OARSI annual meeting, 2020.

79

MENDELIAN RANDOMIZATION IDENTIFIES A CAUSAL ROLE FOR SERUM INSULIN-LIKE GROWTH FACTOR-1 IN HIP OSTEOARTHRITIS

A.E. Hartley, E. Sanderson, L. Paternoster, R. Granell, J.H. Tobias, C.L. Gregson. *Univ. of Bristol, Bristol, United Kingdom*

Purpose: Individuals with acromegaly (characterised by elevated circulating IGF-1) are at an increased risk of secondary osteoarthritis (OA), but epidemiological evidence for an association between serum insulin-like growth factor-1 (IGF-1) and OA in the general population is conflicting. We determined the observational associations between serum IGF-1 and hospital-diagnosed (HD) hand, hip and knee and hand OA in UK Biobank (UKBB). We performed Mendelian Randomization (MR) to determine if observed associations represent a true causal effect.

Methods: Serum IGF-1 was assessed by chemiluminescent immunoassay. HD hip, knee and hand OA were determined using linked hospital inpatient records. Observational associations between serum IGF-1 and HD OA variables were determined by multivariable logistic regression, adjusting for age, sex, ethnicity, oestrogen use and BMI. We performed one-sample (1SMR) using two-stage least-squares regression, with an unweighted allele score generated from the eight single nucleotide polymorphisms (SNPs) robustly associated with IGF-1 in the largest genome-wide association study (GWAS) meta-analysis, as an instrument. MR is a form of instrumental variable regression which uses genetic variants robustly related to the exposure as instruments, providing an estimate of the causal effect which is unbiased by confounding and reverse causality. Multivariable MR (MVMR) determined the BMI-independent effect of IGF-1, by including BMI as an additional exposure, instrumented by an unweighted BMI allele score generated from 69 independent loci. MR analyses were adjusted for sex, genotyping chip and 10 principal components (PCs) to account for population stratification.

Results: 421,572 individuals had complete data for the observational analyses, of whom 332,092 (79%) had genetic data, were unrelated and of European ancestry, suitable for MR. The mean (SD) ages of the observational and MR populations were 56.4 (8.1) and 56.5 (8.0) years respectively, with 54% female in both populations. Median (interquartile range) IGF-1 concentration was 21.3 (17.6, 24.9) nmol/L in both populations. In the observational population, 3.1% had HD hip OA (3.2% in the MR population); 0.7% had hand OA and 5.4% knee OA in both populations. In analyses adjusted for age, sex, ethnicity and oestrogen use, serum IGF-1 concentration was associated with a decreased odds of HD OA (OR_{hand}=0.82 [0.77, 0.88] $p=3x10^{-9}$, OR_{hip}=0.94 [0.91, 0.97] $p=4x10^{-4}$, OR_{knee}=0.81 [0.80, 0.83] $p=1x10^{-64}$; OR per doubling in IGF-1 concentration). After additional adjustment for BMI, serum IGF-1 remained associated with a reduced odds of hand OA; however, it was then associated with an *increased* odds of hip OA (OR_{hip}=1.04 [1.01, 1.07] p=0.014), with little evidence of an association with knee OA. Using 1SMR, we found strong evidence for increased risk of hip OA with higher IGF-1 concentrations (risk difference per SD increase in IGF-1=0.009 [0.004, 0.015] p=0.001, corresponding to an approximate OR_{hip} 1.36 [1.13, 1.63]), and also evidence for an increased risk of knee OA (risk difference=0.009 [0.001, 0.016] p=0.019). In contrast, point estimates suggested a decreased risk of hand OA, although confidence intervals were wide, reflecting the low prevalence of HD hand OA. When testing the assumptions of MR, we found evidence for an association between the IGF-1 allele score and BMI, which violates the assumption that an instrument is unrelated to any confounders of the exposure-outcome relationship. We therefore performed MVMR analyses to determine the BMI-independent effect; the effect size for IGF-1 on hip OA was unchanged (risk difference=0.009 [0.003, 0.014] p=0.003); whereas, the effect of IGF-1 on knee OA was attenuated by one-third (risk difference=0.006 [-0.001, 0.014] p=0.076).

Conclusions: Our MR analyses provide strong evidence that higher concentrations of serum IGF-1 are a causal risk factor for hip OA in a very large UK population, with weaker evidence for a causal role in knee OA and very little evidence for an effect on hand OA. Our MVMR analyses estimate the direct effect of IGF-1 on OA conditional on BMI, these results suggest that this causal role of IGF-1 is independent of BMI, consistent with our observational analyses. Further study is justified to determine the mechanism underlying this association.

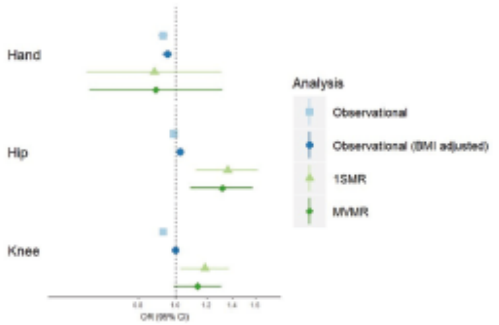

Summary of associations between serum IGF-1 and hospital diagnosed OA in UKBB from observational and MR analyses.
Points represent the odds ratio per SD increase in IGF-1. Horizontal bars represent 95% confidence intervals. Observational analyses are adjusted for age, sex, history of oestrogen replacement use and ethnicity. MR analyses are adjusted for sex, genotyping chip and 10 Principal Components.

80

TEMPORAL RELATIONSHIP BETWEEN OSTEOARTHRITIS AND COMORBIDITIES: A COMBINED CASE CONTROL AND COHORT STUDY IN THE UNITED KINGDOM PRIMARY CARE SETTING

S. Swain [1], C. Coupland [1], C. Mallen [2], C. Fu Kuo [3], A. Sarmanova [4], M. Doherty [1], W. Zhang [1]. [1] *Univ. of Nottingham, Nottingham, United Kingdom;* [2] *Keele Univ., Keele, United Kingdom;* [3], *Chang Gung Mem. Hosp., Taiwan, Taiwan;* [4] *Univ. of Bristol, Bristol, United Kingdom*

Purpose: To determine the temporal relationship between osteoarthritis (OA) and comorbidities.

Methods: During a 20 years period (1997-2017), we identified 222,290 incident OA cases and 222,290 age (+/-2 years), sex and practice matched controls (non-OA) from the UK Clinical Practice Research Datalink (CPRD). Controls were assigned with an index date, same as OA diagnosis date in matched cases. For the follow-up analysis, 27,932 incident OA patients and 27,932 age (+/-2 years), sex and practice matched controls without selected comorbidities at or before OA diagnosis were identified. The association (Odds Ratio (ORs)) of OA with 47 identified comorbidities and with multi-morbidity (≥2 comorbidities) prior to diagnosis, and the risks (hazard ratio (HRs)) of developing these comorbidities after OA diagnosis, were estimated and adjusted for age, sex, diagnosis year, body mass index, smoking and alcohol consumption. The false discovery rate method was used to obtain adjusted P values to account for multiple testing.

Results: Within the 20 years observational period prior to the index date, the prevalence of multi-morbidity among OA cases and controls was 53.1% and 41.8% respectively. The adjusted OR was 1.71 (95% CI 1.69-1.74). Of 47 chronic conditions studied, 39 had significant associations with OA before the diagnosis, including rheumatoid arthritis, fibromyalgia, polymyalgia, back pain, Sjogren's syndrome, systemic lupus erythematosus, ankylosing spondylitis, gout, heart failure, depression and peripheral vascular diseases. [Figure 1] After the index date, the median time to develop multi-morbidity was 7 years in people with OA whereas it was 9 years in people without OA. The adjusted HR was 1.43 (95% CI 1.32-1.54). The cumulative probabilities of having at least two comorbidities at 5 years, 15 years and 20 years following the index date were 0.64%, 22.14% and 52.93% in patients with incident OA and 0.25%, 15.53% and 38.00% in controls, respectively [Figure 2] Patients with incident OA were significantly more likely to develop 21 comorbidities than non-OA controls. Leading comorbidities were fibromyalgia, rheumatoid arthritis, dementia, ankylosing spondylitis, sleep problems, benign prostate disease, anaemia, crystal arthropathy, peripheral vascular disease, depression, gall bladder disease and cancer. [Figure 1]

Appendix 7: Questionnaire sent to all consenting HBM participants at follow-up.

University of BRISTOL

The High Bone Mass Study

Follow-up Questionnaire 2016

Please complete this questionnaire as thoroughly and as accurately as you can to help us with our research. Some questions on different pages may seem similar but please try to complete the whole questionnaire. To help you complete some of the questions, it may be useful to have details of your medicines/ prescriptions with you.
All your answers will be treated as **strictly confidential** and will only be seen by the research team.

This questionnaire will take approximately **30 minutes** to complete.
If you have any difficulties with the questions, please contact the research team:
Email: **high-bone-mass@bristol.ac.uk**
Telephone: **0117 414 7861**

Thank you very much for your continuing participation in this study

We very much appreciate you taking the time to fill in this questionnaire

Arthritis Research UK

wellcome trust

This questionnaire has **7 sections**. The first **6 sections are for male and female** participants and the **final section is for female participants only**.

Please fill in your personal details on this page **before** completing the questionnaire. This page will be separated from the rest of the questionnaire to ensure that your responses remain **confidential**.

Please use **black pen** and make sure you **cross inside** the boxes, not next to them. Thank you!

First name:

Last name:

Your date of birth: / /

Today's date: / /

Your Postcode:

Please ensure you have filled in your name and other details on the previous page.

Section 1: Personal Information

1A. What is your height today?

_ _ . _ _ metres **OR** _ _ feet _ _ inches

1B. How much do you currently weigh?

_ _ _ kilograms **OR** _ _ stone _ _ pounds

2. What is the highest level of education or training that you have successfully completed?

CSE/ School Certificate	☐ 11	Higher degree (e.g. Master's/ PhD)	☐ 41
GCSE/ O Level	☐ 12	PGCE- Postgraduate Cert. of Education	☐ 42
Apprenticeship	☐ 21	Other teaching qualification	☐ 43
GCE/ A Level/ Scottish Highers	☐ 22	State enrolled nurse	☐ 51
Diploma of Higher Education	☐ 31	State registered nurse	☐ 52
Bachelor's degree (e.g. BA, BSc)	☐ 32	Other para-medical qualification	☐ 53
Other degree level qualification (e.g. graduate membership of a professional institute)	☐ 33	Qualifications in shorthand typing or other skills (e.g. hairdressing)	☐ 61
Other ☐ 71 _		None of these	☐ 0

Section 2: Your Joints

3A. Have you ever been told by a doctor that you have **arthritis**?

Yes ☐ 1 Year Diagnosed _ _ _ _ No ☐ 0 Don't know ☐ 99

***If No**, please go to question 4A (page 4)*

Question 3 continues on page 4

4 876419 181113

3B. If Yes, please give the type of arthritis (if known):

Osteoarthritis ☐ 1 Rheumatoid arthritis ☐ 2 Other ☐ 3 Don't know ☐ 99

If Other, please specify: _____

3C. Which joints are affected? (Please tick all that apply).

Knees ☐ Hips ☐ Hands/ Wrists ☐ Back ☐

Neck ☐ Shoulders ☐ Ankles/ Feet ☐ Other ☐

If Other, please specify: _____

4A. Have you ever had a joint replacement?

Yes ☐ 1 No ☐ 0 ***If No,*** *please go to question 5A (below)*

4B. If Yes, please provide details below, indicating which joint was replaced, the year the joint replacement operation was performed and the reason for the joint replacement:

	0 **No**	1 **Yes**	**Year**	**Reason (*e.g. arthritis, fracture*)**
Right hip	☐	☐	_____	_____
Left hip	☐	☐	_____	_____
Right knee	☐	☐	_____	_____
Left knee	☐	☐	_____	_____
Other	☐	☐	_____	_____

If Other, please specify: _____

5A. Have you ever had any operations on your **spine**?

Yes ☐ 1 No ☐ 0 Don't know ☐ 99

5B. If Yes, please specify: _____

5C. Have you ever had an injection in your **spine** to relieve pain from **arthritis**?

Yes ☐ 1 No ☐ 0 Don't know ☐ 99

Your knees

6. Have you ever had any of the following procedures performed on your **knee(s) for arthritis**? **If Yes**, please indicate which knee:

	0 No	1 Yes, Left	2 Yes, Right	3 Yes, Both	99 Don't know
Steroid injection	☐	☐	☐	☐	☐
Cartilage operation	☐	☐	☐	☐	☐
Knee washout/ lavage/ arthroscopy	☐	☐	☐	☐	☐

7. The following questions concern the amount of pain you have experienced in your **knees**. For each situation please enter the amount of pain experienced in the **last 48 hours**.

Question: How much pain do you have?

7A. Walking on a flat surface

None ☐0 Mild ☐1 Moderate ☐2 Severe ☐3 Extreme ☐4

7B. Going up or down stairs

None ☐0 Mild ☐1 Moderate ☐2 Severe ☐3 Extreme ☐4

7C. At night while in bed

None ☐0 Mild ☐1 Moderate ☐2 Severe ☐3 Extreme ☐4

7D. Sitting or lying

None ☐0 Mild ☐1 Moderate ☐2 Severe ☐3 Extreme ☐4

7E. Standing upright

None ☐0 Mild ☐1 Moderate ☐2 Severe ☐3 Extreme ☐4

8. The following questions concern the amount of stiffness (not pain) you have experienced in the **last 48 hours** in your **knees**. Stiffness is a sensation of restriction or slowness in the ease with which you move your joints.

8A. How **severe** is your knee stiffness **after** first **wakening** in the morning?

None ☐0 Mild ☐1 Moderate ☐2 Severe ☐3 Extreme ☐4

8B. How **severe** is your knee stiffness after sitting, lying or resting **later in the day**?

None ☐0 Mild ☐1 Moderate ☐2 Severe ☐3 Extreme ☐4

9. The following questions concern your physical function. By this we mean your ability to move around and to look after yourself. For each of the following activities, please indicate the degree of difficulty you have experienced in the **last 48 hours** due to your **knees**.

Question: What degree of difficulty do you have with:

9A. Ascending stairs

None ☐0 Mild ☐1 Moderate ☐2 Severe ☐3 Extreme ☐4

9B. Rising from sitting

None ☐0 Mild ☐1 Moderate ☐2 Severe ☐3 Extreme ☐4

9C. Walking on flat

None ☐0 Mild ☐1 Moderate ☐2 Severe ☐3 Extreme ☐4

9D. Getting in/ out of car

None ☐0 Mild ☐1 Moderate ☐2 Severe ☐3 Extreme ☐4

9E. Putting on socks/ stockings

None ☐0 Mild ☐1 Moderate ☐2 Severe ☐3 Extreme ☐4

9F. Rising from bed

None ☐0 Mild ☐1 Moderate ☐2 Severe ☐3 Extreme ☐4

9G. Sitting

None ☐0 Mild ☐1 Moderate ☐2 Severe ☐3 Extreme ☐4

10. In the **past week**, how much has **knee pain** affected your sleep?

Not at all ☐0 Mildly ☐1 Moderately ☐2 Severely ☐3 Extremely ☐4

Your hips

11. The following questions concern the amount of pain you have experienced in your **hips**. For each situation please enter the amount of pain experienced in the **last 48 hours**.

Question: How much pain do you have?

11A. Walking on a flat surface

None ☐0 Mild ☐1 Moderate ☐2 Severe ☐3 Extreme ☐4

11B. Going up or down stairs

None ☐0 Mild ☐1 Moderate ☐2 Severe ☐3 Extreme ☐4

11C. At night while in bed

None ☐0 Mild ☐1 Moderate ☐2 Severe ☐3 Extreme ☐4

11D. Sitting or lying

None ☐0 Mild ☐1 Moderate ☐2 Severe ☐3 Extreme ☐4

11E. Standing upright

None ☐0 Mild ☐1 Moderate ☐2 Severe ☐3 Extreme ☐4

12. The following questions concern the amount of stiffness (not pain) you have experienced in the **last 48 hours** in your **hips**.

12A. How **severe** is your hip stiffness **after** first **wakening** in the morning?

None ☐0 Mild ☐1 Moderate ☐2 Severe ☐3 Extreme ☐4

12B. How **severe** is your hip stiffness after sitting, lying or resting **later in the day**?

None ☐0 Mild ☐1 Moderate ☐2 Severe ☐3 Extreme ☐4

13. The following questions concern your physical function. For each of the following activities, please indicate the degree of difficulty you have experienced in the **last 48 hours** due to your **hips**.

Question: What degree of difficulty do you have with:

13A. Ascending stairs

None ☐0 Mild ☐1 Moderate ☐2 Severe ☐3 Extreme ☐4

13B. Rising from sitting

None ☐0 Mild ☐1 Moderate ☐2 Severe ☐3 Extreme ☐4

13C. Walking on flat

None ☐0 Mild ☐1 Moderate ☐2 Severe ☐3 Extreme ☐4

13D. Getting in/ out of car

None ☐0 Mild ☐1 Moderate ☐2 Severe ☐3 Extreme ☐4

13E. Putting on socks/ stockings

None ☐0 Mild ☐1 Moderate ☐2 Severe ☐3 Extreme ☐4

13F. Rising from bed

None ☐0 Mild ☐1 Moderate ☐2 Severe ☐3 Extreme ☐4

13G. Sitting

None ☐0 Mild ☐1 Moderate ☐2 Severe ☐3 Extreme ☐4

14. In the **past week**, how much has **hip pain** affected your sleep?

Not at all ☐0 Mildly ☐1 Moderately ☐2 Severely ☐3 Extremely ☐4

Section 3: Your Bones

15A. Has a doctor told you that you have broken, fractured or chipped any bones as an adult **(since the age of 18)**?

Yes ☐1 No ☐0 Don't know ☐99

***If No** or **Don't know**, please go to question 16A (page 9)*

Question 15 continues on page 9

15B. If Yes, please provide details (please include all fractures, including those you have already told us about):

Bone (*e.g. finger, rib*)	Age when fracture/ break occurred	Cause (*e.g. fall from standing height/ off ladder*)	Office use
_____	⌊__⌋	_____	☐☐
_____	⌊__⌋	_____	☐☐
_____	⌊__⌋	_____	☐☐
_____	⌊__⌋	_____	☐☐
_____	⌊__⌋	_____	☐☐

16A. Have either of your parents or any of your brothers or sisters fractured/ broken a bone as an adult?

Yes ☐1 No ☐0 Don't know ☐99

***If No** or **Don't know**, please go to question 17A (page 10)*

16B. If Yes, please provide details:

Relative	Bone (*e.g. finger, rib*)	Age	Cause (*e.g. fall from standing height/ off ladder*)	Office use
_____	_____	⌊__⌋	_____	☐☐☐
_____	_____	⌊__⌋	_____	☐☐☐
_____	_____	⌊__⌋	_____	☐☐☐
_____	_____	⌊__⌋	_____	☐☐☐
_____	_____	⌊__⌋	_____	☐☐☐
_____	_____	⌊__⌋	_____	☐☐☐

Medications for your bones

17A. Have you ever taken calcium/ vitamin D supplements?

Yes, currently taking ☐1 Yes, taken in the past ☐2 No ☐0 Don't know ☐99

17B. If Yes, how long did you take/ have you been taking them for?

|_|_| years |_|_| months Don't know ☐99

18A. Have you ever been told by a doctor that you have **osteoporosis (brittle bones)**?

Yes ☐1 Year Diagnosed |_|_|_|_| No ☐0 Don't know ☐99

***If No**, please go to Section 4: Your Health (page 11)*

18B. Have you ever taken a Bisphosphonate tablet for osteoporosis? *(e.g. Risedronate/ Actonel, Alendronate/ Alendronic acid/ Fosamax, Ibandronate/ Boniva)*

Yes, currently taking ☐1 Yes, taken in the past ☐2 No ☐0 Don't know ☐99

18C. If Yes, how long did you take/ have you been taking one for?

|_|_| years |_|_| months Don't know ☐99

18D. Have you ever had an intravenous Zoledronate/ Zolendronic acid (Aclasta) infusion/ injection?

Yes ☐1 No ☐0 Don't know ☐99

18E. If Yes, how long did you receive/ have you been receiving these infusions/ injections for?

|_|_| years |_|_| months Don't know ☐99

18F. Have you ever had a Denosumab (Prolia) injection?

Yes ☐1 No ☐0 Don't know ☐99

18G. If Yes, how long did you receive/ have you been receiving these injections for?

|_|_| years |_|_| months Don't know ☐99

Section 4: Your Health

19A. How would you describe your **current health**?

Very Good ☐ 1 Good ☐ 2 Fair ☐ 3 Poor ☐ 4 Very Poor ☐ 5

19B. Do you **have** or **have you ever had** any of the following diseases?

	0 No	1 Yes	If Yes, please specify which disease or type:
1. Diabetes	☐	☐	
2. Cancer	☐	☐	
3. Stroke/ Transient Ischaemic Attack (TIA)	☐	☐	
4. Depression/ Anxiety	☐	☐	
5. Spinal stenosis	☐	☐	
6. Carpal tunnel syndrome	☐	☐	
7. Acromegaly	☐	☐	
8. Fibromyalgia	☐	☐	
9. Gout	☐	☐	

20A. Have you ever been on steroids (Prednisolone) for longer than three months?

Yes, currently taking ☐ 1 Yes, taken in the past ☐ 2 No ☐ 0 Don't know ☐ 99

***If No** or **Don't know**, **Male** participants please go to question 21A (page 12) and **Female** participants please go to question 22A (page 12)*

20B. If Yes, how long did you take/ have you been taking steroids?

|__|__| years |__|__| months Don't know ☐ 99

20C. Why did you take steroids?

Female participants please go to question 22A (page 12)

21A. Male participants only: Have you ever received hormone treatment/ injections for prostate cancer? (*e.g. Goserelin/ Zoladex, Buserelin/Suprefact, Histrelin/ Vantas, Leuprorelin/ Prostap, Triptorelin/ Decapeptyl*)

Yes, currently receiving ☐1 Yes, received in the past ☐2 No ☐0 Don't know ☐99

21B. If Yes, how long did you receive/ have you been receiving it for?

|_|_| years |_|_| months Don't know ☐99

22A. Are you currently taking any other medicines (including prescribed and over-the-counter medicines)?

Yes ☐1 No ☐0 ***If No,*** *please go to question 23 (page 13)*

22B. Do you regularly take medication for pain (at least twice a week)?

Yes ☐1 No ☐0

22C. Please list **all** medications below, including any pain medications (*if you need more space, please write on page 18*):

Name of medication (*please copy name in full from container*)	**Dosage (*e.g. 50mg*)**	**Number of tablets taken in ONE WEEK**	**Reason for taking**
		|_|_|	
		|_|_|	
		|_|_|	
		|_|_|	
		|_|_|	
		|_|_|	
		|_|_|	
		|_|_|	
		|_|_|	
		|_|_|	

23. Under each heading, please cross the ONE box that best describes you health TODAY.

23A. Mobility

- I have no problems in walking about ☐ 1
- I have slight problems in walking about ☐ 2
- I have moderate problems in walking about ☐ 3
- I have severe problems in walking about ☐ 4
- I am unable to walk about ☐ 5

23B. Self-care

- I have no problems washing or dressing myself ☐ 1
- I have slight problems washing or dressing myself ☐ 2
- I have moderate problems washing or dressing myself ☐ 3
- I have severe problems washing or dressing myself ☐ 4
- I am unable to wash or dress myself ☐ 5

23C. Usual activities *(e.g. work, study, housework, family or leisure activities)*

- I have no problems doing my usual activities ☐ 1
- I have slight problems doing my usual activities ☐ 2
- I have moderate problems doing my usual activities ☐ 3
- I have severe problems doing my usual activities ☐ 4
- I am unable to do my usual activities ☐ 5

23D. Pain/ discomfort

- I have no pain or discomfort ☐ 1
- I have slight pain or discomfort ☐ 2
- I have moderate pain or discomfort ☐ 3
- I have severe pain or discomfort ☐ 4
- I have extreme pain or discomfort ☐ 5

23E. Anxiety/ depression

- I am not anxious or depressed ☐ 1
- I am slightly anxious or depressed ☐ 2
- I am moderately anxious or depressed ☐ 3
- I am severely anxious or depressed ☐ 4
- I am extremely anxious or depressed ☐ 5

23F. We would like to know how good or bad your health is TODAY.
This scale is numbered from 0 to 100.
100 means the best health you can imagine.
0 means the worst health you can imagine.
Mark an X on the scale to indicate how your health is TODAY.

Now, please write the number you marked on the scale in the box below.

Your health today = ☐

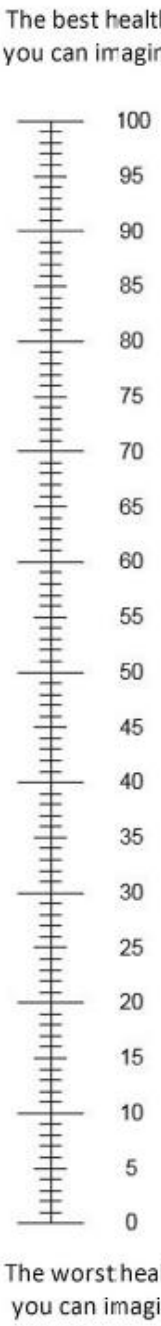

Section 5: Your Physical Activity

24. Do you regularly use a mobility aid?

No ☐ 0 | Yes, walking stick ☐ 1 | Yes, zimmer frame/ trolley ☐ 2 | Yes, mobility scooter ☐ 3 | Yes, wheelchair ☐ 4

25. For approximately how long can you walk on your own, before you need to stop and rest?

Less than 1 minute ☐ 5 | 1 to 5 minutes ☐ 4 | 5 to 10 minutes ☐ 3 | 10 to 20 minutes ☐ 2 | More than 20 minutes ☐ 1

26. Think about all the **vigorous** activities that you did in the **last 7 days**. **Vigorous** physical activities are activities that take hard physical effort and make you breathe much harder than normal. Think *only* about those physical activities that you did for at least 10 minutes at a time.

26A. During the **last 7 days**, on how many days did you do **vigorous** physical activities like heavy lifting, digging, aerobics or fast bicycling?

___ days per week

No vigorous physical activities *(skip to question 27, below)* ☐

26B. How much time did you usually spend doing **vigorous** physical activities on one of those days?

___ ___ hours per day ___ ___ minutes per day Don't know/ not sure ☐ 99

27. Think about all the **moderate** activities that you did in the **last 7 days**. **Moderate** physical activities are activities that take moderate physical effort and make you breathe somewhat harder than normal. Think *only* about those physical activities that you did for at least 10 minutes at a time.

27A. During the **last 7 days**, on how many days did you do **moderate** physical activities like carrying light loads, bicycling at a regular pace, or doubles tennis?

___ days per week

No moderate physical activities *(skip to question 28, page 16)* ☐

27B. How much time did you usually spend doing **moderate** physical activities on one of those days?

___ ___ hours per day ___ ___ minutes per day Don't know/ not sure ☐ 99

28. Think about the time you spent **walking** in the **last 7 days**. This includes at work and at home, walking to travel from place to place, and any other walking that you might do just for recreation, sport, exercise or leisure.

28A. During the **last 7 days**, on how many days did you **walk** for at least 10 minutes at a time?

___ days per week

No walking *(skip to Section 6, below)* ☐

28B. How much time did you usually spend **walking** on one of those days?

___ hours per day ___ minutes per day Don't know/ not sure ☐99

Section 6: Your Lifestyle

29A. Are you a current smoker?

Yes ☐1 No ☐0 ***If No**, please go to question 30A (below)*

29B. If Yes, how much do you smoke in a **normal day**? *(If you smoke roll-ups, cigars or pipes, please give the equivalent number of cigarettes)*

1-5 ☐1 6-10 ☐2 11-20 ☐3 More than 20 ☐4

29C. How old were you when you started smoking?

___ years Can't remember ☐99

30A. Have you **ever** smoked cigarettes regularly (at least one cigarette a day for 12 months or more)?

Yes ☐1 No ☐0

30B. If Yes, how long ago did you give up smoking?

___ years ___ months Can't remember ☐99

31A. Would you describe your present alcohol intake as:

Daily/ most days ☐4 Weekends only ☐3 Once or twice a month ☐2 Special occasions ☐1 Never ☐0

31B. How much alcohol do you drink during an **average week**? *(**one** drink is: **half** a pint of beer, a **single** whickey/ gin etc. or **one** glass of wine sherry)*

___ drinks Don't know ☐99

8 876419 181126

Section 7: Female participants only

32. How old were you when you first started having periods?

|__|__| years Can't remember ☐99

33A. Have you passed the menopause?

Yes ☐1 Current ☐2 No ☐0 Don't know ☐99

33B. If Yes, how old were you when your periods stopped (approximately)?

|__|__| years Can't remember ☐99

34A. Have you had a hysterectomy?

Yes ☐1 No ☐0

34B. If Yes, how old were you?

|__|__| years Can't remember ☐99

35. Have you had any ovaries removed?

Yes, one ☐1 Yes, both ☐2 No ☐0 Don't know ☐99

36. Have you ever used Hormone Replacement Therapy (HRT)?

Yes, patches ☐1 Yes, tablets ☐2 Yes, implant ☐3 No ☐0 Don't know ☐99

37A. Have you ever taken an Aromatase inhibitor for breast cancer? *(e.g. Anastrozole/ Arimidex, Letrozole/Femara, Exemestane/ Aromasin)*

Yes, currently taking ☐1 Yes, taken in the past ☐2 No ☐0 Don't know ☐99

37B. If Yes, how long did you take/ have you been taking it for?

|__|__| years |__|__| months Can't remember ☐99

Thank you for completing this questionnaire

Please use this space to write anything else you feel is relevant

Please post this questionnaire, with your signed consent form, in the freepost envelope provided

If you have any questions, please contact Jon Tobias via April Hartley:

Email: high-bone-mass@bristol.ac.uk

Telephone: 0117 414 7861

Appendix 8: Inter- and intra-rater reliability statistics for the standardization set of knee radiographs.

	Inter-rater				**Intra-rater**			
	ICC	**95% CI**			**ICC**	**95% CI**		
Medial minimal JSW	0.787	0.689, 0.885			0.955	0.933, 0.977		
Maximum tibial plateau width	0.986	0.979, 0.993			0.994	0.991, 0.997		
	Unweighted		**Weighted**		**Unweighted**		**Weighted**	
	kappa	**95% CI**	**kappa**	**95% CI**	**Kappa**	**95% CI**	**kappa**	**95% CI**
KL grade	0.607	0.479, 0.739	0.861	0.787, 0.890	0.803	0.734, 0.909	0.952	0.946, 0.959
Medial femoral osteophyte	0.521	0.406, 0.560	0.614	0.573, 0.697	0.745	0.670, 0.867	0.865	0.822, 0.878
Lateral femoral osteophyte	0.772	0.666, 0.957	0.951	0.920, 0.961	0.683	0.652, 0.765	0.919	0.881, 0.945
Medial tibial osteophyte	0.628	0.459, 0.777	0.839	0.798, 0.853	0.669	0.579, 0.711	0.853	0.806, 0.884
Lateral tibial osteophyte	0.533	0.453, 0.636	0.792	0.688, 0.870	0.822	0.755, 0.849	0.899	0.839, 0.972
Medial JSN	0.636	0.459, 0.689	0.86	0.626, 0.928	0.652	0.630, 0.786	0.867	0.782, 0.892
Lateral JSN	0.517	0.265, 0.550	0.684	0.366, 0.848	0.747	0.474, 0.926	0.826	0.698, 0.910
Medial subchondral sclerosis	0.483	-0.131, 1			0.792	0.396, 1.000		
Lateral subchondral sclerosis	1	1,1			0.659	0.036, 1.000		
Chondrocalcinosis	0.459	0.114, 0.805			0.869	0.692, 1.000		

Appendix 9: Intra-rater reliability statistics for knee variables after first grading attempt.

	N	Unweighted		Weighted	
		Kappa	**95% CI**	**Kappa**	**95% CI**
KL	69	0.544	0.409, 0.694	0.828	0.736, 0.898
medial femoral osteophyte	69	0.838	0.638, 0.963	0.947	0.861, 0.989
medial tibial osteophyte	69	0.82	0.691, 0.937	0.917	0.847, 0.973
lateral femoral osteophyte	69	0.645	0.359, 0.858	0.877	0.628, 0.967
lateral tibial osteophyte	69	0.71	0.498, 0.884	0.845	0.689, 0.943
medial JSN	69	0.418	0.149, 0.661	0.704	0.377, 0.886
lateral JSN	69	0.242	0, 0.496	0.796	0,0.895
medial sclerosis	69	0.489	-0.111, 1		
lateral sclerosis	69	0.660	0.038, 1		
Chondrocalcinosis	69	0.850	0.561, 1		
Any OA (>=2)	69	0.820	0.684, 0.957		
Severe OA (>=3)	69	0.573	0.337, 0.808		
Any osteophyte (>=1)	69	0.820	0.684, 0.957		
Moderate osteophyte (>=2)	69	0.832	0.647, 1		
Any JSN (>=1)	69	0.422	0.184, 0.659		
Moderate JSN (>=2)	69	1	1,1		
Any sclerosis	69	0.653	0.209, 1		
		ICC	**95% CI**		
minimal JSW	139	0.995	0.993, 0.998		
max tibial plateau width	139	1	1.000, 1.000		

Appendix 10: Intra-rater reliability statistics between second and third gradings of the 10% sample.

	N	Unweighted		weighted	
		Kappa	95% CI	Kappa	95% CI
KL	69	0.762	0.643, 0.879	0.923	0.875, 0.963
medial femoral osteophyte	69	0.811	0.610, 0.955	0.942	0.868, 0.988
medial tibial osteophyte	69	0.822	0.664, 0.935	0.912	0.806, 0.970
lateral femoral osteophyte	69	0.817	0.578, 1	0.962	0.854, 1
lateral tibial osteophyte	69	0.909	0.729, 1	0.945	0.810, 1
medial JSN	69	0.752	0.474, 0.941	0.887	0.643, 0.978
lateral JSN	69	0.327	0, 0.496	0.855	0.795, 0.900
medial sclerosis	69	0.660	0.038, 1		
lateral sclerosis	69	1	1, 1		
Chondrocalcinosis	69	1	1, 1		
Any OA (>=2)	69	0.877	0.759, 0.994		
Severe OA (>=3)	69	0.818	0.619, 1		
Any osteophyte (>=1)	69	0.877	0.759, 0.994		
Moderate osteophyte (>=2)	69	0.939	0.821, 1.000		
Any JSN (>=1)	69	0.758	0.560, 0.956		
Moderate JSN (>=2)	69	1	1, 1		
Any sclerosis	69	0.793	0.398, 1		

Appendix 11: Analyses of agreement of baseline measurements of minimal joint space width and maximal tibial plateau width between myself and Dr Hardcastle.

Appendix 9a: Scatterplot of Dr Hardcastle's original mJSW measurements and my measurements for the same radiographs.

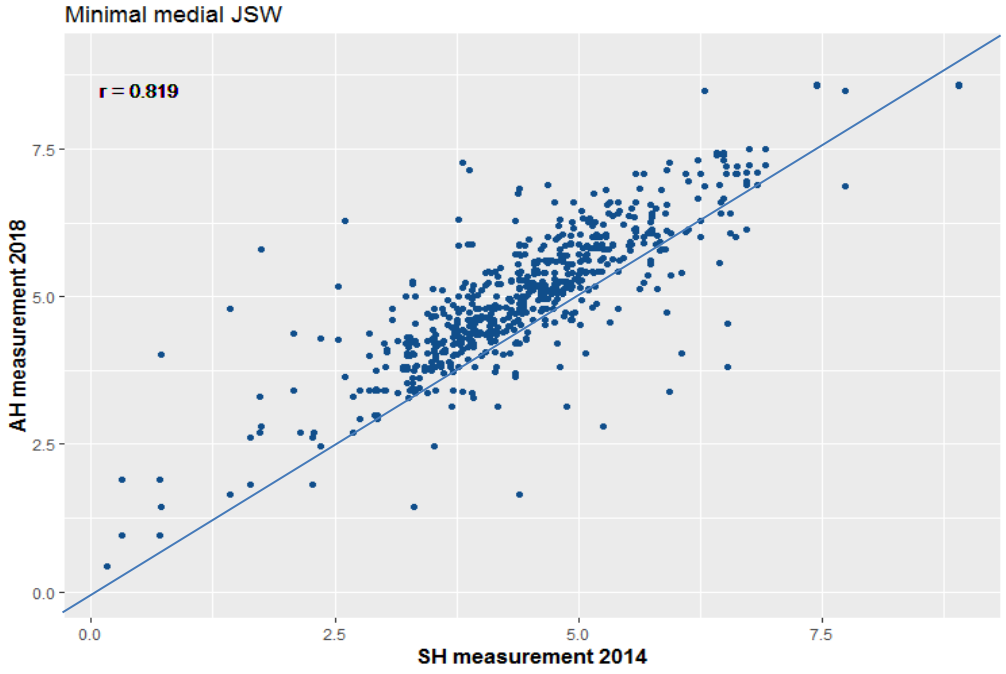

Appendix 9b: Scatterplot of Dr Hardcastle's original maximal tibial plateau width measurements and my measurements for the same radiographs.

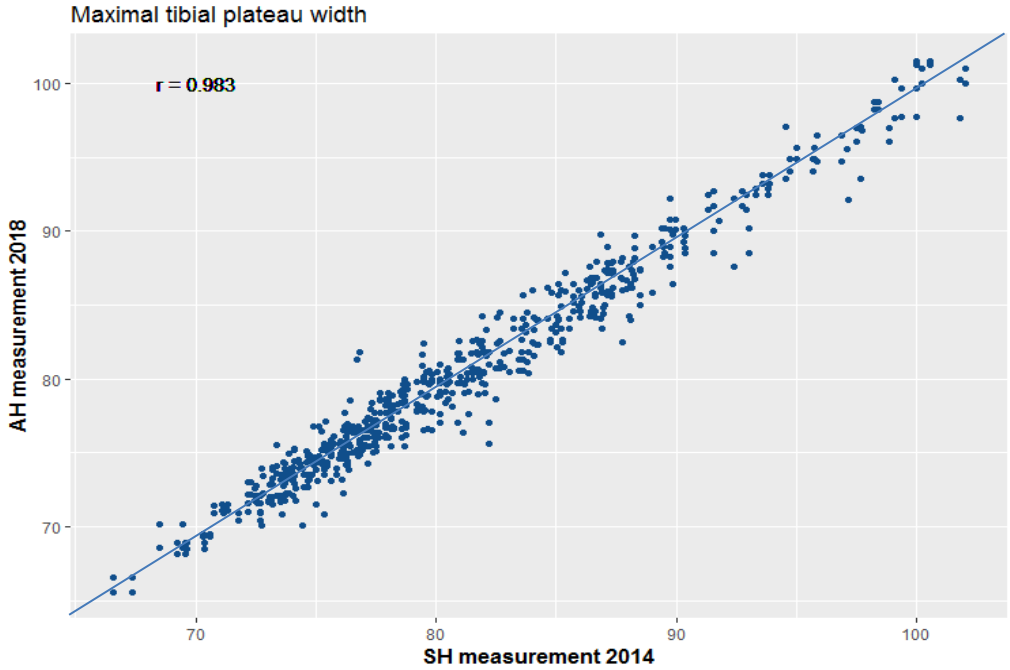

Appendix 9c: Bland Altman plot displaying agreement between myself and Dr Hardcastle for measurements of mJSW.

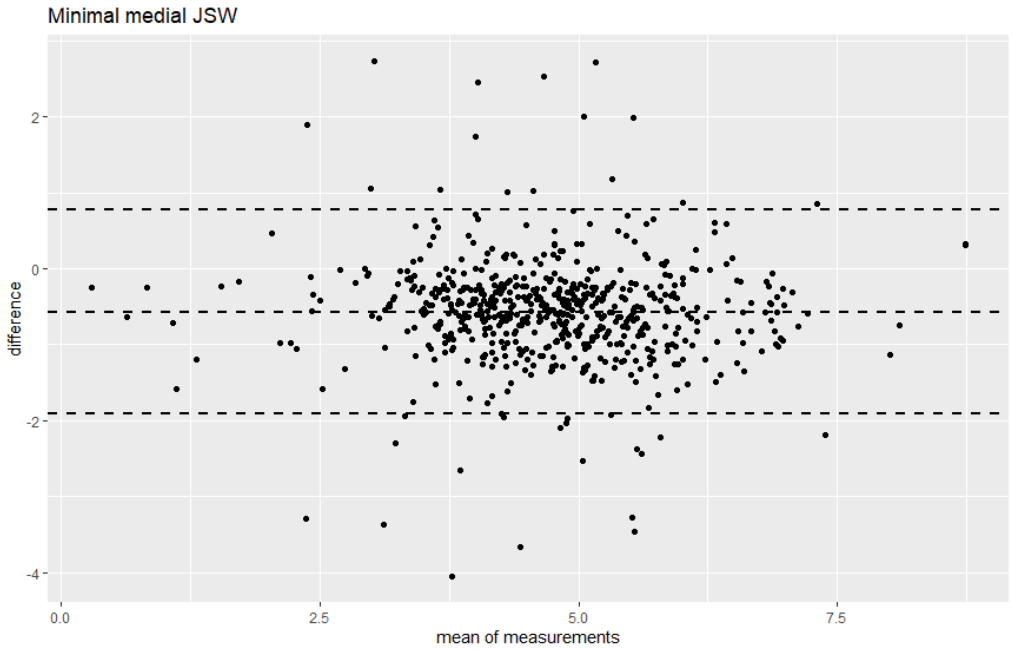

Appendix 9d: Bland Altman plot displaying agreement between myself and Dr Hardcastle for measurements of maximal tibial plateau width.

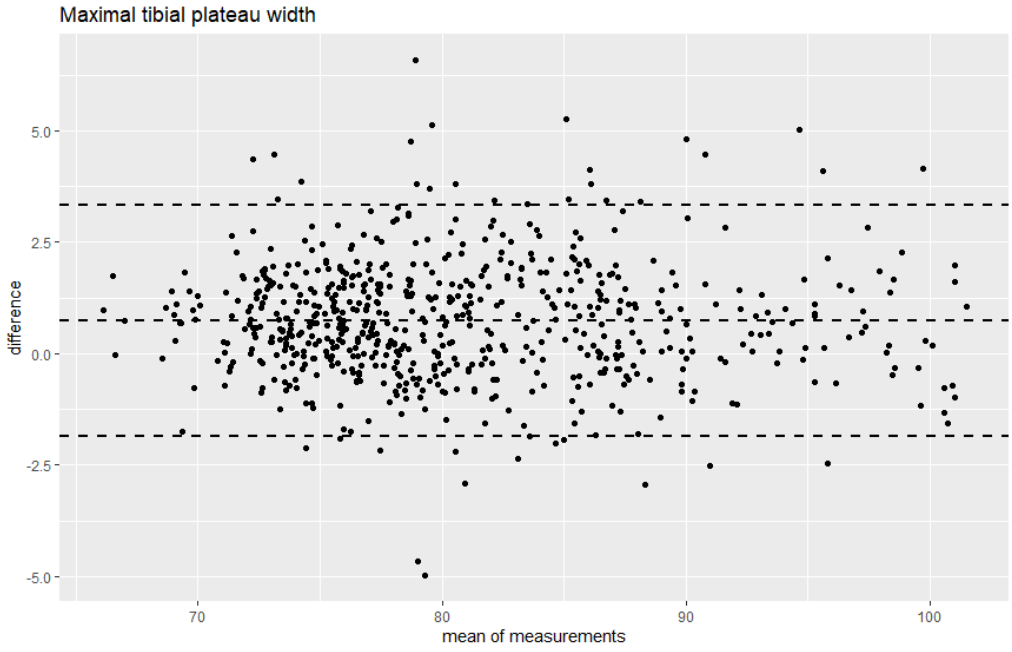

Appendix 9e: Correlation between maximum tibial plateau width assessed at baseline and follow-up.

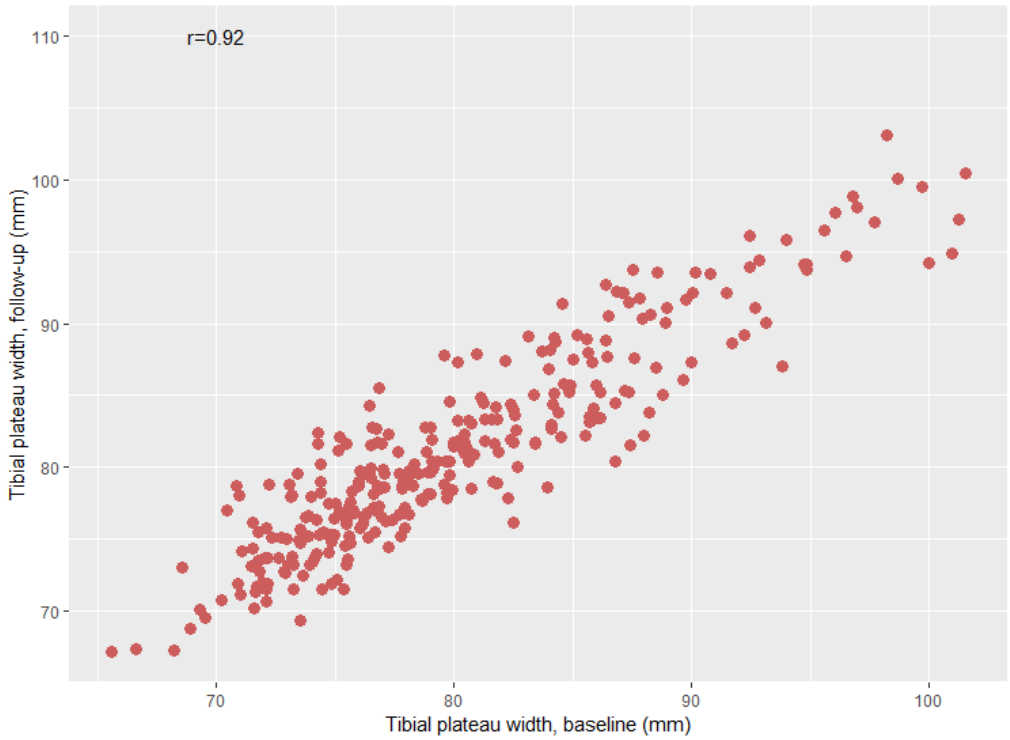

Appendix 12: Standard operating procedure for measuring hip minimal joint space width.

Version 1 20th June 2019
April Hartley

SOP for measuring hip superior minimal joint space width with BoneFinder

1. Launch BoneFinder from \\ads.bris.ac.uk\filestore\BRMS\Research\MRU\Rheum\HBM_Study\HBM2\Anonymous Xrays\hip_mjsw\BoneFinder_Markup-Tool_WINv1.0.2\64bit

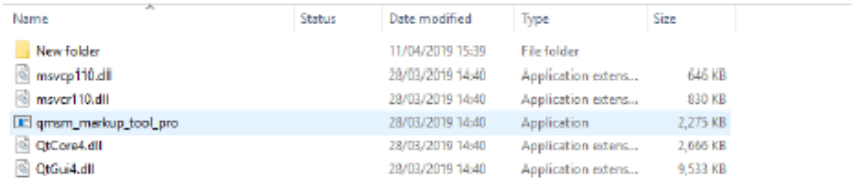

2. Use File→Open Image to open a pelvic radiograph: you will need to navigate to the DICOM image location (\\ads.bris.ac.uk\filestore\BRMS\Research\MRU\Rheum\HBM_Study\HBM2\Anonymous Xrays\pooled baseline and followup xrays, anonymised\hips)
3. To adjust brightness, select this icon:

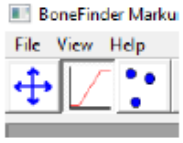

Right click and drag the mouse up/down as required

4. To zoom in on the left or right hip, move the wheel on the mouse downwards
5. Select the points button:

And place a point at the superior lateral curvature of the femoral head:

1

6. Select the curve button:

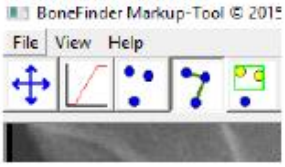

Place 15 additional points around the femoral head at evenly spaced intervals, ending with the superior medial curvature of the femoral head:

Tip: it is best to place all points first and then move them to be evenly spaced using the hand tool to click on the points and drag them:

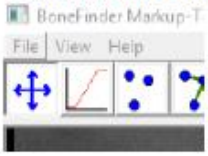

7. Use the point tool to place a point on the lateral edge of the sourcil (acetabular eyebrow). Mark on the lowest point of the sclerotic line where the acetabular roof meets (in order of importance) 1. The posterior wall, 2. The anterior wall, OR 3. The most lateral part of the brightest sclerotic line:

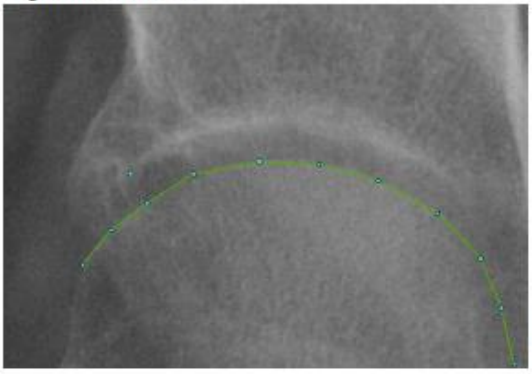

8. Add seven additional evenly space points along the lowest point of the sclerotic line ending at the medial edge of the sourcil where there is a break in the line AND/OR where the sourcil distinctly changes thickness/angle:

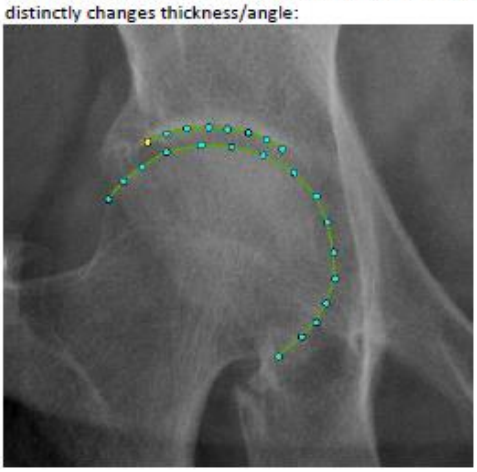

9. Save the points file using File→Save points as. Save in \\ads.bris.ac.uk\filestore\BRMS\Research\MRU\Rheum\HBM_Study\HBM2\Anonymous Xrays\hip_mjsw\bonefinder_points_curves as the three letter code followed by the side: e.g. AAA_right or AAA_left

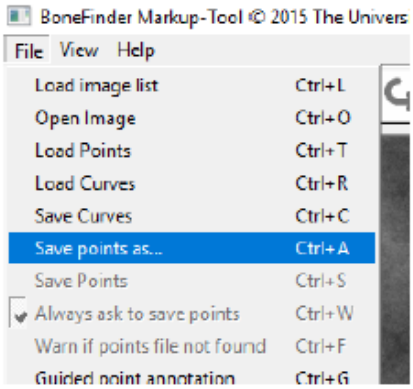

Save the curves in the same place using the same labelling system:

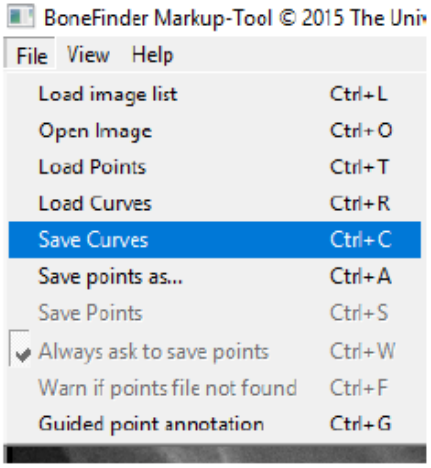

10. Select 'Clear' and move to the opposite side. Repeat steps 5 to 9.

Appendix 13: Correlation between the HipMorf baseline mJSW measurements and the BoneFinder baseline mJSW measurements.

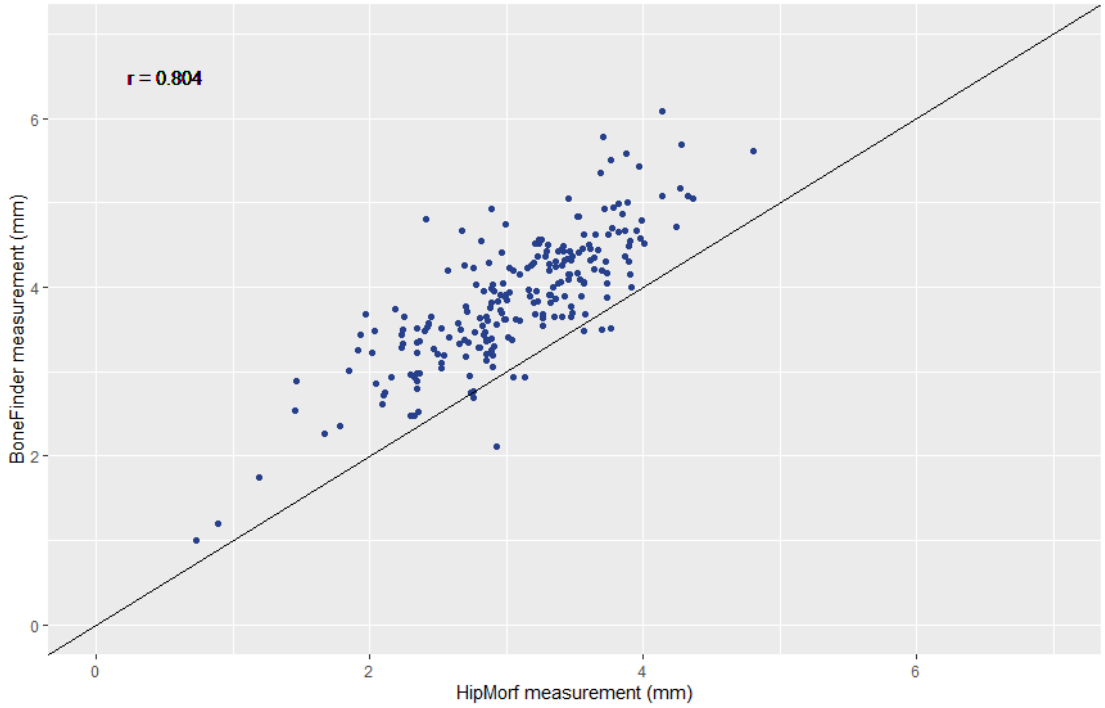

Appendix 14: Bland-Altman plot presenting agreement between the BoneFinder and HipMorf methods for measuring mJSW.

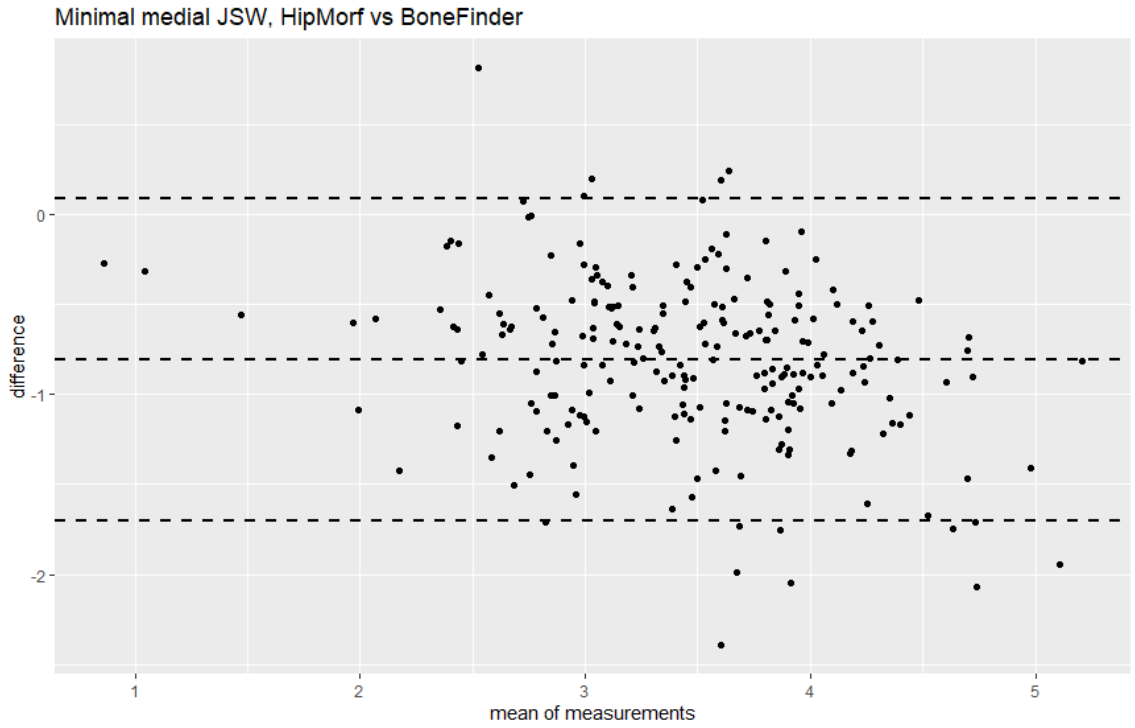

Appendix 15: Inter- and intra-rater reliability statistics for the standardization set of hip radiographs.

	Inter-rater				**Intra-rater**			
	Unweighted		**Weighted**		**Unweighted**		**weighted**	
	kappa	**95% CI**	**Kappa**	**95% CI**	**kappa**	**95% CI**	**kappa**	**95% CI**
Croft score	0.477	0.288, 0.622	0.799	0.671, 0.865	0.698	0.541, 0.811	0.863	0.751, 0.938
Superior femoral osteophyte	0.584	0.333, 0.735	0.844	0.647, 0.917	0.81	0.623, 0.945	0.925	0.875, 1
Inferior femoral osteophyte	0.544	0.317, 0.745	0.838	0.717, 0.928	0.89	0.698, 1	0.956	0.847, 1
Superior acetabular osteophyte	0.369	0.227, 0.561	0.692	0.528, 0.833	0.81	0.661, 0.935	0.926	0.856, 0.983
Inferior acetabular osteophyte	0.48	0.177, 0.783			0.88	0.717, 1		
Superior JSN	0.813	0.643, 1	0.859	0.732, 0.972	0.782	0.538, 0.943	0.828	0.617, 0.968
Medial JSN	0.662	0.454, 0.826	0.835	0.662, 0.924	0.7	0.525, 0.937	0.831	0.695, 0.942
Acetabular subchondral sclerosis	-0.035	-0.093, 0.023			0.651	0.205, 1		
Femoral subchondral sclerosis	-0.028	-0.083, 0.027			0.304	-0.076, 0.683		
Subchondral cysts	-0.026	-0.079, 0.026			0			

Appendix 16: Histograms of the Nightingale health-assessed metabolic traits in the HBM population.

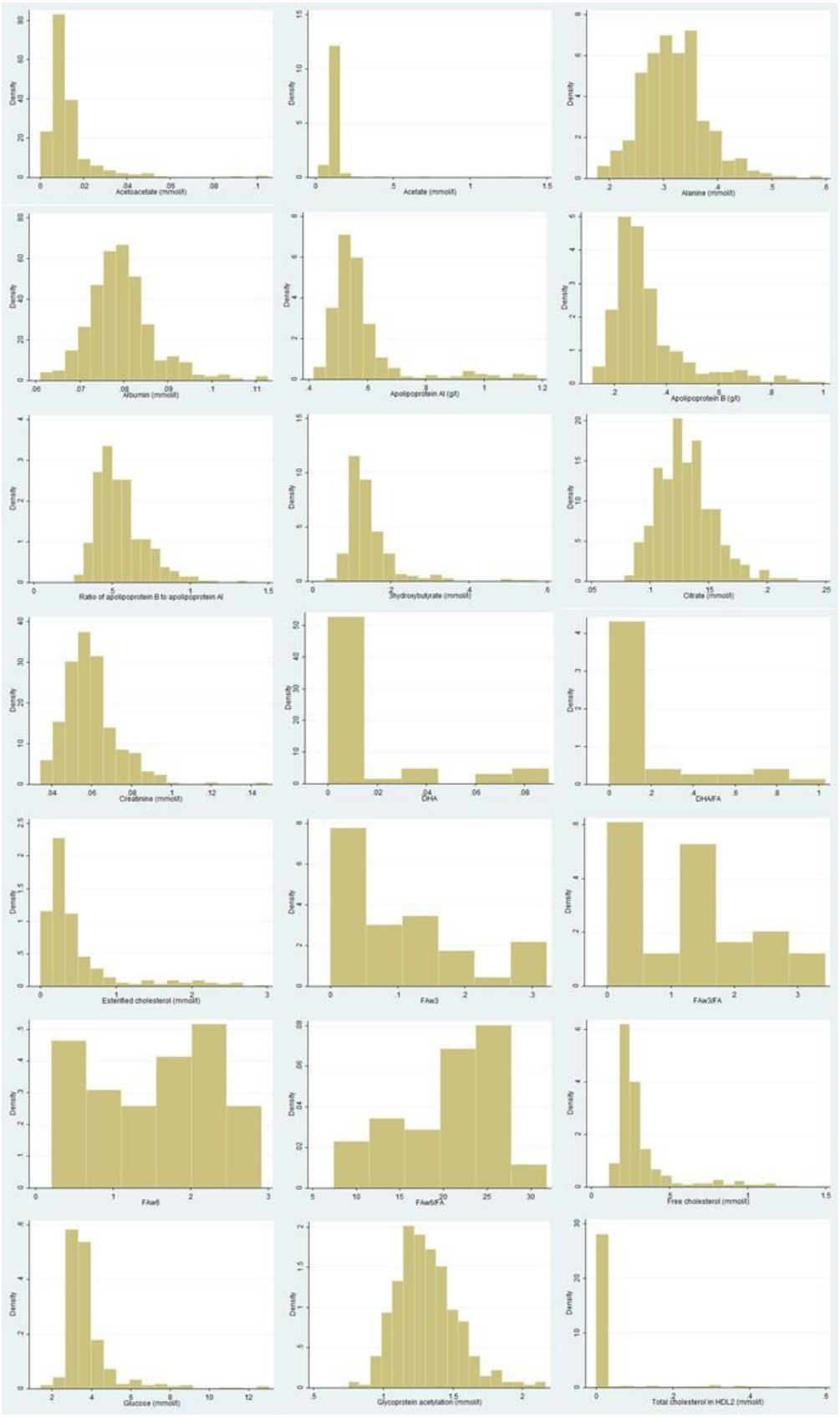

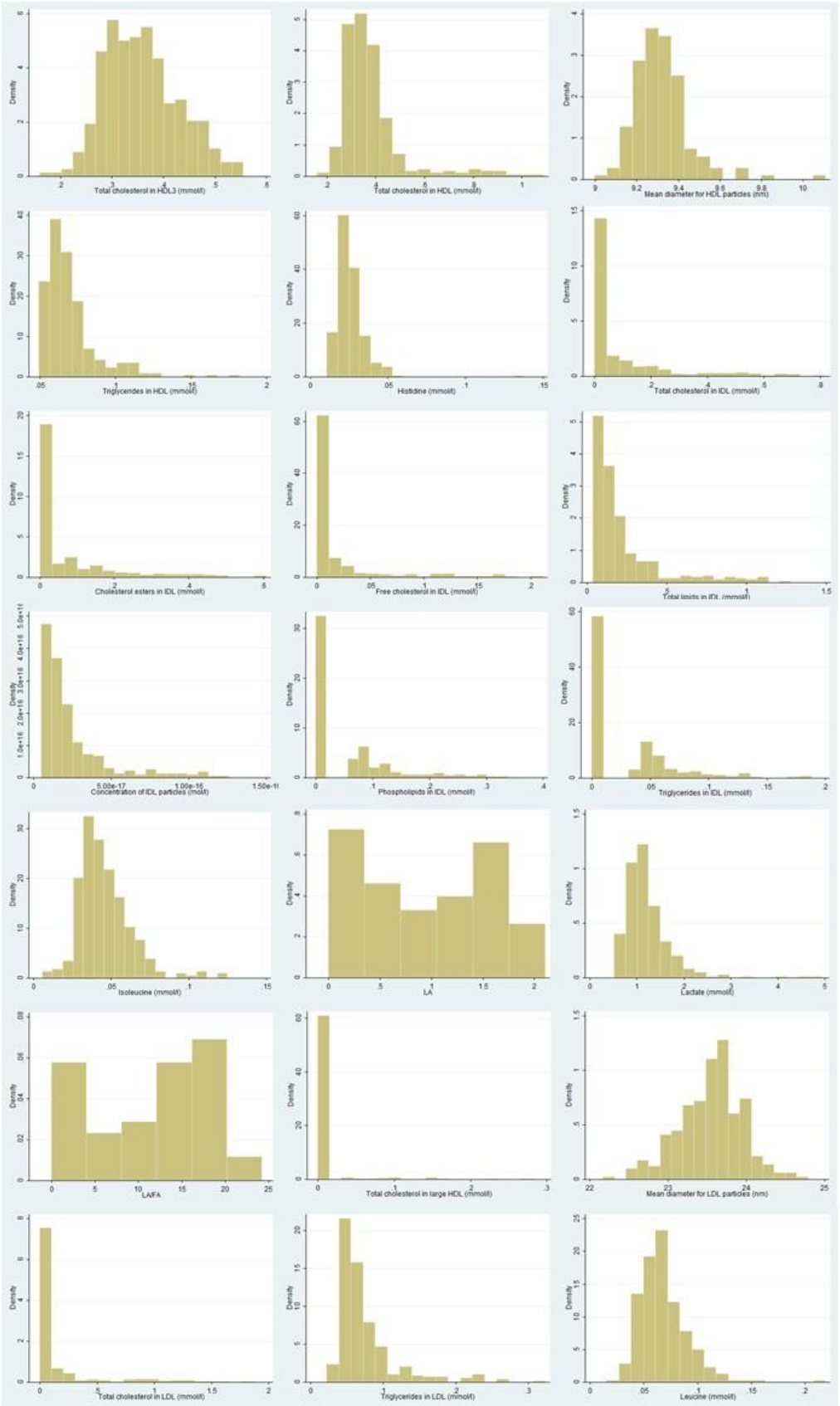
Density
Total cholesterol in HDL3 (mmol/l)
Total cholesterol in HDL (mmol/l)
Mean diameter for HDL particles (nm)
Triglycerides in HDL (mmol/l)
Histidine (mmol/l)
Total cholesterol in IDL (mmol/l)
Cholesterol esters in IDL (mmol/l)
Free cholesterol in IDL (mmol/l)
Concentration of IDL particles (mol/l)
Phospholipids in IDL (mmol/l)
Triglycerides in IDL (mmol/l)
Isoleucine (mmol/l)
LA
Lactate (mmol/l)
LA/FA
Total cholesterol in large HDL (mmol/l)
Mean diameter for LDL particles (nm)
Total cholesterol in LDL (mmol/l)
Triglycerides in LDL (mmol/l)
Leucine (mmol/l)


Density
Total cholesterol in large HDL (mmol/l)
Cholesterol esters in large HDL (mmol/l)
Free cholesterol in large HDL (mmol/l)
Total lipids in large HDL (mmol/l)
Concentration of large HDL particles (mol/l)
Phospholipids in large HDL (mmol/l)
Triglycerides in large HDL (mmol/l)
Total cholesterol in large LDL (mmol/l)
Cholesterol esters in large LDL (mmol/l)
Free cholesterol in large LDL (mmol/l)
Total lipids in large LDL (mmol/l)
Concentration of large LDL particles (mol/l)
Phospholipids in large LDL (mmol/l)
Triglycerides in large LDL (mmol/l)
Total cholesterol in large VLDL (mmol/l)
Cholesterol esters in large VLDL (mmol/l)
Free cholesterol in large VLDL (mmol/l)
Total lipids in large VLDL (mmol/l)
Concentration of large VLDL particles (mol/l)
Phospholipids in large VLDL (mmol/l)
Triglycerides in large VLDL (mmol/l)

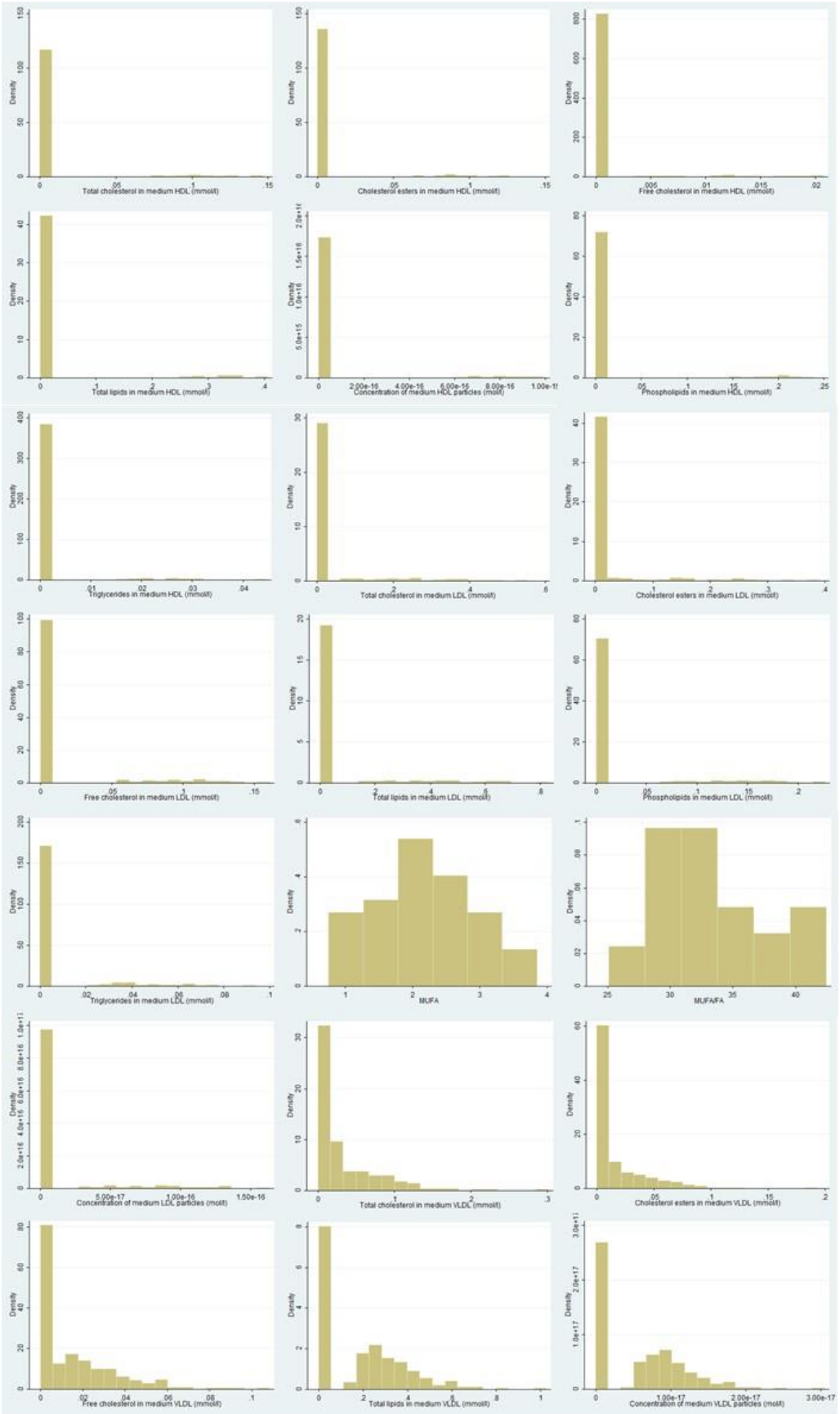
Density
Total cholesterol in medium HDL (mmol/l)
Cholesterol esters in medium HDL (mmol/l)
Free cholesterol in medium HDL (mmol/l)
Total lipids in medium HDL (mmol/l)
Concentration of medium HDL particles (mol/l)
Phospholipids in medium HDL (mmol/l)
Triglycerides in medium HDL (mmol/l)
Total cholesterol in medium LDL (mmol/l)
Cholesterol esters in medium LDL (mmol/l)
Free cholesterol in medium LDL (mmol/l)
Total lipids in medium LDL (mmol/l)
Phospholipids in medium LDL (mmol/l)
Triglycerides in medium LDL (mmol/l)
MUFA
MUFA/FA
Concentration of medium LDL particles (mol/l)
Total cholesterol in medium VLDL (mmol/l)
Cholesterol esters in medium VLDL (mmol/l)
Free cholesterol in medium VLDL (mmol/l)
Total lipids in medium VLDL (mmol/l)
Concentration of medium VLDL particles (mol/l)

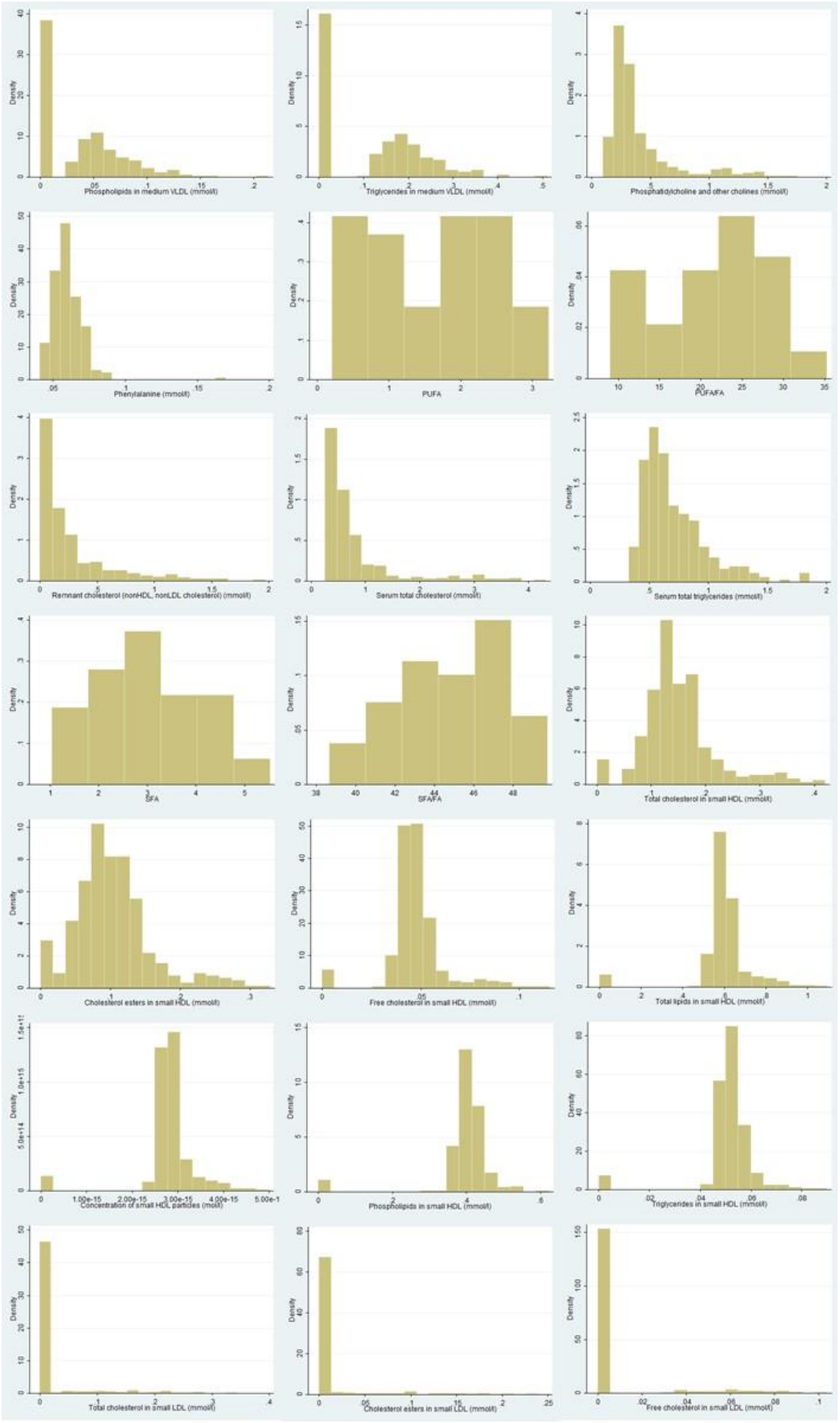
Density
Phospholipids in medium VLDL (mmol/l)
Triglycerides in medium VLDL (mmol/l)
Phosphatidylcholine and other cholines (mmol/l)
Phenylalanine (mmol/l)
PUFA
PUFA/FA
Remnant cholesterol (nonHDL, nonLDL cholesterol) (mmol/l)
Serum total cholesterol (mmol/l)
Serum total triglycerides (mmol/l)
SFA
SFA/FA
Total cholesterol in small HDL (mmol/l)
Cholesterol esters in small HDL (mmol/l)
Free cholesterol in small HDL (mmol/l)
Total lipids in small HDL (mmol/l)
Concentration of small HDL particles (mol/l)
Phospholipids in small HDL (mmol/l)
Triglycerides in small HDL (mmol/l)
Total cholesterol in small LDL (mmol/l)
Cholesterol esters in small LDL (mmol/l)
Free cholesterol in small LDL (mmol/l)


Density
Total lipids in small HDL (mmol/l)
Concentration of small HDL particles (mol/l)
Phospholipids in small HDL (mmol/l)
Triglycerides in small HDL (mmol/l)
Total cholesterol in small LDL (mmol/l)
Cholesterol esters in small LDL (mmol/l)
Free cholesterol in small LDL (mmol/l)
Total lipids in small LDL (mmol/l)
Concentration of small LDL particles (mol/l)
Phospholipids in small LDL (mmol/l)
Triglycerides in small LDL (mmol/l)
Sphingomyelins (mmol/l)
Total cholesterol in small VLDL (mmol/l)
Cholesterol esters in small VLDL (mmol/l)
Free cholesterol in small VLDL (mmol/l)
Total lipids in small VLDL (mmol/l)
Concentration of small VLDL particles (mol/l)
Phospholipids in small VLDL (mmol/l)
Triglycerides in small VLDL (mmol/l)
TG/PG
Total cholines (mmol/l)

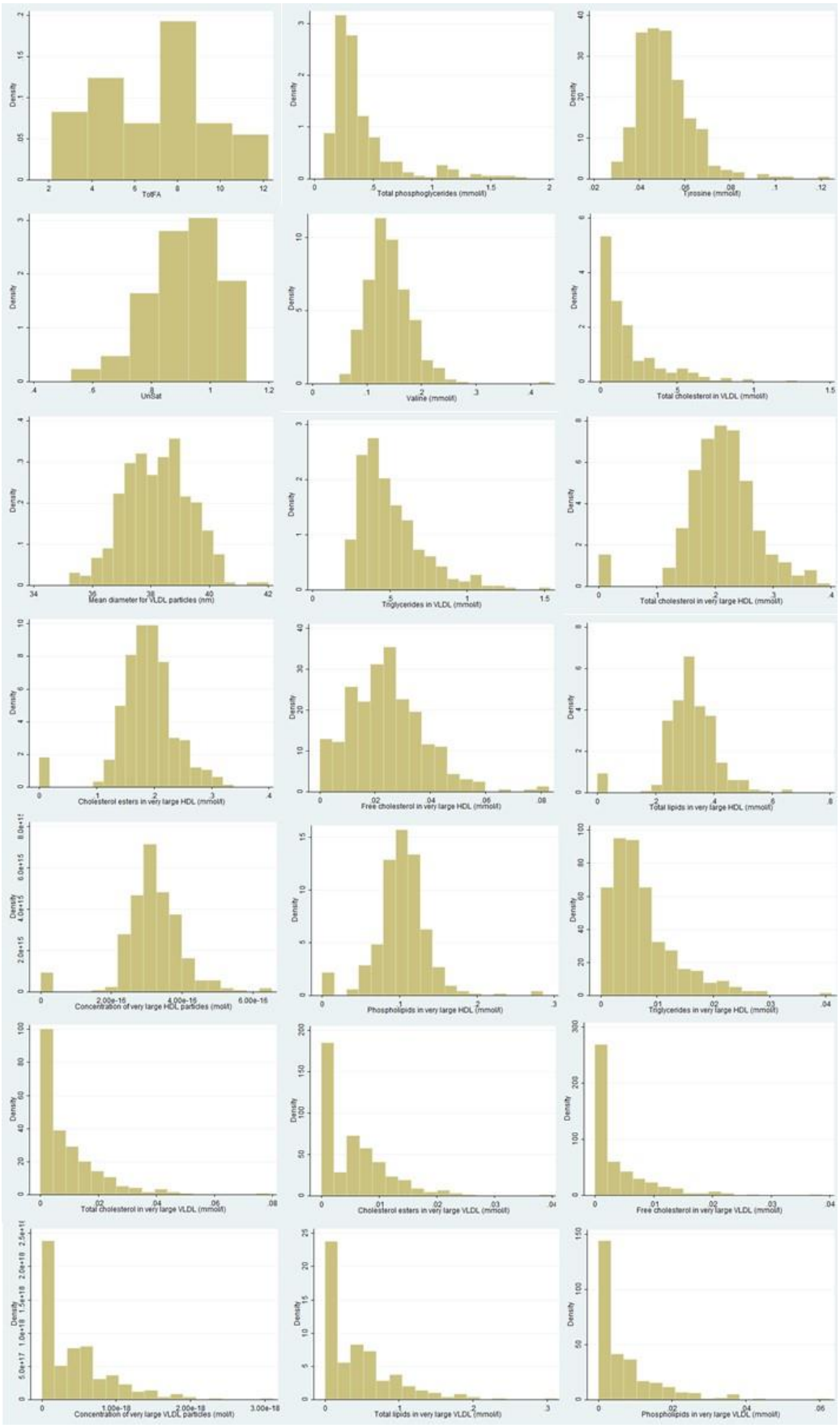
Density
TotFA
Total phosphoglycerides (mmol/l)
Tyrosine (mmol/l)
UnSat
Valine (mmol/l)
Total cholesterol in VLDL (mmol/l)
Mean diameter for VLDL particles (nm)
Triglycerides in VLDL (mmol/l)
Total cholesterol in very large HDL (mmol/l)
Cholesterol esters in very large HDL (mmol/l)
Free cholesterol in very large HDL (mmol/l)
Total lipids in very large HDL (mmol/l)
Concentration of very large HDL particles (mol/l)
Phospholipids in very large HDL (mmol/l)
Triglycerides in very large HDL (mmol/l)
Total cholesterol in very large VLDL (mmol/l)
Cholesterol esters in very large VLDL (mmol/l)
Free cholesterol in very large VLDL (mmol/l)
Concentration of very large VLDL particles (mol/l)
Total lipids in very large VLDL (mmol/l)
Phospholipids in very large VLDL (mmol/l)

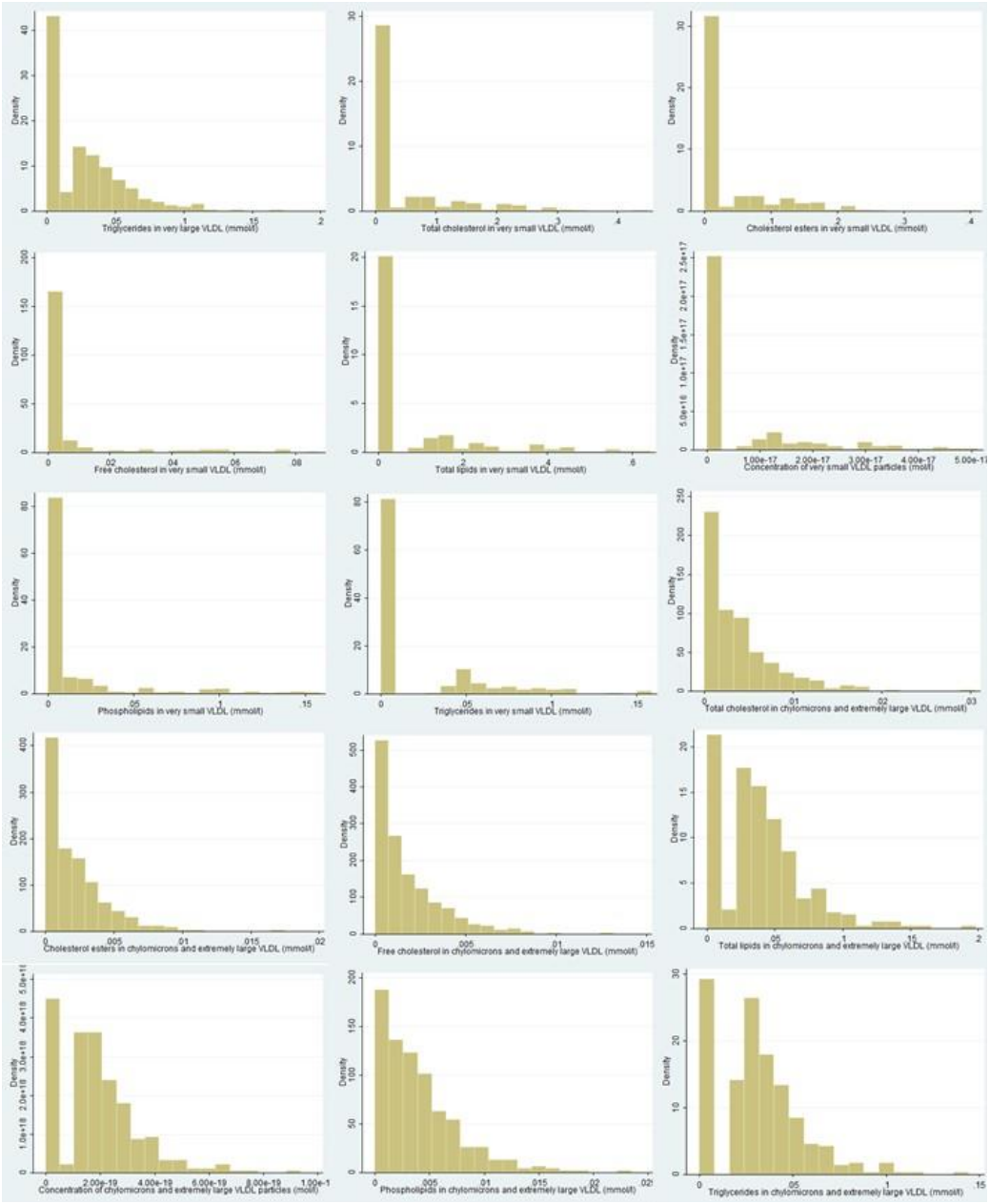
Density
Triglycerides in very large VLDL (mmol/l)
Total cholesterol in very small VLDL (mmol/l)
Cholesterol esters in very small VLDL (mmol/l)
Free cholesterol in very small VLDL (mmol/l)
Total lipids in very small VLDL (mmol/l)
Concentration of very small VLDL particles (mol/l)
Phospholipids in very small VLDL (mmol/l)
Triglycerides in very small VLDL (mmol/l)
Total cholesterol in chylomicrons and extremely large VLDL (mmol/l)
Cholesterol esters in chylomicrons and extremely large VLDL (mmol/l)
Free cholesterol in chylomicrons and extremely large VLDL (mmol/l)
Total lipids in chylomicrons and extremely large VLDL (mmol/l)
Concentration of chylomicrons and extremely large VLDL particles (mol/l)
Phospholipids in chylomicrons and extremely large VLDL (mmol/l)
Triglycerides in chylomicrons and extremely large VLDL (mmol/l)

Appendix 17: Final numbers with available measurements after excluding those samples that were not immediately frozen after collection and summary data for each of the metabolic traits.

	All samples immediately frozen						Removing 7SD outliers		
Metabolic traits	**N**	**Mean**	**SD**	**Median**	**LQ**	**UQ**	**N**	**Mean**	**SD**
Lipoprotein particle size									
Mean diameter for VLDL particles (nm)	326	38.35	1.05	38.32	37.57	39.06			
Mean diameter for LDL particles (nm)	326	23.53	0.42	23.55	23.26	23.82			
Mean diameter for HDL particles (nm)	326	9.30	0.10	9.30	9.23	9.36			
Cholesterol									
Serum total cholesterol (mmol/l)	326	0.61	0.37	0.50	0.40	0.72			
Total cholesterol in VLDL (mmol/l)	326	0.14	0.15	0.10	0.04	0.18			
Remnant cholesterol (nonHDL, nonLDL cholesterol) (mmol/l)	326	0.20	0.23	0.13	0.04	0.27			
Total cholesterol in LDL (mmol/l)	326	0.07	0.12	0.03	0.01	0.07			
Total cholesterol in HDL (mmol/l)	326	0.35	0.06	0.34	0.30	0.39			
Total cholesterol in HDL3 (mmol/l)	326	0.35	0.06	0.34	0.30	0.39			
Esterified cholesterol (mmol/l)	326	0.34	0.28	0.28	0.19	0.44			
Free cholesterol (mmol/l)	326	0.27	0.10	0.25	0.21	0.30			
Glycerides and Phospholipids									
Serum total triglycerides (mmol/l)	326	0.67	0.24	0.61	0.51	0.78			
Triglycerides in VLDL (mmol/l)	326	0.49	0.20	0.43	0.35	0.58			
Triglycerides in LDL (mmol/l)	326	0.07	0.03	0.06	0.05	0.07			
Triglycerides in HDL (mmol/l)	326	0.07	0.01	0.06	0.06	0.07			
Total phosphoglycerides (mmol/l)	326	0.34	0.17	0.29	0.23	0.40			
Phosphatidylcholine and other cholines (mmol/l)	326	0.33	0.16	0.29	0.23	0.37			
Sphingomyelins (mmol/l)	326	0.21	0.11	0.19	0.17	0.22	325	0.20	0.07
Total cholines (mmol/l)	326	0.69	0.40	0.62	0.53	0.74	325	0.67	0.25
Apolipoproteins									
Apolipoprotein AI (g/l)	326	0.55	0.05	0.54	0.51	0.58			
Apolipoprotein B (g/l)	326	0.30	0.10	0.28	0.23	0.34			
Ratio of apolipoprotein B to apolipoprotein AI	326	0.54	0.15	0.51	0.44	0.60			
Glycolysis-related metabolites									
Glucose (mmol/l)	319	3.77	1.36	3.42	3.10	3.91			
Lactate (mmol/l)	319	1.23	0.52	1.13	0.94	1.42	318	1.22	0.48
Citrate (mmol/l)	326	0.13	0.02	0.13	0.11	0.14			

Amino acids									
Alanine (mmol/l)	326	0.32	0.06	0.31	0.28	0.35			
Histidine (mmol/l)	326	0.02	0.01	0.02	0.02	0.03			
Branched-chain									
Isoleucine (mmol/l)	326	0.04	0.02	0.04	0.03	0.05			
Leucine (mmol/l)	326	0.07	0.02	0.06	0.05	0.08			
Valine (mmol/l)	326	0.14	0.04	0.14	0.11	0.16	325	0.14	0.04
Aromatic									
Phenylalanine (mmol/l)	308	0.06	0.01	0.06	0.05	0.07	307	0.06	0.01
Tyrosine (mmol/l)	326	0.05	0.01	0.05	0.04	0.06			
Ketone bodies									
Acetate (mmol/l)	322	0.12	0.08	0.11	0.10	0.13	320	0.12	0.03
Acetoacetate (mmol/l)	325	0.01	0.01	0.01	0.01	0.01	324	0.01	0.01
3hydroxybutyrate (mmol/l)	326	0.14	0.07	0.13	0.11	0.16			
Fluid balance									
Creatinine (mmol/l)	321	0.06	0.01	0.06	0.05	0.07			
Albumin (mmol/l)	326	0.08	0.01	0.08	0.07	0.08			
Inflammation									
Glycoprotein acetylation (mmol/l)	326	1.31	0.21	1.29	1.16	1.43			

Missing values in the removing 7SD outliers column represent no outliers.

Appendix 18: Comparing metabolomic associations in HBM to previously published work.

To check the reliability of the metabolomic data, I compared associations with BMI, stratified by gender, to previously published results from adolescents (342). I performed linear regression modelling, with standardized metabolic traits as the exposure and BMI as the outcome, adjusting for age at blood sample collection, stratifying by gender and with robust SEs (Figure). Overall results were consistent, in direction of effect and difference in magnitude between men and women, with the previously published results (provided in Figure 2 of Wurtz *et al* (342)). The sample size was much smaller for HBM (206 HBM women and 114 men *vs* 6,468 women and 6,196 men, meaning CIs were wider and some results were null. The only difference between the HBM results and those previously published was a stronger association between BMI and glycoprotein acetyls in HBM women compared to men, whereas the opposite pattern was seen in the Wurtz population. This could reflect the much smaller sample size for HBM men or the older age of the HBM men compared to the adolescents and young adults studied by Wurtz *et al*.

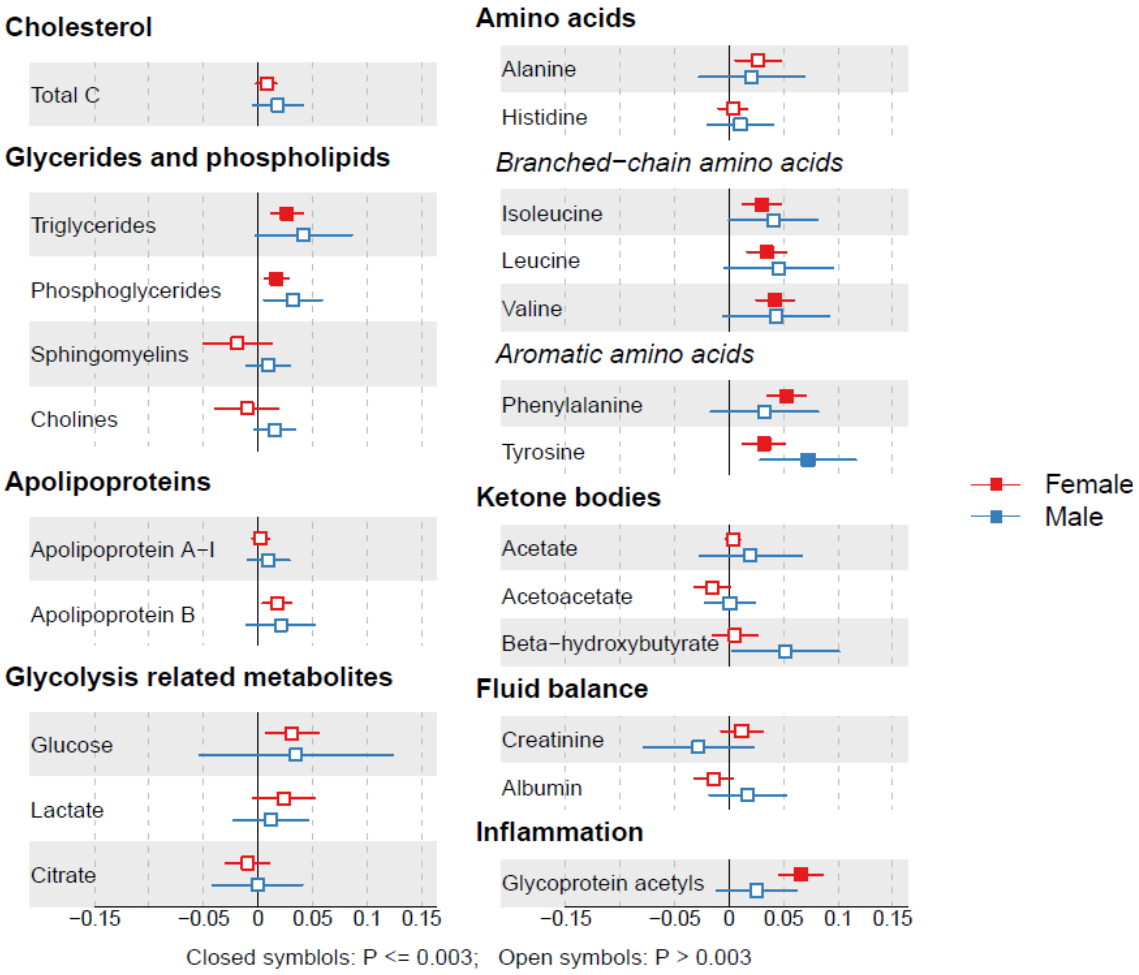

Figure 1: Associations between BMI and metabolic traits in the HBM population, stratified by gender.
Points represent the SD increase in metabolic trait per 1kg/m²increase in BMI.

I analysed differences in metabolic traits between those individuals ever taking statins and those individuals who had never taken a statin and compared results to those previously published (451). I created a variable for statin use based on recorded medications at baseline. I identified statins based on a BNF code of 02.12(s). Other lipid-lowering medications (ezetimibe and fibrates) were identified based on free-text responses. I assessed differences in mean concentrations of metabolic traits between those who had ever taken a lipid-lowering medication and those who had never taken one, in SD units, using linear regression, adjusting for age and sex, and using robust SEs (Figure). Sample sizes were much smaller in HBM and therefore results were closer to the

null. However, the direction of associations with statins were similar to the published literature (Presented in Figures 1 and 3 of Wurtz *et al* (451)).

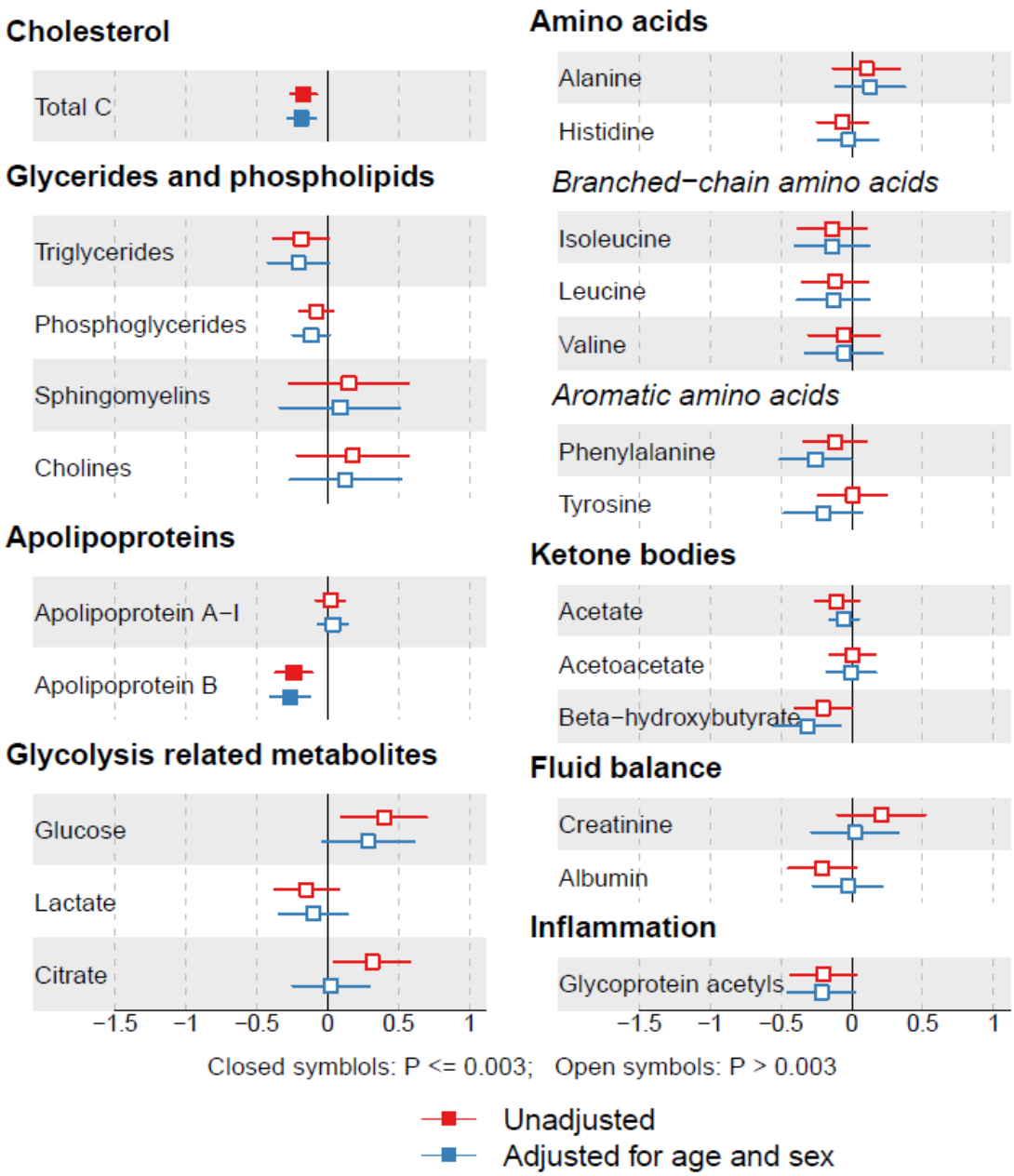

Figure 2: Associations between statin use and metabolic traits in the HBM population. Points represent the mean difference in SD units between those taking statins and those not taking statins.

Appendix 19: Histograms of the 23 metabolic traits analysed in Chapter 8.

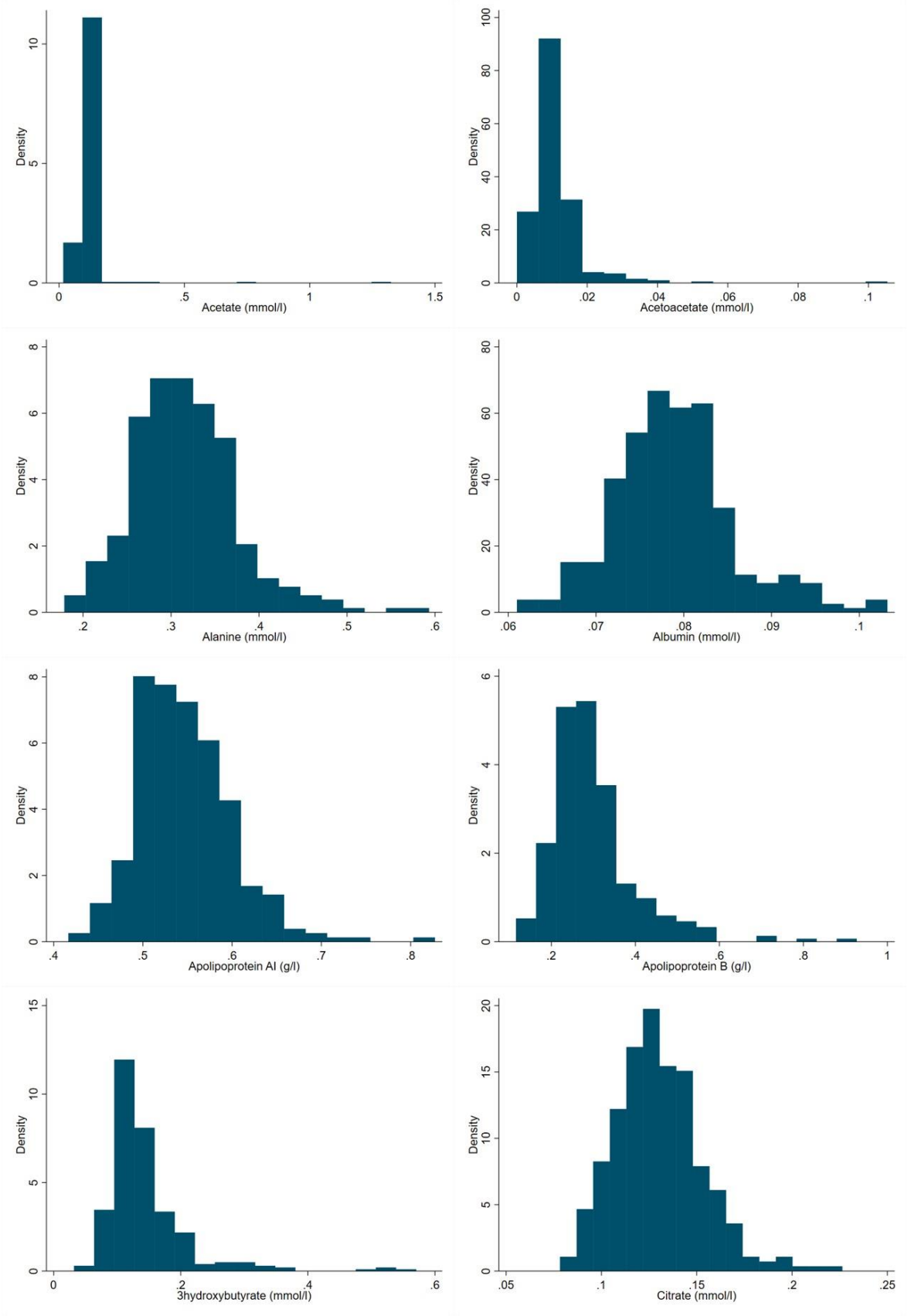

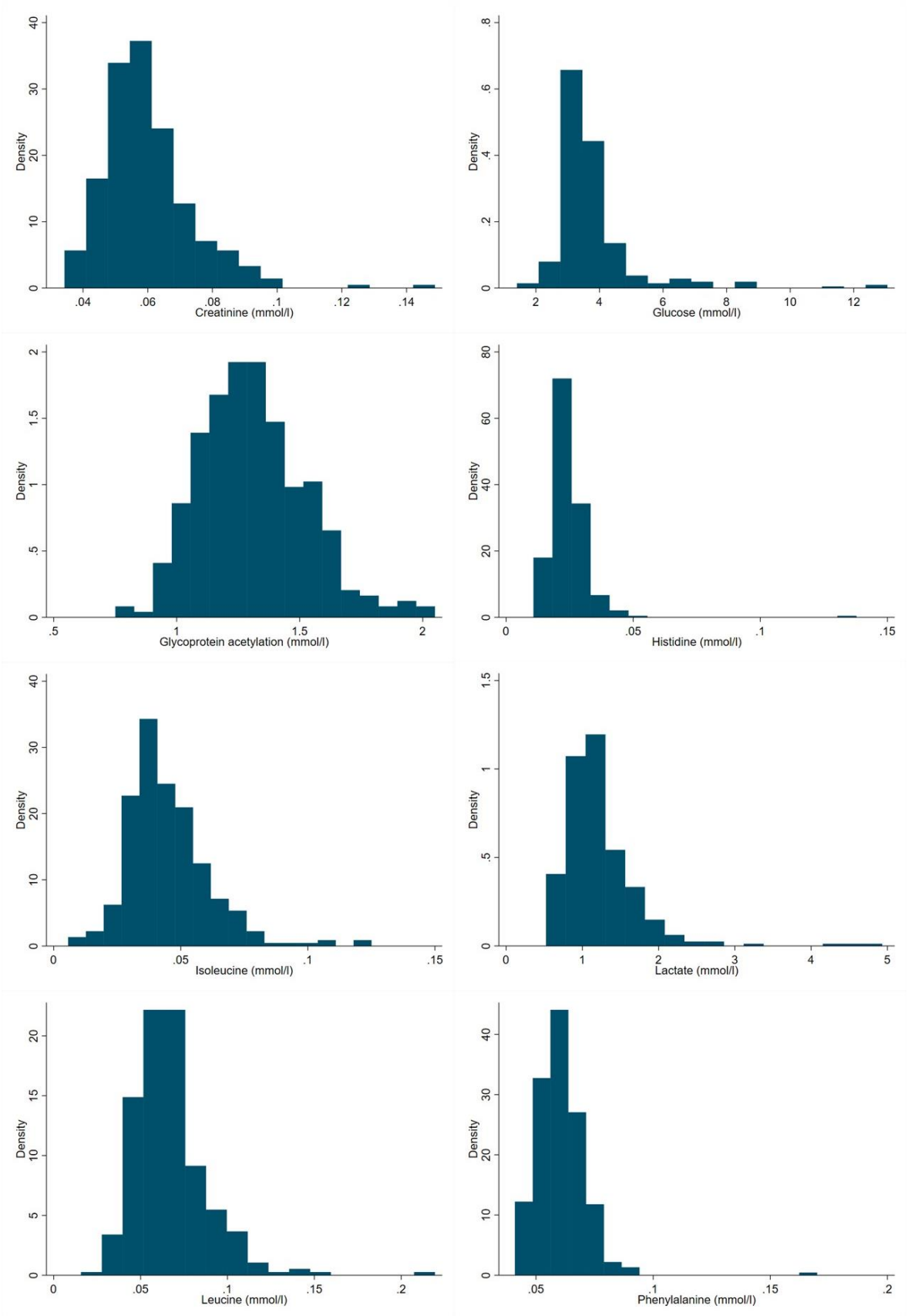
Density
Creatinine (mmol/l)
Glucose (mmol/l)
Glycoprotein acetylation (mmol/l)
Histidine (mmol/l)
Isoleucine (mmol/l)
Lactate (mmol/l)
Leucine (mmol/l)
Phenylalanine (mmol/l)

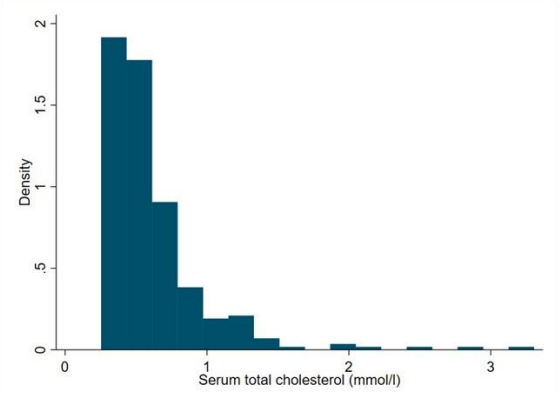
Density
0
.5
1
1.5
2
0
1
2
3
Serum total cholesterol (mmol/l)

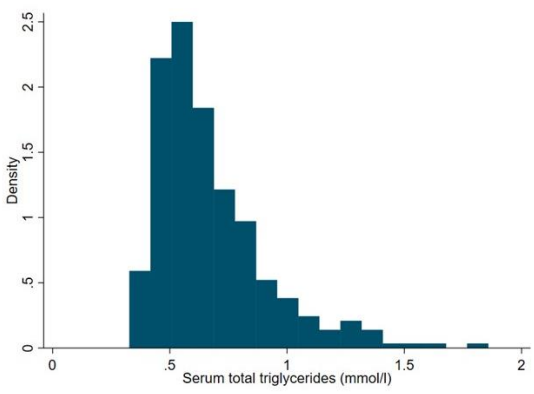
Density
0
.5
1
1.5
2
2.5
0
.5
1
1.5
2
Serum total triglycerides (mmol/l)

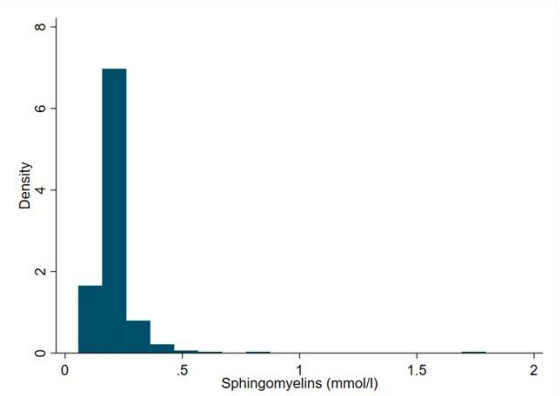
Density
0
2
4
6
8
0
.5
1
1.5
2
Sphingomyelins (mmol/l)

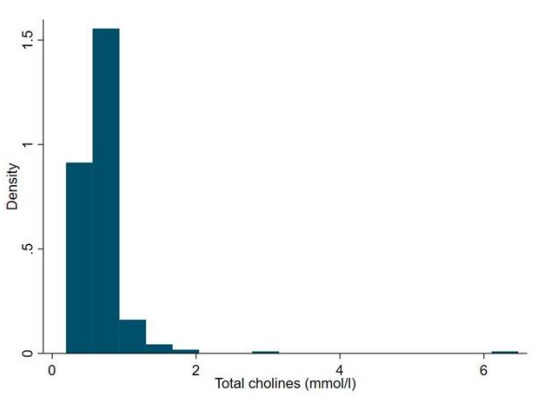
Density
0
.5
1
1.5
0
2
4
6
Total cholines (mmol/l)

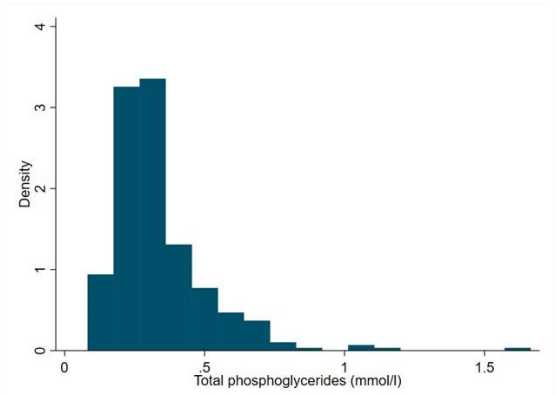
Density
0
1
2
3
4
0
.5
1
1.5
Total phosphoglycerides (mmol/l)

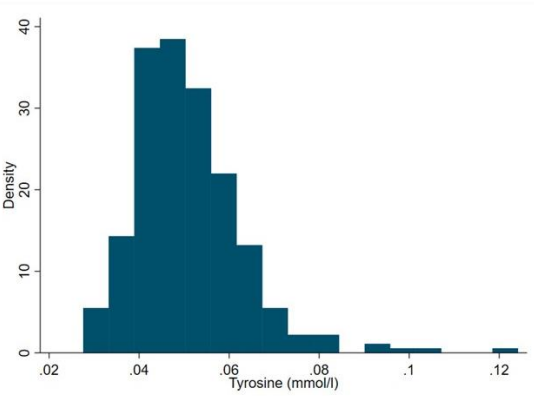
Density
0
10
20
30
40
.02
.04
.06
.08
.1
.12
Tyrosine (mmol/l)

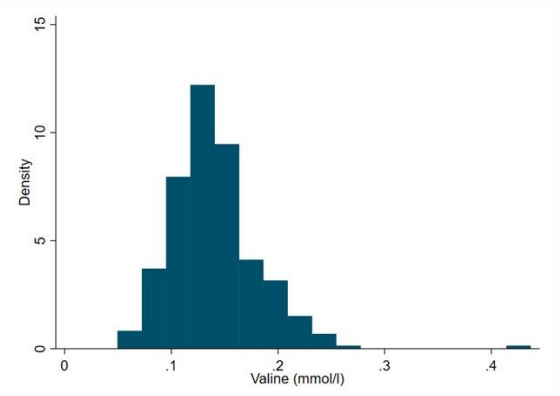
Density
0
5
10
15
0
.1
.2
.3
.4
Valine (mmol/l)

Appendix 20: Descriptive characteristics of the HBM metabolomics study population, stratified by HBM status.

	Total HBM cohort analysed (N=320)	**HBM individuals (N=198)**	**Family members with normal BMD (N=122)**	***p*-value for difference**
	Mean (SD)	**Mean (SD)**	**Mean (SD)**	
Age (years)	59.1 (15.0)	61.6 (13.7)	55.0 (16.2)	1.26×10^{-4}
Height (cm)	168.7 (9.9)	166.9 (8.9)	171.7 (10.5)	1.45×10^{-5}
Weight (kg)	84.5 (17.0)	84.9 (16.8)	84.0 (17.4)	0.664
BMI (kg/m^2)	29.7 (5.6)	30.5 (5.8)	28.4 (4.9)	0.001
L1-BMD	1.28 (0.22)	1.40 (0.16)	1.08 (0.16)	1.34×10^{-50}
L1-BMD Z-score	2.53 (2.14)	3.85 (1.34)	0.36 (1.25)	5.36×10^{-69}
Max TH-BMD	1.15 (0.21)	1.25 (0.18)	0.99 (0.14)	3.13×10^{-34}
Max TH-BMD Z-score	2.07 (1.61)	3.02 (1.16)	0.53 (0.89)	1.55×10^{-57}
Physical Activity (MET-minutes/week)	3740.5 (4414.6)	3479.0 (3293.0)	4155.7 (5760.0)	0.804
		Median (IQR)	**Median (IQR)**	
β-CTX (µg/L)[a]	0.18 (0.12, 0.27)	0.17 (0.12, 0.25)	0.20 (0.11, 0.28)	0.214
P1NP (µg/L)[a]	33.0 (25.0, 44.0)	32.0 (23.0, 44.0)	34.0 (26.0, 44.0)	0.339
Osteocalcin (µg/L)[a]	16.9 (13.8, 21.7)	16.6 (13.1, 21.2)	18.0 (14.6, 23.0)	0.007
		N (%)	**N (%)**	
Female	206 (64.4)	152 (76.8)	54 (44.3)	3.69×10^{-9}
Postmenopausal[b]	159 (77.2)	130 (85.5)	29 (53.7)	1.70×10^{-6}
History of bisphosphonate use	10 (3.1)	8 (4.0)	2 (1.6)	0.231
History of oral glucocorticoid use	66 (20.6)	48 (24.2)	18 (14.8)	0.042
Prior/current smoking	172 (53.9)	114 (57.6)	58 (47.5)	0.080
Alcohol Consumption				
None	78 (24.4)	57 (28.8)	21 (17.2)	
Occasional	32 (10.0)	22 (11.1)	10 (8.2)	0.002
Regular	160 (50.0)	99 (50.0)	61 (50.0)	
Heavy	50 (15.6)	20 (10.1)	30 (24.6)	

[a]p-value represents difference in log-transformed concentrations due to skewed distributions; [b]individuals currently going through menopause included in this category. Max TH BMD is the highest recorded BMD from the left and right hips. Total weekly MET-minutes is calculated as the energy requirement of each activity type multiplied by duration and summed across all three activity types. History of oral glucocorticoid use is based on self-report of current or past oral glucocorticoid use for any duration.

Appendix 21: Full results of the metabolomics analysis with HBM as the exposure.

	Model 1					Model 3				Excluding outliers					Excluding tagged samples				
Outcome	**N**	**B**	**LCI**	**UCI**	**p**	**β**	**LCI**	**UCI**	**p**	**N**	**β**	**LCI**	**UCI**	**p**	**N**	**β**	**LCI**	**UCI**	**p**
Acetoacetate	319	0.098	-0.036	0.232	0.153	0.140	-0.010	0.291	0.068	318	0.087	-0.024	0.198	0.124	311	0.116	-0.036	0.269	0.136
Acetate	316	0.018	-0.207	0.244	0.873	0.173	-0.215	0.561	0.383	314	0.016	-0.065	0.096	0.703	311	0.154	-0.246	0.554	0.451
Alanine	320	-0.369	-0.582	-0.157	0.001	-0.382	-0.607	-0.156	0.001	320	-0.382	-0.607	-0.156	0.001	311	-0.255	-0.465	-0.046	0.017
Albumin	320	-0.196	-0.418	0.026	0.083	0.006	-0.249	0.262	0.962	320	0.006	-0.249	0.262	0.962	311	0.075	-0.160	0.311	0.529
Apolipoprotein A1	320	-0.127	-0.222	-0.032	0.009	-0.100	-0.196	-0.003	0.042	320	-0.100	-0.196	-0.003	0.042	311	-0.060	-0.148	0.029	0.190
Apolipoprotein B	320	-0.036	-0.210	0.139	0.688	-0.062	-0.228	0.105	0.468	320	-0.062	-0.228	0.105	0.468	311	0.028	-0.126	0.182	0.724
Beta hydroxybutyrate	320	0.309	0.109	0.509	0.002	0.299	0.057	0.542	0.015	320	0.299	0.057	0.542	0.015	311	0.266	0.023	0.508	0.032
Citrate	320	0.194	0.017	0.370	0.031	-0.001	-0.194	0.193	0.994	320	-0.001	-0.194	0.193	0.994	311	0.016	-0.178	0.211	0.868
Creatinine	315	-0.067	-0.300	0.166	0.573	0.149	-0.078	0.375	0.198	315	0.149	-0.078	0.375	0.198	311	0.167	-0.057	0.391	0.144
Glucose	313	-0.031	-0.271	0.209	0.800	-0.096	-0.330	0.137	0.418	313	-0.096	-0.330	0.137	0.418	311	-0.099	-0.332	0.134	0.405
Glycoprotein acetyls	320	0.109	-0.119	0.337	0.348	-0.018	-0.266	0.231	0.890	320	-0.018	-0.266	0.231	0.890	311	0.061	-0.170	0.292	0.606
Histidine	320	0.057	-0.121	0.235	0.532	0.103	-0.089	0.296	0.292	319	0.054	-0.103	0.211	0.503	311	0.145	-0.040	0.330	0.125
Isoleucine	320	-0.082	-0.319	0.155	0.498	-0.033	-0.291	0.224	0.799	320	-0.033	-0.291	0.224	0.799	311	0.002	-0.257	0.261	0.986
Lactate	313	-0.147	-0.373	0.079	0.202	-0.098	-0.437	0.240	0.569	312	0.006	-0.274	0.287	0.964	311	-0.093	-0.432	0.245	0.590
Leucine	320	-0.176	-0.419	0.067	0.156	-0.128	-0.420	0.163	0.389	320	-0.128	-0.420	0.163	0.389	311	-0.058	-0.347	0.231	0.694
Phenylalanine	302	0.229	0.006	0.451	0.044	0.011	-0.270	0.292	0.937	301	-0.087	-0.299	0.126	0.423	295	0.026	-0.257	0.308	0.858
Total cholesterol	320	-0.040	-0.173	0.093	0.556	-0.059	-0.179	0.061	0.336	320	-0.059	-0.179	0.061	0.336	311	0.011	-0.095	0.117	0.844
Triglycerides	320	-0.024	-0.250	0.202	0.835	0.021	-0.185	0.227	0.843	320	0.021	-0.185	0.227	0.843	311	0.122	-0.074	0.318	0.224
Sphingomyelins	320	-0.180	-0.447	0.087	0.187	-0.286	-0.636	0.064	0.109	319	-0.127	-0.286	0.033	0.120	311	-0.274	-0.638	0.090	0.140
Cholines	320	-0.173	-0.420	0.075	0.172	-0.285	-0.612	0.041	0.087	319	-0.135	-0.280	0.009	0.066	311	-0.263	-0.603	0.078	0.130
Phosphoglycerides	320	-0.050	-0.203	0.103	0.521	-0.099	-0.229	0.032	0.138	320	-0.099	-0.229	0.032	0.138	311	-0.051	-0.184	0.083	0.455
Tyrosine	320	-0.001	-0.240	0.237	0.991	-0.194	-0.464	0.076	0.160	320	-0.194	-0.464	0.076	0.160	311	-0.139	-0.401	0.123	0.299
Valine	320	-0.126	-0.363	0.110	0.295	-0.074	-0.365	0.217	0.619	319	0.038	-0.170	0.246	0.717	311	-0.014	-0.305	0.278	0.925

Appendix 22: Full results of the metabolomics analysis with TB-BMD as the exposure.

	Model 1					Model 3				Excluding outliers					Excluding tagged samples				
Outcome	**N**	**β**	**LCI**	**UCI**	**p**	**β**	**LCI**	**UCI**	**p**	**N**	**β**	**LCI**	**UCI**	**p**	**N**	**β**	**LCI**	**UCI**	**p**
Acetoacetate	318	-0.019	-0.065	0.026	0.406	0.013	-0.067	0.094	0.743	317	-0.018	-0.065	0.029	0.459	310	0.008	-0.082	0.098	0.866
Acetate	315	0.055	-0.037	0.147	0.241	-0.004	-0.051	0.043	0.865	314	-0.014	-0.050	0.023	0.470	310	-0.010	-0.062	0.042	0.704
Alanine	319	0.006	-0.092	0.105	0.898	-0.114	-0.217	-0.010	0.031	319	-0.114	-0.217	-0.010	0.031	310	-0.080	-0.189	0.028	0.147
Albumin	319	0.036	-0.052	0.123	0.423	-0.042	-0.148	0.065	0.442	319	-0.042	-0.148	0.065	0.442	310	-0.036	-0.139	0.068	0.502
Apolipoprotein A1	319	-0.014	-0.059	0.030	0.531	-0.047	-0.097	0.003	0.065	319	-0.047	-0.097	0.003	0.065	310	-0.031	-0.075	0.013	0.170
Apolipoprotein B	319	-0.005	-0.076	0.065	0.878	-0.053	-0.136	0.030	0.209	319	-0.053	-0.136	0.030	0.209	310	-0.020	-0.095	0.054	0.593
Beta hydroxybutyrate	319	-0.027	-0.118	0.063	0.555	-0.008	-0.117	0.101	0.881	319	-0.008	-0.117	0.101	0.881	310	-0.014	-0.137	0.109	0.822
Citrate	319	-0.109	-0.218	0.000	0.050	-0.031	-0.137	0.075	0.565	319	-0.031	-0.137	0.075	0.565	310	-0.048	-0.165	0.069	0.423
Creatinine	314	0.137	0.008	0.267	0.038	0.049	-0.072	0.170	0.428	314	0.049	-0.072	0.170	0.428	310	0.055	-0.086	0.196	0.444
Glucose	312	-0.027	-0.144	0.090	0.650	-0.118	-0.249	0.013	0.078	312	-0.118	-0.249	0.013	0.078	310	-0.130	-0.273	0.013	0.075
Glycoprotein acetyls	319	-0.003	-0.092	0.086	0.947	-0.092	-0.189	0.004	0.061	319	-0.092	-0.189	0.004	0.061	310	-0.088	-0.188	0.012	0.085
Histidine	319	-0.011	-0.082	0.061	0.768	-0.023	-0.097	0.051	0.548	318	-0.027	-0.100	0.047	0.479	310	-0.008	-0.083	0.067	0.833
Isoleucine	319	0.034	-0.078	0.147	0.552	-0.076	-0.188	0.037	0.188	319	-0.076	-0.188	0.037	0.188	310	-0.076	-0.198	0.047	0.225
Lactate	312	-0.031	-0.197	0.135	0.716	-0.121	-0.287	0.045	0.153	311	-0.063	-0.181	0.056	0.298	310	-0.138	-0.331	0.055	0.161
Leucine	319	-0.022	-0.159	0.114	0.749	-0.148	-0.275	-0.021	0.022	319	-0.148	-0.275	-0.021	0.022	310	-0.136	-0.263	-0.009	0.036
Phenylalanine	301	-0.032	-0.136	0.072	0.550	-0.077	-0.176	0.021	0.123	300	-0.074	-0.172	0.024	0.141	294	-0.095	-0.206	0.015	0.091
Total cholesterol	319	-0.019	-0.069	0.031	0.465	-0.050	-0.113	0.012	0.114	319	-0.050	-0.113	0.012	0.114	310	-0.019	-0.071	0.032	0.459
Triglycerides	319	0.055	-0.034	0.145	0.225	-0.019	-0.121	0.082	0.712	319	-0.019	-0.121	0.082	0.712	310	0.013	-0.085	0.110	0.799
Sphingomyelins	319	-0.102	-0.212	0.009	0.071	-0.087	-0.193	0.020	0.110	318	-0.052	-0.130	0.027	0.196	310	-0.083	-0.202	0.036	0.170
Cholines	319	-0.097	-0.194	-0.001	0.047	-0.099	-0.190	-0.007	0.034	318	-0.065	-0.124	-0.006	0.031	310	-0.092	-0.195	0.010	0.078
Phosphoglycerides	319	-0.035	-0.086	0.017	0.188	-0.078	-0.135	-0.021	0.007	319	-0.078	-0.135	-0.021	0.007	310	-0.059	-0.119	0.000	0.051
Tyrosine	319	-0.135	-0.248	-0.022	0.019	-0.191	-0.316	-0.066	0.003	319	-0.191	-0.316	-0.066	0.003	310	-0.184	-0.312	-0.056	0.005
Valine	319	0.020	-0.118	0.158	0.776	-0.113	-0.235	0.009	0.070	318	-0.073	-0.168	0.021	0.128	310	-0.102	-0.226	0.023	0.109

Appendix 23: Full results of the metabolomics analysis with L1-BMD as the exposure.

	Model 1					Model 3				Excluding outliers					Excluding tagged samples				
Outcome	**N**	**β**	**LCI**	**UCI**	**p**	**β**	**LCI**	**UCI**	**p**	**N**	**β**	**LCI**	**UCI**	**p**	**N**	**β**	**LCI**	**UCI**	**p**
Acetoacetate	317	0.046	-0.039	0.130	0.290	0.065	-0.032	0.162	0.186	316	0.023	-0.027	0.073	0.365	309	0.055	-0.045	0.155	0.281
Acetate	314	0.003	-0.058	0.064	0.921	0.002	-0.069	0.073	0.963	313	-0.017	-0.077	0.042	0.568	309	-0.003	-0.075	0.069	0.935
Alanine	318	-0.135	-0.234	-0.036	0.008	-0.171	-0.264	-0.079	<0.001	318	-0.171	-0.264	-0.079	<0.001	309	-0.114	-0.209	-0.019	0.018
Albumin	318	-0.038	-0.158	0.081	0.529	-0.012	-0.132	0.109	0.850	318	-0.012	-0.132	0.109	0.850	309	0.008	-0.107	0.123	0.893
Apolipoprotein A1	318	-0.036	-0.087	0.016	0.173	-0.037	-0.088	0.014	0.155	318	-0.037	-0.088	0.014	0.155	309	-0.013	-0.056	0.030	0.558
Apolipoprotein B	318	-0.032	-0.127	0.063	0.507	-0.055	-0.150	0.041	0.261	318	-0.055	-0.150	0.041	0.261	309	-0.012	-0.100	0.076	0.789
Beta hydroxybutyrate	318	0.107	0.011	0.202	0.029	0.096	-0.010	0.203	0.076	318	0.096	-0.010	0.203	0.076	309	0.087	-0.023	0.197	0.121
Citrate	318	0.016	-0.081	0.112	0.749	-0.006	-0.097	0.086	0.902	318	-0.006	-0.097	0.086	0.902	309	-0.010	-0.102	0.083	0.840
Creatinine	313	0.053	-0.071	0.177	0.404	0.048	-0.054	0.151	0.355	313	0.048	-0.054	0.151	0.355	309	0.059	-0.046	0.163	0.271
Glucose	311	-0.010	-0.133	0.113	0.869	-0.059	-0.178	0.059	0.328	311	-0.059	-0.178	0.059	0.328	309	-0.059	-0.177	0.060	0.333
Glycoprotein acetyls	318	0.038	-0.073	0.149	0.499	-0.025	-0.134	0.083	0.649	318	-0.025	-0.134	0.083	0.649	309	-0.006	-0.112	0.101	0.919
Histidine	318	0.002	-0.079	0.083	0.959	0.004	-0.088	0.095	0.939	317	-0.017	-0.097	0.064	0.685	309	0.028	-0.059	0.114	0.529
Isoleucine	318	0.012	-0.105	0.129	0.841	-0.019	-0.141	0.104	0.765	318	-0.019	-0.141	0.104	0.765	309	-0.001	-0.122	0.120	0.982
Lactate	311	-0.099	-0.255	0.058	0.216	-0.123	-0.286	0.041	0.142	310	-0.058	-0.167	0.050	0.292	309	-0.122	-0.286	0.041	0.142
Leucine	318	-0.056	-0.188	0.076	0.409	-0.088	-0.224	0.049	0.208	318	-0.088	-0.224	0.049	0.208	309	-0.061	-0.193	0.071	0.365
Phenylalanine	300	0.041	-0.071	0.152	0.477	-0.038	-0.154	0.077	0.517	299	-0.072	-0.168	0.023	0.135	293	-0.040	-0.158	0.077	0.501
Total cholesterol	318	-0.042	-0.114	0.031	0.265	-0.055	-0.128	0.018	0.140	318	-0.055	-0.128	0.018	0.140	309	-0.018	-0.082	0.047	0.592
Triglycerides	318	0.013	-0.103	0.129	0.832	-0.011	-0.125	0.103	0.851	318	-0.011	-0.125	0.103	0.851	309	0.033	-0.076	0.141	0.558
Sphingomyelins	318	-0.148	-0.344	0.048	0.138	-0.150	-0.339	0.038	0.118	317	-0.056	-0.119	0.007	0.081	309	-0.138	-0.336	0.059	0.169
Cholines	318	-0.138	-0.319	0.044	0.138	-0.148	-0.323	0.027	0.097	317	-0.060	-0.117	-0.003	0.038	309	-0.131	-0.313	0.052	0.160
Phosphoglycerides	318	-0.039	-0.118	0.041	0.340	-0.064	-0.142	0.013	0.104	318	-0.064	-0.142	0.013	0.104	309	-0.035	-0.113	0.043	0.380
Tyrosine	318	-0.021	-0.144	0.103	0.743	-0.080	-0.206	0.046	0.213	318	-0.080	-0.206	0.046	0.213	309	-0.051	-0.170	0.068	0.403
Valine	318	-0.028	-0.161	0.105	0.682	-0.066	-0.205	0.074	0.355	317	-0.023	-0.137	0.090	0.690	309	-0.044	-0.182	0.094	0.529

Appendix 24: Full results of the metabolomics analysis with TH-BMD as the exposure.

	Model 1					Model 3				Excluding outliers					Excluding tagged samples				
Outcome	**N**	**β**	**LCI**	**UCI**	**p**	**β**	**LCI**	**UCI**	**p**	**N**	**B**	**LCI**	**UCI**	**p**	**N**	**β**	**LCI**	**UCI**	**p**
Acetoacetate	314	-0.001	-0.061	0.060	0.978	0.026	-0.053	0.106	0.514	313	0.003	-0.061	0.067	0.922	306	0.015	-0.065	0.096	0.706
Acetate	311	0.009	-0.051	0.068	0.779	-0.022	-0.087	0.043	0.505	310	-0.021	-0.082	0.041	0.508	306	-0.034	-0.096	0.029	0.291
Alanine	315	-0.015	-0.122	0.093	0.786	-0.079	-0.187	0.029	0.153	315	-0.079	-0.187	0.029	0.153	306	-0.023	-0.129	0.082	0.664
Albumin	315	0.054	-0.053	0.161	0.325	0.023	-0.086	0.132	0.678	315	0.023	-0.086	0.132	0.678	306	0.051	-0.053	0.155	0.339
Apolipoprotein A1	315	-0.032	-0.075	0.010	0.133	-0.050	-0.095	-0.005	0.029	315	-0.050	-0.095	-0.005	0.029	306	-0.032	-0.073	0.008	0.116
Apolipoprotein B	315	-0.026	-0.091	0.039	0.433	-0.064	-0.138	0.009	0.086	315	-0.064	-0.138	0.009	0.086	306	-0.028	-0.097	0.042	0.436
Beta hydroxybutyrate	315	0.010	-0.091	0.110	0.849	0.012	-0.108	0.132	0.847	315	0.012	-0.108	0.132	0.847	306	-0.003	-0.125	0.119	0.961
Citrate	315	-0.065	-0.170	0.039	0.219	-0.008	-0.113	0.097	0.881	315	-0.008	-0.113	0.097	0.881	306	-0.001	-0.110	0.108	0.981
Creatinine	310	0.102	-0.020	0.224	0.101	0.097	-0.020	0.215	0.105	310	0.097	-0.020	0.215	0.105	306	0.104	-0.016	0.223	0.088
Glucose	308	-0.077	-0.208	0.054	0.251	-0.128	-0.262	0.006	0.061	308	-0.128	-0.262	0.006	0.061	306	-0.130	-0.265	0.004	0.058
Glycoprotein acetyls	315	0.056	-0.049	0.162	0.296	-0.031	-0.130	0.068	0.542	315	-0.031	-0.130	0.068	0.542	306	-0.002	-0.100	0.096	0.974
Histidine	315	0.040	-0.037	0.116	0.306	0.034	-0.048	0.116	0.418	314	0.022	-0.056	0.100	0.572	306	0.049	-0.030	0.129	0.222
Isoleucine	315	0.049	-0.059	0.158	0.371	-0.010	-0.116	0.096	0.854	315	-0.010	-0.116	0.096	0.854	306	0.008	-0.096	0.112	0.879
Lactate	308	0.024	-0.132	0.180	0.763	-0.016	-0.170	0.138	0.839	307	0.009	-0.135	0.153	0.900	306	-0.012	-0.166	0.142	0.879
Leucine	315	-0.015	-0.145	0.116	0.822	-0.077	-0.195	0.041	0.203	315	-0.077	-0.195	0.041	0.203	306	-0.043	-0.157	0.070	0.452
Phenylalanine	297	0.025	-0.095	0.144	0.686	-0.038	-0.144	0.069	0.488	296	-0.059	-0.155	0.038	0.234	290	-0.031	-0.141	0.078	0.572
Total cholesterol	315	-0.031	-0.079	0.017	0.209	-0.056	-0.112	0.000	0.049	315	-0.056	-0.112	0.000	0.049	306	-0.027	-0.079	0.024	0.300
Triglycerides	315	0.012	-0.078	0.102	0.795	-0.038	-0.132	0.057	0.433	315	-0.038	-0.132	0.057	0.433	306	0.003	-0.088	0.094	0.951
Sphingomyelins	315	-0.139	-0.319	0.042	0.132	-0.122	-0.286	0.042	0.146	314	-0.044	-0.103	0.014	0.139	306	-0.116	-0.286	0.054	0.180
Cholines	315	-0.133	-0.300	0.034	0.117	-0.130	-0.283	0.023	0.095	314	-0.056	-0.107	-0.006	0.029	306	-0.120	-0.279	0.038	0.135
Phosphoglycerides	315	-0.046	-0.102	0.009	0.101	-0.079	-0.141	-0.018	0.012	315	-0.079	-0.141	-0.018	0.012	306	-0.060	-0.122	0.003	0.061
Tyrosine	315	-0.089	-0.205	0.027	0.134	-0.121	-0.240	-0.002	0.047	315	-0.121	-0.240	-0.002	0.047	306	-0.100	-0.217	0.017	0.093
Valine	315	0.028	-0.104	0.160	0.679	-0.039	-0.158	0.081	0.525	314	0.005	-0.093	0.103	0.917	306	-0.010	-0.128	0.108	0.866

Appendix 25: Full results of the metabolomics analysis with hip osteophytes as the outcome.

	Model 1					Model 3				Excluding outliers					Excluding tagged samples				
Outcome	**N**	**OR**	**LCI**	**UCI**	**p**	**OR**	**LCI**	**UCI**	**p**	**N**	**OR**	**LCI**	**UCI**	**p**	**N**	**OR**	**LCI**	**UCI**	**p**
Acetoacetate	519	0.672	0.486	0.930	0.017	0.670	0.465	0.964	0.031	517	0.685	0.449	1.045	0.079	503	0.665	0.460	0.962	0.031
Acetate	513	1.108	0.902	1.360	0.328	1.108	0.905	1.357	0.319	509	0.589	0.288	1.205	0.147	503	1.094	0.899	1.332	0.371
Alanine	521	1.139	0.885	1.466	0.312	1.069	0.831	1.374	0.605	521	1.069	0.831	1.374	0.605	503	1.172	0.907	1.516	0.225
Albumin	521	0.904	0.720	1.134	0.383	0.985	0.778	1.247	0.900	521	0.985	0.778	1.247	0.900	503	1.014	0.795	1.293	0.912
Apolipoprotein A1	521	1.089	0.617	1.921	0.769	1.000	0.580	1.725	1.000	521	1.000	0.580	1.725	1.000	503	1.278	0.686	2.380	0.440
Apolipoprotein B	521	1.247	0.891	1.746	0.198	1.205	0.877	1.655	0.250	521	1.205	0.877	1.655	0.250	503	1.444	0.991	2.104	0.056
Beta hydroxybutyrate	521	1.011	0.794	1.286	0.932	0.992	0.791	1.243	0.942	521	0.992	0.791	1.243	0.942	503	0.984	0.786	1.234	0.892
Citrate	521	1.103	0.861	1.413	0.437	0.979	0.752	1.275	0.875	521	0.979	0.752	1.275	0.875	503	0.994	0.757	1.304	0.963
Creatinine	511	1.182	0.918	1.522	0.195	0.957	0.729	1.258	0.754	511	0.957	0.729	1.258	0.754	503	0.936	0.713	1.228	0.632
Glucose	507	1.684	1.264	2.245	<0.001	1.492	1.136	1.960	0.004	507	1.492	1.136	1.960	0.004	503	1.473	1.124	1.931	0.005
Glycoprotein acetyls	521	1.282	1.013	1.624	0.039	1.285	1.009	1.637	0.042	521	1.285	1.009	1.637	0.042	503	1.323	1.025	1.707	0.031
Histidine	521	0.951	0.827	1.092	0.476	0.979	0.855	1.122	0.762	519	0.998	0.701	1.422	0.993	503	1.011	0.878	1.165	0.875
Isoleucine	521	1.042	0.833	1.304	0.717	0.990	0.784	1.251	0.935	521	0.990	0.784	1.251	0.935	503	1.022	0.806	1.297	0.856
Lactate	507	1.063	0.812	1.390	0.657	1.027	0.786	1.342	0.846	505	1.178	0.924	1.500	0.186	503	1.021	0.780	1.338	0.878
Leucine	521	1.069	0.854	1.338	0.559	1.004	0.796	1.268	0.970	521	1.004	0.796	1.268	0.970	503	1.058	0.828	1.354	0.651
Phenylalanine	491	1.157	0.912	1.469	0.230	1.120	0.868	1.444	0.383	489	1.085	0.788	1.492	0.618	477	1.116	0.867	1.438	0.395
Total cholesterol	521	1.158	0.763	1.759	0.490	1.147	0.770	1.709	0.499	521	1.147	0.770	1.709	0.499	503	1.540	0.868	2.733	0.140
Triglycerides	521	1.271	0.975	1.657	0.077	1.225	0.955	1.571	0.111	521	1.225	0.955	1.571	0.111	503	1.374	1.042	1.811	0.024
Sphingomyelins	521	1.089	0.900	1.316	0.380	1.093	0.880	1.358	0.422	520	1.041	0.737	1.470	0.819	503	1.127	0.872	1.456	0.360
Cholines	521	1.226	0.909	1.652	0.182	1.200	0.896	1.607	0.220	520	1.177	0.815	1.698	0.385	503	1.305	0.903	1.885	0.156
Phosphoglycerides	521	1.456	0.915	2.316	0.113	1.367	0.882	2.119	0.162	521	1.367	0.882	2.119	0.162	503	1.697	0.947	3.042	0.075
Tyrosine	521	1.178	0.915	1.517	0.203	1.064	0.821	1.380	0.639	521	1.064	0.821	1.380	0.639	503	1.106	0.838	1.459	0.477
Valine	521	1.097	0.875	1.374	0.424	1.031	0.816	1.303	0.795	519	0.993	0.757	1.304	0.962	503	1.067	0.835	1.362	0.605

Appendix 26: Full results of the metabolomics analysis with hip JSN as the outcome.

	Model 1					Model 3				Excluding outliers					Excluding tagged samples				
Outcome	**N**	**OR**	**LCI**	**UCI**	**p**	**OR**	**LCI**	**UCI**	**p**	**N**	**OR**	**LCI**	**UCI**	**P**	**N**	**OR**	**LCI**	**UCI**	**p**
Acetoacetate	519	1.090	0.799	1.487	0.588	1.110	0.827	1.488	0.488	517	1.307	0.867	1.971	0.201	503	1.131	0.841	1.521	0.417
Acetate	513	1.110	0.966	1.276	0.141	1.150	0.987	1.340	0.072	509	0.367	0.143	0.945	0.038	503	1.158	0.990	1.355	0.067
Alanine	521	1.132	0.893	1.433	0.306	1.101	0.865	1.403	0.434	521	1.101	0.865	1.403	0.434	503	1.150	0.863	1.533	0.341
Albumin	521	0.898	0.697	1.156	0.404	0.985	0.759	1.277	0.908	521	0.985	0.759	1.277	0.908	503	0.972	0.736	1.282	0.838
Apolipoprotein A1	521	1.021	0.586	1.780	0.941	0.941	0.515	1.717	0.842	521	0.941	0.515	1.717	0.842	503	1.047	0.522	2.100	0.896
Apolipoprotein B	521	0.981	0.699	1.378	0.913	0.993	0.678	1.455	0.973	521	0.993	0.678	1.455	0.973	503	1.011	0.663	1.544	0.958
Beta hydroxybutyrate	521	1.049	0.804	1.369	0.724	1.019	0.784	1.324	0.890	521	1.019	0.784	1.324	0.890	503	1.056	0.824	1.355	0.666
Citrate	521	0.940	0.719	1.228	0.649	0.807	0.607	1.073	0.140	521	0.807	0.607	1.073	0.140	503	0.793	0.589	1.067	0.126
Creatinine	511	0.950	0.765	1.178	0.639	0.718	0.544	0.947	0.019	511	0.718	0.544	0.947	0.019	503	0.712	0.536	0.945	0.019
Glucose	507	1.117	0.863	1.446	0.399	1.069	0.794	1.439	0.661	507	1.069	0.794	1.439	0.661	503	1.062	0.785	1.436	0.697
Glycoprotein acetyls	521	0.959	0.744	1.237	0.749	0.983	0.739	1.308	0.905	521	0.983	0.739	1.308	0.905	503	0.945	0.710	1.257	0.697
Histidine	521	0.984	0.798	1.213	0.878	1.008	0.820	1.238	0.943	519	1.184	0.810	1.730	0.383	503	1.027	0.833	1.266	0.806
Isoleucine	521	1.076	0.802	1.444	0.624	1.072	0.780	1.472	0.669	521	1.072	0.780	1.472	0.669	503	1.091	0.792	1.502	0.595
Lactate	507	0.926	0.724	1.185	0.542	0.901	0.680	1.193	0.466	505	0.937	0.680	1.291	0.690	503	0.906	0.684	1.200	0.492
Leucine	521	1.144	0.874	1.496	0.328	1.121	0.845	1.486	0.429	521	1.121	0.845	1.486	0.429	503	1.142	0.853	1.530	0.372
Phenylalanine	491	1.080	0.895	1.303	0.424	1.047	0.859	1.276	0.651	489	1.013	0.678	1.512	0.951	477	1.035	0.846	1.267	0.735
Total cholesterol	521	0.964	0.606	1.532	0.875	1.005	0.612	1.651	0.985	521	1.005	0.612	1.651	0.985	503	1.070	0.623	1.837	0.806
Triglycerides	521	0.993	0.753	1.308	0.958	0.986	0.721	1.348	0.929	521	0.986	0.721	1.348	0.929	503	0.978	0.699	1.369	0.899
Sphingomyelins	521	1.155	0.993	1.342	0.061	1.169	0.988	1.383	0.069	520	1.017	0.704	1.468	0.929	503	1.180	0.998	1.395	0.053
Cholines	521	1.224	1.038	1.443	0.017	1.234	1.028	1.482	0.024	520	1.113	0.757	1.637	0.587	503	1.253	1.037	1.515	0.020
Phosphoglycerides	521	1.140	0.811	1.602	0.452	1.129	0.771	1.656	0.533	521	1.129	0.771	1.656	0.533	503	1.193	0.815	1.747	0.364
Tyrosine	521	1.251	0.986	1.588	0.065	1.182	0.910	1.536	0.211	521	1.182	0.910	1.536	0.211	503	1.209	0.916	1.595	0.180
Valine	521	1.228	0.962	1.566	0.099	1.202	0.940	1.537	0.143	519	1.100	0.824	1.468	0.518	503	1.220	0.946	1.573	0.125

Appendix 27: Full results of the metabolomics analysis with knee osteophytes as the outcome.

	Model 1					Model 3				Excluding outliers					Excluding tagged samples				
Outcome	**N**	**OR**	**LCI**	**UCI**	**p**	**OR**	**LCI**	**UCI**	**p**	**N**	**OR**	**LCI**	**UCI**	**P**	**N**	**OR**	**LCI**	**UCI**	**p**
Acetoacetate	599	1.002	0.738	1.360	0.990	1.070	0.750	1.527	0.710	596	1.094	0.652	1.837	0.733	583	1.024	0.698	1.504	0.902
Acetate	593	0.864	0.702	1.064	0.168	0.926	0.609	1.410	0.722	588	1.047	0.530	2.067	0.895	583	0.886	0.536	1.464	0.636
Alanine	601	1.026	0.818	1.286	0.827	0.984	0.741	1.307	0.910	600	0.984	0.741	1.309	0.914	583	0.985	0.723	1.342	0.922
Albumin	601	0.705	0.532	0.933	0.015	0.956	0.691	1.322	0.784	600	0.954	0.687	1.325	0.778	583	0.939	0.666	1.324	0.720
Apolipoprotein A1	601	0.968	0.565	1.661	0.907	1.063	0.594	1.902	0.837	600	1.127	0.630	2.017	0.687	583	1.109	0.594	2.070	0.746
Apolipoprotein B	601	0.976	0.736	1.293	0.863	0.894	0.617	1.296	0.555	600	0.897	0.618	1.301	0.565	583	0.895	0.611	1.312	0.569
Beta hydroxybutyrate	601	1.121	0.890	1.411	0.333	0.968	0.714	1.313	0.836	598	0.857	0.600	1.223	0.394	583	0.962	0.709	1.306	0.804
Citrate	601	1.358	1.072	1.719	0.011	0.965	0.738	1.262	0.797	600	0.970	0.742	1.268	0.824	583	0.978	0.746	1.283	0.874
Creatinine	591	1.171	0.940	1.459	0.160	1.107	0.836	1.465	0.477	590	1.113	0.841	1.471	0.454	583	1.110	0.840	1.468	0.464
Glucose	588	1.011	0.839	1.218	0.908	0.747	0.550	1.016	0.063	587	0.746	0.552	1.009	0.057	583	0.747	0.551	1.011	0.059
Glycoprotein acetyls	601	1.101	0.882	1.374	0.395	0.949	0.699	1.289	0.737	600	0.941	0.691	1.282	0.702	583	0.954	0.694	1.311	0.770
Histidine	601	0.726	0.512	1.029	0.072	0.737	0.512	1.061	0.100	598	0.736	0.496	1.091	0.127	583	0.683	0.465	1.003	0.052
Isoleucine	601	0.848	0.681	1.055	0.139	0.793	0.613	1.025	0.077	600	0.784	0.604	1.016	0.066	583	0.784	0.604	1.017	0.067
Lactate	588	0.903	0.724	1.126	0.364	0.868	0.646	1.166	0.347	585	0.783	0.564	1.089	0.146	583	0.893	0.673	1.183	0.430
Leucine	601	0.925	0.744	1.150	0.483	0.854	0.673	1.084	0.196	600	0.846	0.665	1.077	0.175	583	0.849	0.669	1.077	0.178
Phenylalanine	565	1.127	0.898	1.413	0.303	0.867	0.663	1.132	0.294	562	0.879	0.626	1.232	0.453	551	0.875	0.671	1.142	0.327
Total cholesterol	601	0.944	0.651	1.368	0.759	0.857	0.527	1.393	0.533	600	0.880	0.543	1.424	0.602	583	0.868	0.522	1.442	0.584
Triglycerides	601	0.931	0.742	1.169	0.540	0.882	0.651	1.195	0.419	600	0.873	0.643	1.186	0.386	583	0.883	0.644	1.211	0.441
Sphingomyelins	601	1.043	0.922	1.180	0.499	1.015	0.809	1.274	0.896	598	0.753	0.456	1.242	0.266	583	1.028	0.839	1.260	0.791
Cholines	601	1.075	0.957	1.207	0.223	1.021	0.810	1.288	0.858	598	0.718	0.407	1.266	0.252	583	1.035	0.841	1.272	0.748
Phosphoglycerides	601	1.041	0.755	1.436	0.805	0.784	0.502	1.225	0.285	600	0.793	0.508	1.240	0.310	583	0.805	0.510	1.271	0.352
Tyrosine	601	1.262	1.014	1.572	0.038	0.934	0.733	1.191	0.583	600	0.929	0.728	1.185	0.553	583	0.944	0.737	1.208	0.644
Valine	601	0.974	0.779	1.218	0.817	0.884	0.689	1.134	0.332	598	0.946	0.702	1.275	0.716	583	0.885	0.689	1.136	0.336

Appendix 28: Full results of the metabolomics analysis with knee JSN as the outcome.

	Model 1					Model 3				Excluding outliers					Excluding tagged samples				
Outcome	**N**	**OR**	**LCI**	**UCI**	**p**	**OR**	**LCI**	**UCI**	**P**	**N**	**OR**	**LCI**	**UCI**	**p**	**N**	**OR**	**LCI**	**UCI**	**p**
Acetoacetate	599	0.933	0.530	1.643	0.811	0.914	0.462	1.808	0.797	596	0.946	0.438	2.043	0.887	583	0.946	0.494	1.811	0.866
Acetate	593	0.664	0.318	1.388	0.276	0.530	0.190	1.478	0.225	588	0.533	0.188	1.508	0.235	583	0.581	0.180	1.879	0.364
Alanine	601	1.100	0.852	1.420	0.463	1.068	0.796	1.434	0.660	600	1.060	0.790	1.422	0.699	583	1.104	0.777	1.569	0.582
Albumin	601	0.776	0.523	1.151	0.208	0.972	0.632	1.496	0.897	600	0.973	0.631	1.502	0.902	583	0.957	0.584	1.566	0.861
Apolipoprotein A1	601	0.589	0.292	1.188	0.139	0.520	0.242	1.116	0.093	600	0.533	0.249	1.143	0.106	583	0.541	0.238	1.230	0.143
Apolipoprotein B	601	0.783	0.505	1.214	0.274	0.708	0.401	1.252	0.235	600	0.705	0.398	1.249	0.231	583	0.675	0.351	1.298	0.239
Beta hydroxybutyrate	601	1.009	0.646	1.577	0.968	0.879	0.530	1.456	0.616	598	0.612	0.355	1.054	0.077	583	0.932	0.598	1.454	0.757
Citrate	601	1.559	1.186	2.048	0.001	1.242	0.917	1.683	0.161	600	1.238	0.907	1.689	0.179	583	1.262	0.916	1.740	0.155
Creatinine	591	1.317	1.009	1.719	0.043	1.160	0.842	1.597	0.364	590	1.163	0.844	1.604	0.356	583	1.175	0.846	1.633	0.336
Glucose	588	1.011	0.783	1.306	0.933	0.829	0.568	1.210	0.331	587	0.821	0.562	1.200	0.309	583	0.808	0.546	1.195	0.285
Glycoprotein acetyls	601	1.026	0.773	1.362	0.860	0.991	0.687	1.431	0.962	600	0.986	0.682	1.427	0.942	583	0.984	0.654	1.478	0.937
Histidine	601	0.692	0.411	1.166	0.167	0.701	0.405	1.211	0.203	598	0.696	0.395	1.229	0.212	583	0.654	0.358	1.193	0.166
Isoleucine	601	0.777	0.519	1.161	0.218	0.744	0.452	1.224	0.244	600	0.747	0.453	1.233	0.254	583	0.757	0.448	1.281	0.300
Lactate	588	0.632	0.425	0.940	0.023	0.571	0.357	0.914	0.020	585	0.568	0.351	0.920	0.022	583	0.595	0.377	0.941	0.026
Leucine	601	0.882	0.615	1.265	0.496	0.838	0.552	1.272	0.407	600	0.842	0.553	1.280	0.420	583	0.853	0.542	1.343	0.493
Phenylalanine	565	1.105	0.879	1.388	0.393	0.957	0.736	1.245	0.746	562	1.026	0.677	1.554	0.905	551	0.946	0.719	1.244	0.690
Total cholesterol	601	0.682	0.367	1.270	0.228	0.602	0.280	1.297	0.195	600	0.606	0.282	1.304	0.200	583	0.571	0.233	1.396	0.219
Triglycerides	601	0.826	0.577	1.183	0.297	0.761	0.470	1.235	0.269	600	0.759	0.467	1.231	0.264	583	0.731	0.418	1.279	0.272
Sphingomyelins	601	1.241	1.039	1.483	0.017	1.268	1.030	1.561	0.025	598	0.755	0.437	1.304	0.313	583	1.276	1.041	1.564	0.019
Cholines	601	1.290	1.069	1.557	0.008	1.305	1.057	1.611	0.013	598	0.754	0.398	1.430	0.387	583	1.315	1.069	1.617	0.010
Phosphoglycerides	601	0.943	0.630	1.412	0.775	0.766	0.434	1.352	0.358	600	0.769	0.436	1.357	0.365	583	0.798	0.443	1.437	0.452
Tyrosine	601	1.068	0.817	1.396	0.631	0.851	0.615	1.179	0.333	600	0.851	0.613	1.182	0.336	583	0.864	0.607	1.230	0.417
Valine	601	0.968	0.704	1.332	0.843	0.913	0.650	1.283	0.600	598	0.957	0.630	1.453	0.835	583	0.922	0.639	1.331	0.665

Appendix 29: Full results of the metabolomics analysis with DIP osteophytes as the outcome.

	Model 1					Model 3				Excluding outliers					Excluding tagged samples				
Outcome	**N**	**OR**	**LCI**	**UCI**	**p**	**OR**	**LCI**	**UCI**	**p**	**N**	**OR**	**LCI**	**UCI**	**p**	**N**	**OR**	**LCI**	**UCI**	**p**
Acetoacetate	318	1.043	0.727	1.497	0.817	1.079	0.760	1.531	0.671	317	1.440	0.853	2.431	0.173	310	1.084	0.760	1.547	0.657
Acetate	315	0.968	0.795	1.179	0.748	1.114	0.918	1.351	0.276	313	0.578	0.304	1.099	0.094	310	1.138	0.952	1.360	0.156
Alanine	319	0.914	0.742	1.127	0.400	0.866	0.647	1.158	0.331	319	0.866	0.647	1.158	0.331	310	0.804	0.585	1.104	0.177
Albumin	319	0.737	0.561	0.969	0.029	1.040	0.769	1.408	0.798	319	1.040	0.769	1.408	0.798	310	0.982	0.733	1.317	0.905
Apolipoprotein A1	319	0.550	0.320	0.944	0.030	0.511	0.255	1.024	0.058	319	0.511	0.255	1.024	0.058	310	0.470	0.211	1.047	0.064
Apolipoprotein B	319	0.915	0.657	1.274	0.597	0.884	0.603	1.294	0.526	319	0.884	0.603	1.294	0.526	310	0.835	0.523	1.334	0.451
Beta hydroxybutyrate	319	1.250	0.968	1.614	0.087	1.210	0.901	1.625	0.204	319	1.210	0.901	1.625	0.204	310	1.234	0.913	1.669	0.172
Citrate	319	1.360	1.077	1.719	0.010	0.806	0.602	1.077	0.145	319	0.806	0.602	1.077	0.145	310	0.782	0.588	1.041	0.093
Creatinine	314	1.360	1.041	1.776	0.024	1.056	0.772	1.444	0.734	314	1.056	0.772	1.444	0.734	310	1.056	0.771	1.444	0.736
Glucose	312	1.045	0.773	1.414	0.775	0.809	0.610	1.073	0.142	312	0.809	0.610	1.073	0.142	310	0.807	0.608	1.071	0.138
Glycoprotein acetyls	319	1.013	0.797	1.287	0.919	0.993	0.751	1.313	0.959	319	0.993	0.751	1.313	0.959	310	0.957	0.716	1.279	0.766
Histidine	319	0.975	0.762	1.247	0.840	1.051	0.831	1.328	0.680	318	0.932	0.596	1.455	0.755	310	1.048	0.824	1.333	0.702
Isoleucine	319	1.021	0.817	1.275	0.855	1.054	0.791	1.404	0.718	319	1.054	0.791	1.404	0.718	310	1.045	0.785	1.392	0.763
Lactate	312	0.733	0.568	0.947	0.018	0.657	0.487	0.886	0.006	311	0.546	0.388	0.767	<0.001	310	0.660	0.491	0.889	0.006
Leucine	319	1.036	0.847	1.267	0.732	1.025	0.794	1.322	0.850	319	1.025	0.794	1.322	0.850	310	0.997	0.773	1.287	0.982
Phenylalanine	301	1.115	0.904	1.377	0.309	0.858	0.668	1.102	0.230	300	0.730	0.514	1.037	0.079	294	0.853	0.661	1.101	0.223
Total cholesterol	319	0.809	0.537	1.221	0.313	0.798	0.466	1.368	0.413	319	0.798	0.466	1.368	0.413	310	0.739	0.359	1.522	0.411
Triglycerides	319	1.064	0.801	1.415	0.667	1.100	0.826	1.466	0.514	319	1.100	0.826	1.466	0.514	310	1.093	0.787	1.520	0.595
Sphingomyelins	319	1.344	0.907	1.991	0.141	1.141	0.876	1.487	0.328	318	1.082	0.746	1.569	0.679	310	1.157	0.872	1.537	0.312
Cholines	319	1.292	0.875	1.907	0.197	1.076	0.838	1.383	0.565	318	0.958	0.592	1.549	0.862	310	1.096	0.837	1.436	0.504
Phosphoglycerides	319	0.964	0.642	1.449	0.861	0.807	0.503	1.293	0.372	319	0.807	0.503	1.293	0.372	310	0.810	0.470	1.397	0.449
Tyrosine	319	1.239	0.982	1.563	0.071	0.865	0.664	1.127	0.283	319	0.865	0.664	1.127	0.283	310	0.855	0.651	1.121	0.257
Valine	319	1.069	0.884	1.293	0.489	1.071	0.808	1.421	0.632	318	1.057	0.786	1.420	0.715	310	1.047	0.789	1.390	0.749

Appendix 30: Full results of the metabolomics analysis with CMC osteophytes as the outcome.

	Model 1					Model 3				Excluding outliers					Excluding tagged samples				
Outcome	**N**	**OR**	**LCI**	**UCI**	**p**	**OR**	**LCI**	**UCI**	**p**	**N**	**OR**	**LCI**	**UCI**	**p**	**N**	**OR**	**LCI**	**UCI**	**p**
Acetoacetate	318	0.775	0.565	1.063	0.114	0.777	0.530	1.138	0.195	317	0.810	0.502	1.306	0.388	310	0.800	0.556	1.153	0.232
Acetate	315	1.040	0.880	1.228	0.647	1.142	0.976	1.336	0.098	313	1.193	0.662	2.149	0.558	310	1.162	0.980	1.378	0.084
Alanine	319	1.100	0.845	1.433	0.478	1.087	0.817	1.445	0.567	319	1.087	0.817	1.445	0.567	310	0.983	0.708	1.365	0.919
Albumin	319	0.847	0.683	1.051	0.131	1.087	0.850	1.391	0.506	319	1.087	0.850	1.391	0.506	310	1.039	0.793	1.361	0.781
Apolipoprotein A1	319	0.769	0.446	1.326	0.345	0.797	0.418	1.521	0.492	319	0.797	0.418	1.521	0.492	310	0.556	0.270	1.147	0.112
Apolipoprotein B	319	1.140	0.814	1.598	0.445	1.104	0.766	1.592	0.595	319	1.104	0.766	1.592	0.595	310	0.953	0.611	1.485	0.830
Beta hydroxybutyrate	319	0.911	0.732	1.135	0.407	0.857	0.659	1.115	0.250	319	0.857	0.659	1.115	0.250	310	0.868	0.663	1.137	0.304
Citrate	319	1.101	0.857	1.413	0.452	0.773	0.582	1.027	0.076	319	0.773	0.582	1.027	0.076	310	0.764	0.574	1.018	0.066
Creatinine	314	1.333	0.961	1.850	0.085	1.186	0.795	1.770	0.404	314	1.186	0.795	1.770	0.404	310	1.173	0.785	1.753	0.436
Glucose	312	1.298	0.903	1.867	0.158	1.095	0.816	1.470	0.546	312	1.095	0.816	1.470	0.546	310	1.100	0.819	1.478	0.526
Glycoprotein acetyls	319	1.168	0.924	1.478	0.194	1.155	0.901	1.482	0.255	319	1.155	0.901	1.482	0.255	310	1.118	0.859	1.456	0.405
Histidine	319	0.814	0.624	1.062	0.130	0.864	0.666	1.122	0.274	318	0.957	0.605	1.512	0.849	310	0.826	0.614	1.112	0.208
Isoleucine	319	1.103	0.883	1.377	0.389	1.112	0.851	1.454	0.436	319	1.112	0.851	1.454	0.436	310	1.079	0.825	1.412	0.578
Lactate	312	1.023	0.804	1.302	0.852	1.054	0.806	1.377	0.703	311	1.028	0.767	1.377	0.853	310	1.044	0.800	1.363	0.750
Leucine	319	1.190	0.953	1.487	0.125	1.197	0.908	1.579	0.203	319	1.197	0.908	1.579	0.203	310	1.142	0.859	1.518	0.362
Phenylalanine	301	1.126	0.791	1.602	0.511	0.930	0.704	1.226	0.605	300	1.097	0.769	1.564	0.611	294	0.930	0.706	1.226	0.607
Total cholesterol	319	1.125	0.737	1.716	0.586	1.110	0.683	1.805	0.674	319	1.110	0.683	1.805	0.674	310	0.877	0.447	1.721	0.704
Triglycerides	319	1.206	0.901	1.614	0.208	1.209	0.898	1.629	0.211	319	1.209	0.898	1.629	0.211	310	1.116	0.805	1.546	0.512
Sphingomyelins	319	1.263	0.858	1.859	0.236	1.117	0.807	1.546	0.505	318	0.999	0.663	1.506	0.997	310	1.076	0.793	1.459	0.638
Cholines	319	1.417	0.864	2.322	0.167	1.182	0.815	1.715	0.379	318	1.075	0.694	1.665	0.745	310	1.119	0.791	1.583	0.525
Phosphoglycerides	319	1.398	0.890	2.196	0.146	1.227	0.798	1.887	0.352	319	1.227	0.798	1.887	0.352	310	1.086	0.675	1.747	0.735
Tyrosine	319	1.385	1.027	1.867	0.033	1.142	0.829	1.573	0.417	319	1.142	0.829	1.573	0.417	310	1.102	0.796	1.526	0.559
Valine	319	1.227	0.982	1.532	0.071	1.235	0.929	1.641	0.147	318	1.210	0.901	1.625	0.206	310	1.192	0.888	1.599	0.242

Appendix 31: Full results of the metabolomics analysis with DIP JSN as the outcome.

	Model 1					Model 3				Excluding outliers					Excluding tagged samples				
Outcome	**N**	**OR**	**LCI**	**UCI**	**p**	**OR**	**LCI**	**UCI**	**P**	**N**	**OR**	**LCI**	**UCI**	**p**	**N**	**OR**	**LCI**	**UCI**	**p**
Acetoacetate	318	1.115	0.790	1.574	0.535	1.184	0.836	1.677	0.341	317	1.474	0.945	2.300	0.087	310	1.219	0.841	1.768	0.296
Acetate	315	0.783	0.591	1.037	0.088	0.760	0.463	1.247	0.277	313	0.777	0.426	1.416	0.410	310	0.762	0.441	1.317	0.330
Alanine	319	0.981	0.773	1.244	0.871	0.959	0.734	1.252	0.756	319	0.959	0.734	1.252	0.756	310	0.890	0.660	1.200	0.445
Albumin	319	0.924	0.729	1.172	0.516	1.273	0.981	1.652	0.069	319	1.273	0.981	1.652	0.069	310	1.255	0.933	1.689	0.134
Apolipoprotein A1	319	0.604	0.331	1.104	0.101	0.568	0.287	1.122	0.104	319	0.568	0.287	1.122	0.104	310	0.442	0.230	0.851	0.015
Apolipoprotein B	319	0.746	0.525	1.061	0.103	0.656	0.421	1.020	0.061	319	0.656	0.421	1.020	0.061	310	0.536	0.317	0.906	0.020
Beta hydroxybutyrate	319	1.158	0.938	1.429	0.172	1.124	0.863	1.463	0.387	319	1.124	0.863	1.463	0.387	310	1.165	0.893	1.521	0.261
Citrate	319	1.199	0.966	1.490	0.100	0.823	0.631	1.072	0.149	319	0.823	0.631	1.072	0.149	310	0.797	0.609	1.043	0.098
Creatinine	314	1.198	0.963	1.491	0.105	0.984	0.777	1.247	0.896	314	0.984	0.777	1.247	0.896	310	0.987	0.782	1.246	0.914
Glucose	312	0.879	0.693	1.115	0.289	0.647	0.464	0.903	0.011	312	0.647	0.464	0.903	0.011	310	0.646	0.461	0.905	0.011
Glycoprotein acetyls	319	0.942	0.753	1.180	0.604	0.915	0.697	1.200	0.520	319	0.915	0.697	1.200	0.520	310	0.859	0.634	1.164	0.326
Histidine	319	1.039	0.808	1.336	0.767	1.126	0.898	1.411	0.304	318	0.963	0.631	1.469	0.861	310	1.109	0.880	1.396	0.381
Isoleucine	319	0.836	0.668	1.047	0.118	0.815	0.643	1.033	0.091	319	0.815	0.643	1.033	0.091	310	0.791	0.620	1.010	0.060
Lactate	312	0.905	0.713	1.149	0.413	0.888	0.647	1.217	0.459	311	0.975	0.702	1.353	0.879	310	0.898	0.656	1.229	0.503
Leucine	319	0.883	0.718	1.087	0.241	0.847	0.681	1.052	0.133	319	0.847	0.681	1.052	0.133	310	0.804	0.638	1.014	0.065
Phenylalanine	301	0.950	0.772	1.170	0.631	0.811	0.634	1.037	0.095	300	0.838	0.615	1.142	0.264	294	0.805	0.622	1.042	0.099
Total cholesterol	319	0.652	0.404	1.052	0.080	0.562	0.294	1.076	0.082	319	0.562	0.294	1.076	0.082	310	0.386	0.185	0.803	0.011
Triglycerides	319	0.957	0.723	1.266	0.757	0.945	0.702	1.274	0.712	319	0.945	0.702	1.274	0.712	310	0.888	0.631	1.250	0.497
Sphingomyelins	319	1.342	0.914	1.970	0.133	1.187	0.934	1.507	0.160	318	1.128	0.797	1.597	0.495	310	1.186	0.937	1.501	0.156
Cholines	319	1.350	0.886	2.056	0.162	1.162	0.909	1.486	0.230	318	1.066	0.704	1.614	0.763	310	1.135	0.910	1.415	0.262
Phosphoglycerides	319	0.909	0.617	1.339	0.629	0.737	0.456	1.190	0.212	319	0.737	0.456	1.190	0.212	310	0.644	0.390	1.061	0.084
Tyrosine	319	0.986	0.798	1.219	0.897	0.742	0.582	0.944	0.015	319	0.742	0.582	0.944	0.015	310	0.680	0.535	0.866	0.002
Valine	319	0.911	0.743	1.117	0.368	0.880	0.694	1.115	0.290	318	0.950	0.727	1.243	0.709	310	0.847	0.662	1.085	0.189

Appendix 32: Full results of the metabolomics analysis with CMC JSN as the outcome.

	Model 1					Model 3				Excluding outliers					Excluding tagged samples				
Outcome	**N**	**OR**	**LCI**	**UCI**	**p**	**OR**	**LCI**	**UCI**	**p**	**N**	**OR**	**LCI**	**UCI**	**p**	**N**	**OR**	**LCI**	**UCI**	**P**
Acetoacetate	318	0.916	0.698	1.202	0.528	0.937	0.672	1.306	0.700	317	1.005	0.637	1.585	0.983	310	0.986	0.717	1.357	0.933
Acetate	315	0.872	0.677	1.124	0.290	0.924	0.704	1.215	0.573	313	1.445	0.766	2.725	0.256	310	0.960	0.752	1.225	0.741
Alanine	319	1.168	0.955	1.428	0.131	1.162	0.919	1.469	0.210	319	1.162	0.919	1.469	0.210	310	1.007	0.762	1.331	0.962
Albumin	319	0.850	0.684	1.055	0.140	1.007	0.801	1.267	0.951	319	1.007	0.801	1.267	0.951	310	0.949	0.732	1.229	0.690
Apolipoprotein A1	319	1.670	0.982	2.842	0.058	1.858	1.029	3.355	0.040	319	1.858	1.029	3.355	0.040	310	1.364	0.712	2.612	0.349
Apolipoprotein B	319	1.267	0.966	1.662	0.087	1.284	0.944	1.748	0.111	319	1.284	0.944	1.748	0.111	310	1.044	0.728	1.496	0.816
Beta hydroxybutyrate	319	1.139	0.912	1.424	0.252	1.111	0.864	1.429	0.410	319	1.111	0.864	1.429	0.410	310	1.166	0.890	1.527	0.265
Citrate	319	1.160	0.953	1.413	0.139	0.919	0.728	1.160	0.475	319	0.919	0.728	1.160	0.475	310	0.909	0.712	1.161	0.444
Creatinine	314	1.183	0.923	1.518	0.184	1.040	0.778	1.392	0.790	314	1.040	0.778	1.392	0.790	310	1.040	0.777	1.392	0.792
Glucose	312	1.008	0.804	1.262	0.947	0.875	0.644	1.190	0.396	312	0.875	0.644	1.190	0.396	310	0.881	0.649	1.196	0.417
Glycoprotein acetyls	319	1.030	0.837	1.267	0.783	1.006	0.796	1.272	0.960	319	1.006	0.796	1.272	0.960	310	0.947	0.730	1.229	0.682
Histidine	319	0.849	0.652	1.105	0.224	0.887	0.696	1.130	0.333	318	0.945	0.650	1.372	0.764	310	0.811	0.612	1.074	0.144
Isoleucine	319	0.996	0.800	1.241	0.975	0.984	0.774	1.252	0.898	319	0.984	0.774	1.252	0.898	310	0.950	0.742	1.218	0.688
Lactate	312	1.095	0.878	1.366	0.422	1.115	0.850	1.464	0.431	311	1.091	0.786	1.515	0.601	310	1.111	0.848	1.457	0.444
Leucine	319	1.134	0.943	1.365	0.182	1.118	0.905	1.380	0.301	319	1.118	0.905	1.380	0.301	310	1.049	0.838	1.312	0.679
Phenylalanine	301	1.242	0.997	1.546	0.053	1.138	0.912	1.420	0.251	300	1.080	0.807	1.445	0.603	294	1.135	0.909	1.419	0.264
Total cholesterol	319	1.537	1.057	2.237	0.025	1.607	1.076	2.401	0.020	319	1.607	1.076	2.401	0.020	310	1.225	0.787	1.906	0.369
Triglycerides	319	1.083	0.871	1.347	0.475	1.087	0.849	1.392	0.507	319	1.087	0.849	1.392	0.507	310	0.928	0.695	1.239	0.612
Sphingomyelins	319	1.204	0.942	1.540	0.139	1.142	0.896	1.454	0.283	318	0.982	0.677	1.425	0.925	310	1.089	0.863	1.375	0.471
Cholines	319	1.319	0.941	1.849	0.108	1.216	0.914	1.618	0.178	318	1.087	0.722	1.638	0.688	310	1.131	0.883	1.448	0.331
Phosphoglycerides	319	1.409	1.018	1.951	0.039	1.327	0.950	1.855	0.097	319	1.327	0.950	1.855	0.097	310	1.108	0.765	1.604	0.587
Tyrosine	319	1.276	1.044	1.559	0.017	1.104	0.891	1.367	0.367	319	1.104	0.891	1.367	0.367	310	1.069	0.865	1.321	0.539
Valine	319	1.111	0.931	1.325	0.243	1.078	0.881	1.318	0.468	318	1.048	0.824	1.332	0.703	310	1.034	0.836	1.279	0.757

Appendix 33: Full results of the metabolomics analysis with P1NP as the exposure.

	Model 1					Model 3				Excluding outliers					Excluding tagged samples				
Outcome	**N**	**β**	**LCI**	**UCI**	**p**	**B**	**LCI**	**UCI**	**p**	**N**	**β**	**LCI**	**UCI**	**p**	**N**	**β**	**LCI**	**UCI**	**p**
Acetoacetate	319	-0.060	-0.173	0.053	0.296	-0.061	-0.173	0.051	0.288	318	-0.018	-0.087	0.051	0.606	311	-0.045	-0.137	0.047	0.341
Acetate	316	-0.021	-0.084	0.043	0.522	-0.005	-0.060	0.049	0.851	314	0.012	-0.031	0.055	0.579	311	-0.001	-0.068	0.065	0.974
Alanine	320	0.132	0.005	0.258	0.042	0.140	0.016	0.263	0.027	320	0.158	0.018	0.298	0.027	311	0.136	0.000	0.273	0.050
Albumin	320	0.051	-0.043	0.145	0.284	0.077	-0.015	0.169	0.103	320	0.081	-0.016	0.179	0.103	311	0.082	-0.016	0.180	0.103
Apolipoprotein A1	320	0.007	-0.096	0.111	0.887	0.019	-0.080	0.119	0.703	320	0.009	-0.037	0.054	0.703	311	-0.010	-0.050	0.031	0.640
Apolipoprotein B	320	-0.040	-0.146	0.066	0.457	-0.037	-0.145	0.071	0.501	320	-0.029	-0.114	0.056	0.501	311	-0.063	-0.132	0.006	0.073
Beta hydroxybutyrate	320	-0.011	-0.125	0.103	0.850	-0.015	-0.123	0.093	0.783	320	-0.018	-0.147	0.111	0.783	311	-0.016	-0.147	0.114	0.805
Citrate	320	0.137	0.029	0.245	0.013	0.106	0.004	0.208	0.042	320	0.118	0.004	0.232	0.042	311	0.132	0.014	0.249	0.028
Creatinine	315	0.137	-0.096	0.370	0.250	0.146	-0.057	0.349	0.160	315	0.170	-0.067	0.406	0.160	311	0.172	-0.069	0.413	0.163
Glucose	313	0.012	-0.102	0.126	0.835	0.006	-0.097	0.108	0.916	313	0.006	-0.107	0.119	0.916	311	0.007	-0.105	0.120	0.898
Glycoprotein acetyls	320	-0.040	-0.131	0.051	0.386	-0.034	-0.121	0.053	0.438	320	-0.038	-0.135	0.058	0.438	311	-0.036	-0.133	0.060	0.460
Histidine	320	0.003	-0.097	0.104	0.951	0.009	-0.093	0.110	0.865	319	0.023	-0.080	0.126	0.661	311	-0.002	-0.109	0.106	0.977
Isoleucine	320	0.110	-0.079	0.300	0.253	0.121	-0.067	0.309	0.207	320	0.135	-0.074	0.344	0.207	311	0.134	-0.080	0.348	0.219
Lactate	313	0.018	-0.093	0.129	0.748	0.031	-0.080	0.142	0.585	312	0.031	-0.093	0.156	0.625	311	0.033	-0.095	0.160	0.615
Leucine	320	0.139	-0.054	0.333	0.159	0.152	-0.037	0.341	0.116	320	0.172	-0.042	0.387	0.116	311	0.172	-0.047	0.391	0.123
Phenylalanine	302	0.100	-0.028	0.228	0.125	0.088	-0.034	0.211	0.158	301	0.103	-0.045	0.252	0.173	295	0.114	-0.032	0.261	0.126
Total cholesterol	320	-0.017	-0.123	0.088	0.747	-0.014	-0.124	0.095	0.796	320	-0.008	-0.072	0.055	0.796	311	-0.039	-0.085	0.008	0.102
Triglycerides	320	-0.039	-0.149	0.071	0.488	-0.029	-0.136	0.078	0.595	320	-0.029	-0.137	0.079	0.595	311	-0.062	-0.162	0.037	0.222
Sphingomyelins	320	-0.004	-0.089	0.081	0.931	-0.013	-0.102	0.075	0.771	319	-0.005	-0.099	0.088	0.915	311	-0.031	-0.130	0.068	0.538
Cholines	320	0.003	-0.085	0.090	0.954	-0.007	-0.098	0.084	0.883	319	0.002	-0.086	0.090	0.972	311	-0.024	-0.117	0.070	0.620
Phosphoglycerides	320	-0.012	-0.136	0.112	0.852	-0.014	-0.138	0.109	0.819	320	-0.010	-0.093	0.073	0.819	311	-0.034	-0.115	0.047	0.406
Tyrosine	320	0.102	-0.059	0.263	0.215	0.087	-0.064	0.237	0.258	320	0.100	-0.074	0.274	0.258	311	0.097	-0.078	0.272	0.276
Valine	320	0.159	-0.025	0.343	0.090	0.173	-0.010	0.355	0.063	319	0.111	-0.038	0.259	0.144	311	0.205	-0.009	0.419	0.060

Appendix 34: Full results of the metabolomics analysis with osteocalcin as the exposure.

	Model 1					Model 3				Excluding outliers					Excluding tagged samples				
Outcome	**N**	**β**	**LCI**	**UCI**	**p**	**B**	**LCI**	**UCI**	**p**	**N**	**β**	**LCI**	**UCI**	**p**	**N**	**β**	**LCI**	**UCI**	**p**
Acetoacetate	319	-0.008	-0.127	0.110	0.891	-0.020	-0.143	0.104	0.755	318	0.011	-0.065	0.087	0.782	311	-0.008	-0.101	0.086	0.873
Acetate	316	-0.033	-0.086	0.021	0.229	-0.018	-0.067	0.031	0.480	314	0.003	-0.031	0.037	0.859	311	-0.015	-0.068	0.037	0.565
Alanine	320	0.020	-0.093	0.134	0.725	0.042	-0.067	0.150	0.453	320	0.044	-0.071	0.158	0.453	311	0.013	-0.095	0.121	0.811
Albumin	320	0.021	-0.077	0.119	0.670	0.036	-0.066	0.138	0.486	320	0.036	-0.064	0.135	0.486	311	0.045	-0.050	0.140	0.355
Apolipoprotein A1	320	-0.036	-0.158	0.087	0.567	-0.022	-0.141	0.096	0.710	320	-0.010	-0.060	0.041	0.710	311	-0.020	-0.064	0.025	0.385
Apolipoprotein B	320	-0.094	-0.200	0.012	0.082	-0.079	-0.187	0.030	0.154	320	-0.057	-0.136	0.022	0.154	311	-0.077	-0.134	-0.020	0.008
Beta hydroxybutyrate	320	0.033	-0.102	0.169	0.628	0.037	-0.095	0.169	0.584	320	0.041	-0.105	0.187	0.584	311	0.041	-0.105	0.188	0.580
Citrate	320	0.158	0.051	0.265	0.004	0.136	0.034	0.239	0.009	320	0.142	0.035	0.248	0.009	311	0.150	0.042	0.259	0.007
Creatinine	315	0.170	-0.042	0.381	0.116	0.187	0.003	0.371	0.047	315	0.203	0.003	0.402	0.047	311	0.200	-0.001	0.401	0.051
Glucose	313	-0.064	-0.167	0.038	0.220	-0.051	-0.135	0.034	0.242	313	-0.052	-0.138	0.035	0.242	311	-0.053	-0.140	0.034	0.232
Glycoprotein acetyls	320	-0.067	-0.177	0.043	0.234	-0.035	-0.140	0.071	0.518	320	-0.036	-0.145	0.073	0.518	311	-0.019	-0.123	0.086	0.728
Histidine	320	0.032	-0.073	0.137	0.550	0.038	-0.066	0.142	0.474	319	0.009	-0.079	0.097	0.846	311	0.026	-0.074	0.127	0.607
Isoleucine	320	-0.047	-0.206	0.113	0.565	-0.023	-0.175	0.130	0.772	320	-0.023	-0.181	0.135	0.772	311	-0.021	-0.183	0.141	0.801
Lactate	313	-0.123	-0.212	-0.034	0.007	-0.105	-0.193	-0.017	0.020	312	-0.096	-0.184	-0.008	0.033	311	-0.115	-0.210	-0.021	0.017
Leucine	320	-0.042	-0.180	0.096	0.549	-0.019	-0.148	0.111	0.778	320	-0.020	-0.157	0.117	0.778	311	-0.012	-0.152	0.128	0.868
Phenylalanine	302	0.012	-0.109	0.132	0.851	0.027	-0.082	0.136	0.630	301	0.046	-0.072	0.163	0.448	295	0.027	-0.095	0.150	0.661
Total cholesterol	320	-0.053	-0.164	0.058	0.352	-0.041	-0.157	0.075	0.490	320	-0.022	-0.085	0.041	0.490	311	-0.040	-0.081	0.001	0.053
Triglycerides	320	-0.124	-0.226	-0.021	0.018	-0.102	-0.198	-0.005	0.039	320	-0.096	-0.187	-0.005	0.039	311	-0.112	-0.186	-0.038	0.003
Sphingomyelins	320	0.020	-0.057	0.097	0.607	0.006	-0.069	0.082	0.871	319	0.007	-0.070	0.085	0.852	311	-0.003	-0.079	0.073	0.938
Cholines	320	0.006	-0.074	0.086	0.885	-0.003	-0.082	0.076	0.938	319	-0.002	-0.077	0.072	0.948	311	-0.012	-0.084	0.061	0.748
Phosphoglycerides	320	-0.068	-0.184	0.049	0.256	-0.053	-0.168	0.062	0.369	320	-0.033	-0.106	0.039	0.369	311	-0.046	-0.111	0.018	0.157
Tyrosine	320	-0.060	-0.173	0.053	0.296	-0.054	-0.159	0.050	0.309	320	-0.058	-0.170	0.054	0.309	311	-0.064	-0.174	0.047	0.258
Valine	320	-0.034	-0.171	0.103	0.628	-0.007	-0.138	0.124	0.915	319	0.003	-0.136	0.142	0.964	311	0.003	-0.142	0.148	0.968

Appendix 35: Full results of the metabolomics analysis with β-CTX as the exposure.

	Model 1					Model 3				Excluding outliers					Excluding tagged samples				
Outcome	**N**	**B**	**LCI**	**UCI**	**p**	**B**	**LCI**	**UCI**	**P**	**N**	**β**	**LCI**	**UCI**	**p**	**N**	**β**	**LCI**	**UCI**	**p**
Acetoacetate	319	0.062	-0.074	0.199	0.373	0.057	-0.083	0.197	0.424	318	0.073	-0.026	0.171	0.147	311	0.049	-0.063	0.161	0.388
Acetate	316	-0.033	-0.070	0.004	0.077	-0.005	-0.047	0.037	0.815	314	-0.016	-0.052	0.021	0.393	311	-0.002	-0.052	0.048	0.945
Alanine	320	-0.077	-0.166	0.013	0.093	-0.056	-0.147	0.036	0.233	320	-0.062	-0.163	0.040	0.233	311	-0.074	-0.175	0.027	0.152
Albumin	320	-0.030	-0.128	0.067	0.543	0.018	-0.085	0.121	0.730	320	0.019	-0.088	0.125	0.730	311	0.032	-0.072	0.135	0.548
Apolipoprotein A1	320	-0.081	-0.177	0.015	0.098	-0.059	-0.152	0.035	0.218	320	-0.026	-0.068	0.015	0.218	311	-0.031	-0.071	0.009	0.128
Apolipoprotein B	320	-0.126	-0.209	-0.042	0.003	-0.118	-0.207	-0.029	0.009	320	-0.091	-0.159	-0.023	0.009	311	-0.093	-0.159	-0.028	0.005
Beta hydroxybutyrate	320	0.179	0.010	0.348	0.038	0.174	0.008	0.341	0.040	320	0.203	0.009	0.398	0.040	311	0.212	0.018	0.406	0.032
Citrate	320	0.235	0.113	0.357	<0.001	0.185	0.071	0.300	0.002	320	0.203	0.078	0.329	0.002	311	0.199	0.072	0.327	0.002
Creatinine	315	0.053	-0.087	0.194	0.456	0.078	-0.053	0.210	0.241	315	0.090	-0.060	0.239	0.241	311	0.096	-0.053	0.246	0.205
Glucose	313	-0.095	-0.190	0.001	0.051	-0.097	-0.182	-0.011	0.026	313	-0.104	-0.196	-0.012	0.026	311	-0.102	-0.193	-0.011	0.028
Glycoprotein acetyls	320	-0.050	-0.143	0.042	0.286	-0.041	-0.133	0.051	0.386	320	-0.044	-0.145	0.056	0.386	311	-0.033	-0.132	0.065	0.508
Histidine	320	-0.055	-0.136	0.025	0.180	-0.048	-0.133	0.037	0.265	319	-0.033	-0.113	0.048	0.423	311	-0.051	-0.137	0.036	0.254
Isoleucine	320	-0.076	-0.200	0.047	0.226	-0.051	-0.174	0.072	0.413	320	-0.056	-0.190	0.078	0.413	311	-0.050	-0.187	0.087	0.474
Lactate	313	-0.086	-0.181	0.010	0.079	-0.065	-0.155	0.025	0.159	312	-0.063	-0.162	0.036	0.214	311	-0.075	-0.178	0.027	0.148
Leucine	320	-0.071	-0.178	0.036	0.196	-0.046	-0.156	0.063	0.409	320	-0.051	-0.174	0.071	0.409	311	-0.041	-0.165	0.083	0.518
Phenylalanine	302	-0.008	-0.111	0.095	0.877	-0.028	-0.126	0.070	0.575	301	-0.004	-0.103	0.094	0.930	295	-0.039	-0.152	0.074	0.496
Total cholesterol	320	-0.076	-0.151	0.000	0.051	-0.068	-0.153	0.016	0.114	320	-0.039	-0.087	0.009	0.114	311	-0.042	-0.088	0.004	0.070
Triglycerides	320	-0.148	-0.227	-0.070	<0.001	-0.129	-0.209	-0.049	0.002	320	-0.128	-0.208	-0.049	0.002	311	-0.129	-0.205	-0.052	0.001
Sphingomyelins	320	-0.016	-0.084	0.052	0.651	-0.035	-0.107	0.037	0.341	319	-0.021	-0.096	0.055	0.590	311	-0.037	-0.117	0.043	0.362
Cholines	320	-0.031	-0.093	0.032	0.336	-0.048	-0.116	0.019	0.158	319	-0.033	-0.096	0.030	0.308	311	-0.048	-0.116	0.019	0.160
Phosphoglycerides	320	-0.095	-0.174	-0.016	0.018	-0.095	-0.180	-0.010	0.029	320	-0.063	-0.119	-0.006	0.029	311	-0.063	-0.120	-0.007	0.028
Tyrosine	320	-0.071	-0.173	0.030	0.169	-0.096	-0.196	0.003	0.057	320	-0.109	-0.221	0.003	0.057	311	-0.099	-0.212	0.013	0.083
Valine	320	-0.066	-0.188	0.055	0.284	-0.040	-0.166	0.085	0.529	319	-0.017	-0.149	0.114	0.795	311	-0.033	-0.178	0.112	0.656

Appendix 36: ICD codes for exclusion of controls in analyses of hospital-diagnosed OA in UK Biobank.

ICD10									**ICD9**			
M111*	M152	M189	M228	M2329	M236	M240*	M2485	M4952	712	7172	7224	7367
M112*	M153	M19	M229	M233	M2360	M241*	M2486	M4953	7121	7173	7225	7368
M118*	M154	M190*	M23	M2330	M2361	M242*	M2489	M4954	7122	7174	7226	7369
M119*	M158	M191*	M230	M2331	M2362	M243	M249	M4955	7123	7175	7229	7543
M13	M159	M192*	M2300	M2332	M2363	M2430	M2490	M4956	7128*	7176	723	75430
M130	M1599	M198*	M2301	M2333	M2364	M2434	M2494	M4957	7129*	7178	7230	75431
M1300	M16	M199*	M2302	M2334	M2365	M2435	M2495	M4958	715	7179	7231	75432
M1305	M160	M20	M2303	M2335	M2366	M2436	M2496	M4959	7150	718	7295*	7544
M1306	M161	M200	M2304	M2336	M2367	M2439	M2499	M498*	7151*	7180*	73100	75440
M1309	M162	M210	M2305	M2337	M2369	M244	M25	M50	7152*	7181*	73101	75441
M131	M163	M2100	M2306	M2339	M238	M2440	M255*	M501	7153*	7182*	73102	75442
M1310	M164	M2105	M2307	M234	M2380	M2444	M256*	M502	7158	7183*	73103	75443
M1314	M165	M2106	M2309	M2340	M2381	M2445	M257*	M503	7159	7184*	73104	75444
M1315	M166	M2109	M231	M2341	M2382	M2446	M258*	M508	7161*	7185*	732	7545
M1316	M167	M211	M2310	M2342	M2383	M2449	M259*	M509	7165	7186*	7320	75450
M1319	M169	M2110	M2311	M2343	M2384	M245	M42	M51	71650	7188*	7321	75451
M138	M17	M2115	M2312	M2344	M2385	M2450	M420*	M949*	71654	7189*	7322	75452
M1380	M170	M2116	M2314	M2345	M2386	M2454	M421*	Q65*	71655	7192*	7323	75453
M1384	M171	M2119	M2315	M2346	M2387	M2455	M429*	V134	71656	7194*	7324	75459
M1385	M172	M212	M2316	M2347	M2389	M2456	M472*	V135	71659	7195*	7325	7546
M1386	M173	M2120	M2317	M2349	M239	M2459	M478*	V136	7166	7196*	7326	75460
M1389	M174	M2124	M2319	M235	M2390	M246	M479	M21	71660	7197	7327*	75461
M139	M175	M2125	M232	M2350	M2391	M2460	M4790		71664	7198*	7328*	75469
M1390	M179	M2126	M2320	M2351	M2392	M2464	M4791		71665	7199*	7329	835
M1394	M18	M2129	M2321	M2352	M2393	M2465	M4792		71666	7200	7339*	8350
M1395	M180	M22	M2322	M2353	M2394	M2466	M4793		71669	721*	736	8351
M1396	M181	M220	M2323	M2354	M2395	M2469	M4794		7168*	722	7362	836
M1399	M182	M221	M2324	M2355	M2396	M247*	M4795		7169*	7220	7363	8360
M15	M183	M222	M2325	M2356	M2397	M248	M4796		717	7221	7364	8361
M150	M184	M223	M2326	M2357	M2399	M2480	M4797		7170	7222	7365	8362
M151	M185	M224	M2327	M2359	M24	M2484	M4798		7171	7223	7366	8366

Represents a wildtype number from 1 to 9.

Appendix 37: Summary statistics for the eBMD SNPs used for two-sample MR analyses.

		Exposure=BMD					Outcome= hip OA					Outcome= knee OA					Outcome=BMI				
SNP	**EA**	**Estrada**	**EAF**	**Beta**	**SE**	**p**	**EAF**	**Beta**	**SE**	**p**	**passed Steiger filtering**	**EAF**	**Beta**	**SE**	**P**	**passed Steiger filtering**	**EAF**	**Beta**	**SE**	**p**	**passed Steiger filtering**
rs10015974	A	0	0.24	0.010	0.002	5.50E-09	0.242	-0.008	0.013	5.58E-01	T	0.246	0.010	0.010	3.26E-01	T	0.3083	0.003	0.004	5.25E-01	T
rs10057211	A	0	0.91	-0.030	0.003	8.40E-18	0.891	0.018	0.018	3.18E-01	T	0.893	0.026	0.015	7.04E-02	T					
rs10145299	T	0	0.51	-0.020	0.002	7.60E-27	0.512	0.010	0.011	3.66E-01	T	0.519	-0.016	0.009	6.85E-02	T	0.5417	0.004	0.004	2.92E-01	T
rs10147522	A	0	0.66	-0.010	0.002	5.00E-09	0.652	-0.022	0.012	6.11E-02	T	0.657	-0.001	0.009	8.86E-01	T	0.7167	0.007	0.004	7.19E-02	T
rs10206992	T	0	0.75	0.020	0.002	5.30E-17	0.733	-0.009	0.013	4.61E-01	T	0.729	0.011	0.010	2.86E-01	T	0.7417	0.004	0.004	2.95E-01	T
rs10239787	C	0	0.67	0.030	0.002	0.00E+00	0.660	-0.019	0.012	1.02E-01	T	0.655	0.001	0.009	8.91E-01	T	0.6083	0.007	0.004	6.35E-02	T
rs10407062	T	0	0.55	0.010	0.002	2.60E-11	0.537	0.011	0.011	3.09E-01	T	0.537	-0.018	0.009	4.76E-02	T	0.5083	-0.003	0.004	4.15E-01	T
rs1042704	G	0	0.78	0.030	0.002	5.20E-28	0.800	-0.007	0.014	6.47E-01	T	0.800	-0.013	0.011	2.37E-01	T	0.75	0.006	0.006	2.78E-01	T
rs1043003	T	0	0.62	0.020	0.002	3.60E-12	0.613	0.011	0.012	3.34E-01	T	0.609	-0.006	0.010	5.21E-01	T	0.6333	0.003	0.004	4.61E-01	T
rs10462395	A	0	0.8	-0.010	0.002	1.60E-05	0.802	0.009	0.014	5.21E-01	T	0.790	-0.013	0.011	2.54E-01	T	0.8333	-0.009	0.005	7.32E-02	T
rs10473868	G	0	0.57	0.010	0.002	1.30E-08	0.556	0.011	0.012	3.63E-01	T	0.557	0.020	0.010	3.83E-02	T	0.5417	0.004	0.004	2.56E-01	T
rs10490046	A	0	0.78	0.030	0.002	7.00E-30	0.761	0.007	0.013	5.67E-01	T	0.759	-0.008	0.010	4.39E-01	T	0.7917	-0.002	0.004	5.85E-01	T
rs10515269	C	0	0.52	-0.020	0.002	3.60E-15											0.625	-0.006	0.004	8.37E-02	T
rs10750766	C	0	0.29	-0.030	0.002	3.60E-27	0.284	0.007	0.012	5.70E-01	T	0.291	-0.004	0.010	7.09E-01	T					
rs10756762	T	0	0.59	-0.020	0.002	2.50E-21	0.589	-0.004	0.012	7.02E-01	T	0.592	-0.007	0.010	4.88E-01	T	0.525	0.006	0.004	9.73E-02	T
rs10764201	C	0	0.48	-0.020	0.002	4.60E-19	0.480	0.006	0.011	5.83E-01	T	0.486	-0.009	0.009	2.93E-01	T	0.45	-0.009	0.004	1.61E-02	T
rs10765568	C	0	0.63	0.020	0.002	2.70E-15	0.639	0.016	0.012	1.65E-01	T	0.633	-0.006	0.009	5.13E-01	T	0.6083	-0.012	0.004	3.18E-03	T
rs10779795	A	0	0.66	0.020	0.002	4.40E-22	0.658	0.022	0.012	7.24E-02	T	0.657	0.010	0.009	3.11E-01	T	0.6667	0.010	0.004	1.24E-02	T
rs10792352	C	0	0.29	-0.010	0.002	3.50E-03	0.296	0.010	0.012	3.97E-01	T	0.306	0.014	0.010	1.58E-01	T					
rs10800531	A	0	0.54	-0.030	0.002	4.50E-35											0.5847	-0.003	0.004	4.45E-01	T
rs10817896	C	0	0.73	-0.020	0.002	3.70E-10	0.718	-0.008	0.012	5.42E-01	T	0.716	0.000	0.010	9.86E-01	T	0.7083	0.002	0.004	5.52E-01	T
rs10842704	T	0	0.76	-0.030	0.002	3.40E-28	0.728	0.015	0.013	2.21E-01	T	0.723	0.017	0.010	8.33E-02	T	0.8167	0.009	0.004	6.46E-03	T
rs10885434	G	0	0.28	0.020	0.002	9.80E-23	0.285	-0.007	0.013	6.01E-01	T	0.297	-0.016	0.011	1.21E-01	T					
rs10893348	C	0	0.56	-0.020	0.002	8.60E-13	0.559	-0.008	0.011	5.02E-01	T	0.564	-0.011	0.009	2.09E-01	T					
rs10917477	A	0	0.52	-0.010	0.002	1.70E-13	0.515	-0.020	0.011	6.96E-02	T	0.522	0.006	0.009	5.33E-01	T	0.5667	0.002	0.004	5.52E-01	T
rs10920352	T	0	0.58	-0.010	0.002	4.00E-10	0.553	0.012	0.012	3.00E-01	T	0.549	0.011	0.009	2.27E-01	T	0.5678	-0.002	0.004	6.53E-01	T
rs10931982	T	0	0.23	-0.050	0.002	0.00E+00	0.204	-0.013	0.015	3.98E-01	T	0.205	0.005	0.013	6.62E-01	T	0.3	0.005	0.008	5.10E-01	T
rs10956974	C	0	0.78	-0.030	0.002	4.00E-27	0.741	-0.005	0.013	6.87E-01	T	0.747	-0.012	0.010	2.46E-01	T	0.7333	0.004	0.004	3.64E-01	T
rs10980517	A	0	0.53	-0.020	0.002	5.40E-13	0.514	0.003	0.011	7.92E-01	T	0.512	-0.002	0.009	7.93E-01	T					
rs11067228	A	0	0.55	-0.020	0.002	2.10E-16	0.568	-0.009	0.012	4.19E-01	T	0.565	0.001	0.009	9.01E-01	T	0.525	-0.001	0.004	8.12E-01	T
rs11073930	G	0	0.45	-0.020	0.002	1.10E-27											0.3583	0.003	0.004	4.66E-01	T
rs11088458	A	0	0.29	0.040	0.002	0.00E+00	0.279	0.002	0.013	8.65E-01	T	0.295	0.001	0.010	9.33E-01	T					
rs11142400	G	0	0.67	-0.010	0.002	2.20E-09	0.644	-0.009	0.012	4.53E-01	T	0.647	-0.004	0.010	7.17E-01	T					
rs11175835	G	0	0.29	0.020	0.002	2.10E-22	0.255	-0.011	0.013	3.96E-01	T	0.264	0.012	0.011	2.89E-01	T	0.325	-0.002	0.004	7.21E-01	T
rs11196170	G	0	0.79	0.030	0.002	2.90E-31	0.799	-0.002	0.015	8.94E-01	T	0.781	-0.007	0.012	5.87E-01	T					
rs112073168	G	0	0.97	0.040	0.006	9.00E-10	0.972	-0.008	0.036	8.15E-01	T	0.973	-0.043	0.029	1.33E-01	T					
rs11228240	C	1	0.72	0.040	0.002	0.00E+00	0.738	0.001	0.013	9.71E-01	T	0.738	0.027	0.010	7.88E-03	T	0.7667	0.001	0.004	8.89E-01	T
rs11238526	A	0	0.94	-0.020	0.004	1.20E-06	0.940	0.015	0.026	5.64E-01	T	0.926	0.009	0.019	6.53E-01	T	0.9083	0.000	0.007	9.96E-01	T
rs11238756	T	0	0.55	-0.010	0.002	5.50E-10	0.539	-0.014	0.011	2.10E-01	T	0.534	-0.006	0.009	4.84E-01	T	0.6333	0.001	0.004	7.05E-01	T
rs112766772	T	0	0.77	-0.020	0.002	3.30E-10	0.782	-0.020	0.018	2.59E-01	T	0.783	0.012	0.017	4.79E-01	T					
rs1133400	A	0	0.78	-0.030	0.002	4.60E-34	0.788	0.020	0.014	1.68E-01	T	0.789	0.013	0.012	2.57E-01	T	NA	-0.012	0.008	1.48E-01	T
rs11576308	G	0	0.39	-0.020	0.002	2.70E-15	0.385	-0.072	0.012	5.87E-09	F	0.384	-0.010	0.010	2.85E-01	T	0.3833	-0.001	0.004	7.72E-01	T
rs11587434	G	0	0.74	-0.010	0.002	1.00E-06	0.745	-0.010	0.014	4.63E-01	T	0.739	-0.031	0.011	4.79E-03	F	NA	-0.024	0.004	2.53E-11	F

rs1159798	A	0	0.22	0.060	0.002	0.00E+00	0.225	-0.011	0.014	4.29E-01	T	0.231	-0.013	0.011	2.25E-01	T	0.2417	0.001	0.006	8.44E-01	T
rs116228246	G	0	0.98	-0.090	0.006	0.00E+00	0.977	-0.005	0.038	8.92E-01	T	0.979	-0.009	0.032	7.80E-01	T					
rs11643240	A	0	0.73	0.020	0.002	2.10E-12	0.749	0.019	0.013	1.37E-01	T	0.737	-0.023	0.010	2.06E-02	T	0.7083	-0.010	0.004	1.33E-02	T
rs116504838	G	0	0.97	-0.030	0.006	1.50E-06	0.976	0.040	0.037	2.80E-01	T	0.975	0.025	0.029	3.94E-01	T					
rs11668064	A	0	0.69	0.030	0.002	0.00E+00	0.709	0.005	0.013	7.16E-01	T	0.699	0.014	0.010	1.81E-01	T	0.7583	-0.003	0.004	4.54E-01	T
rs11670562	T	0	0.74	-0.010	0.002	3.00E-11	0.742	-0.002	0.013	8.56E-01	T	0.740	-0.011	0.010	2.87E-01	T					
rs11675489	A	0	0.54	0.010	0.002	1.30E-09	0.562	0.015	0.011	1.91E-01	T	0.561	-0.018	0.009	4.16E-02	T	0.4833	-0.002	0.004	5.52E-01	T
rs11679303	C	0	0.78	0.010	0.002	8.40E-09	0.771	0.001	0.013	9.18E-01	T	0.774	-0.004	0.011	6.74E-01	T	0.7417	-0.002	0.004	5.70E-01	T
rs11688492	T	0	0.54	0.010	0.002	2.30E-11	0.557	0.011	0.012	3.62E-01	T	0.557	0.001	0.010	9.23E-01	T					
rs11696009	A	0	0.66	-0.020	0.002	2.30E-14	0.671	-0.009	0.012	4.76E-01	T	0.675	-0.004	0.009	6.86E-01	T	0.6083	-0.001	0.004	8.61E-01	T
rs117111740	T	0	0.97	0.110	0.006	0.00E+00	0.965	0.024	0.034	4.90E-01	T	0.969	0.036	0.030	2.28E-01	T					
rs11729023	C	0	0.88	-0.030	0.003	1.30E-14	0.879	-0.013	0.017	4.49E-01	T	0.880	-0.002	0.014	8.64E-01	T	0.8583	-0.008	0.006	1.75E-01	T
rs11743474	A	0	0.84	0.020	0.003	4.80E-09	0.836	-0.018	0.016	2.42E-01	T	0.840	0.000	0.013	9.75E-01	T	0.8083	0.003	0.005	6.24E-01	T
rs117481343	C	0	0.97	-0.130	0.006	0.00E+00	0.967	0.064	0.034	6.35E-02	T	0.971	0.037	0.029	1.95E-01	T					
rs118115924	G	0	0.99	0.200	0.009	0.00E+00	0.988	-0.013	0.057	8.26E-01	T	0.989	0.023	0.050	6.46E-01	T					
rs11814082	T	0	0.82	-0.010	0.002	2.30E-05	0.825	-0.019	0.015	2.02E-01	T	0.820	-0.022	0.012	6.05E-02	T	0.8167	0.000	0.005	9.84E-01	T
rs11880992	G	0	0.59	0.020	0.002	2.20E-15	0.595	0.037	0.012	1.37E-03	T	0.582	-0.017	0.009	6.23E-02	T	0.625	-0.002	0.004	6.36E-01	T
rs11881367	G	0	0.91	-0.100	0.003	0.00E+00	0.908	0.046	0.020	1.97E-02	T	0.903	0.004	0.015	8.18E-01	T	0.9083	0.000	0.005	9.83E-01	T
rs11915970	A	0	0.88	-0.040	0.003	0.00E+00	0.868	-0.035	0.017	3.55E-02	T	0.872	0.001	0.013	9.65E-01	T	0.875	-0.009	0.006	1.05E-01	T
rs11934731	G	1	0.32	0.040	0.002	0.00E+00	0.312	0.003	0.012	7.99E-01	T	0.313	0.000	0.010	9.88E-01	T	0.3417	-0.007	0.004	8.22E-02	T
rs1206755	C	0	0.53	-0.020	0.002	1.90E-15											0.5	-0.005	0.004	1.44E-01	T
rs12228756	G	0	0.93	-0.030	0.004	5.10E-13	0.937	0.025	0.023	2.75E-01	T	0.922	0.010	0.018	5.88E-01	T	0.95	-0.008	0.008	3.30E-01	T
rs12251299	C	0	0.87	0.100	0.003	0.00E+00	0.865	0.002	0.017	8.81E-01	T	0.864	-0.004	0.013	7.68E-01	T	0.8333	0.004	0.006	5.46E-01	T
rs12452440	T	0	0.42	-0.020	0.002	5.60E-21	0.424	0.005	0.012	6.76E-01	T	0.421	0.005	0.010	5.74E-01	T					
rs12462380	A	0	0.58	-0.010	0.002	1.00E-05	0.561	-0.012	0.012	2.92E-01	T	0.564	-0.002	0.009	8.25E-01	T					
rs12487905	T	0	0.79	-0.010	0.002	4.80E-08	0.803	-0.001	0.014	9.34E-01	T	0.797	-0.010	0.011	3.82E-01	T	0.8	0.005	0.005	2.97E-01	T
rs12534970	A	0	0.51	-0.010	0.002	6.00E-09	0.500	-0.007	0.012	5.45E-01	T	0.497	0.008	0.010	4.32E-01	T					
rs12545602	C	0	0.87	-0.020	0.003	8.40E-13	0.866	-0.030	0.017	6.81E-02	T	0.869	0.005	0.013	6.77E-01	T	0.875	-0.001	0.006	8.58E-01	T
rs12616772	A	0	0.35	0.010	0.002	5.50E-09	0.337	-0.014	0.012	2.33E-01	T	0.342	0.002	0.009	8.41E-01	T	0.3417	-0.005	0.003	1.14E-01	T
rs12673062	G	0	0.78	-0.010	0.002	6.80E-06	0.782	-0.021	0.014	1.35E-01	T	0.785	-0.002	0.011	8.71E-01	T	0.7833	-0.002	0.005	7.44E-01	T
rs12756373	A	0	0.91	-0.020	0.003	1.80E-10	0.905	-0.014	0.020	4.95E-01	T	0.914	-0.003	0.017	8.82E-01	T	0.8917	-0.004	0.009	6.58E-01	T
rs12811685	C	0	0.66	0.020	0.002	1.70E-14	0.672	-0.013	0.013	3.33E-01	T	0.671	0.007	0.010	5.21E-01	T	0.725	-0.005	0.004	2.40E-01	T
rs1286075	C	1	0.83	-0.030	0.002	3.00E-30	0.824	-0.045	0.015	2.47E-03	T	0.813	-0.016	0.011	1.55E-01	T	0.7917	-0.007	0.005	1.23E-01	T
rs1286662	A	0	0.82	0.020	0.002	8.20E-16	0.820	0.006	0.014	6.82E-01	T	0.816	0.010	0.012	3.86E-01	T	0.8417	0.000	0.005	9.35E-01	T
rs12942736	C	0	0.76	0.020	0.002	3.80E-23	0.776	0.001	0.016	9.42E-01	T	0.780	0.018	0.015	2.19E-01	T	0.725	-0.005	0.005	2.59E-01	T
rs12945403	T	0	0.34	0.020	0.002	6.20E-17	0.333	0.006	0.012	6.00E-01	T	0.342	0.009	0.010	3.62E-01	T					
rs13002567	T	0	0.67	-0.020	0.002	5.60E-17	0.663	0.014	0.012	2.54E-01	T	0.670	0.016	0.009	9.03E-02	T	0.6583	-0.002	0.004	6.35E-01	T
rs13070996	G	0	0.72	0.010	0.002	9.70E-10	0.703	0.007	0.013	5.65E-01	T	0.697	0.003	0.010	7.63E-01	T	0.6917	0.005	0.004	2.62E-01	T
rs13072536	A	0	0.78	-0.020	0.002	2.20E-09	0.761	-0.036	0.013	6.27E-03	T	0.752	-0.014	0.010	1.76E-01	T	0.8	-0.011	0.004	8.02E-03	T
rs13088318	A	0	0.66	-0.020	0.002	9.20E-12	0.662	-0.012	0.012	3.32E-01	T	0.664	0.009	0.010	3.84E-01	T	0.6833	0.006	0.004	1.54E-01	T
rs13179493	T	0	0.71	-0.030	0.002	0.00E+00	0.728	-0.003	0.015	8.42E-01	T	0.726	-0.004	0.014	7.39E-01	T	0.7333	0.001	0.005	8.70E-01	T
rs13201764	T	0	0.85	-0.030	0.003	4.30E-20	0.857	0.020	0.016	2.08E-01	T	0.854	0.013	0.013	3.06E-01	T	0.8083	-0.003	0.005	5.21E-01	T
rs13220896	G	0	0.96	0.040	0.005	1.00E-11	0.962	0.022	0.038	5.60E-01	T	0.962	-0.010	0.030	7.42E-01	T					
rs13225158	G	0	0.65	0.010	0.002	2.70E-05	0.655	0.001	0.012	9.30E-01	T	0.659	-0.006	0.009	5.14E-01	T	0.6167	0.000	0.004	9.20E-01	T
rs13334558	T	0	0.21	-0.020	0.002	1.70E-13	0.200	0.013	0.016	4.18E-01	T	0.197	0.006	0.014	6.83E-01	T	0.2333	0.001	0.005	8.28E-01	T
rs134613	T	0	0.35	0.040	0.002	0.00E+00	0.359	0.005	0.012	6.61E-01	T	0.353	0.005	0.009	5.73E-01	T	0.2833	-0.001	0.004	8.81E-01	T
rs1386625	A	0	0.1	0.050	0.003	0.00E+00	0.086	-0.046	0.021	2.86E-02	T	0.081	-0.025	0.017	1.50E-01	T	0.0917	-0.017	0.007	1.17E-02	T
rs139603701	A	0	0.98	0.110	0.007	0.00E+00	0.984	0.007	0.048	8.88E-01	T	0.985	-0.021	0.041	6.18E-01	T					
rs1414660	C	0	0.81	-0.080	0.002	0.00E+00	0.811	0.008	0.014	5.80E-01	T	0.799	-0.005	0.011	6.24E-01	T	0.8417	0.001	0.006	8.16E-01	T

rs1428968	C	0	0.82	-0.020	0.002	7.20E-19	0.822	-0.028	0.015	6.16E-02	T	0.825	-0.009	0.012	4.30E-01	T	0.875	-0.009	0.005	6.25E-02	T
rs142971131	G	0	0.99	0.120	0.010	1.00E-21	0.977	-0.066	0.050	1.85E-01	T	0.980	-0.032	0.046	4.87E-01	T					
rs144412371	C	0	0.96	0.040	0.005	6.60E-13	0.968	-0.060	0.036	1.02E-01	T	0.967	-0.029	0.029	3.26E-01	T					
rs144832051	C	0	0.98	-0.180	0.006	0.00E+00	0.973	0.029	0.037	4.40E-01	T	0.975	-0.045	0.031	1.52E-01	T					
rs1463598	C	0	0.64	-0.020	0.002	2.30E-13	0.609	0.002	0.012	8.57E-01	T	0.600	0.013	0.009	1.72E-01	T	0.5833	0.002	0.004	6.34E-01	T
rs1475120	G	0	0.45	-0.010	0.002	1.60E-10	0.465	0.017	0.011	1.33E-01	T	0.453	-0.001	0.009	9.04E-01	T	0.5167	-0.004	0.004	2.84E-01	T
rs1502199	A	0	0.25	0.020	0.002	2.40E-16	0.264	0.015	0.013	2.22E-01	T	0.267	-0.005	0.010	6.29E-01	T	0.3083	-0.006	0.004	1.53E-01	T
rs150445982	C	0	0.98	-0.100	0.006	2.00E-36	0.978	0.020	0.041	6.28E-01	T	0.979	-0.038	0.034	2.55E-01	T					
rs1548607	A	0	0.67	0.020	0.002	1.10E-14	0.674	0.007	0.013	5.87E-01	T	0.675	0.002	0.010	8.87E-01	T	0.7	-0.001	0.005	8.38E-01	T
rs1550270	T	0	0.7	-0.020	0.002	7.30E-15	0.687	0.009	0.012	4.60E-01	T	0.682	0.005	0.009	6.17E-01	T	0.6917	-0.003	0.004	4.24E-01	T
rs1575667	A	0	0.12	0.020	0.003	1.40E-13	0.113	0.002	0.018	9.17E-01	T	0.120	-0.006	0.014	6.47E-01	T	0.175	0.011	0.006	6.05E-02	T
rs1581630	C	0	0.23	0.020	0.002	2.10E-19	0.242	0.043	0.013	8.74E-04	T	0.257	0.012	0.010	2.52E-01	T	0.2417	-0.002	0.004	6.93E-01	T
rs167365	C	0	0.38	0.020	0.002	1.90E-15	0.359	0.002	0.012	8.75E-01	T	0.363	-0.013	0.009	1.64E-01	T	0.3559	0.006	0.004	1.40E-01	T
rs16878921	G	0	0.9	-0.030	0.003	3.80E-26	0.898	-0.034	0.019	6.31E-02	T	0.899	-0.020	0.015	1.78E-01	T	0.875	0.002	0.006	7.59E-01	T
rs17010957	T	0	0.85	-0.030	0.003	1.10E-28	0.851	-0.023	0.016	1.43E-01	T	0.853	0.006	0.013	6.41E-01	T	0.9167	-0.004	0.004	4.35E-01	T
rs17035323	G	0	0.84	0.020	0.002	6.20E-14	0.842	0.005	0.015	7.56E-01	T	0.840	-0.001	0.012	9.29E-01	T	0.8583	-0.005	0.005	3.17E-01	T
rs1706708	G	1	0.67	0.030	0.002	0.00E+00	0.687	0.002	0.012	8.74E-01	T	0.691	0.006	0.010	5.63E-01	T					
rs17173698	G	0	0.97	-0.050	0.006	9.70E-15	0.979	0.031	0.040	4.36E-01	T	0.979	0.009	0.032	7.73E-01	T	0.9569	-0.013	0.017	4.49E-01	T
rs17265513	T	0	0.8	0.030	0.002	4.70E-36	0.789	0.018	0.014	1.96E-01	T	0.791	0.008	0.011	4.95E-01	T	0.8417	0.001	0.004	7.42E-01	T
rs1736213	T	0	0.44	0.010	0.002	6.30E-11	0.419	0.008	0.011	4.59E-01	T	0.423	0.015	0.009	8.69E-02	T	0.4417	0.004	0.004	2.69E-01	T
rs17507577	G	0	0.93	-0.060	0.004	0.00E+00	0.911	0.019	0.020	3.47E-01	T	0.913	0.010	0.016	5.23E-01	T	0.9417	-0.004	0.008	5.99E-01	T
rs17514738	T	0	0.6	0.020	0.002	7.00E-21	0.579	0.004	0.011	7.26E-01	T	0.584	-0.010	0.009	2.54E-01	T	0.6167	0.002	0.004	5.45E-01	T
rs1777277	C	0	0.55	0.010	0.002	7.50E-09	0.538	-0.004	0.011	6.88E-01	T	0.545	0.005	0.009	5.83E-01	T	0.3966	-0.003	0.003	4.01E-01	T
rs1904398	A	0	0.49	-0.020	0.002	1.50E-15	0.517	0.002	0.011	8.48E-01	T	0.508	0.000	0.009	9.73E-01	T	0.5	-0.002	0.003	4.22E-01	T
rs1907310	G	0	0.17	0.020	0.002	9.40E-15	0.180	-0.017	0.015	2.51E-01	T	0.200	0.021	0.012	8.64E-02	T	0.1333	-0.005	0.005	3.07E-01	T
rs1991431	G	0	0.56	0.020	0.002	2.40E-16	0.562	-0.008	0.011	4.55E-01	T	0.575	-0.021	0.009	2.29E-02	T	0.5167	-0.007	0.004	7.45E-02	T
rs2052480	G	0	0.71	-0.030	0.002	3.60E-31	0.719	0.009	0.012	4.65E-01	T	0.717	0.004	0.010	6.96E-01	T	0.7167	0.007	0.004	1.11E-01	T
rs2069442	G	0	0.75	0.020	0.002	1.60E-16	0.702	-0.002	0.012	8.46E-01	T	0.714	-0.010	0.010	3.19E-01	T	0.775	0.001	0.004	8.91E-01	T
rs2091624	G	0	0.9	0.030	0.003	1.50E-12	0.900	0.010	0.019	5.83E-01	T	0.881	-0.005	0.014	7.04E-01	T	0.925	0.002	0.006	7.59E-01	T
rs2095931	A	0	0.16	-0.020	0.003	6.10E-13	0.147	0.004	0.016	8.02E-01	T	0.145	-0.020	0.013	1.33E-01	T	0.125	-0.005	0.006	4.22E-01	T
rs210374	A	0	0.27	-0.010	0.002	2.30E-09	0.300	0.011	0.013	3.81E-01	T	0.309	0.007	0.011	5.25E-01	T	0.25	-0.001	0.004	9.05E-01	T
rs212417	G	0	0.33	0.030	0.002	0.00E+00	0.351	0.007	0.012	5.25E-01	T	0.358	-0.003	0.009	7.43E-01	T	0.375	-0.004	0.004	3.17E-01	T
rs215226	A	0	0.6	-0.020	0.002	4.00E-32	0.597	-0.007	0.011	5.68E-01	T	0.598	-0.024	0.009	7.39E-03	T	0.6333	0.006	0.004	1.10E-01	T
rs2153672	C	0	0.9	-0.020	0.003	1.60E-10	0.900	-0.001	0.019	9.51E-01	T	0.900	0.006	0.015	7.07E-01	T	0.9167	-0.004	0.006	5.25E-01	T
rs2174633	A	0	0.26	-0.020	0.002	3.70E-11	0.264	0.000	0.013	9.76E-01	T	0.267	0.008	0.010	4.33E-01	T	0.3417	0.000	0.004	9.43E-01	T
rs2204015	C	0	0.21	0.010	0.002	2.00E-09	0.202	0.015	0.015	3.10E-01	T	0.219	-0.001	0.012	9.28E-01	T	0.225	-0.005	0.005	2.68E-01	T
rs2216949	C	0	0.88	-0.030	0.003	1.40E-19	0.844	0.001	0.016	9.30E-01	T	0.835	0.004	0.012	7.28E-01	T	0.8667	0.000	0.005	9.85E-01	T
rs2227607	C	0	0.89	0.020	0.003	1.60E-09	0.900	0.007	0.019	7.25E-01	T	0.898	-0.009	0.015	5.34E-01	T	0.85	0.009	0.006	1.19E-01	T
rs2235485	A	0	0.84	0.020	0.002	4.80E-16	0.850	-0.001	0.016	9.61E-01	T	0.850	0.023	0.013	7.54E-02	T	0.8	-0.005	0.005	3.27E-01	T
rs2271329	G	0	0.81	-0.040	0.002	0.00E+00	0.792	-0.030	0.014	3.00E-02	T	0.802	0.011	0.011	3.33E-01	T	0.8417	-0.006	0.005	1.97E-01	T
rs2303696	T	0	0.62	-0.020	0.002	2.00E-14	0.619	-0.005	0.012	6.90E-01	T	0.625	0.002	0.010	8.38E-01	T	0.65	-0.003	0.004	4.68E-01	T
rs2375683	G	0	0.75	0.010	0.002	2.70E-10	0.742	-0.002	0.013	8.70E-01	T	0.738	0.005	0.010	6.09E-01	T	0.7833	0.002	0.005	6.96E-01	T
rs2423151	G	0	0.35	0.040	0.002	0.00E+00	0.352	0.032	0.012	6.19E-03	T	0.343	0.017	0.009	7.24E-02	T	0.3667	-0.001	0.004	8.61E-01	T
rs2430689	C	0	0.61	0.020	0.002	3.00E-16	0.622	0.033	0.012	4.67E-03	T	0.623	0.021	0.009	2.12E-02	T	0.6417	0.002	0.004	6.17E-01	T
rs2442599	G	0	0.28	-0.020	0.002	1.20E-10	0.269	-0.002	0.013	8.98E-01	T	0.273	-0.009	0.010	3.91E-01	T	0.2667	-0.010	0.004	1.73E-02	T
rs2491105	T	0	0.77	-0.020	0.002	9.40E-21	0.773	-0.016	0.014	2.51E-01	T	0.780	-0.013	0.011	2.36E-01	T					
rs2546984	T	0	0.22	0.010	0.002	3.70E-08	0.221	-0.008	0.014	5.66E-01	T	0.219	0.005	0.011	6.44E-01	T	0.1583	0.000	0.005	1.00E+00	T
rs2553772	T	0	0.46	-0.030	0.002	0.00E+00	0.459	0.009	0.011	4.11E-01	T	0.451	0.006	0.009	4.88E-01	T	0.3917	-0.002	0.004	5.17E-01	T
rs2566752	T	1	0.62	-0.040	0.002	0.00E+00	0.616	-0.042	0.012	2.99E-04	T	0.616	-0.006	0.009	5.04E-01	T					

rs2566774	T	0	0.19	0.040	0.002	0.00E+00	0.184	0.015	0.014	2.81E-01	T	0.185	0.010	0.012	3.62E-01	T	0.1379	-0.002	0.005	7.39E-01	T
rs2639953	G	0	0.48	0.030	0.002	0.00E+00	0.479	0.001	0.011	9.30E-01	T	0.481	0.010	0.009	2.42E-01	T	0.4667	-0.004	0.004	2.80E-01	T
rs2647462	T	0	0.17	0.030	0.002	4.60E-38	0.167	0.014	0.015	3.74E-01	T	0.168	0.019	0.012	1.15E-01	T	0.1897	0.002	0.005	7.29E-01	T
rs2653559	C	0	0.84	0.030	0.002	2.50E-26	0.848	0.009	0.016	5.88E-01	T	0.827	0.010	0.012	4.13E-01	T	NA	0.004	0.008	6.30E-01	T
rs2707518	G	1	0.61	-0.170	0.002	0.00E+00	0.631	0.002	0.012	8.92E-01	T	0.618	-0.002	0.009	7.90E-01	T	0.625	-0.004	0.004	2.95E-01	T
rs2737252	G	1	0.72	-0.030	0.002	0.00E+00	0.718	-0.007	0.012	5.58E-01	T	0.724	-0.002	0.010	8.27E-01	T	0.725	0.010	0.003	2.63E-03	T
rs2741856	G	1	0.92	-0.070	0.003	0.00E+00	0.911	-0.055	0.020	5.81E-03	T	0.916	-0.019	0.017	2.69E-01	T	0.9083	-0.002	0.007	8.03E-01	T
rs2761884	G	0	0.55	0.050	0.002	0.00E+00	0.558	0.022	0.011	5.54E-02	T	0.567	0.027	0.009	3.16E-03	T	0.55	-0.001	0.004	8.95E-01	T
rs2830913	G	0	0.56	-0.020	0.002	2.30E-30	0.573	0.000	0.011	9.77E-01	T	0.573	0.008	0.009	3.56E-01	T	0.65	-0.001	0.003	8.04E-01	T
rs28362709	G	0	0.77	0.040	0.002	0.00E+00	0.790	0.033	0.015	2.45E-02	T	0.791	0.010	0.012	3.67E-01	T					
rs28364580	G	0	0.75	0.020	0.002	1.00E-19	0.755	0.008	0.013	5.44E-01	T	0.751	-0.003	0.010	7.44E-01	T					
rs28373428	G	0	0.86	-0.020	0.003	8.80E-15	0.854	-0.013	0.016	4.16E-01	T	0.853	-0.027	0.013	2.99E-02	T					
rs28498618	G	0	0.79	0.020	0.002	9.30E-15	0.783	-0.012	0.014	3.98E-01	T	0.790	-0.001	0.011	9.09E-01	T	0.7	-0.002	0.004	7.16E-01	T
rs28732148	C	0	0.93	-0.020	0.004	6.40E-08	0.939	0.044	0.029	1.26E-01	T	0.925	0.019	0.022	3.82E-01	T	0.9333	-0.018	0.008	3.62E-02	T
rs2929308	T	0	0.49	0.040	0.002	0.00E+00											0.475	0.009	0.004	1.55E-02	T
rs2944590	G	0	0.56	-0.020	0.002	5.40E-24	0.557	0.003	0.011	7.94E-01	T	0.557	0.009	0.009	3.24E-01	T					
rs3118906	G	0	0.72	-0.030	0.002	7.30E-35	0.737	0.013	0.013	3.05E-01	T	0.733	0.026	0.010	9.67E-03	T	0.7583	0.004	0.003	2.65E-01	T
rs3127084	G	0	0.48	0.010	0.002	3.90E-08	0.487	-0.023	0.012	4.93E-02	T	0.488	-0.003	0.009	7.53E-01	T	0.45	0.004	0.004	2.58E-01	T
rs34123233	T	0	0.82	-0.020	0.002	3.60E-17	0.837	0.014	0.016	3.86E-01	T	0.831	-0.005	0.013	7.10E-01	T	0.9	0.009	0.004	3.86E-02	T
rs34324915	A	0	0.64	-0.020	0.002	6.00E-21	0.651	0.016	0.012	1.60E-01	T	0.651	0.011	0.009	2.60E-01	T					
rs34396633	C	0	NA	-0.160	0.018	6.60E-13	0.977	-0.127	0.068	5.95E-02	T	0.873	-0.117	0.050	1.78E-02	F	0.975	-0.021	0.011	5.30E-02	T
rs344078	C	0	0.83	0.040	0.002	0.00E+00	0.824	0.011	0.015	4.70E-01	T	0.822	-0.011	0.012	3.58E-01	T	0.8417	-0.006	0.005	2.11E-01	T
rs34553872	A	1	0.82	-0.060	0.002	0.00E+00	0.835	-0.013	0.015	3.94E-01	T	0.831	0.016	0.012	1.90E-01	T	0.875	0.004	0.005	4.19E-01	T
rs34583478	C	0	0.92	0.040	0.003	3.50E-19	0.930	0.001	0.022	9.74E-01	T	0.930	0.021	0.018	2.40E-01	T					
rs35264941	G	0	0.98	0.060	0.007	1.20E-11	0.983	0.020	0.045	6.59E-01	T	0.977	-0.013	0.034	6.93E-01	T	0.9667	-0.006	0.014	6.83E-01	T
rs35308216	T	0	0.92	0.060	0.003	0.00E+00	0.924	-0.023	0.022	2.84E-01	T	0.916	0.000	0.017	9.83E-01	T					
rs35531047	T	1	0.78	-0.050	0.002	0.00E+00	0.767	-0.011	0.014	4.31E-01	T	0.769	0.002	0.011	8.36E-01	T	0.7417	-0.006	0.005	1.92E-01	T
rs36010930	T	0	0.72	-0.010	0.002	2.70E-10	0.719	-0.007	0.013	5.51E-01	T	0.705	-0.020	0.010	4.37E-02	T					
rs36016056	G	0	0.75	-0.020	0.002	2.90E-13	0.735	-0.002	0.013	8.61E-01	T	0.742	0.017	0.010	9.31E-02	T	0.7583	0.000	0.004	9.63E-01	T
rs368510	G	0	0.67	-0.020	0.002	1.30E-29	0.653	-0.003	0.014	8.39E-01	T	0.659	0.019	0.013	1.26E-01	T	0.6917	0.001	0.004	9.05E-01	T
rs370387	G	1	0.44	-0.050	0.002	0.00E+00	0.459	-0.008	0.011	4.52E-01	T	0.466	-0.015	0.009	8.89E-02	T	NA	-0.006	0.006	3.66E-01	T
rs3740861	G	0	0.7	-0.010	0.002	8.40E-07	0.707	0.000	0.012	9.93E-01	T	0.713	0.012	0.010	2.19E-01	T	0.725	-0.003	0.004	4.21E-01	T
rs3760456	C	0	0.56	0.020	0.002	1.30E-26	0.551	-0.016	0.011	1.61E-01	T	0.559	-0.009	0.009	3.37E-01	T	0.5833	-0.007	0.004	8.24E-02	T
rs3763745	A	0	0.75	-0.010	0.002	6.30E-09	0.757	-0.009	0.013	4.86E-01	T	0.757	0.014	0.010	1.95E-01	T	0.7167	-0.001	0.004	7.80E-01	T
rs3765971	C	0	0.35	-0.030	0.002	1.90E-37	0.343	-0.007	0.012	5.45E-01	T	0.330	-0.018	0.009	5.23E-02	T	0.3333	0.005	0.004	2.11E-01	T
rs3790608	G	0	0.85	-0.040	0.003	0.00E+00	0.864	0.028	0.016	8.89E-02	T	0.860	-0.003	0.013	8.17E-01	T					
rs3801427	C	0	0.24	-0.030	0.002	0.00E+00	0.227	-0.014	0.013	2.81E-01	T	0.233	-0.019	0.011	6.93E-02	T	0.2583	-0.010	0.004	2.56E-02	T
rs3829849	C	0	0.63	-0.010	0.002	4.60E-14	0.644	0.049	0.012	3.71E-05	F	0.647	-0.025	0.009	7.36E-03	T	0.675	-0.015	0.003	2.17E-06	T
rs3848474	G	0	0.56	-0.020	0.002	1.80E-11	0.572	0.018	0.012	1.34E-01	T	0.576	0.013	0.009	1.71E-01	T					
rs4081747	G	0	0.38	0.010	0.002	2.80E-10	0.383	0.009	0.012	4.33E-01	T	0.384	0.007	0.009	4.39E-01	T	0.375	0.000	0.004	9.46E-01	T
rs4233949	C	0	0.39	0.070	0.002	0.00E+00	0.372	0.014	0.012	2.35E-01	T	0.376	0.004	0.009	7.06E-01	T	0.3917	0.003	0.004	4.77E-01	T
rs42916	C	0	0.26	-0.020	0.002	7.30E-17	0.231	0.019	0.013	1.48E-01	T	0.249	0.039	0.010	1.68E-04	T	0.2083	0.002	0.004	5.70E-01	T
rs4360494	G	0	0.44	-0.020	0.002	2.50E-23											0.4483	-0.006	0.003	5.64E-02	T
rs4418639	G	0	0.41	0.020	0.002	1.70E-13	0.391	0.001	0.011	9.24E-01	T	0.390	0.001	0.009	8.85E-01	T	0.45	0.000	0.003	9.13E-01	T
rs4496284	G	0	0.57	-0.020	0.002	2.50E-19	0.576	0.014	0.011	2.17E-01	T	0.577	0.008	0.009	3.96E-01	T					
rs4505759	C	1	0.69	-0.060	0.002	0.00E+00	0.693	-0.004	0.012	7.32E-01	T	0.695	-0.018	0.010	6.30E-02	T	0.675	-0.007	0.005	1.60E-01	T
rs45573936	T	0	0.97	0.040	0.006	3.00E-11	0.972	-0.065	0.035	5.86E-02	T	0.973	-0.038	0.029	1.87E-01	T					
rs4635400	G	1	0.64	0.050	0.002	0.00E+00	0.640	-0.013	0.012	2.69E-01	T	0.626	-0.025	0.009	7.61E-03	T	0.6	0.002	0.004	5.45E-01	T
rs4664604	C	0	0.17	-0.020	0.002	3.30E-11	0.159	0.025	0.015	1.10E-01	T	0.169	-0.013	0.012	2.86E-01	T	0.1833	-0.003	0.005	6.17E-01	T

rs4669522	T	0	0.21	-0.020	0.002	1.90E-10	0.191	-0.017	0.014	2.40E-01	T	0.187	-0.001	0.012	9.16E-01	T	0.1583	-0.011	0.005	2.72E-02	T
rs4683184	G	0	0.36	-0.010	0.002	5.00E-10	0.374	0.009	0.012	4.44E-01	T	0.370	0.003	0.009	7.32E-01	T	0.3583	-0.013	0.004	5.13E-04	T
rs4739697	A	0	0.34	0.020	0.002	3.70E-18	0.331	-0.009	0.012	4.45E-01	T	0.324	-0.009	0.010	3.27E-01	T	0.325	0.000	0.004	9.20E-01	T
rs4743930	C	0	0.75	-0.030	0.002	3.80E-35	0.746	-0.009	0.013	4.59E-01	T	0.740	0.026	0.010	1.10E-02	T	0.675	-0.013	0.004	2.31E-03	T
rs4782351	A	0	0.39	0.010	0.002	4.00E-13	0.382	-0.002	0.012	8.41E-01	T	0.396	-0.002	0.009	8.26E-01	T					
rs4806862	G	0	0.67	-0.020	0.002	2.30E-22	0.657	0.008	0.012	4.89E-01	T	0.652	-0.003	0.010	7.83E-01	T	0.6917	0.005	0.004	2.52E-01	T
rs4821797	T	0	0.67	0.020	0.002	6.80E-24	0.662	0.023	0.012	5.92E-02	T	0.654	-0.007	0.009	4.65E-01	T	0.6667	0.001	0.004	7.64E-01	T
rs482339	C	0	0.69	0.070	0.002	0.00E+00	0.689	-0.003	0.012	8.11E-01	T	0.677	-0.003	0.010	7.20E-01	T	0.6583	-0.002	0.004	6.43E-01	T
rs4849701	T	0	0.48	0.020	0.002	3.90E-17	0.468	0.007	0.011	5.40E-01	T	0.481	0.000	0.009	9.64E-01	T	0.45	-0.004	0.004	2.58E-01	T
rs4876858	G	0	0.21	0.020	0.002	4.40E-19	0.205	0.011	0.015	4.38E-01	T	0.219	-0.007	0.012	5.64E-01	T	0.125	-0.005	0.005	2.59E-01	T
rs4878008	C	0	0.61	0.010	0.002	8.80E-10	0.608	0.008	0.012	4.72E-01	T	0.622	-0.002	0.009	8.59E-01	T	0.6083	0.000	0.004	9.79E-01	T
rs4912085	G	0	0.43	0.020	0.002	1.10E-21											0.4661	-0.001	0.004	7.32E-01	T
rs4964511	T	0	0.49	0.010	0.002	4.50E-10	0.504	-0.018	0.011	1.21E-01	T	0.486	-0.004	0.009	6.40E-01	T	NA	0.019	0.007	6.52E-03	F
rs4979905	C	0	0.82	0.030	0.002	5.60E-24	0.819	-0.035	0.015	1.68E-02	T	0.798	-0.027	0.012	1.66E-02	T	0.7917	-0.008	0.005	1.04E-01	T
rs55787537	T	0	0.83	0.030	0.002	1.00E-19	0.833	-0.015	0.016	3.46E-01	T	0.832	0.018	0.013	1.89E-01	T					
rs56225285	A	0	0.7	-0.020	0.002	1.70E-17	0.681	0.002	0.014	8.76E-01	T	0.688	0.014	0.013	2.67E-01	T					
rs56240884	C	0	0.71	-0.020	0.002	5.50E-23	0.716	-0.027	0.014	4.73E-02	T	0.711	-0.006	0.011	5.55E-01	T	0.6333	-0.014	0.004	8.33E-04	T
rs56320441	T	0	0.91	-0.020	0.003	5.20E-12	0.914	-0.042	0.020	3.78E-02	T	0.913	0.012	0.016	4.72E-01	T					
rs56682471	A	1	0.79	-0.030	0.002	7.20E-30	0.781	-0.020	0.013	1.38E-01	T	0.781	-0.018	0.011	9.70E-02	T	0.8417	0.007	0.005	1.28E-01	T
rs56940811	C	0	0.93	-0.030	0.004	1.10E-08	0.932	-0.015	0.025	5.34E-01	T	0.902	-0.005	0.018	8.00E-01	T					
rs57043009	C	0	0.85	-0.050	0.003	0.00E+00	0.844	-0.003	0.015	8.40E-01	T	0.843	-0.001	0.012	9.49E-01	T	0.8583	0.001	0.005	8.75E-01	T
rs571356	G	0	0.68	0.020	0.002	1.40E-12	0.691	-0.036	0.012	3.12E-03	T	0.688	-0.024	0.010	1.33E-02	T	0.6667	0.001	0.004	9.03E-01	T
rs5735	T	0	0.69	0.020	0.002	8.10E-16	0.679	-0.006	0.012	6.05E-01	T	0.681	-0.006	0.010	5.49E-01	T	0.7167	0.001	0.004	8.84E-01	T
rs5754387	G	0	0.8	0.020	0.002	1.20E-09	0.788	-0.004	0.014	7.82E-01	T	0.781	-0.009	0.011	3.89E-01	T	0.8583	-0.015	0.005	9.52E-04	T
rs5770908	G	0	0.67	0.020	0.002	7.10E-19	0.664	0.016	0.012	1.85E-01	T	0.662	-0.002	0.010	8.23E-01	T	0.6833	0.004	0.004	3.53E-01	T
rs603424	G	0	0.83	0.030	0.002	4.80E-27	0.842	-0.005	0.016	7.38E-01	T	0.826	0.002	0.013	9.07E-01	T	0.8	0.002	0.004	7.33E-01	T
rs6086143	A	0	0.56	0.000	0.002	3.50E-01	0.578	0.014	0.011	1.97E-01	F	0.567	-0.006	0.009	4.91E-01	F	0.6167	-0.002	0.004	4.99E-01	T
rs60891864	C	0	0.6	-0.030	0.002	0.00E+00	0.584	0.031	0.012	7.22E-03	T	0.587	0.004	0.009	6.64E-01	T	0.5667	-0.005	0.004	1.63E-01	T
rs6117294	T	0	0.6	0.020	0.002	2.60E-13	0.596	-0.025	0.012	2.67E-02	T	0.595	-0.011	0.009	2.25E-01	T	0.6083	0.002	0.004	5.63E-01	T
rs6120804	C	0	0.82	-0.030	0.002	1.30E-22	0.814	-0.012	0.014	4.09E-01	T	0.811	0.003	0.011	7.95E-01	T	0.8	-0.006	0.005	2.09E-01	T
rs6129493	A	0	0.72	0.010	0.002	5.30E-09	0.731	-0.013	0.013	3.26E-01	T	0.735	0.012	0.010	2.38E-01	T	0.75	0.004	0.004	2.84E-01	T
rs61733768	G	0	0.97	0.080	0.006	7.70E-36	0.963	0.027	0.030	3.77E-01	T	0.965	-0.004	0.025	8.76E-01	T	0.975	-0.002	0.008	8.20E-01	T
rs61780429	T	0	0.78	0.020	0.002	2.40E-13	0.788	-0.021	0.014	1.35E-01	T	0.790	-0.032	0.011	4.46E-03	T	0.7963	-0.004	0.005	3.84E-01	T
rs6185	C	0	0.75	0.020	0.002	5.50E-16	0.728	-0.027	0.013	4.49E-02	T	0.725	0.012	0.011	2.68E-01	T	0.775	0.000	0.004	9.64E-01	T
rs61998565	G	0	0.85	0.020	0.003	1.40E-07	0.849	-0.008	0.018	6.50E-01	T	0.847	0.005	0.017	7.60E-01	T	0.8583	0.001	0.006	9.31E-01	T
rs62007684	T	0	0.66	0.040	0.002	0.00E+00	0.645	0.029	0.012	1.40E-02	T	0.643	0.018	0.009	5.48E-02	T	0.625	0.014	0.004	3.18E-04	T
rs62182131	G	0	0.92	0.030	0.003	6.40E-13	0.914	-0.036	0.021	8.13E-02	T	0.918	-0.002	0.017	8.99E-01	T	0.8917	0.010	0.007	1.57E-01	T
rs62271373	T	0	0.94	-0.030	0.004	1.50E-12	0.955	-0.019	0.028	4.98E-01	T	0.955	0.023	0.022	3.10E-01	T					
rs62302300	C	0	0.84	0.020	0.003	1.50E-14	0.850	0.008	0.016	6.15E-01	T	0.846	0.020	0.013	1.01E-01	T	0.8083	-0.008	0.005	1.36E-01	T
rs62321667	G	0	0.88	0.020	0.003	3.80E-13	0.896	-0.007	0.018	7.09E-01	T	0.891	0.001	0.014	9.47E-01	T					
rs62453057	A	0	0.82	-0.020	0.002	1.20E-16	0.808	0.005	0.015	7.50E-01	T	0.819	0.012	0.012	3.06E-01	T	0.7833	0.000	0.005	9.35E-01	T
rs630539	C	0	0.05	-0.030	0.004	3.30E-09	0.057	-0.002	0.025	9.41E-01	T	0.055	-0.006	0.020	7.51E-01	T	0.0333	-0.001	0.009	9.26E-01	T
rs6471752	C	0	0.85	0.020	0.003	5.20E-14	0.837	-0.018	0.015	2.40E-01	T	0.833	0.024	0.012	4.09E-02	T	0.7833	-0.004	0.005	4.80E-01	T
rs6485702	T	1	0.34	0.030	0.002	0.00E+00	0.343	-0.001	0.012	9.49E-01	T	0.344	0.002	0.009	8.22E-01	T	0.225	-0.002	0.003	4.72E-01	T
rs6542920	A	0	0.35	-0.010	0.002	6.60E-10	0.353	-0.027	0.012	2.33E-02	T	0.356	-0.015	0.009	1.06E-01	T	0.3	-0.003	0.004	5.00E-01	T
rs6546334	C	0	0.66	0.020	0.002	1.40E-16	0.638	-0.019	0.012	1.07E-01	T	0.640	-0.024	0.009	8.56E-03	T	0.6833	0.001	0.004	8.61E-01	T
rs6564890	C	0	0.46	0.020	0.002	6.80E-28	0.471	0.010	0.011	3.56E-01	T	0.478	0.010	0.009	2.46E-01	T	0.4417	-0.002	0.003	5.53E-01	T
rs6583866	T	0	0.46	0.010	0.002	2.10E-11											0.4917	-0.002	0.004	6.08E-01	T
rs660240	T	0	0.22	0.010	0.002	4.10E-09	0.216	0.039	0.013	3.82E-03	T	0.213	0.008	0.011	4.80E-01	T	0.2845	0.006	0.004	9.16E-02	T

rs6664489	G	0	0.22	-0.010	0.002	1.30E-08	0.237	0.015	0.013	2.51E-01	T	0.233	0.010	0.011	3.41E-01	T	0.2167	0.003	0.004	4.53E-01	T
rs6716216	A	0	0.88	-0.030	0.003	1.20E-25	0.874	-0.017	0.017	3.21E-01	T	0.875	-0.029	0.014	3.62E-02	T					
rs6722557	G	0	0.75	-0.020	0.002	4.60E-14	0.732	-0.031	0.013	1.29E-02	T	0.735	-0.005	0.010	6.13E-01	T	0.7083	0.003	0.004	5.45E-01	T
rs6761320	C	0	0.57	-0.010	0.002	1.20E-06	0.583	-0.009	0.012	4.55E-01	T	0.573	-0.032	0.009	5.85E-04	F	0.5167	-0.003	0.004	4.00E-01	T
rs6769511	T	0	0.69	-0.010	0.002	3.30E-08	0.694	-0.018	0.012	1.43E-01	T	0.692	-0.004	0.010	6.98E-01	T	0.7083	0.010	0.003	2.61E-03	T
rs6782178	C	0	0.58	-0.010	0.002	1.00E-14	0.606	0.002	0.012	8.49E-01	T	0.605	0.004	0.009	6.73E-01	T					
rs6794670	C	0	0.8	0.010	0.002	8.40E-11	0.781	0.002	0.014	8.68E-01	T	0.771	-0.020	0.011	8.59E-02	T	0.7917	0.004	0.005	4.31E-01	T
rs6839437	T	0	0.16	-0.030	0.002	9.00E-36	0.169	-0.019	0.015	2.11E-01	T	0.177	0.000	0.012	9.93E-01	T					
rs6861681	G	0	0.7	-0.010	0.002	3.70E-08	0.681	-0.008	0.012	5.15E-01	T	0.690	0.007	0.010	4.56E-01	T	0.7083	0.011	0.003	9.49E-04	T
rs6864688	C	0	0.47	0.010	0.002	2.70E-13	0.484	0.014	0.011	2.16E-01	T	0.478	0.012	0.009	1.72E-01	T	0.475	0.004	0.004	2.24E-01	T
rs687914	G	0	0.75	0.020	0.002	7.50E-20	0.769	0.014	0.015	3.61E-01	T	0.773	0.046	0.013	5.30E-04	T					
rs6882422	G	0	0.88	0.030	0.003	1.90E-19	0.895	0.016	0.018	3.69E-01	T	0.897	0.014	0.015	3.45E-01	T	0.9167	0.012	0.006	5.49E-02	T
rs6885822	G	0	0.84	0.020	0.003	2.90E-20	0.864	-0.012	0.017	4.62E-01	T	0.862	-0.007	0.013	5.72E-01	T	0.8	0.005	0.005	3.26E-01	T
rs6901631	T	0	0.87	-0.010	0.003	3.70E-08	0.872	-0.024	0.017	1.62E-01	T	0.869	0.003	0.013	8.39E-01	T	0.8583	-0.001	0.006	9.18E-01	T
rs6903443	A	0	0.46	0.050	0.002	0.00E+00	0.430	0.025	0.011	2.71E-02	T	0.437	0.012	0.009	1.91E-01	T	0.45	-0.001	0.004	7.92E-01	T
rs6930181	A	0	0.54	0.010	0.002	1.10E-07											0.5333	-0.002	0.004	6.27E-01	T
rs6931664	A	0	0.4	-0.070	0.002	0.00E+00	0.390	-0.004	0.011	6.94E-01	T	0.404	-0.014	0.009	1.34E-01	T	0.4333	0.006	0.004	9.21E-02	T
rs6938070	T	0	0.3	0.020	0.002	1.70E-24	0.295	0.024	0.012	4.57E-02	T	0.291	-0.001	0.010	9.61E-01	T	0.2417	-0.001	0.004	8.30E-01	T
rs6965122	A	0	0.67	0.050	0.002	0.00E+00	0.676	0.027	0.012	2.58E-02	T	0.673	-0.011	0.009	2.59E-01	T	0.725	0.007	0.004	9.72E-02	T
rs6985616	A	0	0.56	-0.010	0.002	8.70E-08	0.552	0.005	0.011	6.45E-01	T	0.548	-0.010	0.009	2.84E-01	T	0.6	-0.002	0.004	5.99E-01	T
rs7000279	C	0	0.73	-0.010	0.002	7.70E-09	0.731	-0.007	0.013	5.70E-01	T	0.734	-0.011	0.010	2.94E-01	T					
rs7014448	T	0	0.32	0.030	0.002	7.00E-28	0.319	0.000	0.012	9.80E-01	T	0.320	0.013	0.010	1.89E-01	T	0.325	-0.002	0.004	5.92E-01	T
rs7017252	C	0	0.62	-0.020	0.002	6.40E-16	0.627	-0.012	0.012	3.00E-01	T	0.620	-0.007	0.009	4.83E-01	T	0.625	0.000	0.004	9.37E-01	T
rs7040344	C	0	0.65	0.030	0.002	0.00E+00	0.658	0.029	0.012	1.50E-02	T	0.652	0.004	0.009	6.61E-01	T	0.6667	0.000	0.003	9.08E-01	T
rs7102	T	0	0.63	0.020	0.002	3.50E-20	0.625	-0.001	0.012	9.64E-01	T	0.625	0.000	0.009	9.78E-01	T	0.6917	0.001	0.003	8.03E-01	T
rs7121378	T	0	0.12	-0.020	0.003	7.50E-11	0.114	-0.024	0.018	1.70E-01	T	0.119	-0.011	0.014	4.51E-01	T	0.1833	0.003	0.006	6.42E-01	T
rs7121746	A	0	0.41	0.060	0.002	0.00E+00	0.381	-0.002	0.012	8.25E-01	T	0.394	0.003	0.009	7.22E-01	T	0.3833	0.005	0.004	2.06E-01	T
rs7135535	G	0	0.55	0.010	0.002	1.20E-10	0.546	-0.003	0.011	7.74E-01	T	0.557	0.004	0.009	6.32E-01	T					
rs71390846	G	1	0.81	0.040	0.002	0.00E+00	0.813	-0.014	0.014	3.19E-01	T	0.813	0.000	0.012	9.89E-01	T					
rs71420186	G	0	0.93	0.030	0.004	3.40E-10	0.923	-0.007	0.022	7.51E-01	T	0.925	-0.009	0.018	5.92E-01	T					
rs7167692	T	0	0.95	0.050	0.004	3.40E-25	0.950	-0.022	0.026	3.86E-01	T	0.949	0.003	0.021	8.99E-01	T	0.9417	-0.004	0.009	6.58E-01	T
rs7170637	G	0	0.84	0.020	0.003	2.80E-10	0.841	-0.028	0.017	9.43E-02	T	0.839	0.012	0.014	3.82E-01	T	0.85	0.010	0.007	2.00E-01	T
rs7175531	T	1	0.35	-0.030	0.002	0.00E+00	0.338	0.009	0.012	4.34E-01	T	0.342	0.033	0.009	4.13E-04	T	0.2833	0.001	0.004	9.05E-01	T
rs7198843	T	0	0.43	-0.020	0.002	6.10E-11	0.427	-0.018	0.012	1.22E-01	T	0.433	-0.015	0.009	9.98E-02	T	0.3917	-0.003	0.004	4.07E-01	T
rs7209460	C	1	0.3	-0.050	0.002	0.00E+00	0.305	-0.032	0.012	8.63E-03	T	0.314	-0.037	0.010	1.15E-04	T	0.3833	-0.007	0.004	7.91E-02	T
rs722526	A	0	0.49	-0.010	0.002	4.10E-05	0.472	-0.018	0.011	1.04E-01	T	0.482	0.011	0.009	2.18E-01	T	0.4333	0.000	0.004	9.57E-01	T
rs7236090	T	0	0.44	-0.010	0.002	1.60E-07	0.479	0.004	0.012	7.58E-01	T	0.475	0.002	0.010	8.35E-01	T	0.55	0.002	0.004	6.01E-01	T
rs7237942	A	0	0.21	0.020	0.002	3.20E-12	0.210	-0.043	0.014	1.94E-03	T	0.207	-0.031	0.011	5.06E-03	T	0.2583	0.007	0.004	7.18E-02	T
rs72656010	T	0	0.87	-0.020	0.003	6.30E-10	0.869	0.019	0.017	2.51E-01	T	0.864	0.032	0.013	1.39E-02	T					
rs72692842	C	0	0.91	0.030	0.003	4.90E-13	0.908	-0.043	0.020	3.06E-02	T	0.910	-0.026	0.017	1.15E-01	T	0.8833	-0.011	0.007	9.36E-02	T
rs7274697	G	0	0.92	-0.020	0.003	8.20E-08	0.913	-0.024	0.020	2.28E-01	T	0.915	-0.016	0.016	3.10E-01	T	0.8917	0.003	0.007	6.37E-01	T
rs72805220	C	0	0.93	0.060	0.004	0.00E+00	0.940	-0.011	0.024	6.55E-01	T	0.939	-0.001	0.019	9.50E-01	T					
rs72813180	C	0	0.85	0.020	0.003	8.20E-09	0.861	0.006	0.016	7.24E-01	T	0.844	0.008	0.013	5.33E-01	T					
rs72868839	A	0	0.93	-0.050	0.004	8.10E-37	0.919	0.059	0.023	8.73E-03	T	0.925	-0.008	0.019	6.59E-01	T	0.8833	0.004	0.007	6.08E-01	T
rs72945685	C	0	0.89	-0.020	0.003	2.00E-12	0.894	-0.010	0.018	5.71E-01	T	0.892	0.003	0.014	8.55E-01	T	0.8917	-0.005	0.006	4.48E-01	T
rs7301013	A	0	0.85	-0.020	0.003	1.30E-18	0.840	-0.001	0.015	9.46E-01	T	0.839	-0.013	0.012	3.01E-01	T	0.8917	-0.004	0.005	4.06E-01	T
rs73029263	A	0	0.87	0.030	0.003	1.80E-26	0.864	-0.051	0.016	1.98E-03	T	0.867	-0.024	0.013	7.20E-02	T					
rs73066226	T	0	0.84	-0.010	0.003	5.30E-08	0.832	0.029	0.015	5.65E-02	T	0.834	-0.001	0.012	9.34E-01	T					
rs73156468	G	0	0.86	0.020	0.003	1.70E-08	0.851	-0.036	0.016	2.01E-02	T	0.855	-0.009	0.013	4.90E-01	T	0.8833	0.004	0.005	4.37E-01	T

rs73238169	G	0	0.87	0.020	0.003	2.10E-10	0.869	0.005	0.016	7.52E-01	T	0.868	0.016	0.013	2.20E-01	T	0.9083	-0.009	0.006	1.00E-01	T
rs73479996	G	0	0.93	0.020	0.004	9.70E-10	0.924	0.005	0.022	8.36E-01	T	0.923	0.037	0.018	3.34E-02	T					
rs737534	A	0	0.81	0.020	0.002	2.40E-07	0.817	0.022	0.015	1.38E-01	T	0.814	0.017	0.012	1.42E-01	T	0.7667	0.000	0.005	9.84E-01	T
rs74119759	C	0	0.84	0.030	0.003	1.70E-26	0.833	0.013	0.015	4.03E-01	T	0.835	0.016	0.012	1.90E-01	T	0.875	0.002	0.005	6.57E-01	T
rs747091	T	0	0.44	-0.010	0.002	7.30E-11	0.450	0.001	0.011	9.41E-01	T	0.441	-0.016	0.009	7.92E-02	T	0.4167	-0.012	0.004	1.30E-03	T
rs7484147	T	0	0.36	0.050	0.002	0.00E+00	0.397	0.017	0.012	1.29E-01	T	0.390	0.011	0.009	2.41E-01	T	0.3667	-0.009	0.004	2.36E-02	T
rs7488974	G	0	0.6	-0.050	0.002	0.00E+00	0.593	-0.023	0.011	3.92E-02	T	0.593	-0.004	0.009	6.96E-01	T	0.6083	0.006	0.003	6.57E-02	T
rs74910854	A	0	0.93	0.020	0.004	2.10E-11	0.937	0.033	0.027	2.22E-01	T	0.937	0.009	0.024	7.12E-01	T					
rs7504492	T	0	0.62	-0.010	0.002	4.60E-10	0.616	-0.017	0.012	1.47E-01	T	0.623	0.016	0.009	9.34E-02	T	0.6083	-0.001	0.004	7.64E-01	T
rs7516171	C	0	0.82	-0.030	0.002	1.10E-21	0.807	-0.013	0.014	3.56E-01	T	0.808	0.007	0.011	5.65E-01	T					
rs751979	C	0	0.65	-0.020	0.002	8.10E-25	0.648	-0.004	0.012	7.17E-01	T	0.641	-0.015	0.009	1.04E-01	T	0.6417	-0.001	0.004	8.68E-01	T
rs75230517	G	0	0.95	0.100	0.004	0.00E+00	0.946	0.035	0.025	1.62E-01	T	0.945	0.000	0.020	9.83E-01	T	0.9417	-0.007	0.008	3.66E-01	T
rs7527300	C	0	0.59	0.030	0.002	3.40E-30	0.577	-0.016	0.011	1.48E-01	T	0.589	0.000	0.009	9.99E-01	T	0.625	-0.001	0.004	8.74E-01	T
rs7546500	T	0	0.67	-0.020	0.002	2.50E-12	0.677	0.023	0.013	8.37E-02	T	0.680	0.003	0.010	7.79E-01	T	0.681	-0.003	0.005	5.37E-01	T
rs75660521	C	0	0.94	0.020	0.004	4.40E-06	0.931	-0.027	0.023	2.47E-01	T	0.926	0.006	0.018	7.59E-01	T	0.925	0.004	0.008	6.51E-01	T
rs7679094	C	0	0.59	0.010	0.002	4.00E-09	0.609	0.004	0.012	7.63E-01	T	0.600	-0.002	0.010	8.80E-01	T	0.6417	0.000	0.004	9.37E-01	T
rs76833657	G	0	0.92	0.040	0.003	1.70E-24	0.929	0.000	0.022	9.93E-01	T	0.905	0.004	0.017	8.08E-01	T	0.9083	-0.019	0.007	1.36E-02	T
rs7694707	A	0	0.38	0.010	0.002	3.00E-08	0.365	0.007	0.012	5.71E-01	T	0.362	-0.013	0.009	1.74E-01	T					
rs76983463	T	0	0.96	-0.040	0.005	3.70E-15	0.970	-0.036	0.034	2.91E-01	T	0.969	-0.002	0.027	9.26E-01	T					
rs7703751	A	0	0.74	0.020	0.002	2.00E-26	0.760	-0.013	0.013	3.25E-01	T	0.758	-0.027	0.010	9.52E-03	T	0.7083	-0.005	0.004	2.55E-01	T
rs77392239	T	0	0.92	-0.040	0.003	1.80E-21	0.928	-0.029	0.024	2.25E-01	T	0.919	0.016	0.020	4.03E-01	T	0.9083	0.009	0.006	1.44E-01	T
rs77431781	A	0	0.92	0.030	0.004	2.00E-12	0.935	0.017	0.023	4.68E-01	T	0.935	0.007	0.019	6.94E-01	T					
rs77718124	A	1	0.94	-0.050	0.004	1.40E-26	0.949	-0.013	0.030	6.58E-01	T	0.951	-0.012	0.026	6.51E-01	T					
rs78015143	G	0	0.9	-0.030	0.003	1.40E-16	0.910	0.008	0.020	7.00E-01	T	0.910	-0.019	0.016	2.50E-01	T					
rs7814941	A	0	0.8	-0.020	0.002	1.30E-13	0.805	0.071	0.014	5.90E-07	F	0.787	0.019	0.011	9.23E-02	T	0.8	-0.006	0.005	1.85E-01	T
rs78150433	G	0	0.97	-0.040	0.006	4.60E-12	0.974	-0.056	0.044	2.05E-01	T	0.977	0.014	0.039	7.27E-01	T					
rs7820881	G	0	0.62	-0.010	0.002	1.50E-07	0.631	-0.039	0.012	7.61E-04	F	0.637	-0.024	0.009	1.02E-02	T	0.55	0.002	0.004	6.17E-01	T
rs78432519	C	0	0.89	0.040	0.003	2.30E-31	0.884	0.030	0.018	9.00E-02	T	0.882	0.017	0.014	2.29E-01	T					
rs785836	C	0	0.65	-0.010	0.002	2.70E-10	0.649	0.024	0.013	5.46E-02	T	0.648	0.010	0.010	3.21E-01	T	0.7	-0.003	0.004	4.38E-01	T
rs7866211	T	1	0.7	0.020	0.002	3.60E-28	0.686	0.002	0.012	8.46E-01	T	0.684	0.013	0.010	1.84E-01	T	0.725	-0.004	0.004	3.67E-01	T
rs78817479	C	0	0.91	-0.030	0.003	2.40E-11	0.913	-0.004	0.020	8.23E-01	T	0.917	0.028	0.016	8.94E-02	T					
rs79016257	G	0	0.96	-0.040	0.005	2.10E-14	0.952	0.006	0.027	8.13E-01	T	0.953	-0.023	0.022	2.93E-01	T					
rs7937689	C	0	0.78	0.020	0.002	1.50E-22	0.786	0.014	0.014	3.10E-01	T	0.787	0.010	0.011	3.55E-01	T	0.8167	-0.005	0.005	3.17E-01	T
rs7953929	C	0	0.8	0.020	0.002	2.10E-12	0.791	0.034	0.014	1.39E-02	T	0.793	0.033	0.011	3.19E-03	T	0.8167	-0.002	0.005	6.17E-01	T
rs7959604	C	0	0.93	0.060	0.004	0.00E+00	0.924	-0.006	0.023	8.02E-01	T	0.915	-0.010	0.018	5.79E-01	T					
rs79719017	T	0	0.7	-0.020	0.002	8.00E-20	0.721	-0.021	0.013	9.84E-02	T	0.726	-0.005	0.010	5.84E-01	T	0.6833	0.008	0.004	6.67E-02	T
rs79730878	T	0	0.77	0.020	0.002	3.90E-22	0.796	-0.008	0.014	5.68E-01	T	0.790	0.014	0.011	2.05E-01	T	0.8	-0.004	0.005	4.19E-01	T
rs798545	C	0	0.7	-0.010	0.002	7.20E-07	0.713	-0.007	0.012	5.54E-01	T	0.712	0.028	0.010	3.72E-03	T	0.7167	0.001	0.004	7.70E-01	T
rs8002850	G	0	0.66	0.030	0.002	1.00E-38	0.683	0.020	0.013	1.17E-01	T	0.677	-0.007	0.010	5.15E-01	T					
rs80222069	C	0	0.89	0.020	0.003	2.30E-10	0.895	-0.062	0.018	7.97E-04	F	0.897	-0.039	0.015	7.92E-03	T	0.9167	0.007	0.006	2.45E-01	T
rs8070737	G	0	0.82	-0.010	0.002	4.40E-09	0.829	-0.001	0.015	9.48E-01	T	0.825	-0.006	0.012	6.32E-01	T	0.8917	-0.001	0.005	9.22E-01	T
rs8095921	G	0	0.78	-0.020	0.002	1.10E-09	0.780	-0.003	0.014	8.46E-01	T	0.784	0.005	0.011	6.21E-01	T	0.7833	-0.001	0.005	8.62E-01	T
rs8121146	C	0	0.46	0.010	0.002	3.80E-08	0.489	0.000	0.011	9.89E-01	T	0.485	0.005	0.009	6.06E-01	T					
rs825453	A	0	0.39	0.020	0.002	1.60E-14	0.385	-0.002	0.011	8.25E-01	T	0.397	0.021	0.009	1.78E-02	T	0.45	0.012	0.004	1.90E-03	T
rs833823	A	0	0.03	0.040	0.006	8.20E-08	0.024	-0.004	0.039	9.20E-01	T	0.026	0.018	0.029	5.38E-01	T	0.0333	-0.007	0.013	5.63E-01	T
rs868127	C	0	0.71	0.020	0.002	9.10E-13	0.721	-0.008	0.015	5.77E-01	T	0.721	-0.006	0.014	6.86E-01	T	0.6917	0.010	0.006	9.21E-02	T
rs884205	A	1	0.25	-0.030	0.002	3.00E-26	0.264	0.008	0.013	5.20E-01	T	0.259	0.006	0.010	5.68E-01	T	0.3	-0.003	0.004	4.29E-01	T
rs890074	G	0	0.52	-0.010	0.002	7.90E-09	0.492	-0.037	0.011	1.07E-03	F	0.486	-0.004	0.009	6.92E-01	T	0.5417	-0.009	0.004	1.74E-02	T
rs899631	G	0	0.61	-0.020	0.002	2.70E-19	0.598	-0.007	0.012	5.95E-01	T	0.597	0.009	0.010	3.85E-01	T	0.6	0.001	0.004	7.13E-01	T

rs901865	T	0	0.17	0.030	0.002	8.40E-22	0.165	0.015	0.015	3.31E-01	T	0.164	-0.026	0.012	3.06E-02	T	0.175	0.000	0.005	9.84E-01	T
rs9290351	G	0	0.88	-0.020	0.003	5.90E-15	0.861	-0.017	0.016	3.04E-01	T	0.850	-0.006	0.013	6.56E-01	T	0.85	0.000	0.006	1.00E+00	T
rs9296151	G	0	0.97	0.040	0.005	4.40E-13	0.965	0.013	0.032	6.83E-01	T	0.962	-0.024	0.024	3.19E-01	T					
rs9364386	T	0	0.82	0.030	0.002	2.30E-26	0.836	0.002	0.015	8.70E-01	T	0.831	0.011	0.012	3.59E-01	T	0.7167	0.009	0.005	6.53E-02	T
rs9378485	T	0	0.62	0.010	0.002	1.50E-11	0.612	-0.004	0.011	7.03E-01	T	0.604	-0.015	0.009	1.06E-01	T	0.6167	-0.003	0.004	4.77E-01	T
rs939666	C	1	0.8	-0.070	0.002	0.00E+00	0.803	-0.014	0.014	3.29E-01	T	0.801	-0.020	0.011	7.33E-02	T	0.7417	0.002	0.005	6.17E-01	T
rs9447004	A	0	0.48	0.020	0.002	1.00E-30	0.503	-0.015	0.011	1.81E-01	T	0.500	-0.004	0.009	6.18E-01	T	0.3917	0.001	0.004	7.46E-01	T
rs945508	T	0	0.47	-0.010	0.002	1.80E-08	0.480	-0.016	0.011	1.40E-01	T	0.469	-0.015	0.009	9.84E-02	T	0.5	-0.001	0.004	8.33E-01	T
rs9466056	A	1	0.38	-0.010	0.002	2.80E-11	0.363	-0.014	0.012	2.40E-01	T	0.370	-0.011	0.009	2.35E-01	T	0.45	0.003	0.004	3.71E-01	T
rs947091	G	0	0.52	-0.040	0.002	0.00E+00	0.549	0.004	0.011	7.30E-01	T	0.546	0.012	0.009	1.85E-01	T	0.55	0.003	0.004	3.71E-01	T
rs9482770	T	0	0.55	-0.070	0.002	0.00E+00	0.548	0.014	0.011	2.00E-01	T	0.552	0.002	0.009	7.99E-01	T	0.525	-0.005	0.004	1.97E-01	T
rs9513510	G	0	0.3	0.040	0.002	0.00E+00	0.324	0.005	0.012	6.75E-01	T	0.321	-0.010	0.009	2.81E-01	T	0.25	-0.001	0.004	8.61E-01	T
rs9521510	T	0	0.68	0.020	0.002	8.50E-22	0.657	-0.009	0.012	4.60E-01	T	0.657	0.005	0.009	5.74E-01	T	0.7083	0.002	0.004	7.08E-01	T
rs9530279	T	0	0.74	0.020	0.002	1.70E-15	0.747	0.005	0.013	7.18E-01	T	0.743	0.018	0.011	9.83E-02	T	0.775	-0.004	0.004	3.17E-01	T
rs9532858	G	0	0.32	0.010	0.002	1.10E-13	0.323	0.010	0.012	4.03E-01	T	0.317	-0.013	0.009	1.60E-01	T	0.325	-0.001	0.004	7.51E-01	T
rs9594738	C	1	0.51	0.050	0.002	0.00E+00	0.483	0.029	0.011	8.65E-03	T	0.502	0.036	0.009	5.20E-05	T	0.5667	0.001	0.004	8.29E-01	T
rs960192	C	0	0.4	-0.020	0.002	9.00E-19	0.396	0.018	0.012	1.21E-01	T	0.402	0.008	0.009	3.69E-01	T	0.4083	-0.004	0.004	3.17E-01	T
rs9606138	G	0	0.89	0.120	0.003	0.00E+00	0.889	0.047	0.019	1.32E-02	T	0.892	0.037	0.016	2.22E-02	T	0.95	0.002	0.008	7.72E-01	T
rs9873544	T	0	0.38	-0.010	0.002	7.10E-13	0.378	-0.001	0.012	9.30E-01	T	0.374	0.009	0.009	3.05E-01	T	0.3167	-0.003	0.004	4.00E-01	T
rs9896306	C	0	0.73	0.030	0.002	4.80E-27	0.723	-0.011	0.013	3.97E-01	T	0.712	-0.007	0.010	4.97E-01	T	0.65	-0.001	0.004	8.86E-01	T
rs9921222	C	1	0.53	0.030	0.002	2.80E-33	0.505	0.019	0.011	9.11E-02	T	0.528	0.011	0.009	2.39E-01	T	0.525	0.003	0.004	4.45E-01	T
rs9927137	A	0	0.52	0.010	0.002	5.50E-11	0.524	-0.011	0.012	3.34E-01	T	0.528	0.014	0.009	1.17E-01	T					
rs9952412	A	0	0.48	-0.020	0.002	6.50E-16	0.489	-0.012	0.012	3.07E-01	T	0.479	-0.005	0.010	5.76E-01	T					
rs9974172	A	0	0.15	-0.020	0.003	3.40E-08	0.134	0.013	0.017	4.58E-01	T	0.133	-0.012	0.014	3.69E-01	T	0.15	-0.003	0.006	6.42E-01	T
rs9975345	T	0	0.46	0.010	0.002	5.70E-09	0.443	0.009	0.011	4.19E-01	T	0.438	-0.006	0.009	5.33E-01	T					

Appendix 38: BMI SNPs used as instruments in two-sample MR analyses.

	Exposure= BMI					Outcome=eBMD					Outcome=hip OA					Outcome=knee OA				
SNP	**EA**	**EAF**	**Beta**	**SE**	**p**	**EAF**	**Beta**	**SE**	**P**	**passed Steiger filtering**	**EAF**	**Beta**	**SE**	**p**	**passed Steiger filtering**	**EAF**	**Beta**	**SE**	**p**	**passed Steiger filtering**
rs1000940	G	0.320	0.019	0.003	1.28E-08	0.301	0.007	0.002	1.50E-03	F	0.302	0.009	0.013	4.80E-01	T	0.301	0.007	0.010	4.74E-01	T
rs10132280	C	0.682	0.023	0.003	1.14E-11	0.700	0.000	0.002	5.50E-01	T	0.699	0.018	0.013	1.66E-01	T	0.700	0.027	0.010	7.54E-03	T
rs1016287	T	0.287	0.023	0.003	2.25E-11	0.299	-0.003	0.002	1.80E-01	T	0.298	-0.010	0.013	4.36E-01	T	0.298	0.019	0.010	6.54E-02	T
rs10182181	G	0.462	0.031	0.003	8.78E-24	0.488	0.004	0.002	7.60E-02	T	0.488	0.016	0.012	1.62E-01	T	0.487	-0.022	0.009	1.73E-02	T
rs10938397	G	0.434	0.040	0.003	3.21E-38	0.434	0.008	0.002	5.10E-05	T	0.473	0.015	0.012	1.93E-01	T	0.473	-0.006	0.009	5.24E-01	T
rs10968576	G	0.320	0.025	0.003	6.61E-14	0.324	0.000	0.002	9.60E-01	T	0.436	0.006	0.012	5.95E-01	T	0.435	0.014	0.009	1.44E-01	T
rs11030104	A	0.792	0.041	0.004	5.56E-28	0.797	-0.010	0.002	7.20E-04	T	0.323	0.020	0.012	1.11E-01	T	0.323	0.010	0.010	3.33E-01	T
rs11057405	G	0.901	0.031	0.006	2.02E-08	0.894	-0.001	0.003	8.50E-01	T	0.797	-0.003	0.015	8.21E-01	T	0.797	0.008	0.012	4.92E-01	T
rs11165643	T	0.583	0.022	0.003	2.07E-12	0.592	0.000	0.002	9.70E-01	T	0.894	0.064	0.019	8.29E-04	F	0.894	0.023	0.015	1.30E-01	T
rs1167827	G	0.553	0.020	0.003	6.33E-10	0.565	0.003	0.002	8.20E-02	T	0.592	0.005	0.012	7.03E-01	T	0.592	0.008	0.009	4.29E-01	T
rs11727676	T	0.910	0.036	0.006	2.55E-08	0.904	-0.018	0.003	1.40E-07	F	0.565	-0.004	0.012	7.06E-01	T	0.566	0.022	0.009	1.68E-02	T
rs12286929	G	0.523	0.022	0.003	1.31E-12	0.526	-0.029	0.002	1.00E-49	F	0.905	-0.088	0.020	9.69E-06	F	0.905	-0.027	0.016	8.93E-02	T
rs12401738	A	0.352	0.021	0.003	1.15E-10	0.383	-0.003	0.002	1.20E-01	T	0.526	0.005	0.012	6.44E-01	T	0.526	0.007	0.009	4.40E-01	T
rs12429545	A	0.133	0.033	0.005	1.09E-12	0.129	0.008	0.003	1.60E-03	F	0.381	-0.018	0.012	1.41E-01	T	0.382	0.036	0.010	1.39E-04	T
rs12940622	G	0.575	0.018	0.003	2.49E-09	0.559	0.003	0.002	1.80E-01	T	0.129	0.004	0.018	8.25E-01	T	0.129	0.022	0.014	1.21E-01	T
rs13021737	G	0.828	0.060	0.004	1.11E-50	0.829	0.015	0.002	3.60E-08	T	0.559	0.025	0.012	3.37E-02	T	0.559	0.015	0.009	1.21E-01	T
rs13078960	G	0.196	0.030	0.004	1.74E-14	0.201	0.004	0.002	3.10E-01	T	0.829	0.028	0.016	6.61E-02	T	0.829	0.023	0.012	6.29E-02	T
rs13107325	T	0.072	0.048	0.007	1.83E-12	0.075	-0.016	0.004	2.50E-05	F	0.202	0.022	0.015	1.30E-01	T	0.201	0.021	0.012	6.51E-02	T
rs13191362	A	0.879	0.028	0.005	7.34E-09	0.875	0.001	0.003	4.80E-01	T	0.075	0.098	0.022	9.53E-06	F	0.075	0.074	0.018	2.69E-05	T
rs1516725	C	0.872	0.045	0.005	1.89E-22	0.863	-0.003	0.003	3.80E-01	T	0.875	-0.006	0.018	7.41E-01	T	0.875	0.040	0.014	4.24E-03	T
rs1528435	T	0.631	0.018	0.003	1.20E-08	0.621	0.004	0.002	5.20E-02	T	0.862	0.036	0.017	3.49E-02	T	0.863	0.048	0.014	4.35E-04	T
rs1558902	A	0.415	0.082	0.003	########	0.402	0.019	0.002	1.20E-19	T	0.621	-0.003	0.012	8.28E-01	T	0.621	0.022	0.010	2.29E-02	T
rs16851483	T	0.066	0.048	0.008	3.55E-10	0.066	0.010	0.004	4.00E-03	F	0.404	0.057	0.012	1.92E-06	T	0.403	0.043	0.010	6.12E-06	T
rs16951275	T	0.784	0.031	0.004	1.91E-17	0.775	0.000	0.002	9.80E-01	T	0.066	0.060	0.024	1.04E-02	T	0.066	0.039	0.019	3.71E-02	T
rs17001654	G	0.153	0.031	0.005	7.76E-09	0.148	-0.001	0.003	8.60E-01	T	0.775	0.009	0.014	5.00E-01	T	0.775	0.021	0.011	6.00E-02	T
rs17024393	C	0.040	0.066	0.009	7.03E-14	0.026	0.004	0.006	7.30E-01	T	0.148	-0.023	0.017	1.74E-01	T	0.148	0.000	0.013	9.92E-01	T
rs17094222	C	0.211	0.025	0.004	5.94E-11	0.213	0.002	0.002	9.50E-01	T	0.027	-0.011	0.037	7.55E-01	T	0.026	0.008	0.029	7.77E-01	T
rs17405819	T	0.700	0.022	0.003	2.07E-11	0.702	0.003	0.002	2.90E-01	T	0.213	0.010	0.014	4.72E-01	T	0.213	0.012	0.011	2.90E-01	T
rs17724992	A	0.746	0.019	0.004	3.42E-08	0.733	0.000	0.002	6.70E-01	T	0.702	-0.019	0.013	1.38E-01	T	0.702	0.002	0.010	8.86E-01	T
rs1808579	C	0.534	0.017	0.003	4.17E-08	0.515	-0.006	0.002	1.00E-02	F	0.733	-0.009	0.013	5.05E-01	T	0.733	0.018	0.011	9.01E-02	T
rs1928295	T	0.548	0.019	0.003	7.91E-10	0.570	0.001	0.002	3.00E-01	T	0.516	0.026	0.012	2.44E-02	T	0.515	0.020	0.009	3.44E-02	T
rs2033529	G	0.293	0.019	0.003	1.39E-08	0.288	0.005	0.002	6.00E-03	F	0.569	0.002	0.012	8.80E-01	T	0.570	0.030	0.009	1.15E-03	T
rs2033732	C	0.747	0.019	0.004	4.89E-08	0.744	0.001	0.002	4.10E-01	T	0.746	0.008	0.013	5.52E-01	T	0.745	0.002	0.011	8.90E-01	T
rs205262	G	0.273	0.022	0.004	1.75E-10	0.267	0.001	0.002	7.90E-01	T	0.268	0.018	0.013	1.71E-01	T	0.268	0.054	0.011	2.88E-07	F
rs2112347	T	0.629	0.026	0.003	6.19E-17	0.640	0.007	0.002	7.40E-04	T	0.640	-0.009	0.012	4.38E-01	T	0.641	0.017	0.010	8.76E-02	T
rs2121279	T	0.152	0.025	0.004	2.31E-08	0.126	-0.002	0.003	4.30E-01	T	0.126	0.021	0.018	2.24E-01	T	0.126	-0.002	0.014	8.62E-01	T
rs2176598	T	0.251	0.020	0.004	2.97E-08	0.246	-0.003	0.002	2.10E-01	T	0.246	-0.010	0.014	4.75E-01	T	0.246	0.015	0.011	1.61E-01	T
rs2207139	G	0.177	0.045	0.004	4.13E-29	0.170	0.000	0.002	4.90E-01	T	0.169	0.017	0.016	2.82E-01	T	0.169	0.019	0.012	1.18E-01	T
rs2245368	C	0.180	0.032	0.006	3.19E-08	0.167	0.008	0.002	1.80E-03	F	0.168	0.036	0.016	1.97E-02	T	0.168	0.040	0.012	1.37E-03	T
rs2287019	C	0.804	0.036	0.004	4.59E-18	0.818	0.006	0.002	3.90E-03	T	0.818	0.026	0.015	8.34E-02	T	0.818	0.003	0.012	8.27E-01	T
rs2365389	C	0.582	0.020	0.003	1.63E-10	0.592	0.007	0.002	1.30E-02	T	0.592	0.034	0.012	3.88E-03	T	0.592	0.012	0.010	2.10E-01	T
rs2820292	C	0.555	0.020	0.003	1.83E-10	0.568	0.006	0.002	2.70E-02	T	0.567	0.017	0.012	1.51E-01	T	0.567	0.019	0.009	3.84E-02	T
rs29941	G	0.669	0.018	0.003	2.41E-08	0.673	0.002	0.002	7.60E-01	T	0.673	0.006	0.012	6.10E-01	T	0.673	0.009	0.010	3.71E-01	T

rs3101336	C	0.613	0.033	0.003	2.66E-26	0.600	0.010	0.002	7.10E-05	T	0.601	0.021	0.012	8.29E-02	T	0.601	0.014	0.010	1.37E-01	T
rs3736485	A	0.454	0.018	0.003	7.41E-09	0.461	0.003	0.002	2.00E-01	T	0.461	0.021	0.012	7.03E-02	T	0.461	0.036	0.009	1.14E-04	T
rs3817334	T	0.407	0.026	0.003	5.15E-17	0.408	-0.001	0.002	9.90E-01	T	0.408	-0.033	0.012	4.90E-03	T	0.408	-0.016	0.009	8.23E-02	T
rs3849570	A	0.359	0.019	0.003	2.60E-08	0.348	-0.002	0.002	3.20E-01	T	0.347	0.002	0.012	8.44E-01	T	0.347	0.010	0.010	3.25E-01	T
rs3888190	A	0.403	0.031	0.003	3.14E-23	0.402	-0.003	0.002	1.90E-01	T	0.400	-0.010	0.012	4.24E-01	T	0.400	0.010	0.010	3.10E-01	T
rs4256980	G	0.646	0.021	0.003	2.90E-11	0.655	0.005	0.002	2.70E-02	T	0.655	0.003	0.012	7.82E-01	T	0.654	-0.007	0.010	4.51E-01	T
rs4740619	T	0.542	0.018	0.003	4.56E-09	0.552	0.004	0.002	5.50E-02	T	0.551	0.013	0.012	2.80E-01	T	0.551	0.010	0.009	2.65E-01	T
rs543874	G	0.193	0.048	0.004	2.62E-35	0.207	0.012	0.002	3.60E-06	T	0.207	0.036	0.014	1.36E-02	T	0.207	0.032	0.012	4.96E-03	T
rs6477694	C	0.365	0.017	0.003	2.67E-08	0.353	0.003	0.002	1.50E-01	T	0.353	0.041	0.012	8.53E-04	F	0.353	0.021	0.010	3.34E-02	T
rs6567160	C	0.236	0.056	0.004	3.93E-53	0.233	0.015	0.002	2.90E-07	T	0.234	0.049	0.014	3.36E-04	T	0.233	0.031	0.011	4.38E-03	T
rs657452	A	0.394	0.023	0.003	5.48E-13	0.391	-0.002	0.002	1.00E+00	T	0.391	-0.010	0.012	4.23E-01	T	0.391	-0.003	0.010	0.7419	T
rs6804842	G	0.575	0.019	0.003	2.48E-09	0.573	0.003	0.002	3.10E-01	T	0.574	-0.003	0.012	7.77E-01	T	0.574	0.019	0.009	0.04028	T
rs7138803	A	0.384	0.032	0.003	8.15E-24	0.368	0.012	0.002	9.20E-07	F	0.369	0.051	0.012	2.85E-05	T	0.368	0.011	0.010	0.2501	T
rs7141420	T	0.527	0.024	0.003	1.23E-14	0.516	0.006	0.002	9.10E-03	T	0.516	0.019	0.012	1.14E-01	T	0.516	0.014	0.009	0.1412	T
rs758747	T	0.265	0.023	0.004	7.47E-10	0.277	0.004	0.002	7.10E-02	T	0.278	-0.012	0.013	3.66E-01	T	0.278	-0.017	0.010	0.113	T
rs7599312	G	0.724	0.022	0.003	1.17E-10	0.732	0.005	0.002	1.50E-01	T	0.732	0.005	0.013	6.85E-01	T	0.732	0.015	0.011	0.1623	T
rs7899106	G	0.052	0.040	0.007	2.96E-08	0.050	0.005	0.004	2.50E-01	T	0.050	-0.007	0.027	7.90E-01	T	0.050	-0.011	0.021	0.6035	T
rs7903146	C	0.713	0.023	0.003	1.11E-11	0.710	-0.011	0.002	8.10E-09	F	0.710	-0.012	0.013	3.42E-01	T	0.710	0.033	0.010	0.001212	T
rs9400239	C	0.688	0.019	0.003	1.61E-08	0.706	-0.006	0.002	3.10E-02	T	0.706	0.028	0.013	2.80E-02	T	0.706	0.022	0.010	0.02979	T

Appendix 39: Hip OA SNPs used in two-sample MR analysis with BMD as the outcome.

		Exposure=Hip OA				Outcome=eBMD				
SNP	**EA**	**EAF**	**Beta**	**SE**	**p**	**EAF**	**Beta**	**SE**	**P**	**Passed Steiger filtering**
rs10843013	A	0.781	-0.105	0.014	8.40E-15	0.794	0	0.002	8.50E-01	T
rs11164653	T	0.418	-0.076	0.011	2.46E-11	0.409	-0.004	0.002	2.40E-02	T
rs12209223	A	0.116	0.125	0.018	8.76E-13	0.102	0.003	0.003	5.10E-01	T
rs13057823	A	0.31	0.073	0.012	1.63E-09	0.304	0.013	0.002	3.60E-06	T
rs1321917	C	0.404	0.067	0.011	2.71E-09	0.408	-0.001	0.002	9.20E-01	T
rs1913707	A	0.599	0.069	0.011	2.09E-09	0.612	-0.001	0.002	9.20E-01	T
rs2078396	T	0.366	-0.074	0.012	2.70E-10	0.383	0.001	0.002	2.30E-01	T
rs2268023	A	0.419	0.066	0.011	7.12E-09	0.395	0.006	0.002	2.30E-02	T
rs111844273	A	0.02	0.26	0.041	3.34E-10	0.021	0.005	0.006	5.70E-01	T

Appendix 40: Summary statistics for the knee OA instruments used in two-sample MR with BMD as the outcome.

		Exposure= knee OA				Outcome=eBMD				
SNP	**EA**	**EAF**	**Beta**	**SE**	**P**	**EAF**	**Beta**	**SE**	**p**	**passed Steiger filtering**
rs143384	A	0.586	0.06	0.009	5.40E-11	0.598	0.003	0.002	3.30E-01	T
rs4548913	A	0.623	-0.053	0.009	6.62E-09	0.639	-0.025	0.002	4.50E-32	F
rs66906321	T	0.172	-0.074	0.012	5.69E-10	0.181	-0.015	0.002	1.10E-08	T
rs9940278	T	0.443	0.064	0.009	6.93E-13	0.421	0.019	0.002	1.60E-19	T

Appendix 41: Hip OA SNPs used in two-sample MR analysis with BMI as the outcome.

		Exposure= hip OA				Outcome= BMI				
SNP	**EA**	**EAF**	**Beta**	**SE**	**P**	**EAF**	**Beta**	**SE**	**P**	**Passed Steiger Filtering**
rs10492367	T	0.19	0.1518	0.0148	1.25E-24	0.175	-0.0017	0.0047	0.7176	T
rs11059094	T	0.4777	0.0759	0.0117	7.38E-11	0.4224	0.0077	0.0043	0.07334	T
rs11583641	T	0.2764	-0.0811	0.0131	5.58E-10	0.25	0.0025	0.0044	0.5699	T
rs12040949	T	0.3843	-0.0665	0.012	2.84E-08	0.3793	0.0046	0.004	0.2501	T
rs12209223	A	0.1032	0.1558	0.0191	3.88E-16	0.1333	-0.0176	0.0062	0.00453	T
rs1913707	A	0.6123	0.0795	0.012	2.96E-11	0.55	-0.0033	0.004	0.4094	T
rs2785988	A	0.2988	0.0828	0.0127	7.30E-11	0.2797	0.0086	0.0034	0.01098	T
rs2836618	A	0.2613	0.0876	0.0132	3.20E-11	0.325	0.0038	0.0042	0.3656	T
rs3774355	A	0.3601	0.0907	0.0121	8.20E-14	0.2917	0.0103	0.0031	0.000986	T
rs4338381	A	0.6319	0.095	0.0121	4.37E-15	0.6121	0.0043	0.0038	0.2578	T
rs62063281	A	0.7771	-0.0964	0.014	5.30E-12	0.8	-0.004	0.0047	0.3947	T
rs7222178	A	0.1991	0.0965	0.0146	3.78E-11	0.1833	0.0082	0.0056	0.1431	T
rs74767794	A	0.6829	0.0751	0.0126	2.56E-09	0.6583	0.0067	0.0033	0.0429	T
rs7571789	T	0.4761	0.0886	0.0117	3.26E-14	0.4583	0.003	0.0037	0.4175	T
rs79056043	A	0.9497	-0.1625	0.0268	1.33E-09	0.9667	0.007	0.0083	0.399	T
rs798748	T	0.3817	-0.0715	0.012	2.50E-09	0.3083	-0.0021	0.0038	0.5805	T
rs80287694	A	0.8869	-0.1093	0.0184	2.66E-09	0.8833	-0.0013	0.0063	0.8365	T

Appendix 42: Knee OA SNPs used in two-sample MR analysis with BMI as the outcome.

		Exposure= Knee OA				Outcome= BMI				
SNP	**EA**	**EAF**	**Beta**	**SE**	**P**	**EAF**	**Beta**	**SE**	**P**	**Passed Steiger Filtering**
rs1078301	A	0.7315	-0.0679	0.0106	1.27E-10	0.7417	-0.0035	0.0044	0.4263	T
rs143384	A	0.5966	0.0935	0.0095	4.77E-23	0.6	-7E-04	0.0033	0.8247	T
rs17567417	C	0.4698	-0.0655	0.0093	1.96E-12	0.4167	-0.0082	0.0038	0.03094	T
rs28817269	C	0.3557	0.0599	0.0097	6.46E-10	0.425	0.0029	0.0044	0.5098	T
rs4775006	A	0.4114	0.0578	0.0094	8.40E-10	0.4224	-0.0052	0.0046	0.2583	T
rs6499244	A	0.5596	0.0622	0.0094	3.88E-11	0.5333	0.0127	0.0037	0.000598	T
rs8067763	A	0.5936	-0.0566	0.0095	2.39E-09	0.6	0.0043	0.0038	0.2578	T
rs8067895	A	0.2858	0.0616	0.0103	1.89E-09	0.2917	0.0045	0.0041	0.2724	T
rs9277552	T	0.2105	-0.064	0.0114	1.97E-08	0.275	-0.0026	0.0044	0.5546	T

Appendix 43: Forest plots of leave-one-out analyses in the bidirectional MR analyses.

Appendix 41a: Forest plot presenting the leave-one-out analysis for the effect of eBMD on hip OA.

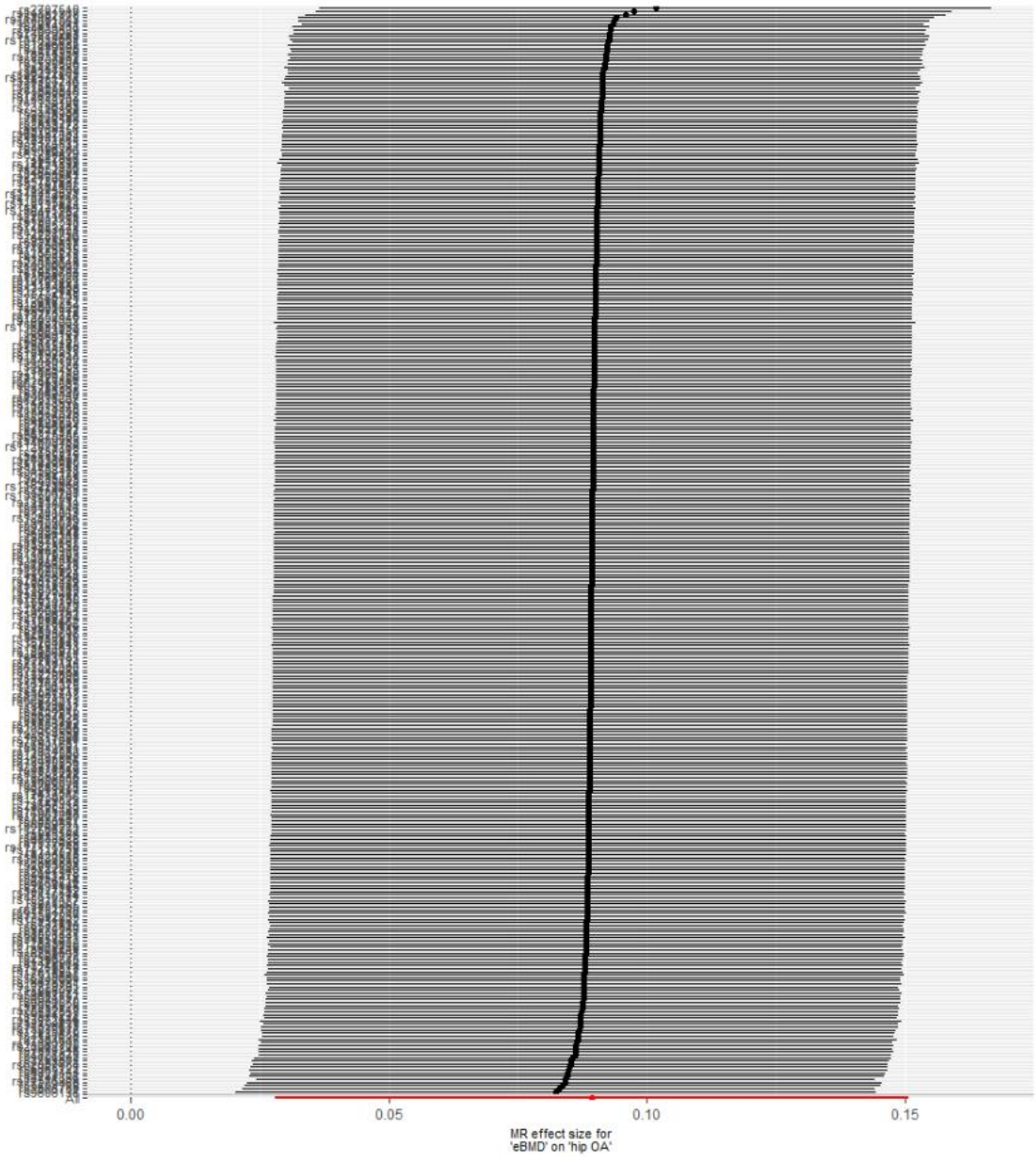

Appendix 41b: Forest plot presenting the leave-one-out analysis for the effect of eBMD on knee OA.

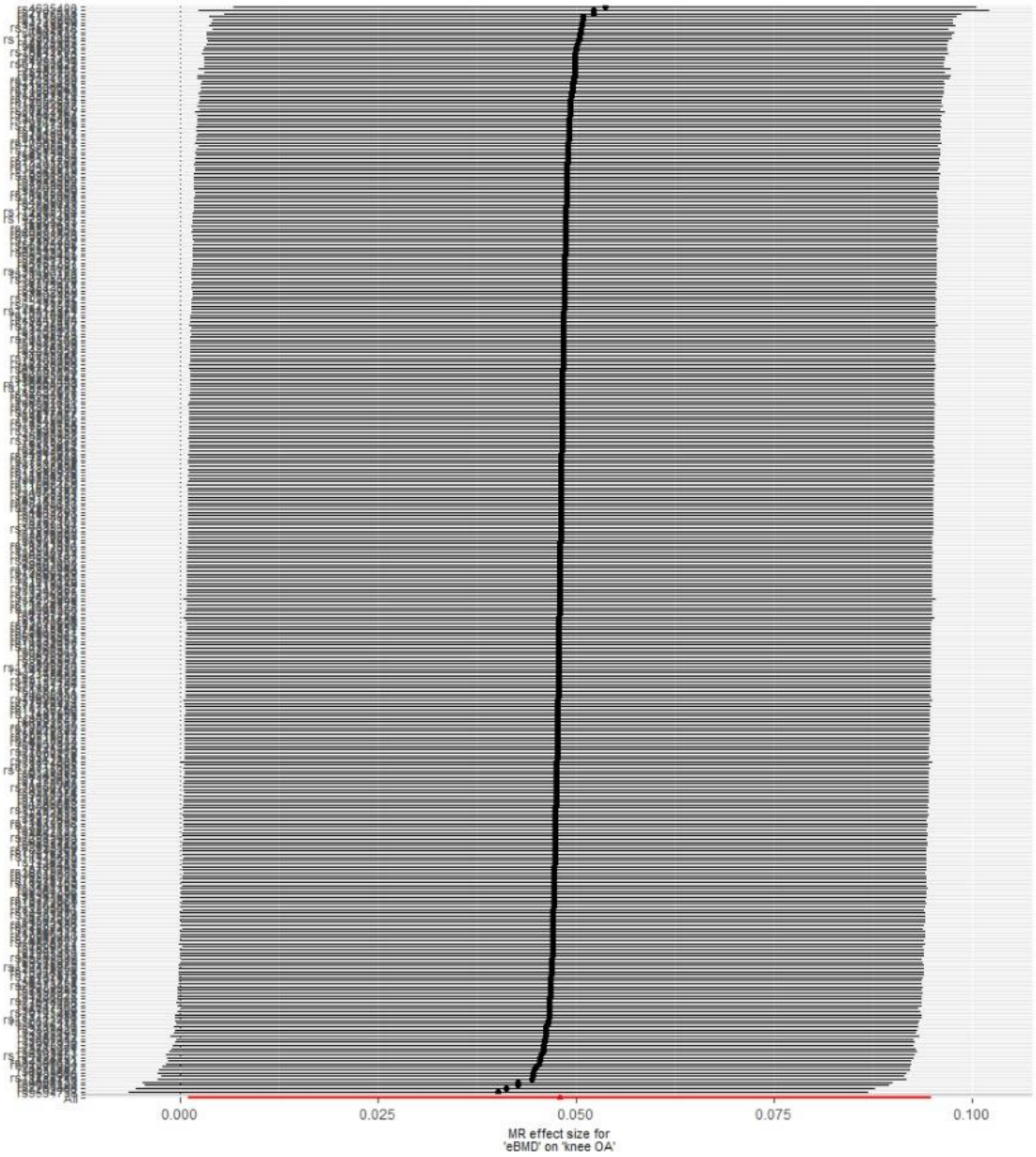

Appendix 41c: Forest plot presenting the leave-one-out analysis for the effect of knee OA on eBMD.

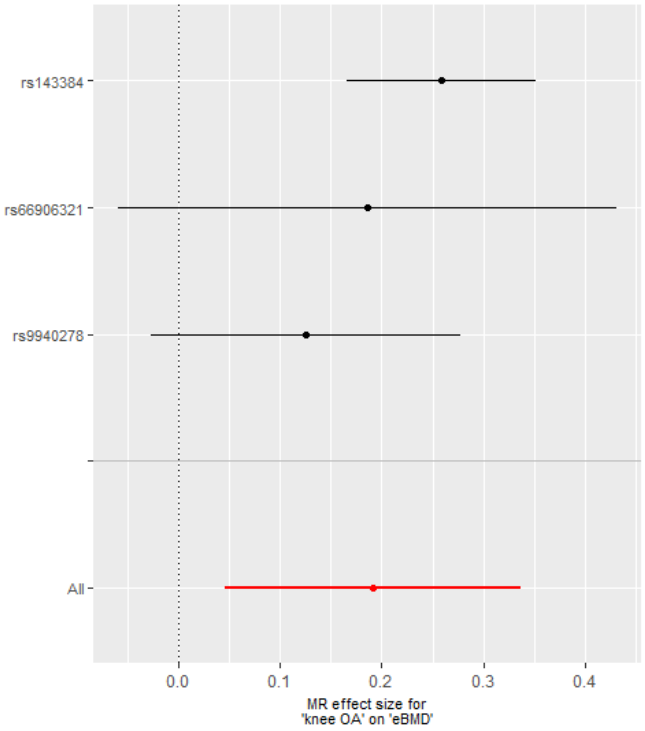

Appendix 41d: Forest plot presenting the leave-one-out analysis for the effect of BMI on hip OA.

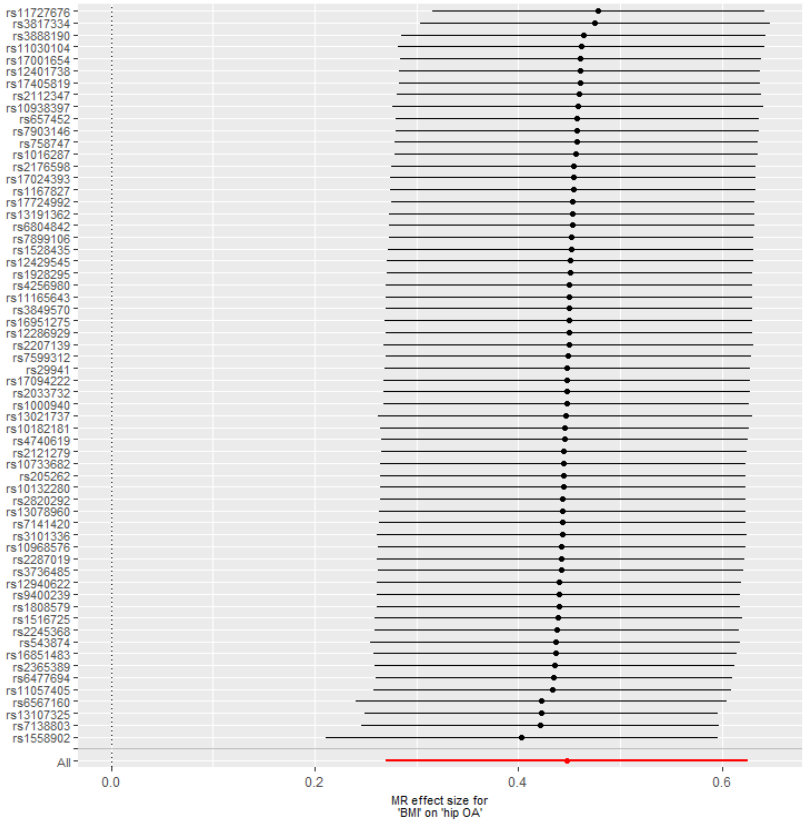

Appendix 41e: Forest plot presenting the leave-one-out analysis for the effect of BMI on knee OA.

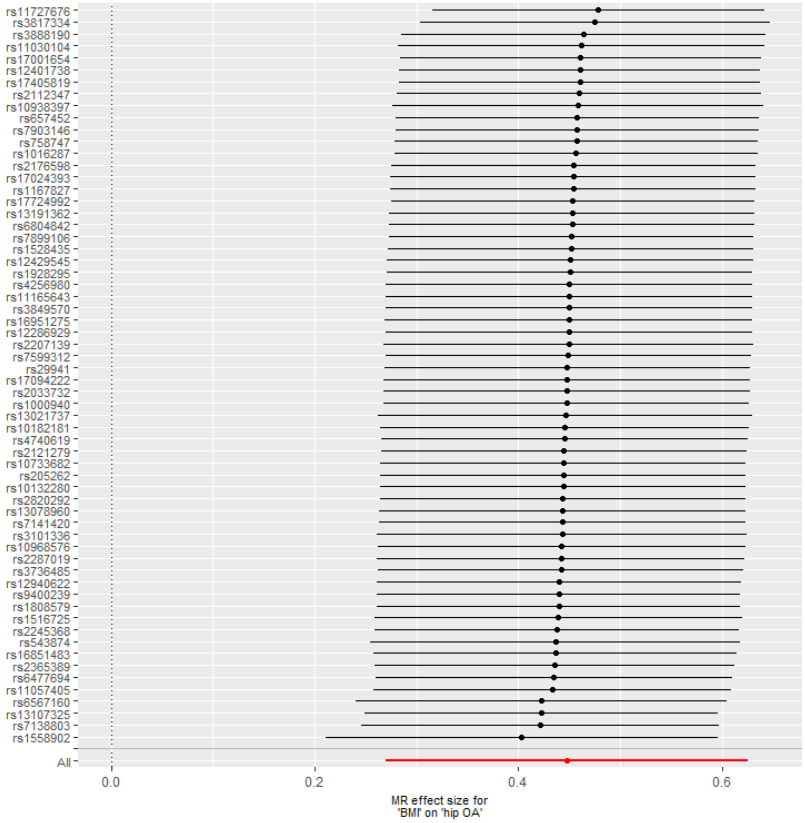

Appendix 41f: Forest plot presenting the leave-one-out analysis for the effect of hip OA on BMI.

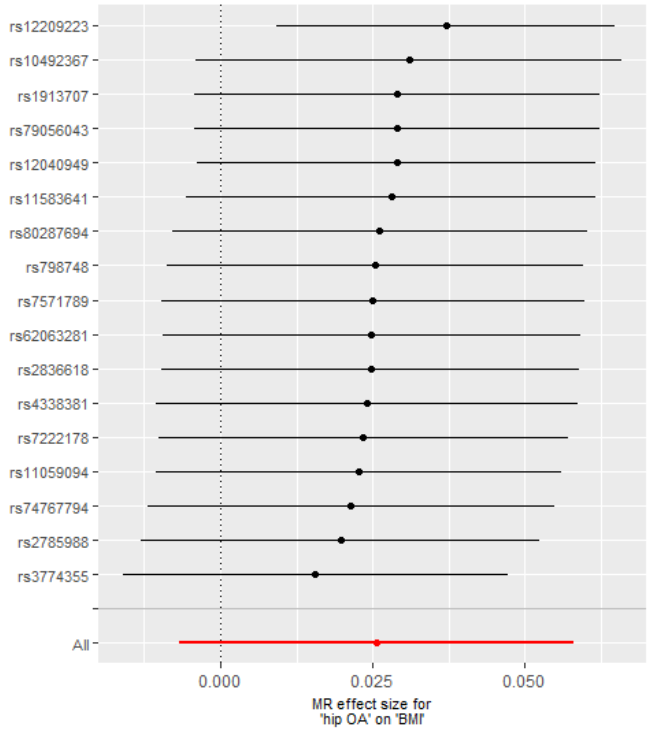

Appendix 41g: Forest plot presenting the leave-one-out analysis for the effect of BMI on eBMD.

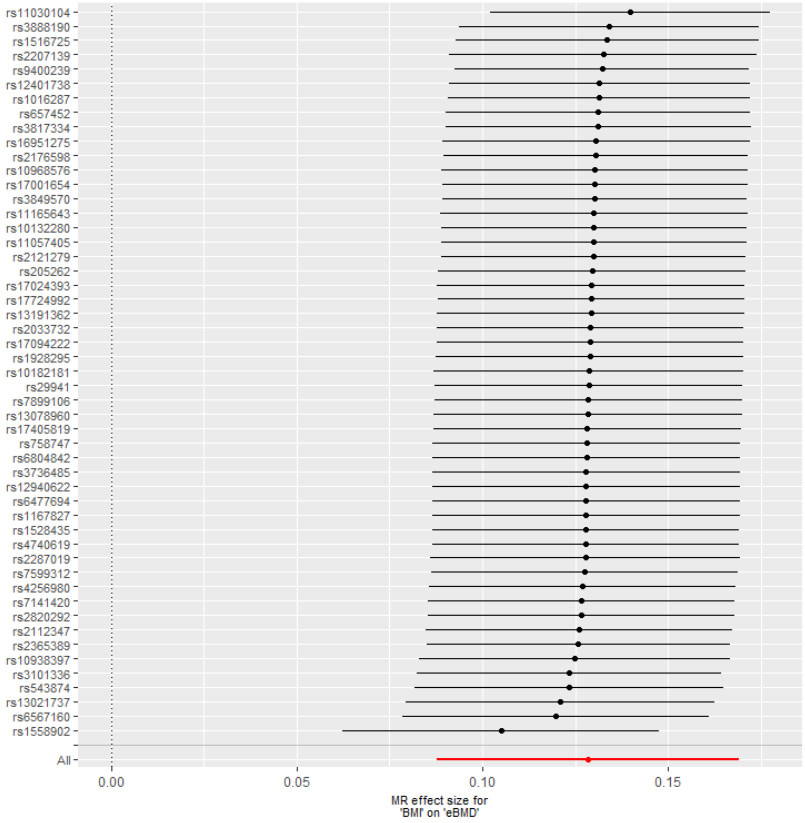

Appendix 44: Miami plots comparing GWAS results without and with adjustment for eBMD for hand (top), hip (middle) and knee (bottom) OA.

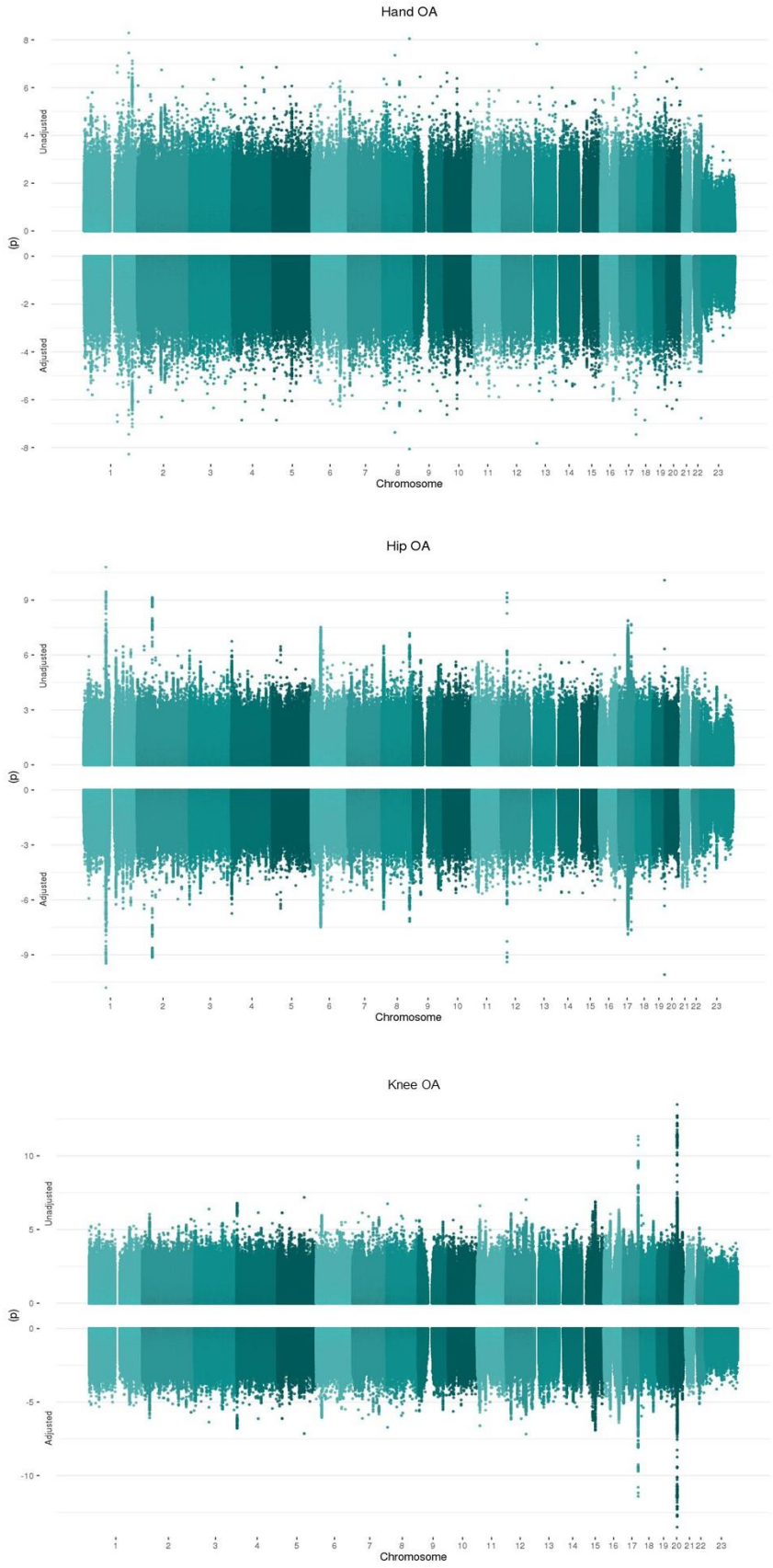

Appendix 45: QQplots for each sub-phenotype GWAS in each Rotterdam study population.

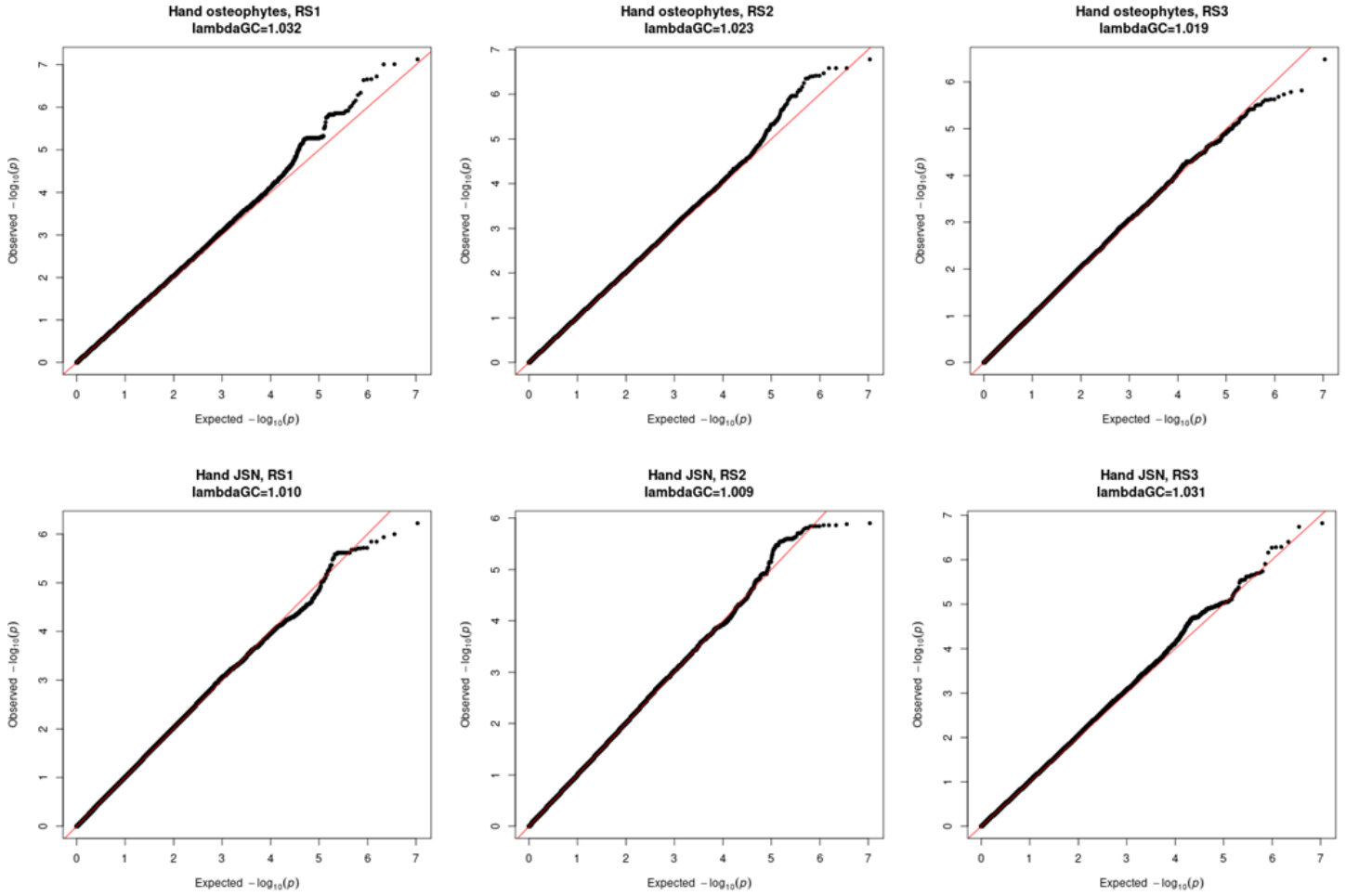

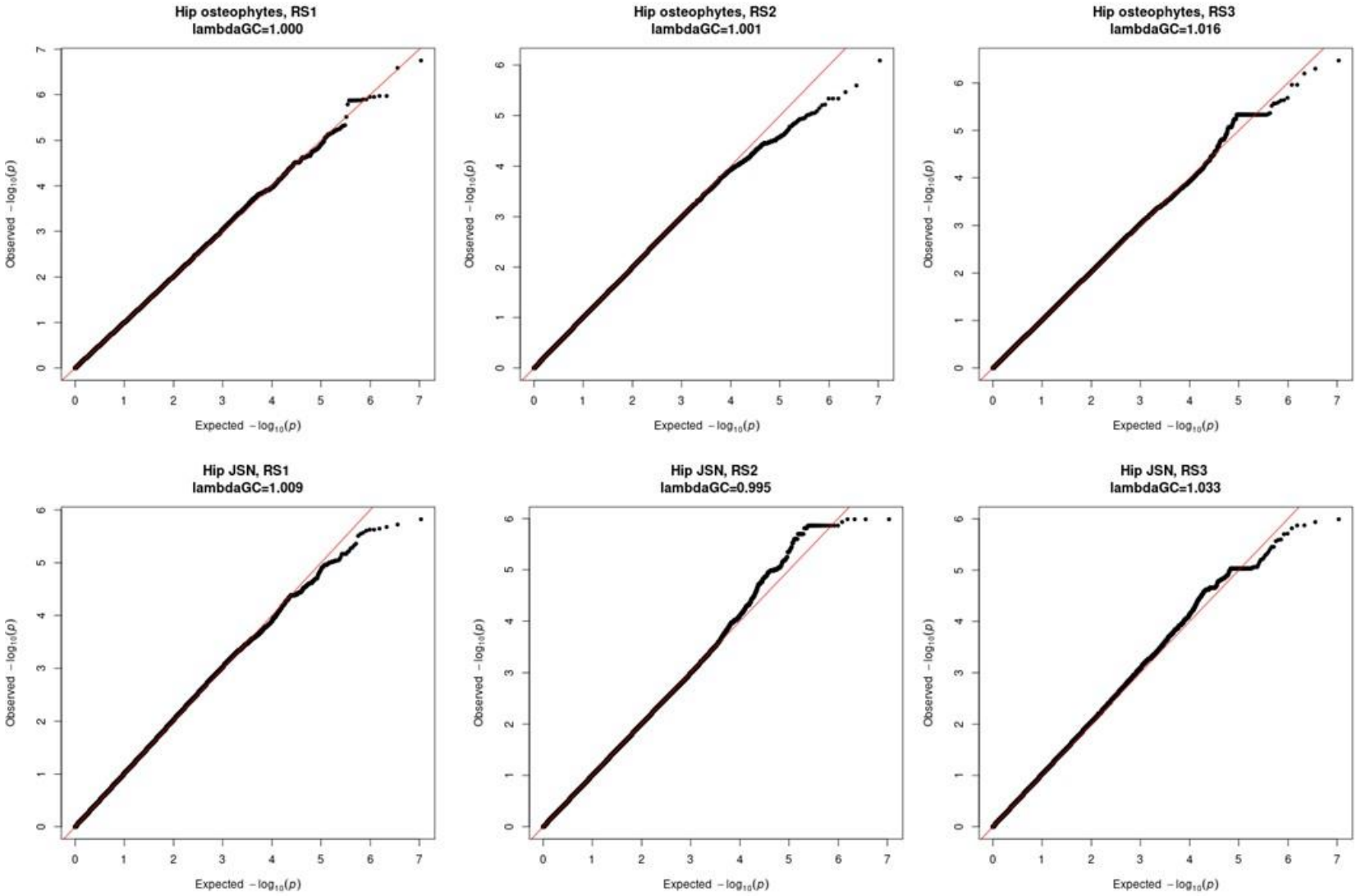
Hip osteophytes, RS1
lambdaGC=1.000
Hip osteophytes, RS2
lambdaGC=1.001
Hip osteophytes, RS3
lambdaGC=1.016
Hip JSN, RS1
lambdaGC=1.009
Hip JSN, RS2
lambdaGC=0.995
Hip JSN, RS3
lambdaGC=1.033
Observed $-\log_{10}(p)$
Expected $-\log_{10}(p)$

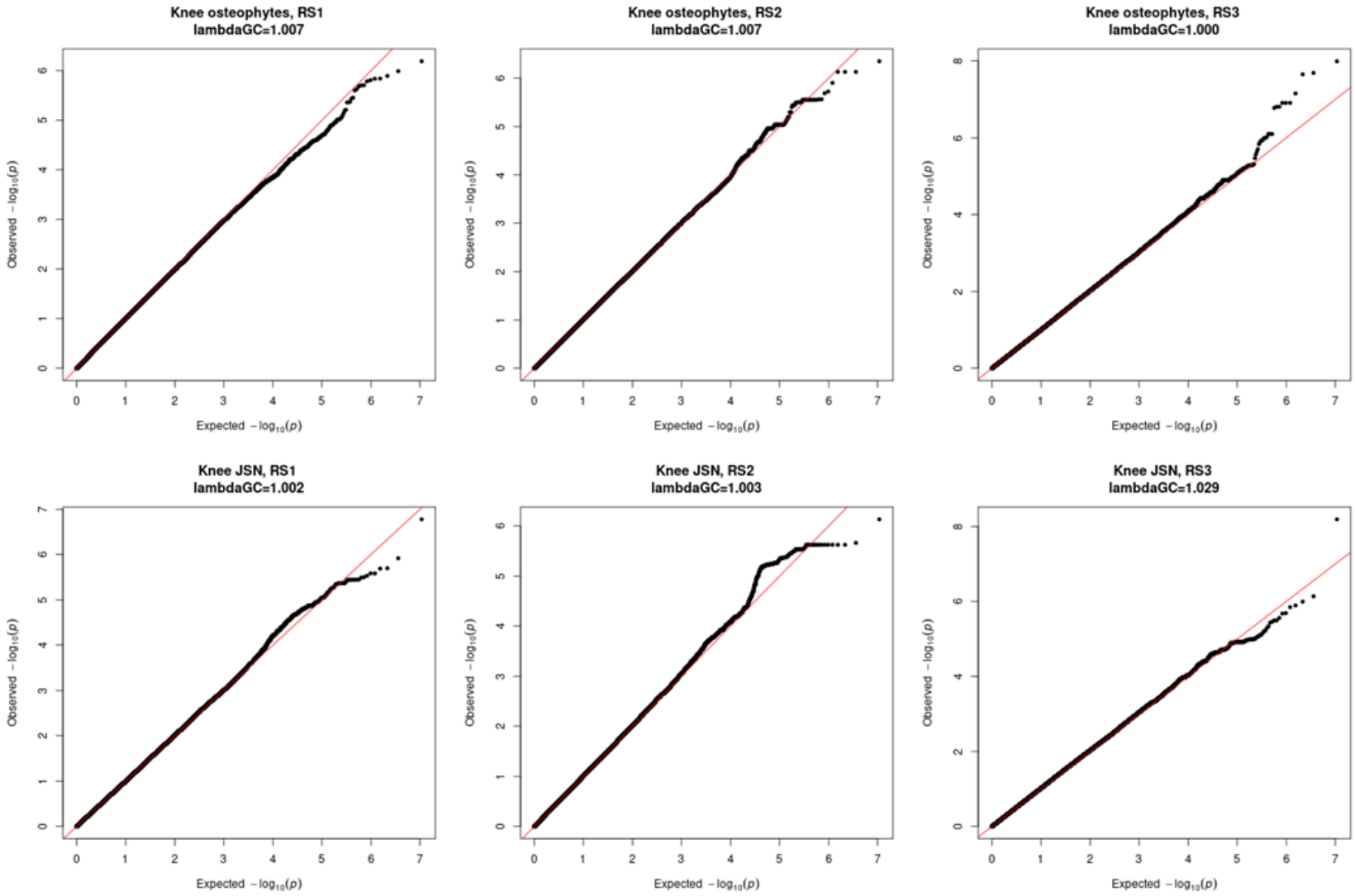
Knee osteophytes, RS1
lambdaGC=1.007
Knee osteophytes, RS2
lambdaGC=1.007
Knee osteophytes, RS3
lambdaGC=1.000
Knee JSN, RS1
lambdaGC=1.002
Knee JSN, RS2
lambdaGC=1.003
Knee JSN, RS3
lambdaGC=1.029
Observed $-\log_{10}(p)$
Expected $-\log_{10}(p)$

Appendix 46: IGF-1-associated SNPs used in 2SMR analyses and their associations with IGF-1 in the GIANT consortium, with hip and knee OA in the GWAS meta-analysis of UK Biobank and arcOGEN and with hand OA in UK Biobank.

SNP	Closest gene	EA	NEA	IGF-1				Hip OA			Knee OA			Hand OA		
				EAF	Beta	SE	*p*	Beta	SE	*p*	Beta	SE	*p*	Beta	SE	*P*
rs1065656*	*NUBP2*	C	G	0.306	-0.054	0.009	$1.17x10^{-8}$	0.006	0.013	0.265	-0.006	0.010	0.568	$1x10^{-4}$	$2x10^{-4}$	0.480
rs2153960	*FOXO3*	A	G	0.687	0.055	0.009	$5.16x10^{-9}$	0.027	0.013	0.033	0.023	0.010	0.028	$-7x10^{-5}$	$2x10^{-4}$	0.750
rs509035	*GHSR*	A	G	0.308	0.051	0.009	$2.09x10^{-8}$	$4x10^{-4}$	0.013	0.976	0.024	0.010	0.017	$1x10^{-4}$	$2x10^{-4}$	0.550
rs646776*	*CELSR2*	T	C	0.785	-0.028	0.010	$6.87x10^{-9}$ [a]	-0.040	0.014	0.004	-0.003	0.011	0.794	$7x10^{-5}$	$2x10^{-4}$	0.760
rs700753*	*TNS3*	C	G	0.347	-0.092	0.009	$1.60x10^{-23}$	0.004	0.012	0.753	0.010	0.010	0.292	$3x10^{-5}$	$2x10^{-4}$	0.860
rs780093	*GCKR*	T	C	0.409	-0.065	0.009	$2.19x10^{-13}$	-0.031	0.012	0.010	-0.023	0.010	0.014	$3x10^{-4}$	$2x10^{-4}$	0.930
rs934073	*ASXL2*	C	G	0.711	-0.053	0.009	$6.48x10^{-9}$	-0.014	0.013	0.265	0.006	0.010	0.563	$-5x10^{-5}$	$2x10^{-4}$	0.820
rs978458	*IGF1*	T	C	0.265	0.057	0.010	$1.56x10^{-10}$	0.038	0.013	0.005	0.013	0.011	0.209	$1x10^{-4}$	$2x10^{-4}$	0.520

[a]*p-value from bivariate analysis. p-value used to estimate beta=0.09.* **SNPs also associated with IGF-BP3 in the CHARGE meta-analysis (514).*

Appendix 47: Associations between BMI instruments and BMI in UK Biobank.

SNP	EA	Beta	SE	*P*
rs1000940	G	0.068	0.013	$5x10^{-8}$
rs10132280	A	-0.107	0.013	$2x10^{-17}$
rs1016287	C	-0.100	0.013	$3x10^{-15}$
rs10182181	G	0.159	0.012	$<1x10^{-300}$
rs10733682	G	-0.061	0.012	$2x10^{-7}$
rs10938397	G	0.152	0.012	$<1x10^{-300}$
rs10968576	G	0.115	0.012	$7x10^{-21}$
rs11030104	G	-0.181	0.014	$8x10^{-37}$
rs11057405	A	-0.127	0.019	$1x10^{-11}$
rs11165643	T	0.086	0.012	$2x10^{-13}$
rs1167827	G	0.099	0.012	$2x10^{-17}$
rs11727676	C	-0.036	0.019	0.061
rs12286929	G	0.085	0.012	$2x10^{-13}$
rs12401738	A	0.082	0.012	$4x10^{-12}$
rs12429545	A	0.122	0.017	$2x10^{-12}$
rs12940622	A	-0.089	0.012	$1x10^{-14}$
rs13021737	G	0.257	0.015	$<1x10^{-300}$
rs13078960	G	0.087	0.014	$1x10^{-9}$
rs13107325	T	0.231	0.022	$6x10^{-26}$
rs13191362	G	-0.093	0.017	$9x10^{-8}$
rs1516725	C	0.159	0.017	$2x10^{-21}$
rs1528435	T	0.077	0.012	$1x10^{-10}$
rs1558902	A	0.354	0.012	$<1x10^{-300}$
rs16851483	T	0.173	0.023	$9x10^{-14}$
rs16951275	C	-0.134	0.014	$2x10^{-22}$
rs17001654	G	0.063	0.016	$1x10^{-4}$
rs17024393	C	0.347	0.036	$1x10^{-21}$
rs17094222	C	0.070	0.014	$5x10^{-7}$
rs17405819	C	-0.094	0.013	$6x10^{-14}$
rs17724992	G	-0.070	0.013	$9x10^{-8}$
rs1808579	T	-0.104	0.012	$2x10^{-19}$
rs1928295	C	-0.058	0.012	$6x10^{-7}$
rs2033529	G	0.094	0.013	$2x10^{-13}$
rs2033732	C	0.050	0.013	$2x10^{-4}$
rs205262	G	0.143	0.013	$2x10^{-28}$
rs2112347	G	-0.141	0.012	$8x10^{-32}$
rs2121279	T	0.054	0.017	0.002
rs2176598	C	-0.083	0.013	$4x10^{-10}$
rs2207139	G	0.199	0.015	$2x10^{-38}$
rs2245368	T	-0.115	0.015	$7x10^{-14}$
rs2287019	T	-0.154	0.015	$7x10^{-25}$
rs2365389	T	-0.063	0.012	$9x10^{-8}$
rs2820292	C	0.090	0.012	$9x10^{-15}$
rs29941	G	0.072	0.012	$4x10^{-9}$
rs3101336	C	0.107	0.012	$1x10^{-19}$
rs3736485	G	-0.076	0.012	$6x10^{-11}$
rs3817334	T	0.114	0.012	$2x10^{-22}$
rs3849570	A	0.053	0.012	$1x10^{-5}$
rs3888190	A	0.124	0.012	$3x10^{-26}$
rs4256980	G	0.080	0.012	$3x10^{-11}$
rs4740619	C	-0.087	0.012	$7x10^{-14}$
rs543874	G	0.224	0.014	$<1x10^{-300}$
rs6477694	T	-0.052	0.012	$2x10^{-5}$
rs6567160	C	0.259	0.014	$<1x10^{-300}$
rs657452	G	-0.069	0.012	$4x10^{-9}$
rs6804842	G	0.059	0.012	$5x10^{-7}$
rs7138803	A	0.127	0.012	$2x10^{-26}$
rs7141420	T	0.096	0.012	$8x10^{-17}$
rs758747	T	0.052	0.013	$6x10^{-5}$
rs7599312	A	-0.078	0.013	$3x10^{-9}$
rs7899106	G	0.122	0.026	$4x10^{-6}$
rs7903146	T	-0.084	0.013	$3x10^{-11}$
rs9400239	C	0.076	0.013	$2x10^{-9}$

Appendix 48: Associations between height instruments and height in UK Biobank.

SNP	Beta	SE	*p* value	EA
rs425277	0.127	0.018	8.98E-13	T
rs2284746	0.283	0.016	<1.00E-300	G
rs2806561	-0.125	0.016	4.33E-15	G
rs2219320	-0.192	0.018	3.22E-26	C
rs7544462	-0.226	0.029	3.31E-15	C
rs6600365	-0.229	0.016	<1.00E-300	T
rs564914	0.135	0.016	5.67E-17	T
rs6691924	0.188	0.025	3.96E-14	T
rs2815379	0.127	0.018	4.68E-13	G
rs17391694	0.231	0.023	1.03E-23	T
rs7551732	0.165	0.016	1.19E-24	A
rs2811594	0.157	0.016	9.5E-22	G
rs7517682	-0.168	0.016	7.55E-26	A
rs1321666	0.081	0.016	3.41E-07	C
rs9428104	0.283	0.018	<1.00E-300	G
rs6658763	-0.135	0.030	6.51E-06	T
rs7534365	0.255	0.023	1.83E-28	C
rs2298265	-0.206	0.025	2.19E-16	T
rs6694089	0.267	0.017	<1.00E-300	A
rs17369123	0.196	0.020	4.5E-22	T
rs4652773	-0.100	0.016	2.93E-10	G
rs3814333	0.320	0.017	<1.00E-300	T
rs10863936	-0.124	0.016	4.02E-15	A
rs1244981	0.067	0.022	0.001996	A
rs991967	0.258	0.017	<1.00E-300	C
rs1544196	-0.145	0.019	6.73E-14	A
rs11799609	0.070	0.022	0.001254	T
rs17038954	0.162	0.033	6.76E-07	T
rs3885668	-0.173	0.016	3.42E-27	T
rs13006748	0.083	0.017	1.84E-06	C
rs2289195	0.265	0.016	<1.00E-300	A
rs711245	-0.160	0.017	2.22E-21	A
rs17511102	0.311	0.028	3.08E-29	T
rs897080	-0.136	0.019	5.32E-13	T
rs354196	0.075	0.016	2.9E-06	G
rs3791679	-0.471	0.019	<1.00E-300	G
rs7568069	-0.238	0.016	<1.00E-300	A
rs11684404	0.197	0.017	3.16E-32	C
rs13388725	0.056	0.016	0.000486	G
rs2166898	-0.196	0.021	1.77E-20	A
rs7567288	0.082	0.020	5.06E-05	C
rs4953951	-0.183	0.030	1.65E-09	T
rs12987566	0.159	0.018	7.94E-19	T
rs6746356	-0.141	0.018	1.69E-14	C
rs12693589	0.098	0.018	5.61E-08	C
rs6435143	-0.053	0.016	0.000891	C
rs994533	-0.209	0.017	9.7E-35	C
rs12470505	-0.275	0.027	3.77E-25	G
rs16859517	0.397	0.042	4.23E-21	T
rs3116168	0.273	0.018	<1.00E-300	C
rs4344931	0.102	0.017	5.09E-09	C
rs2633761	0.068	0.016	2.26E-05	A
rs13078528	0.233	0.037	2.16E-10	A
rs2597513	-0.272	0.026	7.96E-26	T
rs9816693	0.165	0.020	8.68E-16	C
rs2581830	-0.225	0.016	<1.00E-300	C
rs9835332	-0.169	0.016	1.52E-26	C
rs17806888	-0.177	0.025	5.28E-13	C
rs12330322	-0.214	0.019	4.39E-29	T
rs9825951	-0.154	0.017	1.19E-20	A
rs1797625	0.134	0.017	1.15E-15	T
rs1546391	0.163	0.030	4.62E-08	G
rs6439168	0.237	0.019	7.93E-36	G
rs724016	0.547	0.016	<1.00E-300	G
rs4325879	-0.119	0.018	5.16E-11	T
rs6441170	0.121	0.016	2.04E-13	C
rs7652177	0.261	0.016	<1.00E-300	G

rs720390	0.205	0.016	3.23E-36	A
rs4686904	-0.161	0.017	2.11E-22	T
rs3958122	0.166	0.017	4.36E-23	T
rs11722554	-0.287	0.041	3.75E-12	A
rs2302580	-0.173	0.016	5.28E-27	T
rs7692995	-0.548	0.022	<1.00E-300	C
rs16994718	-0.134	0.024	1.34E-08	T
rs1996422	0.088	0.017	5E-07	G
rs17081935	0.233	0.020	2.08E-30	T
rs9993613	-0.214	0.016	<1.00E-300	G
rs17556750	0.286	0.017	<1.00E-300	A
rs6813055	-0.129	0.016	3.05E-16	T
rs12639764	-0.232	0.016	<1.00E-300	C
rs1562975	0.130	0.017	4.78E-14	A
rs6838153	0.128	0.017	4.13E-14	G
rs12513181	-0.108	0.018	2.39E-09	A
rs1812175	0.589	0.021	<1.00E-300	G
rs13150868	0.079	0.016	7.94E-07	T
rs955748	0.155	0.018	3.84E-17	G
rs9292468	-0.238	0.016	<1.00E-300	C
rs3812040	-0.170	0.018	4.32E-22	C
rs7716219	-0.232	0.017	<1.00E-300	C
rs2662027	-0.134	0.026	2.25E-07	T
rs9291926	-0.120	0.016	3.78E-14	G
rs34651	-0.275	0.029	3.72E-21	T
rs6894139	-0.198	0.016	7.03E-36	G
rs13177718	-0.236	0.030	2.31E-15	T
rs6887276	0.098	0.016	5.83E-10	G
rs7701414	0.262	0.016	<1.00E-300	G
rs165189	0.129	0.023	1.46E-08	G
rs4624820	0.074	0.016	2.83E-06	A
rs4620037	-0.223	0.019	1.02E-30	C
rs12153391	-0.172	0.018	6E-21	A
rs4868126	0.247	0.017	<1.00E-300	G
rs422421	0.292	0.019	<1.00E-300	C
rs4246079	0.239	0.024	4.59E-23	G
rs9392918	0.294	0.016	<1.00E-300	C
rs1047014	0.232	0.018	2.1E-36	C
rs806794	-0.370	0.018	<1.00E-300	G
rs2857693	-0.264	0.016	<1.00E-300	T
rs12214804	-0.601	0.028	<1.00E-300	T
rs16895130	0.155	0.018	2.84E-18	G
rs10948222	0.139	0.016	7.11E-18	C
rs12190423	-0.080	0.016	1.02E-06	C
rs648831	0.191	0.016	4.17E-33	T
rs310421	0.194	0.016	2.31E-34	T
rs314263	-0.332	0.017	<1.00E-300	T
rs6920372	-0.168	0.016	1.8E-25	A
rs389663	-0.104	0.017	7.27E-10	C
rs1155939	0.318	0.016	<1.00E-300	A
rs1415701	-0.294	0.018	<1.00E-300	A
rs4896582	-0.368	0.017	<1.00E-300	A
rs6902771	0.230	0.016	<1.00E-300	T
rs1832871	-0.142	0.017	2.39E-17	G
rs991946	-0.121	0.016	1.81E-14	T
rs2763273	-0.199	0.019	4.71E-26	T
rs798497	-0.408	0.017	<1.00E-300	G
rs4725061	0.152	0.016	1.51E-21	G
rs3807931	0.167	0.016	5.26E-26	A
rs12538407	-0.217	0.016	<1.00E-300	G
rs552707	-0.355	0.017	<1.00E-300	C
rs6974574	0.170	0.017	9.99E-25	T
rs1113765	-0.112	0.021	6.05E-08	A
rs17807185	0.094	0.016	6.23E-09	G
rs42039	0.427	0.018	<1.00E-300	T
rs2188177	0.090	0.016	1.67E-08	T
rs6952113	-0.121	0.016	8.4E-14	A
rs6962887	-0.130	0.017	4.1E-14	G
rs273945	0.112	0.016	3.08E-12	C
rs6955948	0.151	0.018	1.27E-17	T

rs4875421	-0.069	0.016	1.59E-05	A
rs429433	-0.197	0.037	8.47E-08	G
rs7823327	0.078	0.016	8.05E-07	T
rs4273857	-0.206	0.019	2.61E-28	G
rs2013265	-0.180	0.018	5.62E-23	T
rs9650315	-0.395	0.023	<1.00E-300	T
rs16939034	0.127	0.029	1.24E-05	T
rs4735677	0.283	0.018	<1.00E-300	T
rs7007200	-0.022	0.017	0.203406	C
rs1599473	-0.201	0.018	1.15E-27	T
rs10283100	0.279	0.035	6.68E-16	G
rs4733724	-0.349	0.020	<1.00E-300	G
rs1036821	-0.227	0.017	<1.00E-300	A
rs7033940	-0.106	0.025	2.56E-05	C
rs2149163	0.106	0.016	6.59E-11	C
rs1576900	-0.062	0.018	0.000448	A
rs3763631	-0.114	0.017	2.32E-11	G
rs11144688	-0.357	0.024	<1.00E-300	A
rs958225	0.184	0.034	7.68E-08	A
rs7043114	-0.143	0.016	2.42E-19	T
rs817300	-0.528	0.030	<1.00E-300	A
rs7870753	0.301	0.019	<1.00E-300	G
rs989393	-0.135	0.017	8.57E-15	C
rs3739707	-0.147	0.018	8.71E-16	A
rs10119624	0.114	0.017	1.09E-11	A
rs7033487	-0.282	0.020	<1.00E-300	C
rs1742829	-0.206	0.028	8.86E-14	A
rs7466269	-0.212	0.017	1.35E-37	G
rs7849585	0.172	0.017	1.01E-24	T
rs12779328	-0.201	0.018	1.82E-30	T
rs7069985	0.129	0.019	1.92E-11	G
rs10995319	-0.152	0.019	3.53E-16	C
rs1171615	-0.185	0.019	6.16E-23	T
rs10997979	0.162	0.016	1.61E-24	G
rs1815314	-0.180	0.016	2.46E-29	A
rs1923367	-0.209	0.016	<1.00E-300	C
rs2631676	0.215	0.020	1.92E-26	G
rs7899004	-0.208	0.016	8.67E-39	C
rs6584575	0.159	0.027	2.38E-09	A
rs291979	0.195	0.019	2.85E-25	A
rs1614303	0.113	0.020	3.03E-08	T
rs7097701	0.151	0.016	1.14E-21	C
rs10794175	0.136	0.016	2.25E-17	T
rs4320932	-0.216	0.020	3.33E-26	C
rs2237886	0.323	0.026	9.04E-36	T
rs2099745	-0.026	0.035	0.460234	A
rs757081	0.117	0.017	2.62E-12	G
rs10767838	-0.103	0.018	9.72E-09	G
rs3802758	0.141	0.029	1.26E-06	A
rs1681630	-0.173	0.017	2.7E-25	C
rs2510396	0.218	0.022	5.19E-23	C
rs2509133	0.108	0.016	8.47E-12	C
rs11236294	0.114	0.018	6.44E-11	T
rs606452	-0.348	0.023	<1.00E-300	C
rs632124	0.145	0.016	2E-19	A
rs11221442	-0.099	0.018	6.44E-08	C
rs11612228	0.176	0.017	6.19E-26	T
rs2856321	-0.194	0.016	3.22E-32	A
rs12228415	0.122	0.016	1.72E-14	G
rs10770705	-0.168	0.017	8.82E-24	C
rs11049611	-0.268	0.017	<1.00E-300	T
rs10843390	0.151	0.018	1.18E-17	T
rs10880969	0.131	0.017	2.68E-14	C
rs2164968	0.132	0.016	6.85E-16	C
rs11175992	-0.226	0.019	1.16E-31	A
rs17783015	-0.069	0.022	0.00182	T
rs3825199	0.381	0.019	<1.00E-300	G
rs7971536	-0.175	0.016	1.89E-28	A
rs2888893	-0.107	0.016	1.4E-11	T
rs4767473	0.165	0.024	2.98E-12	A

rs7980687	0.255	0.020	9.79E-39	A
rs11057552	0.126	0.021	1.56E-09	A
rs1199734	0.141	0.021	1.74E-11	G
rs12323101	0.110	0.016	2.19E-11	A
rs3118905	-0.368	0.018	<1.00E-300	A
rs4883972	-0.034	0.016	0.032816	G
rs3818416	0.116	0.019	4.74E-10	C
rs7319045	-0.187	0.016	2.09E-30	G
rs7985356	-0.142	0.019	3.66E-14	A
rs8017130	0.141	0.017	2.08E-16	G
rs1950500	-0.184	0.017	4.18E-26	C
rs12435366	-0.084	0.019	7.24E-06	T
rs10131337	0.130	0.018	2.28E-12	T
rs8006657	0.106	0.016	9.67E-11	G
rs11624136	0.079	0.016	6.35E-07	A
rs2093210	-0.285	0.016	<1.00E-300	T
rs2058092	-0.060	0.016	0.000176	C
rs862034	0.188	0.016	3.23E-30	G
rs7154721	-0.211	0.016	<1.00E-300	C
rs1190545	0.156	0.018	3.41E-18	C
rs12882130	-0.182	0.016	2E-28	G
rs10152739	0.087	0.018	2.48E-06	T
rs316618	-0.125	0.019	9.56E-11	A
rs16964211	-0.357	0.037	1.78E-21	A
rs7177711	-0.144	0.016	1.41E-19	G
rs7162825	0.040	0.016	0.012057	T
rs731874	0.131	0.017	2.77E-14	A
rs5742915	0.215	0.016	<1.00E-300	C
rs7162542	0.343	0.016	<1.00E-300	G
rs2238300	-0.071	0.016	1.18E-05	A
rs2871865	-0.414	0.025	<1.00E-300	G
rs4246302	0.128	0.017	8.69E-14	G
rs11648796	0.257	0.020	<1.00E-300	G
rs26868	0.166	0.016	1.24E-25	A
rs960006	0.091	0.016	9.93E-09	C
rs1659127	0.163	0.017	3.62E-22	A
rs11642612	0.150	0.016	1.35E-20	C
rs9929889	-0.082	0.016	3.16E-07	T
rs8058684	0.190	0.017	1.34E-28	A
rs3790086	-0.155	0.016	1.71E-22	G
rs217181	0.104	0.020	1.98E-07	T
rs2326458	-0.138	0.018	2.94E-14	A
rs8052560	0.168	0.019	2.24E-19	A
rs9217	0.226	0.016	<1.00E-300	C
rs8067165	0.145	0.016	4.44E-19	G
rs3760318	-0.317	0.016	<1.00E-300	A
rs2028067	0.139	0.022	1.22E-10	C
rs584828	-0.165	0.016	1.49E-24	T
rs4986172	-0.198	0.017	1.05E-32	T
rs227724	0.147	0.017	1.25E-18	T
rs1401795	-0.187	0.016	8.2E-32	G
rs2079795	-0.303	0.017	<1.00E-300	C
rs2070776	0.315	0.017	<1.00E-300	G
rs2072268	-0.101	0.016	1.98E-10	A
rs1552173	-0.110	0.016	4.77E-12	T
rs4239020	-0.088	0.017	1.79E-07	T
rs888403	0.092	0.017	2.8E-08	G
rs14062	0.025	0.017	0.130853	G
rs4369779	0.476	0.019	<1.00E-300	C
rs2337143	-0.108	0.017	1.26E-10	G
rs9967417	-0.237	0.016	<1.00E-300	C
rs11152213	0.203	0.019	1.22E-27	C
rs8097893	-0.149	0.039	0.000155	G
rs11659752	-0.138	0.017	5.53E-16	G
rs11880992	0.244	0.016	<1.00E-300	A
rs1346490	-0.079	0.016	1.59E-06	C
rs4072910	-0.200	0.016	1.92E-36	C
rs8103992	-0.162	0.020	2.53E-16	C
rs7253628	0.154	0.021	2.78E-13	G
rs4803468	-0.175	0.016	2.67E-27	G

rs11880124	-0.167	0.028	4.01E-09	G
rs7273787	0.195	0.017	8.08E-32	G
rs1884897	-0.319	0.016	<1.00E-300	G
rs6085662	0.110	0.016	3.06E-11	C
rs7261425	-0.107	0.018	1.25E-09	G
rs1074683	-0.294	0.018	<1.00E-300	G
rs143384	0.590	0.016	<1.00E-300	G
rs17450430	0.248	0.019	<1.00E-300	T
rs6020202	-0.134	0.019	1.5E-12	A
rs2057291	-0.110	0.017	3.03E-11	G
rs6061231	-0.087	0.017	6.64E-07	A
rs2834442	0.145	0.016	1.36E-18	A
rs9977276	0.130	0.019	5.81E-12	G
rs5757318	0.145	0.022	4.08E-11	T
rs738288	-0.046	0.016	0.004089	A